Animal Models in Cardiovascular Research

Third Edition

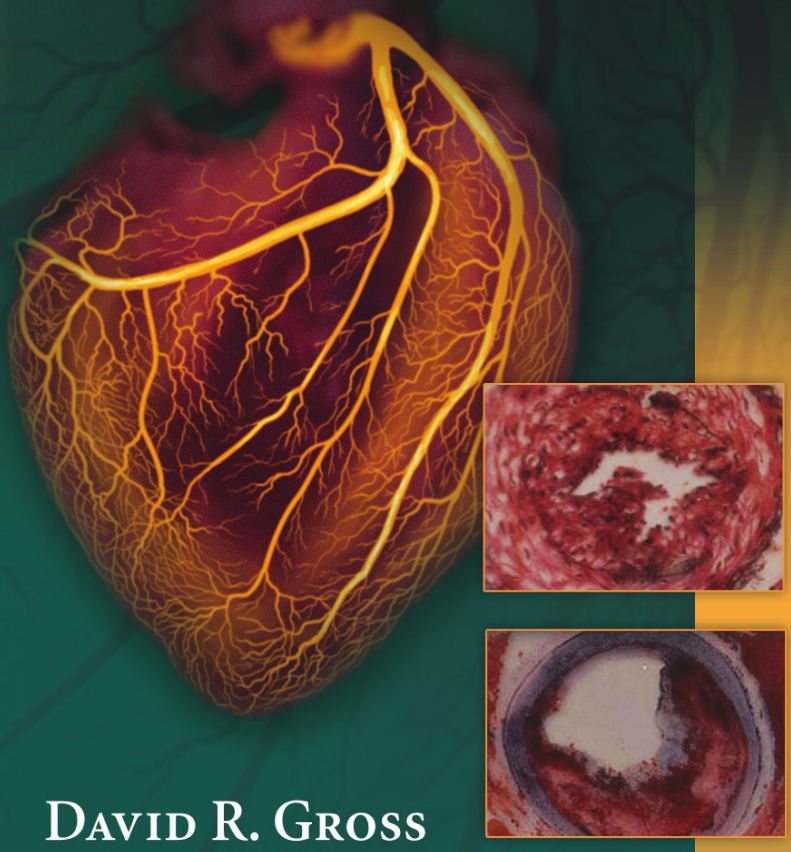

David R. Gross

Springer

Animal Models in Cardiovascular Research

David R. Gross

Animal Models in Cardiovascular Research

Third Edition

Springer

David R. Gross
Professor Emeritus
University of Illinois
Urbana Champaign
College of Veterinary Medicine
Department of Veterinary Biosciences
2001 S. Lincoln Ave.
Urbana IL 61802
USA

ISBN: 978-0-387-95961-0 e-ISBN: 978-0-387-95962-7
DOI: 10.1007/978-0-387-95962-7
Springer Dordrecht Heidelberg London New York

Library of Congress Control Number: 2009927491

© Springer Science+Business Media, LLC 2009
All rights reserved. This work may not be translated or copied in whole or in part without the written permission of the publisher (Springer Science+Business Media, LLC, 233 Spring Street, New York, NY 10013, USA), except for brief excerpts in connection with reviews or scholarly analysis. Use in connection with any form of information storage and retrieval, electronic adaptation, computer software, or by similar or dissimilar methodology now known or hereafter developed is forbidden.
The use in this publication of trade names, trademarks, service marks, and similar terms, even if they are not identified as such, is not to be taken as an expression of opinion as to whether or not they are subject to proprietary rights.

Printed on acid-free paper

Springer is part of Springer Science+Business Media (www.springer.com)

To Drs. Theodore S. Gross and Jeffrey M. Gross who continue the family obsession for the acquisition and dissemination of new knowledge.

Preface

This new edition of *Animal Models in Cardiovascular Research* describes historical and recent advances in our understanding of the cardiovascular system from studies conducted in a variety of animal models. Since the last edition, we have witnessed an explosion in the use of both congenic and transgenic animals. The use of specific knock-in and knock-out transgenic models has resulted in an avalanche of genetic, molecular, and protein-based information that, potentially, could result in an amazing new array of treatment and management options. However, the results of these studies also introduce a sometime bewildering array of redundant, overlapping, and competing molecular pathways involved in both physiological and pathological responses.

This third edition is designed to provide a better basis for understanding and using animal models in the current climate of background knowledge and information. It is significantly different than the previous two editions. Chapter 1 is updated from the previous editions addressing general principles of animal selection. It also provides expanded tables of normal physiological values for easy reference. Chapter 2 covers preoperative care, preanesthesia, and chemical restraint, and includes a significantly expanded section on pain recognition and analgesia particularly in rodents. Chapter 3 provides a summary of normal cardiovascular parameters obtained from intact, awake animals. The data have been rearranged in outline rather than the previous tabular form hopefully resulting in easier reference.

Chapter 4 addresses the techniques, problems, and pitfalls of measuring cardiac function in animals. There is an emphasis on the proper use of these measurements to develop new treatment and management strategies as well as using them to study mechanisms of disease. Chapter 5 emphasizes the techniques, problems, and pitfalls involved in the measurement of arterial function and ventricular/arterial coupling dynamics. Again the emphasis is on the use of these parameters to develop new treatment and management strategies and for studying the mechanisms of disease. Chapter 6 is an all new chapter dealing specifically with the problems and pitfalls inherent in using isolated heart preparations. The need for this chapter became apparent because so much information was published using obviously nonphysiologic preparations. The use of both pumping and nonpumping preparations is described along with techniques necessary for using hearts from larger species where oxygen-carrying capacity of the perfusate is critical. The importance of hypoxia and anoxia in the interpretation of results is discussed.

Chapter 7 focuses on the cardiovascular effects of the postoperative analgesic drugs commonly used today and how to avoid potential problems resulting from these effects when reporting experimental data. These data are also presented in outline form rather than the tabular format used in the two previous editions. Chapter 8 addresses the use of naturally occurring animal models of valvular and infectious cardiovascular disease. The information presented has been updated and expanded from the second edition. Chapter 9 examines iatrogenic models of ischemic heart disease.

Chapter 10 is new. It provides a review of iatrogenic, transgenic, and naturally occurring animal models of cardiomyopathy and heart failure. Chapter 11 includes new, updated, and revised information reviewing iatrogenic and transgenic models of hypertension. Chapter 12 contains new and updated information on iatrogenic and transgenic models of atherosclerotic disease.

Chapter 13 is completely a new material dealing with animal models for the study of neurohumeral and central nervous system control of the cardiovascular system. Chapter 14 is also new. It provides examples of cardiovascular studies involving the use of specific transgenic models that are not normally associated with the cardiovascular system, such as estrogen receptor knockouts, to study cardiovascular function.

Urbana, IL David R. Gross

Acknowledgements

Rosalie Gross has supported, encouraged, loved and endured since April of 1960. Our journey together continues.

Special thanks are owed to Professor Gary A. Iwamoto. Chapter 13 benefited significantly from his critical review and insightful suggestions.

Introduction

Animal rights activist organizations lobbied for and obtained significantly more restrictive regulations from governments worldwide since the last edition of this text. The agenda of most animal rights groups is to stop our use of animals. If biomedical science is to advance, we must understand the complexities and interrelationships of the various physiological control mechanisms that regulate living whole animal systems. It is more essential than ever that we persevere.

"Old guard" physiologists, pharmacologists, and toxicologists, familiar with whole animal homeostatic control mechanisms, believe some "new breed" scientists working at the molecular level are so focused in their particular area of expertise they have little appreciation for the potential effects of the iatrogenic changes they induce on the whole animal. Frequently lost in the landslide of new information is an understanding of how any particular gene, molecule, and/or protein fits into our broad understanding of the basic physiology of the animal species and how that relates to the human species. A few scientists even seem unaware that most, if not all, physiological systems have multiple and redundant control mechanisms that adjust any particular organ or system behavior to the homeostatic requirements of the whole animal.

Physiological systems may have several stimulatory and inhibitory controls that operate at some constant level of activity. The same physiological response is therefore possible by increasing stimulation or decreasing inhibition or vice versa. At the molecular and cellular level, the more information we obtain the more apparent it becomes that multiple pathways are present to achieve the same response. When cells, or organ systems, are perturbed by interrupting, knocking out, or upregulating a specific molecular or genetic pathway, redundant pathway(s) are, appropriately, up- or downregulated in response to maintain homeostasis.

A significant number of the animal models described in this text have been derived using either congenic or transgenic techniques. It is therefore appropriate to provide an abbreviated description of how these animals are produced.

Congenic strains of animals are developed by mating two inbred strains and then backcrossing the descendants for at least five and up to ten or more generations with one of the original strains. At each step, selections are made for the specific phenotype or genotype of interest. This allows the phenotype or genotype to pass from the donor strain onto an otherwise uniform recipient strain. The congenic

strain can then be compared to the pure recipient strain to determine phenotypical or genetic differences. Producing large numbers of eggs via superovulation in females and then using microsatellite or nucleotide polymorphism markers to track the genes of interest can speed up specific congenic strain development.

Transgenic animals are generally created using one of two different protocols. The first uses recombinant DNA methodology to insert (knock in) or remove (knock out) a specific gene or protein from the genome. The DNA used usually includes a structural gene, as well as other sequences, that enables it to be incorporated into the DNA of the host and to be expressed by the particular cells of interest. The most common method of producing a transgenic animal model involves harvesting embryonic stem cells from the inner cell mass of blastocysts. When these cells are grown in culture, they retain their ability to produce all the cells of the mature animal. The cultured cells are then exposed to the DNA of interest and those cells that successfully incorporate the DNA are identified and separated. These isolated cells are then injected into the inner cell mass of blastocysts. The resulting embryos are transplanted into a pseudopregnant dam. It is uncommon, at least in mice, for more than a third of the embryos thus transplanted to develop into healthy offspring. The next step is to test all the offspring to identify those with the desired gene. Usually, no more than 10–20% will have that gene and they will be heterozygous for it. The next step is to mate two heterozygous mice and screen their offspring for the one in four that will be homozygous for the transgene of interest. Mating homozygous animals produces the transgenic strain.

A second method of producing transgenic animals involves the same preparation of the DNA of interest and then harvesting freshly fertilized eggs before the sperm head has become a pronucleus. The male pronucleus is injected with the DNA of interest, and when the pronuclei have fused to form diploid zygote nuclei, the zygote is allowed to divide by mitosis to form a two-cell embryo. The two-cell embryo is then implanted in the pseudopregnant foster mother and the same steps used in the embryonic stem cell method are followed.

Contents

About the Author

Dr. David Gross entered private veterinary practice after earning the DVM degree from Colorado State University in 1960. In 1974 he was awarded the Ph.D. degree in physiology from the Ohio State University beginning a 36-year career in academics that culminated as professor and head of the Department of Veterinary Biosciences in the College of Veterinary Medicine, University of Illinois, Urbana-Champaign. Dr. Gross' research career encompassed 58 funded projects totaling over $5.5 million and 91 papers published in refereed journals using a wide variety of animal models. Ironically, his three most-cited research papers received no external funding. He and his colleagues showed that feeding dietary cholesterol to rabbits induced Alzheimer's-like lesions in the brain. Their work also showed that surgery involving cardiopulmonary bypass resulted in Alzheimer's-like brain lesions in pigs. With another group of colleagues, he helped pioneer minimally invasive coronary artery bypass grafting techniques using the pig as a model.

Chapter 1
General Principles of Animal Selection and Normal Physiological Values

Animals used in meaningful experiments must be held long enough in approved facilities to insure that they are not incubating infectious diseases. If the animal care facility does not require this, responsible investigators must still make certain these precautions are taken. Animals should be vaccinated, or tested and certified to be free of the diseases most likely to cause a problem in that species or that can be transmitted to personnel working with them. They should be verified free of both internal and external parasites. Prior to use they should be given a complete physical exam. Normal physiological parameters for the most commonly used species are in this chapter. Depending upon the experimental design, it might be prudent to collect blood samples and establish normal hematological and/or serum enzyme levels for each individual animal used. Although these precautions can be time consuming and expensive, the costs are minimal when compared with the overall cost of conducting experiments where the results are suspect because the physical condition or general health of the subject animals is a problem.

One of the most neglected aspects of a physical examination conducted on animals used in research protocol is a history. Significant information can be gleaned by talking with observant animal care personnel about the appetite of the animal(s) and the character of the urine and feces. It is the responsibility of the principle investigator to ascertain that the animal care personnel are, in fact, observant and have been properly trained to record their observations appropriately for each individual animal or cage of grouped animals.

The physical examination of each animal should include the rectal temperature and an evaluation of the mucous membranes. Particular notice should be taken of abnormal discharges from the eyes, nose, and other orifices. Animals with inflamed mucous membranes should be examined more closely to determine the cause. Judicious use of the stethoscope can rule out the possibility of using animals with congenital or acquired valvular disease, unless the model is of particular interest. Dogs that originate from areas where heartworms are endemic and animals that originate from areas where parasitic blood diseases are a problem must be shown to be free of those afflictions. It can be a good idea to record an ECG to rule out congenital or acquired arrhythmias that might render the animal unfit for a particular protocol.

Hydration is an important consideration. Any animal used in an experimental protocol should be well hydrated. If the preparation of the animal model requires

D.R. Gross, *Animal Models in Cardiovascular Research*,
DOI: 10.1007/978-0-387-95962-7_1, © Springer Science + Business Media, LLC 2009

extensive surgery or if the experimental protocol is of long duration, the state of hydration must be maintained. Although these considerations may seem obvious, they are, too often, ignored or forgotten. The choice of hydrating fluid is dependent upon the experimental protocol but care must be taken to avoid iatrogenic changes in acid–base or electrolyte balance. Most surgical procedures or experimental protocols do not require that animals be without water prior to anesthesia. Free choice of water to a healthy subject should insure normal hydration. As a matter of convenience, and to prevent inspiration of ingesta, it is usually wise to withhold food overnight or for 12 h prior to general anesthesia.

If it is necessary to draw blood for hematological or serum enzyme studies, investigators should be aware that many sedatives and anesthetic agents commonly used to restrain animals for this purpose will lower most CBC parameters. Other special considerations are related to the use of less usual animal models. Ferrets, for example, are obligate carnivores with extremely short digestive tracts. If food is not available ferrets have the ability to mobilize peripheral fat stores very quickly. When this happens, the liver experiences a fat overload resulting in hepatic swelling, and this can result in the leakage of membrane enzymes such as alanine aminotransferase (ALT). If the swelling persists, the bile canaliculi can be obstructed and alkaline phosphatase levels in the serum will rise significantly. Ferrets are also subject to insulinomas, the most common neoplasm in this species. Prior to use in experiments, these animals should be evaluated for the possibility of this tumor.

Normal reference ranges for hematological and serum enzyme levels for various species should be used with caution. Values can and do vary between laboratories dependent upon the methodology and instrumentation used. This is particularly true for serum enzymes. Comparisons of dog and cat serum in analyzers using wet reagents and dry reagents demonstrated that alkaline phosphatase, alanine aminotransferase, feline amylase, urea nitrogen, cholesterol, creatinine, glucose, total canine bilirubin, calcium, albumin, potassium, and feline total bilirubin were all comparable between the two methods. However, determinations of albumin, potassium, and calcium did not correlate between the two methods.[1] Normal ranges must be established for each species for each specific analytical laboratory or, preferably, investigators must take care to establish normal values for each animal used in a study prior to any perturbations.

Providing ranges of normal physiological parameters is useful only for purposes of comparison. If results obtained from any individual animal or group of animals to be used in a study vary significantly from published normal ranges, investigators should take the time and make the effort to establish that their animals are normal and the results obtained are useful.

Special Requirement Considerations

Sometimes the selection of an appropriate animal model is dictated by characteristic behaviors of a species. If the experimental design requires that data be collected over a prolonged period of time from an intact awake animal at rest, it is necessary

to select a species that can be trained to remain quiet for prolonged periods with minimal physical restraint. When the protocol requires exercise, a species that can be trained to exercise on an appropriate device must be selected. If a particular experimental design can best be served by using a particular animal model, it is always possible to learn to handle the use that species or line. Unfortunately, the animal model is often chosen because the investigator and/or members of the laboratory are most familiar with that species, the normal physiological parameters for the species are known, and previous experience has been good. These are all valid reasons but should not dictate the choice when other factors are involved. Experiments where the function of the thermoregulatory system is important to the outcome of the study should be conducted in a species that has thermoregulatory responses most similar to that of humans, assuming the data are to be extrapolated to the human condition. Dogs and cats have only a few sweat glands in their paws and rely on panting for thermal regulation. Pigs are unable to thermo regulate efficiently because of thick subcutaneous fat deposits and poorly developed sweating capability. Malignant hyperthermia is a practical problem in this species. Most herbivores and carnivores do not develop atherosclerosis as a naturally occurring disease. Omnivores such as swine can develop this disease with age, and the disease process can be accelerated significantly with a high cholesterol and high fat diet. The coronary circulation of pigs is similar to that of man as are the size and shape of the swine cardiovascular system. Blood coagulation mechanisms in swine are also very similar to those in humans.[2] The pathways of ventricular excitation and distribution of Purkinje fibers in swine, cattle, sheep and goats are different than those in humans but those in dogs are similar.[3]

Some physiological parameters are constant from mice to elephants. *Cardiac output*, for example, averages *50–100 mL/kg body weight/minute*. Normal left ventricular *Ejection Fractions*=40–80%. *Blood volumes* are, *roughly 7–9% of the body weight* (L/kg). Normal arterial $pH = 7.40 \pm 0.05$, arterial $pO_2 = 85–100$ *mmHg*, arterial pCO_2 = 35–45 mmHg, and arterial $HCO_3^- = 12.6–40$ *mEq/L* across all mammalian species where reliable values for normal animals have been reported. Venous blood gases will vary considerably depending upon the metabolic state of the animal (Tables1.1–1.4).

Normal Physiological Data

Taking data from many different studies and using the ranges of those numbers as a true representation can lead to erroneous conclusions. For example in Table 1.4 the ranges of values for heart rates in awake dogs are taken from 93 different reports. These include different conditions of ambient temperature, different levels of excitement of the animals, different ages, and, most importantly, different breeds and sizes of animals. The same is true for the aortic pressure values. These data are provided only to give a feeling for a range of values that could be expected (Tables 1.5 and 1.6).

Platelet numbers can be estimated with fair accuracy from a stained blood smear but only if the platelets are distributed randomly throughout the smear and in the absence of any clumping. The feathered edge of the smear should be examined for

Table 1.1 Normal ranges for body weight, birth weight, breeding age[4,5]

Species	Weight (kg)	Birth weight (gm)	Breeding age (months)	Estrus cycle duration (days)
Rats	0.07–0.23	4–6	2–3	4–5
Mice	0.020–0.050	0.0015	2	4-5
Rabbits	3.7 (1.5)	75–125	6–7	~15 (irregular)
Dogs (Beagles)	9–19	1,100–2,200	9	22
Cats	2.1–4.5	120–130	10	15–28
Guinea pigs	0.330–0.530	75–100	3	16–19
Pigs (2–6 months)	15–125	200–400	6	21
Calves	40–80	25–35 (kg)	Na	na
Sheep (adult)	26–54	1,000–3,000	5–12	17
Goats (adult)	6–36	750–2,000	5–12	21
Primates (Rhesus)	2.5–4.5	500–700	54	28

Table 1.2 Daily food consumption, nitrogen intake, urinary nitrogen, fecal nitrogen[4,5]

Species	Daily intake (gm)	Nitrogen intake (gm/day)	Urinary nitrogen excretion (gm/day)	Fecal nitrogen excretion (gm/day)
Rats (adult)	10	0.37 ± 0.19	0.10 ± 0.08	0.06 ± 0.04
Mice (adult)	5	Nf	Nf	Nf
Rabbits (adult)	180	Nf	Nf	Nf
Dogs (adult)	400	Nf	Nf	Nf
Cats (adult)	100	Nf	Nf	Nf
Guinea pigs (adult)	12	Nf	Nf	Nf
Pigs	Nf	31 ± 10	15 ± 7	3 ± 0.6
Calves	Nf	32 ± 20	14 ± 7	11 ± 0.6
Sheep (adult)	Nf	12 ± 6	7 ± 3	3 ± 2
Goats (adult)	Nf	8 ± 5	5 ± 0.6	3 ± 3
Primates (Rhesus)	150	Nf	Nf	Nf

Nf not found.

Table 1.3 Adult metabolism, food consumption, water consumption, urine output[4]

Species	Metabolism (Cal/kg/day)	Food consumption (% of body wt/day)	Water consumption (% of body wt/day)	Urine output (ml/kg/day)
Rats	130	20–30	10–15	0.55
Mice	60	15	15	0.08
Rabbits	110	5–10	5–10	0.5
Dogs	80	5–10	5–10	0.4–0.7
Cats	80	5–10	5–10	0.4–0.6
Guinea Pigs	100	5	5–10	0.5
Primates	158	2–4	5–10	Nf

Nf not found.

Table 1.4 Ranges for normal rectal temperatures, respiratory rate, heart rate, blood pressure[4,6,7]

Species	Rectal temp (°C)	Respiratory rate (breaths/min)	Heart rate (b/min)	Blood pressure (mmHg, systolic/diastolic)
Rats	38.1–38.5	65–110	305–500	153/51
Mice	37.1–37.5	80–240	580–680	120/75
Rabbits	39.1–39.5	40–65	205–306	118/67
Dogs	37.9–39.9	10–30	62–170	183/51
Cats	38.1–39.2	20–30	100–259	155/68
Guinea pigs	38.4–38.8	70–100	240–300	140/90
Pigs	38.7–39.8	45–60	74–116	169/55
Calves	36.7–39.1	25–40	75–146	140/70
Sheep	38.3–39.9	15–20	63–210	140/80
Goats	38.5–39.7	15–20	80–120	140/90
Primates (Rhesus)	38.4–38.8	40–60	180–210	160/125

Table 1.5 Ranges for normal red blood cell parameters[4,6-23]

Species	Hematocrit (%)	Hemoglobin (g/100 mL)	RBC ($\times 10^6/\mu L$)	Mean corpuscular volume (μm^3)	Mean corpuscular Hb conc (g%)
Rats	40–51	13–15	8–9	54–58	30–31.5
Mice	40–43	11–12	8–10	48–57	25–27
Rabbits	40–42	13–14	6–7	61–63	31–33
Dogs	22–65	5–18	5.8–9.2	59–78	15–37
Cats	15–56	10–16	5–10	39–55	13–36
Guinea pigs	43–51	14–15.3	5–6.1	40–50	24.6–33
Pigs	37–42	11.2–14	5.4–8	50–76.7	26.7–35
Calves	24–46	5.6–12.5	5.2–8.6	49–65	30–36
Sheep	27–45	9–15	8–10	28–40	31–34
Goats	19–58	8–9	8–9	15–40	31.5-42
Primates (Rhesus)	17–48	5–12.5	2–5	54–56	15–39

Table 1.6 Ranges for normal blood count parameters[4,6-8,10,12-15,18-21,23-25]

Species	WBC ($\times 10^3$ mm^{-3})	Neutro (%)	Lympho (%)	Mono (%)	Eosino (%)	Platelets ($\times 10^3$ mm^{-3})
Rats	4.7–10	14.5–26	73–85	0.3–4.5	0.4–1.2	690–1,190
Mice	13–14	17–18	72–77	2–4	2–3	400–600
Rabbits	8–9	40–46	40–42	8–9	2–4	150–550
Dogs	6–17	60–77	12–30	3–10	2–10	135–400
Cats	5–19.5	35–75	20–55	1–4	2–12	200–300
Guinea pigs	11–12	35–37	55–57	3–4	3–4	375–525
Pigs	6.7–15	20–35	54–56	3–4	0.2–1	275–600
Calves	4–12	15–45	45–75	2–7	2–20	415–1,095
Sheep	4–12	31–33	55–60	3–4	5–6	520–750
Goats	4–13	11–48	50–85	0.5–5	0–8	148–390
Primates (Rhesus)	5.5–19.5	21–69	20.5–70	0–8.5	0–6	205–607

the absence of platelet clumps prior to using the slide for counting. Platelet clumps occur with frequency if there is any difficulty with the venipuncture and are more common in blood drawn from small peripheral veins or veins from small species. Cat platelets are exceedingly reactive and clump readily during sample collection. Improved estimates of platelet counts can be obtained using a Unopette system and counting platelets in a hemacytometer manually or by using an electronic cell counter but the latter will underestimate counts if the platelets are large or if there are clumps. Some cats and some breeds of dogs have unusually large platelets and counts using electronic cell counters are often erroneously low in these animals (Table 1.7).

Prothrombin and activated prothrombin times are very dependent upon the particular batch or species of thromboplastin used. A recent study designed to determine the international sensitivity index of various sources of thromboplastin found an international normalized ratio (INR) bias of 6.0%. Studies that require exact measurements of clotting parameters must be aware of these limitations.[50]

It is important to note that some enzyme levels, particularly in dogs and cats, have shown a dependency on the age of the animals (Tables 1.8–1.11).[155] C-reactive protein levels vary with the type of anticoagulant used.[108]

Table 1.7 Ranges for normal coagulation parameters and blood glucose, activated partial thromboplastin time (aPPT), prothrombin time (PT), fibrinogen, and glucose (T)[8-10,13,26-49]

Species	aPPT (s)	PT (s)	Fibrinogen (mg/dL)	Glucose (mg/dL)
Rats	20–30	9–48	215–294	100–264
Mice	23	11.9–13	178–329	112–135
Rabbits	19–34	7–12	223–314	125–175
Dogs	10–15	7.5–9	120–290	80–106
Cats	14–25	16.5–27.5	100–300	90–140
Guinea pigs	25–30	32–38	125–150	139–149
Pigs	10–25	10–12	160–390	84–139
Calves	30.7–90.7	21.9–40.6	160–560	95–111
Sheep	30–36	14.7–15.9	211–360	35–55
Goats	25–35	12–16	180–400	38–72
Primates (Rhesus)	22–38	10–18	175–295	55–75

Table 1.8 Ranges for normal plasma electrolytes[6,10,13,17,18,51-57]

Species	Na^+ (mEq/L)	K^+ (mEq/L)	Cl^- (mEq/L)	Mg^{++} (mg/dL)	Ca^{++} (mg/dL) or (mmol/L)
Rats	143–156	5.4–7.0	100–110	1.6–4.4	9.5–10.3
Mice	128–145	4.8–5.8	105–110	0.8–3.9	2.4–2.6
Rabbits	138–155	3.7–6.8	92–112	2.0–5.4	6.4–6.9
Dogs	139–153	3.6–5.2	103–121	1.5–2.8	10.1–10.5
Cats	137–164	3.5–4.7	109–127	2–3	10.5–11.1
Guinea pigs	120–146	3.8–8.0	90–115	1.8–3.0	2.4–2.6
Pigs	135–152	4.9–7.1	94–106	1.2–3.7	2.8–3.0
Calves	132–152	3.9–5.8	97–111	2.5–3.1	9.5–10.1
Sheep	140–164	4.2–6.7	113–121	1.8–2.4	2.3–2.6
Goats	136–155	3.1–6.7	98–111	2.8–3.6	3.9–6.0
Primates (Rhesus)	143–164	3.8–6.7	103–118	1.0–2.7	9.5–10.8

Table 1.9 Ranges for normal blood chemistry, blood urea nitrogen (BUN), creatinine (CR), total cholesterol (TC), triglycerides (TG), high density lipoprotein (HDL), total protein (TP), albumin (ALB)[4,6-8,10,11,13,18,21,23,31,32,35,45,48,49,53,54,58-84]

Species	BUN (mg/dL)	CR (mg/dL)	TC (mg/dL) or (mmol/L)	TG (mg/dL) or (mmol/L)	HDL (mg/dL) or (mmol/L)	TP (g/dL)	ALB (g/dL)
Rats	10–54	0.2–0.8	10–126	6.7–86.2	31.9–51.0	7.0–7.7	2.2–3.9
Mice	14–28	0.3–1.0	26–98	65–152	46.1–63.9	6.9–7.9	3.4–3.6
Rabbits	13–29	0.5–2.6	5–80	12–152	10–29	4.7–7.3	
Dogs	10–26	0.8–1.7	115–275	22.5–46	35.1–48.7	5.3–8.0	3.2–3.5
Cats	14–32	0.8–1.8	83–135 2.03-5.15	0.18–0.40	0.67–2.0	5.0–8.0	2.8–3.6
Guinea pigs	9–31	0.6–2.2	16–43	33–104 0.8–1.2	0.5–1.5	4.9–5.5	3.0–4.1
Pigs	4–22	1.2–6	76–174 2.2–2.6	37.0–49.2 0.35–0.57	40.6–55.3	4.8–7.7	3.1–3.6
Calves	6–26	1.0–2.0	78–173 0.25–3.84	25.8–37.4 0.11–0.46	83.7–84.5	4.2–7.5	3.0–4.7
Sheep	15–36	0.7–3.0	50–140 0.92–2.07	7.0–29.0	33–60.3	5.2–11.4	0.68–3.7
Goats	10–27	0.2–2.2	55–210 1.01–3.44	0.26–2.02	47–74.6	5.0–9.3	2.2–4.9
Primates (Rhesus)	7–23	1–2	125–270	20–121	68–96	5.1–8.2	1.9–5.3

Table 1.10 Blood chemistry, ranges of enzyme levels, aspartate aminotransaminase (AST), alanine aminotransaminase (ALT), alkaline phosphatase (ALP), serum glutamic oxaloacetic transaminase (SGOT), serum glutamic pyruvic transaminase (SGPT), tumor necrosis factor-α (TNF-α)[4,6,8-10,12-16,18,20,22-24,28,34,35,41,45,53,54,60,74-76,79,80,85-97,97-107]

Species	AST (IU/L)	ALT (IU/L)	ALP (IU/L)	SGOT (IU/L)	SGPT (IU/L)	TNF-α (pg/mL)
Rats	76–197	28–60	99–381	101–184	68–78	0–40
Mice	16–83	1–13	296–326	23–178	32–60	0–20
Rabbits	1.5–30	1–50	102–179	25–98	27–80	0–19
Dogs	10–70	1–100	20–190	1–7	3–8	239–314
Cats	20–50	41–86	10–40	20–83	0–5	0–4
Guinea pigs	45–68	25–40	62–252	16–67	500–1000	0–10
Pigs	0–131	23–95	62–152	15–72	12–26	0–25
Calves	25–110	6–36	64–222	26–58	18–70	11–139
Sheep	29–101	9–25	45–208	40–123	41–67	0–15
Goats	68–531	12–57	2–964	43–131	4–251	0–18
Primates (Rhesus)	25–105	5–75	1,900–2,800	12–45	10–18	1–23

Other important sources of new information are available on the Internet. For example, the PhysGen program at the Medical College of Wisconsin has developed a number of different consomic rat models. Information concerning these animals,

Table 1.11 Blood chemistry, ranges of normal levels, creatine phosphokinase (CPK), cortisol, T_3, T_4, interleukin-10 (IL-10), interleukin-6 (IL-6), C-reactive protein (CRP)[4,6,23,35,45-47,54,76,86,97,100,104,105,108-154]

Species	CPK (IU/L) or (μmol × 10^{-3} of P/min)	Cortisol (μgm/dL) or (nmol/L)	T_3 (nmol/L) or (ngm/mL)	T_4 (nmol/L) or (μgm/dL)	IL-10 (pgm/mL)	IL-6 (pgm/mL)	CRP (mgd/L)
Rats	9–12	3.8–11.2	0.9–2.1	27.9–37.6	23.7–25.1	90–250	0.67–0.79
Mice	6100–7900	1.4–4.6	2.1–3.9	4.0–8.0	442–478	10–19	0.09–0.1
Rabbits	106–495	9.1–15.1	7.4–9.3	25.3–30.3	[a]	0–20	0.28–0.40
Dogs	47–329	2–144	1–2	15–48	15.6–76	0–24	0.28–3.12
Cats	0–363	57–114	0.6–1	17–38	0[b]	0[b]	1.3–1.9
Guinea pigs	10–300	125–290	1.5–2.6	12–30	0[b]	0[b]	0[b]
Pigs	300–400	0.5–50	1.4–1.8	57–69	0[b]	0–50	0[b]
Calves	41–200	4–6.5	2.1–3.4	83–104	0.1–0.5	0[b]	0[b]
Sheep	102–358	11–29	0.8–1.7	4.2–6.7	0[b]	55.9–109.5	0.3–0.62
Goats	228–3,432	1.5–20 93.1–2,252	0.9–1.4	7.1–7.9	0[b]	0[b]	0.55–0.72
Primates (Rhesus	500–1,000	1.5–25	100–152	6–9	0[b]	1–11	0.5–5.5

[a]Values are available using molecular techniques and measurement of DNA and/or mRNA. These values should be reported as units of activity/units of DNA or mRNA.
[b]Values below the detection levels.

their phenotypical hematological and enzymatic characteristics, and using them to increase our understanding of the genetic mechanistic pathways of the cardiovascular, pulmonary and renal systems is available at http://pga.mcw.edu/.

References

1. Sutton A, Dawson H, Hoff B, Grift E, Shoukri M. Analyte comparisons between 2 clinical chemistry analyzers. *Can Vet J*. 1999;40:255–260.
2. Gross DR. Thromboembolic phenomena and the use of the pig as an appropriate animal model for research on cardiovascular devices. *Int J Artif Organs*. 1997;20:195–203.
3. Hamlin RL, Smith CR. Categorization of common domestic mammals based upon their ventricular activation process. *Ann N Y Acad Sci*. 1965;127:195–203.
4. Gross DR. Unpublished data.
5. Kohn RA, Dinneen MM, Russek-Cohen E. Using blood urea nitrogen to predict nitrogen excretion and efficiency of nitrogen utilization in cattle, sheep, goats, horses, pigs, and rats. *J Anim Sci*. 2005;83:879–889.
6. Gross DR. *Animal Models in Cardiovascular Research, 2nd Revised Edition.* Boston: Kluwer Academic Publishers; 1994.
7. Singh A, Singh J, Grewal AS, Brar RS. Studies on some blood parameters of crossbred calves with experimental theileria annulata infections. *Vet Res Commun*. 2001;25:289–300.
8. Chen CM, Hou CC, Cheng KC, Tian RL, Chang CP, Lin MT. Activated protein C therapy in a rat heat stroke model. *Crit Care Med*. 2006;34:1960–1966.

9. Ballantyne B, Snellings WM, Norris JC. Respiratory peripheral chemosensory irritation, acute and repeated exposure toxicity studies with aerosols of triethylene glycol. *J Appl Toxicol*. 2006;26:387–396.
10. Ramirez JH, Palacios M, Tamayo O, Jaramillo R, Gutierrez O. Acute and subacute toxicity of salvia scutellarioides in mice and rats. *J Ethnopharmacol*. 2007;109:348–356.
11. Albarellos G, Montoya L, Ambros L, Kreil V, Hallu R, Rebuelto M. Multiple once-daily dose pharmacokinetics and renal safety of gentamicin in dogs. *J Vet Pharmacol Ther*. 2004;27:21–25.
12. Niwetpathomwat A, Kaewthamasorn M, Tiawsirisup S, Techangamsuwan S, Suvarnvibhaja S. A retrospective study of the clinical hematology and the serum biochemistry tests made on canine dirofilariasis cases in an animal hospital population in Bangkok, Thailand. *Res Vet Sci*. 2007;82:364–369.
13. Chengelis CP, Kirkpatrick JB, Marit GB, Morita O, Tamaki Y, Suzuki H. A chronic dietary toxicity study of DAG (diacylglycerol) in beagle dogs. *Food Chem Toxicol*. 2006;44:81–97.
14. Senturk S. Evaluation of the anti-endotoxic effects of polymyxin-E (colistin) in dogs with naturally occurred endotoxic shock. *J Vet Pharmacol Ther*. 2005;28:57–63.
15. Chikamune T, Katamoto H, Nomura K, Ohashi F. Lipoprotein profile in canine pancreatitis induced with oleic acid. *J Vet Med Sci*. 1998;60:413–421.
16. Parton K, Balmer TV, Boyle J, Whittem T, MacHon R. The pharmacokinetics and effects of intravenously administered carprofen and salicylate on gastrointestinal mucosa and selected biochemical measurements in healthy cats. *J Vet Pharmacol Ther*. 2000;23:73–79.
17. Aumann M, Worth LT, Drobatz KJ. Uroperitoneum in cats: 26 cases (1986–1995). *J Am Anim Hosp Assoc*. 1998;34:315–324.
18. Kitagaki M, Yamaguchi M, Nakamura M, Sakurada K, Suwa T, Sasa H. Age-related changes in haematology and serum chemistry of weiser-maples guinea pigs (cavia porcellus). *Lab Anim*. 2005;39:321–330.
19. Gundersen Y, Vaagenes P, Thrane I, et al. Response of circulating immune cells to major gunshot injury, haemorrhage, and acute surgery. *Injury*. 2005;36:949–955.
20. Ohtsuka G, Nakata K, Yoshikawa M, et al. Long-term in vivo left ventricular assist device study for 284 days with gyro PI pump. *Artif Organs*. 1999;23:504–507.
21. Rerat M, Zbinden Y, Saner R, Hammon H, Blum JW. In vitro embryo production: Growth performance, feed efficiency, and hematological, metabolic, and endocrine status in calves. *J Dairy Sci*. 2005;88:2579–2593.
22. Al-Habsi K, Johnson EH, Kadim IT, et al. Effects of low concentrations of dietary cobalt on liveweight gains, haematology, serum vitamin B(12) and biochemistry of omani goats. *Vet J*. 2007;173:131–137.
23. Lopez-Olvera JR, Marco I, Montane J, Lavin S. Haematological and serum biochemical values of southern chamois (rupicapra pyrenaica). *Vet Rec*. 2006;158:479–484.
24. Lozano FS, Cascajo C, Garcia-Sanchez E, et al. Bacterial translocation as a source of dacron-graft contamination in experimental aortic operation: The importance of controlling SIRS. *Surgery*. 2006;140:83–92.
25. Kramer JK, Sauer FD, Farnworth ER, Wolynetz MS, Jones G, Rock GA. Hematological and lipid changes in newborn piglets fed milk replacer diets containing vegetable oils with different levels of n-3 fatty acids. *Lipids*. 1994;29:859–868.
26. Tunali-Akbay T, Sener G, Salvarli H, Sehirli O, Yarat A. Protective effects of ginkgo biloba extract against mercury(II)-induced cardiovascular oxidative damage in rats. *Phytother Res*. 2007;21:26–31.
27. Ikeguchi H, Maruyama S, Morita Y, et al. Effects of human soluble thrombomodulin on experimental glomerulonephritis. *Kidney Int*. 2002;61:490–501.
28. Bolkent, S, Arda-Pirincci, P, Bolkent, S, Yanardag, R, Tunali, S, Yildirim, S. Influence of zinc sulfate intake on acute ethanol-induced liver injury in rats. *World J Gastroenterol*. 2006;12:4345–4351.
29. Tanaka-Azevedo AM, Tanaka AS, Sano-Martins IS. A new blood coagulation inhibitor from the snake bothrops jararaca plasma: Isolation and characterization. *Biochem Biophys Res Commun*. 2003;308:706–712.

30. Hu Z, Garen A. Targeting tissue factor on tumor vascular endothelial cells and tumor cells for immunotherapy in mouse models of prostatic cancer. *Proc Natl Acad Sci U S A*. 2001;98:12180–12185.
31. Portilla D, Li S, Nagothu KK, et al. Metabolomic study of cisplatin-induced nephrotoxicity. *Kidney Int*. 2006;69:2194–2204.
32. Liu SX, Hou FF, Guo ZJ, et al. Advanced oxidation protein products accelerate atherosclerosis through promoting oxidative stress and inflammation. *Arterioscler Thromb Vasc Biol*. 2006;26:1156–1162.
33. Cam Y, Cetin E, Ica A, Atalay O, Cetin N. Evaluation of some coagulation parameters in hepatic coccidiosis experimentally induced with eimeria stiedai in rabbits. *J Vet Med B Infect Dis Vet Public Health*. 2006;53:201–202.
34. Kroeze EJ, Zentek J, Edixhoven-Bosdijk A, Rothuizen J, van den Ingh TS. Transient erythropoietic protoporphyria associated with chronic hepatitis and cirrhosis in a cohort of german shepherd dogs. *Vet Rec*. 2006;158:120–124.
35. Hryszko T, Inaba K, Ihara H, Suzuki Y, Mogami H, Urano T. Nafamostat attenuated the impairment of fibrinolysis in animal sepsis model by suppressing the increase of plasminogen activator inhibitor type 1. *J Trauma*. 2006;60:859–864.
36. Ontachi Y, Asakura H, Takahashi Y, et al. No interplay between the pathways mediating coagulation and inflammation in tissue factor-induced disseminated intravascular coagulation in rats. *Crit Care Med*. 2006;34:2646–2650.
37. Windberger U, Bartholovitsch A, Plasenzotti R, Korak KJ, Heinze G. Whole blood viscosity, plasma viscosity and erythrocyte aggregation in nine mammalian species: Reference values and comparison of data. *Exp Physiol*. 2003;88:431–440.
38. Kaplan B, Karabay G, Zagyapan RD, Ozer C, Sayan H, Duyar I. Effects of taurine in glucose and taurine administration. *Amino Acids*. 2004;27:327–333.
39. Kessler CM, Tang Z, Jacobs HM, Szymanski LM. The suprapharmacologic dosing of antithrombin concentrate for staphylococcus aureus-induced disseminated intravascular coagulation in guinea pigs: Substantial reduction in mortality and morbidity. *Blood*. 1997;89:4393–4401.
40. de Groot GH, Reuvers CB, Schalm SW, et al. A reproducible model of acute hepatic failure by transient ischemia in the pig. *J Surg Res*. 1987;42:92–100.
41. Nieuwoudt M, Kunnike R, Smuts M, et al. Standardization criteria for an ischemic surgical model of acute hepatic failure in pigs. *Biomaterials*. 2006;27:3836–3845.
42. Irmak K, Sen I, Col R, et al. The evaluation of coagulation profiles in calves with suspected septic shock. *Vet Res Commun*. 2006;30:497–503.
43. Sano H, Fujita T. Effect of supplemental calcium propionate on insulin action to blood glucose metabolism in adult sheep. *Reprod Nutr Dev*. 2006;46:9–18.
44. Robinson MH, Twigg LE, Wheeler SH, Martin GR. Effect of the anticoagulant, pindone, on the breeding performance and survival of merino sheep, ovis aries. *Comp Biochem Physiol B Biochem Mol Biol*. 2005;140:465–473.
45. Yokus B, Cakir DU, Kanay Z, Gulten T, Uysal E. Effects of seasonal and physiological variations on the serum chemistry, vitamins and thyroid hormone concentrations in sheep. *J Vet Med A Physiol Pathol Clin Med*. 2006;53:271–276.
46. Katoh K, Yoshida M, Kobayashi Y, Onodera M, Kogusa K, Obara Y. Responses induced by arginine-vasopressin injection in the plasma concentrations of adrenocorticotropic hormone, cortisol, growth hormone and metabolites around weaning time in goats. *J Endocrinol*. 2005;187:249–256.
47. Kannan G, Terrill TH, Kouakou B, et al. Transportation of goats: Effects on physiological stress responses and live weight loss. *J Anim Sci*. 2000;78:1450–1457.
48. Tigno XT, Gerzanich G, Hansen BC. Age-related changes in metabolic parameters of nonhuman primates. *J Gerontol A Biol Sci Med Sci*. 2004;59:1081–1088.
49. Winegar DA, Brown PJ, Wilkison WO, et al. Effects of fenofibrate on lipid parameters in obese rhesus monkeys. *J Lipid Res*. 2001;42:1543–1551.
50. Poller L, Keown M, Chauhan N, et al. European concerted action on anticoagulation. A multicentre calibration study of WHO international reference preparations for thromboplastin, rabbit (RBT/90) and human (rTF/95). *J Clin Pathol*. 2005;58:667–669.

51. Pederson BA, Schroeder JM, Parker GE, Smith MW, DePaoli-Roach AA, Roach PJ. Glucose metabolism in mice lacking muscle glycogen synthase. *Diabetes*. 2005;54:3466–3473.
52. Liesegang A, Loch L, Burgi E, Risteli J. Influence of phytase added to a vegetarian diet on bone metabolism in pregnant and lactating sows. *J Anim Physiol Anim Nutr (Berl)*. 2005;89:120–128.
53. Cole NA, Brown MA, Phillips WA. Genetic x environment interactions on blood constituents of angus, Brahman, and reciprocal-cross cows and calves grazing common Bermuda grass or endophyte-infected tall fescue. *J Anim Sci*. 2001;79:1151–1161.
54. Dubreuil P, Arsenault J, Belanger D. Biochemical reference ranges for groups of ewes of different ages. *Vet Rec*. 2005;156:636–638.
55. Chang JM, Hwang SJ, Tsai JC, Lai YH. In vivo effect of endothelin-1 on plasma calcium and parathyroid hormone concentrations. *J Endocrinol*. 2000;165:179–184.
56. Funaba M, Hashimoto E, Iriki T, Abe M. Utilization of nitrogen and macro-minerals in response to nutritional status in clinically normal adult cats. *Exp Anim*. 1998;47:143–149.
57. Symonds HW, Treacher RJ. The responses of goats to the experimental induction of hypocalcaemia with cation-exchange columns. *J Physiol*. 1968;198:193–201.
58. Reid K, Tsung A, Kaizu T, et al. LIVER I/R injury is improved by the arginase inhibitor, n-omega-hydroxy-nor-l-arginine (NOR-NOHA). *Am J Physiol Gastrointest Liver Physiol*. 2007;292:G512–517.
59. Yogeeta SK, Hanumantra RB, Gnanapragasam A, Senthilkumar S, Subhashini R, Devaki T. Attenuation of abnormalities in the lipid metabolism during experimental myocardial infarction induced by isoproterenol in rats: Beneficial effect of ferulic acid and ascorbic acid. *Basic Clin Pharmacol Toxicol*. 2006;98:467–472.
60. He SX, Luo JY, Wang YP, et al. Effects of extract from ginkgo biloba on carbon tetrachloride-induced liver injury in rats. *World J Gastroenterol*. 2006;12:3924–3928.
61. Jatwa R, Kar A. Cardio-protective role of terazosin is possibly mediated through alteration in thyroid function. *Eur J Pharmacol*. 2006;551:87–91.
62. Andrzejczak D, Gorska D, Czarnecka E. Influence of amlodipine and atenolol on lipopolysaccharide (LPS)-induced serum concentrations of TNF-alpha, IL-1beta, IL-6 in spontaneously hypertensive rats (SHR). *Pharmacol Rep*. 2006;58:711–719.
63. Penza M, Montani C, Romani A, et al. Genistein affects adipose tissue deposition in a dose-dependent and gender-specific manner. *Endocrinology*. 2006;147:5740–5751.
64. den Boer MA, Voshol PJ, Schroder-van der Elst JP, et al. Endogenous interleukin-10 protects against hepatic steatosis but does not improve insulin sensitivity during high-fat feeding in mice. *Endocrinology*. 2006;147:4553–4558.
65. Pinelli A, Trivulzio S, Tomasoni L, et al. Drugs modifying nitric oxide metabolism affect plasma cholesterol levels, coagulation parameters, blood pressure values and the appearance of plasma myocardial necrosis markers in rabbits: Opposite effects of L-NAME and nitroglycerine. *Cardiovasc Drugs Ther*. 2003;17:15–23.
66. Wei J, Ma C, Wang X. Simvastatin inhibits tissue factor and plasminogen activator inhibitor-1 expression of glomerular mesangial cells in hypercholesterolemic rabbits. *Biomed Res*. 2006;27:149–155.
67. Gupta RK, Kesari AN, Watal G, Murthy PS, Chandra R, Tandon V. Nutritional and hypoglycemic effect of fruit pulp of annona squamosa in normal healthy and alloxan-induced diabetic rabbits. *Ann Nutr Metab*. 2005;49:407–413.
68. Wu X, Wang J, Fan J, et al. Localized vessel expression of lipoprotein lipase in rabbits leads to rapid lipid deposition in the balloon-injured arterial wall. *Atherosclerosis*. 2006;187:65–73.
69. Liu H, Zheng F, Cao Q, et al. Amelioration of oxidant stress by the defensin lysozyme. *Am J Physiol Endocrinol Metab*. 2006;290:E824–E832.
70. Prasad K, Lee P. Suppression of hypercholesterolemic atherosclerosis by pentoxifylline and its mechanism. *Atherosclerosis*. 2007;192:313–322.
71. Juzwiak S, Wojcicki J, Mokrzycki K, et al. Effect of quercetin on experimental hyperlipidemia and atherosclerosis in rabbits. *Pharmacol Rep*. 2005;57:604–609.
72. Asanuma K, Adachi K, Sugimoto T, Chiba S. Effects of lysine-induced acute renal failure in dogs. *J Toxicol Sci*. 2006;31:87–98.

73. Fettman MJ, Stanton CA, Banks LL, et al. Effects of neutering on bodyweight, metabolic rate and glucose tolerance of domestic cats. *Res Vet Sci*. 1997;62:131–136.
74. Drochner W, Schollenberger M, Gotz S, Lauber U, Tafaj M, Piepho HP. Subacute effects of moderate feed loads of isolated fusarium toxin deoxynivalenol on selected parameters of metabolism in weaned growing piglets. *J Anim Physiol Anim Nutr (Berl)*. 2006;90:421–428.
75. Quigley JD, Wolfe TA, Elsasser TH. Effects of additional milk replacer feeding on calf health, growth, and selected blood metabolites in calves. *J Dairy Sci*. 2006;89:207–216.
76. Husier BR, Blum JW. Metabolic and endocrine changes in response to endotoxin administration with or without oral arginine supplementation. *J Dairy Sci*. 2002;85:1927–1935.
77. Fernandez A, Mensua C, Biescas E, Lujan L. Clinicopathological features in ovine AA amyloidosis. *Res Vet Sci*. 2003;75:203–208.
78. Rier SE, Turner WE, Martin DC, Morris R, Lucier GW, Clark GC. Serum levels of TCDD and dioxin-like chemicals in rhesus monkeys chronically exposed to dioxin: Correlation of increased serum PCB levels with endometriosis. *Toxicol Sci*. 2001;59:147–159.
79. Tyagi A, Rajalakshmi M, Jeyaraj DA, Sharma RS, Bajaj JS. Effects of long-term use of testosterone enanthate. II. effects on lipids, high and low density lipoprotein cholesterol and liver function parameters. *Int J Androl*. 1999;22:347–355.
80. Wu JB, Lin WL, Hsieh CC, Ho HY, Tsay HS, Lin WC. The hepatoprotective activity of kinsenoside from *Anoectochilus formosanus*. *Phytother Res*. 2007;21:58–61.
81. Green TJ, Moghadasian MH. Species-related variations in lipoprotein metabolism: The impact of FER(HDL) on susceptibility to atherogenesis. *Life Sci*. 2004;74:2441–2449.
82. Quinet EM, Savio DA, Halpern AR, et al. Liver X receptor (LXR)-beta regulation in LXRalpha-deficient mice: Implications for therapeutic targeting. *Mol Pharmacol*. 2006;70:1340–1349.
83. Kristensen F, Barsanti JA. Analysis of serum proteins in clinically normal pet and colony cats, using agarose electrophoresis. *Am J Vet Res*. 1977;38:399–402.
84. Schurman SJ, McAdams AJ, Beischel L, Davis AE,3rd, Welch TR. C3-independent glomerulonephritis in guinea pigs: Dependence upon primary humoral response. *Clin Immunol Immunopathol*. 1995;74:51–58.
85. El-Samaligy MS, Afifi NN, Mahmoud EA. Evaluation of hybrid liposomes-encapsulated silymarin regarding physical stability and in vivo performance. *Int J Pharm*. 2006;319:121–129.
86. Ke QH, Zheng SS, Liang TB, Xie HY, Xia WL. Pretreatment of hypertonic saline can increase endogenous interleukin 10 release to attenuate hepatic ischemia reperfusion injury. *Dig Dis Sci*. 2006;51:2257–2263.
87. Paul SC, Lv P, Xiao YJ, An P, Liu SQ, Luo HS. Thalidomide in rat liver cirrhosis: Blockade of tumor necrosis factor-alpha via inhibition of degradation of an inhibitor of nuclear factor-kappaB. *Pathobiology*. 2006;73:82–92.
88. Schomburg L, Riese C, Michaelis M, et al. Synthesis and metabolism of thyroid hormones is preferentially maintained in selenium-deficient transgenic mice. *Endocrinology*. 2006;147:1306–1313.
89. Wang J, Bo H, Meng X, Wu Y, Bao Y, Li Y. A simple and fast experimental model of myocardial infarction in the mouse. *Tex Heart Inst J*. 2006;33:290–293.
90. Wang F, Xu ZR, Su JH. Effect of HCH contamination of diet on the growth performance and immune and antioxidant ability in growing/finishing pigs. *Vet Res Commun*. 2006;30:645–654.
91. Jayakumar T, Ramesh E, Geraldine P. Antioxidant activity of the oyster mushroom, pleurotus ostreatus, on CCl(4)-induced liver injury in rats. *Food Chem Toxicol*. 2006;44:1989–1996.
92. Thejass P, Kuttan G. Allyl isothiocyanate (AITC) and phenyl isothiocyanate (PITC) inhibit tumour-specific angiogenesis by down regulating nitric oxide (NO) and tumour necrosis factor-alpha (TNF-alpha) production. *Nitric Oxide*. 2007;16:247–257.
93. de Bem AF, de Lima Portella R, Perottoni J, et al. Changes in biochemical parameters in rabbits blood after oral exposure to diphenyl diselenide for long periods. *Chem Biol Interact*. 2006;162:1–10.
94. Efstathopoulos N, Tsaganos T, Giamarellos-Bourboulis EJ, et al. Early apoptosis of monocytes contributes to the pathogenesis of systemic inflammatory response and of bacterial translocation in an experimental model of multiple trauma. *Clin Exp Immunol*. 2006;145:139–146.

95. Giamarellos-Bourboulis EJ, Baziaka F, Antonopoulou A, et al. Clarithromycin co-administered with amikacin attenuates systemic inflammation in experimental sepsis with escherichia coli. *Int J Antimicrob Agents*. 2005;25:168–172.
96. Zhao SP, Wu J. Fenofibrate reduces tumor necrosis factor-alpha serum concentration and adipocyte secretion of hypercholesterolemic rabbits. *Clin Chim Acta*. 2004;347:145–150.
97. Ilcol YO, Yilmaz Z, Ulus IH. Endotoxin alters serum-free choline and phospholipid-bound choline concentrations, and choline administration attenuates endotoxin-induced organ injury in dogs. *Shock*. 2005;24:288–293.
98. Davidson MG, Lappin MR, Rottman JR, et al. Paradoxical effect of clindamycin in experimental, acute toxoplasmosis in cats. *Antimicrob Agents Chemother*. 1996;40:1352–1359.
99. Lehmann R, Joller H, Haagmans BL, Lutz H. Tumor necrosis factor alpha levels in cats experimentally infected with feline immunodeficiency virus: Effects of immunization and feline leukemia virus infection. *Vet Immunol Immunopathol*. 1992;35:61–69.
100. Wang JF, Wang M, Ma JL, Jiao LG, Zhou XY, Lindberg JE. The influence of intramammary lipopolysaccharide infusion on serum ca, P, vitamin D, cytokines and cortisol concentrations in lactating sows. *J Vet Med A Physiol Pathol Clin Med*. 2006;53:113–118.
101. Teague BD, Court FG, Morrison CP, Kho M, Wemyss-Holden SA, Maddern GJ. Electrolytic liver ablation is not associated with evidence of a systemic inflammatory response syndrome. *Br J Surg*. 2004;91:178–183.
102. Dai YB, Liu XY, Liu M, Tao JP. Pathogenic effects of the coccidium eimeria ninakohlyakimovae in goats. *Vet Res Commun*. 2006;30:149–160.
103. Wisloff H, Flaoyen A, Ottesen N, Hovig T. Narthecium ossifragum (L.) huds. causes kidney damage in goats: Morphologic and functional effects. *Vet Pathol*. 2003;40:317–327.
104. Horney B. Clinical pathology interpretation. *Can Vet J*. 1996;37:244–245.
105. Ashok BT, Tadi K, Banerjee D, Konopa J, Iatropoulos M, Tiwari RK. Pre-clinical toxicology and pathology of 9-(2′-hydroxyethylamino)-4-methyl-1-nitroacridine (C-1748), a novel anticancer agent in male beagle dogs. *Life Sci*. 2006;79:1334–1342.
106. Singh RP, Khanna R, Kaw JL, Khanna SK, Das M. Comparative effect of benzanthrone and 3-bromobenzanthrone on hepatic xenobiotic metabolism and anti-oxidative defense system in guinea pigs. *Arch Toxicol*. 2003;77:94–99.
107. Gadina M, Bertini R, Mengozzi M, Zandalasini M, Mantovani A, Ghezzi P. Protective effect of chlorpromazine on endotoxin toxicity and TNF production in glucocorticoid-sensitive and glucocorticoid-resistant models of endotoxic shock. *J Exp Med*. 1991;173:1305–1310.
108. Martinez-Subiela S, Ceron JJ. Effects of hemolysis, lipemia, hyperbilirrubinemia, and anticoagulants in canine C-reactive protein, serum amyloid A, and ceruloplasmin assays. *Can Vet J*. 2005;46:625–629.
109. Fascetti AJ, Mauldin GE, Mauldin GN. Correlation between serum creatine kinase activities and anorexia in cats. *J Vet Intern Med*. 1997;11:9–13.
110. Zhang QY, Ge JB, Chen JZ, et al. Mast cell contributes to cardiomyocyte apoptosis after coronary microembolization. *J Histochem Cytochem*. 2006;54:515–523.
111. Carroll JA, Carter DB, Korte SW, Prather RS. Evaluation of the acute phase response in cloned pigs following a lipopolysaccharide challenge. *Domest Anim Endocrinol*. 2005;29:564–572.
112. Sudhahar V, Kumar SA, Varalakshmi P. Role of lupeol and lupeol linoleate on lipemic-oxidative stress in experimental hypercholesterolemia. *Life Sci*. 2006;78:1329–1335.
113. Piao F, Yokoyama K, Ma N, Yamauchi T. Subacute toxic effects of zinc on various tissues and organs of rats. *Toxicol Lett*. 2003;145:28–35.
114. Cai X, Wong YF, Zhou H, et al. Manipulation of the induction of adjuvant arthritis in sprague-dawley rats. *Inflamm Res*. 2006;55:368–377.
115. Peng N, Liu JT, Gao DF, Lin R, Li R. Angiotensin II-induced C-reactive protein generation: Inflammatory role of vascular smooth muscle cells in atherosclerosis. *Atherosclerosis*. 2007;193:292–298.
116. Kim AJ, Park S. Mulberry extract supplements ameliorate the inflammation-related hematological parameters in carrageenan-induced arthritic rats. *J Med Food*. 2006;9:431–435.

117. Ray S, Phadke S, Patel C, Hackman RM, Stohs S. Short-term and long-term in vivo exposure to an ephedra- and caffeine-containing metabolic nutrition system does not induce cardiotoxicity in B6C3F1 mice. *Arch Toxicol*. 2005;79:330–340.
118. Oguri S, Motegi K, Iwakura Y, Endo Y. Primary role of interleukin-1 alpha and interleukin-1 beta in lipopolysaccharide-induced hypoglycemia in mice. *Clin Diagn Lab Immunol*. 2002;9:1307–1312.
119. Hernandez A, Martinez ME, Fiering S, Galton VA, St Germain D. Type 3 deiodinase is critical for the maturation and function of the thyroid axis. *J Clin Invest*. 2006;116:476–484.
120. Zhou X, Zhao X, Tang L, et al. Immunomodulatory activity of the rhizomes of impatiens pritzellii var. hupehensis on collagen-induced arthritis mice. *J Ethnopharmacol*. 2007;109:505–509.
121. You Q, Cheng L, Reilly TP, Wegmann D, Ju C. Role of neutrophils in a mouse model of halothane-induced liver injury. *Hepatology*. 2006;44:1421–1431.
122. Elovitz MA, Mrinalini C. The use of progestational agents for preterm birth: Lessons from a mouse model. *Am J Obstet Gynecol*. 2006;195:1004–1010.
123. Hu A, Jiao X, Gao E, et al. Chronic beta-adrenergic receptor stimulation induces cardiac apoptosis and aggravates myocardial ischemia/reperfusion injury by provoking inducible nitric-oxide synthase-mediated nitrative stress. *J Pharmacol Exp Ther*. 2006;318:469–475.
124. Yu L, Pragay DA, Chang D, Wicher K. Biochemical parameters of normal rabbit serum. *Clin Biochem*. 1979;12:83–87.
125. de Prada TP, Pozzi AO, Coronado MT, et al. Atherogenesis takes place in cholesterol-fed rabbits when circulating concentrations of endogenous cortisol are increased and inflammation suppressed. *Atherosclerosis*. 2007;191:333–339.
126. Min X, Xiaohui Z, Zhaixiang D, Ming O. Effect of the yang tonifying herbs on myocardial beta-adrenoceptors of hypothyroid rabbits. *J Ethnopharmacol*. 1998;60:43–51.
127. Czako L, Hegyi P, Takacs T, et al. Effects of octreotide on acute necrotizing pancreatitis in rabbits. *World J Gastroenterol*. 2004;10:2082–2086.
128. Bauersachs J, Hiss K, Fraccarollo D, Laufs U, Ruetten H. Simvastatin improves left ventricular function after myocardial infarction in hypercholesterolemic rabbits by anti-inflammatory effects. *Cardiovasc Res*. 2006;72:438–446.
129. Kjelgaard-Hansen M, Luntang-Jensen M, Willesen J, Jensen AL. Measurement of serum interleukin-10 in the dog. *Vet J*. 2007;173:361–365.
130. Kearns RJ, Hayek MG, Turek JJ, et al. Effect of age, breed and dietary omega-6 (n-6): Omega-3 (n-3) fatty acid ratio on immune function, eicosanoid production, and lipid peroxidation in young and aged dogs. *Vet Immunol Immunopathol*. 1999;69:165–183.
131. Osuka K, Suzuki Y, Tanazawa T, et al. Interleukin-6 and development of vasospasm after subarachnoid haemorrhage. *Acta Neurochir (Wien)*. 1998;140:943–951.
132. Gunn-Moore DA, Caney SM, Gruffydd-Jones TJ, Helps CR, Harbour DA. Antibody and cytokine responses in kittens during the development of feline infectious peritonitis (FIP). *Vet Immunol Immunopathol*. 1998;65:221–242.
133. Waner T, Avidar Y, Peh HC, Zass R, Bogin E. Hematology and clinical chemistry values of normal and euthymic hairless adult male dunkin-hartley guinea pigs (Cavia porcellus). *Vet Clin Pathol*. 1996;25:61–64.
134. Gosiewska A, Wilson S, Kwon D, Peterkofsky B. Evidence for an in vivo role of insulin-like growth factor-binding protein-1 and -2 as inhibitors of collagen gene expression in vitamin C-deficient and fasted guinea pigs. *Endocrinology*. 1994;134:1329–1339.
135. Weishaupt A, Jander S, Bruck W, et al. Molecular mechanisms of high-dose antigen therapy in experimental autoimmune encephalomyelitis: Rapid induction of Th1-type cytokines and inducible nitric oxide synthase. *J Immunol*. 2000;165:7157–7163.
136. Siegel J, Rent R, Gewurz H. Interactions of C-reactive protein with the complement system. I. Protamine-induced consumption of complement in acute phase sera. *J Exp Med*. 1974;140:631–647.

137. Castella M, Buckberg GD, Tan Z. Neurologic preservation by Na+-H+ exchange inhibition prior to 90 minutes of hypothermic circulatory arrest. *Ann Thorac Surg*. 2005;79:646–54; discussion 646-54.
138. D'Allaire S, DeRoth L. Physiological responses to treadmill exercise and ambient temperature in normal and malignant hyperthermia susceptible pigs. *Can J Vet Res*. 1986;50:78–83.
139. Carroll JA, Veum TL, Matteri RL. Endocrine responses to weaning and changes in post-weaning diet in the young pig. *Domest Anim Endocrinol*. 1998;15:183–194.
140. Stevenson LS, McCullough K, Vincent I, et al. Cytokine and C-reactive protein profiles induced by porcine circovirus type 2 experimental infection in 3-week-old piglets. *Viral Immunol*. 2006;19:189–195.
141. Thom ML, Hope JC, McAulay M, et al. The effect of tuberculin testing on the development of cell-mediated immune responses during mycobacterium bovis infection. *Vet Immunol Immunopathol*. 2006;114:25–36.
142. Yamanaka H, Hagiwara K, Kirisawa R, Iwai H. Transient detection of proinflammatory cytokines in sera of colostrum-fed newborn calves. *J Vet Med Sci*. 2003;65:813–816.
143. Schroedl W, Fuerll B, Reinhold P, Krueger M, Schuett C. A novel acute phase marker in cattle: Lipopolysaccharide binding protein (LBP). *J Endotoxin Res*. 2001;7:49–52.
144. Nakajima Y, Momotani E, Murakami T, et al. Induction of acute phase protein by recombinant human interleukin-6 (IL-6) in calves. *Vet Immunol Immunopathol*. 1993;35:385–391.
145. Bloomfield FH, Oliver MH, Hawkins P, et al. Periconceptional undernutrition in sheep accelerates maturation of the fetal hypothalamic-pituitary-adrenal axis in late gestation. *Endocrinology*. 2004;145:4278–4285.
146. Ulutas PA, Ozpinar A. Effect of mannheimia (pasteurella) haemolytica infection on acute-phase proteins and some mineral levels in colostrum-breast milk-fed or colostrum-breast milk-deprived sheep. *Vet Res Commun*. 2006;30:485–495.
147. Marques PR, Illner P, Williams DD, et al. Hypothalamic control of endocrine thermogenesis. *Am J Physiol*. 1981;241:E420–E427.
148. Maudsley S, Baltz ML, Munn EA, et al. Isolation and characterization of goat C-reactive protein. *Biochim Biophys Acta*. 1987;924:75–80.
149. Eisner JR, Barnett MA, Dumesic DA, Abbott DH. Ovarian hyperandrogenism in adult female rhesus monkeys exposed to prenatal androgen excess. *Fertil Steril*. 2002;77:167–172.
150. Sawhney RC, Rastogi I, Rastogi GK. Effect of estrogens on thyroid function. II. alterations in plasma thyroid hormone levels and their metabolism. *Metabolism*. 1978;27:279–288.
151. Asiedu CK, Goodwin KJ, Balgansuren G, et al. Elevated T regulatory cells in long-term stable transplant tolerance in rhesus macaques induced by anti-CD3 immunotoxin and deoxyspergualin. *J Immunol*. 2005;175:8060–8068.
152. Varnavski AN, Zhang Y, Schnell M, et al. Preexisting immunity to adenovirus in rhesus monkeys fails to prevent vector-induced toxicity. *J Virol*. 2002;76:5711–5719.
153. Riley RF, Coleman MK. Isolation of C-reactive proteins of man, monkey, rabbit and dog by affinity chromatography on phosphorylated cellulose. *Clin Chim Acta*. 1970;30:483–496.
154. Fitzgerald JT, Sena MJ, Vandewalker KN, et al. Occult pretransplantation systemic inflammation and post transplantation vascular changes in a primate arterial allograft model. *Transplantation*. 2004;78:367–374.
155. Kraft W, Hartmann K, Dereser R. Dependency on age of laboratory values in dogs and cats. 1. Enzyme activities in blood serum. *Tierarztl Prax*. 1995;23:502–508.

Chapter 2
Preanesthesia, Anesthesia, Chemical Restraint, and the Recognition and Treatment of Pain and Distress

The reader is referred to two standard veterinary textbooks for in-depth information about the pharmacodynamics, pharmacokinetics, and practical use of anesthetic and analgesic agents in animals.[1,2] The preanesthetic, anesthetic, chemical restraint, and analgesic regimens cited in this chapter have received approval from an Institutional Animal Care and Use Committee (IACUC) or similar body with the same responsibilities or have been published by board certified veterinary anesthesiologists.

There is increasing pressure, primarily a response of Institutional Animal Care and Use Committees to external pressure, to require that any procedure conducted in animals that could be considered to cause pain or distress to a human be conducted with the benefit of anesthesia or analgesia. This policy can and does result in some anesthetic deaths, stress associated with the anesthetic procedure, and/or confounding drug-induced changes in the animal that may be more severe than the procedure to be conducted. In some instances, proper prior training and acclimation of the animals, particularly of the larger species, to the procedure can result in fewer problems than tranquilizing, sedating, or anesthetizing the animal. It might still be necessary to provide chemical restraint for a variety of reasons including humane considerations. For most circumstances, the same agents used for anesthesia and/or analgesia can be used for chemical restraint.

General Principles of Pain Recognition in Animals

There is an absolute need for anyone conducting animal research to be able to recognize pain and treat the individual animal appropriately. Acute pain is usually accompanied by changes in the autonomic nervous system, does not last beyond the time needed for the injury to heal, and responds to treatment with analgesics. Acute recurrent pain is the term generally used to describe prolonged pain such as that associated with some neoplasms. Chronic pain is classified as long-term pain with no obvious cause or onset in time. Somatic pain is usually localized while visceral pain is not.

The International Association for the Study of Pain (ISAP) defines pain as "…an unpleasant, sensory, emotional experience associated with actual or potential tissue damage or described in terms of such damage…" This definition is open to criticism

D.R. Gross, *Animal Models in Cardiovascular Research*,
DOI: 10.1007/978-0-387-95962-7_2, © Springer Science + Business Media, LLC 2009

since individual animals, including humans, perceive and communicate pain uniquely, as individuals, reacting to the particular circumstance(s) as individuals. There is a well documented body of literature indicating cognitive modulation of pain influenced by attention, distraction, environment, and prior experience.[3] The ISAP guidelines for the effective diagnosis and treatment of pain were specifically developed to provide a formal evaluation process for analgesic agents. The protocol states that the subject should be compared with clinically normal animals of the same species using some quantitative measure of behavioral parameters such as movement, grooming, and sleep, and by physiological parameters such as EEGs, hormone concentrations, and measures of the autonomic nervous system. Whatever parameters used they are then measured again following treatment with an agent being evaluated for analgesic effect.[3]

Pain can be objectively measured by recording increased afferent nerve activity from nociceptors. Changes in the autonomic nervous system in response to pain can be manifest by changes in heart rate, pupillary diameter, skin resistance, and peripheral blood flow. Pain-induced changes in the hypothalamic-pituitary-adrenal axis can be estimated by measuring circulating levels of corticosteroids. Postural changes in response to pain can be voluntary or involuntary. They include hyperreflexia, the adoption of an immobile stance, abnormal postures during Recumbency and/or abnormal positioning of limbs, head, and/or neck. Pain associated locomotor activity changes include movements such as restlessness, kicking, stamping, rolling, jumping, licking or biting at the site of injury or pain, and excessive tail wagging or "wringing". Pain is frequently manifested as a lack of appetite and/or thirst, although some animals may "play" with water without drinking it.[4, 5]

Some general signs of animal well-being and absence of pain are common to most species used as animal models for cardiovascular research. Pain-free animals will keep themselves well groomed, have normal movement, eat and drink normally, and demonstrate normal reproduction. They will interact with cage mates and/or handlers and will exhibit curiosity by exploration of their surroundings, particularly when placed in a new, nonthreatening environment. There is an evolving nomenclature associated with the recognition of pain in animals. "Guarding" is any attempt to protect itself or a specific anatomical area. Animals will move away or display aggressive behavior when guarding. "Vocalization" involves crying out when manipulated or when forced to use an affected anatomical area. "Mutilation" involves repetitive licking, biting, scratching, shaking, or rubbing an affected area. "Restlessness" includes relentless pacing, lying down and getting up, or shifting of weight. "Sweating" from the paws in dogs and cats, sweating from the skin in horses, and panting despite cool or comfortable housing conditions for most species can indicate pain. "Recumbency" involves animals lying down for unusual lengths of time for the species. "Depression" is usually manifested as reluctance to move or difficulty in rising. "Postures" including holding the head down, the abdomen tucked up, a hunched over stance, facial distortions, and pallor of mucous membranes are all considered "abnormal appearance". Signs of pain are often not all present at the same time and those observed at one particular time may not be present the next time the animal is examined. Investigators have the responsibility to become familiar with the normal condition and behavior of the animals they are using and understand that signs of pain involve a complex group of changes that must be considered as a whole.

Recognizing, assessing, and evaluating pain and discomfort in animal models is not as straightforward as some animal rights activists maintain. Beynen et al.[6] created a model of gallstones in mice. They critically evaluated vocalization, magnitude of abdominal muscular contractions, stance, response to abdominal palpation, and at least five other parameters. They found that abdominal palpation was the only parameter routinely effective in differentiating between mice with and without gallstones. Lariviere et al.[7] determined there are heritable aspects of nociception that could indicate genetic sources of variation in individual responses to painful stimuli. Anil et al.[8] claim the assessment of the degree of pain in domestic animals is subjective, not reliable, and has not made much progress since the 1940s.

The fact that the recognition and assessment of pain in animals used for research is difficult must not deter us from making those evaluations. No small part of the problem comes because of the regulatory view, based on pure anthropomorphic thought, that any procedure or condition likely to cause pain in humans will do the same in animals. Flecknell suggests the use of a "critical anthropomorphic approach," an approach that considers differences in anatomy, posture, and behavior in the framework of a pain assessment scheme.[9, 10] To make matters more complicated distinction between distress, suffering, and stress in animals tend to be blurred and the terms are frequently used synonymously. It would be very helpful to develop species-specific pain scoring systems to facilitate the evaluation of pain and its rationale treatment. This is extremely important in cardiovascular studies since, as will be discussed in Chap. 7, almost all drugs used for chemical restraint or for analgesia in research animals have significant cardiovascular effects.[11]

There are three pain-scoring systems commonly used for humans and animals: the simple descriptive scale (SDS), the numeric rating scale (NRS), and the visual analogue scale (VAS). All three of these scales were developed for use by human patients to record the intensity of their own pain. Physicians, parents, and nurses interacting with pediatric patients use the same scoring systems. McGrath and colleagues have studied pain recognition in pediatric patients. They describe three aspects of pain, cognitive or phenomenological, behavioral, and physiological. Each of these aspects may require a different method of measurement. They developed the Children's Hospital of Eastern Ontario Pain Scale (CHEOPS), a NRS that assigns a score to various behaviors for pediatric patients. A study conducted after major surgery in 3 to 7-year-old patients found that two different self-report scales used were strongly and significantly correlated but there was little relationship between the scores for the self-reports and the behavioral measures. Many of these patients who reported severe pain manifested few of the behavioral indicators used by CHEOPS.[12] Another study by the same group found that parents tended to overestimate their child's pain whereas nurses were less consistent in their scoring and tended to underestimate.[13] Another scoring system, the Non-Communicating Children's Pain Checklist, was used by caregivers to discriminate between pain and distress in children with cognitive impairments. Seven of the items in this checklist: "Cranky, Seeking Comfort, Change in the Eyes, Less Active, Gesture to Part That Hurts, Tears, and Gasping" significantly predicted numerical pain ratings by caregivers.[14] Studies have also demonstrated a relationship between maternal behavior and infant pain during immunization in human patients tested at 6 months

and again at 18 months of age comparing measured vagal tone and "infant difficultness." At 6 months, 44% of the variability between biologically based infant variables (measured vagal tone and infant difficultness) and maternal contextual variables (maternal behavior during pain to the infant and maternal sensitivity) was predicted by infant difficultness and mothers' vocalizations during immunization.[15]

The advent of patient-controlled analgesia (PCA) has enabled many studies that all emphasize the psychological aspects of pain perception in human patients. This technique gives control of the frequency of analgesic administration to the patient. Patients with higher anxiety levels and less social support use more PCA. Older patients usually report less pain but use the same amount of analgesic as younger patients. Music decreased the amount of PCA in one group of patients. Females use significantly less PCA than males but the state of preoperative anxiety in women receiving abdominal hysterectomy correlated with increased PCA use.[3]

Even objective tests for the relief of pain are sometimes less than reliable. Changes in motor reflexes, autonomic reflexes, and neuroendocrine responses that mimic pain and severe distress can be induced just by approaching and handling animals that are not well acclimated to some level of human interaction. The use of parameters such as heart rate, respiratory rate, body temperature, and salivation will be unreliable as measures of postoperative pain unless considerable time and effort is expended to tame, handle, and train each animal preoperatively. The Bispectral Index Score (BIS) is a software program used to quantitate electroencephalographic data for the purpose of evaluating the hypnotic state during anesthesia. A recent study determined the relationship between BIS values and the minimum alveolar concentration (MAC), using isoflurane in cats and concluded that the BIS endpoints used to titrate anesthetic agents in humans may not be applicable to cats.[16]

Pain is a natural phenomenon that results in injured anatomical sites being protected and allowed to heal. Following surgery it might be beneficial for an animal, or human, to not move about normally and thus to protect the incision site. There is increasing evidence that performance animals particularly racehorses, routinely treated with Nonsteroidal anti-inflammatory drugs (NSAIDs) such as phenylbutazone, for supposedly minor injuries suffer more catastrophic injuries while performing. It is also true that excessive pain can be detrimental and even life threatening, particularly in animals considered as prey species, such as rabbits. Excessive pain prolongs recovery from illness or injury. Excessive pain will stop an animal from eating and may lead to GI shut down and even death. Some species, particularly rabbits and sheep, can go into shock from excessive pain and die, even though the illness or injury might not have been life-threatening. Decisions regarding the administration of analgesia must involve clinical judgment.

Anyone who works with or lives with a variety of individual animals or animal species on a regular basis realizes that individual animals have different personalities. These differences extend to the demonstration and even perception of pain. Some individuals are stoic while others are crybabies, and the response to pain can vary with the circumstances in any one individual. Although there are definite species differences in pain demonstration, individual variations within a species are sometimes greater than between species differences. There is clear evidence that the perceived intensity and tolerance of pain varies among individuals. There are also significant

differences between quadrupeds and bipeds related to postoperative pain. Abdominal surgery is apparently less painful in quadrupeds than in bipeds since the latter use their abdominal muscles to a greater extent to maintain posture and while ambulating. A median sternotomy produces low to moderate pain in humans but significant pain in animals because quadrupeds use their forelimbs for walking. A lateral thoracotomy is less painful in quadrupeds since they rely more on abdominal respiration and bipeds more on thoracic respiration.[5]

Female subjects apparently experience greater analgesia from κ-opioid analgesics such as nalbuphine and butorphanol than do male subjects.[17] The same research group conducted a double-blind, placebo-controlled study to evaluate the analgesic efficacy of the combination of a μ-opioidergic analgesic (morphine) and pentazocine (a κ-opioidergic agent) and found a level of analgesia significantly greater than could be accounted for by the addition of the analgesic effects of each opioid alone.[18] The effects of gonadal hormones on persistent pain has also been demonstrated in rats.[19]

The use of the tricyclic antidepressants, anticonvulsants, *N*-methyl-D-aspartic acid receptor antagonists, and low-dose intravenous local anesthetics for analgesia is increasing in veterinary and laboratory animal medicine. These agents have proved to be efficacious in relieving certain types of pain, particularly neuropathic and cancer pain in humans, but their effectiveness in laboratory animals has not been totally evaluated.

The Use of Anti-Cholinergic Drugs for Preanesthesia

Atropine sulfate has a long history of veterinary use as a routine adjunct to general anesthesia, particularly with the use of inhalant anesthetic agents. Because ether and other early inhalant anesthetic agents were very irritating to mucous membranes, atropine was useful for controlling salivary and respiratory tract secretions. Atropine also blocks the so-called "laryngeal reflex," purported to result in cardiac arrest. Modern inhalant anesthetic agents produce minimal respiratory tract irritation and secretions.

Atropine does have significant effects on the cardiovascular system. The usual doses recommended for preanesthesia do not markedly affect blood pressure but do cause tachycardia. Individual animals will have varying degrees of tachycardia depending upon the normal degree of vagal tone in that individual. As a result of the tachycardia, cardiac output tends to increase. The cardiac vagal efferent nerves are blocked so atropine interferes with the response to any vagally-mediated perturbation. The pressor effects of catecholamines are accentuated. Large doses of atropine can act as direct cardiac depressants.[20]

Atropine has other effects of possible concern in animals being surgically prepared for follow-up studies. It can cause inhibition of GI smooth muscle motility resulting in postoperative GI stasis. This is of particular concern with ruminants. GI secretions are also blocked by atropine, and this can add to postoperative GI problems, particularly in ruminants where salivary secretions high in bicarbonate are important to normal rumen pH and function. Atropine decreases bronchial and tracheal secretions, dilates bronchioles, and changes the viscosity of bronchial and tracheal secretions and the muco-ciliary blanket resulting in prolonged muco-ciliary clearance.

The respiratory effects can lead to atelectasis. Atropine can also lead to urinary retention, and there is a definite anhydrotic effect. There seems to be more reasons not to use atropine as a preanesthetic agent than reasons to do so.

General Comments on Preanesthetic Agents

The psychotropic agents have been used extensively in veterinary medicine since the 1950s when reserpine and the phenothiazine derivatives were first widely accepted for use. These agents are valuable in quieting and calming animals but are most effective when used in animals that are reasonably calm at the time the agents are administered. If the animal is very agitated before the agent is given, the beneficial effects are sometimes mitigated. The major advantage of these agents as preanesthetics is to make induction of anesthesia easier, smoother, and to reduce the total dose of anesthetic agent needed. Drug interactions can occur and if the cardiovascular studies are being conducted while the animal is anesthetized, it becomes difficult to separate drug effects from physiological responses to the perturbations introduced. Many of the tranquilizers used today are α-adrenergic blocking agents, and therefore have a direct effect on blood pressure and, in some cases, heart rate. When used in combinations with other agents, it is difficult to identify which drugs are responsible for the cardiovascular responses observed.

Preanesthesia and Anesthesia in Rats and Mice

The following agents are used and recommended for anesthesia in rats and mice:

Buprenorphine (0.05 mg/kg) administered 1 h prior to administration of Ketamine (45 mg/kg) and medetomidine (0.3 mg/kg), IP. This combination resulted in significantly longer duration of anesthesia than ketamine/medetomidine alone, significant respiratory depression, and two anesthetic deaths.[21]

Chloral hydrate (300 mg/kg) IP: This mixture should be diluted since concentrations above 2% can result in peritonitis.

ChloroPentR (3.0 mL/kg) IP: This is a mixture of chloral hydrate (42.5 mg/mL), sodium pentobarbital (8.86 mg/mL) and $MgSO_4$ (21.2 mg/mL) (Very similar to the old Equithesin sold in the 1950s and 1960s, ouch!)

Diethyl-ether (Avertin) (200–300 mg/kg) IP: Must be stored in a lightproof container under refrigeration. Induction with Avertin in rats combined with orbital puncture for obtaining 0.5 mL of blood caused more distress than did tail vein puncture under nitrous oxide/halothane anesthesia or saphenous vein puncture in untreated rats.[22]

Halothane, same as Isoflurane, but does not seem to be as effective and is more dangerous to laboratory personnel over long periods of use.

Isoflurane induce in a chamber or with a mask using 5 vol% then reduce and maintain in a surgical plane with 1.25–2.5 vol% to effect.

Ketamine (40–80 mg/kg) + Xylazine (5–10 mg/kg) IP

Ketamine (40–80 mg/kg) + ValiumR (5–10 mg/kg) IP

Ketamine (31.25 mg/kg) + Xylazine (6.25 mg/kg) + Acepromazine (1.25 mg/kg), SQ[23]

Ketamine (60 mg/kg) medetomidine (0.4 mg/kg) IP[21]: A gender based difference in this combination when used for short-term chemical restraint was noted. Male mice required a dose of ketamine (50 mg/kg)/medetomidine (10 mg/kg), IP, while female mice needed 75 mg/kg of ketamine to produce the same level of restraint and anesthesia. Atipamezole (1–2.5 mg/kg, IP) effectively reversed the anesthesia by ketamine/medetomidine with males recovering more rapidly than females.[24]

Oxygen + nitrous oxide + halothane, induction with high concentrations of halothane, then reduce to maintain in a surgical plane.

Sodium pentobarbital (35–45 mg/kg) IP or IV

Sufentanil/medetomidine at 0.04/0.15 mg/kg, or 0.50/0.15 mg/kg, IP or 0.8/0.3 mg/kg, SQ all produced a surgical plane of anesthesia. All three combinations also resulted in marked respiratory depression. The SQ method was recommended since it resulted in a more reliable and more rapid induction. The administration of butorphanol and atipamezole (0.2/0.5 mg/kg) caused rapid reversal of anesthesia.[25]

Chemical Restraint (Sedation) in Rats and Mice

All of the above agents and combinations can be used for chemical restraint as well as the following agents:

Acetylpromazine (Acepromazine): 1.0–5.0 mg/kg, SQ, IM, IP, bid.

Diazepam: 5.0–15.0 mg/kg, SQ, IM, IP, bid. Only adequate sedation for minor procedures.[26]

Droperidol: 0.5–2.0 mg/kg, SQ. Doses above 0.5 mg/kg cause subcutaneous inflammation. Allows easier manipulation of the animal for minor procedures but not sufficient sedation for tail-vein or orbital bleeding.[26]

Methimazole: 10–100 mg/kg, IP.

Methohexitone sodium: 44 mg/kg, IP provided < 5 min of immobilization in female C3H/Neu mice. Complete recovery was achieved in 10–15 min.[27]

Pain and Distress Recognition in Rats and Mice

Rats and mice pose some special problems regarding the recognition of pain. Mice, as prey animals, have a genetic predisposition not to display pain behavior since this will signal them out to predators. They are less likely to limp or display other obvious signs of pain than other species. Rats are genetically predisposed to aggressive behavior against injured individuals of their own species, so they also tend to hide injuries.

The detection and appropriate treatment of postoperative pain in rats and mice presents a common problem for cardiovascular researchers. Investigators should devise, adopt, or adapt a pain scale appropriate to their situation. When the experimental

protocol requires surgery, the animals should be observed and scored in their normal environment, when first brought to the laboratory or surgery room, again postoperatively on a regular and ongoing schedule for a period of time depending upon the severity of the insult, until they recovered fully. When the total postoperative score is greater than the preoperative score, animals should be treated with appropriate analgesics. This approach does not exclude preemptive, presurgical use of analgesics in a standardized protocol. Preemptive use is an effective strategy particularly when the drug(s) and dose are predetermined to be effective and safe for the particular procedure and will not interfere with the measurements to be obtained. Martini et al.[28] describe a system that includes code values for observed changes in such parameters as body weight, food consumption, water consumption, body temperature, level of hydration, heart rate, respiratory rate, urine output, feces output, behavior, body positioning, piloerection, ataxia, hyper reactivity, vocalization, and teeth grinding. When rodents demonstrate pain with rapid and shallow respiration, it can be accompanied by grunting or chattering on expiration. Tearing can occur and, in albinos, porphyrin secretion or "red tears" can be observed. Vocalization in rats and mice in acute pain can be at very high frequencies, above human perception. Studies using high frequency recordings have demonstrated this in the absence of other signs. Abnormal feeding behaviors, such as eating their bedding or cannibalism of offspring, can sometimes be observed. If housed with other animals, individuals might separate themselves from the rest of the animals in the cage or attempt to hide.[5]

Distress identification is very difficult. Studies have shown that the area under the corticosterone concentration vs. time curve can be used to model and predict the effects of restraint stress and chemical stressors.[29] Unfortunately, obtaining blood from rats and mice to generate these curves is highly stressful.

Behavioral psychologists have used a wide range of maze testing, learned behavior, and observational studies to characterize anxiety, stress, and distress-related behaviors in rats and mice. Prolonged exposure of female mice to psycho emotional conditions, such as housing aggressive males in proximity separated only by a perforated partition, causes marked anxiety in the females with inhibition of both motor and investigative activity.[30] Male mice exposed to repeated aggression by other male mice demonstrate signs of anxiety determined by various methods of psychological testing, primarily learning, risk avoidance, and problem solving behaviors. The level of anxiety and its behavioral manifestation depends upon the duration of aggression exposure and the genetic strain of the mice.[31, 32] Male mice of two different strains were separated at 4 weeks of age and kept in individual cages for 7 weeks. All mice exhibited signs of chronic anxiety as determined by various psychological tests but there were strong strain and test-specific effects on emotional behavior and memory in these animals.[33]

The following system for evaluating pain and related stress in rats and mice was approved by the IACUC at the University of Illinois and has been used successfully in our lab for the past few years. It is not perfect. Many other schemes have been devised that work just as well or better. The strength of this system is that it became routine for our lab. Laboratory personnel became familiar with it and comfortable using it so it served its purpose. It works best if the animals are scored prior to being moved from the animal care facility, again shortly after arriving at the laboratory or surgery room, after recovery from anesthesia and at regular intervals thereafter until the animals recover and are pain free.

Animal # _____Treatment: _____Date:_____

Circle the appropriate score

Parameter	Descriptors	Score
Comfort when placed in a new, clean cage	Normal investigation and movement during introduction to new surroundings, interested in surroundings, normal grooming, face washing, asleep or calm, resting, moving about normally	1
	Relatively uninterested in surroundings, reluctant to move about, more than normal grooming, chewing, awake but depressed	2
	Uninterested in new surroundings, apparently agitated and restless, incessant grooming	3
Movement once acclimated to new surroundings	Normal	1
	Restless, pacing continuously, getting up and down repeatedly	2
	Face twitching, large muscle twitching	3
	Rolling, thrashing, whole body twitching, losing balance, falling over	4
Appearance or posture	Normal (on sternum or curled up)	1
	Eyelids partially closed, ears flattened or carried abnormally, twitching	2
	Abnormal posture, prayer position, back arching and/or stretching, abnormal facial expression, abnormal leg positioning, grunting, teeth grinding, piloerection, uncontrollable twitching	3-4
Physiological	Normal pupils	1
	Abnormally dilated pupils	2
	No visible salivation	1
	Abnormal salivation	2
8 + h evaluations	Not eating	3
	Eating less than normal	2
	Eating normally	1
	No water intake	3
	Less than normal water intake	2
	Normal water intake	1
	Normal feces	1
	Abnormal feces	2
	Normal urination	1
	no sign of urination	3
Mental status	Same as preop	1
	Submissive or wary compared to preop	2
	Aggressive	3
Vocalization	None	1
	Vocalizes only when touched	2
	Intermittent vocalization	3
	Continuous vocalization	4
Response to palpation of incision site	No change from preop	1
	Pulls away when touched, looking at incision site when moving about	2
	Vocalizes when incision touches, reluctant to move unless prodded	3
	Violent reaction to palpation, vocalizes without wound being touched, snapping or hissing when trying to handle	4
	Extremely restless and violent or aggressive when trying to handle, freezes when palpated	5
Total score**:**		

Treatment of Pain in Rats and Mice

The following drugs and range of doses are recommended by several IACUC Websites, the NIH Website, and journal articles:

Local Anesthetic Agents

Bupivicaine: Local infiltration along the surgery site during closure
Lidocaine: Local infiltration, short duration anesthesia for minor procedures such as skin biopsies.

Nonsteroidal Anti-Inflammatory Drugs

NSAIDs, particularly the derivatives of propionic acid, have been shown to provide postsurgical pain relief at least equivalent to the opioids for certain surgical models in mice.[34] The same conclusions have been made using colorectal distension models in rats.[35-37] The NSAIDs can, however, result in gastrointestinal bleeding and other signs of GI toxicosis, some at therapeutic doses in rodents.[36, 37]

Acetaminophen (Tylenol Pediatric Suspension): No longer recommended since latest data indicate it is not effective in rats and mice.
Aspirin: 100–400 mg/kg, PO, once or twice daily
Carprofen: 5–15 mg/kg, SQ or IM, q 4–5 h, 5–10 mg/kg in water or jello, once daily. (Nonsteroidal anti-inflammatory agent, NSAID), analgesia lasted 4–5 h at 5 mg/kg dose[38]
Ibuprofen: Mice, 30 mg/kg, PO, (NSAID), once daily; Rats, 15 mg/kg, PO, once daily[39]
Flunixin-meglumine (Banamine): 2.5 mg/kg, SQ or IM, bid
Ketoprofen: 5–15 mg/kg, SQ or PO, q 4–5 h (NSAID), analgesia 4–5 h at 5 mg/kg dose[38]
Ketorolac: 5 mg/kg, IM (NSAID)[23]
Meloxicam: 1.0 mg/kg, SQ or PO (NSAID), once daily

Narcotics

Studies conducted on F344, Sprague–Dawley, Long–Evans, and Lewis rats using tail withdrawal from 50, 52, and 55°C water concluded that there is a hierarchy of antinociceptive effects of μ-opioids in rats with morphine and levorphanol demonstrating high potency, buprenorphine intermediate potency, and butorphanol and

nalbuphine low potencies. There were also differences in species sensitivity to these drugs. Morphine and levorphanol were most potent in F344 and least potent in Lewis rats. Butorphanol produced maximal effects in F344 and Sprague-Dawley at relatively low doses and half-maximal effects in Long-Evans at very high doses, but no effect in Lewis rats. Nalbuphine administration elicited near maximal effects in F344 and Sprague-Dawley and no effects in Long-Evans or Lewis strains. Similar effects were found with intermediate doses for these agents. These studies indicate a rank order of intrinsic efficacy in rats as: levorphanol > morphine > dezocine > buprenorphine > butorphanol > nalbuphine. Each of these drugs were found to have significant affinity for other types of opioid receptors, such as κ-receptors, but the antinociceptive effects, in these studies, was mediated by action at the μ-opioid receptor. Because these drugs differ in intrinsic efficacy, they are variously called agonists, partial agonists, to agonist/antagonists.[40, 41]

Buprenorphine continues to be recommended as the analgesic of choice for laboratory rodents at many institutions. A rat model of visceral pain induced by laporotomy and intestinal resection was used to evaluate treatment with buprenorphine (0.5 mg/kg, q 6 h, SQ). The animals exhibited behavior and appearance consistent with pain and distress for as long as 32 h postop. Animals in the same study treated with oxymorphone (0.03 mg/kg/h by continuous IV infusion) showed no signs of pain or distress.[42] Our experience with buprenorphine administered prior to surgery, or just prior to closure of thoracotomy incisions for control of postoperative pain, has not been good. We used recommended doses of buprenorphine in a mouse model of cardiac arrest and resuscitation and in a rat model of coronary ligation. We recorded significant increases in time to recovery and mortality in both models compared with animals treated with local anesthesia of the surgical site and NSAIDs.[43] This agrees with the high mortality rates previously reported on the use of buprenorphine in conjunction with ketamine/medetomidine anesthesia.[21, 44]

There are substantial differences in reports documenting the affects of opioids on both locomotor activity and food and water consumption in laboratory rodents. Morphine significantly decreases gastric emptying times in mice.[45] Because butorphanol and buprenorphine resulted in reduced food intake in rats, it has been concluded that water consumption was a more reliable parameter than food intake for evaluating postoperative pain.[46, 47] However, it has also been reported that butorphanol administered to normal rats results in significant increases in food intake via direct stimulation of the CNS.[45] Recommended drugs are:

Buprenorphine (Buprenex): 0.01–0.5 mg/kg, SQ, IM, or IP bid tid or q 6–12 h depending upon the extent and location of the procedure (0.1–0.25 mg/kg, PO, bid or tid, 0.01–0.02 mg/mL in drinking water, 0.5 mg/kg in jello).

Butorphanol (Torbugesic): 1.0-2.0 mg/kg, SQ, only provides 1–2 h of analgesia in both rats and mice.[48]

Dezocine: 1.0-5.0 mg/kg, PO, high concentrations detected in 15 min after dosing, concentrations in the brain significantly higher than those in the plasma.[49, 41]

Etorphine: 0.05–0.5 mg/kg, IP or Intrathecal[50]

Fentanyl: 0.01–0.3 mg/kg, SQ, provides 2–4 h of analgesia

Levorphanol: 0.5–5.0 mg/kg, IP[41]
Meperidine (Demerol): 2–4 mg/kg, bid
Morphine: 5.0–10.0 mg/kg, SQ or intrathecal, provides 2–3 h of analgesia but the level of analgesic effect is greater than that provided by buprenorphine or butorphanol[48, 51]
Nalbuphine: 2.5, 25, and 250 μmol/kg, IP resulted in 1.5, 2, and 4 h of analgesia, respectively
Naloxone: 0.1–10 mg/kg, SQ, provides 2–4 h of analgesia.[52] Potentiates pentazocine, fentanyl, methadone, and levorphanol analgesia but attenuates morphine, etorphine, propoxyphene analgesia[18]
Oxymorphone: 0.03 mg/kg, Alzet mini-pump, bolus IV injection or continuous IV infusion[42]
Pentazocine: 2 mg/kg, IV
Propoxyphene: 100 mg/kg/day, PO[53]

There is good evidence for antinociceptive synergy between opioid agonists and local anesthetics,[54] and institutional veterinarians and veterinary anesthesiologists are now recommending these combinations for use more frequently. Newer agents including 5–hydroxytryptamine receptor antagonists[55] and specific blockers of pain perception such as capsaicin and serotonin antagonists, as well as other antagonists of peripheral sensitization are being discussed and new agents are being developed.[56] Cyclooxygenase–2 inhibitors and *N*-methyl-D-aspartate receptor antagonists are coming to the market for use in laboratory animals and will require critical review for use in this setting. Agents that selectively block ectopic discharge are also being developed.[56]

Preanesthesia and Anesthesia in Rabbits

The following agents are recommended for use in rabbits:

Fentanyl (0.4 mg/mL) + Droperidol (20 mg/mL) administered at 0.3–0.5 mL/kg, IM will provide a surgical plane of anesthesia. Dosage of 0.125 mL/kg of this mixture will provide sedation and also results in vasodilation and easy blood collection from the central ear artery.
Isoflurane (1.25–2.5 vol%, to effect) following Ketamine/Xylazine or Ketamine/ValiumR will provide a good plane of surgical anesthesia for more prolonged procedures. A mask can be used for isoflurane delivery but intubation of the trachea is preferred. When used exclusively masking with isoflurane for induction results in severe apnea and struggling, hypercapnia, acidosis, and bradycardia. Induction with isoflurane is not recommended.[57]
Ketamine (35 mg/kg) + ValiumR (5–10 mg/kg), IM
Ketamine (44 mg/kg) + Xylazine (5 mg/kg), IM

Pentobarbital sodium (35–45 mg/kg), IV, the barbiturates should always be administered with half the dose given rapidly and the rest of the calculated dose given slowly to effect. Apnea is common with pentobarbital.

Servoflurane can be used as an inhalant anesthetic agent but as with isoflurane animals should not be induced using this agent.[57]

Chemical Restraint (Sedation) in Rabbits

Acepromazine: 1.0 mg/kg, SQ, IM, IV, bid

Diazepam: 2.0 mg/kg, IM, IV, bid

Telazol (combination of tiletamine and zolazepam) was found to be nephrotoxic at doses of 32 or 64 mg/kg and produced no analgesia at those doses. Its use is contraindicated in rabbits.[58, 59]

Pain Recognition in Rabbits

Normal rabbits are bright, alert, active, inquisitive, have a smooth hair coat and a good body condition. Pain in rabbits can be evidenced by limping or a change in gait, the withdrawal or protection of an injured part, awkward or abnormal postures, or by licking, rubbing, or scratching the area of injury. Decreased eating and drinking often accompanies chronic pain in rabbits. Rabbits can demonstrate pain by an anxious or apprehensive appearance, inactivity, and a hunched appearance. They sometimes attempt to hide and/or to vocalize. Some individuals might demonstrate aggressive behavior with increased activity, excessive scratching and/or licking. Reactions to being handled might become exaggerated and result in "screaming." Some rabbits will grind their teeth and salivate excessively when experiencing abdominal pain. Respiratory rates can increase. Anxious rabbits, or rabbits in distress, will sometimes cannibalize their young. Severe distress and pain can result in the tonic immobility reflex (playing dead). This phenomenon is thought to block pain in prey species.[5]

Treatment of Pain in Rabbits

Local Anesthetics

Bupivicaine: Longer acting local anesthetic. This agent is very useful for infusion along an incision site to provide postoperative analgesia.

Lidocaine: 2% for local infusion. Provides short-term anesthesia adequate for biopsies or minor procedures.

Nonsteroidal Anti-Inflammatory Drugs (NSAIDs)

Aspirin: Usually use liquid baby aspirin, 100–400 mg/kg, PO
Carprofen: 1–5 mg/kg, PO, bid
Flunixin: 1–2 mg/kg, SQ or IM, bid
Ketoprofen: 1–3 mg/kg, IM
There is no real reason that other NSAIDs cannot be used, but dosages need to be established.

Narcotics

Buprenorphine: 0.01–0.1 mg/kg, SQ or IM, q 6–12 h
Butorphanol: 0.1–0.5 mg/kg, SQ, IV, IM, q 2–4 h

Alpha–Agonists

Xylazine: 20 mg/kg, IM
These agents are powerful analgesics, particularly for abdominal organ pain, but also produce significant sedation, bradycardia, and hypotension and are therefore rarely used as analgesics.

Preanesthesia and Anesthesia in Dogs

Entering "general anesthesia, dog" into PubMed yielded 2,373 references. Many different techniques and agents for anesthesia in dogs are available. Board certified veterinary anesthesiologists are working hard to refine and develop techniques for safe and effective anesthesia and analgesia in dogs to cope with a wide variety of health status issues. Anesthesia of the critically ill or injured animal is especially problematic. Veterinary anesthesiologists have taken the same tack as human anesthesiologists using a variety of different agents in combination to achieve

balanced anesthesia with minimal adverse effects. For cardiovascular researchers, the most important aspect relating to the choice of anesthetic regimen to use is to have great familiarity and maximum comfort level with the choice. The following anesthetic protocols all provide reasonable results in dogs:

*Acepromazine (0.2 mg/kg) + Butorphanol (0.4 mg/kg), IM followed by inhalation anesthesia.

*Acepromazine (0.05 mg/kg), IM + Oxymorphone (0.05–0.2 mg/kg) IV for induction, followed by inhalation anesthesia (Isoflurane, Halothane, Sevoflurane, or Desflurane)

Acepromazine (0.025 mg/kg) + Pethidine (Meperidine) (3.5 mg/kg), IM + thiopental (10 mg/kg), effects of varying the rate of infusion of thiopental were studied. It was found that a slow rate of thiopental infusion (0.1 mL/kg/min) reduced the induction dose of thiopental required but the quality of induction was inferior to a faster rate of thiopental infusion (0.4 mL/kg/min).[60]

*Acepromazine (0.05 mg/kg), IM followed by Propofol (4–6 mg/kg), IV

*Acepromazine (0.05 mg/kg), IM followed by thiopental (8–20 mg/kg), IV for induction, followed by inhalation anesthesia

Aflaxan (steroid anesthetic agent) (2.0–10.0 mg/kg), IV. The duration of anesthesia was dose dependent. It was found that the agent provided rapid and smooth induction with satisfactory conditions for endotracheal intubation and a short duration of anesthesia, 26.2 ± 7.5 min.[61]

Chloralose (60 mg/kg) + Urethane (200 mg/kg): IV is the classical anesthesia used to maintain autonomic control during acute cardiovascular experiments. Dogs do not recover well from this regimen.

Chlorpromazine (0.5 mg/kg), IV + Ketamine (2 mg/kg), IV + Midazolam (0.5 mg/kg), IV

Chlorpromazine (0.5 mg/kg), IV + Propofal (5 mg/kg), IV

Chlorpromazine (0.5 mg/kg), IV + Thiopental (8 mg/kg), IV

Desmedetomidine (α–2–adrenoceptor agonist, active enantiomer of medetomidine) (1.0–2.0 μg/kg) IV, followed by propofol induction (2.3–3.3 mg/kg), IV, followed by desflurane, to effect. Determined to be effective and safe for induction and maintenance of general anesthesia in healthy dogs.[62]

Fentanyl (5.0–10.0 μg/kg/h) + isoflurane or sevoflurane

Fentanyl (10.0 μg/kg), IV bolus + fentanyl (10.0 μg/kg/h) continuous infusion, resulted in sedation but no anesthesia.[63]

Hydromorphone (0.1 mg/kg) + Diazepam (0.2 mg/kg), IV, followed by inhalation anesthetic

*Ketamine (4–8 mg/kg) + Diazepam (0.2–0.4 mg/kg), IV

Oxymorphone (0.05 mg/kg) + Diazepam (0.2 mg/kg), IM, followed by inhalation anesthetic

Pentobarbital sodium (20–30 mg/kg): IV, half the calculated dose is administered and the remainder to effect

Propofol (6–8 mg/kg), IV for induction, maintained at 24 mg/kg/h constant infusion

Propofol (24 mg/kg/h) + Fentanyl (5.0 μg/kg/h) continuous infusion, IV
Romifidine (0.04–0.08 mg/kg) + propofol (6–8 mg/kg), IV for induction followed by isoflurane to effect. This regimen was determined to by effective for induction and maintenance of general anesthesia in healthy dogs.[64]
Telazol (tiletamine/zolazepam) (6–20 mg/kg), IV[65, 66]
Telazol (10 mg/kg) + Etomidate (0.3 mg/kg), IV[67]
Telazol (10 mg/kg), IV + Medetomidine (30 μg/kg), IM[65]
Telazol (10 mg/kg), IV + Xylazine (1.1 mg/kg), IM[65]
*Thiopental (8–20 mg/kg): IV, half the calculated dose then to effect. Thiopental is usually used for induction followed by intubation of the trachea and then maintenance with inhalation anesthetic.

The seven protocols marked with an asterisk (*) were compared for arytenoid cartilage motion immediately after induction and no differences were found.[68] It is common to add N_2O (nitrous oxide) to halothane, isoflurane, and sevoflurane. The use of N_2O reduces the requirements for the inhalation anesthetics, i.e., less concentration required to maintain the same plane of anesthesia in dogs. N_2O with isoflurane caused increases in heart rate and arterial blood pressure, less of this reaction with sevoflurane and was not observed with halothane.[69] Combinations of acepromazine with butorphanol and induction with thiopental or propofol were compared with premedication with medetomidine and butorphanol and induction with ketamine and diazepam. In all cases, anesthesia was maintained with halothane. It was found that the use of medetomidine, diazepam, and ketamine produced increased splenic volumes.[70] Combinations of hydromorphone + diazepam and oxymorphone + diazepam were found to be safe in hypovolemic dogs.[71]

Chlorpromazine + thiopental, chlorpromazine + ketamine + midazolam, and chlorpromazine + propofal were compared in an evaluation of neurological reflexes in puppies taken by caesarian section. The neurological reflexes in the puppies were most depressed with chlorpromazine + ketamine/midazolam, next most depressed with chlorpromazine + thiopental and least depressed with chlorpromazine + propofal. The absolute least amount of neurological depression was seen in puppies taken from dams with epidural anesthesia.[72]

Skarda et al.[73] published a retrospective report on 137 dogs and 13 cats with congenital or acquired cardiac disease that were anesthetized for diagnostic, therapeutic, or surgical interventions. The most commonly used drugs were a combination of midazolam + oxymorphone for premedication, thiopental or etomidate (remifentanil HCl, a μ-opioid agonist with rapid onset and short duration of action) for induction, and isoflurane for maintenance of anesthesia.

Chemical Restraint (Sedation) in Dogs

Any of the drugs and drug combinations used as preanesthetic regimens listed previously can and are used for chemical restraint in dogs. Some of the most often mentioned agents are:

Acepromazine (0.05–0.2 mg/kg), IM
Acepromazine (0.05 mg/kg) + Butorphanol (0.2 mg/kg), IM
Acepromazine (0.05 mg/kg) + Oxymorphone (0.2 mg/kg), IM
Innovar vet (mixture of Fentanyl + Droperidol) (0.05–0.2 mL/kg), IM
Medetomidine (20 μg/kg), IM
Medetomidine (20 μg/kg) + Butorphanol (0.2 mg/kg), IM
Medetomidine (20 μg/kg) + Hydromorphone (0.1 mg/kg), IM

Medetomidine + hydromorphone and medetomidine + butorphanol provided a longer duration of sedation and better quality of analgesia than medetomidine alone.[74] The combination of acepromazine with butorphanol resulted in a lower incidence of temporary excitement and less panting in dogs after injection compared with the acepromazine oxymorphone combination. There were no significant differences in the degree of sedation, response to noise or manipulation, vocalization, or defecation between the two.[75] When three different sedation protocols were compared for their ability to restrain dogs well enough to make a correct diagnosis of hip dysplasia, it was found that medetomidine and butorphanol were significantly better for this purpose than acepromazine.[76] The combination of medetomidine + butorphanol increased total GFR in healthy dogs but the effect was blocked by the concomitant administration of atropine.[77]

Fentanyl + droperidol (the mixture marketed as Innovar-vet) (0.05 and 0.1 mL/kg), IM were compared with two different doses of medetomidine (0.75 and 1.0 mg/kg). Excellent chemical restraint was achieved with all four regimens. The medetomidine-treated dogs had lower respiratory rates, longer durations of the analgesic effects, but an increased incidence of bradycardia, vomiting, and twitching. Medetomidine-treated dogs shivered less and were less responsive to noisy stimuli than the Innovar-treatment groups. There was also an increased incidence of second-degree heart block in the low dose medetomidine group.[78]

The cardiopulmonary effects of medetomidine (20 μg/kg) + midazolam (0.3 mg/kg) were compared with medetomidine alone (80 μg/kg), both administered IM, in another study. Both protocols caused bradycardia and a transient pressor response but the combination of medetomidine + midazolam provided changes that were less intense than those resulting from the medetomidine alone.[79] Acepromazine (0.1 mg/kg), IM did not have any effect on intravenous glucose tolerance testing in dogs.[80]

Pain Recognition in Dogs

The behavior of dogs with other dogs and with humans can be unique to the type of pain the animal is experiencing. The personality of the individual animal and the intensity of the pain also play a role. Postural changes can include a hunched back, guarding or protecting the painful area, assuming a “praying” position, sitting or lying down in abnormal ways, or head hanging. Movement changes can include

stiffness, not bearing weight on an affected limb, limping, restless thrashing, trembling or shaking, less than normal tail wagging or carrying the tail abnormally low, reluctance to move about when awake, and being slow to rise. Vocalization signs of pain can include screaming, whining, crying, barking, howling or growling, or a lack of expected vocalization in an animal that is normally vocal. Other behavior keys can be abnormal agitation, poor or no self-grooming, a decrease or complete lack of appetite, a dull attitude, inappropriate urination or defecation or not moving away from it, licking or biting of the affected area, or behavior out of character such as a normally gentle dog becoming aggressive.

Hudson et al.[81] assessed the repeatability and validity of using a VAS to evaluate pain and lameness in dogs. The results were compared with objective measures of lameness made using a force-plate. A rather sophisticated statistical analysis enabled them to conclude that a number of behavioral observations were highly and rather easily correlated with a presumption of pain and/or lameness validating their VAS.

Treatment of Pain in Dogs

Local Anesthetics

Infusion of local anesthetics, particularly bupivicane, in surgical incision sites, particularly when combined with NSAIDs or narcotics can be particularly effective for pain relief in dogs.

NSAIDs

Carprofen: 1–5 mg/kg, PO, bid
Flunixin meglumine: (1 mg/kg), IV or IM oid, do not treat for more than 5 days
Ketoprofen: (1.0 mg/kg), IM, bid
Other NSAIDs such as aspirin, ibuprofen, and acetaminophen seem to have more limited effects in dogs.

Narcotics

Buprenorphine: (0.01–0.04 mg/kg), SQ every 8–12 h
Butorphanol: (0.2–0.4 mg/kg), SQ, IM, or IV every 2–5 h

Fentanyl patch: (25, 50, 75, or 100 μg/h sizes, depending upon the size of the dog, <10 kg, 11–20 kg, 20–30 kg, >30 kg, respectively)
Meperidine: (2–10 mg/kg), IM or SQ every 2–3 h

Alpha-Agonists

Most are very effective analgesics but the sedative effects are so strong such that they are usually not very useful for this purpose.

Preanesthesia and Anesthesia in Cats

Many of the same agents used for anesthesia in dogs are used in cats. Cats do, however, pose certain handling problems since they tend to react in a negative way to physical restraint. There are, therefore, great advantages to using preanesthetic regimens that can be administered SQ or IM, and obtaining a level of sedation that makes the placement of an intravenous catheter easier. With the IV catheter in place, it is easy to induce anesthesia, intubate the trachea, and maintain anesthesia using an inhalant anesthetic agent.

*Acepromazine (10 μg/kg) + Buprenorphine (10 μg/kg), IM + induction with Etomidate (1–2 mg/kg), IV
Desflurane induction with facemask, endotracheal intubation, and maintenance with Desflurane. Mean alveolar concentrations over 5 h of anesthesia were 10.27% ± 1.06%. Rapid induction and recovery were observed.[82]
Ketamine: (10 mg/kg), IM, used at times but not recommended for surgical anesthesia when given alone.
Medetomidine (0.02 mg/kg), IV + Propofol (8–10 mg/kg), IV + Sevoflurane[83]
*Medetomine (1.5 mg/M^2 body surface area), IM + Propofol (1–2 mg/kg) for induction
*Midazolam (1.0 mg/kg) + Ketamine (10.0 mg/kg), IM for induction
Midazolam (0.3–1.0 mg/kg) + Ketamine (2–3 mg/kg) + Butorphanol (0.4 mg/kg), IV, tracheal intubation and anesthesia with Isoflurane to effect[84, 85]
Midazolam (1.0 mg/kg) + Ketamine (2.0 mg/kg) + Butorphanol (0.4 mg/kg), IV + induction with Propofol (8–10 mg/kg), IV and anesthesia maintained with a continuous rate of infusion (CRI) of Fentanyl (0.02 mg/kg/h) or Fentanyl (0.02 mg/kg/h) + Servoflurane to effect, or CRI of Propofol (12 mg/kg/h). All regimens are used to effect to maintain the desired plane of surgical anesthesia and the gas anesthetic or propofol is adjusted to maintain the predetermined level.[85]

Pentobarbital sodium: (20–30 mg/kg), IV, half the calculated dose rapidly and the remainder given to effect.
Propofol (5.7–12.9 mg/kg), IV + endotracheal intubation and maintenance with desflurane, sevoflurane, isoflurane or halothane[86, 87]
Sevoflurane or Isoflurane induction with facemask followed by endotracheal intubation and maintenance. Sevoflurane provided more rapid induction.[16, 88]
Sevoflurane + N_2O for induction and maintenance, induction and recovery were both smooth and rapid.[89]
Telazol (combination of tiletamine a dissociative anesthetic agent and zolazepam an alpha–agonist) (10 mg/kg), IV + inhalation anesthesia
Xylazine (0.02 mg/kg), IV + Propofol (8–10 mg/kg), IV + Sevoflurane[83]
The three regimens marked with an asterisk (*) were compared for use in cats diagnosed with cardiomyopathy. The combination of acepromazine-buprenorphine was determined to be preferred because heart rate, blood pressure, and respiratory effects were minimal.[90]

Chemical Restraint (Sedation) in Cats

Acepromazine: (0.03–2.2 mg/kg), SQ, IM, or IV[43, 91]
Diazepam: (1.0 mg/kg), IM or IV
Hydromorphone (0.1 mg/kg) + Glycopyrrolate (0.01 mg/kg), SQ, glycopyrrolate is an anticholinergic agent, parasympatholytic.[92]
Hydromorphone: (0.1 mg/kg), SQ[92]
Ketamine: (3.0–30.0 mg/kg), IM[91, 93]
Medetomidine: (20 μg/kg), IM, determined to be safe in cats with left ventricular hypertrophy[94]
Morphine: (0.1 mg/kg), IM[91]
Telazol (combination of tiletamine and zolazepam): (6–20 mg/kg), IM or IP
Telazol (10 mg/kg) + Etomidate (0.3 mg/kg), IM or IP
Thiopental sodium: (10–20 mg/kg), IV[91]
Xylazine: (2.2 mg/kg), IM[91]

Niedfeldt and Robertson[95] report a correlation between postanesthesia hyperthermia and hydromorphone in cats, while acepromazine, acepromazine + buprenorphine, and acepromazine + buprenorphine + ketoprofen did not show these effects. Ketamine has been associated with nonreversible cerebellar damage in Persian-cross cats.[96] The combination of midazolam + oxymorphone for preanesthesia sedation, thiopental or etomidate for induction and isoflurane for anesthesia was found to be the most commonly used regimen for anesthesia in cats with congenital or acquired heart disease.[73] Thiopental sodium, ketamine, acetylpromazine, xylazine, and morphine chemical restraint were evaluated, and all of these agents interfered with glucose tolerance testing in cats.[91]

Pain Recognition in Cats

Cats are, by nature, much more stoic than dogs and other species. A cat experiencing pain is generally quiet. Some individuals may have an apprehensive facial expression, including the appearance of a creased forehead. Pain in the head or ears can cause the animal to tilt the head toward the affected side. Generalized pain in the thorax and/or abdomen can cause the animal to crouch or hunch its back. If the pain is only thoracic, the head, neck, and body can be extended. Cats with abdominal or back pain sometimes stand with the back arched and walk with a stiff or stilted gait. General postural changes can include a hunched back with lowered head, guarding or protecting the painful area, sitting or laying in abnormal positions for that individual. Movement changes can include stiffness, limping, or reluctance to bear weight on a limb including resting with the affected limb raised, restlessness and thrashing, trembling or shaking, reluctance to move when awake, and/or a slowness to rise when stimulated to do so. Vocalization changes include screaming, yowling, hissing, or crying, especially when a painful area is palpated. An individual that is normally vocal, purring, etc. may not vocalize. Behavioral changes include hyperventilation, an agitated state, lack of grooming, loss of appetite and weight loss, dull attitude, excessive sleeping, noticeably less activity, inappropriate urination or defecation and not moving away from soiled areas, excessive licking of an area, hiding and vigorous attempts to escape when handled.

Treatment of Pain in Cats

Local Anesthetics

Same as for other animals, i.e. local infusion at incision sites before closing.

NSAIDs

Carprofen: (4 mg/kg, initial dose followed by 1.4 mg/kg, tid)[97]
Flunixin meglumine: (1 mg/kg), IV or IM oid, do not treat for more than 5 days[43]
Ketoprofen: (1.0 mg/kg), IM, bid[43]

Narcotics

Buprenorphine: (0.004–0.01 mg/kg), SQ every 8–12 h[43]
Butorphanol: (0.1–0.4 mg/kg), SQ, every 6 h[43]
Levomethadone: (0.3 mg/kg), SQ every 8 h[97]
Morphine: (0.1 mg/kg), SQ every 4–6 h[43]

Alpha-Agonists

Same as for dogs, good analgesia but too much sedation for most applications. Midazolam (0.652 mg/kg) prevented conscious perception of a stimulus to the ulnar nerve in 95% of cats tested. Nine of 12 cats exhibited an abnormal arousal state with four being restless and five being sedated. Seven of the 12 cats exhibited abnormal behaviors when approached and 8 of the 12 abnormal behaviors when restrained. Five of the 12 cats vocalized more during recovery.[93]

Preanesthesia and Anesthesia in Guinea Pigs

Anesthetizing guinea pigs is reported to be difficult and induction times, depth of anesthesia, and recovery times can vary.

Ketamine (35 mg/kg), IP + Xylazine (5 mg/kg), IP[43]
Pentobarbital sodium (35–45 mg/kg), IP[43]
Telazol (10 mg/kg) + Medetomidine (20 μg/kg), IM[98, 99]
Telazol (10 mg/kg) + Xylazine (5 mg/kg), IM[98]
Telazol (100 mg/kg) + Xylazine (10 mg/kg), IP[100]
Telazol (60 mg/kg), IP + Xylazine (5 mg/kg), IP + Butorphanol (0.1 mg/kg), IM, provided smooth induction and recovery with deep surgical anesthesia of long duration[101]

Radde et al.[102] compared telazol at two different dosages, pentobarbital, methoxyflurane, and three different doses of ketamine/xylazine and ketamine/xylazine + methoxyflurane. They found that telazol induced a short period of chemical restraint but lacked analgesic effects at the doses used. Pentobarbital induced prolonged chemical restraint but the analgesic effects were brief. Methoxyflurane induced transient anesthesia and analgesia but is no longer on the market. The ketamine/xylazine combinations all produced good analgesia and chemical restraint but at low doses were suitable only for mildly painful procedures.

Chemical Restraint (Sedation) in Guinea Pigs

The same agents used for anesthesia are used for chemical restraint in this species.

Pain Recognition in Guinea Pigs

Normal guinea pigs will stampede and squeal when frightened or when attempts are made by strangers to handle them. Some animals may run to hide, squealing when strangers enter the room. Sick guinea pigs or guinea pigs in pain will usually

hide and be quiet. Other signs of pain in guinea pigs are similar to those observed in rats and mice.

Treatment of Pain in Guinea Pigs

Local Anesthetic Agents

The same as for other species, infusion of incision sites before closure.

NSAIDs

Flunixin: (2.5–5.0 mg/kg), SQ, every 12–24 h, maximum of 5 days of treatment.
Other NSAIDs can be used at the same dosages cited for rats and mice.

Narcotics

Buprenorphine: (0.1–0.5 mg/kg), SQ every 8–12 h
Meperidine: (10–20 mg/kg), SQ or IM, every 2–3 h
Morphine: (2–5 mg/kg), SQ or IM, every 4 h

Alpha-Agonists

Products and doses the same as for rats and mice.

Preanesthesia and Anesthesia in Pigs

Malignant hyperthermia is a genetic disorder of skeletal muscle and is seen in susceptible pigs exposed to inhalation anesthetics, particularly halothane, and some depolarizing muscle relaxants.[103] Malignant hyperthermia susceptible and malignant hyperthermia nonsensitive pigs are being bred and used for a variety of studies aimed at understanding and diagnosing this condition.[103–105]

Our experience is that positive end-expiratory pressure (PEEP) needs to be employed (3–7 cm H_2O) to maintain adequate pulmonary function and normal acid-base balance during general anesthesia, particularly when associated with open thorax

procedures in pigs, sheeps, and goats.[106-108] The following anesthetic regimens are used in swine:

Acepromazine (2 mg/kg) + Ketamine (10 mg/kg) + atropine (0.05 mg/kg), IM + isoflurane by mask, tracheal intubation and maintenance with Isoflurane to effect[109]

Acepromazine (4 mg/kg), IM + Metomidate (10 mg/kg), IP + Etomidate (0.3 mg/kg), IV + Fentanyl (10 μg/kg), IV + continuous infusion of Etomidate (2.5 mg/kg/h) and Fentanyl (50 μg/kg/h) + N_2O (66%) in oxygen[104]

Diazepam (0.25 mg/kg) + atropine (0.005 mg/kg), IM + sodium Thiopental (30 mg/kg), IV + additional doses of thiopental as needed[110]

Isoflurane (2 vol%) by face mask for induction) + tracheal intubation and Isoflurane (0.5 vol%) for maintenance[111]

Ketamine (22 mg/kg) + Acepromazine (1.1 mg/kg), IM + Pentobarbital sodium (20 mg/kg), IV the latter given to effect

Ketamine (10 mg/kg) + Diazepam (0.5 mg/kg), IM + Thiopental (5 mg/kg), IV to effect + tracheal intubation and Isoflurane (0.8–1.5 vol%) + Fentanyl (5 μg/kg/h)[112]

Ketamine (15 mg/kg) + halothane (1.0 vol%), oxygen (59 vol%) and N_2O (40 vol%)[113]

Ketamine (20 mg/kg) + Midazolam (0.1 mg/kg), Atropine (0.25 mg/kg), IM + induction with Midazolam (0.1 mg/kg) + Sufentanil (0.5 mg/kg), IV + maintenance with continuous infusion of Midazolam (0.15 mg/kg/h) + Sufentanil (0.5 μg/kg/h), IV[114]

Ketamine (8–10 mg/kg), IM + Propofol (0.2–0.4 mg/kg/min), IV[103]

Ketamine (10 mg/kg) + Xylazine (4 mg/kg), IM + alpha-chloralose (50 mg/kg), rapid IV infusion + alpha-chloralose (40 mg/kg/h) continuous IV infusion[115]

Ketamine (20 mg/kg) + Xylazine (0.05 mg/kg), IM + induction with Isoflurane (5 vol%) by face mask and maintenance with isoflurane (1.5–2.5 vol%) to effect[116]

Medetomidine (80 μg/kg) + Ketamine (10 mg/kg) + Butorhanol (200 μg/kg), IM + tracheal intubation and isoflurane to effect[117]

Midazolam (1.5 mg/kg) + Ketamine (20 mg/kg), IM + Atropine (0.05 mg/kg), IV + tracheal intubation and ventilation with oxygen (30 vol%), N_2O (67 vol%), and Isoflurane (3 vol%)[118]

Propofol (2.5–15 mg/kg), IV[119]

Telazol (4.4 mg/kg) + Ketamine (2.2 mg/kg) + Xylazine (2.2 mg/kg), IM + tracheal intubation and inhalation anesthetic[120, 121]

Telazol (4.4 mg/kg) + Xylazine (2.2 mg/kg), IM + tracheal intubation and inhalation anesthetic[120, 121]

Telazol (4.4 mg/kg) + Xylazine (2.2 mg/kg) + atropine (0.04 mg/kg), IV + tracheal intubation and Isoflurane (1–3 vol%) to effect[122]

Thiamyl sodium (30 mg/kg), IV + tracheal intubation and halothane anesthesia (0.5–1.5 vol%, to effect)[123]

A novel new inhaler system used to administer isoflurane to piglets for minor surgical procedures such as castration was recently described. The system consists of a mask, a center body with a valve that can be opened or closed, a vaporization

chamber with a wick system and an injection port, and a rebreathing bag. Isoflurane is delivered via the injection port and the rebreathing bag is filled with oxygen. The mask is fitted over the piglet's nose, the valve is opened and the respiration of the pig moves gases in and out of the inhaler and rebreathing bag. The system provides economical, safe and rapid induction and a safe, smooth recovery in piglets.[124]

Chemical Restraint (Sedation) in Pigs

Many of the same protocols described previously for preanesthesia in pigs can and are used for sedation. Other agents for sedation in pigs have also been approved by animal care and use committees and published. These include:

Acepromazine: (0.04–0.06 mg/kg), SQ, IM or IV, bid
Diazepam: (0.5–8.5 mg/kg), IV, bid[43, 123]
Medetomidine (80 μg/kg) + Ketamine (10 mg/kg), IM[125]
Medetomidine (80 μg/kg) + Midazolam (0.1 mg/kg), IM[126]
Telazol: (4.0–5.0 mg/kg), IM[120, 121, 127]
Telazol (4.4 mg/kg) + Ketamine (2.2 mg/kg), IM[120, 121]
Telazol (3.3 mg/kg) + Xylazine (1.3 mg/kg), IM using blow darts on wild pigs. It was found that some of the wild pigs were only partially immobilized at this dose so the authors recommended 4.0 mg/kg Telazol + 2.0 mg/kg Xylazine[128]
Xylazine (5 mg/kg) + Ketamine (10 mg/kg), IM[125]

Pain Recognition in Pigs

Pigs in pain usually demonstrate changes in their social behavior, (i.e., interactions with other pigs), gait, and posture. They will frequently not indulge in bed making behavior. They normally squeal and attempt to escape when handled and pain will usually accentuate those behaviors. They will usually squeal or grunt loudly when a painful area is palpated and may exhibit loud and persistent vocalization. Adult animals may become aggressive, hide, or be reluctant to move about. They will act dull and depressed with the head held low. They may exhibit rapid shallow respirations, excessive grunting, and/or grinding of the teeth.[5]

Treatment of Pain in Pigs

Local Anesthetic Agents

The same as for other species, the use of local anesthetics by infusion along incision sites before surgical closure has proven to be very effective.

NSAIDs

Flunixin-meglumine: (0.5-1.5 mg/kg), SQ or IV, every 12-24 h, five day maximum
Flunixin-meglumine (1.1 mg/kg) + Ceftiofur (Naxcel) (2.2 mg/kg), IV[117]
Ketoprofen: (1.0 mg/kg), IM, bid
Phenylbutazone: (1.0-4.0 mg/kg), IV or PO, every 12 h

Narcotics

Buprenorphine: (0.005–0.01 mg/kg), SQ or IM every 6–12 h
Butorphanol (0.1–0.3 mg/kg), IM or IV every 8–12 h
Fentanyl patch (25, 50, 75, or 100 μg/h patches) depending upon the size of the animal
Meperidine (2.0–10.0 mg/kg), IM or SQ, every 2–4 h

Alpha-Agonists

Acepromazine: (0.1–1.1 mg/kg), IM
Midazolam: (0.1–0.5 mg/kg), IM or IV
Xylazine: (0.2–2.0 mg/kg), IM

Preanesthesia and Anesthesia in Calves, Sheep, and Goats

Small ruminants are usually docile enough to make induction of anesthesia with Isoflurane or Desflurane very easy using a facemask (3–5 vol%) followed by tracheal intubation and maintenance with low levels (0.5–2.0 vol%) of the same agent. The advantage of the technique is smooth induction and very fast recovery from anesthesia. Many animal care and use committees consider these to be the agents of choice for general anesthesia in calves, sheep, and goats.[43, 129, 130] Other anesthetic regimens include the prior use of sedatives as preanesthetic agents and combinations of agents for either preanesthesia, including enough sedation to make tracheal intubation possible, or anesthesia with additional doses of one or more agents. These protocols include:

Diazepam (0.25 mg/kg) + Ketamine (4 mg/kg), IV, tracheal intubation + Halothane (2 vol%) for maintenance[131]

Halothane (4 vol%) + N_2O (50 vol%) for induction + maintenance with Halothane (1.0–2.0 vol%) to effect[132]
Ketamine (15 mg/kg) + Acepromazine (0.5 mg/kg) + atropine (2 mg/kg), tracheal intubation + maintenance of anesthesia in a surgical plane with Halothane to effect[133]
Ketamine (5–15 mg/kg) + Xylazine (0.1–0.2 mg/kg), IM[134]
Ketamine (20 mg/kg) + Xylazine (0.5 mg/kg), IM + Isoflurane to effect[106]
Propofol (2.5–15 mg/kg), IV induction and continuous infusion[119]
Telazol (13.2 mg/kg) + Xylazine (0.11 mg/kg), IV produced good muscle relaxation and a usefully long duration of anesthesia but a high incidence of apnea lasting as long as 2 min in sheep[135]
Thiopental: (25 mg/kg), IV, half dose rapidly and then to effect, for induction of anesthesia, since intravenous injections are done very easily in small ruminants this technique can be very useful
Xylazine (0.2 mg/kg), IM + a mixture of Xylazine (0.1 mg/mL) + Guaiphenesin (50 mg/mL) + Ketamine (1 mg/mL) was continuously infused at 1.1 mL/kg/h[136]
Xylazine (0.1 mg/kg), IM + Ketamine (5–20 mg/kg), IV until a surgical plane of anesthesia is achieved[137]

Chemical Restraint (Sedation) in Small Ruminants

Acepromazine: (0.05–0.2 mg/kg), IM or SQ
Diazepam: (0.5–1.5 mg/kg), IM or IV
Midazolam: (0.4–1.3 mg/kg), IV
Telazol: (5–13.2 mg/kg), high doses frequently result in apnea[135]
Xylazine: (0.05–0.3 mg/kg), IM or SQ

Recognition of Pain in Small Ruminants

When experiencing pain, small ruminants will often appear dull and depressed with changes in posture and movement. Knowledgeable caretakers often report changes in facial expression by these species when in pain. Heads may be held low and the animals may demonstrate a lack of interest shown in their surroundings or when approached. There is almost always a loss of appetite and weight loss. Severe pain may be manifest in rapid, shallow breathing. When handled calves, sheep, and goats might react violently or adopt a very rigid posture designed to immobilize the region of pain. Grunting and teeth grinding may accompany pain. These species will demonstrate restlessness by repeatedly lying down then getting up indicating an inability to become comfortable. Localized pain can be associated with persistent

licking, nuzzling, or kicking at the injured area. This is especially common with joint pain in goats. If pain is severe it can be expressed by excessive vocalization, bellowing in calves, bleating in sheep and goats.

A study by Kock et al.[138] compared physiological parameters including; pulse rates, rectal temperatures and respiratory rates and selected biochemical measurements including; cortisol, CPK, AP, BUN and others, in free-ranging bighorn sheep captured with drop-nets, drive-nets, net-guns, and chemical immobilization with Telazol. They determined that chemical immobilization resulted in the largest changes in the various parameters measure.

Treatment of Pain in Small Ruminants

Local Anesthetic Agents

Local infiltration of surgical incisions with long acting local anesthetic agents has been repeatedly shown to result in significant pain reduction.

NSAIDs

Flunixin-meglumine: (1.0–2.0 mg/kg), IV, tid
Phenylbutazone: (1.0–4.0 mg/kg), IV, tid

Narcotics

Buprenorphine: (0.005–0.015 mg/kg), SQ or IM every 4–12 h
Butorphanol: (0.2–0.5 mg/kg), SQ or IM every 4 h
Fentanyl patch: (25, 50, 75, or 100 μg/h patches depending upon body weight). Do not forget to shave the area before applying the patch.
Meperidine: (2–10 mg/kg), SQ or IM every 4 h, do not exceed 200 mg total dose

Alpha-Agonists

Acepromazine: (0.04–0.06 mg/kg), SQ, IM or IV, bid
Diazepam: (0.5–1.5 mg/kg), IV, bid

Preanesthesia and Anesthesia in Rhesus Monkeys

Although nonhuman primates of other species are used for cardiovascular studies, their use is becoming more difficult and less common. Significant numbers of Rhesus monkeys are still being used and for this reason, and because more data are available for this species, only Rhesus will be discussed in this text. However, many of the agents described in this section can be and are used in other species of nonhuman primates and at similar doses.

Glycopyrrolate (0.01 mg/kg) + Ketamine (15 mg/kg), IM + Fentanyl (3 μg/kg) + Thiopental (5 mg/kg), IV + Isoflurane + Fentanyl (3 μg/kg/h)[139]

Ketamine (15 mg/kg), IM[140]

Ketamine (15 mg/kg), IM + Glycopyrrolate (12.5 μg/kg), IV + Halothane (1–2 vol%) to effect[141]

Ketamine (15 mg/kg), IM + Halothane (1.5–2.5 vol%) to effect[142]

Ketamine (10 mg/kg) + Xylazine (0.25–2.0 mg/kg), IM

Isoflurane, Desflurane, Halothane, or Sevoflurane delivered by face mask for induction (4–5 vol%) and then maintained with lower concentrations (1.5–2.5 vol%) to effect[140, 143–145]

Pentobarbital sodium (25 mg/kg), IV, half of dose delivered rapidly the remainder slowly to effect, additional doses as required to maintain the desired plane of anesthesia[143, 146, 147]

Chemical Restraint (Sedation) in Rhesus Monkeys

Acepromazine: (0.2 mg/kg), SQ, IM, or IV
Diazepam: (1.0 mg/kg), IM or IV
Ketamine: (5–10 mg/kg), IM

Pain Recognition in Rhesus Monkeys

This species can demonstrate very little reaction to surgical procedures or injury, especially when they are aware of human observation. Experienced investigators feel that viewing animals from a distance or with video makes it more likely to make the necessary observations to diagnose pain. Loud and persistent vocalization is more likely to signify alarm or anger than pain in this species. In general, these animals will have a general appearance of misery and dejection when in pain. They might huddle in a crouched posture and hold their arms across their chest with the head bent forward. Some observers report a “sad” facial expression or grimacing and/or a glassy eyed appearance. The animal might moan or scream, particularly

with acute severe pain. There is a tendency to avoid companions in the cage and to stop grooming activities. When in pain they may also attract altered attention from cage mates varying from lack of normal social grooming to attacks. Acute abdominal pain can be demonstrated by facial contortions, clenching or grinding of teeth, general restlessness, and shaking, accompanied by grunts and moans. When in pain these animals will generally refuse food and water.[5]

There have been some interesting studies conducted regarding stress and distress in Rhesus monkeys. When Ketamine was used to restrain animals not preconditioned to handling, definitive baseline plasma glucose tolerance curves could not be established. When the same animals were conditioned and trained in restraint chairs, clear baseline control data were obtained.[148] Similar results were obtained for hematological, biochemical, and ECG data but a minimum of 3 months of training (conditioning) was required.[149] A large number of adult male Rhesus monkeys were studied for behavioral and hypothalamic-pituitary-adrenal activity as a result of seven consecutive days of physical restraint. These data showed that behavior was not necessarily an indicator of underlying physiological processes and the observed reduction in hypothalamic-pituitary-adrenal activity that was observed with repeated restraint was due to a physiological adaptation to the high cortisol concentrations and not to psychological habituation to the restraint procedures.[150]

Treatment of Pain in Rhesus Monkeys

Local Anesthetics

As in all other species where it has been evaluated infusion of surgical incisions during closure is quite effective.

NSAIDs

Flunixin meglumine: (1.1 mg/kg), IV or IM every 24 h or (0.3–1.0 mg/kg) SQ or IV every 12–24 h, five days maximum of treatment
Tylenol Pediatric Suspension (Acetaminophen): (5–10 mg/kg), PO every 6–12 h

Narcotics

Buprenorphine: (0.01–0.04 mg/kg), SQ, every 6–12 h
Butorphanol: (0.1–0.2 mg/kg), IM, every 12–48 h
Meperidine: (2.0–4.0 mg/kg), IM, every 8–12 h

Conclusions

It is clear from the studies reported in this chapter that many different drugs, drug combinations, and drug dosages are being used for anesthesia, chemical restraint, and analgesia in animals for a wide variety of experimental procedures. The treatment of pain in animals is becoming a subspecialty within veterinary anesthesiology. We can expect considerable new understanding and the development of new and more effective protocols as the science matures. Many analgesics are now available that have not yet been fully tested in all animal species. Investigators must and should consult with knowledgeable sources when making a choice about anesthesia, chemical restraint, or analgesia.

References

1. Adams HR. *Veterinary Pharmacology and Therapeutics, 8th Edition*. Ames, Iowa: Blackwell Publishing; 2001.
2. Thurmon JC, Tranquilli WJ, Benson GJ. *Essentials of Small Animal Anesthesia and Analgesia*. Ames, Iowa: Blackwell Publishing; 1999.
3. Gross DR, Tranquilli WJ, Greene SA, Grimm KA. Critical anthropomorphic evaluation and treatment of postoperative pain in rats and mice. *J Am Vet Med Assoc*. 2003;222:1505–1510.
4. Molony V, Kent JE. Assessment of acute pain in farm animals using behavioral and physiological measurements. *J Anim Sci*. 1997;75:266–272.
5. National Research Council. *Recognition and Assessment of Pain and Distress in Laboratory Animals, Recognition and Alleviation of Pain and Distress in Laboratory Animals.* Washington, DC: National Academy Press; 1992.
6. Beynen AC, Baumans V, Bertens AP, Havenaar R, Hesp AP, Van Zutphen LF. Assessment of discomfort in gallstone-bearing mice: A practical example of the problems encountered in an attempt to recognize discomfort in laboratory animals. *Lab Anim*. 1987;21:35–42.
7. Lariviere WR, Wilson SG, Laughlin TM, et al. Heritability of nociception. III. Genetic relationships among commonly used assays of nociception and hypersensitivity. *Pain*. 2002;97:75–86.
8. Anil SS, Anil L, Deen J. Challenges of pain assessment in domestic animals. *J Am Vet Med Assoc*. 2002;220:313–319.
9. Flecknell PA. Refinement of animal use--Assessment and alleviation of pain and distress. *Lab Anim*. 1994;28:222–231.
10. Flecknell P, Waterman-Pearson A. *Pain Management in Animals*. London: W.B. Saunders Co.; 2000.
11. Parker JL, Adams HR. The influence of chemical restraining agents on cardiovascular function: A review. *Lab Anim Sci*. 1978;28:575–583.
12. Beyer JE, McGrath PJ, Berde CB. Discordance between self-report and behavioral pain measures in children aged 3-7 years after surgery. *J Pain Symptom Manage*. 1990;5:350–356.
13. Demyttenaere S, Finley GA, Johnston CC, McGrath PJ. Pain treatment thresholds in children after major surgery. *Clin J Pain*. 2001;17:173–177.
14. Breau LM, Camfield C, McGrath PJ, Rosmus C, Finley GA. Measuring pain accurately in children with cognitive impairments: Refinement of a caregiver scale. *J Pediatr*. 2001;138:721–727.
15. Sweet SD, McGrath PJ, Symons D. The roles of child reactivity and parenting context in infant pain response. *Pain*. 1999;80:655–661.

16. Lamont LA, Greene SA, Grimm KA, Tranquilli WJ. Relationship of feline bispectral index to multiples of isoflurane minimum alveolar concentration. *Comp Med*. 2005;55:269–274.
17. Gear RW, Miaskowski C, Gordon NC, Paul SM, Heller PH, Levine JD. Kappa-opioids produce significantly greater analgesia in women than in men. *Nat Med*. 1996;2:1248–1250.
18. Levine JD, Gordon NC. Synergism between the analgesic actions of morphine and pentazocine. *Pain*. 1988;33:369–372.
19. Ceccarelli I, Scaramuzzino A, Aloisi AM. Effects of gonadal hormones and persistent pain on non-spatial working memory in male and female rats. *Behav Brain Res*. 2001;123:65–76.
20. Gross DR. *Animal Models in Cardiovascular Research, 2nd Revised Edition*. Boston: Kluwer Academic Publishers; 1994.
21. Hedenqvist P, Roughan JV, Flecknell PA. Effects of repeated anaesthesia with ketamine/medetomidine and of pre-anaesthetic administration of buprenorphine in rats. *Lab Anim*. 2000;34:207–211.
22. Van Herck H, Baumans V, Brandt CJ, et al. Blood sampling from the retro-orbital plexus, the saphenous vein and the tail vein in rats: Comparative effects on selected behavioural and blood variables. *Lab Anim*. 2001;35:131–139.
23. Welberg LA, Kinkead B, Thrivikraman K, Huerkamp MJ, Nemeroff CB, Plotsky PM. Ketamine-xylazine-acepromazine anesthesia and postoperative recovery in rats. *J Am Assoc Lab Anim Sci*. 2006;45:13–20.
24. Cruz JI, Loste JM, Burzaco OH. Observations on the use of medetomidine/ketamine and its reversal with atipamezole for chemical restraint in the mouse. *Lab Anim*. 1998;32:18–22.
25. Hedenqvist P, Roughan JV, Flecknell PA. Sufentanil and medetomidine anaesthesia in the rat and its reversal with atipamezole and butorphanol. *Lab Anim*. 2000;34:244–251.
26. Quinn RH, Danneman PJ, Dysko RC. Sedative efficacy of droperidol and diazepam in the rat. *Lab Anim Sci*. 1994;44:166–171.
27. Dorr W, Weber-Frisch M. Short-term immobilization of mice by methohexitone. *Lab Anim*. 1999;33:35–40.
28. Martini L, Lorenzini RN, Cinotti S, Fini M, Giavaresi G, Giardino R. Evaluation of pain and stress levels of animals used in experimental research. *J Surg Res*. 2000;88:114–119.
29. Schwab CL, Fan R, Zheng Q, Myers LP, Hebert P, Pruett SB. Modeling and predicting stress-induced immunosuppression in mice using blood parameters. *Toxicol Sci*. 2005;83:101–113.
30. Avgustinovich DF, Kovalenko IL. Formation of behavioral pathology in female C57BL/6J mice exposed to prolonged negative psycho emotional conditions. *Neurosci Behav Physiol*. 2005;35:959–967.
31. Kudryavtseva NN, Bondar NP, Avgustinovich DF. Effects of repeated experience of aggression on the aggressive motivation and development of anxiety in male mice. *Neurosci Behav Physiol*. 2004;34:721–730.
32. Kudryavtseva NN, Bondar NP, Avgustinovich DF. Association between experience of aggression and anxiety in male mice. *Behav Brain Res*. 2002;133:83–93.
33. Voikar V, Polus A, Vasar E, Rauvala H. Long-term individual housing in C57BL/6J and DBA/2 mice: Assessment of behavioral consequences. *Genes Brain Behav*. 2005;4:240–252.
34. Hayes KE, Raucci JA, Jr, Gades NM, Toth LA. An evaluation of analgesic regimens for abdominal surgery in mice. *Contemp Top Lab Anim Sci*. 2000;39:18–23.
35. Maves TJ, Pechman PS, Meller ST, Gebhart GF. Ketorolac potentiates morphine antinociception during visceral nociception in the rat. *Anesthesiology*. 1994;80:1094–1101.
36. de la Lastra CA, Nieto A, Motilva V, et al. Intestinal toxicity of ketoprofen-trometamol vs its enantiomers in rat. role of oxidative stress. *Inflamm Res.* 2000;49:627–632.
37. Holzer P, Jocic M, Cabre F, Mauleon D. Estimation of acute flurbiprofen and ketoprofen toxicity in rat gastric mucosa at therapy-relevant doses. *Inflamm Res*. 2001;50:602–608.
38. Roughan JV, Flecknell PA. Behavioural effects of laporotomy and analgesic effects of ketoprofen and carprofen in rats. *Pain*. 2001;90:65–74.
39. Shah A, Jung D. Dose-dependent pharmacokinetics of ibuprofen in the rat. *Drug Metab Dispos*. 1987;15:151–154.

40. Morgan D, Cook CD, Picker MJ. Sensitivity to the discriminative stimulus and antinociceptive effects of mu opioids: Role of strain of rat, stimulus intensity, and intrinsic efficacy at the mu opioid receptor. *J Pharmacol Exp Ther*. 1999;289:965–975.
41. Morgan D, Cook CD, Smith MA, Picker MJ. An examination of the interactions between the antinociceptive effects of morphine and various mu-opioids: The role of intrinsic efficacy and stimulus intensity. *Anesth Analg*. 1999;88:407–413.
42. Gillingham MB, Clark MD, Dahly EM, Krugner-Higby LA, Ney DM. A comparison of two opioid analgesics for relief of visceral pain induced by intestinal resection in rats. *Contemp Top Lab Anim Sci*. 2001;40:21–26.
43. Gross DR. Unpublished data.
44. Roughan JV, Ojeda OB, Flecknell PA. The influence of pre-anaesthetic administration of buprenorphine on the anaesthetic effects of ketamine/medetomidine and pentobarbitone in rats and the consequences of repeated anaesthesia. *Lab Anim*. 1999;33:234–242.
45. Yeung CK, McCurrie JR, Wood D. A simple method to investigate the inhibitory effects of drugs on gastric emptying in the mouse in vivo. *J Pharmacol Toxicol Methods*. 2001;45:235–240.
46. Liles JH, Flecknell PA. The effects of buprenorphine, nalbuphine and butorphanol alone or following halothane anaesthesia on food and water consumption and locomotor movement in rats. *Lab Anim*. 1992;26:180–189.
47. Flecknell PA, Roughan JV, Stewart R. Use of oral buprenorphine ('buprenorphine jello') for postoperative analgesia in rats--A clinical trial. *Lab Anim*. 1999;33:169–174.
48. Gades NM, Danneman PJ, Wixson SK, Tolley EA. The magnitude and duration of the analgesic effect of morphine, butorphanol, and buprenorphine in rats and mice. *Contemp Top Lab Anim Sci*. 2000;39:8–13.
49. Sisenwine SF, Tio CO. The metabolic disposition of dezocine in rhesus monkeys and female rats given 14C-dezocine intragastrically. *Drug Metab Dispos*. 1981;9:37–42.
50. Mucha RF, Kalant H. Log dose/response curve flattening in rats after daily injection of opiates. *Psychopharmacology (Berl)*. 1980;71:51–61.
51. Tong C, Conklin D, Eisenach JC. A pain model after gynecologic surgery: The effect of intrathecal and systemic morphine. *Anesth Analg*. 2006;103:1288–1293.
52. Olson GA, Delatte SW, Kastin AJ, McLean JH, Phillpott DF, Olson RD. Naloxone and fluid consumption in rats: Dose-response relationships for 15 days. *Pharmacol Biochem Behav*. 1985;23:1065–1068.
53. Buttar HS, Moffatt JH. Pre- and postnatal development of rats following concomitant intrauterine exposure to propoxyphene and chlordiazepoxide. *Neurobehav Toxicol Teratol*. 1983;5:549–556.
54. Maves TJ, Gebhart GF. Antinociceptive synergy between intrathecal morphine and lidocaine during visceral and somatic nociception in the rat. *Anesthesiology*. 1992;76:91–99.
55. Pappas TN, Mangel AW, Lawson C. Review article: Evaluation of drugs in experimental gut distension models. *Aliment Pharmacol Ther.* 1999;13 Suppl 2:54–56.
56. Muir WW, III, Woolf CJ. Mechanisms of pain and their therapeutic implications. *J Am Vet Med Assoc*. 2001;219:1346–1356.
57. Flecknell PA, Roughan JV, Hedenqvist P. Induction of anaesthesia with sevoflurane and isoflurane in the rabbit. *Lab Anim*. 1999;33:41–46.
58. Brammer DW, Doerning BJ, Chrisp CE, Rush HG. Anesthetic and nephrotoxic effects of telazol in new Zealand white rabbits. *Lab Anim Sci*. 1991;41:432–435.
59. Doerning BJ, Brammer DW, Chrisp CE, Rush HG. Nephrotoxicity of tiletamine in New Zealand white rabbits. *Lab Anim Sci*. 1992;42:267–269.
60. Dugdale AH, Pinchbeck GL, Jones RS, Adams WA. Comparison of two thiopental infusion rates for the induction of anaesthesia in dogs. *Vet Anaesth Analg*. 2005;32:360–366.
61. Ferre PJ, Pasloske K, Whittem T, Ranasinghe MG, Li Q, Lefebvre HP. Plasma pharmacokinetics of alfaxalone in dogs after an intravenous bolus of alfaxan-CD RTU. *Vet Anaesth Analg*. 2006;33:229–236.
62. Gomez-Villamandos RJ, Palacios C, Benitez A, et al. Dexmedetomidine or medetomidine premedication before propofol-desflurane anaesthesia in dogs. *J Vet Pharmacol Ther*. 2006;29:157–163.

63. Sano T, Nishimura R, Kanazawa H, et al. Pharmacokinetics of fentanyl after single intravenous injection and constant rate infusion in dogs. *Vet Anaesth Analg*. 2006;33:266–273.
64. Gomez-Villamandos RJ, Dominguez JM, Redondo JI, et al. Comparison of romifidine and medetomidine pre-medication in propofol-isoflurane anaesthetised dogs. *J Vet Med A Physiol Pathol Clin Med*. 2006;53:471–475.
65. Jang HS, Kwon YS, Lee MG, Jang KH. The effect of tiletamine/zolazepam (Zoletile) combination with xylazine or medetomidine on electroencephalograms in dogs. *J Vet Med Sci*. 2004;66:501–507.
66. Hellyer P, Muir WW, III, Hubbell JA, Sally J. Cardiorespiratory effects of the intravenous administration of tiletamine-zolazepam to dogs. *Vet Surg*. 1989;18:160–165.
67. Pablo LS, Bailey JE. Etomidate and telazol. *Vet Clin North Am Small Anim Pract*. 1999;29:779–792.
68. Jackson AM, Tobias K, Long C, Bartges J, Harvey R. Effects of various anesthetic agents on laryngeal motion during laryngoscopy in normal dogs. *Vet Surg*. 2004;33:102–106.
69. Duke T, Caulkett N, Tataryn J. The effect of nitrous oxide on halothane, isoflurane and sevoflurane requirements in ventilated dogs undergoing ovariohysterectomy. *Vet Anaesth Analg*. 2006;33:343–350.
70. Wilson DV, Evans ATER, Mullineaux DR. The effect of four anesthetic protocols on splenic size in dogs. *Vet Anaesth Analg.* 2004;31:102–108.
71. Machado CG, Dyson DH, Mathews KA. Evaluation of induction by use of a combination of oxymorphone and diazepam or hydromorphone and diazepam and maintenance of anesthesia by use of isoflurane in dogs with experimentally induced hypovolemia. *Am J Vet Res*. 2005;66:1227–1237.
72. Luna SP, Cassu RN, Castro GB, Teixeira Neto FJ, Silva Junior JR, Lopes MD. Effects of four anaesthetic protocols on the neurological and cardiorespiratory variables of puppies born by caesarean section. *Vet Rec*. 2004;154:387–389.
73. Skarda RT, Bednarski RM, Muir WW, Hubbell JA, Mason DE. Sedation and anesthesia in dogs and cats with cardiovascular diseases. I. Anesthesia plan considering risk assessment, hemodynamic effects of drugs and monitoring. *Schweiz Arch Tierheilkd.* 1995;137:312–321.
74. Kuo WC, Keegan RD. Comparative cardiovascular, analgesic, and sedative effects of medetomidine, medetomidine-hydromorphone, and medetomidine-butorphanol in dogs. *Am J Vet Res*. 2004;65:931–937.
75. Dyson DH, Atilola M. A clinical comparison of oxymorphone-acepromazine and butorphanol-acepromazine sedation in dogs. *Vet Surg*. 1992;21:418–421.
76. Malm S, Strandberg E, Danell B, Audell L, Swenson L, Hedhammar A. Impact of sedation method on the diagnosis of hip and elbow dysplasia in Swedish dogs. *Prev Vet Med*. 2007;78:196–209.
77. Grimm JB, Grimm KA, Kneller SK, et al. The effect of a combination of medetomidine-butorphanol and medetomidine, butorphanol, atropine on glomerular filtration rate in dogs. *Vet Radiol Ultrasound*. 2001;42:458–462.
78. Pettifer GR, Dyson DH. Comparison of medetomidine and fentanyl-droperidol in dogs: Sedation, analgesia, arterial blood gases and lactate levels. *Can J Vet Res*. 1993;57:99–105.
79. Hayashi K, Nishimura R, Yamaki A, et al. Cardiopulmonary effects of medetomidine, medetomidine-midazolam and medetomidine-midazolam-atipamezole in dogs. *J Vet Med Sci*. 1995;57:99–104.
80. Ionut V, Kirkman EL, Bergman RN. Investigation of the effect of acepromazine on intravenous glucose tolerance tests in dogs. *Am J Vet Res*. 2004;65:1124–1127.
81. Hudson JT, Slater MR, Taylor L, Scott HM, Kerwin SC. Assessing repeatability and validity of a visual analogue scale questionnaire for use in assessing pain and lameness in dogs. *Am J Vet Res*. 2004;65:1634–1643.
82. Barter LS, Ilkiw JE, Pypendop BH, Steffey EP. Evaluation of the induction and recovery characteristics of anesthesia with desflurane in cats. *Am J Vet Res*. 2004;65:748–751.

83. Selmi AL, Mendes GM, Lins BT, Figueiredo JP, Barbudo-Selmi GR. Comparison of xylazine and medetomidine as premedicants for cats being anaesthetised with propofol-sevoflurane. *Vet Rec*. 2005;157:139–143.
84. Auer U, Mosing M. A clinical study of the effects of rocuronium in isoflurane-anaesthetized cats. *Vet Anaesth Analg*. 2006;33:224–228.
85. Liehmann L, Mosing M, Auer U. A comparison of cardiorespiratory variables during isoflurane-fentanyl and propofol-fentanyl anaesthesia for surgery in injured cats. *Vet Anaesth Analg*. 2006;33:158–168.
86. Souza AP, Guerrero PN, Nishimori CT, et al. Cardiopulmonary and acid-base effects of desflurane and sevoflurane in spontaneously breathing cats. *J Feline Med Surg*. 2005;7:95–100.
87. Sano T, Nishimura R, Mochizuki M, Hara Y, Tagawa M, Sasaki N. Clinical usefulness of propofol as an anesthetic induction agent in dogs and cats. *J Vet Med Sci*. 2003;65:641–643.
88. Lerche P, Muir WW, Grubb TL. Mask induction of anaesthesia with isoflurane or sevoflurane in premedicated cats. *J Small Anim Pract*. 2002;43:12–15.
89. Tzannes S, Govendir M, Zaki S, Miyake Y, Packiarajah P, Malik R. The use of sevoflurane in a 2:1 mixture of nitrous oxide and oxygen for rapid mask induction of anaesthesia in the cat. *J Feline Med Surg*. 2000;2:83–90.
90. Akkerdaas LC, Mioch P, Sap R, Hellebrekers LJ. Cardiopulmonary effects of three different anaesthesia protocols in cats. *Vet Q*. 2001;23:182–186.
91. Hsu WH, Hembrough FB. Intravenous glucose tolerance test in cats: Influenced by acetylpromazine, ketamine, morphine, thiopental, and xylazine. *Am J Vet Res*. 1982;43:2060–2061.
92. Smith AA, Posner LP, Goldstein RE, et al. Evaluation of the effects of premedication on gastroduodenoscopy in cats. *J Am Vet Med Assoc*. 2004;225:540–544.
93. Ilkiw JE, Suter C, McNeal D, Farver TB, Steffey EP. The optimal intravenous dose of midazolam after intravenous ketamine in healthy awake cats. *J Vet Pharmacol Ther*. 1998;21:54–61.
94. Lamont LA, Bulmer BJ, Sisson DD, Grimm KA, Tranquilli WJ. Doppler echocardiographic effects of medetomidine on dynamic left ventricular outflow tract obstruction in cats. *J Am Vet Med Assoc*. 2002;221:1276–1281.
95. Niedfeldt RL, Robertson SA. Postanesthetic hyperthermia in cats: A retrospective comparison between hydromorphone and buprenorphine. *Vet Anaesth Analg*. 2006;33:381–389.
96. Shamir M, Goelman G, Chai O. Postanesthetic cerebellar dysfunction in cats. *J Vet Intern Med*. 2004;18:368–369.
97. Mollenhoff A, Nolte I, Kramer S. Anti-nociceptive efficacy of carprofen, levomethadone and buprenorphine for pain relief in cats following major orthopaedic surgery. *J Vet Med A Physiol Pathol Clin Med*. 2005;52:186–198.
98. Buchanan KC, Burge RR, Ruble GR. Evaluation of injectable anesthetics for major surgical procedures in guinea pigs. *Contemp Top Lab Anim Sci*. 1998;37:58–63.
99. Wright BS, Rezk PE, Graham JR, et al. Acute lung injury following inhalation exposure to nerve agent VX in guinea pigs. *Inhal Toxicol*. 2006;18:437–448.
100. Sendowski I, Raffin F, Clarencon D. Spectrum of neural electrical activity in guinea pig cochlea: Effects of anaesthesia regimen, body temperature and ambient noise. *Hear Res*. 2006;211:63–73.
101. Jacobson C. A novel anaesthetic regimen for surgical procedures in guinea pigs. *Lab Anim*. 2001;35:271–276.
102. Radde GR, Hinson A, Crenshaw D, Toth LA. Evaluation of anaesthetic regimens in guinea pigs. *Lab Anim*. 1996;30:220–227.
103. Bina S, Cowan G, Karaian J, Muldoon S, Mongan P, Bunger R. Effects of caffeine, halothane, and 4-chloro-m-cresol on skeletal muscle lactate and pyruvate in malignant hyperthermia-susceptible and normal swine as assessed by microdialysis. *Anesthesiology*. 2006;104:90–100.
104. Gerbershagen MU, Wappler F, Fiege M, et al. Effects of a 5HT(2) receptor agonist on anaesthetized pigs susceptible to malignant hyperthermia. *Br J Anaesth*. 2003;91:281–284.

105. Gerbershagen MU, Wappler F, Fiege M, Weihorn R, Kolodzie K, Schulte Esch J. Inhibition of sarcoplasmic Ca2+ adenosine triphosphatase in porcine skeletal muscle samples with cyclopiazonic acid enables in vitro malignant hyperthermia discrimination. *Anesthesiology*. 2004;101:1475–1477.
106. Gross DR, Dewanjee MK, Zhai P, Lanzo S, Wu SM. Successful prosthetic mitral valve implantation in pigs. *ASAIO J*. 1997;43:M382–6.
107. Gross DR, Salley RK, Maley RH, Arden WA, Nammalwar P. Effects of internal mammary artery pedicle coronary artery bypass grafting on aortic valve leaflet positioning. *J Heart Valve Dis*. 1995;4:313–320.
108. Robinson MC, Gross DR, Thielmeier KA, Hill BB, Zeman WF. Development of a minimally invasive technique for coronary revascularization in a porcine model. *Ann Thorac Surg*. 1997;64:64–69.
109. Tobari S, Ikeda Y, Takami H. Beneficial effects of intravenous administration of lipo-prostaglandin E1 on the ischemic gastric tube in pigs. *J Surg Res*. 2005;129:79–84.
110. Tsatsaris A. Effect of temperature increase on the distensibility of porcine thoracic aorta. *Artif Organs*. 2005;29:887–891.
111. Kurita T, Morita K, Fukuda K, et al. Landiolol, an ultra-short-acting beta 1-adrenoceptor antagonist, does not alter the electroencephalographic effect of isoflurane in swine model. *Br J Anaesth*. 2006;96:602–607.
112. Kostopanagiotou G, Theodoraki K, Pandazi A, Arkadopoulos N, Costopanagiotou C, Smyrniotis V. Changes in oxyhemoglobin dissociation curve in intra-abdominal organs during pig experimental orthotopic liver transplantation. *Liver Transpl*. 2005;11:760–766.
113. Louail B, Sapoval M, Bonneau M, Wasseff M, Senechal Q, Gaux JC. A new porcine sponge material for temporary embolization: An experimental short-term pilot study in swine. *Cardiovasc Intervent Radiol*. 2006;29:826–831.
114. Kerbaul F, Bellezza M, Mekkaoui C, et al. Sevoflurane alters right ventricular performance but not pulmonary vascular resistance in acutely instrumented anesthetized pigs. *J Cardiothorac Vasc Anesth*. 2006;20:209–216.
115. Mader TJ, Menegazzi JJ, Betz AE, Logue ES, Callaway CW, Sherman LD. Adenosine A(1) receptor antagonism hastens the decay in ventricular fibrillation waveform morphology during porcine cardiac arrest. *Resuscitation*. 2006;71:254–259.
116. Sparks DL, Gross DR, Hunsaker JC. Neuropathology of mitral valve prolapse in man and cardiopulmonary bypass (CPB) surgery in adolescent Yorkshire pigs. *Neurobiol Aging*. 2000;21:363–372.
117. Radcliffe JS, Rice JP, Pleasant RS, Apgar GA. Technical note: Improved technique for fitting pigs with steered ileocecal valve cannulas. *J Anim Sci*. 2005;83:1563–1567.
118. Klaessens JH, Hopman JC, van Wijk MC, Djien Liem K, Thijssen JM. Assessment of local changes of cerebral perfusion and blood concentration by near infrared spectroscopy and ultrasound contrast densitometry. *Brain Dev*. 2005;27:406–414.
119. Grossherr M, Hengstenberg A, Meier T, Dibbelt L, Gerlach K, Gehring H. Discontinuous monitoring of propofol concentrations in expired alveolar gas and in arterial and venous plasma during artificial ventilation. *Anesthesiology*. 2006;104:786–790.
120. Ko JC, Williams BL, Rogers ER, Pablo LS, McCaine WC, McGrath CJ. Increasing xylazine dose-enhanced anesthetic properties of telazol-xylazine combination in swine. *Lab Anim Sci*. 1995;45:290–294.
121. Ko JC, Williams BL, Smith VL, McGrath CJ, Jacobson JD. Comparison of telazol, telazol-ketamine, telazol-xylazine, and telazol-ketamine-xylazine as chemical restraint and anesthetic induction combination in swine. *Lab Anim Sci*. 1993;43:476–480.
122. Wagh MS, Merrifield BF, Thompson CC. Survival studies after endoscopic transgastric oophorectomy and tubectomy in a porcine model. *Gastrointest Endosc*. 2006;63:473–478.
123. Ragan HA, Gillis MF. Restraint, venipuncture, endotracheal intubation, and anesthesia of miniature swine. *Lab Anim Sci*. 1975;25:409–419.
124. Hodgson DS. An inhaler device using liquid injection of isoflurane for short term anesthesia in piglets. *Vet Anaesth Analg*. 2006;33:207–213.

125. Sakaguchi M, Nishimura R, Sasaki N, Ishiguro T, Tamura H, Takeuchi A. Chemical restraint by medetomidine-ketamine and its cardiopulmonary effects in pigs. *Zentralbl Veterinarmed A*. 1995;42:293–299.
126. Nishimura R, Kim H, Matsunaga S, et al. Sedative effect induced by a combination of medetomidine and midazolam in pigs. *J Vet Med Sci*. 1993;55:717–722.
127. Ashley DW, Mix JW, Christie B, et al. Removal of the OptEase retrievable vena cava filter is not feasible after extended time periods because of filter protrusion through the vena cava. *J Trauma*. 2005;59:847–852.
128. Sweitzer RA, Ghneim GS, Gardner IA, Van Vuren D, Gonzales BJ, Boyce WM. Immobilization and physiological parameters associated with chemical restraint of wild pigs with telazol and xylazine hydrochloride. *J Wildl Dis*. 1997;33:198–205.
129. Keegan RD, Greene SA, Valdez RA, Knowles DK. Cardiovascular effects of desflurane in mechanically ventilated calves. *Am J Vet Res*. 2006;67:387–391.
130. Casas F, Reeves A, Dudzinski D, et al. Performance and reliability of the CPB/ECMO initiative forward lines casualty management system. *ASAIO J*. 2005;51:681–685.
131. Ahmed AF, Constable PD, McCallister MM, Misk NA. Abomasal cannulation in the milk-fed calf using a 7 mm polyurethane tube. *J Vet Med A Physiol Pathol Clin Med*. 2005;52:39–42.
132. Kawahito S, Takano T, Nakata K, et al. Analysis of the arterial blood pressure waveform during left ventricular nonpulsatile assistance in animal models. *Artif Organs*. 2000;24:816–820.
133. Tozzi P, Corno AF, Lapanashvili LV, Von Segesser LK. Muscular counterpulsation: Preliminary results of a non-invasive alternative to intra-aortic balloon pump. *Eur J Cardiothorac Surg*. 2004;26:726–729.
134. Blaze CA, Holland RE, Grant AL. Gas exchange during xylazine-ketamine anesthesia in neonatal calves. *Vet Surg*. 1988;17:155–159.
135. Lin HC, Tyler JW, Wallace SS, Thurmon JC, Wolfe DF. Telazol and xylazine anesthesia in sheep. *Cornell Vet*. 1993;83:117–124.
136. Picavet MT, Gasthuys FM, Laevens HH, Watts SA. Cardiopulmonary effects of combined xylazine-guaiphenesin-ketamine infusion and extradural (inter-coccygeal lidocaine) anaesthesia in calves. *Vet Anaesth Analg*. 2004;31:11–19.
137. Aithal HP, Singh GR, Hoque M, et al. The use of a circular external skeletal fixation device for the management of long bone osteotomies in large ruminants: An experimental study. *J Vet Med A Physiol Pathol Clin Med*. 2004;51:284–293.
138. Kock MD, Jessup DA, Clark RK, Franti CE, Weaver RA. Capture methods in five subspecies of free-ranging bighorn sheep: An evaluation of drop-net, drive-net, chemical immobilization and the net-gun. *J Wildl Dis*. 1987;23:634–640.
139. Pfeuffer J, Juchem C, Merkle H, Nauerth A, Logothetis NK. High-field localized 1H NMR spectroscopy in the anesthetized and in the awake monkey. *Magn Reson Imaging*. 2004;22:1361–1372.
140. Ghoniem GM, Shoukry MS, Monga M. Effects of anesthesia on urodynamic studies in the primate model. *J Urol*. 1996;156:233–236.
141. Farber DM, Giussani DA, Jenkins SL, et al. Timing of the switch from myometrial contractures to contractions in late-gestation pregnant rhesus monkeys as recorded by myometrial electromyogram during spontaneous term and androstenedione-induced labor. *Biol Reprod*. 1997;56:557–562.
142. Sanders EA, Gleed RD, Nathanielsz PW. Anesthetic management for instrumentation of the pregnant rhesus monkey. *J Med Primatol*. 1991;20:223–228.
143. Tsukada H, Nishiyama S, Kakiuchi T, et al. Isoflurane anesthesia enhances the inhibitory effects of cocaine and GBR12909 on dopamine transporter: PET studies in combination with microdialysis in the monkey brain. *Brain Res*. 1999;849:85–96.
144. Yoshikawa T, Ochiai R, Kaneko T, et al. The effect of sevoflurane on regional cerebral metabolism and cerebral blood flow in rhesus monkeys. *Masui*. 1997;46:237–243.
145. Baranov MV, Lenskii VV, Goncharov IB. Peculiarities of anesthesia and systemic hemodynamics in experiment with 30 days head-down immobilization of monkeys. *Aviakosm Ekolog Med*. 2000;34:37–40.

146. Hansen BC, Pek S, Koerker DJ, Goodner CJ, Wolfe RA, Schielke GP. Neural influences on oscillations in basal plasma levels of insulin in monkeys. *Am J Physiol*. 1981;240:E5–E11.
147. Zola-Morgan S, Micheletti C. Respiration rate, heart rate, and body temperature values in cynomolgus monkeys (macaca fascicularis) during barbiturate anesthesia. *J Med Primatol*. 1986;15:399–408.
148. Streett JW, Jonas AM. Differential effects of chemical and physical restraint on carbohydrate tolerance testing in nonhuman primates. *Lab Anim Sci*. 1982;32:263–266.
149. Hassimoto M, Harada T, Harada T. Changes in hematology, biochemical values, and restraint ECG of rhesus monkeys (macaca mulatta) following 6-month laboratory acclimation. *J Med Primatol*. 2004;33:175–186.
150. Ruys JD, Mendoza SP, Capitanio JP, Mason WA. Behavioral and physiological adaptation to repeated chair restraint in rhesus macaques. *Physiol Behav*. 2004;82:205–213.

Chapter 3
Normal Cardiac Function Parameters

The normal values found in this chapter are provided to serve as a quick and easy reference. Investigators might find these values useful to be able to compare to the data they acquire. Manuscripts that report results from animals or preparations significantly different than these ranges could be problematic (Tables 3.1-3.6).

Table 3.1 Ranges of normal cardiac function parameters, left ventricular peak systolic pressure (LVPSP), left ventricular end-diastolic pressure (LVEDP), left ventricular +dP/dt (LV +dP/dt), left ventricular −dP/dt (LV −dP/dt), left ventricular velocity of shortening (LVVS), left ventricular fractional shortening (LVFS)[1,21]

Species	LVPSP (mmHg)	LVEDP (mmHg)	LV +d*P*/d*t* (mmHg/s)	LV −d*P*/d*t* (mmHg/s)	LVVS (mm/s)	LVFS (%)
Rats	124–159[a]	0–16[a]	1,600–4,500[a]	1,480–3,460[a]	21–112[a]	52–59[a]
Mice	100–122[a]	2.0–5.2[a]	8,084–17,916[a]	6,282–14,136[a]	17–21	49–57[a]
Rabbits	90–118[a]	0–8[a]	1,640–3,810[a]	1,570–4,090[a]	18–114[a]	29.6–39.4[a]
Dogs	99–161[a]	0.5–15[a]	1,740–5,295[a]	1,915–3,111[a]	20–118[a]	33–39
Cats	105–135[a]	0–10[a]	1,550–3,500[a]	1,490–4,375[a]	25–110[a]	24–44
Guinea pigs	65.8–77.2	5.0–5.6	2,940–3,600	1,870–2,370	19–93	49–60
Pigs	112–169[a]	5–15[a]	1,790–3,875[a]	1,410–4,487[a]	20–116[a]	36–46
Calves	110–146[a]	5.5–11.5[a]	2,160–3,574[a]	2,109–5,025[a]	16–125[a]	27–47
Sheep	85–118[a]	0–16[a]	1,680–4,525[a]	1,610–2,990[a]	20–115[a]	34–38
Goats	71–116	4–10	1,750–4,225	1,059–1,579	18–105	33–40
Primates (Rhesus)	105–178[a]	0–12[a]	1,678–4,238[a]	1,532–4,720[a]	22–128[a]	12.6–41.2

[a]Data from intact awake, previously instrumented animals; other data from anesthetized animals; depth of anesthesia not reported

D.R. Gross, *Animal Models in Cardiovascular Research*,
DOI: 10.1007/978-0-387-95962-7_3, © Springer Science + Business Media, LLC 2009

Table 3.2 Ranges of normal cardiac function parameters, left ventricular end-diastolic volume (LVEDV), left ventricular segmental shortening (LVSS), left ventricular preload recruitable stroke work (LV-PRSW), systemic resistance (Rao), pulmonary resistance (Rpa), Emax (Emax)[1,2,5,15,17,20,22-57]

Species	LVEDV (ml) or (μl)	LVSS (%)	LV-PRSW (mmHg × ml) or (mW × s/ml)	Rao (dyn × s × cm^{-5}) or (mmHg/ml/min)	Rpa (dyn × s × cm^{-5}) or (mmHg/ml/min)	Emax (mmHg/ml) or (mmHg/μl) or (*mmHg × g/ml*)
Rats	160–180	22–24	52.6–87	0.59–0.77	0.19–0.21	*2,000–2,700*
Mice	15.4–65.0[a]	25–27	65–135[a]	0.38–0.67	1.7–2.3	5.9–10.5
Rabbits	1.4–2.8	16–20	18–27.6	0.30–0.34	60–70	3.9–5.5
Dogs (15–30 kg)	50.6–61.8[a]	9.8–38.0[a]	47–563[a]	1,805–7,269[a]	122–236[a]	1.1–72[a]
Cats	8–22[a]	9.2–27.4[a]	50–520[a]	2,110–5,600[a]	146–228[a]	5–65[a]
Guinea Pigs	Nf	Nf	Nf	57,511–69,791	0.04–0.05[d]	*608–724*
Pigs	71.3–95.3	12.7–26.5	27–35 3.8–6.4	511–605	250–500	2.1–2.9
Calves	3.9–4.9[b]	Nf	Nf	1,361–2,297	390–576	7.1–7.5
Sheep	163–263	13.0–27	53–75	1,091–1,783	410–650	0.36–2.6
Goats	62–156.9	39.4–41.8	Nf	452–578	452–578	1.6–2.4
Primates (Rhesus)	1.38–1.98[b]	12.6–31.2	Nf	1,932–3,170[c]	125–352	*157–435*

Nf not found

[a]Data from intact, awake, previously instrumented animals; other data from anesthetized animals; depth of anesthesia not reported

[b]Left ventricular end-diastolic diameter in cm

[c]Systemic vascular resistance index (dyn × s × m^2/cm^5)

[d]Pulmonary vascular resistance index (mmHg × min × kg^{-1} × ml^{-1})

Table 3.3 Ranges of normal cardiac function parameters, stroke volume (SV), left ventricular power (LVPower), rate pressure product (RPP), myocardial oxygen consumption ($MyoVO_2$), peak velocity of early left ventricular filling (E wave), peak velocity of late left ventricular filling (A wave)[1,2,5,7,15,17,20,22,25,38,58-91]

Species	SV (ml) or (μl)	LVPower ($\times 10^4$ dyn × cm × s^{-1})	RPP (b/min × mmHg × 10^3)	$MyoVO_2$ (ml O_2/min/100 g) or μmol/min/100 g)	E wave (mitral) cm/s)	A wave (mitral) (cm/s)
Rats	150–200	30–50[c]	42–48	0.1–0.7[m]	60–91	39–76
Mice	10.0–14.4	33.0–36.8	22.6–32.2	0.6–0.9[m]	59.5–79.3	29.2–42.5
Rabbits	1.3–2.26[a]	1.71–1.81[d]	22–29	569–665[e]	52.8–60.2	36.2–41.6
Dogs (15–30 kg)	9.4–77.6[a]	17.5–52.9[a]	6.7–21.4[a]	6.9–13.5[a]	39–61	20–38
Cats	3.8–23.0[a]	15.4–48.9[a]	5.4–19.8[a]	7.2–10.6[a]	66–74	25–33
Guinea Pigs	0.52–0.58	100–120[f]	18.9–20.8[k]	18.6–20.2[k]	77–83	0.29–0.31
Pigs	21.8–26.2	2.0–2.5[g] 0.6–1.5[i]	10.9–13.6	103–127[h]	Nf	Nf
Calves	309.1–317.5	Nf	12.8–16.3	Nf	Nf	Nf
Sheep	49–89	170–209.6[j]	9.4–11.4[l]	418–532	24–68.4	34.7–51.3
Goats	42–110	Nf	11.3–18.0	0.8–1.2[n]	Nf	Nf
Primates (Rhesus)	0.40–0.44[b]	Nf	14.2–34.6	Nf	Nf	Nf

Nf not found

[a]Data from intact, awake, previously instrumented animals; other data from anesthetized animals; depth of anesthesia not reported

[b]Stroke volume normalized by body weight in kg (stroke volume index)

[c]Preload adjusted maximal power ($mW/\mu l^2$)

[d]Left ventricular power ($J \times min^{-1}$) in isolated working heart preparation

[e]$\mu l \times g\ dry\ wt^{-1} \times min^{-1}$)

[f]$mJ \times g^{-1} \times min^{-1}$ in isolated heart preparation

[g]Maximal power × EDV^{-2} ($mmHg \times ml^{-1}$)

[h]Anterior wall MVO_2 ($\mu mol \times min^{-1}$)

[i]Preload adjusted maximal power, i.e., maximal hydraulic power output normalized by EDV ($mW \times ml^{-2}$)

[j]$mmHg \times l \times min^{-1} \times m^{-2}$

[k]Isolated heart preparation

[l]Lambs

[m]$\mu mol \times beat^{-1} \times g^{-1}$

[n]Normalized value[85]

Table 3.4 Ranges of normal values for other cardiovascular indices, left ventricular mass/body weight (*LV/body wt*), right ventricular mass/body weight (*RV/body wt*), P-R interval (*P-R*), QRS duration (*QRS*), left ventricular time constant of relaxation (τ)[1,2,12,17,34,43,64,89,92,93-116]

Species	LV/body wt (g/kg) or (mg/g)	RV/body wt (g/kg) or (mg/g)	P-R (ms)	QRS (ms)	τ (ms)
Rats	1.9–2.1	0.5–0.67	39.9–69	31–33	0.9–23.5
Mice	2.7–3.08	0.02–1.0	27.6–33.8	8.4–10.0	3.9–6.5[a]
Rabbits	1.24–1.28	0.47–0.53	60–65	20–22	13.1–14.9
Dogs	3.6–4.9	1.0–1.8	99.8–124.2[a]	55–65	65–501[a]
Cats	1.51–1.58	0.6–0.66	57–75	25–39	42.4–49.0
Guinea Pigs	1.9–2.15	0.33–0.42	49–57	39–41	57.6–71
Pigs	1.35–1.47	0.59–0.63	112–138	34.2–82.0	25–27
Calves	1.42–1.67	1.0–1.5	245–360	58–113	27.9–51.7
Sheep	1.63–1.65	0.57–0.59	107–119	71–77	16.0–18.0
Goats	Nf	0.55–0.60	78–86	31–35	20.1–33.5
Primates (Rhesus)	2.0–2.78	Nf	81–85	48–50	Nf

Nf not found

[a]Data from intact, awake, previously instrumented animals; other data from anesthetized animals; depth of anesthesia not reported

Table 3.5 Normal ranges of blood flow distribution in ml/min/100 g of tissue[1,117-121]

Species	Heart	Kidneys	Liver	GI tract	Spleen
Rats	291–698[a]	140–973[a]	4–182[a]	134–308[a]	32–393[a]
Mice	404–597	106–582	206–245	335–411	89–126
Rabbits	134–545[a]	214–1,044[a]	5–149[a]	72–1,113[a]	41–1,487[a]
Dogs	360–490[a]	214–685[a]	15–55[a]	25–90[a]	64–353[a]
Cats	134–316[a]	235–361[a]	2.8–41[a]	77–123[a]	4.1–260.6[a]
Guinea Pigs	Nf	20–42	Nf	Nf	Nf
Pigs	114–154[a]	379–523[a]	5–11[a]	29–156[a]	172–268[a]
Calves	Nf	Nf	Nf	Nf	Nf
Sheep	83–184[a]	514–930[a]	Nf	46–100[a]	35–265[a]
Goats	Nf	Nf	Nf	Nf	Nf
Primates (Rhesus)	224–508[a]	577–1,665[a]	4–78[a]	48–108[a]	Nf

Nf not found

[a]Data from intact, awake, previously instrumented animals; other data from anesthetized animals; depth of anesthesia not reported

Table 3.6 Normal ranges of blood flow distribution in ml/min/100 g tissue[1,117,119,120,122-125]

Species	Skin	Brain	Bone	Skeletal muscle	Adrenal	Pancreas
Rats	6–31[a]	15–200[a]	10–43	6–106[a]	68–228[a]	28–92[a]
Mice	3–7	51–85	8–27	10–21	140–167	69–98
Rabbits	12–17	50–62	5–33	22–26	Nf	Nf
Dogs	2–21[a]	23–105[a]	3–13[a]	1–108[a]	142–502[a]	20–205[a]
Cats	2–19[a]	41–55[a]	3–4[a]	24–44[a]	152–475[a]	11–198[a]
Guinea Pigs	Nf	Nf	Nf	Nf	Nf	Nf
Pigs	20–30	69–99[a]	10–20	3–37[a]	95–213[a]	124–190[a]
Calves	Nf	Nf	Nf	Nf	Nf	Nf
Sheep	2–8[a]	38–73[a]	Nf	4–43[a]	59–246[a]	139–225[a]
Goats	Nf	Nf	Nf	Nf	Nf	Nf
Primates (Rhesus)	20–30[a]	25–94[a]	Nf	19–39[a]	163–371[a]	Nf

Nf not found

[a]Data from intact, awake, previously instrumented animals; other data from anesthetized animals; depth of anesthesia not reported

References

1. Gross DR. *Animal Models in Cardiovascular Research, Second Revised Edition.* Boston: Kluwer; 1994.
2. Gross DR. Unpublished data.
3. Ishizaka S, Sievers RE, Zhu BQ, et al. New technique for measurement of left ventricular pressure in conscious mice. *Am J Physiol Heart Circ Physiol*. 2004;286:H1208–H1215.
4. Wang Q, Brunner HR, Burnier M. Determination of cardiac contractility in awake unsedated mice with a fluid-filled catheter. *Am J Physiol Heart Circ Physiol*. 2004;286:H806–H814.
5. Stein AB, Tiwari S, Thomas P, et al. Effects of anesthesia on echocardiographic assessment of left ventricular structure and function in rats. *Basic Res Cardiol*. 2007;102(1):28–41.
6. Gao Z, Xing J, Sinoway LI, Li J. P2X receptor-mediated muscle pressor reflex in myocardial infarction (MI). *Am J Physiol Heart Circ Physiol*. 2007;292(2):H939–H945.
7. Stypmann J, Engelen MA, Breithardt AK, et al. Doppler echocardiography and tissue Doppler imaging in the healthy rabbit: Differences of cardiac function during awake and anaesthetised examination. *Int J Cardiol*. 2007;115(2):164–170.
8. Chetboul V, Escriou C, Tessier D, et al. Tissue Doppler imaging detects early asymptomatic myocardial abnormalities in a dog model of Duchenne's cardiomyopathy. *Eur Heart J*. 2004;25:1934–1939.
9. Nishijima Y, Feldman DS, Bonagura JD, et al. Canine nonischemic left ventricular dysfunction: A model of chronic human cardiomyopathy. *J Card Fail*. 2005;11:638–644.
10. Uechi M, Hori Y, Fujimoto K, Ebisawa T, Yamano S, Maekawa S. Cardiovascular effects of a phosphodiesterase III inhibitor in the presence of carvedilol in dogs. *J Vet Med Sci*. 2006;68:549–553.
11. Ishikawa Y, Uechi M, Hori Y, et al. Effects of enalapril in cats with pressure overload-induced left ventricular hypertrophy. *J Feline Med Surg*. 2007;9(1):29–35.
12. Ramirez-Gil JF, Trouve P, Mougenot N, Carayon A, Lechat P, Charlemagne D. Modifications of myocardial Na+, K(+)-ATPase isoforms and Na+/Ca2+ exchanger in aldosterone/salt-induced hypertension in guinea pigs. *Cardiovasc Res*. 1998;38:451–462.
13. Kostelec M, Covell J, Buckberg GD, Sadeghi A, Hoffman JI, Kassab GS. Myocardial protection in the failing heart: I. Effect of cardioplegia and the beating state under simulated left ventricular restoration. *J Thorac Cardiovasc Surg*. 2006;132:875–883.
14. Chee HK, Tuzun E, Ferrari M, et al. Baseline hemodynamic and echocardiographic indices in anesthetized calves. *ASAIO J*. 2004;50:267–271.
15. Power JM, Raman J, Dornom A, et al. Passive ventricular constraint amends the course of heart failure: A study in an ovine model of dilated cardiomyopathy. *Cardiovasc Res*. 1999;44:549–555.
16. Kim WG, Cho SR, Sung SH, Park HJ. A chronic heart failure model by coronary artery ligation in the goat. *Int J Artif Organs*. 2003;26:929–934.
17. Vaitkevicius PV, Lane M, Spurgeon H, et al. A cross-link breaker has sustained effects on arterial and ventricular properties in older rhesus monkeys. *Proc Natl Acad Sci USA*. 2001;98:1171–1175.
18. Sebag IA, Handschumacher MD, Ichinose F, et al. Quantitative assessment of regional myocardial function in mice by tissue Doppler imaging: Comparison with hemodynamics and sonomicrometry. *Circulation*. 2005;111:2611–2616.
19. Kuma F, Ueda N, Ito H, et al. Effects of ultrasound energy application on cardiac performance in open-chest guinea pigs. *Circ J*. 2006;70:1356–1361.
20. Bolotin G, Lorusso R, Schreuder JJ, et al. Perioperative hemodynamic and geometric changes of the left ventricle during cardiomyoplasty in goats with dilated left ventricle. *Chest*. 2002;121:1628–1633.
21. Lorusso R, van der Veen F, Schreuder JJ, et al. Hemodynamic effects in acute cardiomyoplasty of different wrapped muscle activation times as measured by pressure-volume relations. *J Card Surg*. 1996;11:217–225.
22. Yan X, Price RL, Nakayama M, et al. Ventricular-specific expression of angiotensin II type 2 receptors causes dilated cardiomyopathy and heart failure in transgenic mice. *Am J Physiol Heart Circ Physiol*. 2003;285:H2179–H2187.

23. Wallis J, Lygate CA, Fischer A, et al. Supranormal myocardial creatine and phosphocreatine concentrations lead to cardiac hypertrophy and heart failure: Insights from creatine transporter-overexpressing transgenic mice. *Circulation*. 2005;112:3131–3139.
24. Westermann D, Rutschow S, Van Linthout S, et al. Inhibition of p38 mitogen-activated protein kinase attenuates left ventricular dysfunction by mediating pro-inflammatory cardiac cytokine levels in a mouse model of diabetes mellitus. *Diabetologia*. 2006;49:2507–2513.
25. Van den Bergh A, Flameng W, Herijgers P. Type II diabetic mice exhibit contractile dysfunction but maintain cardiac output by favorable loading conditions. *Eur J Heart Fail*. 2006;8: 777–783.
26. Rodriguez F, Langer F, Harrington KB, et al. Alterations in transmural strains adjacent to ischemic myocardium during acute midcircumflex occlusion. *J Thorac Cardiovasc Surg*. 2005;129:791–803.
27. Coates BJ, Broderick TL, Batia LM, Standley CA. MgSO4 prevents left ventricular dysfunction in an animal model of preeclampsia. *Am J Obstet Gynecol*. 2006;195:1398–1403.
28. Faber MJ, Dalinghaus M, Lankhuizen IM, et al. Right and left ventricular function after chronic pulmonary artery banding in rats assessed with biventricular pressure-volume loops. *Am J Physiol Heart Circ Physiol*. 2006;291:H1580–H1586.
29. Jegger D, Jeanrenaud X, Nasratullah M, et al. Noninvasive Doppler-derived myocardial performance index in rats with myocardial infarction: Validation and correlation by conductance catheter. *Am J Physiol Heart Circ Physiol*. 2006;290:H1540–H1548.
30. Baber SR, Deng W, Master RG, et al. Intratracheal mesenchymal stem cell administration attenuates monocrotaline-induced pulmonary hypertension and endothelial dysfunction. *Am J Physiol Heart Circ Physiol*. 2007;292(2):H1120–H1128.
31. Susic D, Varagic J, Ahn J, Matavelli LC, Frohlich ED. Long-term mineralocorticoid receptor blockade reduces fibrosis and improves cardiac performance and coronary hemodynamics in elderly SHR. *Am J Physiol Heart Circ Physiol*. 2007;292(1):H175–H179.
32. Noguchi T, Ikeda K, Sasaki Y, et al. Effects of vitamin E and sesamin on hypertension and cerebral thrombogenesis in stroke-prone spontaneously hypertensive rats. *Hypertens Res*. 2001;24:735–742.
33. Matsushita T, Takaki M, Fujii W, Matsubara H, Suga H. Left ventricular mechanoenergetics under altered coronary perfusion in guinea pig hearts. *Jpn J Physiol*. 1995;45:991–1004.
34. Royse CF, Royse AG. The myocardial and vascular effects of bupivacaine, levobupivacaine, and ropivacaine using pressure volume loops. *Anesth Analg*. 2005;101:679–87.
35. Roosens CD, Ama R, Leather HA, et al. Hemodynamic effects of different lung-protective ventilation strategies in closed-chest pigs with normal lungs. *Crit Care Med*. 2006;34: 2990–2996.
36. Huang W, Kingsbury MP, Turner MA, Donnelly JL, Flores NA, Sheridan DJ. Capillary filtration is reduced in lungs adapted to chronic heart failure: Morphological and haemodynamic correlates. *Cardiovasc Res*. 2001;49:207–217.
37. Christiansen S, Redmann K, Autschbach R. Intrathoracic implantation of a continuous flow left ventricular assist device – the microdiagonal blood pump. *J Cardiovasc Surg (Torino)*. 2006;47:329–335.
38. Olsson K, Hansson A, Hydbring E, von Walter LW, Haggstrom J. A serial study of heart function during pregnancy, lactation and the dry period in dairy goats using echocardiography. *Exp Physiol*. 2001;86:93–99.
39. Kramer CM, Ferrari VA, Rogers WJ, et al. Angiotensin-converting enzyme inhibition limits dysfunction in adjacent noninfarcted regions during left ventricular remodeling. *J Am Coll Cardiol*. 1996;27:211–217.
40. Liakopoulos OJ, Tomioka H, Buckberg GD, Tan Z, Hristov N, Trummer G. Sequential deformation and physiological considerations in unipolar right or left ventricular pacing. *Eur J Cardiothorac Surg*. 2006;29(Suppl 1):S188–S197.
41. Lewis CW, Atkins BZ, Hutcheson KA, et al. A load-independent in vivo model for evaluating therapeutic interventions in injured myocardium. *Am J Physiol*. 1998;275:H1834–H1844.

42. Rodriguez F, Langer F, Harrington KB, et al. Importance of mitral valve second-order chordae for left ventricular geometry, wall thickening mechanics, and global systolic function. *Circulation*. 2004;110:II115–II122.
43. Schmidt MR, Smerup M, Konstantinov IE, et al. Intermittent peripheral tissue ischemia during coronary ischemia reduces myocardial infarction: First demonstration of remote ischemic perconditioning. *Am J Physiol Heart Circ Physiol*. 2007;292(4):H1883–H1890.
44. Joho S, Ishizaka S, Sievers R, Foster E, Simpson PC, Grossman W. Left ventricular pressure-volume relationship in conscious mice. *Am J Physiol Heart Circ Physiol*. 2007;292(1):H369–377.
45. Yin GQ, Qiu HB, Du KH, Tang JQ, Lu CP, Fang ZX. Endotoxic shock model with fluid resuscitation in macaca mulatta. *Lab Anim*. 2005;39:269–279.
46. Wauthy P, Pagnamenta A, Vassalli F, Naeije R, Brimioulle S. Right ventricular adaptation to pulmonary hypertension: An interspecies comparison. *Am J Physiol Heart Circ Physiol*. 2004;286:H1441–H1447.
47. Mutschler D, Wikstrom G, Lind L, Larsson A, Lagrange A, Eriksson M. Etanercept reduces late endotoxin-induced pulmonary hypertension in the pig. *J Interferon Cytokine Res*. 2006;26:661–667.
48. Katsuda S, Miyashita H, Takazawa K, et al. Mild hypertension in young kurosawa and kusanagi-hypercholesterolaemic (KHC) rabbits. *Physiol Meas*. 2006;27:1361–1371.
49. Stoyanova E, Trudel M, Felfly H, Garcia D, Cloutier G. Characterization of circulatory disorders in {beta}-thalassemic mice by non-invasive ultrasound biomicroscopy. *Physiol Genomics*. 2007;29:84–90
50. Dekker AL, Reesink KD, van der Veen FH, et al. Intra-aortic balloon pumping in acute mitral regurgitation reduces aortic impedance and regurgitant fraction. *Shock*. 2003;19:334–338.
51. Reitan O, Steen S, Ohlin H. Left ventricular heart failure model for testing cardiac assist devices. *ASAIO J*. 2002;48:71–75.
52. Zuckerman BD, Orton EC, Latham LP, Barbiere CC, Stenmark KR, Reeves JT. Pulmonary vascular impedance and wave reflections in the hypoxic calf. *J Appl Physiol*. 1992;72:2118–2127.
53. Markov AK, Warren ET, Cohly HH, Sauls DJ, Skelton TN. Influence of fructose-1,6-diphosphate on endotoxin-induced lung injuries in sheep. *J Surg Res*. 2007;138(1):45–50.
54. Hassoun PM, Thompson BT, Hales CA. Partial reversal of hypoxic pulmonary hypertension by heparin. *Am Rev Respir Dis*. 1992;145:193–196.
55. Deb B, Bradford K, Pearl RG. Additive effects of inhaled nitric oxide and intravenous milrinone in experimental pulmonary hypertension. *Crit Care Med*. 2000;28:795–799.
56. Tuchscherer HA, Vanderpool RR, Chesler NC. Pulmonary vascular remodeling in isolated mouse lungs: Effects on pulsatile pressure-flow relationships. *J Biomech*. 2007;40(5):993–1001.
57. Kawaguchi O, Pae WE, Daily BB, Pierce WS. Ventriculoarterial coupling with intra-aortic balloon pump in acute ischemic heart failure. *J Thorac Cardiovasc Surg*. 1999;117:164–171.
58. Shiomi T, Tsutsui H, Hayashidani S, et al. Pioglitazone, a peroxisome proliferator-activated receptor-gamma agonist, attenuates left ventricular remodeling and failure after experimental myocardial infarction. *Circulation*. 2002;106:3126–3132.
59. Gonon AT, Bulhak A, Broijersen A, Pernow J. Cardioprotective effect of an endothelin receptor antagonist during ischaemia/reperfusion in the severely atherosclerotic mouse heart. *Br J Pharmacol*. 2005;144:860–866.
60. Tsutsumi YM, Patel HH, Lai NC, Takahashi T, Head BP, Roth DM. Isoflurane produces sustained cardiac protection after ischemia-reperfusion injury in mice. *Anesthesiology*. 2006;104:495–502.
61. Buchanan J, Mazumder PK, Hu P, et al. Reduced cardiac efficiency and altered substrate metabolism precedes the onset of hyperglycemia and contractile dysfunction in two mouse models of insulin resistance and obesity. *Endocrinology*. 2005;146:5341–5349.

62. Zhou YQ, Foster FS, Parkes R, Adamson SL. Developmental changes in left and right ventricular diastolic filling patterns in mice. *Am J Physiol Heart Circ Physiol*. 2003;285:H1563–H1575.
63. Amory H, McEntee K, Linden AS, et al. Comparative assessment of right ventricular performance from the pressure-volume relationship in double-muscled and conventional calves. *Can J Vet Res*. 1995;59:135–141.
64. Mather LE, Duke CC, Ladd LA, Copeland SE, Gallagher G, Chang DH. Direct cardiac effects of coronary site-directed thiopental and its enantiomers: A comparison to propofol in conscious sheep. *Anesthesiology*. 2004;101:354–364.
65. Cohen JE, Atluri P, Taylor MD, et al. Fructose 1,6-diphosphate administration attenuates post-ischemic ventricular dysfunction. *Heart Lung Circ*. 2006;15:119–123.
66. Murashita T, Kempsford RD, Hearse DJ. Oxygen supply and oxygen demand in the isolated working rabbit heart perfused with asanguineous crystalloid solution. *Cardiovasc Res*. 1991;25:198–206.
67. Squires JE, Sun J, Caffrey JL, Yoshishige D, Mallet RT. Acetoacetate augments beta-adrenergic inotropism of stunned myocardium by an antioxidant mechanism. *Am J Physiol Heart Circ Physiol*. 2003;284:H1340–H1347.
68. Ramirez-Gil JF, Delcayre C, Robert V, et al. In vivo left ventricular function and collagen expression in aldosterone/salt-induced hypertension. *J Cardiovasc Pharmacol*. 1998;32:927–934.
69. Pestel GJ, Hiltebrand LB, Fukui K, Cohen D, Hager H, Kurz AM. Assessing intravascular volume by difference in pulse pressure in pigs submitted to graded hemorrhage. *Shock*. 2006;26:391–395.
70. Chandler MP, Chavez PN, McElfresh TA, Huang H, Harmon CS, Stanley WC. Partial inhibition of fatty acid oxidation increases regional contractile power and efficiency during demand-induced ischemia. *Cardiovasc Res*. 2003;59:143–151.
71. Segers P, Tchana-Sato V, Leather HA, et al. Determinants of left ventricular preload-adjusted maximal power. *Am J Physiol Heart Circ Physiol*. 2003;284:H2295–H2301.
72. Portman MA, Xiao Y, Broers BG, Ning XH. Hypoxic pHi and function modulation by Na+/H+ exchange and alpha-adrenoreceptor inhibition in heart in vivo. *Am J Physiol*. 1997;272:H2664–H2670.
73. Saitoh T, Nakajima T, Takahashi T, Kawahara K. Changes in cardiovascular function on treatment of inhibitors of apoptotic signal transduction pathways in left ventricular remodeling after myocardial infarction. *Cardiovasc Pathol*. 2006;15:130–138.
74. Tracey WR, Treadway JL, Magee WP, et al. Cardioprotective effects of ingliforib, a novel glycogen phosphorylase inhibitor. *Am J Physiol Heart Circ Physiol*. 2004;286:H1177–H1184.
75. Marktanner R, Nacke P, Feindt P, Hohlfeld T, Schipke JD, Gams E. Delayed preconditioning via angiotensin-converting enzyme inhibition: Pros and cons from an experimental study. *Clin Exp Pharmacol Physiol*. 2006;33:787–792.
76. Shen W, Tian R, Saupe KW, Spindler M, Ingwall JS. Endogenous nitric oxide enhances coupling between O2 consumption and ATP synthesis in guinea pig hearts. *Am J Physiol Heart Circ Physiol*. 2001;281:H838–H846.
77. Wang X, Hu Q, Mansoor A, et al. Bioenergetic and functional consequences of stem cell-based VEGF delivery in pressure-overloaded swine hearts. *Am J Physiol Heart Circ Physiol*. 2006;290:H1393–H1405.
78. Lin HC, Thurmon JC, Tranquilli WJ, Benson GJ, Olson WA. Hemodynamic response of calves to tiletamine-zolazepam-xylazine anesthesia. *Am J Vet Res*. 1991;52:1606–1610.
79. Toorop GP, Hardjowijono R, Dalinghaus M, et al. Myocardial blood flow and VO2 in conscious lambs with an aortopulmonary shunt. *Am J Physiol*. 1987;252:H681–H686.
80. Hikasa Y, Okuyama K, Kakuta T, Takase K, Ogasawara S. Anesthetic potency and cardiopulmonary effects of sevoflurane in goats: Comparison with isoflurane and halothane. *Can J Vet Res*. 1998;62:299–306.
81. Talan MI, Engel BT. Learned control of heart rate during dynamic exercise in nonhuman primates. *J Appl Physiol*. 1986;61:545–553.
82. Kobayashi S, Yoshikawa Y, Sakata S, et al. Left ventricular mechanoenergetics after hyperpolarized cardioplegic arrest by nicorandil and after depolarized cardioplegic arrest by KCl. *Am J Physiol Heart Circ Physiol*. 2004;287:H1072–H1080.

83. Noguchi T, Chen Z, Bell SP, Nyland L, LeWinter MM. Activation of PKC decreases myocardial O2 consumption and increases contractile efficiency in rats. *Am J Physiol Heart Circ Physiol*. 2001;281:H2191–H2197.
84. Palmer BM, Noguchi T, Wang Y, et al. Effect of cardiac myosin binding protein-C on mechanoenergetics in mouse myocardium. *Circ Res*. 2004;94:1615–1622.
85. Dankelman J, Van der Ploeg CP, Spaan JA. Transients in myocardial O2 consumption after abrupt changes in perfusion pressure in goats. *Am J Physiol*. 1996;270:H492–H499.
86. Boluyt MO, Converso K, Hwang HS, Mikkor A, Russell MW. Echocardiographic assessment of age-associated changes in systolic and diastolic function of the female F344 rat heart. *J Appl Physiol*. 2004;96:822–828.
87. Motte S, Mathieu M, Brimioulle S, et al. Respiratory-related heart rate variability in progressive experimental heart failure. *Am J Physiol Heart Circ Physiol*. 2005;289:H1729–H1735.
88. Courtois M, Vered Z, Barzilai B, Ricciotti NA, Perez JE, Ludbrook PA. The transmitral pressure-flow velocity relation. Effect of abrupt preload reduction. *Circulation*. 1988;78:1459–1468.
89. Bright JM, Herrtage ME, Schneider JF. Pulsed Doppler assessment of left ventricular diastolic function in normal and cardiomyopathic cats. *J Am Anim Hosp Assoc*. 1999;35:285–291.
90. Teyssier G, Fouron JC, Maroto E, Lessard M, Bard H, van Doesburg NH. Cardiac two-dimensional imaging and reference values for blood flow velocities in the ovine fetus. *J Dev Physiol*. 1992;17:21–27.
91. Kirberger RM, van den Berg JS. Pulsed wave Doppler echocardiographic evaluation of intracardiac blood flow in normal sheep. *Res Vet Sci*. 1993;55:189–194.
92. Rennison JH, McElfresh TA, Okere IC, et al. High fat diet post infarction enhances mitochondrial function and does not exacerbate left ventricular dysfunction. *Am J Physiol Heart Circ Physiol*. 2007;292(3): H1498–H1506.
93. Rungwerth K, Schindler U, Gerl M, et al. Inhibition of Na+-H+ exchange by cariporide reduces inflammation and heart failure in rabbits with myocardial infarction. *Br J Pharmacol*. 2004;142:1147–1154.
94. Rhodes SS, Ropella KM, Camara AK, Chen Q, Riess ML, Stowe DF. How inotropic drugs alter dynamic and static indices of cyclic myoplasmic [Ca2+] to contractility relationships in intact hearts. *J Cardiovasc Pharmacol*. 2003;42:539–553.
95. White DJ, Carlson D, Ordway GA, Horton JW. Protective role of heat stress in burn trauma. *Crit Care Med*. 2004;32:1338–1345.
96. Mueller XM, Tevaearai HT, Tucker O, Boone Y, von Segesser LK. Reshaping the remodeled left ventricle: A new concept. *Eur J Cardiothorac Surg*. 2001;20:786–791.
97. McConnell PI, del Rio CL, Jacoby DB, et al. Correlation of autologous skeletal myoblast survival with changes in left ventricular remodeling in dilated ischemic heart failure. *J Thorac Cardiovasc Surg*. 2005;130:1001.
98. Manohar M, Parks CM, Busch MA, et al. Regional myocardial blood flow and coronary vascular reserve in unanesthetized young calves exposed to a simulated altitude of 3500 m for 8–10 weeks. *Circ Res*. 1982;50:714–726.
99. Lee JC, Taylor FN, Downing SE. A comparison of ventricular weights and geometry in newborn, young, and adult mammals. *J Appl Physiol*. 1975;38:147–150.
100. Taillefer M, Di Fruscia R. Benazepril and subclinical feline hypertrophic cardiomyopathy: A prospective, blinded, controlled study. *Can Vet J*. 2006;47:437–445.
101. Steudel W, Scherrer-Crosbie M, Bloch KD, et al. Sustained pulmonary hypertension and right ventricular hypertrophy after chronic hypoxia in mice with congenital deficiency of nitric oxide synthase 3. *J Clin Invest*. 1998;101:2468–2477.
102. Hohimer AR, Mysliwiec M, Lee K, Davis LE, Pantely GA. Perinatal hypoxia causes ventricular enlargement associated with increased atrial natriuretic peptide (ANP) mRNA levels in newborn mice. *High Alt Med Biol*. 2003;4:241–254.
103. Emoto N, Raharjo SB, Isaka D, et al. Dual ECE/NEP inhibition on cardiac and neurohumoral function during the transition from hypertrophy to heart failure in rats. *Hypertension*. 2005;45:1145–1152.

104. Howard PG, MacLeod BA, Walker MJ. Quinacainol, a new antiarrhythmic with class I antiarrhythmic actions in the rat. *Eur J Pharmacol*. 1992;219:1–8.
105. Aberra A, Komukai K, Howarth FC, Orchard CH. The effect of acidosis on the ECG of the rat heart. *Exp Physiol*. 2001;86:27–31.
106. Appleton GO, Li Y, Taffet GE, et al. Determinants of cardiac electrophysiological properties in mice. *J Interv Card Electrophysiol*. 2004;11:5–14.
107. Chiba K, Sugiyama A, Hagiwara T, Takahashi S, Takasuna K, Hashimoto K. In vivo experimental approach for the risk assessment of fluoroquinolone antibacterial agents-induced long QT syndrome. *Eur J Pharmacol*. 2004;486:189–200.
108. Dhein S, Krusemann K, Schaefer T. Effects of the gap junction uncoupler palmitoleic acid on the activation and repolarization wavefronts in isolated rabbit hearts. *Br J Pharmacol*. 1999;128:1375–1384.
109. Pereira GG, Larsson MH, Yamaki FL, et al. Effects of propofol on the electrocardiogram and systolic blood pressure of healthy cats pre-medicated with acepromazine. *Vet Anaesth Analg*. 2004;31:235–238.
110. Winterton SJ, Turner MA, O'Gorman DJ, Flores NA, Sheridan DJ. Hypertrophy causes delayed conduction in human and guinea pig myocardium: Accentuation during ischaemic perfusion. *Cardiovasc Res*. 1994;28:47–54.
111. Rang WQ, Du YH, Hu CP, et al. Protective effects of calcitonin gene-related peptide-mediated evodiamine on guinea-pig cardiac anaphylaxis. *Naunyn Schmiedebergs Arch Pharmacol*. 2003;367:306–311.
112. Cojoc A, Reeves JG, Schmarkey L, et al. Effects of single-site versus biventricular epicardial pacing on myocardial performance in an immature animal model of atrioventricular block. *J Cardiovasc Electrophysiol*. 2006;17:884–889.
113. Gelzer AR, Attmann T, Radicke D, Nydam D, Candinas R, Lutter G. Effects of acute systemic endothelin receptor blockade on cardiac electrophysiology in vivo. *J Cardiovasc Pharmacol*. 2004;44:564–570.
114. Weber KT, Dennison BH, Fuqua JM, Jr, Speaker DM, Hastings FW. Hemodynamic measurements in unanesthetized calves. *J Surg Res*. 1971;11:383–389.
115. Mohan NH, Niyogi D, Singh HN. Analysis of normal electrocardiograms of jamunapari goats. *J Vet Sci*. 2005;6:295–298.
116. Chaves AA, Keller WJ, O'Sullivan S, et al. Cardiovascular monkey telemetry: Sensitivity to detect QT interval prolongation. *J Pharmacol Toxicol Methods*. 2006;54:150–158.
117. Dowell RT, Gairola CG, Diana JN. Reproductive organ blood flow measured using radioactive microspheres in diestrous and estrous mice. *Am J Physiol*. 1992;262:R666–R670.
118. Sarin SK, Sabba C, Groszmann RJ. Splanchnic and systemic hemodynamics in mice using a radioactive microsphere technique. *Am J Physiol*. 1990;258:G365–G369.
119. Chung CS, Yang S, Song GY, et al. Inhibition of Fas signaling prevents hepatic injury and improves organ blood flow during sepsis. *Surgery*. 2001;130:339–345.
120. Bauerfeind P, Hof R, Hof A, et al. Effects of hCGRP I and II on gastric blood flow and acid secretion in anesthetized rabbits. *Am J Physiol*. 1989;256:G145–G149.
121. Curran-Everett D, Morris KG, Jr, Moore LG. Regional circulatory contributions to increased systemic vascular conductance of pregnancy. *Am J Physiol*. 1991;261:H1842–H1847.
122. Bloomfield SA, Hogan HA, Delp MD. Decreases in bone blood flow and bone material properties in aging fischer-344 rats. *Clin Orthop Relat Res*. 2002;396:248–257.
123. Seifert EL, Sant Anna GM, Rohlicek CV. Effect of body warming on regional blood flow distribution in conscious hypoxic one-month-old rabbits. *Biol Neonate*. 2006;90:104–112.
124. Eckardt H, Lind M, Christensen KS, Hansen ES, Hvid I. Mid-tibial distraction osteogenesis redistributes bone blood flow: A microsphere study in rabbits. *Acta Orthop*. 2005;76:459–464.
125. Vertrees RA, Bidani A, Deyo DJ, Tao W, Zwischenberger JB. Venovenous perfusion-induced systemic hyperthermia: Hemodynamics, blood flow, and thermal gradients. *Ann Thorac Surg*. 2000;70:644–652.

Chapter 4
Measuring Cardiac Function

The normal cardiovascular system is a finely tuned pump and delivery system functioning together, with optimal efficiency, to match cardiac output to the integrated metabolic demands of the entire corpus. The inherent physical properties of the two systems contribute to the efficiency, and the physiological coordination of central and local control mechanisms assure that all tissues are supplied with appropriate blood supply. Under normal circumstances, local demands for blood flow are met by locally controlled adjustments and diversion of flow to metabolically active tissues without the need to increase pump function. When metabolic demands increase significantly, cardiac output must increase to meet the demand. If the heart is unable to meet the demand, the corpus is, by definition, in heart failure.

The problem for the physician treating patients and for the researcher studying the mechanisms and/or the treatment of cardiovascular disease is to be able to understand and quantify changes in or loss of function.

Hill[1] first described the force-velocity relationship of skeletal muscle, and Katz[2] determined that stretching of the muscle to different lengths before stimulating it produced increased force of the contraction. Subsequent studies revealed that sudden length changes at high stretching velocities resulted in a slightly concave force-extension relationship.[3] Significant work directed at characterizing the elastic properties and mechanical analogs of cardiac muscle has been done but part of the ambiguity and nonuniqueness of the classic concepts that have been described is attributable to the complex structure and difficulty in maintaining all aspects of a normal environment for the experimental preparations, usually isolated papillary muscle, ventricular strips or atrial strips, used to do these basic studies. All of these preparations include a large series elastic element of unknown nature and a nonuniformity of sarcomere lengths that make precise measurements of force, length, and velocity as functions of time difficult, if not impossible.

Contractility of cardiac muscle is defined as the ability to generate force and shorten. It is a function of the original length of the muscle (preload) and the interval between previous contractions (rate). It is dependent upon environmental conditions such as the ionic composition, the presence or absence of exogenous inotropic agents, the temperature, and the relative concentrations of an increasing number of identified endogenous substances and their receptors. Contractility is also dependent

D.R. Gross, *Animal Models in Cardiovascular Research*,
DOI: 10.1007/978-0-387-95962-7_4, © Springer Science + Business Media, LLC 2009

upon the load against which the muscle is contracting, the afterload. The quantification of afterload will be discussed in the next chapter.

Assessment of the mechanical properties of cardiac muscle is currently based on concepts derived from the mathematical theory of elasticity. This theory defines, in quantitative terms, the state of deformation within a solid body subjected to the action of a system of forces in equilibrium. The terminology of elasticity theory can be confusing. The following list of definitions might be helpful.

Elasticity is the property of recovery of a material to its initial configuration when stresses are applied and then removed. If the material assumes its initial form exactly it is "perfectly elastic," otherwise it is termed "inelastic."

Stress is defined as force/unit cross-sectional area of a material. It is generally resolved into normal or perpendicular, shear or torsional stress.

Strain is the deformation of a material produced by application of stress and is usually expressed as a percentage change from the unstressed dimensions. *Lagrangian strain* is expressed as $E_L = (l - l_0)/l_0$ where l_0 is the length corresponding to zero stress and l is the instantaneous (stretched) length. Lagrangian strain is most often used in studies of materials where deformations are small, i.e., metals. Zero state lengths are, technically, all but impossible to obtain in biological tissues.

Natural strain is more appropriately used when deformation is large. It is usually expressed as $E_N = \ln (l/l_0)$. In this case l is the stretched length and l_0 is the length at zero stress determined at a transmural, in the case of the heart ventricular, pressure of 0 mmHg. Sometimes l_0 is replaced with the preload length, with the end-diastolic dimension, or with l_{max}, the length at which maximum active tension is developed. These expedients violate the fundamental principle of elastic theory that says that when the stress is zero the Lagrangian strain should be zero.

Tension is a force that produces an extension; it is not the same as stress and has units of dynes or gram weight.

Compliance is defined as a change in volume in response to a change in pressure, dV/dP, and applies to hollow structures.

Distensibility is defined as a change in volume due to a change in pressure normalized by the original volume ($dV/V_o dP$) and is a more appropriate measure for both the heart and blood vessels.

Volume elasticity is the reciprocal of distensibility ($V_o dP/dV$) and has the same dimensions as stress.

Stress relaxation describes the decrease of stress with time when a material is held at a constant strain after a sudden increase in strain.

Creep is time-dependent elongation while held at a constant stress after a rapid change in stress. Both stress relaxation and creep are characteristic behaviors of biological materials.

Isotropy occurs when the elastic properties of a material are the same in all directions, common in gelatin, uncommon in biological tissues.

Anisotropy exists when the elastic properties of a material vary with direction.

Nonhomogeneous material is a description of a material when a small element from an elastic body does not possess the same specific physical properties as the original body.

Incompressibility describes a material when the volume elements are conserved during deformation.

Quantification of myocardial elasticity depends on the wall stress and the ratio of volume to mass, in addition to the change in pressure with changes in volume. Elasticity of the left, or right ventricle, is most commonly determined by changing the preload conditions, recording multiple pressure/volume loops, then connecting the end-systolic points of the pressure/volume loops. Compliance or distensibility can only be evaluated during diastole and cannot be determined at any single point in time. Recent advances in transgenic technology and the use of this technology to address specific mechanistic questions about cardiac performance using transgenic mice models have emphasized the importance of in vivo phenotyping of cardiovascular function. This poses a host of very specific technological problems because of the high heart rates and small size of the animals being used. These technological problems exist when making the necessary measurements in human subjects and larger animal models but are especially problematic in smaller species. Many of the citations that follow are from work done in mice. The same techniques are more easily applied, because of fewer technical limitations, to larger species.

The Pressure–Volume Relationship

Daniel Burkhoff, Israel Mirsky, and Hiroyuki Suga have provided an outstanding review for the assessment of both systolic and diastolic properties of the left ventricle using the pressure-volume analysis.[4] The reader is referred to this article for an understanding of the basic concepts that govern the use of the pressure-volume relationship, how real-life applications of the concepts differ from the ideal conditions, how to appropriately analyze the end-systolic and end-diastolic information generated, and to become aware of the most common problems associated with the application of the theoretical concepts.

Several studies have demonstrated that the end-systolic pressure-diameter relationship is only approximately linear and in many instances is distinctly nonlinear, particularly in mice.[4,5] When the end-systolic pressure-volume relationship (ESPVR) is used to compare contractility between experimental groups both the slope (E_{es}) and volume axis intercept (V_0) should be reported. This is somewhat problematic because, in many individuals of all species, the linear extrapolation of the slope of the ESPVR to zero pressure provides a negative volume. This is, obviously, a physical impossibility.

The statistical analysis of these data is frequently done using the Student's *t* test and this is not correct. Multiple linear regression analysis (analysis of covariance) is more appropriate. If the appropriate statistical analysis demonstrates that the ESPVR is significantly different due to some perturbation or change of condition, the average values of E_{es} and V_0 can be used to describe the direction the curves have shifted but only within the range of the actually measured values.[4]

It seems clear that the currently cited approaches for normalizing E_S to reflect the influence of chamber size and geometry are inadequate. Because this is true, current thinking is that myocardial contractility should be evaluated using the concept of the end-systolic myocardial stress-strain relationship. This method of evaluation yields a measure of myocardial stiffness at end-systole. The chamber stiffness index (β_w) and myocardial stiffness index (k) provide parameters of passive chamber and myocardial properties that are both load and chamber-size independent. These indices should also be statistically evaluated using multiple linear regression techniques.[4]

The end-diastolic pressure-volume relationship (EDPVR) is clearly nonlinear but provides a measure of passive ventricular diastolic properties. Because of the nonlinear character of this relationship, it is imperative that statistical tests used to evaluate changes must account for covariance in parameter values. When the question posed by the experiment is dependent upon the size of the heart, a measure of compliance (capacitance) or distensibility at a specified filling pressure is appropriate. This parameter can be measured under most experimental conditions and differences can, appropriately, be determined using the Student's t test.[4]

Another Measure of Ventricular Elasticity

A technique based on modeling the actual long axis displacement of the mitral annulus as a linear damped oscillator with time-varying coefficients has been published. The technique is reported to estimate viscoelastic properties as well as the elastic component. In this model, elastic deformations resulting from changes in the mechanical properties of the left ventricular myocardium are represented as a time-varying spring and the relaxation and a time-varying viscous damper represents frictional energy losses. The advantage of this technique is that it could be applied noninvasively using ultrasound diagnostics. Time will tell whether this model will be accepted and used by researchers.[6]

Measurement of Electrical Activity

Berul and colleagues[7,8] used epicardial and six-lead body surface ECG data to characterize normal cardiac conduction properties in mice. They were able to determine AV conduction properties as well as atrial, AV, and ventricular effective refractory periods. ECGs were monitored on an oscilloscope and recorded at 100 mm/s paper speeds. Pacing thresholds were determined for each lead and stimulation performed for 1.0 ms pulse widths at 2× the diastolic threshold. They were able to determine the ECG frontal axes (P and QRS) and time intervals (PR, QRS, QT, JT, and RR). They derived the QT_c as the rate corrected QT interval as described by Bazett[9] and the JT_c as the rate corrected JT interval ($JT/RR^{1/2}$).[7]

Two different 8-electrode catheters (2 F, CIB'ER, NuMed, Hopkinton, NY or the 1.1 F, EPR-100, Millar Instruments, Houston, TX) were used to record ECG signals and for pacing. Recordings were made from the right ventricle and from catheter placement in the esophagus over the heart. Minimum current amplitude required for capture during intracardiac pacing was approximately 100 μA and for transesophageal pacing approximately 800 μA. All standard ECG time intervals were successfully determined and Qt_c values calculated. After recording a period of normal, sinus rhythm hearts were paced for 10 s and the cycle length was decremented by 10 ms segments. The sinus node recovery time (SNRT) was determined for each pacing cycle length and corrected by subtracting the intrinsic cardiac cycle length from the recovery interval. The hearts were paced at rapid rates to assess A-V conduction properties. The maximum cycle lengths resulting in Wenckebach and in 2:1 A-V conduction were determined. Refractory periods were determined by delivering an 8-stimulus drive train at a 100 ms cycle length followed by a premature stimulus that was progressively decremented in 5 ms intervals. A-V nodal, atrial, and ventricular effective refractory periods were defined as the longest drive train to premature stimulus coupling interval for each region that failed to generate a propagated beat.[10]

Hofer et al.[11] describe a flexible sensor used to measure the surface potential and its electric near field on the epicardial surface. During depolarization, the electric near field describes a vector loop. Using this information, they were able to compute the magnitude of local conduction velocities. The sensor consists of four recording electrodes (14×14 μm^2) separated by 50 μm conducting leads on a 50-μm thick polyimide film. The low mass and flexibility of the sensor allows it to ride beating mouse hearts without significant displacement even at heart rates of 600 beats/min.

Telemetry is an effective way to monitor ECG data in small rodents. A commercially available system is available (Data Sciences, St. Paul, MN) that uses an implantable radio frequency transmitter weighing just over 3.5 gm. A receiver for the system can be placed near the cage of each animal being studied. The system produces a high-level, single-channel, 1-100 Hz band pass filtered ECG. The analog signal can be digitized at 500 Hz using an A/D converter and recorded digitally. The resulting ECGs can then be analyzed by signal-averaging software to produce signal-averaged complexes for analysis and comparison.[12]

Measurement of Pressure

Hellige[13] determined the dynamic response characteristics of 38 fluid-filled catheter manometer systems. The worst of the systems were only flat to 5 Hz and the best were flat to 26 Hz. This means, of the systems tested, most were only satisfactory for recording pressures in human subjects at rest. The more high frequency systems were capable of recording dP/dt accurately at moderately high heart rates induced by inotropic stimulation of the heart. Phase distortion was also negligible in this

range of heart rates. Low compliance transducers yielded the best results. The lower frequency response systems overestimate dP/dt_{max}. The use of low frequency pass filters to attenuate high frequency artifacts is not effective. Another study by the same author[14] compared fluid-filled to catheter tip manometer systems. This study indicated that the fluid-filled systems resulted in appreciable errors in dP/dt_{max} because of the inadequate dynamic response characteristics of these systems in relation to the frequency content of the pressure curves. Normal heart rates in human subjects yielded errors in dP/dt_{max} of <10% if the frequency response of the system was flat to 10 Hz, equal to the first 10 harmonics of the heart rate. If we assume that these heart rates were in the range of 100 beats/min, we can extrapolate that in mice, with heart rates of 400-600 beats/min we need a catheter system flat to >60 Hz. Both fluid-filled and catheter-tip manometer systems were sensitive to temperature and should be equilibrated at the normal body temperature of the subject animal prior to use.[14]

Using a hydraulic sinusoidal pressure wave generator, Branzi et al.[15] found that systems used clinically that were flat to 5 Hz measured left ventricular pressure waves adequately, but dP/dt measurements with a Cook 5.2 F, 105 cm fluid-filled catheter and manometer system had a 28-31% error. The most commonly used catheter-tip manometer systems for mice, 1.2-2.0 F (Millar MIKRO-TIP, Millar Instruments, Houston, TX) is advertised to have a frequency response flat to 10,000 Hz, and is capable of accurately measuring pressure fluctuations in animals with very high heart rates, particularly when coupled to a system capable of recording at a sampling rate >1 kHz.[16-18]

The usual parameters derived from measurements of ventricular pressures are systolic pressure, end-diastolic pressure, the maximum and minimum values of the first derivatives of pressure (dP/dt_{max} and dP/dt_{min}), and the time needed for relaxation of 50% of maximal ventricular pressure to baseline (tau, τ).[19] Wang and colleagues[20] developed a new catheter for the measurement of left ventricular pressures in conscious mice. They used the balloon-pop test and demonstrated that their "Pebax" catheter with an internal diameter of 0.3 mm had a flat frequency response to 50.5 ± 0.6 Hz and found no difference in measurements between their system and a 1.4 F Millar catheter-tip manometer system during measurements of heart rate, left ventricular systolic pressure, LV dP/dt_{max}, LV dP/dt_{min}, ejection time or τ in mice.

Echocardiography

History

Behm described the use of ultrasound to measure ocean depths in 1921. In 1929, Sokoloff used the technology to detect flaws in materials. In 1946, Denier suggested that ultrasound might be able to produce images of internal organs. Keidel first described the use of ultrasound to record volume changes with each beat of the

heart in 1950. He was not able to quantitate the volume changes because of some technical problems such as the inhomogeneity of the beam he used, the formation of standing waves, and the insufficient beam width. Ludwig and Struthers reported the practical use of reflected ultrasound in 1949. They used a combined transmitter and receiver to generate very short pulses of ultrasound and record the echo signal received on an oscilloscope screen. They repeated the procedure 200 times per second and thus described the first A-scan or A-mode (Amplitude) echogram. The first cardiovascular related use of diagnostic ultrasound was for the diagnosis of pericardial effusion and mitral valve disease reported by Edler in 1955. Hertz and Edler borrowed an ultrasonic reflectoscope from the Siemens Corporation in 1953. This device had the capability of varying pulse length and intensity. The pulse repetition rate was fixed at 200/s and the pulse intensity could be raised to a maximum of approximately 2 W/cm^2. Ultrasound frequencies of 0.5, 1.0, 2.5, and 5.0 MHz could be generated. The transducer was a quartz crystal with a surface diameter of 12 mm. The A-scan (amplitude-modulated) produced by this machine provided only information about the distance between the transducer surface and the echo-producing structure. Hertz built a camera and was able to feed 35-mm film through it at a constant speed. Using a horizontal slit in the image plane of the camera objective and placing the camera in front of the oscilloscope, he was able to record motion of the heart and this display was later dubbed "motion-mode" (M-mode). An improvement was made when echo and the ECG were simultaneously recorded. In 1958, Siemens supplied a new type of piezoelectric transducer using barium titanate instead of quartz. The new transducers made recordings of more heart structures possible, including the aortic outflow tract and all of the cardiac valves.[21]

Feigenbaum and colleagues were able to generate considerable interest in the use of ultrasound technology as a noninvasive technique for measuring left ventricular function.[22-25] Interestingly, the first paper describing the measurement of the internal dimensions between the interventricular septum and the posterior left ventricular wall was rejected by all of the major cardiology journals. R.L. Popp, who was a cardiology fellow at Indiana with Feigenbaum, went on to Stanford and repeated the studies he helped with in Feigenbaum's laboratory. He was able to publish the techniques and results only after Feigenbaum reviewed and accepted the manuscript.[21]

Wild and Reid developed the first two-dimensional ultrasound imaging system in 1952, but their system could not produce the large number of images per second required to produce real-time images. Hertz and Olofsson developed a system that scanned the heart using an oscillating ultrasonic mirror system that used separate transmitting and receiving transducers with an elliptic, hyperbolic mirror. Immersing the mirror-transducer system in a water bath provided acoustic coupling between the various components of this system. A rubber bellows was used to couple the system to the transducer. The entire transducer system was rocked back and forth in the water bath. The lateral resolution of the system was very good but its inertia limited the frame rate that was attainable. At 1-MHz it was possible to achieve lateral resolution of about 2 mm at depths from 50 to 110 mm into the thorax with a longitudinal resolution of about 3 mm. In 1967, Asberg was able to scan the heart

at rates of 6-7 frames/s. Despite excellent lateral resolution, high sensitivity, and the large aperture angle provided by the optical mirror system, it resulted in distorted images because of the low frame-rate and because the narrow reflected beam fell mainly on the transmitting transducer shielding the receiving transducer. Hertz and Lindström developed a system consisting of six separate mirror elements. The driving shaft was rotated so the focal point of the upper ultrasound mirror described an approximately flat scanning movement for a part of the rotation. The next mirror then came into position and was activated and so on. A single transducer was used for both transmission and reception. The system was originally designed for 16 frames/s but the speed was increased to 25 frames/s. The latter system provided real time heart images without excessive dynamic distortion or flickering. However, the large scanning head required that the patient be positioned head down on a special bed with a hole through the mattress. The hole allowed the water-filled rubber bellows needed for acoustical coupling to be placed in contact with the chest wall.[21]

Ebina et al. performed experiments on excised human hearts and living dogs. Their real time 2D system had poor penetration at 10 MHz and poor resolving power at 1 MHz. They used 2.25 or 5 MHz with a repetition rate of 500/s in their studies and produced the first gated studies obtaining good images of the heart, great vessels, intra-cardiac structures, sizing of the cardiac chambers, and measuring the thickness of the cardiac and vascular walls.[21]

Nicolass Bom presented the first real-time linear array images of the moving heart in 1971. He used 20, parallel, single-element, brightness-modulated lines (B-modes) that were activated sequentially but almost instantaneously. Each transducer element had a separate excitation stage and reception circuit so each, in sequence, transmitted a short acoustic pulse and received the echoes. The depth of the structures was indicated on the horizontal axis of an oscilloscope while the vertical position of each line corresponded to the position of the respective element in the transducer. He achieved a scan rate of 150 frames/s and obtained information of anatomical relationships of the major cardiac structures, valve motion, and thickening and calcification of valves.[21]

Griffith and Henry published a sector scanning method for 2D cardiac images in 1974. They developed a scanner modified with a mechanical motor that oscillated a standard transducer through either a 30° or 45° sector. They were able to achieve about 30 frames/s and there was no significant signal loss or distortion caused by the scanning motion. The high line density and well-collimated beam produced high quality frames superior to those achievable with the multielement system.[21]

Physics of Echo Technology

Range resolution is the minimum distance between two point targets at which separate registrations can be distinguished. Distance resolution is determined by the shape, amplitude, and length of the ultrasound pulse. A pulse length or distance resolution of about 1 mm is probably short enough to separate echoes from within the human-sized

heart. That distance can be achieved using a 1-MHz transducer while a 2-MHz transducer results in a 3-dB distance resolution of about 0.75 mm. The amplitude of the echo signal also varies as the structures within the heart move. A change in echo amplitude of about 20 dB introduces a positional error in range resolution of 0.3-0.5 mm. A transducer disc diameter of 0.5 in. at 1 MHz produces an ultrasound beam with a 15° divergence. A narrower beam can be achieved at higher frequencies but higher frequencies do not penetrate tissues as well as lower frequencies.

Echo signals returning from various structures in the beam arrive at the transducer at different times, depending upon their location. The system must include delays in the processing of the echoes received so that the effective orientation of the array during reception corresponds to the orientation of the transmission. These delays must be varied so that the echoes returning from different depths in a particular direction will arrive at the summing amplifier in phase. After summation the signal is processed while echoes from all other directions will not be in phase and therefore will be partially ignored.

Ha et al.[26] assumed that there is a degree of finite noise in frame-to-frame motion estimation and that speckle partially decorrelates between successive frames during freehand scanning. Components of diagonal motion due to the limitations of manual transducer movement were assumed to be responsible for decorrelation. They determined that an optimal step size exists and is dependent upon the signal to noise ratio, angle of the diagonal motion transducer geometry, lens focusing parameters, transducer operating frequency, and beam forming parameters. They also found that the optimal step size requires using every available image frame.

The average speed of ultrasound in soft tissue is 1,540 m/s. In man, the distance from the chest wall to the posterior heart wall is about 15 cm. The distance the ultrasound wave has to travel is, therefore, 30 cm, out and back. Thus the time required is 0.3/1,540 approximately 195 μs. In this instance, the maximum number of pulses that can be transmitted is 5,000/s. The maximum repetition frequency is also limited by the dead time necessary to convert from receiver to transmitter. The frame rate is very important when recording rapidly moving structures. In man at resting heart rates, the aortic leaflets open at about 300 mm/s. The movement amplitude of each leaflet is about 10 mm so the full excursion of the leaflet takes about 33 ms. To analyze the movement pattern of a leaflet a frame rate of >30 frames/s is necessary. Although increasing the frame rate allows more detailed motion analysis, it decreases the number of lines available for each individual frame. With pulse repetition frequencies of 4,500 lines/s and a frame rate of 100/s, there are only 45 lines per frame. When the lines per frame are reduced the quality of the images is also reduced.

High-frequency ultrasound biomicroscopy technology has been stimulated by the need for cardiovascular phenotyping of mice, particularly transgenic mice, serving as models of human disease. This high-resolution technology is also useful in ophthalmology, dermatology, and for the measurement of microvascular flow. Several systems capable of operating in the 20-75 MHz range are now available commercially. These systems offer 2D (B-scan) and power Doppler capability. Color flow imaging and elastographic imaging will be available. Most of the echocardiographic

data now published for mice is performed using a single-element transducer and mechanical sweep-scan techniques. With B-scan imaging the frame rate of the imaging system is an important limitation. Typical frame rates of the high-frequency systems now available range from 30 to 60 frames/s and are dependent upon the scan width, scan depth, and transducer beam width. To image mice hearts with a scan width of 10 mm, a scan depth of 9-18 mm, a transducer beam width of 180 μm, and a lateral step size of 25 μm, the estimated maximal frame rate would be about 100 Hz. At that frame rate, an adult mouse heart would be imaged at only 10-20 frames per beat. A frame rate that low drastically reduces the ability to quantify wall and valve motion and spatial-temporal artifacts will result in artifactual geometrical deformations of the heart during both systole and diastole. This occurs because at a frame rate of 100 Hz, the collection of single frame RF data occurs over 10 ms and during that amount of time the mouse heart undergoes significant shape changes.[27]

Doppler Flow Velocity and Tissue Doppler Imaging

History

At a meeting of the Royal Bohemian Society of Sciences in Prague on May 25, 1842, Christian Doppler presented a paper entitled, "On the colored light of double stars and some other stars on the heaven." On the basis of his observations and calculations, he concluded that changes in wavelength of light from stars were related to changes of relative motion between the observer and the light source. He suggested that if a light source and an observer are both stationary the observed frequencies of the light are the same. If the observer moves toward the light source the frequency increases and moving away the frequency decreases. In 1845 and 1848, Doppler's theory was tested in similar experiments by Christoph Ballot and Scott Russell who used moving train locomotives. Ballot used two musicians with perfect pitch, one on a moving locomotive blowing a single note on a horn, the other stationary as the locomotive approached and passed, reporting on the pitch of the note. Russell observed a significant difference between the tones of his locomotive's whistle blowing continuously as it passed through a tunnel at high speed. In 1956, Howard Hardy was granted a US patent for an apparatus for measuring vibrations. That application said, in part; "…Due to what is known as the 'Doppler' effect, the frequency of the reflected sound will deviate from the fixed frequency of the transmitted wave in direct proportion to the velocity of the movable or vibrating surface…" The same year Dr. Shigeo Satomura published his work for the design of a device using ultrasonic Doppler techniques and suggested it might prove useful for cardiac applications. He worked in collaboration with Dr. Yasuharu Nimura and his department chair, Professor Tsuneo Yoshida. They reported cardiac data obtained using a 3.5 MHz transducer at the 20th Annual Meeting of the Japanese Circulation

Society in March 1956. Drs. Nimura and Satomura continued their collaboration and published results demonstrating that the time interval between closing and opening of the heart valves could be used to determine the duration of isometric contraction and relaxation of the ventricles and the clinical significance of prolonged relaxation.[21]

Dr. Eng. Kanemasa Kato constructed the first apparatus to combine echo and Doppler technologies. In 1960, he reported on a probe with an inner disc-like transducer and outer disc arranged concentrically. The inner, 3 MHz, disc was used for the Doppler signaling and the outer one for the pulse-echo at 2 MHz. The pulse repetition rate of his device was 1,000-2,000 cycles/s with an impulse length of 20 μs. The Doppler signals from this device were processed using both a band pass filter and a sound spectrograph or sonogram. The sonogram represented time on the abscissa and frequency on the ordinate. The density of color corresponded to the frequency. During the same timeframe, Dr. Satomura and his colleagues developed techniques for studying peripheral blood flow. Dr. Kato and coworkers were able to demonstrate that the Doppler velocity signals resulted primarily from scattering of ultrasound by red blood cells and that the power of the Doppler output was proportional to the number of RBCs per unit volume. This finding was the basis for the quantitative measurement of blood flow developed by Franklin and his colleagues and reported in 1961 and 1966. The combination of continuous wave Doppler and 2D imaging in 1982 made use of the technology widely available. Color-coded Doppler, reported in 1984, increased the usefulness of the technology making it possible to record velocities and to obtain noninvasive estimates of pressure drops across valves and between chambers, the assessment of valve lesions, and congenital lesions as well as important information during both diastole and systole.[21]

Physics of Doppler Technology

Color flow imaging is limited by the sweep-scan technique since the motion of the transducer causes a broadening of the tissue and blood Doppler spectra resulting in spectral overlap. This is a particular problem when trying to measure slow flows as in the microvasculature. It is possible to prevent transducer motion artifact by tissue clutter filtering but this significantly reduces sensitivity to slow flow.[27]

Errors caused by intrinsic spectral broadening (ISB) are related to the Doppler angle. In general, experienced users of Doppler technology keep the Doppler angle under 60° but even at this angle ISB can produce a 40% overestimation of peak velocities. Ideally a Doppler angle of 45° or less would reduce this source of error but technical problems make this difficult in most applications. Using the transverse Doppler equation as a correction for ISB, in conjunction with the classical Doppler equation, apparently improves the accuracy of peak velocity measurements.[28]

The time-frequency of the Doppler blood flow signal is normally computed by using the short time or fast Fourier transform (FFT). This transform assumes stationarity of the signal during a finite time interval imposing constraints on the estimate.

Additionally, the FFT has a fixed time-frequency window, which means it cannot be used to accurately analyze signals with a relatively wide bandwidth that change rapidly with time. Use of the wavelet transform, with a flexible time-frequency window, can be used as a signal-processing tool for Doppler blood flow signals and can generate a time-frequency representation with better resolution than the FFT.[29]

The precision of the velocity estimate increases with the ensemble size used for the estimation. When the sweep-scan technique is used the maximum ensemble size depends upon the beam width, transducer sweep velocity, and pulse repetition frequency (PRF). This same set of parameters also determines the frame rate, thus the choice of an ensemble size also limits the frame rate. Estimation of blood velocities up to 10 mm/s using a 40 MHz transducer with a 100-μm focal spot dictates a maximum frame rate of approximately 0.3 frames per second (fps). This assumes an ensemble size of 50 and a field of view of 4×4 mm^2. This poses significant problems when using the technology on mice. The low frame rate produces significant spatial-temporal artifacts because the blood velocities displayed on a single frame would be estimated over a period significantly longer than the mouse heart cycle period. The sweep velocity and frame rate could be increased by decreasing the ensemble size but this would result in lower precision of the velocity estimate. If the PRF is increased the result is a lower resolution of the Doppler spectrum. Increasing the sweep velocity would also cause an increase in tissue and blood spectrum broadening. These difficulties can be addressed by using a technique involving ECG-gating data acquisition. The ECG is used to trigger the transmission of pulse ensembles at successive positions while the transducer is kept in a fixed position. These data are then reassembled, line-by-line, according to the time of acquisition relative to the ECG trigger signal. Cine loops of B-scan images or color flow images are produced at a frame rate equal to the PRF. The technique is referred to as retrospective B-scan imaging (RBI) and retrospective color flow imaging (RCFI).[27] Unfortunately, as this is being written, most investigators using duplex technology in mice are not yet using RBI and RCFI.

Tissue Doppler Imaging

Hartley and colleagues first described the technique using a single-crystal ultrasound device to integrate the velocity of the various myocardial layers that pass back and forth through a range-gated sample volume located within the myocardium at a fixed distance from the epicardial surface. This method of measuring displacement does not require accurate tracking of an interface, a significant problem with echo tracking of endocardial motion in animals with high heart rates, and is less sensitive to changes in echo amplitude as the interface moves and changes orientation.[30,31]

Tissue Doppler imaging (TDI) was used to measure endocardial and epicardial systolic velocities and strain rates in mice. Low measurement variability was reported and the technique was able to track changes in the parameters with dobutamine,

esmolol, and endotoxin perturbations.[32] The technique is also able to detect torsion. This is important since recent work demonstrates that untwisting of the left ventricle appears to be linked, temporally, with early diastolic base-to-apex pressure gradients that may assist efficient left ventricular filling. Left ventricular torsion and subsequent rapid untwisting appear to be manifestations of elastic recoil and link systolic contraction to diastolic filling.[33] TDI obtained parameters have been shown to be more independent of pre and afterload than the usual Doppler-derived cardiac measurements.[34]

Examples of Ultrasound Data Reported Using <20-MHz Transducers

Liu et al. used an Acuson c256 with a 15-MHz linear transducer to estimate ejection fractions (EF) from short-axis views on LV diastolic area and LV systolic area in mice. Tracing the chamber outlines manually then digitizing with software installed in the unit made dimension measurements. Three beats were averaged for each measurement.[35]

A Hitachi EUB 8000 was used for transthoracic echocardiography using a 13-MHz linear scanner. M-mode echocardiograms were used to record the left ventricular end-diastolic dimensions and percent fractional shortening in hamsters.[36] Another group used a standoff with a 15-MHz linear array transducer and a Power Vision 8000 unit from Toshiba in mice. Depth was set at 2 cm in the zoom mode to optimize resolution and penetration. Short-axis 2D images were acquired at the level of the papillary muscles at a sweep speed of 100 mm/s. Measurements of the thickness of the left ventricular anterior and posterior walls in both systole and diastole were made.[37]

Using a Sequoia C256 System with a 15-MHz linear array transducer 2D-guided M-mode and Doppler echocardiographic studies of aortic and transmitral flows were performed in rats. End-diastolic and end-systolic dimensions were measured using software included with the equipment. The percent fractional shortening was calculated from the dimension measurements. Ejection time and the isolvolumic contraction and relaxation times were calculated from three consecutive beats and averaged to calculate a myocardial performance index (MPI), the sum of the isovolumic contraction and relaxation times divided by the ejection time.[38]

Rats were studied using a HDI 5000 SonoCT ultrasound system, a 12.5-MHz phased-array transducer with a 0.3 cm standoff and a 15.7-MHz broadband linear transducer. Two-D, M-mode, and color and spectral Doppler images were acquired from the parasternal short-axis, modified parasternal long-axis and modified apical four-chamber views. Parameters of left ventricular function were peak E-wave velocities, peak A-wave velocities, and the E/A ratios. At high heart rates the fusion of E and A-waves made A-wave measurements unreliable. Left ventricular volumes were estimated using the Teichholz Method, the area-length method (using a prolate ellipsoid model), and the modified Simpson's method. All were compared with the

LV volume measured by morphometry. Measurements were also made of LV fractional shortening, fractional area change, ejection fraction, anterior wall thickness, end-diastolic diameter, and cross-sectional area.[39]

C57BL/6N mice were used to evaluate the effect of anesthesia on echocardiographic parameters. A Sonos 5500, with L15/6-MHz transducer, was used to obtain LV M-mode images with the mice in the left lateral decubitus position. A parasternal short-axis view at the papillary muscle level was used. Measurements were estimated for heart rate, end-diastolic dimension, percent fractional shortening, and aortic ejection times. The group reported intraobserver variability for LV chamber diameter measurements in this strain of mice of 0.9% ± 8.2%.[40]

Two-dimensional guided M-mode tracings of the LV were obtained with sweep speeds of 100 mm/s using a Sonos 5500 ultrasound machine and a 15-MHz linear-array transducer. Using the leading edge technique, values were determined for LV internal dimensions and wall thickness during both systole and diastole. Measurements were taken from two cardiac cycles and averaged. Following the M-mode recordings long-axis 2D image guided color Doppler recordings were obtained. Peak flow velocities, isovolumic-relaxation time, and E-wave deceleration times were calculated as the average of 7-10 cycles.[41]

Echocardiography using a VIVID 7 and a 13-MHz linear array transducer was performed on mice. Right ventricular 2D images were obtained in the short-axis view that also provided a transverse section of the LV at the mitral valve end of the papillary muscle. The transverse diameter of the RV, including the free wall, was found to be a more accurate measure than separately measuring the cavity and free wall diameters since there was difficulty in discriminating the RV free wall in some animals. Intra and interscorer reliability for RV measurements was found to be acceptable with a mean difference of <10%.[42]

In human subjects, very high quality data are obtained with lower frequencies. Short-axis parasternal views for effective mitral valve area determination and transmitral pulsed-Doppler flow velocity images were recorded using a model C256 Acuson Sequoia equipped with a 2-MHz transducer. Twenty to thirty consecutive heartbeats were digitally stored for analysis. Transmitral Doppler E and A-waves were used in a model-based image processing procedure extensively tested in this laboratory. The conclusions reached were that an in vivo validation of average, early, and passive chamber stiffness could facilitate quantitative, noninvasive diastolic function, based on an analysis of transmitral flow.[43]

Examples of Ultrasound Data Reported Using 20-MHz (or Greater) Transducers

Zhou and colleagues used aVS40, VisualSonics biomicroscope with a transducer frequency of 40-MHz to image murine embryonic hearts. They were able to obtain lateral resolution of 68 μm and axial resolution of 38 μm. The pulsed Doppler operating frequency was set at 20 MHz for blood flow velocity measurements. The

Doppler sample volume was $104 \times 257\ \mu m^2$, and the PRF was set at 25 kHz, which enabled the measurement of velocities up to 50 cm/s. They were able to record flow velocities from both the mitral and tricuspid valves of embryonic hearts.[44]

A Vevo 660 VisualSonics ultrasound machine with a single element oscillating transducer with a center frequency of 35-MHz, a focal length of 10 mm and frame rate of 30 Hz was used to image mice. The lateral and axial resolutions for the probe used were $115 \times 55\ \mu m^2$. The axial dimension of the sample volume when used in the pulsed-wave Doppler mode was set at 0.3 mm for recordings made in the common carotid artery and to 0.51 mm for recordings in the ascending and abdominal aorta. Images of the heart were obtained in B-mode using the parasternal long-axis view. The M-mode sampling line was perpendicular to the ascending aorta so that changes in aortic diameters could be visualized. For Doppler recordings the beam angle was $<60°$.[45]

The Vevo 660 VisualSonics with a 30-MHz transducer was used by Zhang et al.[46] for measurements in mice. They used the parasternal long-axis, parasternal short-axis, and apical four-chamber 2D views to measure LV end-systolic, end-diastolic volume, ejection fraction, fractional shortening, LV mass, a wall motion score index (WMSI), a myocardial performance index (MPI), E-wave peak velocities, A-wave peak velocities, and E/A.

Transcutaneous blood velocity waveforms were obtained from the ascending thoracic aorta of mice using a 20-MHz pulsed Doppler system with a hand-held probe. Ascending aortic diameters were measured during systole from an image of the long-axis of the LV outflow tract using 19 and 30-MHz transducers. Waveform data were analyzed to calculate heart rate, stroke distance, i.e., the velocity envelope integrated over the ejection time and mean velocities. Mean velocity and stroke distance were multiplied by cross-sectional area to determine stroke volumes and cardiac output. The mitral flow velocity recordings were analyzed to obtain peak and time durations for E- (early diastole) and A- (atrial contraction) waves.[47]

Recently a group from Baylor College of Medicine reported on the development of a high frequency, high-resolution Doppler spectrum analyzer (DSPW). They compared the performance of this device to an adapted clinical Medasonics spectrum analyzer and a zero-crossing interval histogram they have used previously. They found the DSPW provided significantly higher values for aortic velocity and aortic acceleration than the other two devices. Aortic ejection times were shorter and isovolumic relaxation was longer with the DSPW. They concluded that the performance of the DSPW was superior to the other two analyzing devices and will prove to be especially valuable for the detection of stenotic jet velocities and vortex shedding frequencies as well as being able to detect subtle changes in wave shapes in peripheral vessels not possible with currently used clinical Doppler systems.[48,49]

Another recent report describes two scanning methods for obtaining cardiac images in mice that do not require high-frequency transducer arrays. The first method uses images from the isovolumic contraction and relaxation phases and simultaneously recorded ECG signals. The ultrasound images are, retrospectively, reconstructed within a relatively short data acquisition time using the ECG to trigger the imaging system. The second method uses the line-scanning mode, with ECG

gating, to acquire and reconstruct the entire cardiac cycle. The effective frame rate is determined by the PRF and can be up to 2 kHz in the system described.[50]

Summary of Information Needed to Ascertain the Reliability of Ultrasound Data

Unfortunately, it is rare to find all the information that should be available to determine how good ultrasound derived data are, in most published reports, especially from animals with high heart rates. Information regarding the acquisition of echo data should include the frequency of the transducer, the range resolution, the distance resolution, the beam width and/or divergence, the PRF, and the frame rate. When reporting Doppler-derived data, it would be very helpful to have information about the transducer frequency, the Doppler sample volume, the PRF, the Doppler angle, the focal spot distance, the frame rate, and the ensemble size.

Techniques for Measuring Ventricular Volumes

The measurement of ventricular volume as a function of time and pressure is of paramount importance for the evaluation of myocardial performance. Left ventricular volume measurements are reasonably straightforward but significant technical difficulties do exist. Accurate right ventricular volume measurements are more problematic because of the complex geometry.

Radiographic

Right ventricular angiography was described in the mid 1940s.[51] Angiographic determination of left ventricular volumes takes advantage of representing the geometry of the ventricle as a prolate ellipsoid. Simple mathematics, using measurements from single plane angiograms, makes the volume calculation straightforward.[52] The advent of biplane angiography allowed the use of the multiple slice technique for measuring the volume of complex geometries.[53] Angiographic techniques are time consuming and require digitization and, in most cases, manual identification of the borders.

Many investigators have used radiopaque markers implanted in the heart to measure dimensions and to evaluate parameters such as wall-thickening, fiber shortening, shortening velocities, and to generate strain data.[54] Problems with this technology involve the necessity for orthogonal imaging to obtain three-dimensional movement, the need for invasive surgical placement of the markers, the possibility of scar formation from the surgery and from the embedded foreign bodies, and the

ability to generate frame rates fast enough to capture the movement in animal models with high heart rates.

Echocardiography and Tissue Doppler Imaging

The previous discussion of these techniques detailed the problems inherent in their use. Ignorance, or lack of reporting, of transducer frequencies, range, and distance resolution, beam width and/or divergence, pulse repetition frequencies, and frame rates for echo-derived data and transducer frequency, Doppler sample volume, PRF, Doppler angles, focal spot distances, frame rates, and ensemble size for Doppler-derived data hamper the use of these technologies. Without this information it is difficult to determine the reliability or accuracy of the measurements. These techniques also require the use of a mathematical expression for the geometry of the ventricle. For the left ventricle, the prolate ellipsoid is probably acceptable but the complex geometry of the right ventricle is problematic. One approach to the determination of right ventricular volumes has been to use 2D echo to measure whole heart volumes from the apical 2 and 4-chamber views then measure the left ventricle, calculate its volume, and subtract this from the whole heart volumes to estimate right ventricular volumes. Two-dimensional echocardiography generally has a low sampling rate. When used in animals with high heart rates, the technique has limited usefulness.[53] The use of automated border detection and three-dimensional reconstruction algorithms is becoming more common but has not yet gained widespread use in animal studies.[55-60]

Sonomicrometry

This technique, first described by Rushmer's group,[61] has been used to measure left ventricular dimensions by taking advantage of the relatively constant rate of propagation of ultrasound waves through tissue. Left ventricular volume measurements are usually calculated using the prolate ellipsoid model while right ventricular volume calculations are difficult. Placement of the crystals directly in line so dimension changes can be recorded throughout the entire cardiac cycle requires some skill and experience. The technique requires invasive surgery and scar formation can be a problem.

Radionuclide Ventriculography

This technique relies on the intravenous injection of a radionuclide tracer and the detection of gamma or X-rays using a scintillation counter or gamma camera. Two methods are used. The first pass method records by recording time activity curves over a region of interest using a counter or camera properly positioned immediately after the rapid intravenous injection of the tracer. This works reasonably well for

the left ventricle because good mixing of the tracer with the blood occurs on its passage through the right heart and lungs. Right ventricular volume determinations are less reliable because complete mixing of the tracer does not occur. Equilibrium studies take advantage of prior labeling of the entire circulating blood volume, usually with technitium-99m. ECG-gating techniques are used to measure time-varying volumes. Count rates are higher and complete mixing is not a problem. The ventricular volume measured is dependent upon correct positioning of the gamma camera. Other technical problems include low frame rates, variation in R-R intervals, and boundary overlap. In general, this technique lacks both the accuracy and temporal resolution necessary to reconstruct reliable time-varying volume curves.[53]

Magnetic Resonance Imaging and Computer-Assisted Tomographry Scan

Clear endocardial and epicardial imaging is possible using magnetic resonance imaging (MRI). Volumes are calculated from simultaneously acquired transverse slices and usually analyzed using Simpson's rule, but intra and interobserver errors in these measurements can be large. The technique is adequate to measure large volume changes but is inadequate for small volume changes. The technology is expensive, time consuming, and much too slow for effective use in animals with high heart rates. Because high quality and dependable simultaneous pressure measurements are difficult, the technique is usually not suitable for constructing pressure-volume loops.[53] It is possible to make reasonably accurate measurements of wall thickness, and LV end-diastolic and end-systolic diameters.[62]

Van der Velde et al.[63] compared left ventricular volume measurements made with cine-CT scans to simultaneous measurements using conduction catheters in seven dogs. They found high correlation coefficients for both total volume and segmental volume estimations, except in the basal segment of the heart. However, they also reported a significant variability in both the slope and intercept between animals. They concluded that the conductance method provided a distinct advantage because of the ability to record continuous values while the cine-CT method provided more anatomical detail.

Conductance-Derived Volume Measurements

The use of conductance catheters is the most popular method currently used in both the clinical and experimental setting. Impedance plethysmography has been known and used since the early 1900s, but was considered too crude a measure to have real value for the accurate measurement of ventricular volumes.[53] In 1953, Rushmer's group fixed electrodes to the endocardial surfaces of both the right and left ventricles

in dogs and recorded time-varying impedance.[64]The conductance catheter system used today for cardiac measurements was originally developed by Jan Baan and colleagues.[65] This group has continued to refine and perfect the system since, using it for both clinical and experimental applications.[66-69] Conductance catheters are usually standard angiographic catheters with platinum electrodes added toward the tip. The tip and last electrode from the tip produce an electric field. The number of sensing electrodes between the two electric field electrodes varies with the size of the ventricle into which it is to fit and the distance between electrodes. The volume of blood between any two sensing electrodes is assumed to be a cylinder bounded by the endothelial surfaces of the ventricle and the equipotential surfaces of the electrodes. The measured columns are stacked to produce a volume. The change in conductance in the cylinder is the result of a change in resistance between the two sensing electrodes as the cross-sectional area of the cylinder changes during the cardiac cycle. For a more complete explanation of the technology and the theory of operation, see the article by White and Redington.[53] Another form of these catheters uses a dual field excitation employing a second electric field of opposite polarity to the original field. The output of this system was compared with the single-excitation conductance system developed previously and with electromagnetic flowmeter determinations of stroke volume. The dual-excitation system was shown to correlate much better with the flow probe data.[70,71] This technology is reported to increase the electric field homogeneity. Conductance catheter volume measurements of right ventricular volumes are not as affected by the geometric shape of the ventricle but is affected by the conductivity and geometry of surrounding structures. Those structures interfere with the homogeneity of the electric field. The technique is based on the assumption that the electric field produced by the catheter is homogeneous and parallel to the long axis of the ventricle. The number of sensing electrodes and their spacing must be such that they are all maintained within the ventricle during the entire cycle. The calculation of ventricular volumes also requires a calibration involving estimation of a parallel conductance offset (V_c) and a dimensionless slope factor generally referred to as α.[53]

Because the electric currents generated by conductance catheters extend beyond the ventricle, they measure the conductivity of adjacent structures such as the myocardium, the adjoining ventricle, atrial volumes, and some lung tissue overestimating the actual ventricular volume. This is the offset volume (V_c). Many investigators choose to ignore the offset volume assuming it to be constant throughout the cycle, not changing with the perturbations of their experiments. Sometimes "relative" volumes are reported. When measuring right ventricular volumes with the conductance catheter respiration, atrial filling, right ventricular ejection, and myocardial blood volume changes can all provide sources of V_c variability. Making the measurements with respiration suspended can minimize the respiratory effects. The actual parallel conductance can be corrected by independent measures of volume in the same subject. The usual technique is to use a saline dilution method. A small bolus of hypertonic saline injected into the ventricle results in an increase in the measured conductance reflected as an increase in amplitude of the right ventricular volume signal but the conductivity of surrounding tissues is not affected. A regression

technique is then used to calculate V_c.[66] The regression technique is most reliable when at least eight data points are used and when the average transient conductance volume changes more than 15%.[72,73] Adequate mixing of the intravenous injection of the hypertonic saline bolus is essential. This is not a problem with left ventricular measurements but can be for the right ventricle.

Correction of conductance-derived volumes is also dependent upon the inhomogeneity of the excitation field. The previously mentioned dimensionless slope factor (α) is an estimate of the slope between the true volume and the conductance-derived volume following the correction for V_c. To be able to report accurate volumes, it is necessary to calculate α by relating the conductance-derived value to an independent method, thermal dilution, echocardiography, or postmortem measurements. Any inherent error in the independent measurement used is a problem and all have such problems. Mur and Baan found a model-derived value of $\alpha = 0.69$.[69] Baan reported an $\alpha = 0.8$ in isolated hearts, ranges in dogs from 0.78 to 1.05 and in humans from 0.44 to 1.05.[66] To provide accurate estimates of ventricular volume using this technique, it is necessary to assess both V_c and α and these values should be reported.[53]

The conductance volume measurement technique was validated in smaller hearts using piglets and lambs, by comparing results with simultaneously recorded biplane cineangiography. Volume changes were induced by vena caval occlusions, aortic occlusions, and intravenous volume infusions with and without dobutamine and propranolol infusions. Raw conductance volumes were nearly identical to those measured cineangiographically but after correction for V_c and α the correlation was not as good. The authors blamed this lack of agreement on the saline technique used to generate the V_c and α correction factors. They also found that reliable and linear ESPVRs were obtained using vena caval and aortic occlusions but not with volume infusions. The E_{es} was 25% less steep when generated by caval occlusion when compared with aortic occlusion.[74]

Millar Instruments (Houston, TX) produces a small (1.0-1.4 F) catheter with four conductance electrodes and a micromanometer for pressure (SPR-719). The distance between the conductance excitation is about equal to the longitudinal base-apex distance in an adult mouse heart. Yang et al.[75] used this system to measure age-related changes in ventricular function in C57BL/s female mice. This study is notable because of the care taken to calibrate volumes using two different methods, calibration with an independent measure of volume, and calibration using the experimental slope coefficient (α) and V_c. They were able to identify several pressure-volume-related parameters that changed as the mice became senescent.

Other Measures of Myocardial Physical Properties

Westerhof[76]suggests that both ventricular pressure and intramyocardial pressure are generated by variations in stiffness of the myocardium during each cardiac cycle. For any intramyocardial space, he says a time-varying pressure-volume relationship comes about from the changes in muscle stiffness, and this results in a time-varying

elastance and a maximal systolic elastance (E_{max}). If any intramyocardial cavity, i.e., the interstitial space and/or capacity of the coronary vasculature, is subjected to isovolumic conditions a high pressure will result. When the volume is decreased during systole the pressures will be lower.

Myocardial Resistivity

Reyes et al.[77] developed a dual-frequency conductance system based on the dual-excitation work previously mentioned.[70,71] Millar Instruments fabricated a tetrapolar resistivity catheter according to the group's specifications, and the system was used to measure myocardial resistivity in mice. The catheter has four parallel platinum electrodes aligned with intraelectrode spacing of 0.25 mm between electrodes 1 and 2, 0.4 mm between electrodes 2 and 3, and 0.25 mm between electrodes 3 and 4. The electrodes are inside a 1 mm diameter plastic tip that also has two vacuum ports. A small vacuum is applied to maintain contact of the catheter tip to the epicardium of the intact beating mouse heart. They used saline of known conductivities to generate a calibration curve for the device and were able to measure time-varying intramyocardial volumes (resistivity). Those measurements were related to stiffness or elasticity parameters.

Tissue Characterization

Changes in soft tissue elasticity can often be related to pathological events. Elastography or elasticity imaging involves at least three different noninvasive techniques used to provide a raster format image of the mechanical properties of tissues in vivo. The approach is to use a known force to displace the tissue of interest, measure its motion, and use those measurements to characterize the elastic properties of the tissue. The force for displacement can be either static or dynamic but dynamic displacement is of greater interest since it allows a more comprehensive characterization of tissue physical properties in a spectrum of frequencies. Ultrasound radiation is an attractive choice for this purpose since it is noninvasive. Existing ultrasound technology and devices are easily modified for this application, the force can be generated externally yet focused at a desired depth and location, and the force can be generated with a range of frequencies and temporal shapes. Three different methods are described; transient methods that use an impulse force and the transient response of the tissue is detected using Doppler techniques, shear-wave methods that apply oscillating forces to the tissue and the resulting shear wave is detected by ultrasound or other methods, and vibro-acoustography. The latter uses a localized oscillating force, and the acoustic response of the tissue is measured using a hydrophone or microphone device.[78]

Measuring Diastolic Dysfunction

Diastolic function is the ability of the heart to fill adequately and at normal pressures. It is dependent upon both active and passive processes that occur at the myocyte, extracellular matrix, and ventricular chamber levels. Left ventricular diastole is also dependent upon right ventricular diastole, pericardial, and other extracardiac constraints, as well as cardiac preload and afterload.[79]

There is, however, some variability in the exact definition of diastolic dysfunction. Some disease processes can produce directionally opposite changes in relaxation and compliance. The quantification of diastolic function is usually based on some assumptions basic to the mathematical model being used and those assumptions might not apply to the particular type of perturbation being studied.[80]

Left ventricular diastole starts at the onset of myocardial relaxation, just prior to aortic valve closure. During isovolumic relaxation the LV pressure declines rapidly following a time course usually modeled by a monoexponential function that yields a decay time constant (τ).[81] This pressure decline is most likely an active process since ATP hydrolysis is required to release the actin-myosin bonds and for calcium uptake into the sarcoplasmic reticulum. It is also dependent upon passive mechanical forces such as elastic recoil. The latter is dependent upon the extent of sarcomere shortening during systole, the state of contractility, the composition of the extracellular matrix proteins, and the viscoelastic properties of the complex structure and geometry. If relaxation is too slow it can be associated with increases in early and/or late diastolic pressures, particularly with high heart rates.[79] Myofilament sensitivity to calcium is another factor that regulates diastolic relaxation.[82]

The second phase of diastole is initiated with opening of the mitral valve and the onset of rapid ventricular filling, during which approximately 80% of ventricular filling occurs. The first phase relaxation results in a large atrio-ventricular pressure gradient that is the driving force for this second filling phase. Any delay in ventricular relaxation, loss of the normal amount of elastic recoil, or any increase in chamber stiffness impairs the formation of the gradient and affects ventricular filling. Diastasis, the third phase, is the period at the end of rapid ventricular filling, when atrial and ventricular pressures equilibrate and there is no additional ventricular inflow. It is the best time to assess the passive diastolic stiffness of the ventricle. Measuring pressures at varying ventricular volumes can do this. The resulting diastolic pressure-volume relation (DPVR) is usually modeled using a monoexponential function (β). Decreased compliance results in increased β. Both human and animal subjects with cardiomyopathy display a rightward shift of the DPVR as a result of dilation.[81]

Atrial contraction normally contributes the other 20% of ventricular filling. Many forms of heart failure, particularly hypertensive heart failure and senescent heart failure in both animals and man, produce limitations on early rapid filling making atrial filling more important. When atrial dilation accompanies this form of disease, it is usually associated with diastolic dysfunction and a poor prognosis.[79]

Ventricular compliance is dependent upon both the composition and structure of the extracellular matrix surrounding cardiac myocytes. The isotype and amount of

collagen present is a determinant but even more important is the amount of glycation cross-linking and the ultrastructural location of the collagen. The deposition of collagen is increased with such pathologies as hypertrophy, aging, heart failure, and myocardial infarction.[79]

Extraventricular forces that have an effect on LV diastolic pressure include right ventricular loading and interactions with the pericardium. These forces can account for as much as 40% of the measured LV pressure, so failure to account for them will lead to significant error in interpretation of diastolic function. DPVR is best evaluated by measuring transmural rather than left ventricular cavity pressures with the right ventricle unloaded. This has been done by measuring beat-to-beat pressure-volume data, with the use of rapid vena caval occlusions, to generate multiple cycles at varying preload volumes.[81] Changes in circulating blood volumes can, particularly when there is neurohumeral hyperactivation, result in increased LV filling pressures without measurable systolic or diastolic dysfunction. Thus the measurement of increased end-diastolic pressures in a heart of normal size does not always justify a conclusion of dysfunction.[79]

Increases in afterload, especially during late ejection, have been shown to have a deleterious effect on the rate of ventricular relaxation in both human and animal subjects. Late systolic loading is particularly important during senescence due to the dilation and stiffening of the arterial tree. Studies in transgenic mice overexpressing cardiac troponin-I suggest that protein kinase A phosphorylation of troponin-I may be an important mediator of the interaction between afterload and ventricular relaxation.[83] However, animal studies have indicated that afterload must be increased to approximately 80% of isovolumic contraction to result in an increase in end-diastolic pressures, again indicating the unreliability of this measure of diastolic dysfunction.[79]

It has been reported that nearly half of all human patients with heart failure have EF within the normal range. This has been termed heart failure with normal ejection fraction (HFnEF) and is frequently assumed to be associated with diastolic dysfunction. The evidence for this assumption is not well documented. Patients studied with single-beat pressure-volume analysis and noninvasive volume measurements demonstrated increased diastolic stiffness when compared with normal controls. Another study used invasive techniques and multibeat DPVR analysis and the HFnEF subjects in this study did not demonstrate increased left-ventricular stiffness. The increased end-diastolic pressures that were observed in these patients were attributed to external forces such as increased epicardial volumes.[79]

References

1. Hill A. The heat of shortening and the dynamic constants of muscle. *Proc R Soc London B*. 1938;126:136–195.
2. Katz B. The relation between force and speed in muscular contraction. *J Physiol*. 1939;96:45–64.

3. Ford A, Huxley A, Simmons R. Tension responses to sudden length change in simulated frog muscle fibers near slack length. *J Physiol*. 1977;269:441–515.
4. Burkhoff D, Mirsky I, Suga H. Assessment of systolic and diastolic ventricular properties via pressure-volume analysis: A guide for clinical, translational, and basic researchers. *Am J Physiol Heart Circ Physiol*. 2005;289:H501–H512.
5. Claessens TE, Georgakopoulos D, Afanasyeva M, et al. Nonlinear isochrones in murine left ventricular pressure-volume loops: How well does the time-varying elastance concept hold? *Am J Physiol Heart Circ Physiol*. 2006;290:H1474–H1483.
6. Kheradvar A, Milano M, Gorman RC, Gorman JH, III, Gharib M. Assessment of left ventricular viscoelastic components based on ventricular harmonic behavior. *Cardiovasc Eng*. 2006;6:30–39.
7. Berul CI, Aronovitz MJ, Wang PJ, Mendelsohn ME. In vivo cardiac electrophysiology studies in the mouse. *Circulation*. 1996;94:2641–2648.
8. Berul CI, Christe ME, Aronovitz MJ, Seidman CE, Seidman JG, Mendelsohn ME. Electrophysiological abnormalities and arrhythmias in alpha MHC mutant familial hypertrophic cardiomyopathy mice. *J Clin Invest*. 1997;99:570–576.
9. Bazett HC. An analysis of the time-relations of electrocardiograms. *Heart*. 1920;7:353–370.
10. Appleton GO, Li Y, Taffet GE, et al. Determinants of cardiac electrophysiological properties in mice. *J Interv Card Electrophysiol*. 2004;11:5–14.
11. Hofer E, Keplinger F, Thurner T, et al. A new floating sensor array to detect electric near fields of beating heart preparations. *Biosens Bioelectron*. 2006;21:2232–2239.
12. Mitchell GF, Jeron A, Koren G. Measurement of heart rate and Q-T interval in the conscious mouse. *Am J Physiol*. 1998;274:H747–H751.
13. Hellige G. Recording of ventricular pressure by conventional catheter manometer systems efficiency of several combinations of conventional catheters, modern transducers and catheter-flush systems. *Basic Res Cardiol*. 1976;71:389–406.
14. Hellige G. Recording of ventricular pressure by conventional catheter manometer systems. I. Minimal requirements of blood pressure recording systems and estimation of frequency response characteristics. *Basic Res Cardiol*. 1976;71:319–336.
15. Branzi A, Zannoli R, Binetti G, Lamberti G, Magnani B. Study of the precision and limitations in measuring left ventricular pressure and its first time-derivative. *G Ital Cardiol*. 1977;7:995–1002.
16. Lorenz JN, Robbins J. Measurement of intraventricular pressure and cardiac performance in the intact closed-chest anesthetized mouse. *Am J Physiol*. 1997;272:H1137–H1146.
17. Azhar G, Zhang X, Wang S, Zhong Y, Quick CM, Wei JY. Maintaining serum response factor activity in the older heart equal to that of the young adult is associated with better cardiac response to isoproterenol stress. *Basic Res Cardiol*. 2007;102:233–244.
18. Van den Bergh A, Flameng W, Herijgers P. Type II diabetic mice exhibit contractile dysfunction but maintain cardiac output by favourable loading conditions. *Eur J Heart Fail*. 2006;8:777–783.
19. Matsushima S, Kinugawa S, Ide T, et al. Over expression of glutathione peroxidase attenuates myocardial remodeling and preserves diastolic function in diabetic heart. *Am J Physiol Heart Circ Physiol*. 2006;291:H2237–H2245.
20. Wang Q, Brunner HR, Burnier M. Determination of cardiac contractility in awake unsedated mice with a fluid-filled catheter. *Am J Physiol Heart Circ Physiol*. 2004;286:H806–H814.
21. Edler I, Lindstrom K. The history of echocardiography. *Ultrasound Med Biol*. 2004;30:1565–1644.
22. Feigenbaum H. Cardiovascular uses of diagnostic ultrasound. *J Indiana State Med Assoc*. 1967;60:1522–1525.
23. Feigenbaum H, Linback RE, Nasser WK. Hemodynamic studies before and after instrumental mitral commissurotomy. A reappraisal of the pathophysiology of mitral stenosis and the efficacy of mitral valvotomy. *Circulation*. 1968;38:261–276.
24. Feigenbaum H, Popp RL, Chip JN, Haine CL. Left ventricular wall thickness measured by ultrasound. *Arch Intern Med*. 1968;121:391–395.

25. Feigenbaum H, Zaky A. Ultrasound as a diagnostic tool in cardiology. A review. *Med Res Eng*. 1968;7:26–31.
26. Ha JS, Walker WF, Hossack JA. Determination of an optimal image frame interval for frame-to-frame ultrasound image motion tracking. *IEEE Trans Ultrason Ferroelectr Freq Control*. 2005;52:386–396.
27. Dawson D, Lygate CA, Saunders J, et al. Quantitative 3-dimensional echocardiography for accurate and rapid cardiac phenotype characterization in mice. *Circulation*. 2004;110:1632–1637.
28. Winkler AJ, Wu J. Correction of intrinsic spectral broadening errors in Doppler peak velocity measurements made with phased sector and linear array transducers. *Ultrasound Med Biol*. 1995;21:1029–1035.
29. Zhang Y, Guo Z, Wang W, He S, Lee T, Loew M. A comparison of the wavelet and short-time Fourier transforms for Doppler spectral analysis. *Med Eng Phys*. 2003;25:547–557.
30. Hartley CJ, Latson LA, Michael LH, Seidel CL, Lewis RM, Entman ML. Doppler measurement of myocardial thickening with a single epicardial transducer. *Am J Physiol*. 1983;245:H1066–H1072.
31. Hartley CJ, Litowitz H, Rabinovitz RS, et al. An ultrasonic method for measuring tissue displacement: Technical details and validation for measuring myocardial thickening. *IEEE Trans Biomed Eng*. 1991;38:735–747.
32. Sebag IA, Handschumacher MD, Ichinose F, et al. Quantitative assessment of regional myocardial function in mice by tissue Doppler imaging: Comparison with hemodynamics and sonomicrometry. *Circulation*. 2005;111:2611–2616.
33. Notomi Y, Martin-Miklovic MG, Oryszak SJ, et al. Enhanced ventricular untwisting during exercise: A mechanistic manifestation of elastic recoil described by Doppler tissue imaging. *Circulation*. 2006;113:2524–2533.
34. Stypmann J, Engelen MA, Breithardt AK, et al. Doppler echocardiography and tissue Doppler imaging in the healthy rabbit: Differences of cardiac function during awake and anaesthetised examination. *Int J Cardiol*. 2007;115:164–170.
35. Liu YH, Carretero OA, Cingolani OH, et al. Role of inducible nitric oxide synthase in cardiac function and remodeling in mice with heart failure due to myocardial infarction. *Am J Physiol Heart Circ Physiol*. 2005;289:H2616–H2623.
36. Shimizu T, Okamoto H, Watanabe M, et al. Altered microvasculature is involved in remodeling processes in cardiomyopathic hamsters. *Jpn Heart J*. 2003;44:111–126.
37. Zhang C, Yasuno S, Kuwahara K, et al. Blockade of angiotensin II type 1 receptor improves the arrhythmia morbidity in mice with left ventricular hypertrophy. *Circ J*. 2006;70:335–341.
38. Rennison JH, McElfresh TA, Okere I, et al. High fat diet post infarction enhances mitochondrial function and does not exacerbate left ventricular dysfunction. *Am J Physiol Heart Circ Physiol*. 2007;292:H1498–H1506.
39. Stein AB, Tiwari S, Thomas P, et al. Effects of anesthesia on echocardiographic assessment of left ventricular structure and function in rats. *Basic Res Cardiol*. 2007;102:28–41.
40. Roth DM, Swaney JS, Dalton ND, Gilpin EA, Ross J, Jr. Impact of anesthesia on cardiac function during echocardiography in mice. *Am J Physiol Heart Circ Physiol*. 2002;282:H2134–40.
41. Du XJ, Samuel CS, Gao XM, Zhao L, Parry LJ, Tregear GW. Increased myocardial collagen and ventricular diastolic dysfunction in relaxin deficient mice: A gender-specific phenotype. *Cardiovasc Res*. 2003;57:395–404.
42. Larsen KO, Sjaastad I, Svindland A, Krobert KA, Skjonsberg OH, Christensen G. Alveolar hypoxia induces left ventricular diastolic dysfunction and reduces phosphorylation of phospholamban in mice. *Am J Physiol Heart Circ Physiol*. 2006;291:H507–H516.
43. Lisauskas JB, Singh J, Bowman AW, Kovacs SJ. Chamber properties from transmitral flow: Prediction of average and passive left ventricular diastolic stiffness. *J Appl Physiol*. 2001;91:154–162.
44. Zhou YQ, Foster FS, Parkes R, Adamson SL. Developmental changes in left and right ventricular diastolic filling patterns in mice. *Am J Physiol Heart Circ Physiol*. 2003;285:H1563–H1575.

45. Stoyanova E, Trudel M, Felfly H, Garcia D, Cloutier G. Characterization of circulatory disorders in beta-thalassemic mice by non-invasive ultrasound biomicroscopy. *Physiol Genomics*. 2007;29:84–90.
46. Zhang Y, Takagawa J, Sievers RE, et al. Validation of the wall motion score and myocardial performance indices as novel techniques to assess cardiac function in mice post myocardial infarction. *Am J Physiol Heart Circ Physiol*. 2007;292:H1187–H1192.
47. Kulandavelu S, Qu D, Adamson SL. Cardiovascular function in mice during normal pregnancy and in the absence of endothelial NO synthase. *Hypertension*. 2006;47:1175–1182.
48. Reddy AK, Jones AD, Martono C, Caro WA, Madala S, Hartley CJ. Pulsed Doppler signal processing for use in mice: Design and evaluation. *IEEE Trans Biomed Eng*. 2005;52:1764–1770.
49. Reddy AK, Taffet GE, Li YH, et al. Pulsed Doppler signal processing for use in mice: Applications. *IEEE Trans Biomed Eng*. 2005;52:1771–1783.
50. Liu JH, Jeng GS, Wu TK, Li PC. ECG triggering and gating for ultrasonic small animal imaging. *IEEE Trans Ultrason Ferroelectr Freq Control*. 2006;53:1590–1596.
51. Chavez I, Dorbecker N, Celis A. Direct intracardiac angiography: Its diagnostic value. *Am Heart J*. 1947;33:560–593.
52. Sandler H, Dodge HT. The use of single plane angiocardiograms for the calculation of left ventricular volume in man. *Am Heart J*. 1968;75:325–334.
53. WhitePA, Redington AN. Right ventricular volume measurement: Can conductance do it better? *Physiol Meas*. 2000;21:R23–R41.
54. Rodriguez F, Langer F, Harrington KB, et al. Alterations in transmural strains adjacent to ischemic myocardium during acute midcircumflex occlusion. *J Thorac Cardiovasc Surg*. 2005;129:791–803.
55. Vogel M, Ho SY, Lincoln C, Yacoub MH, Anderson RH. Three-dimensional echocardiography can simulate intraoperative visualization of congenitally malformed hearts. *Ann Thorac Surg*. 1995;60:1282–1288.
56. Vogel M, White PA, Redington AN. In vitro validation of right ventricular volume measurement by three-dimensional echocardiography. *Br Heart J*. 1995;74:460–463.
57. Knackstedt C, Franke A, Mischke K, et al. Semi-automated 3-dimensional intracardiac echocardiography: Development and initial clinical experience of a new system to guide ablation procedures. *Heart Rhythm*. 2006;3:1453–1459.
58. Watanabe T, Omata S, Odamura M, Okada M, Nakamura Y, Yokoyama H. Three-dimensional quantification of cardiac surface motion: A newly developed three-dimensional digital motion-capture and reconstruction system for beating heart surgery. *J Thorac Cardiovasc Surg*. 2006;132:1162–1171.
59. Lang RM, Mor-Avi V, Sugeng L, Nieman PS, Sahn DJ. Three-dimensional echocardiography: The benefits of the additional dimension. *J Am Coll Cardiol*. 2006;48:2053–2069.
60. Gu L, Xu J, Peters TM. Novel multistage three-dimensional medical image segmentation: Methodology and validation. *IEEE Trans Inf Technol Biomed*. 2006;10:740–748.
61. Ellis RM, Franklin DL, Rushmer RF. Left ventricular dimensions recorded by sonocardiometry. *Circ Res*. 1956;4:684–688.
62. Diez-Freire C, Vazquez J, Correa de Adjounian MF, et al. ACE2 gene transfer attenuates hypertension-linked pathophysiological changes in the SHR. *Physiol Genomics*. 2006;27:12–19.
63. van der Velde ET, van Dijk AD, Steendijk P, et al. Left ventricular segmental volume by conductance catheter and cine-CT. *Eur Heart J*. 1992;13 Suppl E:15–21.
64. Rushmer RF, Crystal DK, Wagner C, Ellis RM. Intracardiac impedance plethysmography. *Am J Physiol*. 1953;174:171–174.
65. Baan J, Jong TT, Kerkhof PL, et al. Continuous stroke volume and cardiac output from intraventricular dimensions obtained with impedance catheter. *Cardiovasc Res*. 1981;15:328–334.
66. Baan J, van der Velde ET, de Bruin HG, et al. Continuous measurement of left ventricular volume in animals and humans by conductance catheter. *Circulation*. 1984;70:812–823.

67. Baan J, Van der Velde, E.T., Steendijk P, Koops J. Calibration and application of the conductance catheter for ventricular volume measurement. *Automedica*. 1989;11:357–365.
68. Burkhoff D, van der Velde E, Kass D, Baan J, Maughan WL, Sagawa K. Accuracy of volume measurement by conductance catheter in isolated, ejecting canine hearts. *Circulation*. 1985;72:440–447.
69. Mur G, Baan J. Computation of the input impedances of a catheter for cardiac volumetry. *IEEE Trans Biomed Eng*. 1984;31:448–453.
70. Steendijk P, Mur G, Van Der Velde ET, Baan J. The four-electrode resistivity technique in anisotropic media: Theoretical analysis and application on myocardial tissue in vivo. *IEEE Trans Biomed Eng*. 1993;40:1138–1148.
71. Steendijk P, Van der Velde ET, Baan J. Left ventricular stroke volume by single and dual excitation of conductance catheter in dogs. *Am J Physiol*. 1993;264:H2198–H2207.
72. Herrera MC, Olivera JM, Valentinuzzi ME. Parallel conductance estimation by hypertonic dilution method with conductance catheter: Effects of the bolus concentration and temperature. *IEEE Trans Biomed Eng*. 1999;46:830–837.
73. Herrera MC, Olivera JM, Valentinuzzi ME. Parallel conductance determination in cardiac volumetry using dilution manoeuvres: Theoretical analysis and practical implications. *Med Biol Eng Comput*. 1999;37:169–174.
74. Teitel DF, Klautz RJ, Cassidy SC, et al. The end-systolic pressure-volume relationship in young animals using the conductance technique. *Eur Heart J*. 1992;13 Suppl E:40–46.
75. Yang B, Larson DF, Watson R. Age-related left ventricular function in the mouse: Analysis based on in vivo pressure-volume relationships. *Am J Physiol*. 1999;277:H1906–H1913.
76. Westerhof N. Physiological hypotheses--intramyocardial pressure. A new concept, suggestions for measurement. *Basic Res Cardiol*. 1990;85:105–119.
77. Reyes M, Steinhelper ME, Alvarez JA, et al. Impact of physiological variables and genetic background on myocardial frequency-resistivity relations in the intact beating murine heart. *Am J Physiol Heart Circ Physiol*. 2006;291:H1659–H1669.
78. Fatemi M, Greenleaf JF. Probing the dynamics of tissue at low frequencies with the radiation force of ultrasound. *Phys Med Biol*. 2000;45:1449–1464.
79. Borlaug BA, Kass DA. Mechanisms of diastolic dysfunction in heart failure. *Trends Cardiovasc Med*. 2006;16:273–279.
80. Senzaki H, Fetics B, Chen CH, Kass DA. Comparison of ventricular pressure relaxation assessments in human heart failure: Quantitative influence on load and drug sensitivity analysis. *J Am Coll Cardiol*. 1999;34:1529–1536.
81. Kass DA. Assessment of diastolic dysfunction. invasive modalities. *Cardiol Clin*. 2000;18:571–586.
82. Kass DA, Solaro RJ. Mechanisms and use of calcium-sensitizing agents in the failing heart. *Circulation*. 2006;113:305–315.
83. Takimoto E, Soergel DG, Janssen PM, Stull LB, Kass DA, Murphy AM. Frequency- and afterload-dependent cardiac modulation in vivo by troponin I with constitutively active protein kinase A phosphorylation sites. *Circ Res*. 2004;94:496–504.

Chapter 5
Measuring Vascular Function and Ventricular/Arterial Coupling Dynamics

History

> "… Now this Velocity is only the Velocity of the Blood at its firft entering into the *Aorta*, in the Time of the Syftole; in confequence of which the Blood in the Arteries, being forcibly propelled forward, with an accelerated *Impetus*, thereby dilates the Canal of the Arteries, which begin again to contract at the Infstant the Syftole ceafes: By which curious Artifice of Nature, the Blood is carried on in the finer Capillaries, with an almoft even Tenor of Velocity, in the fame manner as the fpouting Water of fome fire-Engines, is contrived to flow with a more even Velocity, not withftanding the alternate Syftoles and Diaftoles of the rifing and falling *Embolus* or Force; and this by the means of a large inverted Globe, wherein the compreffed Air alternately dilating or contracting, in Conformity to the workings to and fro of the *Embolus*, and thereby impelling the Water more equably than the *Embolus* alone would do, pufhes it out in a more nearly equal Spout.…"[1]

The above quote is probably the first ever published description of the arterial system working in combination with the heart to deliver blood to the peripheral tissues. It may also be the first published use of a model to describe a physiological phenomenon. Stephen Hales work was eventually translated into German and this led to the use of the term "windkessel" to describe the workings of the elastic (compliant) aorta and large arteries, by Otto Frank in 1899.[2]

Frank and his colleagues described the arterial system using a two-element windkessel model consisting of a lumped resistance and a lumped compliance. Thomas Young described the connection between the elastic behavior of the arterial wall and the pulse wave velocity (PWV).[3] In 1878, Moens built on Young's work and published a mathematical expression of PWV in terms of vessel elasticity and dimensions. The same concepts were, independently, derived by Korteweg and the relationships are now known as the Moens-Korteweg equation.[4,5] Our understanding of the details of arterial behavior was enhanced by the work of McDonald and Womersley, who described a linear solution to the Navier-Stokes equations for arterial flow. This work led to the concept of arterial input impedance.[6]

The three-element windkessel model proposed by Westerhof is most often used to characterize both the systemic and pulmonary arterial systems.[7] The pulsatile motion of blood can be analyzed in a more general way by applying the laws of classical mechanics. The methods were adopted by scientists with an interest in the

D.R. Gross, *Animal Models in Cardiovascular Research*,
DOI: 10.1007/978-0-387-95962-7_5, © Springer Science + Business Media, LLC 2009

details of the propagation phenomena of the aortic pressure and flow waveforms including Noordergraff, Taylor, Westerhof, and Avolio.[8–11] These models embody the nonuniform, distributed, branching properties of the arterial system but are overly complex when the need is to study the behavior of the system when seen from the aortic or pulmonary valves.[11] Work on models has also focused on a series of so-called "tube" models. These vary from the single uniform elastic tube loaded with a resistive load,[9,10] two elastic tubes in parallel (the T-tube model),[11,12] two elastic tubes in series,[13] and a uniform tube loaded with a complex load.[11,14,15] All of these models have limitations in their ability to describe pressure and flow waveforms and related propagation phenomena during a variety of perturbations to the system, i.e., the solutions are not unique.[11] Some of the limitations of these models can be overcome when two tubes loaded with complex loads are connected in parallel.[16]

The purpose of physiological modeling is to enable us to describe the function of a system in precise terms. One can then use this description to generalize and predict system behavior. A good model codifies our current knowledge of system behavior. The model is a simplified version of reality, one that we can comprehend ourselves and communicate to others. However, an overly simplified model may not provide a satisfactory explanation for system behavior under all, or even most, circumstances, since physiological systems are complex with redundant mechanisms for controlling responses to physiological and pathological perturbations. The most desirable model is one that constitutes the best compromise between simplicity and the ability to explain the system's essential properties and behavior.[17] Any realistic model of the systemic or pulmonary arterial systems must include both compliance and inertial (inductive) components along with a description of the total cross-sectional area through which the blood is pumped (resistance) and the response of these systems to neural-humoral control, body position, exercise (both acute and long-term effects), and the influence of physiological and pathological states such as aging, atherosclerosis, diabetes, hypertension, arrhythmias, heart failure, with and without normal ejection fractions, and abnormal environments such as hyper- and hypo-baric conditions.[17]

Quantification of Arterial Compliance

Before it is possible to discuss the physiological or pathological roles of arterial compliance, the compliance must be quantified. This is not a trivial problem. Early attempts to accomplish this were based on estimates of aortic wall properties by measuring pulse wave velocities but the relationship between wall stiffness, as indexed by PWV, and compliance is not straightforward. Lumped parameter model estimations of compliance with variations of the windkessel model also fall short. Five general methods have been described to measure compliance: (1) Using the ratio of stroke volume to pulse pressure. This method implicitly assumes that compliance over the pressure range as measured is independent of the mean distending pressure. (2) Assuming that the diastolic aortic pressure decay is a monoexponential

function with a time constant (τ) equal to resistance × compliance. This assumption has several flaws. When measured with very high-frequency devices, the diastolic pressure decay is frequently not close to being an exponential function, particularly when there are late wave reflections that distort the diastolic pressure. Even in those cases where the pressure decay appears to be exponential, it is often not mono exponential. Regression of the log of pressure vs. time to obtain the time constant, the most common method, implicitly assumes that the pressure asymptotically decays to zero. The technique is very sensitive to any noise in the measurement and the method implicitly assumes that compliance is independent of the mean distending pressure. (3) Using the low frequencies of the impedance modulus spectrum for a compliance estimate. (4) Parameter estimation techniques using various models of the system. (5) Using a two-element model of the vasculature and an analysis of any particular two points of area under the diastolic portions of a high-fidelity recording of the pressure tracing. The basis for this is expressed as:

$$A/[R\ (P_1 - P_2\ 0]$$

where A is the area under the diastolic pressure-time tracing between times t_1 and t_2, any two points easily identified and arbitrary, P_1 and P_2 are the diastolic pressures corresponding to these times, and R is peripheral resistance. All of the five methods are applicable only to steady-state conditions.[18]

Force-Displacement Measurements

Patel and colleagues measured longitudinal strain, circumferential strain, lateral intravascular pressure, blood velocity, and longitudinal motion and their relationships to each other in the aortas of 25 dogs in situ. The diameter and length were measured with two electrical recording calipers consisting of two bonded wire strain gauges cemented to each side of a piece of curved brass shim stock suspended between the hinged legs of the caliper. The legs had eyelets for suturing to the vessel wall. Any displacement of the legs of the caliper with respect to each other was reflected by a change in resistance. They were able to demonstrate that with inspiration the thoracic aorta increased in length while the abdominal aorta shortened. During the cardiac cycle, the thoracic aorta increased as pressure increased and the abdominal aorta segmental length decreased. The shortening of the abdominal aorta was attributed to the elongating strain of the thoracic aorta. Percent change in volume, per centimeter H_2O pressure change, for the descending thoracic aorta was in the range of $0.3\% \pm 0.1\%$ with mean distending pressures of 140–189 cm H_2O. As the mean distending pressure was increased the percent change in volume decreased.[19]

In a subsequent study, Patel and colleagues determined the dynamic mechanical properties of the middle descending thoracic aorta (MDTA) of dogs, in vitro. The instrumentation consisted of a sinusoidal driver, a coupling assembly and a displacement measuring device consisting of a thin brass shim on which were mounted

two SR-4 strain gauges wired to form a half-bridge. The static elastic modulus (E) was calculated from:

$$E = s/e = (\Delta F/A)/(\Delta h/h_o)$$

where s is the stress, e is the strain, ΔF is the change in force, A is the area of the hammer portion of the coupling assembly, Δh is the change in thickness, and h_o is the the thickness of the material prior to any force being applied. A segment of aorta with a measured in vivo length (L) and diameter (D) was removed and placed in Ringer's solution. The volume (V) was determined by measuring the volume of Ringer's solution displaced. The h_o was calculated from:

$$h_o = V/\pi DL$$

since the vessel is incompressible.

The segment was then cut longitudinally, stretched to its in vivo dimension and mounted into the apparatus. Small sinusoidal radial strains were superimposed on the prestrained specimen at a variety of frequencies. The resulting forces were subjected to harmonic analysis and the mechanical impedance (Z) was calculated as the complex ratio of stress to strain. For a material that behaves like a spring and dashpot in parallel (Voigt model) the real part of Z (E') represents the dynamic elastic properties of the tissue and the imaginary part of Z (E'') represents the viscous properties. The values of E' obtained in these studies were within 6% of the values for static radial elastic modulus obtained in situ from the same animals.[20]

Patel and colleagues also isolated a segment in the canine MDTA and used a mechanical device to measure force and length changes in situ. They were able to quantitate the dynamic anisotropic viscoelastic properties of the aorta in these circumstances in a living animal and found reasonable agreement with in vitro studies.[21,22]

Gentile et al. used ultrasonic dimension gauges and a high-fidelity catheter-tip manometer system to measure changes in segment length, diameter, and intravascular pressure in intact anesthetized dogs. Volume distensibility (E_v) was calculated for the ascending aorta (AA), the upper descending thoracic aorta (UDTA) and the MDTA as the sum of circumferential extensibility (E_c), longitudinal extensibility (E_l) and combined second and third-order extensibilities (E_k). The inner wall radius (R_i) was calculated from:

$$R_i = R_o/(1 + d),$$

where R_o is the outer wall radius and d is the ratio of wall thickness to inner wall radius. The value for d was obtained by removing segments, of the same in vivo length, from the descending thoracic aorta of six dogs, cleaning them of all perivascular connective tissue and using the volume displacement technique to determine the volume. Responding to transluminal pressure changes from end-diastole to peak systole the inner wall radius, axial length and intraluminal volume changes are indicated by ΔR_i, ΔL, and ΔV, respectively. The volume distensibility (E_v) was

defined as the percent volume change per mmHg ΔP and the following equations were derived:

$$\begin{aligned} E_v &= (\Delta V / V)(100\,\Delta P) \\ &= (2\,\Delta P_i / R_i)(100\,\Delta P) + (\Delta L / L)(100\,\Delta P) \\ &+ \Delta R_i^2 / R_i^2 + 2(\Delta R_i / R_i)(\Delta L / L)(100 / \Delta P) \\ &+ (\Delta R_i^2\ \Delta L) / (R_i^2\ L)(100 / \Delta P). \end{aligned}$$

The first and second-order terms are linear expressions that represent the contributions of changes in circumference and segment length as a result of the pulse pressure. The circumferential and longitudinal extensibilities, E_c and E_L are defined by the following relationships:

$$E_c = 2\,(dR_i / dP)\,(100/R_i),$$

$$E_L = (dL / dP)\,(100/L)$$

When the length change during systole is compressed rather than elongated, as has been shown previously by Patel et al., the ΔL term is negative and yields a negative value for the E_L term. The higher order extensibilities (E_k, combined second and third order) accounted for the percentage volume changes per mmHg pulse pressure due to the interactions between E_c and E_L. The mean E_v values were 1.62% ± 0.31% ΔV/mmHg for the AA, 0.84% ± 0.08% ΔV/mmHg for the UDTA and 0.62% ± 0.08% ΔV/mmHg for the MDTA. Since the E_c values for these segments of the thoracic aorta were very similar the longitudinal wall motion is an important determinant of the mechanical behavior of this vessel.[23,24]

Pulse Wave Velocity

This is the speed at which pressure, velocity, or flow waves travel along a given arterial segment. Sir Isaac Newton described the physics of the relationship between the speed at which a physical disturbance travels in some medium being dependent upon the elasticity and density of that medium.[25] This led to the work by Young, Moens, Korteweg, and others describing the PWV (C) in mathematical terms:

$$C = \sqrt{}\, Eh/2R\rho,$$

where E is the elastic modulus, h is the wall thickness, $2R$ is the internal diameter, and ρ is the density of the blood. The application of this relationship assumes that: (1) the tube is perfectly elastic, infinitely long, and homogenous; (2) the wall thickness is small with respect to the diameter; and (3) that the fluid within the lumen is incompressible. It should be apparent that this measurement has significant limitations since the arterial system is viscoelastic, branching, anything but homogenous, and

at the level of the peripheral vessels, away from the major conduit vessels, the ratio of wall thickness to diameter increases markedly.[25]

The practical problems associated with using the Moens–Korteweg equation and PWV to estimate the elastic modulus, aside from the previously mentioned theoretical limitations, are related to the difficulty of exactly measuring the distance along the longitudinal axis of the vessel between the two measuring points and difficulties in identifying the foot velocity, or some other identical point on both recordings. Latham describes an intersecting-slope technique for accomplishing this involving extrapolating the end-diastolic portion of the pressure pulse and identifying the point of intersection with another line drawn though the initial rapid upstroke to define the foot.[25] Pressure waveforms recorded using two or more micro-tip manometers placed a known distance apart on the same catheter make it simple to know the distance between the measuring points. This is an invasive technique but has been used to good advantage to quantify changes in arterial mechanical behavior in a variety of circumstances.[26–28]

Because PWV measurements can be made noninvasively, the technique has attracted significant attention and use. The most common methods of measurement involve the use of pressure-sensitive external transducers or Doppler ultrasound technology. Reddy et al. recently reported using a high frequency, high-resolution Doppler spectrum analyzer to record aortic velocities. They compared this method to using a clinical spectrum analyzer and the zero-crossing interval histogram method to measure peak flow velocities in mice. They obtained virtually the same results, approximately 374–414 cm/s. It is difficult to align two transducers an exactly known distance along the longitudinal axis of the vessel but this is essential if one is to be able to measure wave velocities and estimate mechanical behavior accurately.[29,30] External pressure recording transducers generally have more limitations than transcutaneous Doppler transducers.[25]

The brachial-ankle PWV was measured using a commercially available system that makes use of pressure cuffs and oscillometry. PWV was calculated by dividing the distance from the aortic valve to the ankle artery by the sum of the difference between the time the pulse waves were transmitted to the brachium and the time the same wave were transmitted to the ankle, and the time difference between the second heart sound, recorded with a phonocardiogram, and the notch of the brachial pulse waves.[31] An ultrasound technique was used to measure carotid-femoral, carotid-radial, and femoral-posterior tibial sites. The conclusion was that carotid-femoral PWV is a better indicator of atherosclerotic disease than either the carotid-radial or femoral-posterior tibial PWV.[32]

Davies et al.[33] measured femoral-tibial PWV in 10 healthy human volunteers. They found that muscle metaboreflex activation results in a stiffening of the arteries measured that can overcome local exercise-induced decreases in arterial PWV. Carotid-femoral PWV was measured noninvasively in 259 people with hypertension and the effects of chronic coffee drinking were evaluated. The device used in the studies is commercially available (Complior, Artech Medical, Pantin, France). Two different pulse waves are obtained simultaneously at two sites, the base of the neck for the common carotid artery and over the right femoral artery. The distance

for calculation of the PWV was defined as the distance from the suprasternal notch to the femoral artery minus the distance from the carotid artery to the suprasternal notch.[34] The flaw in all of these measurements is the inherent errors involved in estimating the distance along the longitudinal axis of the vessel(s) of interest. Measuring this distance from superficial or external measurements on the subject generally underestimates the true path length, particularly in senescent subjects with tortuous vessels.[25] However, when PWV is carefully measured, it is significantly altered with aging, hypertension, and atherosclerosis.[25] There is rarely any mention of corrections made for variations in blood viscosity or density that might occur from differences in hematocrit, serum protein, cholesterol levels, or other factors when measuring PWV.

Modeling Techniques for Estimating Vascular Mechanical Behavior

Although the dynamics of the arterial systems of different animal species are of interest to veterinary scientists, the major reason for the use of animal models is to obtain meaningful measurements that enable modeling of the human system. Because of this it is important that the information gained from the animal model being used be easily extrapolated to the human situation. The animal model must be appropriate.

Morphologically, the arteries of various species of animals can differ significantly. Cross-sectional areas of the thoracic aorta comparing cow, dog, rabbit, pig, and human were stained with elastic van Gieson stain and evaluated. The relative amount of collagen varied with the species, as did the distribution of the collagen. The thickness of the thoracic aorta also varies significantly with species.[24] We have demonstrated significant morphological and compliance changes in pigs fed a high fat diet for 16 weeks. These animals did not demonstrate any signs of atherosclerotic disease.[35]

There are several reports published that indicate that 50–60% of the total systemic arterial compliance sensed by the ejecting heart may be contained in the AA, aortic arch, and the major branches of the aortic arch.[25] Input impedance can be used to express the relationship between mean pressure and flow and pulsatile pressure and flow in the root of the aorta or the pulmonary artery and has been used to describe both the static and dynamic physical properties of the arterial system being evaluated.[12,36,37] Input impedance describes the arterial system in terms of frequency response and is determined by relating corresponding frequency components of arterial pressure and flow waves. The ratio of the amplitude of the pressure harmonics to the amplitude of the corresponding flow harmonics provides an impedance modulus as a function of frequency. The delay between the flow and pressure harmonics provides the impedance phase angle. The impedance model includes a measure of resistance (mean pressure/mean flow), compliance of the vessel wall, and the inertial effects of the blood and wave reflections.[11] The phase angle between the pressure

and flow waveforms is usually negative at low frequencies, with flow leading pressure, and becomes positive at higher frequencies. The zero crossing of the phase angle usually occurs at about the same frequency as the minimum of the impedance modulus. The impedance modulus usually falls sharply from the value at zero frequency. The amplitude at zero frequency represents the total peripheral resistance. The minimum value usually occurs between 2 and 4 Hz. There is generally a second maximum and minimum and leveling off between 5 and 10 Hz. The average of the amplitudes values between 5 and 10 Hz is usually identified as the characteristic impedance and relates to compliance.[11] When measuring pressure and flow to determine input impedance, it is imperative that both be measured at the same site.[38]

Recently, the viscous Navier-Stokes equations were used to model flow and the linearly viscoelastic membrane equations were used to model the mechanical properties in medium to large arteries. Asymptotic and homogenization theory was used to generate a "one-and-one half dimensional" model that was able to describe the viscous dissipation of the fluid, the viscoelastic nature of the blood flow/vessel wall interaction, the hysteresis loop in arterial wall behavior, and two-dimensional flow effects. The model outputs were compared with ultrasound imaging and Doppler flow measurements and excellent agreement was found between the model and the experiments.[39]

An adaptive identification procedure was used to obtain an instantaneous impulse-response representation of the systemic arterial system. A three-element windkessel model was used to calculate instantaneous compliance. Most techniques for the identification of windkessel models rely on generating frequency spectra of the arterial pressure and flow waveforms using Fourier transform techniques. These techniques assume no time variations in the pressure or flow cycle lengths. To meet this requirement, the usual practice is to average data over several cycles and compile "idealized" pressure and flow waves. This is necessary because sequential cardiac cycles are rarely of exactly the same length violating a basic assumption of Fourier transform. Time-domain techniques must assume an invariant system during at least one cycle, even when used to study transient phenomena. The algorithm used in this study was adaptive. It estimated the impulse response (IR) of the system and provided an update at every data point or at every instant during a beat in which data were recorded. A compliance estimate was calculated as the ratio of the maximum derivative of aortic root pressure over the maximum derivative of aortic root flow. Basic assumptions were that optimal coupling occurs when the energy required for the pumping of a given amount of blood is minimal and that the ventricle produces all of its stroke work during ejection. This work examined the possibility of an optimal arterial compliance as a function of time minimizing the work of ejection. We concluded that arterial compliance does not remain constant. It attains a maximum value during systole and a minimum value after end-ejection. The time trajectory of the arterial compliance is similar to the theoretical optimum compliance trajectory and the increase in compliance during systole results in energy savings.[40]

As previously described, lumped and partially distributed models of the input impedance of the pulmonary and systemic arterial beds have been widely used.[11,15,28,41–51] There has been less use of these applications for peripheral beds, even though the

viscoelastic behavior of a particular circulatory bed could be of significant importance particularly in the presence of peripheral vascular disease.[51–56]

The input impedance of the carotid circulation was compared in pigs fed a control diet and pigs fed a hyperlipidemic diet for 16 weeks. Previously calibrated ultrasonic transit-time flowmeter transducers and catheter-tip manometers were located at the origin of both left and right carotid arteries. A lumped, five-parameter model was used to characterize the pressure-flow relationships between the two groups of animals. The model contained a peripheral resistance term (R_p), an overall inertance term (L) and a Ranke model consisting of a resistor (R_d) and two capacitors (representing compliance) (C) and (C_d). The term C represents the overall static compliance of the carotid bed and the parallel capacitor (C_d) and resistance (R_d) account for viscous effects. R_p was calculated as the ratio between mean pressure and mean flow. The other four parameters were estimated by fitting measured to model predicted flows. The average static compliance was reduced by 40% between the normal diet and hyperlipidemic diet-fed pigs. There was a significant reduction in the overall cross-sectional area in the hyperlipidemic diet-fed pigs inferred from a 53% increase in L but R_p, representing resistance vessel tone, was unchanged. No signs of occlusive disease were found in any of the animals used in this study.[35]

Ventricular/Vascular Coupling

In Chap. 4 ventricular function was described using the end-systolic pressure/volume relationship (E_{es}). Arterial function can likewise be described in terms of a pressure/volume relationship (E_a) and the ratio between the two (E_a/E_{es}) describes the coupling between the two systems. The normal operating range of E_a/E_{es} occurs when the coupled system works with maximum efficiency. Values outside the normal range are associated with pathology. Two different methods of estimating E_a are commonly used.

Ventricular/Vascular Coupling Determined Using the Input Impedance

De Tombe et al.[57] used isolated, blood-perfused dog hearts pumping into a simulated three-element windkessel hydraulic system where they could control and vary E_a. Maximal stroke work and optimal ventricular efficiency (stroke work/myocardial oxygen consumption) occurred at E_a/E_{es} ratios of 0.3–1.3. This corresponded with ejection fractions of about 40-80%.

Wistar rats were used to study the effects of reduced arterial compliance as a result of hypervitaminosis D and nicotine. Aortic pressures and flows were simultaneously recorded. The characteristic impedance was used to estimate arterial compliance. E_a/E_{es} increased significantly in the treated rats. The treated group also demonstrated

increases in the wave reflection coefficient, PWV, and a decrease in total arterial compliance. All of the changes were associated with systolic hypertension.[58]

Baboons were used to assess left ventricular/vascular coupling in the supine and upright positions. Aortic pressure and flow were measured to obtain input and characteristic impedances. Ventricular/vascular coupling was evaluated using the ratio of pulsatile power to total left ventricular power (W_p/W_t). No significant change in efficiency of left ventricular/vascular coupling or input impedance was seen with postural changes.[59]

Ventricular/vascular coupling in the presence of aortic stenosis was evaluated using a model that incorporated the time-varying elastance of the LV, the instantaneous net pressure gradient across the aortic valve and the three-element windkessel model for the systemic arterial load. Six human patients with severe aortic stenosis were evaluated a short time before and just after valve replacement surgery. No significant changes in the combined model were observed but this could have been due to the short time interval following cardiopulmonary bypass and surgery with resultant adverse effects on the myocardium. A long-term follow-up study on these patients might have provided more interesting results.[60]

Pigs were used to measure right ventricular/pulmonary artery coupling before and after acute pulmonary hypertension by injecting glass microspheres. E_a was obtained from pulmonary artery pressure and flow measurements, E_{es} from pressure/volume loops. Stroke work was calculated from the pressure/volume loop and oxygen consumption was estimated from the pressure/volume area. Efficiency was defined as the ratio between stroke work and oxygen consumption. Prior to the iatrogenic pulmonary hypertension (control measurements), the right ventricle operated at maximum efficiency and submaximal work output. Decreased compliance associated with pulmonary hypertension decoupled the right ventricle from its vascular load with the maximum stroke work against the afterload shifted and right ventricular stroke volume decreased.[61]

Ventricular/Vascular Coupling Determined Using the Ratio of Ventricular End-Systolic Pressure and Stroke Volume (P_{es}/SV) Designated E_a

Describing afterload in terms of pressure and volume accomplishes several worthwhile goals. When the ratio of ventricular end-systolic pressure and stroke volume is calculated, the resulting expression for E_a represents various aspects of the total arterial input impedance as an effective stiffness parameter. The expression includes arterial resistance as well as the pulsatile components of the load and thus also reflects compliance of the vasculature and wave reflections. Most importantly the estimate of E_a can be coupled to the pressure/volume characterization of the ventricle. E_a/E_{es} ratios in normal humans are generally 0.7–1.0, well within the range of optimal function. Patients with congestive heart failure typically measure values as high as 4.0 because of the relative decline in ventricular contractile function and the concomitant increase in afterload.[62]

Two groups of mice, 6-month old and 16-month old (senescent), were compared using a 1.4 F micromanometer and conductance catheter combination. E_a/E_{es} ratios were increased three times in the senescent mice compared with the controls. The senescent mice also demonstrated significant decreases in stroke volume index, ejection fraction, cardiac output index, stroke work index, and dP/dt_{max}. The load independent measures of preload recruitable stroke work and E_{es} were significantly lower in the senescent mice but heart rate and E_a were not significantly different.[63]

Recently, Frenneaux and Williams[64] reported on E_a/E_{es} ratios in patients with HFnEF (heart failure, normal ejection fractions). E_a was calculated as the ratio of systolic pressure and stroke volume. Patients with HFnEF demonstrated much larger increases in LV end-systolic pressure for any given increase in stroke volume, but the increase in E_{es} was disproportionate to the rise in E_a resulting in a decrease in E_a/E_{es}. During handgrip exercise, the patients had a hypertensive response that correlated with the high basal E_{es} and demonstrated a significantly greater increase in LV end-systolic pressure than healthy control subjects. Figure 3 in the Frenneaux and Williams paper is an example of the problem with real life pressure/volume loops. The linear extrapolation of E_{es} to zero pressure provides a physically impossible negative volume.

Pigs at 1, 2, 4, and 6 weeks of age were catheterized and measurements made of E_{es} and E_a at rest and during isoproterenol and propranolol treatments. Resting heart rate and cardiac index decrease between 1 and 6 weeks. One-week old pigs showed no change in E_{es} from isoproterenol but other indices of contractility, preload-recruitable stroke work, dP/dt_{max}, the dP/dt_{max}-end-diastolic volume relation, cardiac index, and heart rate did increase. E_a decreased with isoproterenol in 1-week-old pigs but did not change in 6-week olds. Contractility indices in pigs at 2, 4, and 6 weeks of age all demonstrated reserve capacity. E_a/E_{es} was higher at rest in 6-week olds than in 1-week olds and fell significantly with isoproterenol in the 6-week olds but not the 1-week olds.[65]

E_a/E_{es} and other ventricular vascular function parameters were measured using a conductance catheter with microtip manometer system in mice with the thorax open. The systemic arterial system was modeled with a four-element windkessel and values for arterial compliance, using impedance measurements, were compared with measurements of E_a obtained with the end-systolic pressure/SV determinations. Occlusion of the aorta resulted in changes in E_a, and input impedance, pulse-wave velocity, and E_{es}, but the E_a/E_{es} ratio was not changed.[66]

Wauthy et al.[67] created acute pulmonary hypertension in dogs, goats, and pigs with hypoxia, distal embolism, and proximal pulmonary arterial constriction. They evaluated right ventricular (RV)/pulmonary arterial (PA) coupling efficiency using right ventricular pressure/volume loops and pulmonary arterial impedance from pressure and flow curves. They found that RV contractility increased proportionally to RV afterload and that optimal coupling was maintained in all three species. Embolization of the pulmonary vasculature increased resistance and wave reflection but not elastance. Proximal constriction of the PA increased resistance, increased and accelerated wave reflection, and resulted in a significant increase in elastance. They concluded that optimal or near-optimal RV/PA coupling was maintained during acute perturbations that resulted in pulmonary vascular hypertension in these three species of animals.

Diastolic Ventricular/Vascular Coupling

Diastolic ventricular/vascular coupling was characterized by comparing the time derivative of left ventricular pressure (d*P*/d*t*) vs. the time-varying pressure to define a "pressure phase plane (PPP)" parameter. The analysis allows determination of a PPP-derived "stiffness analog" during isovolumic contraction and relaxation. LV relaxation was characterized using tau, the time constant of isovolumic relaxation, and vascular relaxation (the aortic pressure decay) was characterized using the exponential decay time constant kappa. The authors provide results that show the PPP-derived systolic and diastolic ventricular and vascular stiffness are strongly coupled with a strong linear correlation between kappa and tau. They conclude that the PPP method provides a tool for quantitative assessment and determination of vascular coupling to diastolic function.[68] Practical problems associated with the determination of tau and kappa were previously discussed in this chapter and Chap. 4.

MRI Imaging for Detection of Ventricular/Vascular Coupling

A non-ferrous catheter-tip manometer was used to measure LV pressures simultaneously with MRI volume determinations in dogs over a wide range of end-systolic pressures produced by pharmaceutical perturbations. Time-varying wall stress did not change from low to medium loads but increased significantly at high end-systolic pressures. The authors concluded that increases in time-varying wall stress resulted from increases in pressure during the latter half of systole and is incompletely offset by shortening and wall thickening.[69]

Tissue Doppler Imaging and Elasticity Imaging

Hartley and colleagues describe a technique for sensing vessel wall motion they call the tissue Doppler displacement method, originally developed to measure ventricular thickening. They applied the technique to record myocardial wall motion in pigs, dogs, and rats.[70–73] Short bursts of ultrasound, two to eight cycles of the carrier frequency are aimed at the tissue of interest. Returning echoes are received by the same transducer. These signals are amplified and mixed with quadrature signals from a reference oscillator and two phase-detected echo signals are produced. The echo signals are sampled using a range-gated pulse delayed from the transmitted burst by an amount corresponding to the echo-return time. The signal is used to generate in-phase and quadrature Doppler signals from a sample volume within the tissue of interest. The in-phase and quadrature signals are viewed on an oscilloscope as *X* and *Y* coordinates of a vector. The technique produces an accurate, high fidelity, measure of the relative motion of any structure it is focused on including the ventricular or arterial walls. The technique was used to compare carotid artery wall motion in 3 to 5-month old wild-type mice, 30-month old senescent mice, apo-lipoprotein E (Apo-E) knockout

mice, and α-smooth muscle actin knockout (α-SMA) mice. Calculated displacement signals from the near and far walls were used to produce a diameter signal, and this was used to generate excursion and augmentation indices. Excursions ranged from 13 μm (Apo-E) to 95 μm (α-SMA). The augmentation index was lowest in the control, wild-type mice and highest in the senescent mice.[74] The technique was also used for noninvasive cardiovascular phenotyping in mice, along with other high-resolution Doppler techniques.[75]

The same technology was used to compare aortic artery wall systolic velocity in human subjects with type 2-diabetes but no coronary artery disease (CAD) (group A), CAD without diabetes (group B), diabetes with CAD (group C) and age and sex matched normal controls. Aortic wall velocities were significantly lower in the three patient groups compared with the control group. Aortic strain, distensibility and systolic velocity showed a strong negative correlation with the duration of the diabetes in the diabetic groups A and C. The conclusion is that aortic stiffening in type 2-diabetes is an early event that might explain the high risk of cardiovascular complications in these patients.[76]

Fatemi and Greenleaf[77] describe three different methods of tissue characterization that can be determined using ultrasound technology. The transient method measures small, transient tissue deformations produced by short transient pressure signals (ultrasound). The shear-wave method uses a short transient excitatory perturbation and measures the resulting shear-wave amplitude and velocity. Vibro-acoustography measures the acoustic field resulting from vibrating the tissue of interest at a specific frequency. Vibro-acoustography can be used to detect particles that do not support shear waves such as gas bubbles. The acoustic emission waves that result from vibrations of the tissue mass have small attenuation in biological tissues and can thus be detected using a hydrophone from a distance, providing a method of evaluating the physical properties of deep tissues or structures, noninvasively.

References

1. Hales S, ed. Statical Essays: Containing Haemastaticks; Or, an Account of Fome Hydraulick and Hydrostatical Experiments made on the Blood and Blood-Veffels of Animals. West-End of St. Paul's, London: Council of the Royal Society; 1733; No. II.
2. Frank O. Die grundform des arteriellen pulses. Z Biol. 1899;37:483.
3. McDonald DA, Taylor MG. The hydrodynamics of the arterial circulation. Prog Biophys Chem. 1959;9:107.
4. Bramwell JC, Hill AV. The velocity of the pulse wave in man. Proc Roy Soc Lond (Biol). 1922;93:298.
5. McDonald DA. Regional pulse-wave velocity in the arterial tree. J Appl Physiol. 1968;24:73–78.
6. McDonald DA. Blood Flow in Arteries, 2nd Edition. Baltimore, MD: Williams & Wilkens; 1974.
7. Westerhof N, Elzinga G, Sipkema P. An artificial arterial system for pumping hearts. J Appl Physiol. 1971;31:776–781.
8. Noordergraaf A, Verdouw PD, van Brummelen AGW, Wiegel FW. Analog of the arterial bed. In: Attinger EO, ed. Pulsatile Blood Flow, 1st Edition. New York, NY: McGraw-Hill; 1964:373.
9. Taylor MG. An approach to an analysis of the arterial pulse wave. II. Fluid oscillations in an elastic pipe. Phys Med Biol. 1957;1:321–329.

10. Taylor MG. An approach to an analysis of the arterial pulse wave. I. oscillations in an attenuating line. Phys Med Biol. 1957;1:258–269.
11. Burattini R. Reduced models of the systemic arterial circulation. In: Westerhof N, Gross DR, eds. Vascular Dynamics; Physiological Perspectives. Life Sciences, Vol. 166. New York: Plenum Press; 1989:69–85.
12. O'Rourke MF. Pressure and flow waves in systemic arteries and the anatomical design of the arterial system. J Appl Physiol. 1967;23:139–149.
13. Wetterer E, Kenner T. Die Dynamik Des Arterienpulses, 1st Edition. Berlin: Springer-Verlag; 1968.
14. Sipkema P, Westerhof N. Effective length of the arterial system. Ann Biomed Eng. 1975;3:296–307.
15. Burattini R, Gnudi G. Computer identification of models for the arterial tree input impedance: Comparison between two new simple models and first experimental results. Med Biol Eng Comput. 1982;20:134–144.
16. Burattini R, Campbell KB. Modified asymmetric T-tube model to infer arterial wave reflection at the aortic root. IEEE Trans Biomed Eng. 1989;36:805–814.
17. Westerhof N, Gross DR. Section I: Conduit and resistive vessel dynamics. In: Westerhof N, Gross DR, eds. Vascular Dynamics; Physiological Perspectives. Life Sciences, Vol. 166. New York: Plenum Press in cooperation with NATO Scientific Affairs Division; 1989:v.
18. Yin CPF, Liu Z. Arterial compliance-physiological viewpoint. In: Westerhof N, Gross DR, eds. Vascular Dynamics, Physiological Perspectives. Life Sciences, Vol. 166. New York: Plenum Press; 1989:9–22.
19. Patel DJ, Mallos AJ, Fry DL. Aortic mechanics in the living dog. J Appl Physiol. 1961;16:293–299.
20. Tucker WK, Janicki JS, Plowman F, Patel DJ. A device to test mechanical properties of tissues and transducers. J Appl Physiol. 1969;26:656–658.
21. Patel DJ, Janicki JS, Carew TE. Static anisotropic elastic properties of the aorta in living dogs. Circ Res. 1969;25:765–779.
22. Patel DJ, Janicki JS, Vaishnav RN, Young JT. Dynamic anisotropic viscoelastic properties of the aorta in living dogs. Circ Res. 1973;32:93–107.
23. Gentile BJ, Gross DR, Chuong CJ, Hwang NH. Segmental volume distensibility of the canine thoracic aorta in vivo. Cardiovasc Res. 1988;22:385–389.
24. Gross DR. Compliance and aging. In: Westerhof N, Gross DR, eds. Vascular Dynamics, Physiological Perspectives. Life Sciences, Vol. 166. New York: Plenum Press; 1989:37–47.
25. Latham RD. Pulse propagation in the systemic arterial tree. In: Westerhof N, Gross DR, eds. Vascular Dynamics; Physiological Perspectives. Life Sciences, Vol. 166. New York: Plenum Press; 1989:49–67.
26. Latham RD, Rubal BJ, Westerhof N, Sipkema P, Walsh RA. Nonhuman primate model for regional wave travel and reflections along aortas. Am J Physiol. 1987;253:H299–H306.
27. Latham RD, Westerhof N, Sipkema P, Rubal BJ, Reuderink P, Murgo JP. Regional wave travel and reflections along the human aorta: A study with six simultaneous micromanometric pressures. Circulation. 1985;72:1257–1269.
28. Latson TW, Hunter WC, Katoh N, Sagawa K. Effect of nitroglycerin on aortic impedance, diameter, and pulse-wave velocity. Circ Res. 1988;62:884–890.
29. Reddy AK, Jones AD, Martono C, Caro WA, Madala S, Hartley CJ. Pulsed Doppler signal processing for use in mice: Design and evaluation. IEEE Trans Biomed Eng. 2005;52:1764–1770.
30. Reddy AK, Taffet GE, Li YH, et al. Pulsed Doppler signal processing for use in mice: Applications. IEEE Trans Biomed Eng. 2005;52:1771–1783.
31. Kubozono T, Miyata M, Ueyama K, et al. Clinical significance and reproducibility of new arterial distensibility index. Circ J. 2007;71:89–94.
32. Tillin T, Chambers J, Malik I, et al. Measurement of pulse wave velocity: Site matters. J Hypertens. 2007;25:383–389.

33. Davies TS, Frenneaux MP, Campbell RI, White MJ. Human arterial responses to isometric exercise: The role of the muscle metaboreflex. Clin Sci (Lond). 2007;112:441–447.
34. Vlachopoulos CV, Vyssoulis GG, Alexopoulos NA, et al. Effect of chronic coffee consumption on aortic stiffness and wave reflections in hypertensive patients. Eur J Clin Nutr. 2007;61:796–802.
35. Burattini R, Montanari L, Mulligan LJ, Cannon MS, Gross DR. Evaluation of hypercholesterol diet-induced changes in viscoelastic properties of carotid circulation in pigs. Am J Physiol. 1992;263:H1919–H1926.
36. Noble MI, Gabe IT, Trenchard D, Guz A. Blood pressure and flow in the ascending aorta of conscious dogs. Cardiovasc Res. 1967;1:9–20.
37. O'Rourke MF. Impact pressure, lateral pressure, and impedance in the proximal aorta and pulmonary artery. J Appl Physiol. 1968;25:533–541.
38. Westerhof N, Noordergraaf A. Errors in the measurement of hydraulic input impedance. J Biomech. 1970;3:351–356.
39. Canic S, Hartley CJ, Rosenstrauch D, Tambaca J, Guidoboni G, Mikelic A. Blood flow in compliant arteries: An effective viscoelastic reduced model, numerics, and experimental validation. Ann Biomed Eng. 2006;34:575–592.
40. Vrettos AM, Gross DR. Instantaneous changes in arterial compliance reduce energetic load on left ventricle during systole. Am J Physiol. 1994;267:H24–H32.
41. Attinger EO, Anne A, McDonald DA. Use of Fourier series for the analysis of biological systems. Biophys J. 1966;6:291–304.
42. Attinger EO, Sugawara H, Navarro A, Riccetto A, Martin R. Pressure-flow relations in dog arteries. Circ Res. 1966;19:230–246.
43. Burattini R, Gnudi G, Westerhof N, Fioretti S. Total systemic arterial compliance and aortic characteristic impedance in the dog as a function of pressure: A model based study. Comput Biomed Res. 1987;20:154–165.
44. Burattini R, Reale P, Borgdorff P, Westerhof N. Dynamic model of the short-term regulation of arterial pressure in the cat. Med Biol Eng Comput. 1987;25:269–276.
45. Defares JG, van der Waal HJ. A method for the determination of systemic arterial compliance in man. Acta Physiol Pharmacol Neerl. 1969;15:329–343.
46. Latham RD, Sipkema P, Westerhof N, Rubal BJ. Aortic input impedance during Mueller maneuver: An evaluation of "effective length". J Appl Physiol. 1988;65:1604–1610.
47. Murgo JP, Westerhof N, Giolma JP, Altobelli SA. Manipulation of ascending aortic pressure and flow wave reflections with the Valsalva maneuver: Relationship to input impedance. Circulation. 1981;63:122–132.
48. Murgo JP, Westerhof N, Giolma JP, Altobelli SA. Aortic input impedance in normal man: Relationship to pressure wave forms. Circulation. 1980;62:105–116.
49. O'Rourke MF, Taylor MG. Input impedance of the systemic circulation. Circ Res. 1967;20:365–380.
50. Patel DJ, Defreitas FM, Fry DL. Hydraulic input impedance to aorta and pulmonary artery in dogs. J Appl Physiol. 1963;18:134–140.
51. Westerhof N, Noordergraaf A. Arterial viscoelasticity: A generalized model effect on input impedance and wave travel in the systematic tree. J Biomech. 1970;3:357–379.
52. Apter JT. Correlation of visco-elastic properties with microscopic structure of large arteries. IV. Thermal responses of collagen, elastin, smooth muscle, and intact arteries. Circ Res. 1967;21:901–918.
53. Apter JT, Marquez E. Correlation of visco-elastic properties of large arteries with microscopic structure. V. Effects of sinusoidal forcings at low and at resonance frequencies. Circ Res. 1968;22:393–404.
54. Bergel DH. The dynamic elastic properties of the arterial wall. J Physiol. 1961;156:458–469.
55. Bergel DH. The static elastic properties of the arterial wall. J Physiol. 1961;156:445–457.
56. Learoyd BM, Taylor MG. Alterations with age in the viscoelastic properties of human arterial walls. Circ Res. 1966;18:278–292.

57. De Tombe PP, Jones S, Burkhoff D, Hunter WC, Kass DA. Ventricular stroke work and efficiency both remain nearly optimal despite altered vascular loading. Am J Physiol. 1993;264:H1817–H1824.
58. Jegger D, da Silva R, Jeanrenaud X, et al. Ventricular-arterial coupling in a rat model of reduced arterial compliance provoked by hypervitaminosis D and nicotine. Am J Physiol Heart Circ Physiol. 2006;291:H1942–H1951.
59. Tran CC, Latham RD, Self DA, Fanton JW, White CD, Owens RW. Effect of upright tilt on ventricular/vascular coupling in chronically instrumented primates. Am J Physiol. 1993;265:H244–H2451.
60. Garcia D, Barenbrug PJ, Pibarot P, et al. A ventricular-vascular coupling model in presence of aortic stenosis. Am J Physiol Heart Circ Physiol. 2005;288:H1874–H1884.
61. Fourie PR, Coetzee AR, Bolliger CT. Pulmonary artery compliance: Its role in right ventricular-arterial coupling. Cardiovasc Res. 1992;26:839–844.
62. Kass DA. Age-related changes in ventricular-arterial coupling: Pathophysiologic implications. Heart Fail Rev. 2002;7:51–62.
63. Yang B, Larson DF, Watson R. Age-related left ventricular function in the mouse: Analysis based on in vivo pressure-volume relationships. Am J Physiol. 1999;277:H1906–H1913.
64. Frenneaux M, Williams L. Ventricular-arterial and ventricular-ventricular interactions and their relevance to diastolic filling. Prog Cardiovasc Dis. 2007;49:252–262.
65. Cassidy SC, Chan DP, Allen HD. Left ventricular systolic function, arterial elastance, and ventricular-vascular coupling: A developmental study in piglets. Pediatr Res. 1997;42:273–281.
66. Segers P, Georgakopoulos D, Afanasyeva M, et al. Conductance catheter-based assessment of arterial input impedance, arterial function, and ventricular-vascular interaction in mice. Am J Physiol Heart Circ Physiol. 2005;288:H1157–H1164.
67. Wauthy P, Pagnamenta A, Vassalli F, Naeije R, Brimioulle S. Right ventricular adaptation to pulmonary hypertension: An interspecies comparison. Am J Physiol Heart Circ Physiol. 2004;286:H1441–H1447.
68. Chung CS, Strunc A, Oliver R, Kovacs SJ. Diastolic ventricular-vascular stiffness and relaxation relation: Elucidation of coupling via pressure phase plane-derived indexes. Am J Physiol Heart Circ Physiol. 2006;291:H2415–H2423.
69. Dell'Italia LJ, Blackwell GG, Thorn BT, Pearce DJ, Bishop SP, Pohost GM. Time-varying wall stress: An index of ventricular vascular coupling. Am J Physiol. 1992;263:H597–H605.
70. Hartley CJ, Litowitz H, Rabinovitz RS, et al. An ultrasonic method for measuring tissue displacement: Technical details and validation for measuring myocardial thickening. IEEE Trans Biomed Eng. 1991;38:735–747.
71. Hartley CJ, Latson LA, Michael LH, Seidel CL, Lewis RM, Entman ML. Doppler measurement of myocardial thickening with a single epicardial transducer. Am J Physiol. 1983;245:H1066–H1072.
72. Zhu WX, Myers ML, Hartley CJ, Roberts R, Bolli R. Validation of a single crystal for measurement of transmural and epicardial thickening. Am J Physiol. 1986;251:H1045–H1055.
73. Doursout MF, Wouters P, Kashimoto S, Hartley CJ, Rabinovitz R, Chelly JE. Measurement of cardiac function in conscious rats. Ultrasound Med Biol. 2001;27:195–202.
74. Hartley CJ, Reddy AK, Madala S, Entman ML, Michael LH, Taffet GE. Noninvasive ultrasonic measurement of arterial wall motion in mice. Am J Physiol Heart Circ Physiol. 2004;287:H1426–H1432.
75. Hartley CJ, Taffet GE, Reddy AK, Entman ML, Michael LH. Noninvasive cardiovascular phenotyping in mice. ILAR J. 2002;43:147–158.
76. Mahfouz Badran H, Elnoamany M. Impact of type 2 diabetes mellitus on aortic elastic properties in normotensive diabetes: Doppler tissue imaging study. J Am Soc Echocardiogr. 2006;19:1471–1481.
77. Fatemi M, Greenleaf JF. Probing the dynamics of tissue at low frequencies with the radiation force of ultrasound. Phys Med Biol. 2000;45:1449–1464.

Chapter 6
Isolated Heart Preparations, Problems, and Pitfalls

Development of the Isolated Heart Preparation

Isolated heart preparations allow many biochemical, physiological, morphological, and pharmacological indices to be evaluated without the confounding effects of other organs, the systemic circulation, and a host of potential confounding responses such as circulating neurohumeral substances. Researchers were able to independently study the role of temperature, oxygen, calcium ions, electrical activity, and autonomic nervous system effects and, more recently, the role of specific genetic variables. When hearts of small laboratory animals are used, the preparations are highly reproducible and can be used quickly in large numbers at relatively low cost. Historically research conducted on isolated hearts led to the discovery of chemical transmission of vagal stimulation, and the importance of preload and afterload to cardiac function. Other important advances include significant understanding of ischemia-reperfusion injury, cell-based therapy, and heart preservation.

The isolated perfused frog heart preparation was first developed at the Physiological Institute, University of Leipzig, under the direction of Carl Ludwig. Elias Cyon, from that institute, published the first description of the technique in 1866.[1] The preparation used was a working heart with serum pumped through an artificial circulation system. Bowditch, also working in Ludwig's lab, modified the preparation and used his iteration to describe the "Treppe" phenomenon, the all-or-none law of the heart and the absolute refractory period.[2] Otto Frank also worked in Ludwig's Physiological Institute developing his own modifications of the isolated frog heart preparation in 1892–1893. Frank further revised the technique after moving to Munich, inserting several valves, stopcocks, and manometers in the perfusion line and was able to measure isovolumetric and isotonic contractions. He published the results of his studies describing the preload dependence of cardiac output in 1895 and in more detail in 1898.[3,4] Carl Wiggers visited Frank's laboratory in 1911 and used many of his techniques in the following years.[1] Howell and Cooke studied the action of inorganic salts and serum on the frog isolated heart preparation.[5,6]

Oscar Langendorff was the first to describe the isolated, retrograde perfused, mammalian heart preparation.[7] Langendorff's method has seen many modifications over the years but the basic concept is the same and the preparation is commonly

D.R. Gross, *Animal Models in Cardiovascular Research*,
DOI: 10.1007/978-0-387-95962-7_6, © Springer Science + Business Media, LLC 2009

known as the Langendorff. Blood or crystalloid perfusate is delivered to the heart via a cannula in the ascending aorta, either at a constant pressure or at a constant flow. Retrograde flow in the aorta closes the aortic valve and the perfusate flows into the coronary vasculature via the coronary ostia. After passing through the coronary circulation, the perfusate mostly drains into the right atrium via the coronary sinus.[8] Some Thebesian venous drainage occurs directly into the right and left ventricles and both atria. Coronary arterioles of most mammalian species also communicate with arteriosinusoidal vessels and arterioluminal vessels that can shunt blood directly into all four cardiac chambers, especially if coronary sinus pressure is elevated or obstructed.

Howell and Duke used an in situ retrograde perfused cat heart preparation to show the relationship between inorganic salts and sympathetic nerve stimulation. They anesthetized the cats with ether, did a sternotomy, ligated the internal mammary arteries, ventilated the lungs, and widely opened the thorax. The brachiocephalic artery was isolated and a cannula inserted. The left subclavian artery was ligated, a loose ligature was placed around the aorta just distal to the left subclavian and the aorta was opened distally. Ringer's solution was run through the brachia-cephalic cannula. After allowing the system to wash out blood, the aorta was ligated and the posterior vena cava was opened to drain all blood. The heart was then beating from the retrograde perfusion of Ringer's solution. Interestingly, they reported that cat hearts were easier to keep functioning than dog hearts.[6]

Martin described a dog in situ isolated heart–lung preparation in 1881. The blood was oxygenated by the lungs and pumped against a controlled resistance. A major problem with Martin's preparation was that a large amount of blood was needed to keep the preparation functioning. Knowlton and Starling adapted the Martin model using a heart–lung preparation from cats to study the influence of temperature and blood pressure on cardiac performance.[9] Knowlton and Starling isolated the heart in situ by ligating the arteries originating from the arch of the aorta and the descending aorta with cannulae placed in the innominate (brachio-cephalic) artery and the anterior vena cava. The cannulae were filled with a solution of hirudin in saline to prevent blood clotting. The blood was pumped into the ascending aorta then through the cannula into a T-tube attached to a mercury manometer to measure the aortic pressure. The other branch of the T-tube was attached to a test tube with an air interface that acted as a "windkessel," a compliance chamber. The pathway "…passes to the resistance *R*. This consists of a thin-walled rubber tube (e.g., a rubber finger-stall) which passes through a wide glass tube T, provided with two lateral tubulures ww. One of these is connected with a mercurial manometer and the other with an air reservoir A, into which air can be pumped by the elastic bellows S. When air is injected into the tube T, the tube R is compressed and will remain so until the pressure of the blood within it is equal or superior to the pressure in the air surrounding it. It is thus possible to vary at will the resistance to the outflow of the blood from the arterial side…." Thus is described the "Starling resistor" well known to a generation of physiologists. After the resistor, the blood was passed into a reservoir from which the blood was siphoned off after a desired amount had been collected. A lateral branch on the siphon tube was attached to a tambour that measured

the change of pressure resulting from the siphoning procedure and thus recorded the volume change per unit time. The siphon discharged the blood into another reservoir kept immersed in a vessel of water that could be maintained at any desired temperature by providing a heat source. From this reservoir the right atrium was supplied with blood via the caval cannula and another mercury manometer attached to the posterior vena cava. Measurements made included arterial pressure, cardiac output (as recorded by the tambour system), and right atrial pressure. Cardiac volumes were measured using a glass cardiometer and a float recorder described in a previous paper by Jerusalem and Starling.[9]

In 1915, E. H. Starling delivered the Linacre Lecture on the Law of the Heart, subsequently published in 1918. He stated the law thus; "…within physiological limits the larger the volume of the heart the greater are the energy of its contraction and the amount of chemical change at each contraction under all conditions of load, output and fatigue the total energy liberated at each beat is determined by the diastolic volume of the heart and therefore by the muscle-fibre length at the beginning of contraction…." He observed that in situ the heart becomes inefficient, i.e., unable to pump blood at the same cardiac output and arterial pressure when diastolic dilation is prevented. These studies were conducted using the previously described heart–lung preparation except that a collapsible rubber sleeve was used as the venous reservoir to prevent any air/blood interface and the potential loss of gases.[10] In this work, Starling cited previous work by Lovatt Evans and colleagues, using a similar heart–lung preparation. Evan's work indicated that any increase in the workload of the heart resulted in an increase in metabolism measured either by oxygen uptake or by carbon dioxide production. Starling confirmed that increased diastolic volume resulted in increased oxygen consumption when the isolated heart was maintained under constant chemical (pH) and temperature conditions. As long as the isolated heart was functioning well, particularly early in the experiment, any increase or decrease in work was accompanied by a proportional increase or decrease in diastolic volume and these changes were proportionally reflected in oxygen consumption. He also observed that at the same diastolic volumes the isolated heart consumed more oxygen per beat when contracting at slower heart rates but that slowing the heart enabled it to do a given amount of work per unit time more economically.[10]

Starling described some problems associated with the isolated heart–lung preparation. Pulmonary edema was common, particularly when the preparation was used over prolonged periods. It was necessary to "…allow for the changes in the elastic tension of the lungs…." Handling of the lungs frequently resulted in atelectasis and a poor preparation. When the beating heart was freed from the pericardium, its contact with the lungs made the spirometer records uneven and difficult to measure. The test for a heart-lung preparation being in "good condition" was that the diastolic volume remained at a steady level when the preload and afterload were held constant. "…In no case does the heart in a heart–lung preparation remain throughout the experiment in this good physiological state, though in many cases during the first one to one and a half hours it deviates but little from this ideal condition. Generally, however, from the very beginning of the experiment, the heart, under even a moderate load, shows a steady slow dilation although the load is maintained con-

stant, and the rate at which this dilatation occurs is much increased by further increase in the strain to which the heart is subjected…."[10]

Retrograde Perfusion Preparations (The Langendorff Preparation)

Two variations of this preparation are commonly used, the pressure-regulated and the flow-regulated. Figure 6.1 is a schematic of the pressure-regulated system and Fig. 6.2 is a schematic of the flow-regulated system. A cannula is inserted into the root of the aorta and perfusate flows directly into the coronary vasculature with the pressure head keeping the aortic valve closed. The typical system consists of a reservoir for the perfusate or a support animal, a warm water reservoir attached to a pump that supplies water jackets around the bulk perfusate reservoir, the heart chamber,

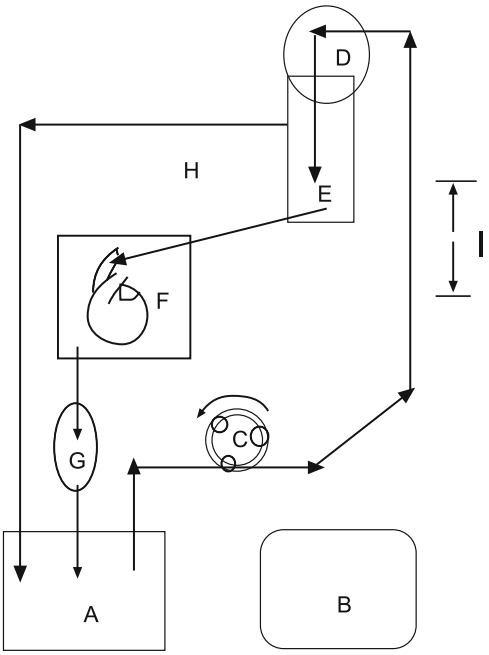

Fig. 6.1 Schematic of the Langendorff-type retrograde pressure-regulated perfusion preparation: (**A**) bulk reservoir for perfusate or a support animal, (**B**) warm water reservoir to supply all water jacketed components, (**C**) pump (also need a pump to circulate warm water through the various components), (**D**) oxygenator (not needed if have a support animal), (**E**) reservoir for the oxygenated perfusate, (**F**) heart chamber, must be temperature controlled, (**G**) coronary outflow from right atrium, coronary sinus and/or pulmonary artery, (**H**) overflow to maintain a constant perfusate level in E, (**I**) method for height adjustment for E to regulate perfusion pressure

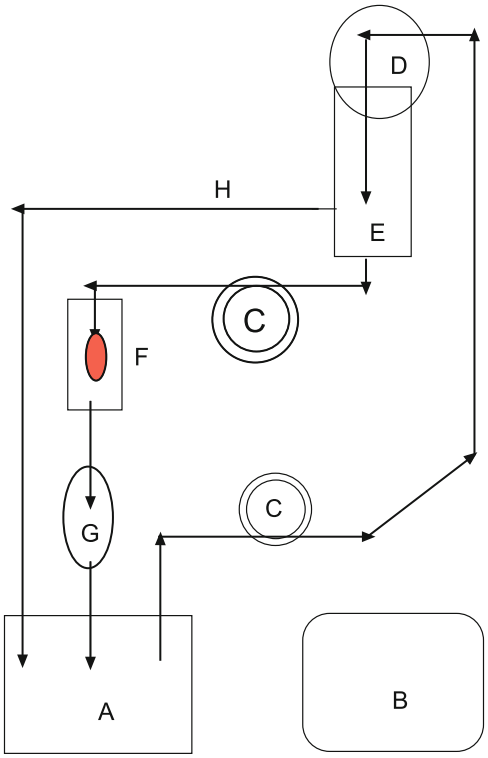

Fig. 6.2 Schematic of the Langendorff-type retrograde flow-regulated perfusion preparation: (**A**) bulk reservoir for perfusate or support animal, (**B**) warm water reservoir for water jackets, (**C**) pumps, (**D**) oxygenator (not needed with support animal), (**E**) reservoir for the oxygenated perfusate, (**F**) heart chamber, (**G**) coronary outflow, (**H**) overflow to maintain a constant perfusate level in (**E**)

and the reservoir for the oxygenated perfusate. Other parts of the system include a pump to deliver perfusate to the oxygenator, an overflow to maintain a constant level in the perfusate reservoir, and a graduated container for measurement of coronary outflow from the right atrium or coronary sinus. The perfusate reservoir needs a method for height adjustment to control the perfusion pressure. The oxygenator system can be as simple as a ceramic gas disperser, bubbler, or a bulb bubbler system when a crystalloid perfusate is used. If whole blood or washed red blood cells are used, a membrane oxygenator is usually preferred since it is less traumatic to the blood components. If a support animal is used, the lungs of that animal serve the purpose. Often a 5–8 μm filter is placed in-line between the bulk reservoir and the oxygenated perfusate reservoir. Appropriately placed taps for pressure and flow transducers are included to measure coronary pressure and flow. Typically a balloon attached to a pressure transducer is placed in the left ventricle to monitor left ventricular pressure and its various derivatives and to control preload.

Choosing between the Pressure-Regulated or Flow-Regulated Langendorff-Type Preparation

Constant flow preparations usually provide more reproducible results, particularly if the experimental design includes low flow perturbations. However, autoregulatory mechanisms that are maintained with constant pressure preparations may be partially or entirely lost with flow-regulated preparations and the heart will not be able to increase flow in response to an increased workload. This could result in ischemia. If regional ischemia is induced when using the constant flow preparation, and the coronary flow rate is not adjusted properly, the same volume of perfusate is forced through a smaller mass of myocardium and flow per gram tissue increases significantly in the perfused zone. These unwanted results do not happen in the constant pressure preparation. The experimental design and the perturbations to be used should dictate the choice of constant pressure or constant flow. In many instances, there is a distinct advantage if one is able to switch instantly between the two modes. There are now commercially available, automatic, feedback computer-controlled systems that can accomplish this.[11,12]

The Isolated, Working, In Situ Heart-Lung Preparation

This preparation was the one used by Starling, and others, to make landmark discoveries about cardiac function.[6,9,10] The basic setup is shown in Fig. 6.3. The heart and lungs are isolated in situ. The lungs are ventilated, and blood flow from the aorta is directed into a compliance chamber, thence into a resistance (both adjustable) then into a reservoir and back into the right atrium. The height of the reservoir is adjustable to control preload. With the appropriate instrumentation aortic pressures and flows, right and left atrial pressures, right and left ventricular pressures and volumes, segmental shortening velocities, and other cardiac parameters can all be measured. A support animal is usually used to provide additional blood to the system as necessary.

The Isolated Working Left Heart Preparation

Some experimental questions can best be addressed using an isolated working left ventricular preparation.[13–16] Crystalloid perfusates have significant advantages and work effectively when used for the hearts of smaller lab animals, particularly mice and rats. The heart is excised, quickly stopped in 4°C balanced salt or cardioplegia solution, cannulated, and then hung in the apparatus and perfused. Some investigators prefer to start and stabilize the preparation using the retrograde perfusion technique of Langendorff and then convert to the working heart mode, others initiate the process by circulating the perfusate through the system.[13,15,17–22] The system generally consists of a reservoir or support animal, a warm water reservoir for circulation through all of the water-jacketed components of the system to maintain a constant

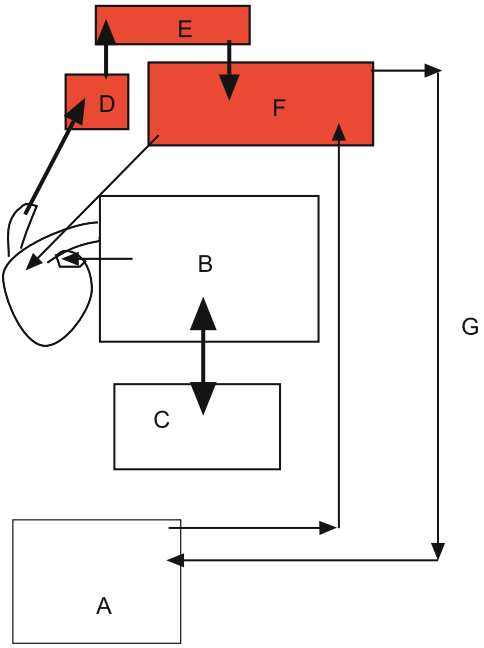

Fig. 6.3 Schematic of the isolated, biventricular working heart-lung preparation: (**A**) support animal, providing arterial blood, (**B**) ventilated isolated lungs, receive blood from the pulmonary artery and return blood to the left atrium of the isolated heart, (**C**) ventilator, (**D**) compliance chamber, amount of air contained can be adjusted to alter the compliance, (**E**) resistance chamber, can be as elegant as the resistor designed by Starling or as simple as a tube clamp, (**F**) reservoir, the height adjusted to provide changes in preload to the right atrium, (**G**) overflow for the reservoir to maintain a constant level of blood

temperature, a pump to move perfusate from the support animal or reservoir to an oxygenator, thence to a reservoir with an adjustable pressure head to control left atrial preload. The left ventricle pumps perfusate into the aorta where it is directed into a compliance chamber, thence into a resistance and then back into the support animal or the reservoir for recirculation. If crystalloid perfusate is used, it is usually wise to put a filter between the pump and the oxygenator. If the preparation is being used for an extended period of time, particularly with blood or RBC-enhanced perfusate, a dialysis system may be included in the loop. The dialysis system is particularly helpful if whole blood is being recirculated without cycling through a support animal.

The Langendorff-Type Perfused Working Left Heart Preparation

This preparation combines the utility of the working heart preparation with the simplicity of retrograde perfusion. It is most useful when working with hearts from larger species since the coronary vasculature can be perfused with blood or

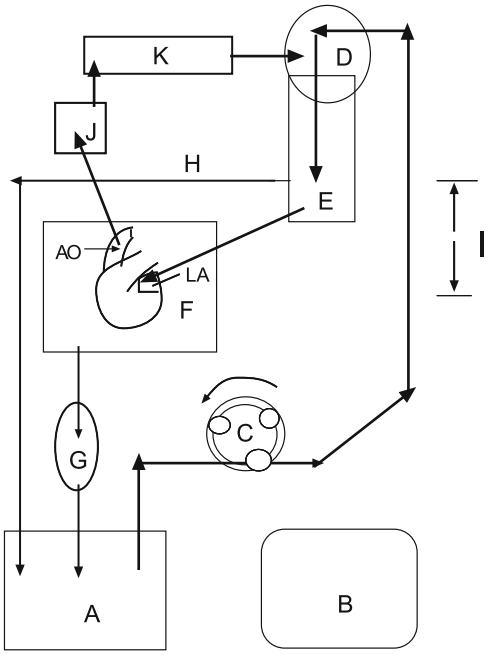

Fig. 6.4 Schematic of the working left heart preparation: (**A**) perfusate reservoir or support animal, (**B**) warm water reservoir, (**C**) pump, (**D**) oxygenator, (**E**) atrial reservoir, (**F**) heart chamber, maintained at a constant temperature (in some cases the heart may be immersed in warm crystalloid solution), (**G**) coronary effluent collection, (**H**) overflow for atrial reservoir to maintain a constant level, (**I**) height adjustment for atrial reservoir, (**J**) compliance chamber, (**K**) resistance

RBC-enhanced perfusate to maintain normoxia while the heart pumps crystalloid. Less blood is necessary to maintain the system so it is easier to maintain the support animal, or the reservoir needed for coronary perfusion. The cannula from the perfusion reservoir to the aorta is usually fitted with at least two different cannulae at the tip, one inserted and fixed in the right coronary artery, the other in the left main coronary artery. Sometimes three cannulae are used and the left circumflex and left anterior descending coronary vessels are cannulated separately (Fig. 6.5).[20]

Igic[23] describes a unique double cannula system with an outer cannula inserted into the aorta and an inner cannula that is advanced into the left ventricle. This "working" left heart ejects the perfusion fluid flowing into the left ventricle during diastole while the outer cannula perfuses the coronary vasculature. Burkhoff et al.[24] described a servo-system employing an electroconductive balloon in the left ventricle and retrograde perfusion of the coronary vasculature. The hearts are made to "eject" and "fill" using a computer-simulated arterial loading system. Complex ejection and filling patterns were created using this system. A similar system was used earlier by Weber et al.[25]

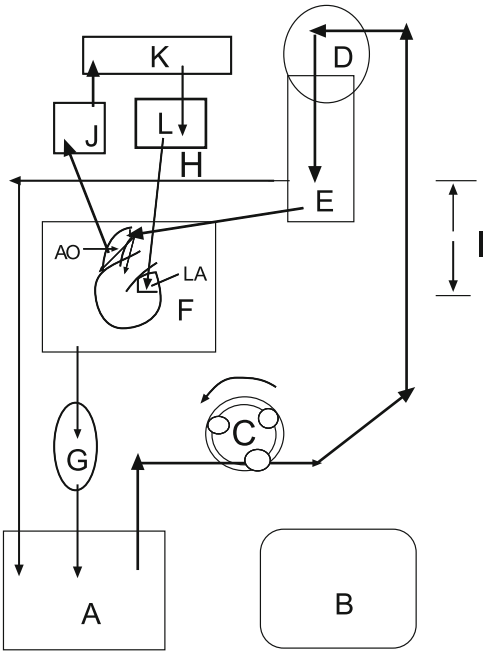

Fig. 6.5 Schematic of the Langendorff-type perfused working left heart preparation: (**A**) perfusate reservoir or support animal, (**B**) warm water reservoir for water-jacketed components, (**C**) pump, (**D**) oxygenator (not needed if support animal is used), (**E**) coronary perfusion reservoir, (**F**) heart chamber, temperature controlled, (**G**) coronary effluent, (**H**) overflow to maintain constant level in perfusion reservoir, (**I**) adjustable apparatus for coronary perfusion pressure (can substitute a pump to provide a flow-regulated system), (**J**) compliance chamber, (**K**) resistance, (**L**) atrial reservoir, also adjustable to control left atrial preload

The Biventricular Isolated Working Heart Preparation

The isolated left working heart preparation is considered to be superior to the Langendorff retrograde perfused preparation for making functional evaluations before and after perturbing the system. Since right ventricular function may be affected independently or may influence left ventricular function, the biventricular isolated working heart model was developed to study total heart function. When an isolated working left heart preparation was converted to a biventricular working preparation, there was an improvement in stroke volume, cardiac output, and pressure development. The same model was used to demonstrate that global ischemia has more of an affect on LV function than RV function.[26,27] An isolated biventricular model was also used to compare the hemodynamic, contractile, and energetic functions of the total isolated heart in ethanol-fed and control rats.[28] Hearts from 1-day, 7-day, 2 weeks, and adult rabbits were compared. The authors demonstrated that fatty acids are the major source of energy used by rabbits up to 2 weeks but the contribution

of glucose oxidation to ATP production was increased from 1-day to 14-days. At 14-days, glucose oxidation rates were still low compared with hearts from adult rabbits.[29] Slight modifications were made in the apparatus and cannulation methods to study norepinephrine-induced expression of cytokines in rat hearts.[30] Isolated biventricular preparations have been used to assess pharmacodynamics, cardiac devices, such as artificial valves, and a range of other studies during the controlled alteration of various determinants of hemodynamic performance. A major advantage of this preparation is the ability to independently control preload and afterload for each ventricle. This preparation was recently used to evaluate the direct myocardial depressant effects of halothane.[31] Most of these preparations are started using a retrograde perfusion mode. Once the heart has recovered and stabilized it is switched to the working mode. These preparations can be instrumented in a wide variety of ways to monitor pressures, flows, volumes, electrical activity, segmental shortening, and any other parameters of interest (Fig. 6.6).[32,33]

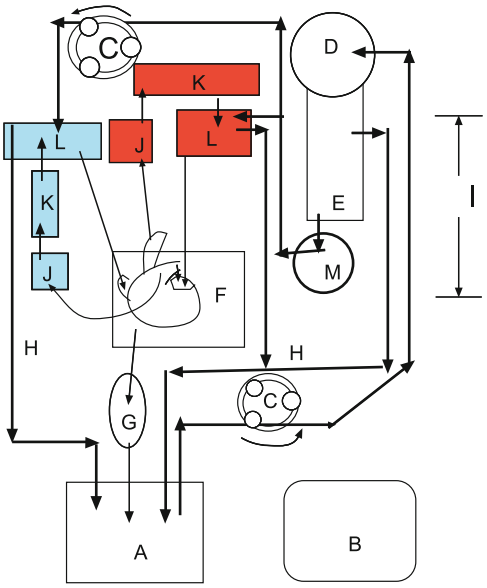

Fig. 6.6 Schematic of the biventricular isolated working heart preparation. (**A**) Reservoir or support animal, (**B**) warm water reservoir to supply all water jackets used in the system, (**C**) pumps, (**D**) oxygenator when whole blood perfusion and a support animal is not used, (**E**) perfusion reservoir, (**F**) temperature controlled chamber for the working heart, (**G**) coronary flow collection if a cannula is placed into the coronary sinus. Otherwise coronary flow must be measured locally with a flow-meter since the coronary outflow is directly into the atria and ventricles and is recirculated, (**H**) overflow to maintain the level in the perfusion reservoir constant, (**I**) apparatus to adjust the height of the perfusion reservoir, (**J**) compliance chambers for both the left and right side, (**K**) resistance for both the right and left side, (**L**) right and left atrial reservoirs that can be height adjusted to control preload to their respective ventricles, (**M**) membrane dialyzer to remove impurities and metabolic waste products

The Biventricular, Retrograde-Perfused, Working Heart Preparation

This model is particularly useful when it is necessary for the heart from a larger species to be used and oxygen carrying capacity must be supplied to prevent hypoxia. The preparation has also been used to pump clear fluid so fiber optic light sources and miniature cameras can be used to record and study natural and prosthetic valve function.[34] However, the blood from the coronary circulation contaminates the clear pumping fluid. This can be partially controlled by cannulation of the coronary sinus but some blood will still enter the pumped fluid from the Thebesian drainage and from arterial venous shunts in the myocardium. The model has been used to study cardiac changes during explantation and the effects of various methods of cardiac preservation for transplantation.[35] This preparation is also useful to separate cardiac responses from systemic responses during pharmacological, electrical, or hemodynamic perturbations (Fig. 6.7).[33]

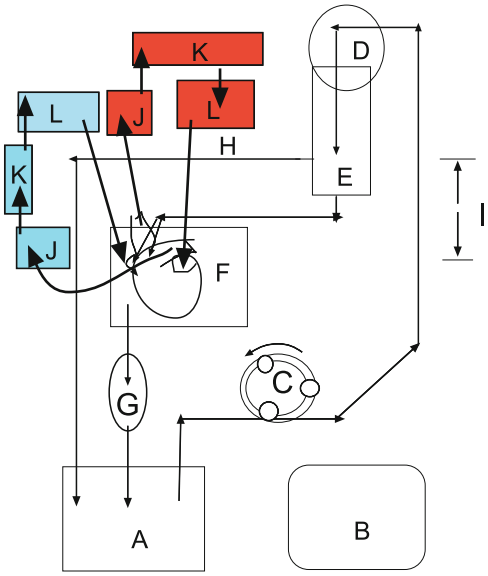

Fig. 6.7 Schematic of the biventricular, retrograde perfused, working heart preparation: (**A**) perfusate reservoir or support animal, (**B**) warm water reservoir, (**C**) pump, (**D**) oxygenator, not required with support animal, (**E**) coronary perfusion reservoir. The cannula supplying the coronary vasculature is divided at the end into two or three cannulae so the coronary arteries can be perfused via the coronary ostia. (**F**) Temperature controlled heart chamber, (**G**) coronary effluent, if the coronary sinus is cannulated, (**H**) overflow to maintain a constant level of coronary perfusate, (**I**) apparatus to enable adjustment of the coronary perfusion pressure, alternatively a pump can be inserted into the system to provide flow-regulation, (**J**) compliance chamber, (**K**) resistance, (**L**) right and left atrial reservoirs. Right and left ventricular preloads and afterloads can be individually adjusted

Perfusion Solutions

The vast majority of isolated heart preparations described in the literature use the bicarbonate buffer perfusion solution as described by Krebs and Henseleit.[36] This perfusion fluid mimics the key ionic content of blood or plasma but Krebs and Henseleit did not account for the fact that approximately half of the calcium in blood is bound to plasma, so their formulation is high in ionized calcium. Because of this many isolated heart preparations have been conducted at the upper limits of the calcium function curve. Ionized calcium concentrations should actually be in the range of 1.2–1.8 mM. Table 6.1 provides a summary of the composition of some recently reported crystalloid perfusion solutions. When preparing solutions that contain both calcium and phosphate ions, it is not uncommon for calcium phosphate particles to be precipitated. If the solution is not filtered, these particles can infarct the coronary vasculature. If they are filtered out, the ionic composition of the perfusate may be different. When preparing a bicarbonate-buffered solution, the calcium component must be the last to be added. The pH must be lowered by bubbling the solution with 95% O_2, 5% CO_2 prior to adding the calcium. Since other particulate impurities are common, even in the most pure commercial chemicals it is prudent to filter (5–8 μm) any perfusion solution prior to use.

Any viable isolated heart preparation must (1) provide enough oxygen to support metabolism, (2) maintain transmembrane ion gradients within normal limits, and (3) provide the energy required to maintain normal contractility. When pure crystalloid is used, oxygenating the buffered solution with 95% O_2, 5% CO_2 will usually maintain the correct pH but this should be monitored, especially during long runs. If fatty acids or protein are added to the buffer, foaming may occur particularly with bubble-type oxygenators. When crystalloid perfusate is used, the pO_2 needs to be >500 mmHg and coronary flow rates must be several times the physiological norm to avoid hypoxia.[11]

The ability to deliver sufficient oxygen to all of the working myocardium with hyperoxygenated crystalloid perfusate, particularly in hearts of larger species, is not trivial. The concern is justified by the rapidity with which cardiac function in hearts from larger species deteriorates when isolated. Perfluorochemicals have been used as emulsions with crystalloid perfusates and the combination does increase the oxygen carrying capacity of the perfusate significantly.[43–46] Perfluorochemical plus 2.9% albumin emulsion-perfused isolated working rabbit hearts demonstrated more stable function over a longer period of time than hearts perfused with the perfluorochemical alone or those perfused with perfluoroc hemical plus 3.4% hydroxyethylstarch or 0.8% hydroxyethylstarch.[47] However, the perfluorochemical compounds foam easily and generally require the use of antifoaming agents. The latter can create unique problems as well. The use of perfluorochemical compounds for the perfusion of isolated heart preparations has not been generally accepted or widely used.

Table 6.1 Perfusate composition

References	NaCl	$NaHCO_3$	KCl	$MgSO_4$	KH_2PO_4	$CaCl_2$	Glucose or dextrose	BSA	Insulin	EDTA	Pyruvate	Mannitol
[36, 15, 37]	118.5	25.0	4.7	1.2	1.2	2.5	11.0	–	–	–	–	–
[12]	118.5	25.0	4.7	1.2	1.2	1.4	11.0	–	–	–	–	–
[17]	118.5	25.0	4.7	1.2	1.2	2.5	5 or 10	2%	0 or 10 μIU/ml	–	–	–
[38]	120.0	25.0	4.7	1.2	1.2	2.5	11.0	–	–	0.5	2.0	–
[35]	118.5	25.0	4.7	1.2	1.2	1.4	–	–	10 IU/l	0.32	2.27	16.0
[19]	118.5	25.0	4.7	1.2	1.2	1.4	5.0	0.5 or 3%	100 μ IU/ml	–	–	–
[20]	118.5	25.0	4.7	1.2	1.2	2.5	11.0	–	–	0.5	–	–
[39]	118.4	25.0	4.7	1.2	1.2	2.5	10	–	–	–	–	–
[40]	133.0	25.0	4.75	1.25	–	1.82	11.1	–	–	–	–	–
[34]	120.0	25.2	4.0	1.3	–	1.2	11.0	–	–	–	–	–
[14]	126.0	24.0	4.7	0.6	1.2	1.25	5.5	–	5.0 IU/l	–	–	0.3
[41]	137.0	15.5	5.0	1.2	1.2	2.5	11.5	–	5.0 IU/l	0.05	16.0	2.0
[42]	108.0	25.0	4.0	–	1.4	2.5	11.0	–	–	–	–	10.0
[18]	118.0	24.0	3.3	1.2	1.2	2.0	10.0	20 mg/l	–	–	–	2.0

All components are in mM/l unless otherwise indicated. *BSA* Bovine serum albumin and *EDTA* chelating agent. All solutions are buffer adjusted for pH in the range of 7.35-7.45

Support Animals

The use of whole blood and a support animal of the same species to provide oxygenated blood and to remove any metabolic waste products generated by the beating heart is an obvious solution. Although the technique seems straightforward, anyone who has used it knows that it is absolutely essential to monitor the support animal carefully and to maintain the support animal within physiological limits. This is not a trivial task.

Sutherland and Hearse[11] have provided details of how to do this using a rat preparation. The support rat is anesthetized and an extracorporeal circuit between the support animal and the Langendorff preparation is primed with a plasma substitute. Flow in the extracorporeal circuit is gradually established until the flow rate is in the range of the expected coronary flow (2–3 ml/min). The gradual increase in flow through the circuit prevents a sudden drop in arterial pressure of the support animal. The support animal can be ventilated or allowed to breathe spontaneously but it is absolutely imperative to maintain its arterial blood gases and blood electrolytes within normal limits. To do this, these parameters must be monitored frequently and adjustments made as necessary. It is frequently necessary to provide blood transfusions to maintain the support animal. Our experience with pigs indicates that it is necessary to provide artificial ventilation to the support animal, with 5-cm H_2O PEEP, to monitor end-expired CO_2 continuously and make any necessary adjustments in ventilation. It is also essential to monitor and correct the rectal temperature of the support animal. It is usually the deterioration of the support animal that limits the experiment. This is particularly true when the experimental design dictates the use of pharmacological agents and blocking agents or results in the release of endogenous substances that can have an adverse effect on the support animal. However, blood-perfused isolated heart preparations, even using rat hearts, are more stable and deteriorate at a much slower rate than the crystalloid-perfused preparations.

Washed Red Blood Cell Addition to the Perfusate

The addition of washed red blood cells to a crystalloid perfusate will also provide oxygen-carrying capacity. When washed RBCs are used, it is generally necessary to use a membrane oxygenator since most bubble oxygenator systems commonly used for crystalloid will exert excessive stress on RBC membranes resulting in rupture, hemolysis, and foaming problems. A simple membrane oxygenator can be constructed using coils of thin-walled silicone rubber tubing and is suitable for mouse and rat heart preparations.[11] If blood from a different species than the isolated heart is being used, it is essential to make certain that the RBCs being used are small enough to pass through the coronary circulation and do not result in capillary embolization. Preparation of the RBC perfusate does require special care. Each liter of fresh blood should be collected into a sterile container containing 5,000 IU heparin. Benzyl penicillin, 0.2 MU/l is usually added and the blood is filtered (200-μm filter) and

centrifuged at 1,000*g* for 20 min. The supernatant and WBCs are removed. The RBCs are resuspended in calcium-free balanced electrolyte solution and centrifuged again. This process is repeated until the supernatant is clear. If the packed cells are to be used at a later time, they are not resuspended and can be stored at 4°C. On the day they are to be used, the RBCs should be washed twice as previously then the packed cells are resuspended 1:1 in a solution made from 250 ml deionized water and 500 ml of a mixture of sterile 6% Dextran and 0.9% sodium chloride. A solution containing NaCl (118.5 mM), KCl (3.8 mM), KH_2PO_4 (1.2 mM), $NaHCO_3$ (25.0 mM), $MgSO_4$ (1.0 mM), and glucose (10.0 mM) is made up and filtered (5-μm filter) then warmed, 3 g of albumin is added, and the warmed solution is mixed with the RBC/Dextran solution. Before being used, the ionic composition must be checked and corrected as needed to match normal blood values for the species. It is particularly important to make certain the ionized Ca^{2+} concentration is within the normal limits. Gentamicin (2 mg/l) is sometimes added to retard bacteria. This detailed protocol will result in a more stable preparation and, almost certainly, more reliable results for any species.[11] Gillis et al.[18] perfused isolated working rabbit hearts with RBCs after filtering heparinized blood through cheesecloth, centrifuging at 2,700*g* for 15 min, removing the plasma and WBCs, washing the RBCs three times with cold 0.9% saline and one time with cold, oxygenated Krebs–Henseleit buffer and then added the RBCs to Krebs–Henseleit buffer solution to obtain a hematocrit of 10%.

Problems and Pitfalls

All isolated heart preparations continuously deteriorate. Standard measures of cardiac function such as developed pressure or dP/dt_{max} in both Langendorff-perfused and working heart preparations can be expected to deteriorate 5–10% per hour. The rate at which any particular preparation being used deteriorates can be very important. It may be necessary to use time-matched controls with corrections for baseline deterioration to achieve statistically significant and meaningful results.[11,32]

Exclusion Criteria

Perhaps the most common problem related to the use of isolated heart preparations is the frequently ignored responsibility to establish and describe exclusion criteria. For a variety of reasons, any particular isolated heart will not be suitable for use. It is incumbent upon investigators not only to describe the lower limits of function that will be accepted but also to reject preparations with very high values that could be the result of inappropriately high $[Ca^{2+}]$, excessive adrenergic stimulation, or other problems with the preparation.[11] It is also prudent to exclude any heart that exhibits a decline in left ventricular function greater than 15% per hour.[12]

Problems Common to Crystalloid Perfusion

Because the osmotic pressure of most crystalloid perfusate solutions is significantly less than the osmotic pressure of plasma, it is safe to assume that all isolated hearts perfused with hypo-osmotic fluid will become edematous. The severity of the edema will be related to the duration of perfusion, the workload, and other aspects of the experimental paradigm.[11,12,18,35,48]

Because of the low oxygen carrying capacity of crystalloid perfusates, we can also assume that isolated hearts perfused in this manner will suffer some degree of hypoxia.[17,18,21,49,50] In hearts from small species, the hypoxia is at least partially compensated for by increased coronary flow, typically 3–4 times higher than in vivo flow rates.

Fatty acids are the preferred substrate for energy production by the aerobic myocardium. When fatty acids are included in crystalloid solutions used for perfusion of isolated hearts it is usually in the form of pyruvate, but its use is not common. More commonly glucose or dextrose is added to the balanced salt solution for energy, but when this is done it is important to also add insulin to enable the sugar to be used by the myocardium.

Contamination

The most common cause of an unstable or failing isolated heart preparation is contamination, particulate, bacterial, or lipopolysaccharide (endotoxin). Bacterial and endotoxin problems are associated with inadequate cleaning or poor design of the apparatus. The latter may include small pockets between oversized tubing and glass components or plastic connectors allowing for "dead" spaces with trapped fluid that allows bacterial growth. The perfusion solution may be contaminated with particulate impurities from the reagents or bacterial contamination occurring during preparation or storage. In most instances, it is advisable to make up a fresh perfusion solution each day, not to store them for more than a few hours. This is particularly important for those perfusates containing substrate or RBCs. Filtering solutions during preparation and including filters in the perfusion circuit will alleviate many problems. Thorough washing of the apparatus with detergent and then flushing with distilled water followed by cleansing with boiling water after every day of use is recommended. If the apparatus does become contaminated, it may be possible to recover it for use by washing with acid or strong detergent followed by repeated rinsing with distilled water and then with boiling water. If any acid or detergent remains it will, obviously, cause problems. A well-designed and properly cleaned and maintained apparatus can be used for years if proper precautions to avoid contamination are used. The inclusion of broad-spectrum antibiotics in the perfusion medium is not a substitute for proper care and maintenance.[11]

Temperature

Table 1.4 provides normal ranges of rectal temperatures for most species commonly used for isolated heart preparations. Despite the fact that normal temperatures can be as high as 39.9°C in dogs and sheep and are at least 38.1°C in other species, except mice isolated heart experiments seem to be routinely conducted at 37°C. It has been clearly shown, particularly, if the experimental paradigm includes ischemic injury, that the isolated rat heart is very sensitive to minor fluctuations in temperature.[51, 52] Buffer-perfused mouse hearts demonstrated a clear dependence of heart rate on temperature with increases of close to 100% as the heart was warmed from 15°C to 40°C. Maximal heart rates were achieved between 37 and 40°C. Left ventricular developed pressures (LVDP) were unchanged between 20 and 37°C and then decreased at 40°C in spontaneously beating hearts, but when the hearts were paced at a constant rate the LVDP demonstrated a clear bell-shaped curve between 27 and 44°C with the maximum at 37°C.[12] It is apparent that temperature is important and it is necessary for investigators to establish an ideal temperature at which to conduct their experiments for the species of heart being used.

Metabolic "Poisoning"

If a recirculating system for perfusion of the isolated heart is used for a prolonged period, be it a balanced salt solution, with or without RBCs, or whole blood, it is possible for the beating or working heart to add enough metabolic waste to gradually poison the system. If a support animal is used, it should be able to remove the metabolic waste but it is extremely important to monitor the support animal and make certain it is not suffering from the exposure. The use of a dialyzer in the circuit can serve the function of metabolic waste removal.

Pacing vs. Spontaneously Beating Preparations

It is generally accepted that healthy hearts exhibit a positive force–frequency relationship, the Treppe effect. Some reports suggest rat and mouse hearts, and failing human hearts demonstrate a negative staircase with increasing rates. Other studies have shown that when temperature, calcium concentration, and heart rates are within normal physiological ranges the positive staircase effect is still present.[12] For most experimental paradigms, it seems advantageous to maintain heart rate, as well as temperature and calcium concentration, within the physiological range so that responses to the experimental perturbations will be maximized. Since spontaneously beating isolated heart preparations are almost always significantly slower than in vivo resting rates for the species pacing at normal rates is prudent.

Frequency Response Testing of Ventricular Pressure Recording Systems

Fluid-filled balloons are the method of choice for the measurement of intraventricular pressures in retrograde-perfused isolated heart experiments. The technique facilitates the measurement of heart rate, systolic, diastolic, and developed pressures, and positive and negative first derivates of pressure. Balloons are constructed of nonelastic plastic film (plastic food wrap), thin silicon rubber, or are latex molded. The latter are available commercially and are the most commonly used. To measure changes in pressure accurately, the balloon must be very flexible and conform to the contours of the endocardium; it must be infinitely compliant and thin and all communication between the balloon and the pressure transducer must have a frequency response that is flat to all frequencies in the range being measured. Unfortunately, particularly when used in hearts from smaller species with high heart rates, the frequency response of the balloon systems are rarely characterized and the fact that they could limit the reliability of the recordings being made is ignored. Sutherland et al.[12] tested the frequency response of their balloon system that uses nonelastic thin plastic film at 9 different balloon volumes between 0 and 80 μl and at 28 frequencies between 1 and 100 Hz. The response of their system was flat to 20 Hz but beyond this the system resonated causing amplification of the signal. Balloon volume did not have a major effect on the frequency-response characteristics but smaller volumes resulted in an underestimation of developed pressure and large volumes can result in endocardial ischemia. Accurate measurement of the derivatives of ventricular pressures, at mouse heart rates, require the ability to record pressure changes with component frequencies in the 50–100 Hz range. The amplification of the signal with the Sutherland et al. system, which is of much higher fidelity than the commercially available latex balloons, ranged from 3.1 to 9.9 dB. Measurements of dP/dt_{max} and dP/dt_{min} using balloons and fluid-filled systems to connect to the pressure transducer in mice, and probably in rats and other species with high heart rates, must therefore be considered suspect.

Heterotopic Transplants

Although it may not be thought of as an isolated heart preparation, the technique of heterotopic transplantation does isolate the heart and allow some specialized studies to be conducted. The technique is primarily used to study immunological responses to transplantation. A new method has been recently described in mice. It uses the suprahepatic inferior vena cava instead of the pulmonary artery of the donor heart for the anastomosis to the infrarenal vena cava of the recipient.[53] Another new method uses improvements on the Ono–Lindsey method based on branch-sparing and venotomy modifications that are reported to decrease the procedure time and thus the ischemic time.[54] Pig to baboon heart transplants were used to conclude that unregulated or disturbed coagulation is closely associated with primary failure of xenotransplants in this model.[55] The receptor for advanced glycation end-products (RAGE) has been shown to play a key role in allorecognition responses.[56]

An improvement in delayed xenograft rejection can probably be achieved by improved immunosuppression.[57] Combined CXCR3 and CCR5 (chemokine receptors) blockade prolonged allograft survival in a mismatched mouse model.[58] Li et al.[59] used a CTLA4-Ig-based conditioning regimen with donor BMT to produce a mixed chimerism and were able to induce donor-specific tolerance to cardiac allografts in rats. Heterotopic transplants using a rat model demonstrated that ERK, JNK, AP-1, and NF-kappaB are all activated during the acute rejection phenomenon indicating that MAPK pathways might play an important role in this.[60] TGF-beta-activated CD8+ T cells mediate antigen-specific, APC-focused patterns of suppression both in vitro and in vivo and thus may play an important role in xenograft survival.[61] Localized IL-10 gene therapy prolongs cardiac allograft survival, possibly by down regulation of perforin production by activated allogenic CD8+ T cells.[62]

The heterotopic heart transplant model is also relevant for studying the effects of chronic unloading of a beating heart. Doenst et al.[63] were able to demonstrate that the genetic responses of both failing human and healthy rat myocardial cells exhibited similar genetic responses to unloading. Normalization of cardiac function, reduction of cardiomyocyte hypertrophy, and cardiac gene expression was demonstrated in a rat model of heterotopic heart transplantation.[64] The rat preparation was also used to demonstrate that physiological doses of thyroid hormone were able to rescue impaired myocyte relaxation and depressed contractile reserve.[65]A rabbit model showed that dopamine infusion has a positive inotropic effect on the postischemic transplanted heart but also increased cardiomyocyte apoptosis. However, the latter was ameliorated by the use of the intravenous anesthetic agent propofol.[66] Studies using a heterotopic swine model of heart transplantation indicated that at least part of the endothelium-dependent relaxations of bradykinin in this model could be attributed to altered EDHF activity and this could occur prior to coronary graft vasculopathy.[67] Mice models were used to provide evidence indicating that extracardiac stem cells, possibly of bone marrow origin, can become cardiac progenitor cells in response to signals from the transplanted heart.[68] Dedja et al.[69] used heterotopic heart xenografts to look for markers of donor and recipient cells. Golden Syrian hamsters or transgenic mice expressing nuclear beta-galactosidase served as organ donors and GFP+ transgenic rats were recipients. GFP+ cells, DC-45+ inflammatory cells and undifferentiated cells that expressed early cardiac markers were demonstrated in xenografts 2 weeks after transplantation. GFP+ mature cardiomyocytes were found in seven of eight hamster xenografts and six of six mouse xenografts. All GFP+ cardiomyocytes also expressed donor markers indicating that they are derived from cell fusion and not from transdifferentiation.

References

1. Zimmer HG. Who discovered the frank-starling mechanism? News Physiol Sci. 2002;17:181–184.
2. Bowditch HP. Uber die eigenthumlichkeiten der reizbarkeit, welche die muskelfasem des herzens zeigen. berichte uber die verhandlungen der koniglich sachsischen gesellschaft zu leipzig. Mathematisch-Physische Classe. 1871;23:652–689.

3. Frank O. Dynamik des herzmuskels. Z Biol. 1895;32:370–437.
4. Frank O. Die grundform des arteriellen pulses. erste abhandlung. mathematische analyse. Z Biol. 1898;37:483–526.
5. Howell WH, Cooke E. Action of the inorganic salts of serum, milk, gastric juice, etc., upon the isolated working heart, with remarks upon the causation of the heart-beat. J Physiol. 1893;14:198–220.
6. Howell WH, Duke WW. Experiments on the isolated mammalian heart to show the relation of the inorganic salts to the action of the accelerator and inhibitory nerves. J Physiol. 1906;35:131–150.
7. Langendorff O. Untersuchungen am uberlebenden saugethierherzen. Pflugers Arch. 1895;61:291–332.
8. Skrzypiec-Spring M, Grotthus B, Szelag A, Schulz R. Isolated heart perfusion according to Langendorff-still viable in the new millennium. J Pharmacol Toxicol Methods. 2007;55:113–126.
9. Knowlton FP, Starling EH. The influence of variations in temperature and blood-pressure on the performance of the isolated mammalian heart. J Physiol. 1912;44:206–219.
10. Starling EH, Visscher MB. The regulation of the energy output of the heart. J Physiol. 1927;62:243–261.
11. Sutherland FJ, Hearse DJ. The isolated blood and perfusion fluid perfused heart. Pharmacol Res. 2000;41:613–627.
12. Sutherland FJ, Shattock MJ, Baker KE, Hearse DJ. Mouse isolated perfused heart: Characteristics and cautions. Clin Exp Pharmacol Physiol. 2003;30:867–878.
13. Grocott-Mason R, Anning P, Evans H, Lewis MJ, Shah AM. Modulation of left ventricular relaxation in isolated ejecting heart by endogenous nitric oxide. Am J Physiol. 1994;267:H1804–H1813.
14. Heindl B, Reichle FM, Zahler S, Conzen PF, Becker BF. Sevoflurane and isoflurane protect the reperfused guinea pig heart by reducing postischemic adhesion of polymorphonuclear neutrophils. Anesthesiology. 1999;91:521–530.
15. How OJ, Aasum E, Kunnathu S, Severson DL, Myhre ES, Larsen TS. Influence of substrate supply on cardiac efficiency, as measured by pressure-volume analysis in ex vivo mouse hearts. Am J Physiol Heart Circ Physiol. 2005;288:H2979–H2985.
16. Petrucci Junior O, Oliveira PP, Carmo MR, Vieira RW, Braile DM. Standardization of an isolated pig heart preparation with parabiotic circulation: Methodological considerations. Braz J Med Biol Res. 2003;36:649–659.
17. Taegtmeyer H, Hems R, Krebs HA. Utilization of energy-providing substrates in the isolated working rat heart. Biochem J. 1980;186:701–711.
18. Gillis AM, Kulisz E, Mathison HJ. Cardiac electrophysiological variables in blood-perfused and buffer-perfused, isolated, working rabbit heart. Am J Physiol. 1996;271:H784–H789.
19. Werner JC, Sicard RE, Schuler HG. Palmitate oxidation by isolated working fetal and newborn pig hearts. Am J Physiol. 1989;256:E315–E321.
20. Casali C, Obadia JF, Canet E, et al. Design of an isolated pig heart preparation for positron emission tomography and magnetic resonance imaging. Invest Radiol. 1997;32:713–720.
21. Modersohn D, Eddicks S, Grosse-Siestrup C, Ast I, Holinski S, Konertz W. Isolated hemo perfused heart model of slaughterhouse pigs. Int J Artif Organs. 2001;24:215–221.
22. Gaffin RD, Gokulan K, Sacchettini JC, et al. Changes in end-to-end interactions of tropomyosin affect mouse cardiac muscle dynamics. Am J Physiol Heart Circ Physiol. 2006;291:H552–H563.
23. Igic R. The isolated perfused "working" rat heart: A new method. J Pharmacol Toxicol Methods. 1996;35:63–67.
24. Burkhoff D, van der Velde E, Kass D, Baan J, Maughan WL, Sagawa K. Accuracy of volume measurement by conductance catheter in isolated, ejecting canine hearts. Circulation. 1985;72:440–447.
25. Weber KT, Janicki JS, Reeves RC, Hefner LL, Reeves TJ. Determinants of stroke volume in the isolated canine heart. J Appl Physiol. 1974;37:742–747.
26. Demmy TL, Magovern GJ, Kao RL. Isolated biventricular working rat heart preparation. Ann Thorac Surg. 1992;54:915–920.
27. Demmy TL, Curtis JJ, Kao R, Schmaltz RA, Walls JT. Load-insensitive measurements from an isolated perfused biventricular working rat heart. J Biomed Sci. 1997;4:111–119.

28. Segel LD. The development of alcohol-induced cardiac dysfunction in the rat. Alcohol Alcohol. 1988;23:391–401.
29. Itoi T, Lopaschuk GD. The contribution of glycolysis, glucose oxidation, lactate oxidation, and fatty acid oxidation to ATP production in isolated biventricular working hearts from 2-week-old rabbits. Pediatr Res. 1993;34:735–741.
30. Briest W, Elsner C, Hemker J, Muller-Strahl G, Zimmer HG. Norepinephrine-induced expression of cytokines in isolated biventricular working rat hearts. Mol Cell Biochem. 2003;245:69–76.
31. Sigg DC, Iaizzo PA. In vivo versus in vitro comparison of swine cardiac performance: Induction of cardiodepression with halothane. Eur J Pharmacol. 2006;543:97–107.
32. Miller WP, Shimamoto N, Nellis SH, Liedtke AJ. Coronary hyperperfusion and myocardial metabolism in isolated and intact hearts. Am J Physiol. 1987;253:H1271–H1278.
33. Yokoyama H, Imagawa JI, Satoh K, Taira N, Tamahashi N. Isolated dog hearts prepared in cold tyrode solution and reperfused with arterial blood are functionally and ultrastructurally normal. Tohoku J Exp Med. 1988;156:121–134.
34. Araki Y, Usui A, Kawaguchi O, et al. Pressure-volume relationship in isolated working heart with crystalloid perfusate in swine and imaging the valve motion. Eur J Cardiothorac Surg. 2005;28:435–442.
35. Chinchoy E, Soule CL, Houlton AJ, et al. Isolated four-chamber working swine heart model. Ann Thorac Surg. 2000;70:1607–1614.
36. Krebs HA, Henseleit K. Untersuchungen ueber die harnstoffbildung im tierkoerper. Hoppe-Seyler's Zeitschrift fur Physiologische Chemie. 1932;210:33–36.
37. Neubauer S, Ingwall JS. The isolated, buffer-perfused ferret heart: A new model for the study of cardiac physiology and metabolism. Lab Anim. 1991;25:348–353.
38. Yang A, Sonin D, Jones L, Barry WH, Liang BT. A beneficial role of cardiac P2X4 receptors in heart failure: Rescue of the calsequestrin overexpression model of cardiomyopathy. Am J Physiol Heart Circ Physiol. 2004;287:H1096–H1103.
39. Tikh EI, Fenton RA, Dobson JG, Jr. Contractile effects of adenosine A1 and A2A receptors in isolated murine hearts. Am J Physiol Heart Circ Physiol. 2006;290:H348–H356.
40. Anderson SE, Liu H, Beyschau A, Cala PM. Effects of cold cardioplegia on pH, Na and Ca in newborn rabbit hearts. Am J Physiol Heart Circ Physiol. 2006;290:H1090–H1097.
41. Fujita S, Roerig DL, Chung WW, Bosnjak ZJ, Stowe DF. Volatile anesthetics do not alter bradykinin-induced release of nitric oxide or L-citrulline in crystalloid perfused guinea pig hearts. Anesthesiology. 1998;89:421–433.
42. Kameyama T, Chen Z, Bell SP, Fabian J, LeWinter MM. Mechanoenergetic studies in isolated mouse hearts. Am J Physiol. 1998;274:H366–H374.
43. Martin SM, Laks H, Drinkwater DC, et al. Perfluorochemical reperfusion limits myocardial reperfusion injury after prolonged hypothermic global ischemia. Biomater Artif Cells Immobilization Biotechnol. 1992;20:985–989.
44. Cornelissen AJ, Spaan JA, Dankelman J, Chan CC, Yin FC. Evidence for stretch-induced resistance increase of proximal coronary microcirculation. Am J Physiol Heart Circ Physiol. 2001;281:H2687–H2696.
45. Kawabata H, Sugiyama K, Katori R. Effect of acetylsalicylic acid on metabolism and contractility in the ischemic reperfused heart. Jpn Circ J. 1996;60:961–971.
46. Snyder DS, Harasawa Y, Sagawa K, Hunter WC. Effects of pentobarbital on inotropic state of isolated canine left ventricle. Heart Vessels. 1993;8:128–135.
47. Segel LD, Ensunsa JL. Albumin improves stability and longevity of perfluorochemical-perfused hearts. Am J Physiol. 1988;254:H1105–H1112.
48. Weng ZC, Nicolosi AC, Detwiler PW, et al. Effects of crystalloid, blood, and university of Wisconsin perfusates on weight, water content, and left ventricular compliance in an edema-prone, isolated porcine heart model. J Thorac Cardiovasc Surg. 1992;103:504–513.
49. Walters HL, III, Digerness SB, Naftel DC, Waggoner JR, III, Blackstone EH, Kirklin JW. The response to ischemia in blood perfused vs. crystalloid perfused isolated rat heart preparations. J Mol Cell Cardiol. 1992;24:1063–1077.
50. Wetstein L, Rastegar H, Barlow CH, Harken AH. Delineation of myocardial ischemia in an isolated blood-perfused rabbit heart preparation. J Surg Res. 1984;37:285–289.

51. Fukunami M, Hearse DJ. The inotropic consequences of cooling: Studies in the isolated rat heart. Heart Vessels. 1989;5:1–9.
52. Cave AC, Hearse DJ. Ischaemic preconditioning and contractile function: Studies with normothermic and hypothermic global ischaemia. J Mol Cell Cardiol. 1992;24:1113–1123.
53. Wu K, Zhang J, Fu J, et al. Novel technique for blood circuit reconstruction in mouse heart transplantation model. Microsurgery. 2006;26:594–598.
54. Wang D, Opelz G, Terness P. A simplified technique for heart transplantation in rats: Abdominal vessel branch-sparing and modified venotomy. Microsurgery. 2006;26:470–472.
55. Wu G, Pfeiffer S, Schroder C, et al. Coagulation cascade activation triggers early failure of pig hearts expressing human complement regulatory genes. Xenotransplantation. 2007;14:34–47.
56. Moser B, Szabolcs MJ, Ankersmit HJ, et al. Blockade of RAGE suppresses alloimmune reactions in vitro and delays allograft rejection in murine heart transplantation. Am J Transplant. 2007;7:293–302.
57. Byrne GW, Davies WR, Oi K, et al. Increased immunosuppression, not anticoagulation, extends cardiac xenograft survival. Transplantation. 2006;82:1787–1791.
58. Schnickel GT, Hsieh GR, Garcia C, Shefizadeh A, Fishbein MC, Ardehali A. Role of CXCR3 and CCR5 in allograft rejection. Transplant Proc. 2006;38:3221–3224.
59. Li S, Salgar SK, Thanikachalam M, et al. CTLA4-ig-based conditioning regimen to induce tolerance to cardiac allografts. J Surg Res. 2006;136:238–246.
60. Hirai H, Shibata T, Aoyama T, Yoshiyama M, Omura T, Suehiro S. Activation of mitogen-activated protein kinases, activator protein-1, and nuclear factor-kappaB during acute rejection after heterotopic heart transplantation in rats. Osaka City Med J. 2006;52:9–19.
61. Kapp JA, Honjo K, Kapp LM, Xu X, Cozier A, Bucy RP. TCR transgenic CD8+ T cells activated in the presence of TGF-beta express FoxP3 and mediate linked suppression of primary immune responses and cardiac allograft rejection. Int Immunol. 2006;18:1549–1562.
62. Oshima K, Cui G, Tung T, Okotie O, Laks H, Sen L. Exogenous IL-10 overexpression reduces perforin production by activated allogenic CD8+ cells and prolongs cardiac allograft survival. Am J Physiol Heart Circ Physiol. 2007;292:H277–H284.
63. Doenst T, Bugger H, Leippert S, Barleon B, Marme D, Beyersdorf F. Differential gene expression in response to ventricular unloading in rat and human myocardium. Thorac Cardiovasc Surg. 2006;54:381–387.
64. Oriyanhan W, Tsuneyoshi H, Nishina T, Matsuoka S, Ikeda T, Komeda M. Determination of optimal duration of mechanical unloading for failing hearts to achieve bridge to recovery in a rat heterotopic heart transplantation model. J Heart Lung Transplant. 2007;26:16–23.
65. Minatoya Y, Ito K, Kagaya Y, et al. Depressed contractile reserve and impaired calcium handling of cardiac myocytes from chronically unloaded hearts are ameliorated with the administration of physiological treatment dose of T3 in rats. Acta Physiol (Oxf). 2007; 189:221–231.
66. Roy N, Friehs I, Cowan DB, Zurakowski D, McGowan FX, del Nido PJ. Dopamine induces postischemic cardiomyocyte apoptosis in vivo: An effect ameliorated by propofol. Ann Thorac Surg. 2006;82:2192–2199.
67. Perrault LP, Aubin MC, Malo O, et al. Status of the endothelium-derived hyperpolarizing factor pathway in coronary arteries after heterotopic heart transplantation. J Heart Lung Transplant. 2007;26:48–55.
68. Li TS, Suzuki R, Ueda K, Murata T, Hamano K. Analysis of the origin and population dynamics of cardiac progenitor cells in a donor heart model. Stem Cells. 2007;25:911–917.
69. Dedja A, Zaglia T, Dall'Olmo L, et al. Hybrid cardiomyocytes derived by cell fusion in heterotopic cardiac xenografts. FASEB J. 2006;20:2534–2536.

Chapter 7
Cardiovascular Effects of Anesthetics, Sedatives, Postoperative Analgesic Agents, and Other Pharmaceuticals

Researchers using animal models must be aware that many of the drugs necessary to provide humane use and care have adverse affects on the cardiovascular system. The use of these agents is absolutely necessary and unavoidable but informed choices can be made to minimize these affects.

Barbiturates

The barbiturates are classified as ultra-short, short-, and long-acting depending upon their fat solubility. The thiobarbiturates are most soluble in fat and therefore provide a surgical plane of anesthesia for less time than the short-acting agents such as pentobarbital sodium. The rate of metabolism for all of these agents is about the same so repeated injections of the ultra-short acting barbiturates can saturate the animal's fat and can result in prolonged anesthetic effects, a potential problem in obese animals.

As a class of drugs, the barbiturates interfere with Ca^{2+} transport in cardiac myocytes and with Ca^{2+} uptake into the sarcoplasmic reticulum. This has an obvious negative inotropic effect that is dose dependent.[1] Pentobarbital has been shown to inhibit nicotinic acetylcholine receptor (nAChR)-induced transients in intracellular free $[Ca^{2+}]_i$ by about 40%.[2]

The barbiturates may also interfere with Ca^{2+}-mediated events in excitation-contraction-coupling and generally tend to result in an increase in preload, a decrease in the various indices of contractility, decreases in afterload, and increases in heart rate.[1,3–8] Barbiturate-induced tachycardia is attributed to a depression of baroreceptor reflex afferent mechanisms. This results in a lack of inhibition of constrictor tone and depression of the vagal and sympathetic components of the baroreceptor-heart rate reflex and can persist after the animal has regained consciousness.[1,5]

In rats, pentobarbital anesthesia coupled with acute coronary artery occlusion is associated with a higher incidence of ischemia-induced arrhythmias. The effects are mitigated in male vs. female rats and by the administration of 17β-estradiol.[9] There is an enhanced incidence of cardiovascular collapse in normotensive Dahl

D.R. Gross, *Animal Models in Cardiovascular Research*,
DOI: 10.1007/978-0-387-95962-7_7, © Springer Science + Business Media, LLC 2009

Salt Sensitive rats compared to Brown Norway rats when dosed with pentobarbital despite nearly identical plasma clearance of the anesthetic agent.[10] Ouabain produces enhanced inotropic effects in dogs following pentobarbital anesthesia.[1]

The barbiturates have also been associated with significant decreases in hepatic artery blood flow and therefore hepatic O_2 supply even when the systemic circulatory effects were minimal.[6] Infusion of thiopental did not block the electroencephalographic burst suppression pattern associated with catecholamine release stimulated by tracheal intubation.[11] Mather et al. compared the effects of coronary artery infusions of R-thiopental, S-thiopental, and rac-thiopental in conscious sheep and found significant dose-dependent decreases in left ventricular dP/dt_{max} and stroke volume and increases in coronary blood flow and heart rate.[7] Thiopental anesthesia induced the release of noradrenaline and cortisol.[12]

Thiopental attenuates the endothelium-dependent component of the potassium ATP^+ channel-induced pulmonary vein vasorelaxation via an inhibitory effect on the nitric oxide pathway and by reducing the levcromakalim-induced decrease in $[Ca^{2+}]_i$ via an inhibitory effect on L-type voltage-gated Ca^{2+} channels.[13] Rat skeletal muscle microcirculation is also affected by thiopental anesthesia. There is dilation of A1 (802–180 μm diameter) and A3 and V3 vessels in WKY rats but in spontaneously hypertensive (SHR) rats there was a dilation of venules accompanied by constriction of A1 and A3 vessels with no increases in macromolecular leak.[14,15]

Pentobarbital alters the effects of endogenous metabolites of the cyclooxygenase pathways that regulate pulmonary vascular pressure/flow relationships in dogs. It completely abolishes mesenteric vessel vasomotion in cats.[1] In rats, pentobarbital-injected IP is associated with a twofold to threefold increase in plasma rennin concentrations and a decrease in cerebral blood flow.[1] When compared to measurements made in conscious rats, pentobarbital lowered ejection fraction, fractional shortening, fractional area change, and velocity of circumferential fiber shortening, but these effects were less with pentobarbital compared to isoflurane or ketamine/xylazine.[16]

Propofol

Propofol is a water immiscible oil formulated as an emulsion and classified as an alkyphenol intravenous sedative-hypnotic agent. It is used for induction and maintenance of general anesthesia. It is reported to attenuate the catecholamine-induced hypertension and tachycardia responses to tracheal intubation better than thiopental.[11] Following injection into the left coronary arteries in conscious sheep, it caused rapid onset decreases in indices of contractility and increases in coronary blood flow and heart rate.[7] Significant decreases in mean arterial pressures, heart rate, and contractility were accompanied by increases in systemic arterial compliance in Rhesus monkeys and isolated rabbit hearts.[17,18] Rats demonstrated significant decreases in blood pressure, heart rate, and renal sympathetic nerve activity following propofol injection.[19] There was a significant, dose-dependent, decrease in stroke volume, while cardiac output did not change, and systemic vascular resistance

decreased at high doses in horses. The pre-ejection period was prolonged and the ratio of pre-ejection period and ejection time increased at the highest dose used.[20,21] The effects of increased cardiac loading on cardiac function following cardiopulmonary bypass were increased by propofol vs. anesthesia with sevoflurane.[22] Depending upon the individual study and the species and dosage used, intravenous injection resulted in increases in pulmonary artery pressures, resistance, O_2 utilization ratio, and $PaCO_2$ and decreases in mean aortic pressures, arterial and venous O_2, and pH. At low doses no changes in these parameters were observed.[1]

Propofol suppresses the release of norepinephrine and cortisol[12] and results in dilation of A3 arterioles and V3 venules with increased effects in SHR vs. WKY rats.[14] It stimulates translocation of protein kinases (PKC) PKC-alpha, PKC-delta, PKC-epsilon, and PKC-zeta to distinct intracellular sites in rat ventricular cardiomyocytes[23]; prevents dopamine-induced apoptosis; and maintains positive inotropy after ischemia in rabbits.[24]

The effects of propofol on sodium currents and single sodium channels were examined using patch-clamp techniques on rat ventricular myocytes. Propofol caused a substantial hyperpolarizing shift in the voltage-dependence of inactivation of sodium currents, a slowing of the macroscopic rate of inactivation, a slowing of the rate of recovery from inactivation, and a reduction in the mean open time of single sodium channels. Single channel conductance was not changed by propofol.[25]

Propofol induces hyperpolarization and relaxation in denervated, small mesenteric vessels from rats by activation of Ca^{2+}- and ATP-activated potassium channels, effects mediated by nitric oxide (NO) and cyclic guanosine monophosphate (cGNP) pathways.[26] Propofol also attenuates the endothelium-dependent component of potassium-ATP^{+} channel-induced pulmonary vein relaxation by inhibition of the NO pathway and a reduction in the levcromakalin-induced decrease in $[Ca^{2+}]_i$ via an inhibitory effect on L-type voltage-gated Ca^{2+} channels.[13]

α-Chloralose

There are dose-response related cardiovascular effects of this agent in dogs. During induction (60 mg/kg, IV), there are transient changes in heart rate, increased LV flow acceleration, increased work and power, and marked sinus arrhythmia. Cardiac output and stroke work decrease transiently but return to baseline within 5 min. At 80 mg/kg, IV, there is a significant decrease in atropine effects on heart rate and A-V conduction but no change in effect following the injection of isoproterenol. Carotid sinus reflexes are well maintained as are mean arterial pressures and peripheral resistance. At 100 mg/kg, IV, there is a marked depression of the response to carotid chemoreceptor stimulation. Stimulation of the carotid sinus nerve enhances the aortic nerve pressor reflex. Dogs premedicated with morphine (5 mg/kg) and then anesthetized with chloralose demonstrate a dose-dependent cardiotoxicity including decreased aortic pressures and LV dP/dt.[27] Cats given 40–250 mg/kg, IV as a bolus and 2 ml/min continuous infusion sustain an increase in renal sympathetic nerve activity. The pressor

response is unaltered in rats given 90 mg/kg, IP + 15 mg/kg per 30 min, IV. At 80 mg/kg, IV, in rabbits, the reflex control of arterial pressure is weakened. Sheep demonstrated significant decreases in baroreflex activity at 30, 60, and 90 mg/kg, IV doses. Given 80 mg/kg, IV, bats demonstrate dilation of the arterioles in the wing.[1]

Urethane

There is no selective blockade of baroreceptor reflexes in cats given 1.25 g/kg, IP, but some of the cats treated with 0.5–21.0 g/kg, IV, of a 20% ethyl carbamate solution dissolved in saline suffered cardiac arrest, depressed ventilation, and transient decreases in renal sympathetic nerve activity but no effects on arterial pressure or heart rate. Rats demonstrated decreases in heart rate, blood pressure, respiratory rates and decreased responsiveness to carotid occlusion, tilt, and chemoreceptor response to sodium cyanide at 750 mg/kg, IV doses. At 1.25 mg/kg, IP, there was no significant change in blood pressure but increased plasma renin activity.[1]

α-Chloralose + Urethane

In dogs, stimulation of the carotid sinus nerve augmented the vasoconstrictor effects of the pressor reflex. In cats, a selective blockade of the baroreceptor reflexes is observed. Rats and mice demonstrate inhibited vasomotion and increased arteriolar vasodilation, decreased cardiac output, and decreased regional blood flows to a wide variety of tissues and the lactate/pyruvate ratio increases. Blood pressure decreases and heart rate increases at higher doses in rats but the pressor response to phenylephrine is not different between conscious and anesthetized rats.[1] The combination decreases arterial pressure, heart rate, mesenteric resistance, and depressor responses to nitroglycerin in chronically instrumented rats but does not alter the baroreflex slope for pressor and depressor stimuli. The sympathoexcitatory response to cerebroventricular angiotensin II is attenuated. Plasma renin activity and the hemodynamic response to peripheral angiotensin-receptor blockade are significantly increased along with vasopressin-dependent vascular tone.[28]

Steroid Anesthetic Agents

Althesin has no effect on arterial pressure or base-line resistance in chronically instrumented rats. There is no effect on regional vascular reactivity to intravenous phenylephrine or nitroglycerin and the slope of the baroreflex curve response to pressor or depressor stimulation is not altered. Plasma renin activity is increased as is the hemodynamic response to peripheral angiotensin-receptor antagonism. Peripheral

neurogenic tone is not altered by althesin in rats.[28] There is a significant depression of cardiac output and stroke volume but no change in cardiac index, heart rate, arterial blood pressure, or systemic vascular resistance in normal adult cats.[29] But in chloralose-anesthetized cats, there is a marked hypotension attributed to a central depressor activity on vasomotor tone, a direct myocardial depressor effect and mild bradycardia.[30] In anesthetized greyhound dogs, althesin produced dose-dependent decreases in arterial pressure, cardiac output, systemic vascular resistance, hepatic artery blood flow, and hepatic O_2 supply.[6] Cardiac sympathetic activity is increased and parasympathetic activity is decreased in rabbits given IV infusions of althesin. Mean arterial pressure and systemic vascular resistance increased.[5]

In guinea pigs, saffan depressed ventilation and arterial blood pressure but did not have an effect on heart rate. The respiratory depression was associated with attenuated responses to hypoxia and hypercapnia.[4] Saffan produces bronchodilation in rhesus monkeys but with minimal cardiovascular effects.[31]

Inhalation Anesthetic Agents

General

All volatile anesthetic agents induce a dose-dependent decrease in myocardial contractility and preload. These changes are associated with decreased myocardial oxygen demand and may, therefore, have a beneficial effect on myocardial oxygen balance during myocardial ischemia. These agents also have direct protective properties against reversible and irreversible ischemic injury to the myocardium. These protective properties have been related to both direct preconditioning effects and an effect on the extent of reperfusion injury.[32–34] Cerebrovascular reactivity to CO_2 in insulin-dependent animals is impaired.[35]

Some volatile anesthetic agents that were previously used extensively are no longer used, for a variety of reasons. Chloroform is actually a good anesthetic agent but when used under hypoxic conditions can cause severe tachyarrythmias including ventricular fibrillation. Ether is now rarely used because of its potential for explosion, especially when combined with oxygen. Methoxyflurane was very popular in veterinary medicine in the 1960s but was withdrawn from the market because fluoride ions are produced when it is metabolized resulting in kidney damage.

The volatile halogenated anesthetic agents are associated with alterations in myofibrillar Ca^{2+} responsiveness but most of their adverse effects are attributed to decreased availability of intracellular Ca^{2+}. They suppress autonomic reflexes and have many indirect actions mediated via these effects on the autonomic system. Marked renal vascular dilation with significant mesenteric constriction is characteristic of the effects of these agents with no changes noted in the coronary circulation. With prolonged anesthesia, there is a progressive increase in aortic pressure and flow but no changes in regional vascular resistance.[1]

Inhalation anesthetics can also sensitize the heart to the arrhythmogenic actions of catecholamines. Two mechanisms have been incriminated for this response. The first mechanism is a reduction in supraventricular driving rate due to the direct depression from the anesthetic and by reflex response to the pressor effects of exogenous or endogenous catecholamines. The second mechanism that predisposes to ventricular tachyarrythmias is the direct depression of the intraventricular conduction system. Halothane appears to have most pronounced effects in this regard.[1]

Halothane

In dogs, halothane has been shown to depress A-V conduction, increase automaticity, and abolish responses to carotid chemoreceptor stimulation by nicotine. There is a sensitive dose-response modification of the hemodynamic response to iatrogenic lowering of arterial pressures, i.e., blocking of the baroreceptor response. There is good documentation for dose-dependent decreases in arterial pressures, cardiac output, stroke volume, and LV contractility indices as well as decreased renal vascular resistance and increased mesenteric resistance.[1,36] Dose-dependent decreases in arterial pressures are associated with decreased myocardial O_2 consumption.[1] Increased epicardial activations times and ventricular functional refractory period have been noted. Increased concentrations of halothane decrease ventricular conduction and shortened the duration of the refractory periods in dogs. There was a decrease in ventricular escape during supramaximal right vagal stimulation, suppressed ectopic pacemaker activity, and markedly decreased ventricular automaticity in halothane-anesthetized dogs given toxic doses of ouabain. This suggests differences in membrane activities due to the halothane anesthesia. Halothane increased the slope of the pulmonary resistance vs. O_2 saturation curve since the reduction in cardiac output caused by the halothane exceeded the decrease in pulmonary arterial pressure.[1] There was no change in cerebral blood flow or epidural pressures noted in fentanyl-induced, halothane-anesthetized dogs and the hemodynamic effects of changes in $[Ca^{2+}]$ were blunted.[1]

Cats demonstrate similar responses to halothane anesthesia including a progressive decrease in maximum diastolic potential, negative chronotropic and dose-dependent decreases in indices of contractility. Severe and sustained ventricular arrhythmias are induced by the rapid IV infusion of guanethidine in halothane-anesthetized cats. The stimulatory effect of catecholamines on myocardial adenylate cyclase is decreased and some indication that the filling of intracellular Ca^2 storage sites is altered. Retinal and cerebral blood flows are increased and choroidal blood flow is decreased by halothane.[1]

In rats, halothane induced marked protection against mortality and renal ischemia during hemorrhagic shock. Cardiac output, mean arterial pressure, and portal venous pressures are decreased in both normal and portal hypertensive rats. Flow is increased to the brain, kidneys, liver, and large intestine and decreased to the heart and skeletal muscle. There is no change in flow to the lungs, skin, spleen, or GI system. There is potent metabolic depression on glucose and fatty acid

metabolism. Halothane reduced the incidence of ventricular fibrillation following acute LAD occlusion.[1] In isolated rat ventricular myocytes, halothane sensitizes the sarcoplasmic reticular Ca^{2+} release process.[37]

Halothane reduces heart rate, left ventricular systolic pressure, LV d*P*/d*t* (both $^{+}$ and $^{-}$), and ejection time and isovolumic relaxation time in previously instrumented mice. An increase in halothane concentration from 0.5 to 1.0 vol% did not result in additional depression of these parameters.[38]

Similar myocardial depression effects of halothane have been recorded in guinea pigs and rabbits.[1] In pigs, halothane also causes dose-dependent negative inotropic effects but provides some protection against hepatic ischemia-reperfusion injury. There is also a dose-dependent decrease in baroreceptor sensitivity and decrease in heart rate.[1,39] Purkinge fiber preparations from sheep exposed to 2% halothane demonstrate decreased duration of the action potential, unchanged resting potential, and decrease in overshoot significantly. One- to three-day-old lambs were anesthetized with halothane. Total body O_2 consumption, cardiac output and aortic pressures. Higher concentrations of halothane decreased blood flow to the brain, heart, kidney, muscle, and GI system. Serum catecholamine concentrations were decreased. Halothane did not prevent the redistribution of blood flow to the heart and brain induced by hypoxia. Similar negative inotropic and blood flow responses to halothane have been observed in horses, primates, ferrets, beaver, and chickens.[1]

Isoflurane

Isoflurane is a popular anesthetic agent for a wide variety of animal studies. In most instances where comparisons have been made, it is less cardiotoxic than halothane. In intact, awake, previously instrumented dogs, isoflurane at 1.25%, end-tidal, results in no significant changes in indices of contractility, but at 2.0% significant decreases occur. At high concentrations up to 3.45%, there is no change in spontaneous cycle length, HIS-Purkinje, or ventricular conduction but A-V conduction increases. There are also significant decreases in aortic pressures, cardiac output, stroke volume, and contractility. At 1.0 and 1.5 MAC, isoflurane causes dose-dependent prolongation of isovolumetric relaxation and LV diastolic compliance. In sarcoplasmic reticulum preparation from dogs, isoflurane stimulated Ca^{2+} uptake at lower concentrations of ATP but no effect at ATP concentrations of 5 and 10 mM, this was less of an effect than enflurane.[1]

Chronically instrumented cats demonstrate an isoflurane dose-dependent attenuation of pressor responses, heart rate responses, and infra renal aortic blood flow responses following direct electrical stimulation of CNS pressor sites.[1] Isoflurane anesthesia in cats is associated with decreases in body temperature, heart rate, mean arterial pressure, mean pulmonary artery pressure, stroke index, cardiac index, hemoglobin, oxygen delivery index, PvO_2 and $PvCO_2$, and circulating levels of dopamine, epinephrine, norepinephrine, and cortisol. Arterial pH and venous pH are also increased.[40]

The reported effects of isoflurane in rats seem mixed varying from reports of no change in blood pressure, heart rate, or cardiac output in previously instrumented

animals before and after anesthesia to decreases in these same parameters when isoflurane was given to rats previously anesthetized with α-chloralose.[1] Stein et al. reported significant isoflurane-induced decreases in echocardiogram-derived indices of contractility compared to conscious rats and rats anesthetized with pentobarbital.[16] In awake rats brain and coronary flow increase in response to hypoxemia, but when the same rats were anesthetized with isoflurane these parameters were decreased. The same study indicated that hypoxemia did not change blood flow to kidneys, GI tract, or liver in conscious rats but blood flow to these organs decreased in response to hypoxemia when the animals were anesthetized with isoflurane.[1] Rats anesthetized with isoflurane maintained autoregulation to all the tissues measured and the autoregulatory coefficient increased in the midbrain and spinal cord at 1 MAC, while cortex flow decreased, subcortex, midbrain, and spinal cord increased. At 2 MAC, blood flow increased to all portions of the brain that were measured.[1] Isoflurane seems to provide the same level of protection against cerebral ischemia-reperfusion injury as halothane with or without hypothermia. Hypocapnia decreases global cerebral blood flow in rats anesthetized with either halothane or isoflurane. There is a dose-dependent decrease in the magnitude of coronary vascular resistance and of coronary flow reserve in isoflurane-anesthetized rats.[1] Both sarcolemmal and mitochondrial K^+ (ATP) channels play essential and distinct roles in the protection against ischemia-reperfusion injury provided by isoflurane. Sarcolemmal K^+ (ATP) channels seem to act as effectors of preconditioning and mitochondrial K^+ (ATP) channels play a dual role as a trigger and as an effector.[41] Remodeling of the myocardium, following LAD ligation, was protected by isoflurane postconditioning. The protection seems to be mediated by protein kinase B/Akt signaling.[42] Isoflurane induced a higher myocardial blood flow and ejection fraction than pentobarbital in healthy rats.[43]

LV function is depressed in mice anesthetized with isoflurane.[44] Delayed cardiac protection mediated by 12-lipoxygenase expression and activity is an important mediator of isoflurane-induced delayed preconditioning in mice.[45] Isoflurane activates K^+ (ATP) channels in vascular smooth muscle cells from mice. This is thought to be the mechanism for isoflurane-induced coronary vasodilation. The sulphonylurea receptor subunit 2B is thought to play an important role in this response.[46] Isoflurane did not exert significant protective effects on left ventricular performance in Langendorff, buffer-perfused, mouse hearts subjected to 45 min of global ischemia followed by 60 min of perfusion.[47] The cardiotoxic effects of isoflurane have also been documented in rabbits, guinea pigs, pigs, sheep, ferrets, ducks, and Sandhills cranes. Most of them demonstrated dose-dependent depression of various indices of contractility, blood pressure, and flow.[1]

Desflurane

Desflurane anesthesia in dogs produces a dose-dependent increase in heart rate and decreases in aortic pressures; systemic resistance; and coronary, renal, hepatic, and cerebral blood flows. LV systolic and diastolic functions are depressed,[1] but the

force-frequency relation is not altered.[36] Heart rate and systolic aortic pressures were reduced while other measured cardiovascular function parameters remained stable when anesthesia was induced with propofol IV and maintained with desflurane at 1.3 MAC in spontaneously breathing cats.[48] Desflurane induced intramyocardial catecholamine release in adult rats but not in senescent rats, accounting for greater myocardial depression in the aged animals.[49] Deformability indices of red blood cells from young rats were significantly increased by desflurane while the same indices from old rat erythrocytes were decreased. This might account for some of the sensitivity to desflurane and other volatile anesthetics in senescent individuals.[50] The nitric oxide synthase inhibitor *N*-nitro-L-arginine blocked desflurane-induced myocardial depression following coronary artery infarction in rabbits.[51]

Sevoflurane

Sevoflurane was shown to be cardioprotective following cardiopulmonary bypass surgery with increased stroke volumes, higher LV dP/dt_{max}, faster rates of relaxation, and lower levels of postoperative circulating troponin I.[22] Autonomic nervous activity and arterial cardiac baroreflex function were evaluated by analyzing blood pressure variability, heart rate variability, and transfer function analysis between the two parameters. Servoflurane (5%) + N_2O (60%) reduced nervous modulation to the heart and reduced sympathetic nervous modulation of the peripheral vasculature.[52]

Conscious dogs paced at various heart rates demonstrated increased dP/dt_{max} as the heart rate was increased. When these animals were anesthetized with sevoflurane, dP/dt_{max} responded to pacing rate but at significantly lower levels and the slope of the regression line correlating dP/dt_{max} and heart rate did not differ. These results indicate that sevoflurane did not alter the force-frequency relationship in dogs.[36] Despite reducing both heart rate and systolic arterial pressure in spontaneously breathing cats, sevoflurane provided stable cardiovascular parameters for short periods of anesthesia but did cause hypercapnia and acidosis.[48] Sevoflurane caused dose-dependent decreases in the magnitude of coronary vascular resistance and coronary flow reserve in rats. It also causes decreases in aortic pressures, cardiac index, and dose-related increases in pCO_2. At higher concentrations, sevoflurane increases cerebral and spinal blood flow as well as coronary and renal arterial flow.[1] Isolated rat ventricular myocytes treated with sevoflurane show inhibited frequency of Ca^{2+} release. When sevoflurane is removed, a burst of spontaneous Ca^{2+} release is initiated.[37] Experiments conducted on right ventricular trabeculae from rats indicate that protein kinase C, mitochondrial K^+ (ATP), and reactive oxygen species are all involved in sevoflurane-induced cardioprotection.[53] The same laboratory showed that sevo flurane-induced cardioprotection depends upon the Na^+/Ca^{2+} exchanger (NCX) preceding protein kinase C-delta (PKC) translocation presumably via increased involvement of the NCX-mediated Ca^{2+} influx. This mode of action seems to be common to many forms of cardiac preconditioning.[54] Sevoflurane produced an increase in action potential duration at concentrations of 0.3-1.0 mM in isolated guinea pig myocytes.

It did not affect the human ether-a-go-go-related gene cardiac potassium channel but did produce a reduction in KvLQT1/minK K^+ channel currents and inhibited the Kv4.3 K^+ channel by speeding its apparent rate of inactivation.[55] Sevoflurane produced significant depression of global right ventricular function in pigs. These changes were associated with a qualitatively different effect on right ventricular inflow and outflow tracts without a change in peripheral vascular resistance.[56]

Ether

Ether had no measurable effects during normoxic conditions in dogs. It depressed cardiac contractility in cats but not as much as halothane or enflurane. It provides protection against mortality and kidney lesions in rats following hemorrhagic shock. There is a significant and sustained increase in plasma renin activity and decrease in arterial pressure in rats anesthetized with ether. Rats also demonstrate dose-dependent increases in heart rate and a high incidence of ventricular tachyarrythmias. Pigs have shown a general depression of the central circulation but no decrease in contractility at 1.3 MAC.[1]

Nitrous Oxide

Nitrous oxide is a poor anesthetic agent but can reduce requirements when used in conjunction with other anesthetic agents. It has been shown to reduce several indices of contractility in dogs. In rats, it produces cerebrovasodilation unrelated to metabolic demand and some blood–brain barrier dysfunction. When added to the regimen in pigs anesthetized with other agents it had no measured effect on the cardiovascular system, but in isolated right ventricular papillary muscle preparations from guinea pigs and ferrets it caused decreased contractility.[1]

Trichloroethylene

This agent is very toxic but is still used in mice by some investigators. Its primary use is as an industrial solvent and is, therefore, of low cost. When used in rats, there was a marked increase in heart rate and little or no protection against mortality or kidney lesions following hemorrhagic shock.[1] When 2.0–3.3-day-old chick embryos were exposed to concentrations >8 parts per billion (ppb) it resulted in valvuloseptal hypercellullarity narrowing outflow tracts, reducing blood flow thereby compromising cardiac output and increasing mortality.[57] Another study conducted in Hamburger and Hamilton stage 13–14 chick embryos at, 10–80 parts per million, reported only a minority of embryos not viable after 24 h of exposure. Those that

were affected exhibited a variety of gross malformations in a dose-dependent manner including a selective reduction in the number of atrioventricular canal mesenchymal cells determined using whole mount confocal microscopy.[58]

The Opioids

There are at least six different factors that contribute to the cardiovascular effects produced by the opioids; existing anesthesia, the species being studied, the dose, the site of action in the brain, any concurrent respiratory system effects, and receptor specificity. Perhaps most important is the existing status of the cardiovascular system, particularly the degree of hypotension or hypertension. Another issue is the plasticity of the opioid receptor system that is capable of changing its level and distribution pattern in response to physiological or pathological perturbations.[59]

The following compilation includes some agents that are more correctly classified as narcotic antagonists. These agents usually compete for the same receptor sites and have some degree of analgesic and/or sedative effects when used alone. The effectiveness of these agents for analgesia, sedation, or chemical restraint varies with species and there is considerable individual preference involved in their use rather than any objective evaluations. In general, the opioids decrease preload, afterload, contractility, and heart rate with a resulting decrease in cardiac output. There are reported incidents of paradoxical excitement and stimulation, probably resulting from central stimulation induced by the individual's response to ataxia, particularly in cats and horses. Opioids also cause central respiratory depression. Fentanyl and other mu-opioid receptor agonists decrease chest wall compliance and increase upper airway resistance, which can result in increased stress on the cardiovascular system.[60]

Morphine

Very young, senescent, and debilitated dogs are more sensitive to opioid-induced respiratory depression. Transient decreases in coronary resistance, left ventricular end-diastolic and end-systolic diameter, increases in heart rate and contractility were measured in previously instrumented conscious dogs dosed at 2 mg/kg, IV. There were no changes in arterial pressure but heart rate decreased at 0.25 mg/kg, IV. A 30% decrease in mesenteric and a 11% decrease in renal vascular resistance were observed at 1 mg/kg, IV, but 3 mg/kg resulted in 120% increase in mesenteric and a 12% decrease in renal vascular resistances. At 3 mg/kg, there was no change in cardiac output, aortic pressure, systemic vascular resistance, or heart rate. In anesthetized dogs, doses of morphine in excess of 0.5 mg/kg, IV, result in hypotension lasting for 10–15 min. Pentobarbital-anesthetized dogs demonstrate hypotension with a compensatory increase in heart rate, increased plasma histamine levels,

increased arterial pCO_2 and pH, and decreased pO_2 when dosed at 2 mg/kg, IV. Dogs anesthetized with thiamylal sodium, ventilated with the thorax open, and dosed at 4 mg/kg, IV, show significant decreases in arterial and vena caval pressures and reservoir volumes, increased central hematocrits, and decreased plasma volumes. There was no change in splanchnic or peripheral compliance or peripheral venous resistance but splanchnic resistance increased at 4 mg/kg, IV. Circulating blood volume decreased by 20% and there was a significant decrease in peripheral perfusion at the latter dose.[1] Epidural administration of morphine (0.1 mg/kg) to spontaneously breathing dogs anesthetized with sevoflurane did not cause any significant changes in the cardiorespiratory measurements made.[61] Hakim et al. examined the effects of morphine (0.6 mg/kg) directly injected into the pulmonary arteries of isolated, perfused, lungs of dogs. The result was a significant constriction of the pulmonary veins associated with histamine release from the lungs.[62]

In cats anesthetized with pentobarbital injections of 0.1–1,000 μg of morphine directly into the carotid artery resulted in variable responses that tended to be biphasic but generally caused inhibition of spontaneous chemoreceptor discharge from the carotid sinus nerve. In decerebrated cats or cats narcotized with ether, urethane, or barbiturates IV doses of ≥0.5 mg/kg morphine resulted in profound hypotension. In cats anesthetized with chloralose 0.5 mg/kg of morphine, Sub-Q, decreased heart rate and blood pressure. Cats anesthetized with chloralose and injected with 400 μg morphine into the lateral ventricle of the brain demonstrated a marked increase in heart rate and a transient increase in blood pressure followed by a subsequent decrease in blood pressure below preinjection levels. Isolated papillary muscle preparations from cats showed dose-dependent decreases in indices of contractility.[1] The rapid administration of morphine sulfate (0.6 mg/kg) directly into the isolated perfused lower lobe of the cat lung produced pulmonary venoconstriction.[62] When morphine was injected into the cerebral ventricles of cats anesthetized with chloralose, it acted on specific sites in the walls of the third ventricle producing a naloxone resistant tachycardia mediated by sympathetic control of the heart. Injections into the cisterna magna, or Sub-Q, resulted in long duration decreases in blood pressure and heart rate mediated by inhibition of sympathetic tone and increased vagal tone via action on structures near the obex at the dorsal surface of the medulla.[63]

At 0.5 mg/kg, Sub-Q, morphine had no effect on the blood pressure of intact awake rats. At 3 mg/kg, Sub-Q, there was a decrease in both blood pressure and heart rate. In midcollicular decerebrate, spontaneously breathing rats 2 mg/kg injected into the right atrium produced dramatic decreases in heart rate and slight, transient, biphasic response in blood pressure.[1] In pithed rats, morphine (1–10 mg/kg, IV) and dermorphin (0.0001–10 μmol/kg, IV), an opioid peptide that is also a selective mu-receptor agonist, had no effect on basal heart rate or blood pressure and failed to modify sympatho-adreno-medullary evoked pressor and tachycardic responses. These results demonstrate that these agents had neither direct peripheral effects on heart rate or blood vessel tone nor any effect on catecholamine release from the sympathetic nerves or adrenal medulla in rats.[64] Dosed at 7.5 mg/kg, IV, conscious rats had significant decreases in heart rate and aortic pressures attributed to increased parasympathetic tone.[1] Chronically administered daily doses of morphine

in rats resulted in dose-dependent, significant, and prolonged increases in aortic pressure and heart rate.[65]

The effects of morphine (3.0 mg/kg, Sub Q) were compared in spontaneously hypertensive (SHR), Wistar–Kyoto (WK), and Sprague–Dawley (SD) rats. SHR had significantly greater hypotension and bradycardia than WK and WK were more effected than SD.[66] Morphine is generally considered to demonstrate cardioprotective effects against ischemia-reperfusion injury and provide slight improvement in cardiac function.[67,68] The mechanism of morphine preconditioning is to prevent ischemia-reperfusion-induced apoptosis via an inositol (1,4,5)-trisphoshate-mediated Ca^{2+} (INS (1,3,5) P_3-dependent Ca^{2+} signaling pathway, in isolated rat ventricular myocytes.[69] Gross et al. suggest that opioid-induced cardioprotection occurs via JAK2 regulation of PI3K pathway-dependent STAT3, Akt, and GSK-3β, with GSK-3β contributing the central role.[70] Using isolated rat cardiac myocytes, Roy et al. showed that morphine decreases hypoxia-induced VEGF(121) and VEGF(165) mRNA expression and VEGF protein concentration through an opioid receptor mechanism, decreased HIF-1alpha protein expression and nuclear protein binding to the VEGF HIP-alpha DNA response element and inhibits phospho-Erk-1,2 MAP kinase and phospho-Akt kinase activity. A rat coronary ligation model used by the same investigators showed that morphine treatment decreased myocardial VEGF protein expression, decreased HIF-lalpha protein expression, and decreased phospho-Erk-1,2 and phospho-Akt expression.[71]

Five days exposure to morphine produced a profound cardioprotective phenotype in mouse hearts. Chronic morphine preconditioning seems to be mediated by a PKC-independent pathway involving PKA, beta(2)-AR, and G(s) proteins, while acute morphine preconditioning is mediated via G(i) proteins and PKC.[72] Morphine pretreatment of mice reduced infarct size in wild-type mice but did not protect iNOS knockout animals.[73] In isolated murine heart preparations, the exogenous activation of both delta- and kappa-opioid receptors provided protection against stunning of the myocardium.[74] Chronic exposure to morphine caused a mouse phenotype that exhibited profound and persistent protections against cardiac ischemia-reperfusion injury.[75]

Rabbits demonstrate dose-related responses to morphine. At doses of 0.5 mg/kg, IV, there was no measured effect on blood pressure while IV doses of 3–4 mg/kg resulted in increased aortic pressures, decreased heart rates, and increased circulating catecholamines and glucose levels. These reactions were enhanced by pretreatment with antihistamines. Urethane-anesthetized rabbits given 9 mg/kg, IV, showed decreases in both blood pressure and heart rate and blocked responses to exogenous catecholamine administration. Microvascular studies using cheek-pouch preparations in hamsters reveal dose-dependent arteriolar dilation. Isolated, spontaneously beating, atrial and papillary muscle preparations from guinea pigs showed decreases in heart rate at lower doses but no effects on action potential parameters or force of contraction. Studies conducted in intact, previously instrumented pigs showed that 1 mg/kg, IV, doses induced small increases in cardiac output but substantial increases in heart rate, systemic and pulmonary artery pressures, left and right ventricular work, and

hematocrit and hemoglobin concentrations. There was no change in stroke volume or systemic vascular resistance.[1]

Awake, pregnant ewes given 5 mg morphine by epidural injection showed no change in either maternal or fetal blood pressures or acid–base parameters. There was a small, but significant, decrease in maternal heart rate and uterine blood flow 120 min postinjection but no changes in maternal central venous pressure, systemic resistance, pulmonary artery pressure, or cardiac output. When previously instrumented pregnant ewes were given 0.6 mg/kg, Sub-Q, there was no change in umbilical blood flow or fetal O_2 consumption. There was a transient hyperglycemia in the ewe with significant decreases in umbilical vein glucose levels and fetal glucose uptake was significantly decreased. Dose-response studies conducted in chronically instrumented fetal lambs, in utero, indicated that doses <0.15 mg/kg, IV, into the fetus, had no effect on fetal heart rate or blood pressure while higher doses increased heart rates with no changes in blood pressure. Intact, awake horses given 0.12 mg/kg, IV, had increased heart rates, increased respiratory rates, and increased cardiac output but no changes in pulmonary arterial pressures, right atrial pressures, arterial pO_2, or pH.[1]

Meperidine (Demerol)

Meperidine at 2 mg/kg, IV, in intact awake dogs reduces cardiac output, aortic pressure, stroke volume, and heart rate; increases pulmonary arterial and systemic resistance; and decreases renal artery resistance with no change in arterial pO_2, pCO_2, or pH. At 6 mg/kg, IV, there was a large renal vascular dilation accompanied by increases in heart rate and a transient increase in cardiac output followed by a significant decrease. There was a decrease in aortic pressure and systemic resistance. The mesenteric vascular bed showed a significant decrease in flow and increase in resistance.[1] Meperidine has a dose-dependent and potent vasodilator effect on the feline pulmonary vasculature responses mediated by opioid and histamine receptor-sensitive pathways.[76] There is a dose-dependent decrease in contractility in isolated papillary muscle preparations from cats but isolated atrial preparations from rats show increases in contractility. Intact, awake horses given meperidine at 1.1 mg/kg, IV, had increased heart rates and cardiac outputs at 5 min postinjection but were back to baseline values at 15 min. There were no measured changes in pulmonary arterial blood gases or respiratory rates.[1]

Methadone

Dose-response studies on methadone in dogs anesthetized with pentobarbital (0.3–5.3 mg/kg, IV) showed decreases in heart rate, cardiac output, and aortic pressure at doses >0.8 mg/kg.[1]

Levomethadone

Levomethadone is a synthetic opioid agonist with high μ-receptor and moderate δ-receptor activities. Cats treated with levomethadone, 0.3 mg/kg, at the time of extubation following major orthopedic surgery and treated with the same dose three times daily on days 2–5 had neither documented changes in the respiratory or cardiovascular parameters measured nor any untoward renal, gastrointestinal, or hepatic effects.[77]

Pentazocine

When dogs were given pentazocine, 5–8 mg/kg, IV, there were transient decreases in heart rate, aortic pressures, arterial pCO_2 and increases in arterial pCO_2 and pH. Horses given pentazocine, 0.9 mg/kg, IV, had transient increases in heart rate and cardiac output, no changes in pulmonary, aortic, or right atrial pressures or blood gases. Isolated atrial strip preparations from guinea pigs showed decreased contractility from pentazocine.[1]

Fentanyl

In dogs and cats, fentanyl patches are most commonly applied to the region between the scapulae to prevent removal or ingestion of the patch by the animal. A recent study indicated that fentanyl is absorbed more quickly and in higher concentrations when the patch was attached to the skin from the groin area compared to the neck or thorax.[78] Fentanyl, 50 μg/kg, IV, given to conscious dogs resulted in decreases in heart rate and respiratory rate. When applied directly to the fourth cerebral ventricle of conscious dogs, fentanyl produced a pronounced bradycardia and significant decreases in blood pressure and the baroreflex. Dogs anesthetized with pentobarbital given fentanyl, IV, showed dose-dependent decreases in indices of contractility, myocardial O_2 consumption, and coronary blood flows at doses ranging from 2.5 to 30 μg/kg but at higher doses (30–160 μg/kg) indices of contractility did not change, nor did left ventricular pressure or aortic pressure. When given 100 μg/kg, IV, fentanyl showed increases in R-R intervals, paced atrial-HIS intervals, AV nodal effective and functional refractory periods, and retrograde ventricular effective refractory periods. There was no effect of fentanyl on isolated coronary artery vascular strips from dogs but autoperfused hindlimb preparations showed a decrease than an increase in precapillary pressure following an intra-arterial dose of 2.5 μg/kg of fentanyl. Dogs anesthetized with ether then rendered decerebrate were given 50 μg/kg, IV, fentanyl. Heart rates and aortic pressures decreased, indicating a peripheral effect. Intact awake dogs given 25–50 μg/kg, IV, over a 10-min period, had increased renal vascular resistance with no change in renal flow, but in anesthetized

dogs dosed with fentanyl renal vascular resistance decreased. At 30 μg/kg, IV, in chloralose-anesthetized dogs, fentanyl caused decreases in heart rate and aortic pressures and increased ventricular fibrillation threshold using the single stimulus technique. There were direct sympatho-inhibitory effects that were not mediated vagally. In another study, chloralose-anesthetized dogs given 5 μg/kg, IV, had augmented bradycardia produced by stimulation of the carotid sinus nerve but no response to stimulation of the nucleus of the solitary tract in the brain.[1] Awake dogs dosed with fentanyl at 0.01 mg/kg, IV, had increased levels of circulating plasma catecholamine, cortisol, and glucose.[79]

Pentobarbital-anesthetized cats given fentanyl at doses of 3 μg/kg, intracisternally, showed a moderate decrease in blood pressure and marked decreases in heart rate, but no change in the baroreceptor response to angiotensin II. In another study from a different lab cats given the same dose, IV, demonstrated only moderate decreases in heart rate and no change in blood pressure. In other studies, fentanyl responses during chloralose and halothane anesthesia in cats were similar to those seen in pentobarbital-anesthetized animals. Isolated papillary muscle preparations from cats showed decreases in contractility when exposed to fentanyl.[1] Baroreceptor reflexes in cats anesthetized with chloralose, with or without nitrous oxide, were well preserved with moderate doses of fentanyl but depressed at high doses.[80] Intravenous fentanyl prolongs the discharges leading to tonic hyperpolarizing synaptic drive potentials and this is thought to explain decreases in chest wall compliance during inspiration.[60] Following IV injection of fentanyl and two of its active metabolites in cats, at relatively high doses, blood pressure decreases were not associated with interactions with opiate receptors in the lower brain stem.[81] Fentanyl vasopressor effects on the pulmonary vascular bed in cats was mediated, or modulated, by both histamine and opiate receptor sensitive pathways.[82]

Fentanyl had no effect on the pulmonary vascular response to hypoxia, no beneficial effects following LAD coronary artery ligation, and no change in coronary blood flow in anesthetized rats. Conscious previously instrumented rabbits dosed with fentanyl (10 and 15 μg/kg, IV) demonstrated decreased heart rates but no change in aortic pressures, cardiac output, peripheral resistance, cerebral blood flow, oxygen transport, oxygen consumption, or GI blood flow. There was a decrease in renal blood flow. Fentanyl significantly attenuated the resistance response and augmented the heart rate following bilateral carotid artery occlusion in these same rabbits. Unanesthetized, previously instrumented sheep given 3.0 mg/kg, IV, fentanyl did not have any change heart rate, cardiac output, aortic pressures, cerebral blood flow, oxygen transport, oxygen consumption, or GI blood flow, but renal blood flow decreased. When the same dose was administered following anesthesia with pentobarbital, there were significant decreases in cerebral blood flow, oxygen transport and consumption, and renal and GI blood flow.[1]

Pigs anesthetized with halothane and nitrous oxide then dosed with fentanyl (50 μg/kg, IV + 100 μg/kg/h, IV, infusion) had no significant changes in heart rate or left ventricular systolic pressure and pressure-time index increased and left ventricular end-diastolic pressure decreased. Coronary artery blood flow and O_2 content increased. In pigs anesthetized with either isoflurane or desflurane fentanyl

at 100 μg/kg, IV, demonstrated modest increases in peripheral resistance but no change in other measured cardiovascular parameters. Intact, awake, previously instrumented primates were given 2, 4, 16, 64, and 128 μg/kg, IV; each dose administered over 1 min with 10 min between doses. Following the final dose stroke volume decreased for 10 min, cardiac output and aortic pressure decreased for 175 min, peripheral resistance decreased for 125 min but central venous pressures and pulmonary arterial wedge pressures did not change.[1]

Butorphanol

Halothane-anesthetized dogs dosed with butorphanol had significant decreases in aortic pressures but no change in cardiac output, stroke volume, peripheral resistance, pH, $PaCO_2$, pO_2, bicarbonate, pulmonary arterial pressures, or pulmonary arterial wedge pressures.[1] When awake dogs were given 0.1 mg/kg, IV, butorphanol, they demonstrated neurohormonal and metabolic changes characteristic of a stress response, i.e., increased circulating catecholamines and cortisol but no significant increase in glucose. Medetomidine blocked these responses.[79] Dogs were anesthetized with propofol, maintained in a state of surgical anesthesia with isoflurane and given butorphanol, 0.4 mg/kg, IV, immediately following endotracheal intubation. The dogs were then subjected to ovariohistorectomy. Various parameters were monitored before and after induction, at the time of the initial incision, when the second ovary was taken, at extubation and every 30 min thereafter for 300 min. There were no significant changes noted in heart rate, blood pressure, or respiratory rate compared to measurements made prior to anesthesia. Plasma cortisol levels were significantly greater at the time of endotracheal extubation and remained higher than baseline levels until 150 min postextubation.[83] Rats and mice dosed with butorphanol, at recommended doses for pain relief following open thorax surgical procedures, had significantly higher mortality rates, serious arrhythmias, and prolonged recovery.[84] Spontaneously beating atrial myocardial strip preparations from guinea pigs showed a dose-dependent decrease in heart rate when exposed to butorphanol.[1]

Buprenorphine

Dogs anesthetized with ketamine and α-chloralose were dosed with buprenorphine at 0.3 mg/kg, IV. Heart rate and aortic pressures were decreased.[1] Following fracture repair cats were given buprenorphine at 0.01 mg/kg at the time of tracheal extubation and the dose was repeated every 8 h for 5 days. There were no significant changes in the cardiovascular or respiratory parameters monitored and no adverse renal, gastrointestinal, or hepatic effects.[77]

Oxymorphone

Intact, awake, previously instrumented dogs were given 0.4 mg/kg as a loading dose + 0.2 mg/kg three times for a total dose of 1 mg/kg, IV. There was a decrease in tidal volume, alveolar total volume, arterial pO_2, and heart rate and a transient decrease in cardiac output. Respiratory rate increased as did arterial pCO_2 physiological dead space, base deficit, hemoglobin concentration, arterial pressures. There were transient increases in peripheral resistance, central venous pressure, pulmonary arterial pressures, and pulmonary wedge pressure.[1] When dogs were anesthetized with halothane and treated with oxymorphone epidurally, heart rate decreased; central venous pressure and systemic vascular resistance increased; and cardiac index, stroke volume, stroke index, and left ventricular work were unchanged.[85] Oxymorphone was administered either IM (0.15 mg/kg) or by epidural (0.05 mg/kg) to dogs undergoing pelvic or hindlimb orthopedic surgery. The dogs were monitored before the drugs were administered and at 15, 30, 60, 90, 120, 180, 240, 300, 360, 420, and 480 min postinjection. There was a significant increase in heart rate and a decrease in blood pressure in both groups.[86] In awake adult horses oxymorphone at 0.03 mg/kg, IV, produced increased heart rates and cardiac output at 5 and 15 min postinjection, but both were back to baseline levels at 30 and 60 min. There was no change in pulmonary arterial, right atrial, or aortic pressures and no change in respiratory rates or blood gases.[1]

Naloxone

When anesthetized dogs were given an IV bolus of 15 mg/kg naloxone heart rate, cardiac output, and mean aortic pressure all increased. There was no change in systemic resistance, or preload-independent contractility. Pentobarbital-anesthetized dogs given 5 mg/kg, IV, showed no changes in the cardiovascular parameters measured but 40 μg/kg doses significantly blunted the baroreceptor response. When anesthetized dogs were put into hemorrhagic shock and treated with naloxone, 2 mg/kg, IV, aortic pressures, cardiac output, contractility, and systemic resistance all increased. Decerebrate dogs given 1 mg/kg, IV, naloxone had increases in aortic pressures, heart rate, and respiratory rate. Intact, awake, previously instrumented dogs given 1 mg/kg + 20 μg/kg/min, IV, had increased plasma β-endorphin and adrenocorticotropic hormone levels but no change in heart rate, aortic pressures, cardiac output, contractility, or plasma catecholamines while at rest. When the same dogs were exercised, the plasma β-endorphin and adrenocorticotropic hormone levels increased following the naloxone treatment. The normal exercise-induced cardiovascular parameters were not blocked by naloxone.[1]

Naloxone and meptazinol (a mixed opioid agonist–antagonist) increased blood pressure and total peripheral resistance but did not evoke significant changes in heart rates of cats or rats following hemorrhage.[87] Intracarotid injections of 0.2 g naloxone in cats produced slight increases in the spontaneous chemoreceptor

discharge rate from the carotid sinus nerve but did not block the excitatory action of adenosine. In chloralose-anesthetized cats, the IV, intra-ventricular, or intra-cisternal injection of 200 μg naloxone had no effect on heart rate or blood pressure. In unanesthetized rats, naloxone, 0.1 mg/kg, IV, reversed the hypotensive effects of endotoxic, hypovolemic, and spinal transection shock. Doses of 2.5–10 mg/kg, IV, in rats anesthetized with thiopental potentiated pressor responses to epinephrine. At 5.0 mg/kg, it potentiated the pressor responses to norepinephrine and phenylephrine and reflex pressor responses to 60 s of carotid occlusion in rats but had no effect on the pressor responses to methoxamine, angiotensin, or isoproterenol. In conscious WKY or SHR rats, doses of 0.03–3.0 mg/kg, IV, showed no change in mean aortic pressure or heart rate. In spontaneously beating isolated atrial strips from rats, there was a dose-dependent decrease in spontaneous rate and an increase in resting tension. Similar preparations from guinea pigs showed a dose-independent decrease in spontaneous rate, lower doses having an enhanced effect. Intact awake rabbits dosed at 4 mg/kg + 0.1 mg/kg/min, IV, had a transient decrease in heart rate, no change in blood pressure or heart rate. Fetal sheep preparations were tested in utero at 1 mg/kg, IV. There were no significant changes in heart rate, aortic pressure, fetal arterial blood gases, or pH. At 2 mg/kg doses, there was still no change in those parameters but there was an augmentation of the catecholamine response to hypoxia. Conscious cynomolgus monkeys given 3–10 mg/kg, IV, had decreased heart rate and aortic pressure responses to angiotensin II.[1]

Other Synthetic Opioids

In anesthetized dogs, alfentanil, 500 μg/kg, IV, decreased heart rate and mean aortic pressures along with decreasing somato-cardiovascular reflexes. In intact, awake, previously instrumented dogs, sufentanil at 25 and 50 μg/kg, IV, caused significant sinus or junctional brady-arrhythmias; no change in systemic or coronary hemodynamics except for a decrease in the rate-pressure product at the high dose. When the autonomic nervous system was blocked in intact, awake dogs, sufentanil, 100–150 μg/kg over 15 min as a loading dose then 150 μg/kg/h, IV, did not change heart rate, left ventricular end-diastolic pressures, cardiac output, stroke volume, pH, arterial pCO_2, contractility, left ventricular systolic pressure, peripheral resistance, or arterial pO_2. Isoflurane-anesthetized dogs dosed with sufentanil at 12.7 ± 6.5 μg/kg + 0.01 ± 0.001 μg/kg/min, titrated to maintain end-tidal CO_2 constant at 50 mmHg had decreased heart rates, arterial pressures, and peripheral resistance with no change in cardiac output. Pulmonary arterial pressures, pulmonary vascular resistance, pulmonary wedge pressures, and central venous pressures were unchanged. There was a reduction in the contribution of central chemoreflexes and a relative increase in the contribution from the peripheral chemoreflexes. Isolated canine cardiac Purkinje fiber preparations show a dose-dependent increase in action potential duration.[1]

Cats were anesthetized with isoflurane and maintained for 60 min at 1.3 MAC. Alfentanil was given IV to achieve plasma concentrations of 500 ng/ml. End-tidal

isoflurane concentration was lowered to 35%. Heart rate, mean arterial pressures, mean pulmonary arterial pressures, stroke index, cardiac index, hemoglobin, oxygen delivery index, PvO_2 and $PvCO_2$, circulating catecholamine, and cortisol levels all increased. Arterial and venous pH both decreased.[40] Kaye et al. studied the effects of sufentanil in cats and determined that it has potent vasodepressor activity in the pulmonary arterial system and the response may be mediated or modulated by both histaminergic and opioid receptor sensitive pathways.[88]

Erythrocyte perfused isolated rabbit hearts were used to study the effects of sufentanil and remifentanil, both of which cause hypotension in intact animals. Neither of the agent caused significant coronary or myocardial changes.[89] Remifentanil (1 mg/kg/min, IV) decreased ventricular and arterial elastance.[90]

Dissociative Anesthetic Agents

True to their name these agents result in dissociation from the environment accompanied by superficial sleep usually accompanied by alternating consciousness and unconsciousness. Animals given these agents maintain pharyngeal, laryngeal, corneal, palpebral and swallowing reflexes and their eyes usually remain open. Muscle tone is increased as are spontaneous involuntary muscle movements. Salivation and lacrimation are usually increased. Somatic analgesia is usually good and visceral analgesia significantly less so.

Ketamine

Ketamine is a congener of phencyclidine and seems to depress the thalamocortical system while stimulating the reticular activating and limbic systems. Ketamine is usually used in combination with a variety of other agents variously classified as tranquilizers, sedatives, anxiolytics, or antipsychotics. This avoids the sometime violent involuntary movements frequently associated with the use of ketamine and seems to prevent emergence hallucinations and delirium. Sedatives with good muscle relaxing properties, such as the benzodiazepines, may be most useful. The effects of ketamine combinations will be discussed in a separate section.

Ketamine itself has marked effects on the cardiovascular system. In clinically normal, intact, awake subjects it increases heart rate, cardiac output, and aortic pressures. These are, most likely, indirect effects that affect the result of sympathetic stimulation and parasympathetic inhibition. There seems to be a direct negative effect on cardiac contractility and this may become significant in animals with compromised cardiac function. The peripheral vasoconstrictor response seen with ketamine is probably centrally mediated but there is no indication of preload increases with this agent. Respiratory rate and minute volume are increased and are associated with decreases in arterial pO_2 and pH and increases in arterial pCO_2.[1]

Dogs treated with ketamine, 10 mg/kg, IM, had increased plasma epinephrine, cortisol, and glucose concentrations a stress-type response.[79] In canine pulmonary arteries, ketamine inhibited K^+ ATP-mediated pulmonary vasorelaxation but did not attenuate the endothelium-dependent component of a lemakalim-induced pulmonary vasorelaxation.[91] In clinically relevant doses, ketamine alters central respiratory activity and diminishes both inspiration-evoked gamma-aminobutyric acid-mediated and glycinergic neurotransmission to parasympathetic cardiac efferent neurons.[92] In sevoflurane-anesthetized cats, ketamine triggered histamine release and induced cardiovascular depression.[93] In neonatal rats, ketamine was shown to inhibit nicotinic acetylcholine receptor-induced transients in intracellular free Ca^{2+} concentrations in intracardiac ganglion neurons.[2] Ketamine can inhibit endotoxin-induced pulmonary inflammation in vivo in adult male Wistar rats, but only at supra-anesthetic dosages.[94] The response of skeletal muscle microcirculation to ketamine was compared in male Wistar–Kyoto (WKY) and Harlan SHR rats. Constriction of A3 arterioles following ketamine was greater in SHR than WKY and this was accompanied by an exaggerated hypertensive response in the SHR.[14,15] When administered during reperfusion following ischemia in isolated, working rat hearts ketamine depressed cardiac function.[95] Ketamine, 100 mg/kg, IP, in male rats increased circulating atrial natriuretic peptide and free fatty acid concentrations in control rats but in 2-kidney, 1-clip animals ketamine did not elicit any additional responses in these parameters.[96] Chronically instrumented intact, awake rats were dosed with ketamine, 5–20 mg/kg. There was a significant, dose-dependent increase in blood pressure, heart rate, and renal sympathetic nerve activity.[19] Intact, awake, previously instrumented rabbits were dosed with ketamine and demonstrated increased heart rates and total peripheral resistance. The heart rate increases were attributed to a reduction in vagal efferent activity.[5] Ketamine produced reversible decreases in left ventricular diastolic pressure, dP/dt and spontaneous heart rate in isolated heart preparations from guinea pigs. These changes were accompanied by dose-dependent increases in the $[Mg^{2+}]_i$ and the total magnesium efflux and activation of p38 MAP kinase and ERK 1–2 pathways.[97]

Ketamine (3 mg/kg) was injected into the subarachnoid space between the last lumbar vertebra and the first sacral vertebra in goats. There was no change in heart rate or arterial pressures.[98] Using COS-7 cells Kawano et al. determined that ketamine-induced inhibition of sarcolemmal K^+ ATP channels. The response was mediated by subunits of inwardly rectifying potassium channels and sulfonylurea receptors.[99] Ketamine (1.5 mg/kg) markedly elevated systemic and pulmonary arterial pressures, heart rate, both systemic and pulmonary vascular resistance, and right and left ventricular filling pressures. These effects were blocked by fentanyl.[100]

Tiletamine

Tiletamine is a dissociative anesthetic agent that provides analgesia and immobilization. The drug produces severe emergence delirium and is not recommended for use alone. It is available commercially mixed with zolazepam, a benzodiazepine derivative

that provides muscle relaxation and tranquilization. This product is marketed as Telazol® and will be covered in the section on drug combinations.

Imidazole and Other Hypnotic, Amnesiac, Anxiolytic, or Antipsychotic Compounds

Etomidate

Etomidate is a carboxylated imidazole derivative classified as a nonbarbiturate hypnotic of ultra-short action. It also inhibits steroid synthesis. It is popular for use in humans as an induction agent and by continuous infusion. The usual induction dose in humans is 0.3 mg/kg but when used in dogs and cats 2–4 mg/kg is needed for induction. Prolonged infusion is known to reduce adrenocortical function and a single IV dose has been shown to suppress adrenal steroidogenesis in dogs and cats for several hours. Recently a single dose in a human patient was reported to cause an acute adrenocortical insufficiency.[101] It produces minimal changes in heart rate, arterial pressures, or myocardial contractility but does induce respiratory depression and apnea upon induction in animals. In veterinary medicine it has not gained significant popularity, because it is more expensive than propofol or thiopental; it can induce sneezing, retching, and myoclonic twitching at induction; and hemolysis and hematuria have been reported following its use in dogs and cats due to its vehicle, propylene glycol. A new formulation using aqueous sulfobutyl ether beta-cyclodextrin resulted in less of a decrease in mean arterial pressure and may be safer than the commercial etomidate that is now available.[102] Etomidate decreases the oxidative phosphorylation in isolated rat liver mitochondria[103] and inhibits K^+ ATP channel activity and angiotensin II-induced Ca^{2+} influx in vascular smooth muscle cells from rats.[104–106] It does not affect mitochondrial adenosine triphospate-sensitive K^+ channels.[107] Isolated pulmonary artery vascular rings from chronically hypoxic rats showed more relaxation from etomidate than did similar rings from human subjects.[108] Pulmonary vascular rings from dogs were used to demonstrate that etomidate (5×10^{-5} M) attenuates the endothelium-dependent component of lemakalim-induced pulmonary vasorelaxation via inhibition of the cyclooxygenase pathway.[91] Etomidate also attenuates pulmonary arterial relaxation responses to acetylcholine and bradykinin by inhibiting both NO- and EDHF-mediated components.[109] When conscious, previously instrumented, rhesus monkeys were treated with etomidate (100 μg/kg), there were significant decreases in mean arterial pressure, heart rate, and myocardial contractility accompanied by increased systemic arterial compliance. There were insignificant changes in left ventricular diastolic pressure, cardiac output, stroke volume, and total peripheral resistance.[17] Mice lacking α2-adrenoceptor subtypes were used to demonstrate that etomidate acts as an agonist at these receptors resulting in an α2B-mediated increase in blood pressure.[110] Both the immobilization and respiratory depression caused by etomidate are mediated by beta3-containing

GABA(A) receptors and hypnotic effects are mediated by both beta3- and beta2-containing GABA(A) receptors. The hypothermic, cardiac depressant, and sedative actions of the drug are largely independent of the beta3-containing GABA(A) receptors.[111] Etomidate (10 μM) did not potentiate epinephrine-induced slowed conduction in canine Purkinje fibers.[112] In rats treated with etomidate, baseline arteriolar diameters were significantly larger than in rats anesthetized with propofol or thiopental. Arteriolar constriction induced by mefenamic acid (20 mmol/l) was significantly greater than that caused by the other two agents.[113]

Metomidate

Metomidate is another imidazole compound that has been used over two decades as a hypnotic agent in pigs. When administered IV it results in minimal respiratory or cardiovascular depression with good hypnosis but analgesia is poor with about a 1-h recovery time. When ketamine and metomidate were compared in pigs with endotoxin-induced shock, the etomidate group had lower cardiac outputs, mean arterial pressures, oxygen delivery, base excesses, and lower survival rates than pigs anesthetized with ketamine.[114] This agent has been withdrawn from the US market and currently is not available.

Benzodiazepines

Midazolam (Versed)

This agent suppresses both norepi and cortisol release.[12] In intact, awake, previously instrumented dogs this drug has dose-dependent effects on heart rate and blood pressure. Lower doses increase heart rate and lower blood pressure. Higher doses may or may not demonstrate a heart rate change while reducing myocardial contractility. There is a direct cardiac inhibition of catecholamine release.[1] Midazolam premedication in dogs may increase the adverse respiratory effects of propofol anesthesia.[115]

In intact, awake, previously instrumented sheep midazolam increased maternal heart rate and also increased mean aortic pressure. Intact, awake pigs were given bupivacaine 2 mg/kg/min until cardiovascular collapse. Midazolam delayed the bupivacaine-induced onset of ventricular arrhythmias, decreased the incidence of clonic-tonic seizures, and prevented increases in blood pressure and heart rate in these pigs.[1] Midazolam does not inhibit the K^+ ATP channel activity in vascular smooth muscle.[104]

Carotid sinus firing frequency was decreased by midazolam in a dose-dependent manner in isolated, perfused carotid bodies from rabbits.[116] Midazolam (3–100 μM) caused a decrease in both peak $[Ca^{2+}]_i$ and shortening in freshly isolated rat ventricular

myocytes.[117] Heart rate variability measurements were used to determine that midazolam induces a predominance of sympathetic activity resulting in increases in heart rate and decreases in blood pressure.[118] Propofol was found to be more potent than midazolam in causing a sympatholytic response in cardiac autonomic nervous system activity during combined spinal and epidural anesthesia.[119] Hyperpolarization of vascular smooth muscle, elicited by activation of the BK ($Ca2^{+}$) K^{+} channel, may contribute to the vasorelaxation effects of midazolam.[120]

Diazepam

Various studies using diazepam produced varying results in intact, awake, previously instrumented dogs. In doses from 0.5 to 2.5 mg/kg, IV, three studies documented an increase in heart rate and one study documented no change. Three studies recorded no change in systemic arterial pressures and another study reported an early increase with a return to baseline with a significant increase in renal blood flow. One study documented a decrease in contractility and another study documented no change. There was an increase in cardiac output and a decrease in contractility in one study and no changes in the other studies. Most studies report a decrease in coronary blood flow and resistance with little or no systemic arterial changes. Ten to forty-eight hours following ligation of the LAD coronary artery in intact, awake dogs, 1 mg/kg, IV, or oral diazepam decreased the frequency of ectopic beats by 80–98%. The infusion of 300 μg to 3 mg diazepam into the A-V nodal artery in anesthetized dogs resulted in third degree A-V block that was not affected by vagotomy and sympathectomy.[1]

In pentobarbital-anesthetized cats 7–10 mg/kg, IV, diazepam had no apparent effect on cardiovascular parameters in cats. Cats anesthetized with halothane, decerebrated and immobilized with gallamine triethiodide given 1 mg/kg, IV, doses of diazepam demonstrated enhanced inhibition of both flexor and extensor monosynaptic reflexes.[1]

Isolated rat hearts exposed to 15 min of global ischemia and then reperfused showed a minor depression of cardiac function when dosed with diazepam during reperfusion.[95] Studies conducted on primary cultures of rat ventricular myocytes exhibited a dose-dependent tachycardia after 1 h of exposure. Longer exposures produced arrhythmias and/or arrest, pseudopodia formation, and increased cytoplasmic granulation of the cells.[1] Diazepam (30 and 100 μM) enhanced excitation-contraction coupling independent of L-type Ca^{2+} channel modulation[117] and augments the inotropic and biochemical effects of dopamine.[121] Doses of 1–10 μM diazepam in whole cell and cell-attached recordings made from labeled paraventricular nucleus neurons (PVN) in hypothalamic brain slices indicated that diazepam suppresses the firing activity of PVN presympathetic neurons by potentiation of GABAergic inputs.[122] In urethane-anesthetized, pancronium-immobilized, artificially ventilated, and bilaterally vagotomized rats, diazepam (1–4 μM/kg, IV) reduced phrenic nerve activity and blood pressure and inhibited the chemoreceptor reflex.[123] In rat aortic rings, a supraclinical concentration of diazepam attenuated phenylephrine-induced contractions

by increasing endothelial nitric oxide activity and by a direct effect on vascular smooth muscle.[124] Rats preconditioned to a noxious stimulus exhibited more freezing behavior and larger increases in blood pressure and heart rate from the stimulus than nonconditioned rats. These effects were blocked by diazepam in the preconditioned rats but not in the controls.[125] In isolated atrial and papillary muscle preparations from rats, doses of 10 μg/ml prevented arrhythmic contractions induced by electrical stimulation in spontaneously beating preparations, increased the refractory period, decreased the maximum driving frequency, and had little effect on the rate of spontaneous contractions. At doses of 30–50 μM, diazepam abolished abnormal rhythm caused by local injury and effectively reduced ectopic automaticity. From 10 to 50 μM, there was a dose-dependent inhibitory effect on ventricular automaticity resulting from inhibition of adenosine uptake. There was also a reduction in the chronotropic responses to norepinephrine via interaction with the cAMP-linked chain of events following β-adrenergic activation. At 0.5–10 μg/ml, there was a dose-dependent increase in contractility but at 20 μg/ml contractility decreased.[1]

Isolated left atrial preparations from mice demonstrated a dose-dependent potentiation of adenosine-mediated reductions in isometric tension. Diazepam also inhibited adenosine uptake in left ventricular slices from mice.[1] In pentobarbital-anesthetized rabbits, there was no effect of diazepam on the carotid sinus baroreflex. Intact, awake, previously instrumented pigs given 0.15 mg/kg, IV, and perturbated by dosing of bupivacaine at 2 mg/kg/min until cardiovascular collapse demonstrated a delayed onset of ventricular arrhythmias and decreased incidence of clonic-tonic seizures. Increases in aortic pressure and heart rate were prevented. In chronically instrumented pregnant ewes 0.2 and 0.5 mg/kg, IV, there was a dose-dependent increase in maternal heart rate and mean aortic pressure. Diazepam causes an increase in fetal heart rate that lasts for more than an hour and a decrease in fetal mean aortic pressure with no change in blood gases in either the dams or the fetuses. Cultured bovine adrenal chromaffin cells in the presence of ouabain showed potentiated effects of GABA on catecholamine release and phosphoinositide metabolism.[1]

Romifidine

In cats sedated with a combination of romifidine and butorphanol, additional doses of romifidine (100 μg/kg, IV) caused a significant decrease in heart rate.[126]

Rilmenidine

This drug is a hybrid ligand that binds to both I1-imadazoline and α-2-adrenergic agonist receptors. In anesthetized rabbits, rilmenidine (1 μg/kg, injected intracisternally) decreased both arterial pressure and heart rate.[127]

α-2 Adrenergic Receptor Agonists

Medetomidine and Dexmedetomidine

Medetomidine is an equal mixture of two optical enantiomers, dexmedetomidine and levomedetomidine. In general, the α-2-adrenoceptor agonists maintain relatively stable systemic blood pressure and heart rate and reduce overall oxygen consumption. They substantially reduce the needed dose of anesthetic agents, thus reducing the potential for adverse reactions and they reduce the risk of postoperative delirium.[128] The α-2 adrenergic receptor agonists are popular in small animal practice because of their potent sedative and analgesic properties. When medetomidine is administered alone, the cardiovascular effects are maximal at a dose of 5 μg/kg and characterized by an initial increase in blood pressure due to peripheral vasoconstriction. The blood pressure then returns to normal or slightly lower than normal levels. The pressor response is generally accompanied by a compensatory decrease in heart rate mediated vagally. A transient change in conductivity of the myocardium may occur resulting in A-V block. There may also be an initial slowing of respiratory rate.[129]

Medetomidine (750 μg/m2, IV) injections in dogs caused a significant decrease in heart rate, cardiac output, and fractional shortening while mean arterial pressure, systemic vascular resistance, and central venous pressure were increased.[130] At doses of 20 μg/kg, IV in dogs, medetomidine was associated with increases in arterial pressures, pulmonary arterial pressures, central venous pressures, systemic vascular resistance, pulmonary vascular resistance, and $PaCO_2$. Heart rate, cardiac output, stroke volume, stroke index, respiratory rate, and arterial pH and PaO_2 all decreased.[131] Medetomidine, 0.02 mg/kg, resulted in hyperglycemia in Beagle dogs.[79] When medetomidine was injected as an epidural, 0.015 mg/kg, dogs demonstrated second degree A-V block associated with sinus arrhythmia during the first 20 min following the injection and blood pressure increased.[86] When medetomidine (0.01 mg/kg) was given IV to healthy German Shepherd dogs breathing spontaneously at 1,486 m above sea level. Heart rate decreased significantly, blood pressure increased, and arterial pO_2 decreased along with a decrease in respiratory rate.[132]

There were significant decreases in heart rate, left ventricular outflow tract velocity, and left ventricular outflow tract pressure gradients in cats given 20 μg/kg medetomidine IM.[133] Dexmedetomidine administered at 10 μg/kg, IM, to cats resulted in decreased heart rates and blood pressures.[134] Goats and sheep were anesthetized with sevoflurane and dosed with dexmedetomidine at 2 μg/kg, IV. Both species showed increases in respiratory resistance, alveolar dead space, and shunt fraction while thoracic compliance decreased. Arterial, pulmonary arterial, pulmonary capillary wedge and central venous pressures all increased while heart rate, cardiac output, and arterial pO_2 also decreased significantly.[135] Continuous infusion of 0.25 μg/kg/min, IV, of dexmedetomidine to rats anesthetized with either halothane or isoflurane resulted in decreased heart rates and arterial blood pressures in the isoflurane-anesthetized rats but not in the halothane-anesthetized animals.[136]

Dogs were pretreated with selegiline (1 mg/kg), a MAO inhibitor once per day by mouth for 44 days then dosed with medetomidine (750 $\mu g/m^2$), IV. The selegiline did

not modify the response to medetomidine. The latter caused a significant decrease in heart rate, cardiac output, and fractional shortening and a significant increase in mean aortic pressure, systemic vascular resistance, and central venous pressure.[130]

Clonidine

Clonidine is a preferential α-2 agonist that has been used for over 35 years as an antihypertensive drug. When used orally, it is an effective anxiolytic agent that also provides stable cardiovascular parameters during venous cannulation procedures.[137] In anesthetized rats, an IV clonidine bolus, 15 μg/kg, evoked prolonged respiratory depression and a significant, but short-term increase in mean arterial pressure followed by a decrease below baseline values.[138]

β-2-Adrenergic Receptor Agonists

Clenbuterol

This β-2 ARA has been shown to have beneficial effects in animal models of heart failure; however, large doses can induce cardiomyocyte death. Subcutaneous injections of 3 mmol/kg in conscious Wistar rats induced cardiomyocyte apoptosis, decreased arterial blood pressures, and increased heart rates.[139] Three hours following subcutaneous administration of 250 μg/kg clenbuterol to rats, taurine levels in cardiac tissue were decreased and remained so at 12 h postadministration. Circulating and skeletal muscle levels of taurine were significantly increased at 3 and 6 h postinjection and serum creatine kinase levels were significantly increased at 12 and 24 h postinjection. These results are important since taurine has been shown to have a protective role in the myocardium.[140] Massive doses of 5 mg/kg, Sub-Q, in Wistar rats resulted in significant myocyte-specific necrosis in both heart and skeletal muscle.[141] Clenbuterol increased electrical field stimulated contractions in mesenteric arteries from both young and old SHR. In the young SHR, clenbuterol seemed to inhibit CGRP release and in old SHR it increased the release and response to norepi while decreasing the release of neuronal NO.[142] Chronic administration of clenbuterol to rats, 2 mg/kg/day for 4 weeks, induced cardiac and skeletal muscle cellular hypertrophy, an increase in oxidative carbohydrate utilization and an increase in sarcoplasmic [Ca^{2+}]. The changes in [Ca^{2+}] were considered to be responsible for an observed increase in Ca^{2+} transients.[143] Rats were dosed with clenbuterol in the range of 1 μg/kg/day to 1 mg/kg/day for 14 days. At doses ≥10 μg/kg/day, the drug increased the protein content of both cardiac and skeletal muscle. Larger doses of 100 μg/kg/day or 1 mg/kg/day resulted in apoptosis and myocyte death in skeletal muscle and significantly increased the area fraction of collagen in the myocardium.[144] BRL-47672 is the pro-drug of clenbuterol. After a single IP

injection of 250 μg/kg, it caused less of an effect on heart rate, arterial blood pressure, and hindquarters vascular conductance than clenbuterol.[145]

A single 15 mg/kg oral dose of clenbuterol in Swiss albino mice caused an increase in collagen distribution in both the subendocardium and left ventricular myocardium. The structural and functional remodeling of the extracellular matrix was attributed to downregulation of MMP-9 activity resulting in impaired collagen turnover.[146] Propofol-induced, isoflurane-anesthetized female dogs given clenbuterol demonstrated a transient decrease in mean arterial blood pressure.[115] Twenty Standardbred female horses were divided into four groups. The first group was dosed with clenbuterol at 2.4 μg/kg, b.i.d for 5 days and exercised on a treadmill for 20 min at 50% VO_2max. The second group was given the clenbuterol at the same dose but not exercised. The third group was exercised but not given clenbuterol and the fourth group served as untreated controls. Both clenbuterol-dosed groups demonstrated significantly higher left ventricular internal dimensions at end diastole and end systole; increased interventricular septal wall thickness at both end diastole and systole; and similar changes in left ventricular posterior wall thickness. There were also increased aortic root dimensions in the clenbuterol-treated animals.[147]

KUR-1246

This new β-2 ARA was administered to conscious dogs at 0.1 and 1.0 μg/kg, IV, with no effects on heart rate, blood pressure, or femoral arterial flow. At higher doses of 10 and 100 μg/kg, IV, there was a significant decrease in blood pressure and increase in heart rate. There were no changes in QT or QTc intervals of ECGs from these animals and at 10 μmol/l concentrations there was no affect on action potential parameters in isolated papillary muscle preparations from guinea pigs.[148]

Fenoterol

Injections of 0.3 mmol/kg of fenoterol induced cardiomyocyte apoptosis in Wistar rats. Higher doses increased heart rate and decreased diastolic blood pressure significantly.[139]

Rauwolfia Derivatives

Reserpine

Numerous studies have confirmed that treatment with reserpine depletes both circulating and tissue catecholamine levels. Intact, awake dogs dosed at 0.03 mg/kg, orally for 6 weeks demonstrated sustained decreases in heart rate and mean aortic pressures.

Arterial tissue levels of K^+, Ca^{2+}, and Mg^{2+} were also decreased along with norepinephrine levels. Pentobarbital-anesthetized dogs demonstrated enhanced vasodilator responses (from doses of 1 mg/kg, 24 h prior to the experimental protocol). Reserpine prevented changes in S-T segments produced by pyridylcarbinol at a dose of 5 mg/kg, IP, for 2 consecutive days prior to the experiment. Pretreatment with 0.3 mg/kg 24 h prior prevented time dependency of the ventricular fibrillation threshold while doses of 0.1 mg/kg, 24 and 48 h prior to the experiment blocked ventricular β-adrenoceptors but 1 mg/kg given 24 h prior did not block the contractile response to norepi. Doses of 3 mg/kg, IV 24 h prior to an experiment had no effect on aortic flow but resulted in a decrease in heart rate, systolic pressure, systemic resistance, left ventricular end-diastolic pressure, and contractility. In both awake and anesthetized dogs in the dose range of 0.03–0.1 mg/kg/day, there were decreases in heart rate and aortic pressures and there was a blockage of α-2 adrenergic mediated responses.[1]

Pentobarbital-anesthetized cats were treated with reserpine (1 mg/kg, IV) 24 h prior to the experiment. The reserpine did not block the effects of angiotensin I or II. Higher doses (3 mg/kg, IP) failed to modify the dose-response curve to 5-HT but produced a significant decrease in the outflow of tritiated norepi induced by 5-HT from isolated pial arteries from cats. Five mg/kg, IP, 15–18 h prior did not block the positive inotropic effects of ammonium vanadate.[1] In rats 3.2 and 2.5 mg/kg/day, IP, pretreatment on days 3, 2, and 1 prior, potentiated α-2 but not α-1 adrenoceptor-mediated responses.[1] Reserpine modified the levels of arginine, cysteine, phenylalanine, tryptophan, isoleucine, and tyrosine in the cytosols of rat atrial and ventricular cardiomyocytes.[149]

Isolated strips of left atrium from rabbits treated with 5 mg/kg reserpine 24 h prior to harvest of the tissues demonstrated depression of tyramine-induced contractions. Isolated saphenous arteries from rabbits treated with 3 mg/kg, IP, 48 h prior and 5 mg/kg, IP, 24 h prior showed substantial contractions produced by stimulation of sympathetic nerves despite a 95.7% increase in norepi content of the tissue.[1] The effects of long-term, low-dose (43 μg/kg/day, continuous SQ infusion), reserpine were studied in New Zealand White rabbits fed a 0.2% cholesterol-enriched diet. Heart rates were decreased significantly but there were no significant effects on blood pressure, the level of lipids in liver or heart, hematocrit, or plasma fibrinogen. The treatment decreased the amount of low-density cholesterol in the aortic walls and the intima–media thickness ratio.[150] The change in content and uptake of dopamine and norepi in the renal, superior mesenteric, and femoral arteries and the abdominal aorta was determined in rabbits following a single 3 mg/kg, IP, dose of reserpine. The recovery of stored dopamine was faster than that of stored norepi following reserpine treatment and the recovery of dopamine uptake after reserpine was slower than norepi uptake.[151] Examination of the ultrastructure of myocardial cells of rabbits 24 h after a single dose of reserpine revealed a decrease in the number and an increase in mitochondrial size, a relaxation of narrowing and ramification of myofibrils and an increase in intracellular lipid content.[152]

Isolated hearts from control and reserpine-treated guinea pigs were retrograde perfused with modified Krebs buffer for 20 min with buffer containing either no milrinone or 1.7×10^{-6} or 1.0×10^{-4} mol/l milrinone. Cyclic AMP content was

significantly lower in the reserpine-treated hearts at each milrinone concentration. Although milrinone significantly increased contractility and ventricular compliance, no difference was observed between the control and reserpine-treated hearts.[153] Isolated atrial preparations from guinea pigs treated with 5 mg/kg, SQ, 24 h prior showed that reserpine pretreatment prevented the release of catecholamines from cardiac sympathetic nerve terminals and prevented increases in contractility induced by hydroxylated metabolites of chlorpromazine. Right ventricular strips from guinea pigs pretreated with 0.1 and 0.03 mg/kg/day for 7 days demonstrated a nonspecific inotropic supersensitivity that was preceded by norepi depletion.[1] Sheep and goats pretreated with 0.02 mg/kg/day for 3 days showed evidence of depleted catecholamine stores and anesthetized monkeys treated with 0.5 mg/kg, IP, 20–24 h pre-experiment demonstrated a blocking of ouabain-induced contractions of the peripheral but not the cerebral arteries.[1] Reserpine pretreatment prevented increases in heart rate, arterial pressure, and left ventricular pressure following 1 ms pulses of 0.1–10 A delivered during ventricular fibrillation in anesthetized pigs following cardiac conversion to normal sinus rhythm.[154]

Phenothiazine Derivatives

These agents can have a significant effect on the cardiovascular system probably linked to the blockade of dopamine within the basal ganglia complex of the CNS. Many of these compounds act as dopamine antagonists acting on dopamine excitatory receptors. In general, these agents decrease preload, contractility, and afterload and increase heart rate. Some are capable of producing arrhythmias, paradoxical to their antiarrhythmic actions. Repolarization abnormalities documented with these agents seem to be dose related. These drugs have strong central α-adrenergic antagonist actions and also block peripheral α-adrenergic receptors. There is also evidence of strong peripheral β_2-adrenergic stimulation resulting in significant vasodilation.[1] Park et al. have shown that there are undesirable and damaging interactions between these agents and cardiac calsequestrin that can result in tachycardia, bradycardia, palpitation and changes in PR, WRS, QTc, and other ECG parameters.[155]

Chlorpromazine and Promazine

Intact, awake, previously instrumented dogs demonstrate a dose-dependent tachycardia and increase in cardiac output with decreased arterial pressures and decreased pulmonary and systemic vascular resistance. Anesthetized dogs given 1 mg/kg, IV, of chlorpromazine also showed decreased contractility, increased conduction time, and decreased conduction velocity in A-V nodal tissue, HIS-Purkinje tissue, and ventricular tissue. The same dose decreased the ventricular multiple response threshold and resulted in mitochondrial dysfunction while decreasing Ca^{2+} binding activity. There was also a dose-dependent inhibition of the Na^{+}/Ca^{2+} exchanger and lysosomal lipase hydrolysis.[1]

Anesthetized cats dosed with 1 mg/kg, IV, chlorpromazine showed a decrease in spontaneous chemoreceptor activity. There was no dose-response sensitivity to ouabain-induced arrhythmias. The intracerebro-ventricular injection of 0.5 mg did not induce arrhythmias or death indicating no central mechanism for the adverse cardiac responses.[1] Urethane-anesthetized cats were used to determine the effect of chlorpromazine on ouabain-induced arrhythmias and death. Chlorpromazine decreased blood pressure without reflex tachycardia suggesting that the drug might interfere with baroreflex function. It was concluded that sudden, unexplained, death in patients given this agent might be due to drug-induced arrhythmias.[156] When rats were injected intravenously with chlorpromazine, local endothelial damage accompanied by thrombus was noted.[157] A range of concentrations of chlorpromazine used to treat rat tissues resulted in decreased Ca^{2+} binding and decreased Mg^{2+}-ATPase and Na^{+}, K^{+}-ATPase activities of the sarcolemma. There was also decreased Ca^{2+} binding and uptake of the microsomal and mitochondrial membranes. At higher concentrations mitochondrial respiratory and oxidative phosphorylation activities were decreased. Intra-arterial injections at a variety of concentrations in a rat hindquarter preparation showed competitive antagonism of the effects of 5-hdroxytryptamine. High doses, 45 mg/kg, IP, an hour prior to coronary artery ligation and every 6 h thereafter reduced ischemic cell death in the myocardium at risk.[1]

Isolated papillary and atrial muscle preparations exposed to 0.001–10 g/ml concentrations of chlorpromazine demonstrated an increased refractory period in rat papillary muscle but no effect on atrial muscle. There was no change in the contractility of the atrial preparations but decreased generated force in the papillary muscle. The treatment did not prevent arrhythmic contractions resulting from electrical stimulation in spontaneously contracting atrial preparations. In vitro rat aortas exposed to 0.25 mM chlorpromazine had a significant decrease in incorporation of labeled acetate into free fatty acids and total phospholipids but not triglycerides. It also altered the pattern of arterial phospholipids synthesized from acetate and decreased acetate incorporation into the combined fractions of sterol esters, hydrocarbons, sterols, and diglycerides.[1]

Isolated right ventricular papillary muscle preparations from guinea pigs showed similar effects of exposure to chlorpromazine, i.e., decreased maximum upstroke velocity, decreased overshoot and decreased resting potential of the action potential, decreased contractility, and suppression of Ca^{2+}-induced contraction.[1] In guinea-pig ventricular myocytes exposed to 2 and 5 μM chlorpromazine, there was blocking of the rapidly activating delayed rectifier K^{+} current. However, the same concen trations failed to block slowly activating delayed rectifier K^{+} currents. These concentrations of the drug also blocked the human ether-a-go-go-related gene (HERG).[158] Chlorpromazine at concentrations of 2 and 5 μM produced early after-depolarizations (EADs), phenomena thought to be associated with the polymorphic ventricular arrhythmia torsades de pointes in humans, in isolated, spontaneously beating guinea pig Purkinje fibers.[159]

A range of chlorpromazine concentrations tested on isolated arterial microsomes from atherosclerotic diet-fed rabbits inhibited cholesterol acyltransferase. In isolated SA-nodal preparations from rabbits, chlorpromazine arrested spontaneous activity that could then be restored with norepi. An isolated, perfused interventricular

septum preparation from rabbits was used to demonstrate that chlorpromazine inhibits Ca^{2+} influx and phospholipase activation.[1] Chlorpromazine also acts as a Ca^{2+}-channel blocking agent in isolated rings of rabbit aorta.[160] Following ischemia, chlorpromazine aided functional recovery of the myocardial tissue and protected against ischemia-induced alterations in structure and membrane permeability. In aortic strips the drug antagonized norepi-, serotonin- and histamine-induced contractions but did not antagonize the PGF_2 or angiotensin II-induced contractions. Isolated pulmonary arterial and aortic preparations from rabbits showed dose-response decreases in contractions evoked by electrical field stimulation, decreased accumulation of tritiated-norepi. This work led to the conclusion that chlorpromazine is a potent inhibitor of postsynaptic α_1-adrenoceptors and also inhibits the reuptake of norepi.[1] Chlorpromazine (0.1 and 1.0 mg/kg, IV) potentiated the decrease in mean blood pressure at 1 min after the onset of head-up tilt in rabbits anesthetized with urethane, urethane + α-chloralose, or nitrous oxide but did not have the effect in conscious rabbits or rabbits anesthetized with a combination of urethane + α-chloralose + morphine.[161]

Promazine given to chronically cannulated pregnant ewes resulted in both maternal and fetal tachycardia and hypotension. It depressed uterine blood flow and fetal pulmonary arterial pO_2 and increased fetal pCO_2.[162] In isolated carotid artery strips from pigs, chlorpromazine treatment resulted in a significant decrease in the tension generated by norepi-induced contractions and inhibited light chain phosphorylation.[1]

Acetylpromazine (Acepromazine)

In intact awake dogs, 0.4 mg/kg, IV, of acetylpromazine caused prolonged hypotension and myocardial depression but offered protection against epinephrine-induced arrhythmias. At a dose of 0.11 mg/kg, IV, mean aortic pressure and arterial pH decreased with no change in arterial pCO_2. At doses of 0.2 mg/kg, IV mean aortic pressures, stroke volume, left ventricular work, respiratory rate, minute ventilation, and oxygen consumption all decreased. There was no change in heart rate, pulmonary arterial pressures, central venous pressures, cardiac output, or peripheral resistance.[1]

Cats anesthetized with chloralose and given 1.5 mg/kg, IV, of acetylpromazine demonstrated increased toxicity to ouabain, decreased blood pressure, and increased heart rates. Similarly anesthetized cats received 500 μg directly into the cerebroventricular space. These animals had decreases in blood pressures but no change in heart rate. Intact, awake cats given 0.2 mg/kg, IM, had decreased cardiac output but no change in stroke volume, heart rate, respiratory rate, or blood gases.[1] Gottingen mini-pigs given acepromazine showed depressed respiratory and cardiovascular function.[163] When acetylpromazine was given to awake sheep, 0.5 mg/kg, IV, it prevented epinephrine-induced arrhythmias.[1,164] Intact, awake horses dosed at 0.5 mg/kg, IM had a slight increase in heart rate and serum cortisol levels but no change in hematocrit. At 0.09 mg/kg, IV, there was no change in heart rate, cardiac output, blood gases, or mean pulmonary arterial pressures but significant decreases in

respiratory rate, central venous pressure, and mean aortic pressure. At 0.1 mg/kg, IV, there was a decrease in mean aortic pressure and partial blockage of the pressor response to adrenalin. Doses of 0.05 mg/kg, IV, resulted in decreased mean aortic pressure and cardiac index with a slight increase in heart rate after 20 min and doses of 0.01 mg/kg, IV, decreased aortic pressures with no change in heart rate.[1]

Other Phenothiazine Derivatives

Triflupromazine, Levomepromazine, Prochlorperazine (thioridazine), Cyamemazine

Triflupromazine is known to induce QT prolongation and torsades de pointes resulting in sudden death in human patients.[165] Rats exposed to a range of intra-arterial doses of triflupromazine demonstrate a strong competitive antagonism of 5-hydroxytryptamine. In isolated right ventricular strip preparations from rats 1–5 μM of triflupromazine improved the recovery of the myocardial tissue following calcium repletion by inhibition of calmodulin. Isolated working rat hearts exposed to 40 min of global ischemia and treated with 2.45 μM triflupromazine either before the ischemia or during reperfusion demonstrated increased membrane stabilization and inhibition of calmodulin and binding to other calcium-dependent proteins. There was no effect on tissue high-energy phosphate levels or mitochondrial oxidative phosphorylation.[1] Spontaneously beating Purkinje fibers of guinea pigs exposed to thioridazine (2 and 5 μM) induced EADs but triflupromazine (2 and 5 μM) did not.[159]

Helical carotid artery strips from pigs exposed to 0.1 mM triflupromazine had a 75% decrease in the tension generated by norepi. At 0.5 mM, there was complete inhibition of generated tension. Isolated cardiac cells from 7-day-old chicks exposed to 10^{-5} M triflupromazine increased incorporation of choline into both phosphocholine and phospholipids and prevented anoxia-induced changes in phosphocholine. At 10^{-4} M, the drug damaged myocardial cells. In guinea-pig ventricular myocytes, doses of 0.5 and 2 μM triflupromazine blocked the rapidly activating delayed rectifier K^+ current but did not block the slowly activating delayed rectifier K^+ current.[165] When Rhesus monkeys were fed an atherosclerotic diet then treated with IM injections of triflupromazine, there was no significant effect on serum cholesterol and triglyceride levels but the formation of atherosclerotic lesions was decreased by decreasing the esterification of cholesterol, inhibiting cholesterol acyltransferase and enhancing the utilization of activating cholesterol ester hydrolase.[166]

Rabbits dosed with levopromazine, 3 mg/kg/day for 3 months, developed endocardial fibrosis.[167] Halothane anesthetized dogs given very high doses of prochlor perazine did not demonstrate cardiohemodynamic collapse while the same model given 0.3-3 mg/kg, IV, developed prolonged ventricular repolarization that could become proarrhythmic.[168] In conscious guinea pigs prochlorperazine prolonged QTc.[169] Guinea pig cardiomyocytes exposed to prochlorperazine at concentrations of 0.5 and 1.0 μM demonstrated blockage of the rapidly activating delayed rectifier

K^+ current, but slowly activating delayed rectifier K^+ currents were not affected.[170] Prochlorperazine blocks K^+ currents and lengthens cardiac repolarization in a concentration-dependent manner.[171] Cyamemazine administered IV to anesthetized guinea pigs did not change QT or QTc but reduced HERG in HEK 293 cells. Human atrial myocytes treated with cyamemazine showed a reduction of native inward Na^+, Ca^{2+}, and K^+ currents.[172]

Butyrophenones

Droperidol

Anesthetized dogs dosed from 500 to 1,000 μg/kg, IV, demonstrated a dose-dependent blockade of α-adrenergic receptors but no effect on baroreceptor function. Experiments conducted using isolated arterial and venous preparations also demonstrated α-adrenergic block. Doses of droperidol injected directly into the sinus node artery resulted in SA nodal arrest followed by HIS bundle rhythm.[1]

Auricular preparations from guinea pigs; papillary muscle from dogs and cats; and Purkinje fiber preparations from dog, cow, and sheep demonstrate that at low concentrations droperidol decreases pacemaker activity and prolongs the effective refractory period. This effect is related to an inhibition of the depolarization process during late diastole. At high concentrations resting potential, action potential amplitude, dV/dt_{max} and conduction velocity are all reduced. There is no negative effect on Ca^{2+}-mediated action potentials. Most of the effects are attributable to droperidol-induced reduction in Na^+ conductance.[173]

In anesthetized cats, droperidol, 250 μg/kg, IV, blocked epinephrine-induced arrhythmias. Low doses of droperidol in pentobarbital-anesthetized cats caused a transient increase in the rate of chemoreceptor afferent activity while high doses caused a transient increase then a decrease. High doses reduced or abolished the normal increase in afferent activity associated with hypoxia. Many different preparations in both rats and rabbits have demonstrated α-adrenergic blocking actions.[1]

Rabbit Purkinje fiber experiments show that droperidol exerts a dual effect on repolarization, prolongation with low concentrations associated with the development of EADs, and subsequent triggered activity. At high concentrations these effects are depressed.[174] Work done at high concentrations using isolated mesenteric artery preparations from rabbits indicated dopamine-receptor and β-adrenergic receptor antagonist activity. Aortic and left atrial strip preparations provide some evidence that droperidol may also inhibit norepi uptake at adrenergic terminals.[1] Work done using isolated ventricular myocytes from guinea pigs indicates that droperidol decreases the time-dependent outward K^+ current elicited by short depolarizations and this result is concentration dependent.[175] Rat ventricular myocytes treated with 0.03-1.0 μM droperidol demonstrate concentration-dependent decreases in both peaks $[Ca^{2+}]_i$ and shortening along with inhibition of 35 mM KCl-induced increases in $[Ca^{2+}]_i$ but there is little direct effect on sarcoplasmic reticulum Ca^{2+} stores.

There is no effect on action potential duration but a rightward shift in the concentration-response curve to extracellular Ca^{2+} for shortening with no concomitant effect on peak $[Ca^{2+}]_i$. There is also a decreased pH_i and an increase in NO production.[176] Intact, awake pigs given droperidol, 0.1, 0.3, and 0.6 mg/kg, IM, showed decreased respiratory rates and body temperature but no significant changes in heart rate.[177]

Haloperidol

Anesthetized dogs demonstrate dose-dependent α-adrenergic blockade from haloperidol resulting in decreased aortic pressure. There is also an increase in conduction time and a decrease in conduction velocity in AV nodal tissue, HIS-Purkinje tissue, and ventricular myocardium.[1] Halothane-anesthetized dogs when given 0.3–3.0 mg/kg, IV, of haloperidol demonstrated dose-dependent decreases in heart rate, contractility, systemic vascular resistance, and blood pressure. There was also delayed intraventricular conduction, and prolongation of ventricular effective refractory period and repolarization phase.[178] Chloralose-anesthetized dogs dosed with 0.15, 0.5, 2.0, and 3.0 mg/kg, IV, haloperidol showed dose-dependent prolongation of QTc, effective refractory periods, and action potential duration at 90% repolarization.[179]

Cats were given 1 mg/kg/day of haloperidol orally for 23 days then anesthetized for the experiments. There was an apparent greater modulation of central α-1 than of α-2 adrenoceptors. The cats had increased aortic pressures, no change in heart rate, and an increased response to bilateral carotid occlusion. There were no changes in response to norepi, angiotensin II, or bradykinin.[180] Haloperidol prolonged the QT interval in cats.[181]

The effects of *N-n*-butyl haloperidol iodide were studied using myocardial ischemia/reperfusion injury (I/R) in a coronary ligation model in rats and the effects on L-type Ca^{2+} current were studied in rat ventricular myocytes. *N-n*-butyl haloperidol reduced the release of creatinine kinase, creatine kinase isoenzyme MB, lactate dehydrogenase, alpha-hydroxybutyrate dehydrogenase, and glutamic-oxaloacetic transaminase. It preserved the activity of superoxide dismutase and decreased the malondialdehyde content in a dose-dependent manner. All of these changes were associated with a reduction in the changes associated with I/R. The drug also decreased L-type Ca^{2+} currents and shifted the current voltage upward without affecting the voltage-dependent properties of these Ca^{2+} currents.[182]

In intact, awake rats haloperidol markedly reduced locomotor activity and significantly reduced cardiovascular responses to stress.[183] Rats dosed at 0.5, 1.0, 2.5, and 5.0 mg/kg/day, IP, for 9 weeks induced a dose-dependent vasoconstriction with decreased lumen diameters of the basilar arteries and a decrease in wall thickness.[184] Right ventricular myocytes from rats were used to demonstrate that haloperidol caused a decrease of amplitude and an acceleration of apparent inactivation of the transient outward K^+ current in a voltage-independent manner.[185] Work done on cultured cardiac myocytes from mice indicates that haloperidol prolongs the diastolic phase of the Ca^{2+} transient with a mid-diastolic re-elevation of $[Ca^{2+}]_i$. The re-elevation of $[Ca^{2+}]_i$ was shown to be provoked by Ca^{2+} release from sarcoplasmic reticulum. This can trigger delayed after-depolarization a major factor in arrhythmogenesis.[186]

Isolated rabbit heart preparations demonstrated dose-dependent negative inotropic effects of haloperidol.[187] Experiments using isolated rings of rabbit thoracic aorta showed that haloperidol is both a Ca^{2+}-channel blocking agent [160] and a 5-hydroxytryptamine (5-HT) receptor antagonist.[188] Rabbits treated with haloperidol, 0.20 mg/kg/day, for 3 months had necrotic lesions in the ventricular myocardium.[167]

Isolated coronary arteries from pigs were used to demonstrate the dopamine-blocking activity of haloperidol.[189] Experiments conducted in tissues from guinea pigs indicate that haloperidol prolongs the action potential, flattens the repolarization phase, and results in decreased myocardial contractility. It also decreases resting potentials, action potential amplitude, and maximum upstroke velocity of the action potential.[1] In conscious, free-moving guinea pigs haloperidol prolongs QTc.[169]

Azaperone

This agent is rarely used alone. It is usually combined with medetomidine or similar drugs for neurolept analgesia/anesthesia. Its effects in combination with other agents will be described later in this chapter. There are a few published reports of the cardiovascular effects of azaperone. Horses dosed at 0.4 and 0.08 mg/kg, IM, showed no change in arterial blood gases, or plasma protein concentration but venous blood hematocrit and hemoglobin decreased for 4 h.[190] In most horses, tested heart rate increased for up to an hour postinjection and aortic blood pressure decreased for at least 4 h with a slight increase in cardiac output. At 0.8 mg/kg, IM, aortic pressure decreased and there was a partial blockade of an epinephrine challenge. At 0.7 mg/kg, IM, there was a significant increase in heart rate and serum cortisol levels and a decrease in hematocrit.[1] The contractile response of isolated rabbit aortic rings to 5-hydroxytryptamine (5-HT) was antagonized by azaperone.[188] Intact, awake pigs were given 5 mg/kg, IM of azaperone. Fifteen minutes later there was a decrease in aortic pressure and cardiac output, an increase in systemic vascular resistance, increased pulmonary arterial blood flow, and decreases in left ventricular myocardial blood flow and vascular conductance of the skin.[1] In thiopentone-anesthetized pigs, azaperone injected IM resulted in α-adrenergic blockade and a mild β-adrenergic blockade.[191] Isolated coronary artery preparations were used to demonstrate that azaperone blocked the vasodilation effects of dopamine.[189]

Other Antipsychotic/Anxiolytic/Antidepressant (Tranquilizer) Drugs

The older generations of tricyclic and butyrophenone tranquilizers inhibit cardiovascular Na^+, Ca^{2+}, and K^+ channels and thus can lead to significant and dangerous cardiac arrhythmias. The selective serotonin reuptake inhibitors (SSRIs) have become more popular because early studies seemed to indicate fewer and more benign cardiovascular and other side effects. More recent case reports indicate that

the SSRIs and other new antipsychotics including clozapine, olanzapine, risperidone, sertindole, aripiprazole, zisprasidone, and quetiapine are increasingly being associated with arrhythmias, prolonged QTc intervals, and orthostatic hypotension even in patients free of preexisting cardiovascular disease.[192,192—194]

Tricyclic Antidepressants

This class of drugs has been associated with tachycardia, bradycardia, cardiac palpitation, changes in PR, QRS, and QTc intervals and even heart failure in human patients. These adverse effects are significantly potentiated by concurrent treatment with antihistamines.[195] These complications are associated with the ability of these agents to bind to cardiac calsequestrin, the same cardiotoxicity mechanism attributed to the phenothiazine derivatives and the anthracycline derivatives.[155] Imipramine, desipramine, trimipramine, clomipramine, lofepramine, amitriptyline, nortriptyline, protriptyline, dothiepin hydrochloride, and doxepin are examples of this class of drugs. Imipramine, amitriptyline, and doxepin were tested in isolated, spontaneously beating Purkinje fiber preparations from guinea pig hearts. EADs were induced by imipramine at doses of 2 and 5 μM, and doxepin at 5 μM but amitriptyline did not induce EADs at either concentration.[159] Inhibition of G protein-activated, inward rectifying K^+ channels (GIRK or Kir3 channels) may contribute to some therapeutic effects of the tricyclic agents but also are associated with adverse effects such as seizures and atrial arrhythmias.[196] Using isolated cardiac myocardium and vascular smooth muscle preparations, Pacher and Kecskemeti [194] found that at concentrations of 0.5–50 μM fluoxetine and citalopram depress Ca^{2+} - and Na^+-dependent electrophysiological parameters as well as cardiac Ca^{2+} currents. At concentrations of 0.1–10 M fluoxetine and citalopram relax both vascular and intestinal smooth muscle.

Selective Serotonin Uptake Inhibitors

This class of drugs includes citalopram, escitalopram oxalate, fluoxetine, fluvoxamine maleate, paroxetine, sertraline, venlafaxin, and dapoxetine. Fluoxetine was found to abbreviate action potential duration rather than lengthening it as has been observed in drugs associated with QT prolongation and potentially fatal arrhythmias.[197] Paroxetine has been associated with digitalis intoxication in a patient treated with both agents.[198] Citalopram and fluoxetine administered IV to achieve a range of clinically relevant plasma concentrations in anesthetized guinea pigs significantly decreased heart rate and/or blood pressure and increased electrical alternans in the high dose range. Venlafaxin increased blood pressure at low dosage levels but did not result in increased electrical alternans even at the highest doses.[199] Isbister et al.[200] studied the effects of overdosing on QTc intervals in patients and

found a rank order of effects for fluoxetine, fluvoxamine, paroxetine, sertraline, and citalopram. Despite serotonin syndrome being a common problem, the conclusion was that these SSRIs were relatively safe when overdosed, except for citalopram that caused significantly prolonged QTc intervals. A retrospective study found no reductions in QTc in patients treated with sertraline, citalopram, paroxetine, or bupropion.[201] Both prospective and retrospective analyses on the effects of citalopram on ECG findings reported a small reduction in heart rate with no significant effects on PQ, QRS, or QTc intervals.[202] However, other work using tissue cultures of rat cardiomyocytes found that citalopram and amitriptyline (a tricyclic) demonstrated the same potency of concentration-dependent inhibition of the L-type Ca^{2+}-channel current.[203] Isolated guinea pig ventricular myocytes were used to demonstrate that citalopram inhibited L-type Ca^{2+} currents. Transfected mammalian cell studies indicate that HERG is blocked with an IC(50) of 3.97 μM.[204] Citalopram altered the cardiac action potential configuration in guinea pig ventricular muscle probably because of an inhibition of cardiac Ca^{2+} and Na^{+} channels.[205] Using an endothelial cell preparation, four different SSRIs were found to induce a fast and reversible block of the volume-sensitive Cl^{-} current.[206]

Spontaneously beating isolated guinea-pig atrial preparations were used to study the inhibition of Na^{+} membrane conductance caused by citalopram. This effect was cited as the probable explanation for a decrease in ouabain-induced arrhythmias.[207,208] Citalopram was shown to be a negative inotropic and chronotropic agent in isolated guinea-pig atrial preparations due to either its ability to block adenosine uptake or its ability to act as an α-1 adenosine receptor antagonist.[207] The immediate-release formulation of venlafaxin caused severe agitation, diarrhea, increased liver enzymes, hypertension, and Hyponatremia while mirtazapine treatment increased liver enzymes, cutaneous edema, and collapse but no hyponatremia.[209] Isolated rat pulmonary and systemic artery preparations from hypoxic and normoxic rats were exposed to citalopram. The drug acted as a 5-HT transporter (SERT) uptake inhibitor.[210] Citalopram and fluoxetine (10 mg/kg/day) prevented hypoxia-induced pulmonary vascular remodeling in mice.[211] Citalopram produced statistically significant age-related changes in bradycardia with greater prevalence in patients >65 years of age.[212]

Paclt et al.[213] compared the effects of dosulepine, a tricyclic antidepressent (50–250 mg/day), citalopram, a SSRI (20-80 mg/day), and lithium (plasma levels of 0.66 ± 0.08 mEq/l) on body surface potential maps generated from electrocardiographic data. Their results indicated a relationship between the dose of dosulepine and the extremes of the isoarea map not seen with citalopram. The repolarization body surface potential map changes were more pronounced in the patients dosed with citalopram while lithium produced only minimal changes in the body surface potential maps. Amitriptyline, dosulepin, citalopram, and lithium effects on the electrocardiogram, vector cardiogram, and body surface maps of patients without cardiovascular disease indicated that the tricyclic agents had increased heart rates with decreased QT and RR intervals. These changes were not recorded in the citalopram- or lithium-treated patients. All of the tested agents decreased the absolute maximum values of depolarization isointegral maps, while lithium and the tricyclic agents reduced the initial and citalopram the later phase of depolarization.

Citalopram slightly diminished the amplitude of the R wave.[214] Fluoxetine did not prolong the action potential duration in cardiac Purkinje fiber preparations from dogs or pigs.[197]

Atypical Antipsychotics

Sertindole

This is one of the newer antipsychotic drugs available. It has activity at dopamine (D2), serotonin (5-HT2), and α-1-adrenergic receptors in the brain and is classified chemically as a phenylindole derivative. In canine and porcine Purkinje fiber preparations, sertindole caused a concentration-dependent prolongation of the action potential duration.[197] Action potential duration at 90% repolarization was significantly prolonged by sertindole in rabbit Purkinje fiber preparations.[215] In Langendorff-perfused isolated rabbit hearts, sertindole exposure resulted in QT prolongation but did not display the proarrhythmic profile typical of other inhibitors of the rapid component of the delayed rectifier K^+ current.[216] In isolated perfused cat, hearts prolongation of the QT interval by sertindole was less than that caused by haloperidol or risperidone.[181]

Pimozide

This drug is a diphenylbutylpiperidine derivative. Its mechanism of action is probably related to its ability to block central dopaminergic receptors but it also has an effect on norepinephrine turnover rates at high doses. Isolated guinea-pig hearts exposed to 100 nmol/l demonstrated reverse rate-dependent prolongation of cardiac repolarization with increases in action potential duration during pacing at 150 or 250 ms cycle lengths. In isolated ventricular myocytes from guinea pigs, pimozide demonstrated a concentration-dependent block of the rapid component of the delayed rectifier K^+ current.[217] Conscious free-moving guinea pigs exposed to pimozide demonstrated prolonged QTc.[169] Pimozide did not demonstrate Ca^{2+}-channel blocking activity in isolated rings of rabbit thoracic aorta.[160]

Clozapine

Clozapine binds to D1, D2, D3, and D5 (dopamine) receptors and has a high affinity for the D4 receptor without inducing catalepsy or inhibiting apomorphine-induced stereotypy in a variety of animal models. It appears to act preferentially at limbic rather than at striatal dopamine receptors. It is also a strong competitive antagonist for various subtypes of adrenergic, cholinergic, histaminergic, and serotonergic

receptors. It prolongs the QT interval in isolated cat hearts.[181] Guinea-pig ventricular myocytes treated with 1 and 5 μM clozapine demonstrated blockade of the rapidly activating delayed rectifier K^+ current but no change in the slowly activating delayed rectifier K^+ currents.[218] Intact, awake rats pretreated with clozapine showed a dose-dependent inhibition of the pressor response, increased heart rates, and increased contractility associated with open field novelty stress.[183]

Risperidone

Risperidone is a very strong dopamine antagonist that also acts as a 5-HT2A antagonist. It is frequently classified as a balanced serotonin/dopamine antagonist. It significantly prolongs the QT interval in isolated Langendorff-perfused cat hearts in a dose-dependent manner.[181] Similar to clozapine risperidone inhibits increases in blood pressure, heart rate, and dP/dt responses induced by environmental stress in rats.[183] Gluais et al. tested risperidone using rabbit Purkinje fibers, ventricular myocardium, and atrial and ventricular myocytes. They found risperidone (0.1–3.0 μM) exerted potent lengthening effects on action potential duration and resulted in the development of EADs at low stimulation rates. At doses of 0.03–0.3 μM, risperidone significantly reduced the current density of the delayed rectifier current, and at 30 μM, it decreased the transient outward and the inward rectifier currents.[219] Prolonged cardiac repolarization with increased action potential duration was observed in isolated guinea-pig hearts paced at 250 ms cycle length exposed to 1.0 μM risperidone. In human ether-a-go-go (HERG)-transfected Chinese hamster ovary cells, risperidone caused concentration-dependent blockade of the rapid component of the delayed rectifier K^+ current.[220] Experiments conducted on isolated canine ventricular myocytes and guinea-pig papillary muscles demonstrated a concentration-dependent lengthening of action potential durations. The effect was reversible and most prominent on the terminal portion of repolarization. In voltage-clamped canine ventricular myocytes, risperidone caused a concentration-dependent block of the rapid component of the delayed rectifier K^+ current not associated with changes in activation or deactivation kinetics. At 10 μM concentrations, risperidone also inhibited the slow component of the delayed rectifier K^+ current.[221] Rabbits dosed at 1.0 mg/kg every 15 days for 3 months with risperidone did not demonstrate ventricular necrosis or endocardial fibrosis.[167]

Amisulpride

This is another antipsychotic drug with a high affinity for D2 and D3 dopaminergic receptors. Rabbits dosed with 15 mg/kg/day for 3 months demonstrated necrotic lesions in the myocardium.[167]

Minaprine

This is another psychotropic drug with dopaminomimetic activity. When administered in vivo in mice, this drug antagonizes the effects of reserpine, blocks the effects of 5-HTP, and activates central dopaminergic transmission but is devoid of adrenergic and anticholinergic effects.[222]

Atypical Antipsychotics

Aripiprazole

Halothane-anesthetized dogs were infused with aripiprazole using escalating doses of 0.03, 0.3, and 3.0 mg/kg each infused over 10 min with 20 min between each dose. There was a dose-dependent increase in heart rate, contractility, and dromotropic effects along with shortening of the ventricular effective refractory period and repolarization phase and a decrease in total peripheral resistance.[178]

Fezolamine

When tested using mouse Purkinje tissue, this agent had less ability to depress myocardial conduction than similar concentrations of standard tricyclic antidepressants. In a cat coronary ligation model much higher doses of fezolamine were needed to induce cardiac depression than were necessary with the tricyclics tested. The drug had no apparent effect on heart rate.[223]

Olanzapine

New Zealand white rabbits dosed with olanzapine (0.3 mg/kg/day for 3 months) demonstrated cardiac hypertrophy.[167]

Lortalamine

In anesthetized dogs, lortalamine antagonizes reserpine-induced ptosis and hypothermia in a dose-dependent manner. It potentiates yohimbine toxicity in mice and in the anesthetized dog. In the anesthetized dog, it diminishes the tyramine pressure response and increases the epinephrine response. However, the effects on cardiac conduction are less than that of imipramine, a tricyclic.[224]

Xylazine

Xylazine is pharmacologically classified as an analgesic, sedative, and skeletal muscle relaxant. It is widely used in large animal species because of its superior effects as a sedative with minimal ataxia. It is a mixed α-adrenergic receptor agonist with an α1–α2 selectivity ratio near unity. It has CNS effects that effectively reduce norepi release. Following IM or IV injection, it causes an initial hypertension followed by a prolonged hypotension; the later most likely associated with its central α2-adrenergic receptor actions. It may potentiate second-degree heart block in horses. It can cause decreases in preload, afterload, and heart rate with no change in contractility due to its effects on the autonomic nervous system. Dogs treated with 1.1 mg/kg, IM, xylazine were more sensitive to epinephrine-induced serious ventricular arrhythmias, including ventricular fibrillation. At the same dose intact, awake, dogs had no change in pulse pressure, stroke volume, or arterial blood gases but a decrease in heart rate and cardiac output and an increase in peripheral resistance.[1] The effects of 2.0 mg/kg, IM, xylazine were studied in intact, awake, dogs. Both systolic and diastolic arterial pressure increased immediately, stayed up for 5–10 min, and then decreased below baseline and did not normalize until 90 min for systolic and 50 min for diastolic.[225]

Left ventricular function was monitored in cats using echocardiography. Xylazine depressed both stroke volume and cardiac output.[226] Goats were given 0.05 mg/kg xylazine as a subarachnoid injection. There was a significant decrease in both heart rate and respiratory rate but no change in blood pressure.[227] Xylazine increased smooth muscle tone of small diameter canine extramural coronary arteries predominantly mediated by its α2-adrenergic receptor agonist action.[228]

Drugs in Combination Providing Neurolept Analgesia/Anesthesia

In recent years, it has become popular to use drugs in combination to provide so-called balanced analgesia/anesthesia. A wide variety of agents are used in a wide variety of dose combinations.

Metomidate + Azaperone

Metomidate (6 mg/kg, IV) and azaperone (5 mg/kg, IM) were studied in conscious pigs. The combination resulted in decreased systemic arterial pressures, an increase in systemic vascular conductance, and a decrease in cardiac output. There was also an increase in arteriovenous shunt blood flow at the expense of nutritional blood

flow. Blood flow to the brain was maintained constant but left ventricular blood flow decreased while vascular conductance to most other organs, except the skin, increased or was maintained constant.[229] Another study in intact, awake, pigs also demonstrated decreases in blood pressure, heart rate, and cardiac index but blood gas and pH measurements detected no significant impairment of pulmonary function.[230] When metomidate and azaperone were given as a continuous IV infusion preceded by atropine pretreatment and followed by halothane + methoxyflurane to Gottingen mini-pigs, there was a mild respiratory acidosis and a gradual increase in blood pressure and heart rate.[163]

Medetomidine + Butorphanol

Medetomidine (20 μg/kg) and butorphanol (0.2 mg/kg) were administered to healthy mixed-breed dogs. Systolic, diastolic, and mean arterial pressures increased as did mean pulmonary arterial pressures, pulmonary capillary wedge pressures, central venous pressures, systemic vascular resistance, pulmonary vascular resistance, and $PaCO_2$. Heart rate, cardiac output, cardiac index, stroke volume, stroke index, respiratory rate, arterial pH, and PaO_2 all decreased. These effects were all statistically equal to the effects of medetomidine alone.[131]

Medetomidine + Butorphanol + Midazolam

Medetomidine was administered to clinically normal dogs. When the effects of the medetomidine were maximal, 20 min postinjection, the dogs were dosed with butorphanol and midazolam. The combination induced respiratory depression, comparable in magnitude to that induced by a combination of acepromazine + butorphanol + thiopental + halothane. There was a significant decrease in respiratory rate, arterial and venous pH, venous oxygen content, oxygen consumption, and oxygen delivery. End-tidal pCO_2, arterial and venous pCO_2, and O_2 extraction increased significantly.[231]

Medetomidine + Buprenorphine + Ketamine

New Zealand White rabbits received an IM injection of medetomidine (0.5 mg/kg), buprenorphine (0.03 mg/kg), and ketamine (35 mg/kg). The animals were intubated and given 0.75% isoflurane in O_2 (1.0 l/min). Systolic, mean, and diastolic arterial pressures were higher with this treatment than in the same rabbits given a combination of ketamine (35 mg/kg) + xylazine (5 mg/kg) and buprenorphine (0.03 mg/kg), IM.[232]

Medetomidine + Midazolam

Medetomidine (20 μg/kg) + midazolam (0.3 mg/kg), IM, administered to dogs resulted in bradycardia, hypertension, decreased cardiac output, and vasoconstriction. These changes were sustained after the induction of anesthesia with thiopental and propofol.[233,234]

Medetomidine + Hydromorphone

Dogs were given medetomidine (20 μg/kg) + hydromorphone (0.1 mg/kg), IV. The result was both systemic and pulmonary hypertension with increases in systemic and pulmonary vascular resistance and decreases in heart rate, cardiac output, stroke volume, and respiratory rate.[131]

Dexmedetomidine + Butorphanol

Healthy cats were given dexmedetomidine (10 μg/kg) + butorphanol (0.2 mg/kg), IM. Heart rate decreased significantly as did systolic and diastolic arterial pressures. After 50 min, mean blood pressure was still depressed in these cats.[134]

Medetomidine + Ketamine

Ponies were dosed with medetomidine (7.0 μg/kg), IV, followed by 2 mg/kg ketamine, IV, 10 min later. The animals were then anesthetized and maintained in a surgical plane of anesthesia for 4 h using 3.5 μg/kg/h medetomidine and propofol (0.2 mg/kg/h), IV. Cardiovascular function was stable with no changes in respiratory rate, PaO_2, $PaCO_2$, heart rate, mean arterial pressures, cardiac index, or mean pulmonary arterial pressures.[235] However, a study in Thoroughbred horses found that the combination of medetomidine (0.005 mg/kg), IV, ketamine (2.5 mg/kg) + midazolam 0.04 mg/kg), IV, followed by a loading dose of propofol (0.5 mg/kg, IV) and a constant infusion of propofol (0.22 mg/kg/min) or a constant infusion of propofol (0.14 mg/kg/min) + ketamine (1 mg/kg/h) + medetomidine (0.00125 mg/kg/h) resulted in lower heart rates, and cardiac index in the horses anesthetized with the propofol, ketamine, medetomidine combination.[21] Chinchillas treated with medetomidine (0.06 mg/kg) + ketamine (5.0 mg/kg), IM, had decreased respiratory and heart rates.[236]

Medetomidine + Ketamine + Midazolam

The combination of medetomidine (0.05 mg/ml), midazolam (0.8 mg/ml), and ketamine (40 mg/ml) was infused IV at 0.025 ml/kg/h in healthy horses anesthetized with sevoflurane in oxygen. Cardiac output and cardiac index were maintained between 65 and 80% of baseline depending upon the horses being in left lateral or dorsal recumbency. Systemic vascular resistance was not altered by the drug combination or position of the animal.[237]

Dexmedetomidine + Ketamine

Systolic and diastolic blood pressures and heart rates decreased significantly in cats treated with dexmedetomidine (10 μg/kg) + ketamine (5.0 mg/kg), IV.[134]

Ketamine in Combination with Tranquilizers

Because of the CNS stimulation and the blockage of catecholamine uptake associated with ketamine, a variety of combinations with various tranquilizers have been used. One of the advantages is that some combinations can be mixed in the same syringe and given as one intramuscular or intraperitoneal injection. However, some combinations can result in chemical interactions resulting in the formation of a precipitate, sludge, or other, less obvious but chemically neutralizing reaction. In laboratory animals, the most common is the combination of ketamine and xylazine.

Ketamine + Acepromazine

Intact, awake, previously instrumented dogs were given 10 mg/kg ketamine + 0.2 mg/kg acepromazine, IV. Heart rate, effective alveolar volume, alveolar-arterial pO_2 gradient, arterial pCO_2, and venous pCO_2 increased while stroke volume, minute ventilation, physiological dead space, and arterial and venous pO_2 decreased.[1] The same combination in mice produced decreases in heart rate and fractional shortening.[3] When xylazine was also included in the mixture given to mice, there was a profound effect on electrophysiological parameters derived from both transesophageal and intracardiac pacing regimens. These workers determined that variations in electrophysiological studies can result from differences in anesthesia, body temperature or the strain or age of the mice used.[238] Cats anesthetized with 13 mg/

kg ketamine and 0.13 mg/kg acepromazine, IV, had decreased aortic pressures, respiratory rate, and arterial pH and pO_2 and a transient increase in heart rate and increased arterial pCO_2. Cats given ketamine (33.6 mg/kg) + acepromazine (1.12 mg/kg), IM, showed similar responses to doses of 20 mg/kg ketamine and 0.5 mg/kg acepromazine, IV, while doses of 11 mg/kg ketamine and 0.11 mg/kg acepromazine, IV, resulted in no significant changes in heart rate or blood pressure.[1]

Ketamine + Xylazine

Intact, awake, previously instrumented dogs given ketamine (10 mg/kg) + xylazine (1.0 mg/kg), IV, developed increases in heart rate, mean aortic pressure, systemic resistance, and tidal volumes and decreases in central venous pressure, stroke volume, left ventricular stroke work, respiratory rate, and minute volume but no change in mean pulmonary arterial pressure or left ventricular work. Similar results were seen in dogs pretreated with atropine and dosed at 11.0 mg/kg ketamine and 1.0 mg/kg xylazine, IV. These dogs also had a significant decrease in LV d*P*/d*t*. The same doses given together IM, or when ketamine was administered 5 min after the IM xylazine and given IV consistently produce both systemic and pulmonary hypotension along with decreased cardiac index and arterial pO_2.[1]

Awake cats when given ketamine (21 mg/kg) + xylazine (2.1 mg/kg), IM, in the same syringe showed hypotension and a decrease in heart rate, respiratory rate, arterial pH and pO_2 and an increase in arterial pCO_2. Two of the ten cats thus treated vomited. When cats were given xylazine (0.3 mg/kg) IM and then 10 min later ketamine (28.7 mg/kg), IM, seven of the ten cats vomited, and aortic pressure decreased prior to the ketamine administration. Heart rate, respiratory rate, and arterial pH all decreased along with arterial pO_2.[1] When the same combination was studied in cats subjected to removal of 25% of their blood volume, there was no significant change in cardiac output, cardiac index, stroke volume, or heart rate, but significant decreases in arterial blood pressures and respiratory rates with arterial pCO_2 increases.[239]

The effects of ketamine (50 mg/kg) and xylazine (5 mg/kg), IP, were studied in male Wistar rats following coronary artery ligation. Heart rate decreased but there was no change in mean arterial pressure, arterial pCO_2, pO_2, pH, or rectal body temperature.[240] Adult male Fischer rats anesthetized with 37 mg/kg ketamine and 7 mg/kg xylazine, IP, had significantly lower cardiac outputs compared to rats lightly anesthetized with pentobarbital. These rats also had significantly lower LV ejection fractions, fractional shortening, fractional area change, and velocity of circumferential fiber shortening corrected for heart rate.[16] Male Sprague–Dawley rats were given two different doses of ketamine (50 and 75 mg/kg) mixed with 5 mg/kg xylazine. There was a decrease in heart rate, cardiac index, and arterial blood pressure.[241] At larger doses ketamine (167 mg/kg) and xylazine (33 mg/kg), Sub-Q, there was a reduction in heart rate, an increase in arterial pO_2, a decrease in arterial pH, in male Wistar rats. There was also a reduction in the constrictive effect of norepi and the dilator effect of bradykinin on isolated mesenteric arteries from rats but no

effect on the vasodilator effects of acetylcholine.[242] Changes in the cardiorespiratory and cerebral oscillator parameters and couplings were studied in rats given a single bolus of ketamine + xylazine. It was determined that respiration drives the cardiac oscillator during deep anesthesia but as the animal awakes during shallow anesthesia the cardiorespiratory interaction becomes insignificant.[243]

Cine MRI was used to determine the effects of ketamine + xylazine anesthesia in mice. There was a significant reduction in heart rate, cardiac output, and wall thickness but an increase in stroke volume and end-diastolic volume. There was no change in ejection fraction or systolic wall thickening.[244] Electrocardiogram- and respiration-gated spin labeling MRI was used to measure myocardial blood flow maps in C57/B16J mice. With ketamine + xylazine anesthesia, the mean blood flow value in the left ventricular myocardium was 6.0 ± 1.9 ml/g/min, not significantly different than the same measurements made under isoflurane anesthesia at 1.25 vol% concentrations. When the isoflurane concentration was increased to 2.0 vol%, myocardial blood flow increased dramatically (16.9 ± 1.8 ml/g/min) with no significant change in heart rate.[245] Ketamine (80 mg/kg) + xylazine (5 mg/kg) was given IP in mice for anesthesia during surgical placement of a high-fidelity left ventricular catheter. There was a significant decrease in heart rate, left ventricular systolic pressure, and dP/dt_{max} that persisted for 3 days following the surgery.[44] When ketamine (100 mg/kg) and xylazine (5 mg/kg) were given IP to mice monitored with echocardiography, cardiac depression was evidenced by a significant decrease in heart rate, percentage of fractional shortening, and increased end-diastolic diameters.[3,8] Diastolic left ventricular function, as determined by tissue Doppler imaging and transthoracic echocardiography, was significantly decreased with ketamine + xylazine anesthesia.[246]

New Zealand White rabbits were examined using tissue Doppler imaging and Doppler-echocardiography. Ketamine + xylazine anesthesia produced significant decreases in fractional shortening, cardiac output, and systolic velocity of the left ventricular free wall as well as a decrease in global left ventricular function.[247] Ketamine (14.6 mg/kg/h) + xylazine (3.7 mg/kg/h), IV, produced a decrease in mean arterial pressure, and heart rate in guinea pigs.[4] Ketamine (40 mg/kg) + xylazine (2.0 mg/kg), IM, decreased respiratory and heart rates in chinchillas.[236]

Anesthesia was induced with ketamine (2.0 mg/kg) + xylazine (1.0 mg/kg), IV, and maintained with ketamine (0.1 mg/kg/min) + xylazine (0.05 mg/kg/min), IV, in horses. There was a significant decrease in cardiac index and left ventricular stroke work and a higher oxygen utilization ratio at 5 and 15 min following induction. Heart rate, arterial pO_2, and arterial blood pressures were decreased from baseline values, while arterial pCO_2 and systemic vascular resistance increased.[248] When intact, awake horses were treated with xylazine (1.1 mg/kg), IV, then after 3 min given ketamine (2.7 mg/kg, IV) there was some degree of second degree A-V heart block in all animals within 22 s after xylazine. During the following 3 min, heart rate decreased. Within 12 s following the administration of ketamine, there was a more severe second degree A-V block with premature ventricular contractions, the later abolished by atropine (0.02 mg/kg), IV. In other studies using horses with the same dose of xylazine but a slightly lower dose of ketamine (2.2 mg/kg, IV),

there was no apparent change in mean aortic pressure, respiratory rate, heart rate, arterial pO_2, pCO_2, cardiac output, pulmonary arterial pressures, central venous pressures, or pulmonary arterial wedge pressures.[1]

Pigs given ketamine (10 mg/kg) + xylazine (1.0 mg/kg), IV, showed no change in mean aortic pressure, pulmonary arterial pressure, arterial pH, pCO_2, plasma glucose, or plasma lactate but cardiac output and arterial pO_2 decreased while systemic vascular resistance increased.[1] Cattle given xylazine (0.2 mg/kg), IM, then ketamine (5 mg/kg), IV, or (10 mg/kg), IM, had decreased respiratory and heart rates after xylazine but both increased toward baseline following ketamine. When cattle were dosed with xylazine (0.088 mg/kg) and ketamine (4.4 mg/kg), IM, there was no change in heart rate, central venous pressure, mean pulmonary arterial pressure, or cardiac output. Mean aortic pressure decreased after 15 min, respiratory rate increased and arterial pO_2 decreased. When Macaca mulatta (rhesus monkeys) were dosed with xylazine (0.6 mg/kg) and ketamine (7 mg/kg), IM, there was a decrease in aortic pressure and heart rate within 30 min along with a decrease in venous pO_2. There were no changes in respiratory rate, arterial pO_2, pCO_2, or pH.[1]

Ketamine + Xylazine + Guaifenesin

Dogs were treated with ketamine (1 mg/ml), xylazine (0.25 mg/ml), and guaifenesin (50 mg/ml) infused at a rate of 2.2 ml/kg/h, IV. There was no change in heart rate, systemic vascular resistance, mean aortic pressure, the rate-pressure product, or arterial pO_2 but a decrease in cardiac index.[1] Previously instrumented awake horses were given ketamine (2 mg/kg), xylazine (0.3 mg/kg), and guaifenesin (100 mg/kg), IV, for induction prior to halothane anesthesia. They showed no changes in aortic pressures, blood gases, or arterial pH but significant ataxia.[1] Awake, previously instrumented calves were infused with ketamine (1 mg/ml), xylazine (0.1 mg/ml), and guaifenesin (50 mg/ml) at a rate of 1.1 ml/kg/h, IV. Heart rate, cardiac output, and cardiac index increased while systemic and pulmonary vascular resistance and mean aortic pressure decreased. Left ventricular stroke work index and arterial pO_2 did not change.[249]

Ketamine + Xylazine + Buprenorphine

Rabbits received ketamine (35 mg/kg), xylazine (5 mg/kg), and buprenorphine (0.03 mg/kg), IM. Blood pressures decreased and heart rates increased.[232]

Ketamine + Diazepam

Twelve adult male Walker Hounds were treated with a combination of ketamine and diazepam. There was inadequate sedation in some dogs and excitement in others. GFR was lowered slightly with a significant increase in aortic blood pressures and

heart rate.[250] Ketamine (50 mg/kg) and diazepam (2.5 mg/kg) were given IP to male Wistar rats and cardiovascular and respiratory function was assessed following coronary artery ligation. The combination resulted in nonsignificant changes in respiratory function, heart rate, arterial pressures, or blood gases.[240]

Midazolam + Butorphanol

The combination of midazolam (0.1 mg/kg) and butorphanol (0.2 mg/kg), IM, in dogs produced decreases in arterial blood pressure and cardiac output. The effects were less than those resulting from treatment with combinations of medetomidine and midazolam or acepromazine and butorphanol.[233,234] Cats treated with midazolam (0.1 mg/kg) and butorphanol (0.4 mg/kg), IV, showed significant decreases in heart rate, mean arterial pressure, and respiratory rate.[251]

Midazolam + Fentanyl + Fluanisone

Langendorff-perfused mouse hearts were subjected to 45 min of global ischemia followed by 60 min of reperfusion. Treatment with this combination of agents did not exert significant protective effects on the ischemia-reperfusion injury.[47] Rabbits were tranquilized by the intramuscular injection of fentanyl/fluanisone (0.2 ml/kg) containing 10 mg/ml fentanyl and 0.2 mg/ml fluanisone. This was followed by an IP injection of midazolam (4 mg/kg) and an additional IM injection of the fentanyl/fluanisone agent (0.1 ml/kg). Minimal changes were observed in the cardiovascular and respiratory parameters monitored and the left ventricle was well perfused.[252]

Midazolam + Methadone + Propofol + Isoflurane + Continuous Infusion of Propofol and Fentanyl

This combination was used for anesthesia in sheep subjected to surgery involving cardiopulmonary bypass. Doses were midazolam (0.1 mg/kg), methadone (0.1 mg/kg), propofol (2–4 mg/kg), isoflurane to effect, propofol (5–7 mg/kg/h), fentanyl (5 μg/kg), and bolus plus (5 μg/kg/h). Electrocardiographic abnormalities were observed during manipulation of the heart in all animals. During the initial phases of the bypass blood, pressure decreased in all animals.[253]

Acepromazine + Meperidine

Healthy cats were injected IM with a combination of acepromazine, meperidine, and atropine. There was a minor degree of respiratory depression and a decrease in cardiac index and stroke volume but no significant changes in heart rate, systemic vascular resistance, or blood pressure.[254]

Fentanyl + Droperidol (Innovar-Vet®)

Intact, awake dogs were given 0.05 ml/kg of the commercial preparation. There was an apparent decrease in heart rate and aortic pressure but no change in cardiac output, stoke volume, or systemic resistance. When given 0.088 ml/kg, there was no change in aortic pressure or arterial pCO_2 but a decrease in pH. The dose of ouabain required to cause ventricular tachycardia was increased. A dose of 0.005 ml/kg resulted in decreased heart rate, mean aortic pressure, LV d*P*/d*t*, and arterial pO_2. There was no change in arterial pH but pCO_2 increased in dogs. When the drugs were dosed at 2 mg/kg droperidol and 40 μg/kg fentanyl, no change was observed in the basic ECG intervals or refractoriness.[1]

Rabbits were treated with 0.2 ml/kg of the standard commercial mixture. Heart rate, mean aortic pressure, LV d*P*/d*t*, and respiratory rate decreased. There was no change in arterial pO_2. When rabbits were dosed with 0.5 ml/kg, there was a greater decrease in heart rate, respiratory rate, and contractility but no change in aortic pressure.

Azaperone + Metomidate

Pigs were dosed with azaperone (2 mg/kg, IM) and metomidate (4 mg/kg, IV) plus 8–10 mg/kg/h metomidate as an IV infusion. There was an initial decrease in heart rate and then a return to baseline. Aortic pressure decreased along with cardiac output and contractility. The peak responses occurred about 10 min following the initial injections. When both the azaperone and metomidate were given IV to pigs, there was a greater increase in mean aortic pressure and the decrease persisted. Heart rate, cardiac index, and stroke index decreased then gradually returned toward baseline.[1]

Acepromazine + Etorphine

Intact, awake horses were dosed with acepromazine (100 μg/kg) and etorphine (24 μg/kg), IV. Heart rate increased, aortic pressure increased then returned to baseline, as did systemic vascular resistance, cardiac output, and stroke volume. When acepromazine was administered (0.1 mg/kg) with etorphine (22 μg/kg), IM, the blood pressure increased less than with the same dose of etorphine alone.[1]

Fentanyl + Morphine

Epidural administration of fentanyl (10 μg/kg) and morphine (0.1 mg/kg) in dogs anesthetized with sevoflurane induced significant decreases in diastolic and mean aortic pressures and total peripheral resistance. Stroke volume did not change, but arterial pCO_2 was increased and arterial pH and pO_2 were decreased along with the heart rate.[61]

Fentanyl + Propofol

The response of the cremaster muscle microcirculation of male Wistar rats to a combination of fentanyl and propofol was dilation of small arterioles.[15] Injured cats were preanesthetized with intravenous midazolam (1 mg/kg), butorphanol (0.4 mg/kg), and ketamine (2 mg/kg), then anesthetized and maintained in a surgical plane of anesthesia with propofol (12 mg/kg/h) + fentanyl (0.02 mg/kg/h). The cats required positive pressure ventilation to maintain end-tidal CO_2 levels below 50 mmHg. The regimen resulted in a mild hypotension.[255]

Xylazine + Morphine

Horses given xylazine (0.66 mg/kg) and morphine (0.12 mg/kg), IV, had decreased heart rates, cardiac output, and respiratory rates; increased central venous pressure; and transient increases in mean aortic and pulmonary arterial pressures. When given the same dose of xylazine and a higher dose of morphine (0.66 mg/kg), there was no change in heart rate but all other parameters were the same as for the lower morphine dosage.[1]

Oxymorphone + Bupivacaine

Halothane-anesthetized dogs were given a combination of oxymorphone and bupivacaine as an epidural injection. Heart rate decreased but central venous pressure and systemic vascular resistance increased.[85]

Tiletamine + Zolazepam (Telazol®, Zoletil®)

Dogs were given three different doses of Telazol (6.6, 13.2, and 19.8 mg/kg, IV) at different times and with residual isoflurane anesthesia following instrumentation and again when fully conscious. Heart rate was increased with all three doses and there was a significant increase in cardiac output with the two larger doses. All doses resulted in a significant transient decrease in arterial blood pressures and LV dP/dt with a return to baseline followed by an increase above baseline. Peripheral vascular resistance increased transiently at the low dose but decreased significantly with the two higher doses. Minute ventilation was decreased only by the 19.8 mg/kg dose.[256] Conscious horses were treated with 0.5 and 1.0 mg/kg Telazol administered as an epidural injection. There were no significant changes in heart rate, respiratory rate, and arterial blood pressures resulting from the treatment.[257] Previously instrumented intact, awake goats treated with either 12 or 24 mg/kg, IV, of the combination had no

changes in heart rate, mean aortic pressures, pulmonary arterial pressures, pulmonary wedge pressures, or pulmonary resistance but there was a decrease in cardiac output and an increase in systemic vascular resistance.[1] Rats given 30, 40, 50, and 60 mg/kg doses of Telazol demonstrated a dose-dependent decrease in heart rate, cardiac output, cardiac index, and stroke index.[241] When Telazol (12 mg/kg, IV) was administered following butorphanol (0.5 mg/kg, IV), awake goats showed significant decreases in cardiac output, mean aortic pressure, an increase in systemic vascular resistance, and mild respiratory acidosis.[1]

Guinea pigs received 60 mg/kg, IP, of the combination, along with xylazine (5 mg/kg, IP) and butorphanol (0.1 mg/kg, IP). There was a minor to moderate effect on the cardiovascular system but a significant depression of respiratory function with attendant changes in blood gases.[258]

Local Anesthetic Agents

Local anesthetic-induced cardiovascular collapse in animals has been repeatedly reported.[259] The vasodilator properties of lidocaine are attributed to the inhibition of action potentials by the blockade of Na+ channels in the vasoconstrictor sympathetic nerves.[260] An epidural bolus administration of 10 ml of 0.2% ropivacaine followed by epidural infusion of 10 ml/h resulted in significant hypotension.[261] However, 2 mg/kg of lidocaine, IV, prior to propofol anesthesia did not result in statistically significant changes in arterial blood pressures in dogs.[262] Excessive prolongation of the action potential duration induced by E-4031, a compound that selectively inhibits the rapid delayed rectifier potassium current, was attenuated by lidocaine in rabbit Purkinje fibers but not in atrial or ventricular tissues.[263] In isolated rat hearts, bupivacaine induced significant cardiac depression.[264] The addition of epinephrine, 1:100,000 and 1:200,000 to 4% articaine resulted in a significant elevation of arterial blood pressure following nerve blocks for dental procedures.[265] The intravenous infusion of rac-bupivacaine (37.5 mg) to conscious sheep decreased myocardial contractility, coronary perfusion, heart rate, and cardiac output.[7] Cardiovascular dose-responses to bupivacaine, levobupivacaine, and ropivacaine were studied in anesthetized, open-thorax rabbits. Levobupivacaine and bupivacaine decreased contractility at doses above 1.32 mg/kg. Bupivacaine decreased ejection fraction and cardiac index and increased systemic vascular resistance. Levobupivacaine reduced ejection fraction and cardiac index and had a biphasic response on vascular resistance, increasing it at high doses. Ropivacaine increased vascular resistance and reduced ejection fraction but had no effect on contractility. Arterial pressures and measures of diastolic function were not affected.[266] Clinically relevant doses of bupivacaine inhibited baroreflex control of heart rate in conscious rats apparently via inhibition of vagal components of the baroreflex.[267]

Non-steroidal Anti-inflammatory Agents

The list of non-steroidal anti-inflammatory agents (NSAIDs) available continues to expand. At this writing they include Aspirin, Carprofen, Celecoxib, Diclofinac, Etodolac, Etomidate, Flunixin, Ibuprofen, Indomethacin, Ketoprofan, Meclofenamate, Meloxicam, Naproxen, Phenylbutazone, Piroxicam, Tenidap, Tenoxicam, and Tolfenamic acid. Many of these agents are now used routinely for the treatment of anticipated postoperative pain in animals used for cardiovascular research so it is important to be aware of any potential effects that could confound the experimental design.[1,268] These agents can produce species-dependent gastroduodenal ulcers probably associated with their ability to induce neutrophilic adhesion to the microvasculature.[269] In human patients, about 25% of NSAID users develop GI ulcers and bleeding presumably by blocking prostaglandin synthesis from cyclooxygenase-1 and -2 (COX-1 and COX-2). The development of COX-2 inhibitors was supposed to reduce the GI side effects but both selective and nonselective NSAIDs inhibit angiogenesis through direct effects on endothelial cells by involving inhibition of MAP kinase ERK2 activity.[270] Teratogenic effects of NSAIDs appear to be species dependent. The offspring of near term female rats were treated with aspirin (14 mg/kg), acetaminophen (14 mg/kg), ibuprofen (6 mg/kg), or indomethacin (0.7 mg/kg). Fetuses collected from these rats at 1, 4, 8, or 24 h posttreatment demonstrated ductal constriction, ventricular dilation, and increased pericardial fluid.[271] Other studies in rats showed increased low-incidence cardiovascular malformations and defects in midline closure.[272] When aspirin was given to pregnant New Zealand White rabbits from gestation days 7–19 at doses of 125, 250, and 350 mg/kg/day or single doses of 500, 700, or 1,000 mg/kg on day 9, 10, or 11, there were toxic effects observed in the dams particularly at the higher doses, mortality, decreased food consumption, and weight loss but no treatment-related external, visceral, or skeletal malformations were observed in the fetuses.[272]

Integrated plasma cortisol levels are decreased in dogs treated with etodolac.[83] Carprofen treatment (4 mg/kg) had no effect on serum biochemical or hematological parameters or GFR in dogs anesthetized with a combination of medetomidine, propofol, and isoflurane.[273] Etomidate produced dose-dependent decreases in mean arterial pressure, cardiac output, liver blood flow, and systemic vascular resistance in greyhounds.[6] When coronary artery thrombosis was induced in dogs by electrolytic injury, COX-2 inhibition with celecoxib or high-dose aspirin (COX-1 and COX-2 inhibition) did not alter time to occlusive thrombus formation but when high-dose aspirin was used after allowing time for endothelial recovery there was a significant increase in time to occlusive thrombus formation.[274]

Cats treated with carprofen following surgical repair of fractures showed no indication of respiratory or cardiovascular depression.[77] However, cats do seem to be more sensitive to the GI complications of the NSAIDs.

When aspirin was combined with an angiotensin converting enzyme (ACE) inhibitor in a rat model of hypertension, the beneficial effects of the ACE inhibitor

were attenuated resulting in the production of massive cardiac necrosis, renal damage, and mortality.[275] When a rat model of iatrogenic portal venous constriction was used to create portal hypertension, mucosal erosions resulting from the stress response to 7 h of physical restraint were augmented by aspirin treatment.[276] Following venous anastomosis in rats, aspirin (5 mg/kg, IV) significantly reduced thrombosis. In the isolated rat, cremaster muscle preparation downstream from an arterial anastomosis aspirin-treated animals demonstrated significantly improved capillary perfusion but only slight increases in arteriolar diameters and reduction in emboli formation.[277] Aspirin (50, 100, or 200 mg/kg, IM) was administered 15 min prior to laser injury of 35–40-μm diameter arterioles. There was an increase in the number of laser injuries required for thrombus formation, a dose-dependent decrease in the duration of embolization and a dose-dependent decrease in the number of emboli formed.[278] In another rat model, aspirin injected at 10 mg/kg had a potent thrombosis effect and decreased bleeding times.[279] A nitric oxide-releasing formulation of aspirin (NCX-4016) reduced experimental restenosis in aged rats and was virtually devoid of GI damage in both young and old animals.[280] Using a rat model of arterial bypass with focal narrowing, Borgdorff et al. were able to demonstrate that COX-2 inhibitors enhanced shear stress-induced platelet aggregation.[281]

Genetically engineered mice with PGI_2 deletions were used to demonstrate an exaggerated response to COX-2 products resulting in elevated blood pressures, accelerated atherogenesis, and thrombus formation.[282] Veins were grafted into the arterial system of rabbits and the animals were treated with either 0.5 mg/kg/day aspirin + 2 mg/kg per 6 h dipyridamole or 40 mg/kg/day + the same dose of dipyridamole. Vein grafts treated with the higher dose of aspirin had significantly less PGI_2 than those treated with the lower dose or the controls and this was associated with significantly more platelet deposition.[283] Rabbits fed an atherogenic diet and treated with 100 mg/kg/day aspirin demonstrated intimal proliferation of the aorta and coronary arteries and increased occurrence and distribution of atheromatous plaques.[284] Selective inhibition, knockout, or mutation of prostaglandin G/H synthase-2 (PGHS-2, also known as COX-2) in mice accelerates thrombogenesis and elevates blood pressure. Knock down of COX-1 mimics the action of low-dose aspirin.[285] Short-term treatment of mice with COX-2 inhibitors reduces monocyte chemotaxis by reducing expression of monocyte chemoattractant protein while long-term treatment results in the opposite effect accelerating atherogenesis.[286]

Aspirin has been shown to protect against myocardial necrosis induced by catecholamine infusion in dogs and rats. NSAIDs also decrease the incidence of arrhythmias and ventricular fibrillation and increase survival rates following coronary occlusions. These effects are probably related to catecholamine blockade not to platelet inhibitory actions. A rank order of potency for the ability to block norepinephrine effects was established in isolated, perfused mesenteric blood vessels from rats: meclofenamate > flufenamate = diclofenac > indomethacin > fenbufen > phenylbutazone > ibuprofen > ketoprofen > naproxen > paracetamol.[1]

The intracoronary infusion of aspirin in dogs (5, 10, 20, and 30 mg) resulted in a dose-dependent reduction of coronary flow and contractility. Doses >10 mg inhibited reactive hyperemia following 15 s of coronary occlusion. Aspirin-treated

cats (650 mg, orally) 24 h prior to the experiment showed an increase in collateral circulation following aortic occlusions. Rats treated with aspirin had no preservation of creatine kinase activity, no protection against isoproterenol-induced hypertrophy, and no increase in cyclic AMP levels. Isolated Purkinje fiber preparations from sheep demonstrated reversibly reduced contractility, resting potential, and action potential duration when treated with aspirin. Pigs treated with 40 mg/kg aspirin had decreased renal PGE_2 excretion but no change in renal blood flow or GFR. Isolated atrial preparations from guinea pigs demonstrated reduced action potential durations in response to aspirin treatment.[1]

Dogs treated with indomethacin (2–20 mg/kg, IV) had variable changes in mean aortic pressures, but significant decreases in cardiac output, heart rate, and stroke volume. Cats anesthetized with pentobarbital showed no hemodynamic effects to treatment with indomethacin other than a dose-dependent mesenteric vasoconstriction. In rats and pigs, indomethacin blocked the pressor effects of norepinephrine and decreased cerebral blood flow. GI blood flow was reduced in rabbits but no other hemodynamic effects were seen. In chronically instrumented fetal lambs, in utero, indomethacin (0.33 ± 0.07 mg/kg of fetal weight) resulted in a significant increase in vascular resistance of both the ductus venosus and the fetal liver.[1]

Neuromuscular Blocking Agents

To combat undesirable movement during anesthesia and to be able to carefully control ventilation and blood gases without having animals struggling breath against the system, a variety of neuromuscular blocking agents are used. These agents can be classified into three types. (1) Competitive or nondepolarizing agents that compete with acetylcholine for available cholinergic receptors at the postsynaptic membrane. The classic example of this type is D-tubocurarine but includes metocurine iodide, gallamine, pancuronium, alcuronium, fazadinium, atracurium, and vecuronium. (2) Depolarizing agents that interfere with the acetylcholine-mediated depolarization of the postsynaptic membrane such as succinylcholine chloride and decamethonium bromide. (3) Aminosteroid drugs including rapacuronium and rocuronium.[1]

These agents have not been thoroughly investigated for cardiovascular effects in all species and reports conflict depending upon species. Gallamine, pancuronium, and alcuronium chloride were reported to have vagolytic effects with increases in heart rate and cardiac output in cats but no effects in dogs.[1,287] Pancuronium and rocuronium have similar effects in high-risk cardiac surgical patients,[288] but early studies reported vagal blockade but no other adverse cardiovascular or respiratory side effects.[289]

Ruminants are more sensitive to neuromuscular blockade and require reduced dosages.[1] Muscle relaxants and their metabolites may have cardiovascular effects by interacting with muscarinic and nicotinic receptors and the ganglionic system. Direct stimulation of mast cells by neuromuscular blockers can also result in histamine release and resultant cardiovascular effects.[290,291] When given as a rapid intravenous

bolus D-tubocurarine induces a transient hypotension in dogs whereas in anesthetized dogs injection of pancuronium caused slight increases in heart rate, blood pressure, and cardiac output, effects blocked by atropine.[1] When mivacurium (0.2 mg/kg, IV) was injected rapidly the incidence and intensity of hypotension was greater in hypertensive than normotensive patients.[292] Atracurium and vecuronium are reported to have minimal effects on blood pressure in dogs while gallamine was shown to have no effect on sympathetic nerve function but with vagolytic effects producing tachycardia without changes in arterial pressures.[1] Laudanosine is a metabolite of atracurium and cisatracurium. It crosses the blood–brain and placental barriers and high plasma concentrations produce hypotension and bradycardia.[293]

Succinylcholine-induced tachyarrythmias are not mediated via direct activation of the autonomic ganglionic $\alpha 3$ or $\beta 4$ subtypes.[294] Succinylcholine administered to awake horses cause an initial decrease in heart rate followed by an increase accompanied by A-V conduction disturbances, extra systoles, and some reports of myocardial damage. Autonomic blockade substantially mollifies these responses in horses suggesting that the adverse effects may be associated with a stress reaction because of the loss of skeletal and respiratory muscle control. When adequate ventilation was provided to awake animals paralyzed with succinylcholine, minimal cardiovascular changes were recorded. Low doses of succinylcholine increase the arrhythmogenicity of epinephrine during light anesthesia with halothane in dogs and increase the susceptibility to digitalis toxicity in horses.[1] While succinylcholine causes a significant increase in heart rate, in many species rocuronium does not.[295]

The cardiopulmonary side effects of a novel nondepolarizing neuromuscular blocking agent (GW280430A), with an ultrashort duration of action were tested in dogs. Bolus dosing had no effects on the cardiovascular parameters monitored until four of six dogs experienced a transient decrease in mean arterial pressure at $25 \times$ ED95. This response was associated with a concomitant increase in plasma histamine concentration.[296] The same drug (GW280430A) tested in cats and rhesus monkeys resulted in approximately four times less hypotension associated with histamine release than was seen with mivacurium.[297] No cardiovascular changes were noted in dogs anesthetized with either propofol or sevoflurane when treated with atracurium.[298] Cats treated with as much as 8× the ED90 with a nondepolarizing muscle relaxant (SZ1677) did not show significant cardiac vagal blocking effects.[287] Vecuronium significantly reduced carotid body neural responses to hypoxia, acetylcholine, and nicotine by inhibiting neuronal nicotinic receptors in the carotid body in rats.[299]

Fifty-two bisquaternary ammonium derivatives of several dicarboxylic acid esters of granatanol and three similar derivatives of pseudogranatanol were recently investigated for neuromuscular blocking potency, onset, and recovery and for cardiovascular side effects. All of the agents were tested first in anesthetized rats and selected compounds were further tested in rabbits, juvenile pigs, cats, dogs, and monkeys. Many, but not all, of these agents produced changes in heart rate and blood pressure associated with vagal blockade.[300]

Aminoglycoside, Fluoroquinolone, and Anthracycline Antibiotics

Experimental animals may require the use of antibiotics for a variety of reasons and a number of these agents have been shown to have adverse cardiovascular effects. The aminoglycosides, neomycin, streptomycin, dihydrostreptomycin, kanamycin, and gentamicin have all been shown to decrease cardiac output, aortic pressure, and left ventricular contractility and to increase heart rate. Penicillin and penicillin-related compounds have been associated with myocardial depression, conduction abnormalities, and vasodilating effects in several species, probably associated with the effect of these agents on Ca^{2+} transport. Chloramphenicol and the tetracyclines, erythromycin, and vancomycin have all been reported to cause myocardial depression. The vehicle in which the xenobiotic is suspended or dissolved may also be a problem. Propylene glycol has well-documented cardiovascular effects.[1]

Erythromycin and the fluoroquinolone antibiotics, sparfloxacin and moxifloxacin, were shown to prolong action potential duration in isolated rabbit, dog, and pig Purkinje fiber preparations. The prolongation was associated with a higher incidence of EADs at 0.2 Hz and prolonged QTc in vivo.[197,215,301,302]

The fluoroquinolone antibiotics sitafloxacin, gatifloxacin, and moxifloxacin were tested in halothane-anesthetized dogs, in dogs with chronic complete A-V block, and in α-chloralose-anesthetized rabbits. In the halothane-anesthetized dogs, gatifloxacin and moxifloxacin (1–3 mg/kg, IV) prolonged the ventricular effective refractory period and the repolarization period; sitafloxacin at the same dose only prolonged the refractory period. In the chronic A-V block dogs, gatifloxacin and moxifloxacin (100 mg/kg by mouth) induced torsades de pointes but sitafloxacin did not. In the rabbits, gatifloxacin, in the presence of methoxamine infusion, induced torsades de pointes but the other two agents did not.[303]

Adriamycin and doxorubicin are anthracycline antibiotics used for chemotherapy with well-documented cardiotoxicity characterized by nuclear DNA fragmentation resulting in cardiomyopathy. Specific DNA lesions include oxidized pyrimidines and 8-hydroxyguanine presumably related to oxidative stress and a pathway involving p53 and the mitochondria.[304-306]

References

1. Gross DR. Animal Models in Cardiovascular Research, 2nd Revised Edition. Boston, MA: Kluwer Academic; 1994.
2. Weber M, Motin L, Gaul S, Beker F, Fink RH, Adams DJ. Intravenous anaesthetics inhibit nicotinic acetylcholine receptor-mediated currents and Ca^{2+} transients in rat intracardiac ganglion neurons. *Br J Pharmacol.* 2005;144:98–107.
3. Rottman JN, Ni G, Khoo M, et al. Temporal changes in ventricular function assessed echocardiographically in conscious and anesthetized mice. *J Am Soc Echocardiogr.* 2003;16:1150–1157.

4. Schwenke DO, Cragg PA. Comparison of the depressive effects of four anesthetic regimens on ventilatory and cardiovascular variables in the guinea pig. *Comp Med.* 2004;54:77–85.
5. Blake DW, Korner PI. Role of baroreceptor reflexes in the hemodynamic and heart rate responses to althesin, ketamine and thiopentone anesthesia. *J Auton Nerv Syst.* 1981;3:55–70.
6. Thomson IA, Fitch W, Hughes RL, Campbell D, Watson R. Effects of certain i.v. anaesthetics on liver blood flow and hepatic oxygen consumption in the greyhound. *Br J Anaesth.* 1986;58:69–80.
7. Mather LE, Ladd LA, Copeland SE, Chang DH. Effects of imposed acid-base derangement on the cardiovascular effects and pharmacokinetics of bupivacaine and thiopental. *Anesthesiology.* 2004;100:1457–1468.
8. Roth DM, Swaney JS, Dalton ND, Gilpin EA, Ross J, Jr. Impact of anesthesia on cardiac function during echocardiography in mice. *Am J Physiol Heart Circ Physiol.* 2002;282:H2134–H2140.
9. Philp KL, Hussain M, Byrne NF, Diver MJ, Hart G, Coker SJ. Greater antiarrhythmic activity of acute 17beta-estradiol in female than male anaesthetized rats: Correlation with Ca^{2+} channel blockade. *Br J Pharmacol.* 2006;149:233–242.
10. Stekiel TA, Contney SJ, Bosnjak ZJ, Kampine JP, Roman RJ, Stekiel WJ. Chromosomal substitution-dependent differences in cardiovascular responses to sodium pentobarbital. *Anesth Analg.* 2006;102:799–805.
11. Mustola ST, Baer GA, Toivonen JK, et al. Electroencephalographic burst suppression versus loss of reflexes anesthesia with propofol or thiopental: Differences of variance in the catecholamine and cardiovascular response to tracheal intubation. *Anesth Analg.* 2003;97:1040–1045, table of contents.
12. Misiolek H, Wojcieszek E, Dyaczynska-Herman A. Comparison of influence of thiopentone, propofol and midazolam on blood serum concentration of noradrenaline and cortisol in patients undergoing non-toxic struma operation. *Med Sci Monit.* 2000;6:319–324.
13. Roh WS, Ding X, Murray PA. Propofol and thiopental attenuate adenosine triphosphate-sensitive potassium channel relaxation in pulmonary veins. *Am J Physiol Lung Cell Mol Physiol.* 2006;291:L636–L643.
14. Brookes ZL, Reilly CS, Brown NJ. Differential effects of propofol, ketamine, and thiopental anaesthesia on the skeletal muscle microcirculation of normotensive and hypertensive rats in vivo. *Br J Anaesth.* 2004;93:249–256.
15. Brookes ZL, Brown NJ, Reilly CS. Response of the rat cremaster microcirculation to hemorrhage in vivo: Differential effects of intravenous anesthetic agents. *Shock.* 2002;18:542–548.
16. Stein AB, Tiwari S, Thomas P, et al. Effects of anesthesia on echocardiographic assessment of left ventricular structure and function in rats. *Basic Res Cardiol.* 2007;102:28–41.
17. Fanton JW, Zarr SR, Ewert DL, Woods RW, Koenig SC. Cardiovascular responses to propofol and etomidate in long-term instrumented rhesus monkeys (macaca mulatta). *Comp Med.* 2000;50:303–308.
18. Chen WH, Lee CY, Hung KC, Yeh FC, Tseng CC, Shiau JM. The direct cardiac effect of propofol on intact isolated rabbit heart. *Acta Anaesthesiol Taiwan.* 2006;44:19–23.
19. Akine A, Suzuka H, Hayashida Y, Kato Y. Effects of ketamine and propofol on autonomic cardiovascular function in chronically instrumented rats. *Auton Neurosci.* 2001;87:201–208.
20. Oku K, Ohta M, Katoh T, Moriyama H, Kusano K, Fujinaga T. Cardiovascular effects of continuous propofol infusion in horses. *J Vet Med Sci.* 2006;68:773–778.
21. Umar MA, Yamashita K, Kushiro T, Muir WW. Evaluation of cardiovascular effects of total intravenous anesthesia with propofol or a combination of ketamine-medetomidine-propofol in horses. *Am J Vet Res.* 2007;68:121–127.
22. Cromheecke S, Pepermans V, Hendrickx E, et al. Cardioprotective properties of sevoflurane in patients undergoing aortic valve replacement with cardiopulmonary bypass. *Anesth Analg.* 2006;103:289–296, table of contents.
23. Wickley PJ, Ding X, Murray PA, Damron DS. Propofol-induced activation of protein kinase C isoforms in adult rat ventricular myocytes. *Anesthesiology.* 2006;104:970–977.
24. Roy N, Friehs I, Cowan DB, Zurakowski D, McGowan FX, del Nido PJ. Dopamine induces postischemic cardiomyocyte apoptosis in vivo: An effect ameliorated by propofol. *Ann Thorac Surg.* 2006;82:2192–2199.

25. Saint DA. The effects of propofol on macroscopic and single channel sodium currents in rat ventricular myocytes. *Br J Pharmacol.* 1998;124:655–662.
26. Nagakawa T, Yamazaki M, Hatakeyama N, Stekiel TA. The mechanisms of propofol-mediated hyperpolarization of in situ rat mesenteric vascular smooth muscle. *Anesth Analg.* 2003;97:1639–1645.
27. Rubal BJ, Buchanan C. Supplemental chloralose anesthesia in morphine premedicated dogs. *Lab Anim Sci.* 1986;36:59–64.
28. Faber JE. Effects of althesin and urethane-chloralose on neurohumoral cardiovascular regulation. *Am J Physiol.* 1989;256:R757–R765.
29. Dyson DH, Allen DG, Ingwersen W, Pascoe PJ, O'Grady M. Effects of saffan on cardiopulmonary function in healthy cats. *Can J Vet Res.* 1987;51:236–239.
30. Al-Khawashki MI, Ghaleb HA, El-Gawhary N, Madkour MK, Radwan AM, El-Sherbiny AM. Pharmacological effects of althesin and its steroidal components on the cardiovascular system. *Middle East J Anaesthesiol.* 1980;5:457–469.
31. Foster A, Zeller W, Pfannkuche HJ. Effect of thiopental, saffan, and propofol anesthesia on cardiovascular parameters and bronchial smooth muscle in the rhesus monkey. *Lab Anim Sci.* 1996;46:327–334.
32. De Hert SG. Volatile anesthetics and cardiac function. *Semin Cardiothorac Vasc Anesth.* 2006;10:33–42.
33. Guarracino F, Landoni G, Tritapepe L, et al. Myocardial damage prevented by volatile anesthetics: A multicenter randomized controlled study. *J Cardiothorac Vasc Anesth.* 2006;20:477–483.
34. Neuhauser C, Muller M, Welters I, Scholz S, Kwapisz MM. Effect of isoflurane on echocardiographic left-ventricular relaxation indices in patients with diastolic dysfunction due to concentric hypertrophy and ischemic heart disease. *J Cardiothorac Vasc Anesth.* 2006;20:509–514.
35. Kadoi Y, Takahashi K, Saito S, Goto F. The comparative effects of sevoflurane versus isoflurane on cerebrovascular carbon dioxide reactivity in patients with diabetes mellitus. *Anesth Analg.* 2006;103:168–172, table of contents.
36. Preckel B, Obal D, Mullenheim J, et al. Effects of halothane, sevoflurane and desflurane on the force-frequency relation in the dog heart in vivo. *Can J Anaesth.* 2006;53:1118–1125.
37. Graham MD, Hopkins PM, Harrison SM. Antagonistic actions of halothane and sevoflurane on spontaneous Ca^{2+} release in rat ventricular myocytes. *Anesthesiology.* 2006;105:58–64.
38. Wang Q, Brunner HR, Burnier M. Determination of cardiac contractility in awake unsedated mice with a fluid-filled catheter. *Am J Physiol Heart Circ Physiol.* 2004;286:H806–H814.
39. Sigg DC, Iaizzo PA. In vivo versus in vitro comparison of swine cardiac performance: Induction of cardiodepression with halothane. *Eur J Pharmacol.* 2006;543:97–107.
40. Pascoe PJ, Ilkiw JE, Fisher LD. Cardiovascular effects of equipotent isoflurane and alfentanil/isoflurane minimum alveolar concentration multiple in cats. *Am J Vet Res.* 1997;58:1267–1273.
41. Marinovic J, Bosnjak ZJ, Stadnicka A. Distinct roles for sarcolemmal and mitochondrial adenosine triphosphate-sensitive potassium channels in isoflurane-induced protection against oxidative stress. *Anesthesiology.* 2006;105:98–104.
42. Feng J, Fischer G, Lucchinetti E, et al. Infarct-remodeled myocardium is receptive to protection by isoflurane postconditioning: Role of protein kinase B/Akt signaling. *Anesthesiology.* 2006;104:1004–1014.
43. Iltis I, Kober F, Dalmasso C, Lan C, Cozzone PJ, Bernard M. In vivo assessment of myocardial blood flow in rat heart using magnetic resonance imaging: Effect of anesthesia. *J Magn Reson Imaging.* 2005;22:242–247.
44. Ishizaka S, Sievers RE, Zhu BQ, et al. New technique for measurement of left ventricular pressure in conscious mice. *Am J Physiol Heart Circ Physiol.* 2004;286:H1208–H1215.
45. Tsutsumi YM, Patel HH, Huang D, Roth DM. Role of 12-lipoxygenase in volatile anesthetic-induced delayed preconditioning in mice. *Am J Physiol Heart Circ Physiol.* 2006;291:H979–H983.
46. Fujita H, Ogura T, Tamagawa M, et al. A key role for the subunit SUR2B in the preferential activation of vascular KATP channels by isoflurane. *Br J Pharmacol.* 2006;149:573–580.

47. Galagudza M, Vaage J, Valen G. Isoflurane and other commonly used anaesthetics do not protect the isolated buffer perfused mouse heart from ischemia-reperfusion injury. *Clin Exp Pharmacol Physiol.* 2006;33:315–319.
48. Souza AP, Guerrero PN, Nishimori CT, et al. Cardiopulmonary and acid-base effects of desflurane and sevoflurane in spontaneously breathing cats. *J Feline Med Surg.* 2005;7:95–100.
49. Rozenberg S, Besse S, Amour J, Vivien B, Tavernier B, Riou B. Effects of desflurane in senescent rat myocardium. *Anesthesiology.* 2006;105:961–967.
50. Yerer MB, Aydogan S, Comu FM, et al. The red blood cell deformability alterations under desflurane anesthesia in rats. *Clin Hemorheol Microcirc.* 2006;35:213–216.
51. Smul TM, Lange M, Redel A, Burkhard N, Roewer N, Kehl F. Desflurane-induced preconditioning against myocardial infarction is mediated by nitric oxide. *Anesthesiology.* 2006;105:719–725.
52. Ogawa Y, Iwasaki K, Shibata S, Kato J, Ogawa S, Oi Y. Different effects on circulatory control during volatile induction and maintenance of anesthesia and total intravenous anesthesia: Autonomic nervous activity and arterial cardiac baroreflex function evaluated by blood pressure and heart rate variability analysis. *J Clin Anesth.* 2006;18:87–95.
53. Bouwman RA, van't Hof FN, de Ruijter W, et al. The mechanism of sevoflurane-induced cardioprotection is independent of the applied ischaemic stimulus in rat trabeculae. *Br J Anaesth.* 2006;97:307–314.
54. Bouwman RA, Salic K, Padding FG, et al. Cardioprotection via activation of protein kinase C-delta depends on modulation of the reverse mode of the Na^+/Ca^{2+} exchanger. *Circulation.* 2006;114:I226–I232.
55. Kang J, Reynolds WP, Chen XL, Ji J, Wang H, Rampe DE. Mechanisms underlying the QT interval-prolonging effects of sevoflurane and its interactions with other QT-prolonging drugs. *Anesthesiology.* 2006;104:1015–1022.
56. Kerbaul F, Bellezza M, Mekkaoui C, et al. Sevoflurane alters right ventricular performance but not pulmonary vascular resistance in acutely instrumented anesthetized pigs. *J Cardiothorac Vasc Anesth.* 2006;20:209–216.
57. Drake VJ, Koprowski SL, Lough J, Hu N, Smith SM. Trichloroethylene exposure during cardiac valvuloseptal morphogenesis alters cushion formation and cardiac hemodynamics in the avian embryo. *Environ Health Perspect.* 2006;114:842–847.
58. Mishima N, Hoffman S, Hill EG, Krug EL. Chick embryos exposed to trichloroethylene in an ex ova culture model show selective defects in early endocardial cushion tissue formation. *Birth Defects Res A Clin Mol Teratol.* 2006;76:517–527.
59. Feuerstein G. The opioid system and central cardiovascular control: Analysis of controversies. *Peptides.* 1985;6 Suppl 2:51–56.
60. Lalley PM. Mu-opioid receptor agonist effects on medullary respiratory neurons in the cat: Evidence for involvement in certain types of ventilatory disturbances. *Am J Physiol Regul Integr Comp Physiol.* 2003;285:R1287–R1304.
61. Naganobu K, Maeda N, Miyamoto T, Hagio M, Nakamura T, Takasaki M. Cardiorespiratory effects of epidural administration of morphine and fentanyl in dogs anesthetized with sevoflurane. *J Am Vet Med Assoc.* 2004;224:67–70.
62. Hakim TS, Grunstein MM, Michel RP. Opiate action in the pulmonary circulation. *Pulm Pharmacol.* 1992;5:159–165.
63. Feldberg W, Wei E. Analysis of cardiovascular effects of morphine in the cat. *Neuroscience.* 1986;17:495–506.
64. Feuerstein G, Zukowska-Grojec Z. Effect of dermorphin and morphine on the sympathetic and cardiovascular system of the pithed rat. *Neuropeptides.* 1987;9:139–150.
65. McNally GP, Carrive P. A telemetric examination of cardiovascular function during the development of, and recovery from, opiate dependence in rats. *Physiol Behav.* 2006;88:55–60.
66. Mahinda TB, Lovell BM, Taylor BK. Morphine-induced analgesia, hypotension, and bradycardia are enhanced in hypertensive rats. *Anesth Analg.* 2004;98:1698–1704, table of contents.
67. Chang WL, Lee SS, Su MJ. Attenuation of post-ischemia reperfusion injury by thaliporphine and morphine in rat hearts. *J Biomed Sci.* 2005;12:611–619.

68. Shi E, Jiang X, Bai H, Gu T, Chang Y, Wang J. Cardioprotective effects of morphine on rat heart suffering from ischemia and reperfusion. *Chin Med J (Engl).* 2003;116:1059–1062.
69. Barrere-Lemaire S, Combes N, Sportouch-Dukhan C, Richard S, Nargeot J, Piot C. Morphine mimics the antiapoptotic effect of preconditioning via an ins(1,4,5)P3 signaling pathway in rat ventricular myocytes. *Am J Physiol Heart Circ Physiol.* 2005;288:H83–H88.
70. Gross ER, Hsu AK, Gross GJ. The JAK/STAT pathway is essential for opioid-induced cardioprotection: JAK2 as a mediator of STAT3, akt, and GSK-3 beta. *Am J Physiol Heart Circ Physiol.* 2006;291:H827–H834.
71. Roy S, Balasubramanian S, Wang J, Chandrashekhar Y, Charboneau R, Barke R. Morphine inhibits VEGF expression in myocardial ischemia. *Surgery.* 2003;134:336–344.
72. Peart JN, Gross GJ. Cardioprotective effects of acute and chronic opioid treatment are mediated via different signaling pathways. *Am J Physiol Heart Circ Physiol.* 2006;291:H1746–H1753.
73. Jiang X, Shi E, Nakajima Y, Sato S. Inducible nitric oxide synthase mediates delayed cardioprotection induced by morphine in vivo: Evidence from pharmacologic inhibition and gene-knockout mice. *Anesthesiology.* 2004;101:82–88.
74. Peart JN, Gross GJ. Exogenous activation of delta- and kappa-opioid receptors affords cardioprotection in isolated murine heart. *Basic Res Cardiol.* 2004;99:29–37.
75. Peart JN, Gross GJ. Morphine-tolerant mice exhibit a profound and persistent cardioprotective phenotype. *Circulation.* 2004;109:1219–1222.
76. Kaye AD, Hoover JM, Baber SR, et al. The effects of meperidine in the pulmonary vascular bed of the cat. *J Cardiothorac Vasc Anesth.* 2006;20:691–695.
77. Mollenhoff A, Nolte I, Kramer S. Anti-nociceptive efficacy of carprofen, levomethadone and buprenorphine for pain relief in cats following major orthopaedic surgery. *J Vet Med A Physiol Pathol Clin Med.* 2005;52:186–198.
78. Mills PC, Magnusson BM, Cross SE. Investigation of in vitro transdermal absorption of fentanyl from patches placed on skin samples obtained from various anatomic regions of dogs. *Am J Vet Res.* 2004;65:1697–1700.
79. Ambrisko TD, Hikasa Y, Sato K. Influence of medetomidine on stress-related neurohormonal and metabolic effects caused by butorphanol, fentanyl, and ketamine administration in dogs. *Am J Vet Res.* 2005;66:406–412.
80. Lennander O, Henriksson BA, Martner J, Biber B. Effects of fentanyl, nitrous oxide, or both, on baroreceptor reflex regulation in the cat. *Br J Anaesth.* 1996;77:399–403.
81. Porsius AJ, Borgdorff P, van Rooij HH, de Neef JH. The inhibitory effect of fentanyl, nicomorphine and 6-nicotinoyl morphine on phrenic nerve activity in relation to their cardiovascular effects in the anaesthetized cat. *Arch Int Pharmacodyn Ther.* 1987;286:123–135.
82. Kaye AD, Hoover JM, Ibrahim IN, et al. Analysis of the effects of fentanyl in the feline pulmonary vascular bed. *Am J Ther.* 2006;13:478–484.
83. Inoue T, Ko JC, Mandsager RE, Payton ME, Galloway DS, Lange DN. Efficacy and safety of preoperative etodolac and butorphanol administration in dogs undergoing ovariohysterectomy. *J Am Anim Hosp Assoc.* 2006;42:178–188.
84. Gross DR, Tranquilli WJ, Greene SA, Grimm KA. Critical anthropomorphic evaluation and treatment of postoperative pain in rats and mice. *J Am Vet Med Assoc.* 2003;222:1505–1510.
85. Torske KE, Dyson DH, Conlon PD. Cardiovascular effects of epidurally administered oxymorphone and an oxymorphone-bupivacaine combination in halothane-anesthetized dogs. *Am J Vet Res.* 1999;60:194–200.
86. Vesal N, Cribb PH, Frketic M. Postoperative analgesic and cardiopulmonary effects in dogs of oxymorphone administered epidurally and intramuscularly, and medetomidine administered epidurally: A comparative clinical study. *Vet Surg.* 1996;25:361–369.
87. Chance E, Paciorek PM, Todd MH, Waterfall JF. Comparison of the cardiovascular effects of meptazinol and naloxone following haemorrhagic shock in rats and cats. *Br J Pharmacol.* 1985;86:43–53.
88. Kaye AD, Phelps J, Baluch A, et al. The effects of sufentanil in the feline pulmonary vascular bed. *Eur J Pharmacol.* 2006;534:159–164.

89. Lecomte P, Ouattara A, Le Manach Y, Landi M, Coriat P, Riou B. The coronary and myocardial effects of remifentanil and sufentanil in the erythrocyte-perfused isolated rabbit heart. *Anesth Analg.* 2006;103:9–14, table of contents.
90. Pittarello D, Bonato R, Armellin G, Sorbara C. Alterations in left ventricular-arterial coupling and mechanical efficiency produced by remifentanil during cardiac anesthesia. *Minerva Anestesiol.* 2001;67:133–147.
91. Sohn JT, Murray PA. Inhibitory effects of etomidate and ketamine on adenosine triphosphate-sensitive potassium channel relaxation in canine pulmonary artery. *Anesthesiology.* 2003;98:104–113.
92. Wang X, Huang ZG, Dergacheva O, et al. Ketamine inhibits inspiratory-evoked gamma-aminobutyric acid and glycine neurotransmission to cardiac vagal neurons in the nucleus ambiguus. *Anesthesiology.* 2005;103:353–359.
93. Costa-Farre C, Garcia F, Andaluz A, Torres R, de Mora F. Effect of H1- and H2-receptor antagonists on the hemodynamic changes induced by the intravenous administration of ketamine in sevoflurane-anesthetized cats. *Inflamm Res.* 2005;54:256–260.
94. Yang J, Li W, Duan M, et al. Large dose ketamine inhibits lipopolysaccharide-induced acute lung injury in rats. *Inflamm Res.* 2005;54:133–137.
95. Oguchi T, Kashimoto S, Yamaguchi T, Kumazawa T, Hashimoto K. Effects of intravenous anesthetics on function and metabolism in the reperfused working rat heart. *Jpn J Pharmacol.* 1995;68:413–421.
96. Saranteas T, Zotos N, Chantzi C, et al. Ketamine-induced changes in metabolic and endocrine parameters of normal and 2-kidney 1-clip rats. *Eur J Anaesthesiol.* 2005;22:875–878.
97. Kim SJ, Kang HS, Lee MY, et al. Ketamine-induced cardiac depression is associated with increase in [Mg2+]i and activation of p38 MAP kinase and ERK 1/2 in guinea pig. *Biochem Biophys Res Commun.* 2006;349:716–722.
98. DeRossi R, Junqueira AL, Beretta MP. Analgesic and systemic effects of ketamine, xylazine, and lidocaine after subarachnoid administration in goats. *Am J Vet Res.* 2003;64:51–56.
99. Kawano T, Oshita S, Takahashi A, et al. Molecular mechanisms underlying ketamine-mediated inhibition of sarcolemmal adenosine triphosphate-sensitive potassium channels. *Anesthesiology.* 2005;102:93–101.
100. Schulte-Sasse U, Hess W, Tarnow J. Hemodynamic analysis of 6 different anesthesia induction procedures in coronary surgery patients. *Anasth Intensivther Notfallmed.* 1982;17:195–200.
101. Lundy JB, Slane ML, Frizzi JD. Acute adrenal insufficiency after a single dose of etomidate. *J Intensive Care Med.* 2007;22:111–117.
102. McIntosh MP, Narita H, Kameyama Y, Rajewski RA, Goto H. Evaluation of mean arterial blood pressure, heart rate, and sympathetic nerve activity in rabbits after administration of two formulations of etomidate. *Vet Anaesth Analg.* 2007;34:149–156.
103. Devin A, Nogueira V, Averet N, Leverve X, Rigoulet M. Profound effects of the general anesthetic etomidate on oxidative phosphorylation without effects on their yield. *J Bioenerg Biomembr.* 2006;38:137–142.
104. Nakamura A, Kawahito S, Kawano T, et al. Differential effects of etomidate and midazolam on vascular adenosine triphosphate-sensitive potassium channels: Isometric tension and patch clamp studies. *Anesthesiology.* 2007;106:515–522.
105. Shin IW, Sohn JT, Kim HJ, et al. Etomidate attenuates phenylephrine-induced contraction in isolated rat aorta. *Can J Anaesth.* 2005;52:927–934.
106. Pili-Floury S, Samain E, Bouillier H, et al. Etomidate alters calcium mobilization induced by angiotensin II in rat aortic smooth muscle cells. *J Cardiovasc Pharmacol.* 2004;43:485–488.
107. Zaugg M, Lucchinetti E, Spahn DR, Pasch T, Garcia C, Schaub MC. Differential effects of anesthetics on mitochondrial K(ATP) channel activity and cardiomyocyte protection. *Anesthesiology.* 2002;97:15–23.
108. Ouedraogo N, Mounkaila B, Crevel H, Marthan R, Roux E. Effect of propofol and etomidate on normoxic and chronically hypoxic pulmonary artery. *BMC Anesthesiol.* 2006;6:2.
109. Ogawa K, Tanaka S, Murray PA. Inhibitory effects of etomidate and ketamine on endothelium-dependent relaxation in canine pulmonary artery. *Anesthesiology.* 2001;94:668–677.

110. Paris A, Philipp M, Tonner PH, et al. Activation of alpha 2B-adrenoceptors mediates the cardiovascular effects of etomidate. *Anesthesiology.* 2003;99:889–895.
111. Zeller A, Arras M, Lazaris A, Jurd R, Rudolph U. Distinct molecular targets for the central respiratory and cardiac actions of the general anesthetics etomidate and propofol. *FASEB J.* 2005;19:1677–1679.
112. Kulier AH, Turner LA, Vodanovic S, Contney S, Lathrop DA, Bosnjak ZJ. Multiple agents potentiate alpha1-adrenoceptor-induced conduction depression in canine cardiac Purkinge fibers. *Anesthesiology.* 2000;92:1713–1721.
113. Bazin JE, Dureuil B, Danialou G, et al. Effects of etomidate, propofol and thiopental anaesthesia on arteriolar tone in the rat diaphragm. *Br J Anaesth.* 1998;81:430–435.
114. Modig J. Positive effects of ketamine v. metomidate anesthesia on cardiovascular function, oxygen delivery and survival. studies with a porcine endotoxin model. *Acta Chir Scand.* 1987;153:7–13.
115. Stegmann GF, Bester L. Some cardiopulmonary effects of midazolam premedication in clenbuterol-treated bitches during surgical endoscopic examination of the uterus and ovariohysterectomy. *J S Afr Vet Assoc.* 2001;72:33–36.
116. Kim C, Shvarev Y, Takeda S, Sakamoto A, Lindahl SG, Eriksson LI. Midazolam depresses carotid body chemoreceptor activity. *Acta Anaesthesiol Scand.* 2006;50:144–149.
117. Kanaya N, Murray PA, Damron DS. Effects of L-type Ca^{2+} channel modulation on direct myocardial effects of diazepam and midazolam in adult rat ventricular myocytes. *J Anesth.* 2006;20:17–25.
118. Win NN, Fukayama H, Kohase H, Umino M. The different effects of intravenous propofol and midazolam sedation on hemodynamic and heart rate variability. *Anesth Analg.* 2005;101:97–102, table of contents.
119. Hidaka S, Kawamoto M, Kurita S, Yuge O. Comparison of the effects of propofol and midazolam on the cardiovascular autonomic nervous system during combined spinal and epidural anesthesia. *J Clin Anesth.* 2005;17:36–43.
120. Klockgether-Radke AP, Pawlowski P, Neumann P, Hellige G. Mechanisms involved in the relaxing effect of midazolam on coronary arteries. *Eur J Anaesthesiol.* 2005;22:135–139.
121. Juan-Fita MJ, Vargas ML, Hernandez J. Diazepam enhances inotropic responses to dopamine in rat ventricular myocardium. *Anesth Analg.* 2006;102:676–681.
122. Zahner MR, Li DP, Pan HL. Benzodiazepine inhibits hypothalamic presympathetic neurons by potentiation of GABAergic synaptic input. *Neuropharmacology.* 2007;52:467–475.
123. Suzuki M, Nishina M, Nakamura S, Maruyama K. Benzodiazepine-sensitive GABA(A) receptors in the commissural subnucleus of the NTS are involved in the carotid chemoreceptor reflex in rats. *Auton Neurosci.* 2004;110:108–113.
124. Park SE, Sohn JT, Kim C, et al. Diazepam attenuates phenylephrine-induced contractions in rat aorta. *Anesth Analg.* 2006;102:682–689.
125. Resstel LB, Joca SR, Moreira FA, Correa FM, Guimaraes FS. Effects of cannabidiol and diazepam on behavioral and cardiovascular responses induced by contextual conditioned fear in rats. *Behav Brain Res.* 2006;172:294–298.
126. Selmi AL, Barbudo-Selmi GR, Moreira CF, et al. Evaluation of sedative and cardiorespiratory effects of romifidine and romifidine-butorphanol in cats. *J Am Vet Med Assoc.* 2002;221:506–510.
127. Sy GY, Bousquet P, Feldman J. Opposite to alpha2-adrenergic agonists, an imidazoline I1 selective compound does not influence reflex bradycardia in rabbits. *Auton Neurosci.* 2006;128:19–24.
128. Aantaa R, Jalonen J. Perioperative use of alpha2-adrenoceptor agonists and the cardiac patient. *Eur J Anaesthesiol.* 2006;23:361–372.
129. Murrell JC, Hellebrekers LJ. Medetomidine and dexmedetomidine: A review of cardiovascular effects and antinociceptive properties in the dog. *Vet Anaesth Analg.* 2005;32:117–127.
130. Dodam JR, Cohn LA, Durham HE, Szladovits B. Cardiopulmonary effects of medetomidine, oxymorphone, or butorphanol in selegiline-treated dogs. *Vet Anaesth Analg.* 2004;31:129–137.
131. Kuo WC, Keegan RD. Comparative cardiovascular, analgesic, and sedative effects of medetomidine, medetomidine-hydromorphone, and medetomidine-butorphanol in dogs. *Am J Vet Res.* 2004;65:931–937.

132. Joubert KE, Lobetti R. The cardiovascular and respiratory effects of medetomidine and thiopentone anaesthesia in dogs breathing at an altitude of 1486 m. *J S Afr Vet Assoc.* 2002;73: 104–110.
133. Lamont LA, Bulmer BJ, Sisson DD, Grimm KA, Tranquilli WJ. Doppler echocardiographic effects of medetomidine on dynamic left ventricular outflow tract obstruction in cats. *J Am Vet Med Assoc.* 2002;221:1276–1281.
134. Selmi AL, Mendes GM, Lins BT, Figueiredo JP, Barbudo-Selmi GR. Evaluation of the sedative and cardiorespiratory effects of dexmedetomidine, dexmedetomidine-butorphanol, and dexmedetomidine-ketamine in cats. *J Am Vet Med Assoc.* 2003;222:37–41.
135. Kutter AP, Kastner SB, Bettschart-Wolfensberger R, Huhtinen M. Cardiopulmonary effects of dexmedetomidine in goats and sheep anaesthetised with sevoflurane. *Vet Rec.* 2006;159:624–629.
136. Rioja E, Santos M, Martinez Taboada F, Ibancovichi JA, Tendillo FJ. Cardiorespiratory and minimum alveolar concentration sparing effects of a continuous intravenous infusion of dexmedetomidine in halothane or isoflurane-anaesthetized rats. *Lab Anim.* 2006;40:9–15.
137. Hall DL, Rezvan E, Tatakis DN, Walters JD. Oral clonidine pretreatment prior to venous cannulation. *Anesth Prog.* 2006;53:34–42.
138. Kaczynska K, Szereda-Przestaszewska M. Clonidine-evoked respiratory effects in anaesthetized rats. *Exp Physiol.* 2006;91:269–275.
139. Burniston JG, Tan LB, Goldspink DF. Relative myotoxic and haemodynamic effects of the beta-agonists fenoterol and clenbuterol measured in conscious unrestrained rats. *Exp Physiol.* 2006;91:1041–1049.
140. Doheny MH, Waterfield CJ, Timbrell JA. The effects of the beta 2-agonist drug clenbuterol on taurine levels in heart and other tissues in the rat. *Amino Acids.* 1998;15:13–25.
141. Burniston JG, Ng Y, Clark WA, Colyer J, Tan LB, Goldspink DF. Myotoxic effects of clenbuterol in the rat heart and soleus muscle. *J Appl Physiol.* 2002;93:1824–1832.
142. Ferrer M, Salaices M, Sanchez M, Balfagon G. Different effects of acute clenbuterol on vasomotor response in mesenteric arteries from young and old spontaneously hypertensive rats. *Eur J Pharmacol.* 2003;466:289–299.
143. Soppa GK, Smolenski RT, Latif N, et al. Effects of chronic administration of clenbuterol on function and metabolism of adult rat cardiac muscle. *Am J Physiol Heart Circ Physiol.* 2005;288:H1468–H1476.
144. Burniston JG, Clark WA, Tan LB, Goldspink DF. Dose-dependent separation of the hypertrophic and myotoxic effects of the beta(2)-adrenergic receptor agonist clenbuterol in rat striated muscles. *Muscle Nerve.* 2006;33:655–663.
145. Jones SW, Baker DJ, Gardiner SM, Bennett T, Timmons JA, Greenhaff PL. The effect of the beta2-adrenoceptor agonist prodrug BRL-47672 on cardiovascular function, skeletal muscle myosin heavy chain, and MyoD expression in the rat. *J Pharmacol Exp Ther.* 2004;311:1225–1231.
146. Patiyal SN, Katoch SS. Tissue specific and variable collagen proliferation in swiss albino mice treated with clenbuterol. *Physiol Res.* 2006;55:97–103.
147. Sleeper MM, Kearns CF, McKeever KH. Chronic clenbuterol administration negatively alters cardiac function. *Med Sci Sports Exerc.* 2002;34:643–650.
148. Furihata Y, Motokawa Y, Murata S, et al. Cardiovascular effects of KUR-1246, a new tetrahydronaphthalen derivative beta2-adrenoceptor agonist and a selective uterine relaxant. *Arzneimittelforschung.* 2006;56:18–24.
149. Gabrys J, Konecki J, Glowacka M, et al. Proteinous amino acids in muscle cytosol of rats' heart, after their treatment with propranolol, pentylenetetrazol or reserpine. *Receptors Channels.* 2004;10:83–90.
150. Shafi S, Stepanova IP, Fitzsimmons C, Bowyer DE, Born GV. Long-term low-dose treatment with reserpine of cholesterol-fed rabbits reduces cholesterol in plasma, non-high density lipoproteins and arterial walls. *J Cardiovasc Pharmacol.* 2002;40:67–79.
151. Okada K, Shinozuka K, Shimoura K, Kobayashi Y, Hattori K, Nakase A. Effects of reserpine on the content and uptake of dopamine and noradrenaline in rabbit arteries. *Clin Exp Pharmacol Physiol.* 1993;20:261–267.

152. Wassilew G, David H, Fitzl G, Beskrownaya N, Sharow V. Ultrastructural morphometric investigation of the heart of rabbits after a single administration of reserpine. *Exp Toxicol Pathol.* 1993;45:217–222.
153. Kehler CH, Hebl JR, Soule CL, Gallagher WJ, Houlton AJ. The effect of reduced myocardial cyclic AMP content on the response to milrinone in the isolated guinea pig heart. *J Heart Lung Transplant.* 1997;16:636–642.
154. Walcott GP, Melnick SB, Killingsworth CR, Smith WM, Ideker RE. Effects of burst stimulation during ventricular fibrillation on cardiac function after defibrillation. *Am J Physiol Heart Circ Physiol.* 2003;285:H766–H774.
155. Park IY, Kim EJ, Park H, Fields K, Dunker AK, Kang C. Interaction between cardiac calsequestrin and drugs with known cardiotoxicity. *Mol Pharmacol.* 2005;67:97–104.
156. Lathers CM, Lipka LJ. Chlorpromazine: Cardiac arrhythmogenicity in the cat. *Life Sci.* 1986;38:521–538.
157. Yabuki M, Tani N, Yoshioka T, Nishibe H, Kanamaru H, Kaneko H. Local thrombus formation in the site of intravenous injection of chlorpromazine: Possible colloid-osmotic lysis of the local endothelial cells. *Biol Pharm Bull.* 2000;23:957–961.
158. Lee SY, Choi SY, Youm JB, et al. Block of HERG human K(+) channel and IKr of guinea pig cardiomyocytes by chlorpromazine. *J Cardiovasc Pharmacol.* 2004;43:706–714.
159. Studenik C, Lemmens-Gruber R, Heistracher P. Proarrhythmic effects of antidepressants and neuroleptic drugs on isolated, spontaneously beating guinea-pig Purkinge fibers. *Eur J Pharm Sci.* 1999;7:113–118.
160. Flaim SF, Brannan MD, Swigart SC, Gleason MM, Muschek LD. Neuroleptic drugs attenuate calcium influx and tension development in rabbit thoracic aorta: Effects of pimozide, penfluridol, chlorpromazine, and haloperidol. *Proc Natl Acad Sci USA.* 1985;82:1237–1241.
161. Takata Y, Kurihara J, Suzuki S, Okubo Y, Kato H. A rabbit model for evaluation of chlorpromazine-induced orthostatic hypotension. *Biol Pharm Bull.* 1999;22:457–462.
162. Cottle MK, Van Petten GR, van Muyden P. Maternal and fetal cardiovascular indices during fetal hypoxia due to cord compression in chronically cannulated sheep. II. responses to promazine. *Am J Obstet Gynecol.* 1983;146:686–692.
163. Svendsen P, Carter AM. Blood gas tensions, acid-base status and cardiovascular function in miniature swine anaesthetized with halothane and methoxyflurane or intravenous metomidate hydrochloride. *Pharmacol Toxicol.* 1989;64:88–93.
164. Rezakhani A, Edjtehadi M, Szabuniewicz M. Prevention of thiopental and thiopental/halothane cardiac sensitization to epinephrine in the sheep. *Can J Comp Med.* 1977;41:389–395.
165. Choi SY, Koh YS, Jo SH. Inhibition of human ether-a-go-go-related gene K^+ channel and IKr of guinea pig cardiomyocytes by antipsychotic drug trifluoperazine. *J Pharmacol Exp Ther.* 2005;313:888–895.
166. Mohindroo A, Ahluwalia P. Effect of trifluoperazine on certain arterial wall lipid-metabolizing enzymes inducing atherosclerosis in rhesus monkeys. *Lipids.* 1997;32:867–872.
167. Belhani D, Frassati D, Megard R, et al. Cardiac lesions induced by neuroleptic drugs in the rabbit. *Exp Toxicol Pathol.* 2006;57:207–212.
168. Satoh Y, Sugiyama A, Takahara A, et al. The antipsychotic and antiemetic drug prochlorperazine delays the ventricular repolarization of the in situ canine heart. *J Pharmacol Sci.* 2005;97:101–106.
169. Shiotani M, Harada T, Abe J, et al. Practical application of guinea pig telemetry system for QT evaluation. *J Toxicol Sci.* 2005;30:239–247.
170. Kim MD, Eun SY, Jo SH. Blockade of HERG human K^+ channel and IKr of guinea pig cardiomyocytes by prochlorperazine. *Eur J Pharmacol.* 2006;544:82–90.
171. Drolet B, Vincent F, Rail J, et al. Thioridazine lengthens repolarization of cardiac ventricular myocytes by blocking the delayed rectifier potassium current. *J Pharmacol Exp Ther.* 1999;288:1261–1268.
172. Crumb W, Llorca PM, Lancon C, Thomas GP, Garay RP, Hameg A. Effects of cyamemazine on hERG, INa, ICa, ito, isus and IK1 channel currents, and on the QTc interval in guinea pigs. *Eur J Pharmacol.* 2006;532:270–278.

173. Carmeliet E, Xhonneux R, Van Glabbeek A, Reneman R. Electrophysiological effects of droperidol in different cardiac tissues. *Naunyn Schmiedebergs Arch Pharmacol.* 1976;293:57–66.
174. Adamantidis MM, Kerram P, Caron JF, Dupuis BA. Droperidol exerts dual effects on repolarization and induces early after-depolarizations and triggered activity in rabbit Purkinge fibers. *J Pharmacol Exp Ther.* 1993;266:884–893.
175. Drolet B, Zhang S, Deschenes D, et al. Droperidol lengthens cardiac repolarization due to block of the rapid component of the delayed rectifier potassium current. *J Cardiovasc Electrophysiol.* 1999;10:1597–1604.
176. Shiga T, Yong S, Carino J, Murray PA, Damron DS. Droperidol inhibits intracellular Ca^{2+}, myofilament Ca^{2+} sensitivity, and contraction in rat ventricular myocytes. *Anesthesiology.* 2005;102:1165–1173.
177. Bustamante R, Valverde A. Determination of a sedative dose and influence of droperidol and midazolam on cardiovascular function in pigs. *Can J Vet Res.* 1997;61:246–250.
178. Sugiyama A, Satoh Y, Hashimoto K. In vivo canine model comparison of cardiohemodynamic and electrophysiological effects of a new antipsychotic drug aripiprazole (OPC-14597) to haloperidol. *Toxicol Appl Pharmacol.* 2001;173:120–128.
179. Rasty S, Amin NB, Sabbah HN, Mishima T, Borzak S, Tisdale JE. Influence of i.v. haloperidol on ventricular repolarization and monophasic action potential duration in anesthetized dogs. *Chest.* 2004;125:1821–1829.
180. Bentley GA, Copeland IW. The effect of chronic haloperidol treatment on some cardiovascular parameters in cats. *Br J Pharmacol.* 1985;86:737–741.
181. Drici MD, Wang WX, Liu XK, Woosley RL, Flockhart DA. Prolongation of QT interval in isolated feline hearts by antipsychotic drugs. *J Clin Psychopharmacol.* 1998;18:477–481.
182. Huang ZQ, Shi GG, Zheng JH, Liu B. Effects of N-n-butyl haloperidol iodide on rat myocardial ischemia and reperfusion injury and L-type calcium current. *Acta Pharmacol Sin.* 2003;24:757–763.
183. van den Buuse M. Acute effects of antipsychotic drugs on cardiovascular responses to stress. *Eur J Pharmacol.* 2003;464:55–62.
184. Gepdiremen A, Aydin N, Halici Z, et al. Chronic treatment of haloperidol causes vasoconstriction on basilar arteries of rats, dose dependently. *Pharmacol Res.* 2004;50:569–574.
185. Bebarova M, Matejovic P, Pasek M, Novakova M. Effect of haloperidol on transient outward potassium current in rat ventricular myocytes. *Eur J Pharmacol.* 2006;550:15–23.
186. Ishida H, Hoshiai K, Hoshiai M, Genka C, Hirota Y, Nakazawa H. Haloperidol prolongs diastolic phase of ca(2+) transient in cardiac myocytes. *Jpn J Physiol.* 1999;49:479–484.
187. Hatip-Al-Khatib I, Bolukbasi-Hatip F. Modulation of the negative inotropic effect of haloperidol by drugs with positive inotropic effects in isolated rabbit heart. *Pharmacology.* 2002;66:19–25.
188. Maayani S, Wilkinson CW, Stollak JS. 5-hydroxytryptamine receptor in rabbit aorta: Characterization by butyrophenone analogs. *J Pharmacol Exp Ther.* 1984;229:346–350.
189. Hapke HJ, Holl C. Effects of dopamine on the coronary vessels of swine. *Dtsch Tierarztl Wochenschr.* 1992;99:66–69.
190. Lees P, Serrano L. Effects of azaperone on cardiovascular and respiratory functions in the horse. *Br J Pharmacol.* 1976;56:263–269.
191. Gregory NG, Wilkins LJ. Effect of azaperone on cardiovascular responsiveness in stress-sensitive pigs. *J Vet Pharmacol Ther.* 1986;9:164–170.
192. Pacher P, Kecskemeti V. Cardiovascular side effects of new antidepressants and antipsychotics: New drugs, old concerns? *Curr Pharm Des.* 2004;10:2463–2475.
193. Pacher P, Ungvari Z, Nanasi PP, Furst S, Kecskemeti V. Speculations on difference between tricyclic and selective serotonin reuptake inhibitor antidepressants on their cardiac effects. is there any? *Curr Med Chem.* 1999;6:469–480.
194. Pacher P, Kecskemeti V. Cardiovascular effects of selective serotonin reuptake inhibitor antidepressants. *Orv Hetil.* 2004;145:425–431.
195. Aubert M, Osterwalder R, Wagner B, et al. Evaluation of the rabbit Purkinge fibre assay as an in vitro tool for assessing the risk of drug-induced torsades de pointes in humans. *Drug Saf.* 2006;29:237–254.

196. Kobayashi T, Washiyama K, Ikeda K. Inhibition of G protein-activated inwardly rectifying K+ channels by various antidepressant drugs. *Neuropsychopharmacology.* 2004;29:1841–1851.
197. Gintant GA, Limberis JT, McDermott JS, Wegner CD, Cox BF. The canine Purkinge fiber: An in vitro model system for acquired long QT syndrome and drug-induced arrhythmogenesis. *J Cardiovasc Pharmacol.* 2001;37:607–618.
198. Bateman DN, Thanacoody HK, Waring WS. Digitalis intoxication induced by paroxetine co-administration. *Lancet.* 2006;368:1962–1963.
199. Fossa AA, Gorczyca W, Wisialowski T, et al. Electrical alternans and hemodynamics in the anesthetized guinea pig can discriminate the cardiac safety of antidepressants. *J Pharmacol Toxicol Methods.* 2007;55:78–85.
200. Isbister GK, Bowe SJ, Dawson A, Whyte IM. Relative toxicity of selective serotonin reuptake inhibitors (SSRIs) in overdose. *J Toxicol Clin Toxicol.* 2004;42:277–285.
201. Goodnick PJ, Jerry J, Parra F. Psychotropic drugs and the ECG: Focus on the QTc interval. *Expert Opin Pharmacother.* 2002;3:479–498.
202. Rasmussen SL, Overo KF, Tanghoj P. Cardiac safety of citalopram: Prospective trials and retrospective analyses. *J Clin Psychopharmacol.* 1999;19:407–415.
203. Hamplova-Peichlova J, Krusek J, Paclt I, Slavicek J, Lisa V, Vyskocil F. Citalopram inhibits L-type calcium channel current in rat cardiomyocytes in culture. *Physiol Res.* 2002;51:317–321.
204. Witchel HJ, Pabbathi VK, Hofmann G, Paul AA, Hancox JC. Inhibitory actions of the selective serotonin re-uptake inhibitor citalopram on HERG and ventricular L-type calcium currents. *FEBS Lett.* 2002;512:59–66.
205. Pacher P, Bagi Z, Lako-Futo Z, Ungvari Z, Nanasi PP, Kecskemeti V. Cardiac electrophysiological effects of citalopram in guinea pig papillary muscle comparison with clomipramine. *Gen Pharmacol.* 2000;34:17–23.
206. Maertens C, Droogmans G, Verbesselt R, Nilius B. Block of volume-regulated anion channels by selective serotonin reuptake inhibitors. *Naunyn Schmiedebergs Arch Pharmacol.* 2002;366:158–165.
207. Pousti A, Deemyad T, Malihi G. Mechanism of inhibitory effect of citalopram on isolated guinea-pig atria in relation to adenosine receptor. *Hum Psychopharmacol.* 2004;19:347–350.
208. Pousti A, Malihi G, Naghibi B. Effect of citalopram on ouabain-induced arrhythmia in isolated guinea-pig atria. *Hum Psychopharmacol.* 2003;18:121–124.
209. Degner D, Grohmann R, Kropp S, et al. Severe adverse drug reactions of antidepressants: Results of the german multicenter drug surveillance program AMSP. *Pharmacopsychiatry.* 2004;37 Suppl 1:S39–S45.
210. Wanstall JC, Fiore SA, Gambino A, Chess-Williams R. Potentiation of 5-hydroxytryptamine (5-HT) responses by a 5-HT uptake inhibitor in pulmonary and systemic vessels: Effects of exposing rats to hypoxia. *Naunyn Schmiedebergs Arch Pharmacol.* 2003;368:520–527.
211. Marcos E, Adnot S, Pham MH, et al. Serotonin transporter inhibitors protect against hypoxic pulmonary hypertension. *Am J Respir Crit Care Med.* 2003;168:487–493.
212. Barak Y, Swartz M, Levy D, Weizman R. Age-related differences in the side effect profile of citalopram. *Prog Neuropsychopharmacol Biol Psychiatry.* 2003;27:545–548.
213. Paclt I, Slavicek J, Dohnalova A, Kitzlerova E, Pisvejcova K. Electrocardiographic dose-dependent changes in prophylactic doses of dosulepine, lithium and citalopram. *Physiol Res.* 2003;52:311–317.
214. Slavicek J, Paclt I, Hamplova J, Kittnar O, Trefny Z, Horacek BM. Antidepressant drugs and heart electrical field. *Physiol Res.* 1998;47:297–300.
215. Lu HR, Vlaminckx E, Teisman A, Gallacher DJ. Choice of cardiac tissue plays an important role in the evaluation of drug-induced prolongation of the QT interval in vitro in rabbit. *J Pharmacol Toxicol Methods.* 2005;52:90–105.
216. Eckardt L, Breithardt G, Haverkamp W. Electrophysiologic characterization of the antipsychotic drug sertindole in a rabbit heart model of torsades de pointes: Low torsadogenic potential despite QT prolongation. *J Pharmacol Exp Ther.* 2002;300:64–71.
217. Drolet B, Rousseau G, Daleau P, Cardinal R, Simard C, Turgeon J. Pimozide (orap) prolongs cardiac repolarization by blocking the rapid component of the delayed rectifier potassium current in native cardiac myocytes. *J Cardiovasc Pharmacol Ther.* 2001;6:255–260.

218. Lee SY, Kim YJ, Kim KT, Choe H, Jo SH. Blockade of HERG human K+ channels and IKr of guinea-pig cardiomyocytes by the antipsychotic drug clozapine. *Br J Pharmacol.* 2006;148:499–509.
219. Gluais P, Bastide M, Caron J, Adamantidis M. Risperidone prolongs cardiac action potential through reduction of K+ currents in rabbit myocytes. *Eur J Pharmacol.* 2002;444:123–132.
220. Drolet B, Yang T, Daleau P, Roden DM, Turgeon J. Risperidone prolongs cardiac repolarization by blocking the rapid component of the delayed rectifier potassium current. *J Cardiovasc Pharmacol.* 2003;41:934–937.
221. Magyar J, Banyasz T, Bagi Z, et al. Electrophysiological effects of risperidone in mammalian cardiac cells. *Naunyn Schmiedebergs Arch Pharmacol.* 2002;366:350–356.
222. Biziere K, Worms P, Kan JP, Mandel P, Garattini S, Roncucci R. Minaprine, a new drug with antidepressant properties. *Drugs Exp Clin Res.* 1985;11:831–840.
223. Baizman ER, Ezrin AM, Ferrari RA, Luttinger D. Pharmacologic profile of fezolamine fumarate: A nontricyclic antidepressant in animal models. *J Pharmacol Exp Ther.* 1987;243:40–54.
224. Depin JC, Betbeder-Matibet A, Bonhomme Y, Muller AJ, Berthelon JJ. Pharmacology of lortalamine, a new potent non-tricyclic antidepressant. *Arzneimittelforschung.* 1985;35:1655–1662.
225. Ilback NG, Stalhandske T. Cardiovascular effects of xylazine recorded with telemetry in the dog. *J Vet Med A Physiol Pathol Clin Med.* 2003;50:479–483.
226. Allen DG, Downey RS. Echocardiographic assessment of cats anesthetized with xylazine-sodium pentobarbital. *Can J Comp Med.* 1983;47:281–283.
227. DeRossi R, Junqueira AL, Beretta MP. Analgesic and systemic effects of xylazine, lidocaine and their combination after subarachnoid administration in goats. *J S Afr Vet Assoc.* 2005;76:79–84.
228. Teng B, Muir WW, 3rd. Effects of xylazine on canine coronary artery vascular rings. *Am J Vet Res.* 2004;65:431–435.
229. van Woerkens LJ, Duncker DJ, Huigen RJ, van der Giessen WJ, Verdouw PD. Redistribution of cardiac output caused by opening of arteriovenous anastomoses by a combination of azaperone and metomidate. *Br J Anaesth.* 1990;65:393–399.
230. Orr JA, Manohar M, Will JA. Cardiopulmonary effects of the combination of neuroleptic azaperone and hypnotic metomidate in swine. *Am J Vet Res.* 1976;37:1305–1308.
231. Pypendop B, Verstegen J. Cardiorespiratory effects of a combination of medetomidine, midazolam, and butorphanol in dogs. *Am J Vet Res.* 1999;60:1148–1154.
232. Difilippo SM, Norberg PJ, Suson UD, Savino AM, Reim DA. A comparison of xylazine and medetomidine in an anesthetic combination in New Zealand white rabbits. *Contemp Top Lab Anim Sci.* 2004;43:32–34.
233. Kojima K, Nishimura R, Mutoh T, Hong SH, Mochizuki M, Sasaki N. Effects of medetomidine-midazolam, acepromazine-butorphanol, and midazolam-butorphanol on induction dose of thiopental and propofol and on cardiopulmonary changes in dogs. *Am J Vet Res.* 2002;63:1671–1679.
234. Kojima K, Nishimura R, Mutoh T, et al. Comparison of cardiopulmonary effects of medetomidine-midazolam, acepromazine-butorphanol and midazolam-butorphanol in dogs. *Zentralbl Veterinarmed A.* 1999;46:353–359.
235. Bettschart-Wolfensberger R, Bowen IM, Freeman SL, Weller R, Clarke KW. Medetomidine-ketamine anaesthesia induction followed by medetomidine-propofol in ponies: Infusion rates and cardiopulmonary side effects. *Equine Vet J.* 2003;35:308–313.
236. Henke J, Baumgartner C, Roltgen I, Eberspacher E, Erhardt W. Anaesthesia with midazolam/medetomidine/fentanyl in chinchillas (chinchilla lanigera) compared to anaesthesia with xylazine/ketamine and medetomidine/ketamine. *J Vet Med A Physiol Pathol Clin Med.* 2004;51:259–264.
237. Kushiro T, Yamashita K, Umar MA, et al. Anesthetic and cardiovascular effects of balanced anesthesia using constant rate infusion of midazolam-ketamine-medetomidine with inhalation of oxygen-sevoflurane (MKM-OS anesthesia) in horses. *J Vet Med Sci.* 2005;67:379–384.
238. Appleton GO, Li Y, Taffet GE, et al. Determinants of cardiac electrophysiological properties in mice. *J Interv Card Electrophysiol.* 2004;11:5–14.
239. Ingwersen W, Allen DG, Dyson DH, Black WD, Goldberg MT, Valliant AE. Cardiopulmonary effects of a ketamine/acepromazine combination in hypovolemic cats. *Can J Vet Res.* 1988;52:423–427.

240. Sumitra M, Manikandan P, Rao KV, Nayeem M, Manohar BM, Puvanakrishnan R. Cardiorespiratory effects of diazepam-ketamine, xylazine-ketamine and thiopentone anesthesia in male Wistar rats - a comparative analysis. *Life Sci.* 2004;75:1887–1896.
241. Saha DC, Saha AC, Malik G, Astiz ME, Rackow EC. Comparison of cardiovascular effects of tiletamine-zolazepam, pentobarbital, and ketamine-xylazine in male rats. *J Am Assoc Lab Anim Sci.* 2007;46:74–80.
242. Rodrigues SF, de Oliveira MA, Martins JO, et al. Differential effects of chloral hydrate- and ketamine/xylazine-induced anesthesia by the s.c. route. *Life Sci.* 2006;79:1630–1637.
243. Musizza B, Stefanovska A, McClintock PV, et al. Interactions between cardiac, respiratory and EEG-delta oscillations in rats during anaesthesia. *J Physiol.* 2007;580:315–326.
244. Kober F, Iltis I, Cozzone PJ, Bernard M. Cine-MRI assessment of cardiac function in mice anesthetized with ketamine/xylazine and isoflurane. *MAGMA.* 2004;17:157–161.
245. Kober F, Iltis I, Cozzone PJ, Bernard M. Myocardial blood flow mapping in mice using high-resolution spin labeling magnetic resonance imaging: Influence of ketamine/xylazine and isoflurane anesthesia. *Magn Reson Med.* 2005;53:601–606.
246. Schaefer A, Meyer GP, Brand B, Hilfiker-Kleiner D, Drexler H, Klein G. Effects of anesthesia on diastolic function in mice assessed by echocardiography. *Echocardiography.* 2005;22: 665–670.
247. Stypmann J, Engelen MA, Breithardt AK, et al. Doppler echocardiography and tissue doppler imaging in the healthy rabbit: Differences of cardiac function during awake and anaesthetised examination. *Int J Cardiol.* 2007;115:164–170.
248. Kerr CL, McDonell WN, Young SS. Cardiopulmonary effects of romifidine/ketamine or xylazine/ketamine when used for short duration anesthesia in the horse. *Can J Vet Res.* 2004;68:274–282.
249. Picavet MT, Gasthuys FM, Laevens HH, Watts SA. Cardiopulmonary effects of combined xylazine-guaiphenesin-ketamine infusion and extradural (inter-coccygeal lidocaine) anaesthesia in calves. *Vet Anaesth Analg.* 2004;31:11–19.
250. Newell SM, Ko JC, Ginn PE, et al. Effects of three sedative protocols on glomerular filtration rate in clinically normal dogs. *Am J Vet Res.* 1997;58:446–450.
251. Gross ME, Smith JA, Tranquilli WJ. Cardiorespiratory effects of combined midazolam and butorphanol in isoflurane-anesthetized cats. *Vet Surg.* 1993;22:159–162.
252. Hexeberg E, Hexeberg S, Hessevik I, Fosse RT. Midazolam in combination with fentanyl/fluanisone and nitrous oxide as anaesthesia in rabbits - cardiovascular parameters. *Lab Anim.* 1995;29:400–406.
253. Schauvliege S, Narine K, Bouchez S, et al. Refined anaesthesia for implantation of engineered experimental aortic valves in the pulmonary artery using a right heart bypass in sheep. *Lab Anim.* 2006;40:341–352.
254. Dyson DH, Allen DG, Ingwersen W, Pascoe PJ. Evaluation of acepromazine/meperidine/atropine premedication followed by thiopental anesthesia in the cat. *Can J Vet Res.* 1988;52:419–422.
255. Liehmann L, Mosing M, Auer U. A comparison of cardiorespiratory variables during isoflurane-fentanyl and propofol-fentanyl anaesthesia for surgery in injured cats. *Vet Anaesth Analg.* 2006;33:158–168.
256. Hellyer P, Muir WW, 3rd, Hubbell JA, Sally J. Cardiorespiratory effects of the intravenous administration of tiletamine-zolazepam to dogs. *Vet Surg.* 1989;18:160–165.
257. Natalini CC, Alves SD, Guedes AG, Polydoro AS, Brondani JT, Bopp S. Epidural administration of tiletamine/zolazepam in horses. *Vet Anaesth Analg.* 2004;31:79–85.
258. Jacobson C. A novel anaesthetic regimen for surgical procedures in guinea pigs. *Lab Anim.* 2001;35:271–276.
259. Foxall G, McCahon R, Lamb J, Hardman JG, Bedforth NM. Levobupivacaine-induced seizures and cardiovascular collapse treated with intralipid. *Anaesthesia.* 2007;62:516–518.
260. Newton DJ, McLeod GA, Khan F, Belch JJ. Mechanisms influencing the vasoactive effects of lidocaine in human skin. *Anaesthesia.* 2007;62:146–150.
261. Gerhardt MA, Gunka VB, Miller RJ. Hemodynamic stability during labor and delivery with continuous epidural infusion. *J Am Osteopath Assoc.* 2006;106:692–698.

262. Braun C, Hofmeister EH, Lockwood AA, Parfitt SL. Effects of diazepam or lidocaine premedication on propofol induction and cardiovascular parameters in dogs. *J Am Anim Hosp Assoc.* 2007;43:8–12.
263. Persson F, Andersson B, Duker G, Jacobson I, Carlsson L. Functional effects of the late sodium current inhibition by AZD7009 and lidocaine in rabbit isolated atrial and ventricular tissue and Purkinge fibre. *Eur J Pharmacol.* 2007;558:133–143.
264. Stehr SN, Ziegeler JC, Pexa A, et al. The effects of lipid infusion on myocardial function and bioenergetics in l-bupivacaine toxicity in the isolated rat heart. *Anesth Analg.* 2007;104:186–192.
265. Hersh EV, Giannakopoulos H, Levin LM, et al. The pharmacokinetics and cardiovascular effects of high-dose articaine with 1:100,000 and 1:200,000 epinephrine. *J Am Dent Assoc.* 2006;137:1562–1571.
266. Royse CF, Royse AG. The myocardial and vascular effects of bupivacaine, levobupivacaine, and ropivacaine using pressure volume loops. *Anesth Analg.* 2005;101:679–687, table of contents.
267. Chang KS, Morrow DR, Kuzume K, Andresen MC. Bupivacaine inhibits baroreflex control of heart rate in conscious rats. *Anesthesiology.* 2000;92:197–207.
268. Borer LR, Peel JE, Seewald W, Schawalder P, Spreng DE. Effect of carprofen, etodolac, meloxicam, or butorphanol in dogs with induced acute synovitis. *Am J Vet Res.* 2003;64:1429–1437.
269. Scheiman JM, Tillner A, Pohl T, et al. Reduction of non-steroidal anti-inflammatory drug induced gastric injury and leucocyte endothelial adhesion by octreotide. *Gut.* 1997;40:720–725.
270. Jones MK, Wang H, Peskar BM, et al. Inhibition of angiogenesis by nonsteroidal anti-inflammatory drugs: Insight into mechanisms and implications for cancer growth and ulcer healing. *Nat Med.* 1999;5:1418–1423.
271. Momma K, Takao A. Transplacental cardiovascular effects of four popular analgesics in rats. *Am J Obstet Gynecol.* 1990;162:1304–1310.
272. Cappon GD, Gupta U, Cook JC, Tassinari MS, Hurtt ME. Comparison of the developmental toxicity of aspirin in rabbits when administered throughout organogenesis or during sensitive windows of development. *Birth Defects Res B Dev Reprod Toxicol.* 2003;68:38–46.
273. Frendin JH, Bostrom IM, Kampa N, Eksell P, Haggstrom JU, Nyman GC. Effects of carprofen on renal function during medetomidine-propofol-isoflurane anesthesia in dogs. *Am J Vet Res.* 2006;67:1967–1973.
274. Hennan JK, Huang J, Barrett TD, et al. Effects of selective cyclooxygenase-2 inhibition on vascular responses and thrombosis in canine coronary arteries. *Circulation.* 2001;104:820–825.
275. Dubey K, Balani DK, Pillai KK. Potential adverse interaction between aspirin and lisinopril in hypertensive rats. *Hum Exp Toxicol.* 2003;22:143–147.
276. Grosfeld JL, Phelps TO, Jesseph JM. Effect of stress and aspirin on extrahepatic portal hypertension in rats. *J Pediatr Surg.* 1975;10:609–615.
277. Peter FW, Franken RJ, Wang WZ, et al. Effect of low dose aspirin on thrombus formation at arterial and venous microanastomoses and on the tissue microcirculation. *Plast Reconstr Surg.* 1997;99:1112–1121.
278. Vesvres MH, Doutremepuich F, Lalanne MC, Doutremepuich C. Effects of aspirin on embolization in an arterial model of laser-induced thrombus formation. *Haemostasis.* 1993;23:8–12.
279. Belougne-Malfatti E, Aguejouf O, Doutremepuich F, Belon P, Doutremepuich C. Combination of two doses of acetyl salicylic acid: Experimental study of arterial thrombosis. *Thromb Res.* 1998;90:215–221.
280. Napoli C, Aldini G, Wallace JL, et al. Efficacy and age-related effects of nitric oxide-releasing aspirin on experimental restenosis. *Proc Natl Acad Sci USA.* 2002;99:1689–1694.
281. Borgdorff P, Tangelder GJ, Paulus WJ. Cyclooxygenase-2 inhibitors enhance shear stress-induced platelet aggregation. *J Am Coll Cardiol.* 2006;48:817–823.
282. Wang D, Wang M, Cheng Y, Fitzgerald GA. Cardiovascular hazard and non-steroidal anti-inflammatory drugs. *Curr Opin Pharmacol.* 2005;5:204–210.
283. Gershlick AH, Syndercombe Court YD, Murday AJ, Lewis CT, Mills PG. Adverse effects of high dose aspirin on platelet adhesion to experimental autogenous vein grafts. *Cardiovasc Res.* 1985;19:770–776.

284. Debons AF, Fani K, Jimenez FA. Enhancement of experimental atherosclerosis by aspirin. *J Toxicol Environ Health.* 1981;8:899–906.
285. Cheng Y, Wang M, Yu Y, Lawson J, Funk CD, Fitzgerald GA. Cyclooxygenases, microsomal prostaglandin E synthase-1, and cardiovascular function. *J Clin Invest.* 2006;116:1391–1399.
286. Fosslien E. Cardiovascular complications of non-steroidal anti-inflammatory drugs. *Ann Clin Lab Sci.* 2005;35:347–385.
287. Vizi ES, Tuba Z, Maho S, et al. A new short-acting non-depolarizing muscle relaxant (SZ1677) without cardiovascular side-effects. *Acta Anaesthesiol Scand.* 2003;47:291–300.
288. Castillo-Zamora C, Lespron Mdel C, Nava-Ocampo AA. Similar preoperative hemodynamic response to pancuronium and rocuronium in high-risk cardiac surgical patients. *Minerva Anestesiol.* 2005;71:769–773.
289. Moore EW, Hunter JM. The new neuromuscular blocking agents: Do they offer any advantages? *Br J Anaesth.* 2001;87:912–925.
290. Kampe S, Krombach JW, Diefenbach C. Muscle relaxants. *Best Pract Res Clin Anaesthesiol.* 2003;17:137–146.
291. Cope TM, Hunter JM. Selecting neuromuscular-blocking drugs for elderly patients. *Drugs Aging.* 2003;20:125–140.
292. Plaud B, Marty J, Debaene B, et al. The cardiovascular effects of mivacurium in hypertensive patients. *Anesth Analg.* 2002;95:379–384, table of contents.
293. Fodale V, Santamaria LB. Laudanosine, an atracurium and cisatracurium metabolite. *Eur J Anaesthesiol.* 2002;19:466–473.
294. Jonsson M, Dabrowski M, Gurley DA, et al. Activation and inhibition of human muscular and neuronal nicotinic acetylcholine receptors by succinylcholine. *Anesthesiology.* 2006;104:724–733.
295. Robertson EN, Driessen JJ, Booij LH. Suxamethonium administration prolongs the duration of action of subsequent rocuronium. *Eur J Anaesthesiol.* 2004;21:734–737.
296. Heerdt PM, Kang R, The' A, Hashim M, Mook RJ, Jr, Savarese JJ. Cardiopulmonary effects of the novel neuromuscular blocking drug GW280430A (AV430A) in dogs. *Anesthesiology.* 2004;100:846–851.
297. Savarese JJ, Belmont MR, Hashim MA, et al. Preclinical pharmacology of GW280430A (AV430A) in the rhesus monkey and in the cat: A comparison with mivacurium. *Anesthesiology.* 2004;100:835–845.
298. Kastrup MR, Marsico FF, Ascoli FO, Becker T, Soares JH, Gomez de Segura IA. Neuromuscular blocking properties of atracurium during sevoflurane or propofol anaesthesia in dogs. *Vet Anaesth Analg.* 2005;32:222–227.
299. Igarashi A, Amagasa S, Horikawa H, Shirahata M. Vecuronium directly inhibits hypoxic neurotransmission of the rat carotid body. *Anesth Analg.* 2002;94:117–122, table of contents.
300. Gyermek L, Lee C, Cho YM, Nguyen N. Quaternary derivatives of granatanol diesters: Potent, ultrashort acting non-depolarizing neuromuscular relaxants. *Life Sci.* 2006;79:559–569.
301. Fazekas T, Krassoi I, Lengyel C, Varro A, Papp JG. Suppression of erythromycin-induced early after-depolarizations and torsades de pointes ventricular tachycardia by mexiletine. *Pacing Clin Electrophysiol.* 1998;21:147–150.
302. Roden DM. Torsade de pointes. *Clin Cardiol.* 1993;16:683–686.
303. Chiba K, Sugiyama A, Hagiwara T, Takahashi S, Takasuna K, Hashimoto K. In vivo experimental approach for the risk assessment of fluoroquinolone antibacterial agents-induced long QT syndrome. *Eur J Pharmacol.* 2004;486:189–200.
304. Hahm S, Dresner HS, Podwall D, et al. DNA biomarkers antecede semiquantitative anthracycline cardiomyopathy. *Cancer Invest.* 2003;21:53–67.
305. Kim C, Kim N, Joo H, et al. Modulation by melatonin of the cardiotoxic and antitumor activities of adriamycin. *J Cardiovasc Pharmacol.* 2005;46:200–210.
306. L'Ecuyer T, Sanjeev S, Thomas R, et al. DNA damage is an early event in doxorubicin-induced cardiac myocyte death. *Am J Physiol Heart Circ Physiol.* 2006;291:H1273–H1280.

Chapter 8
Naturally Occurring and Iatrogenic Animal Models of Valvular, Infectious, and Arrhythmic Cardiovascular Disease

Congenital Cardiac Defects, General Information

Most naturally occurring congenital cardiovascular entities found in humans have been identified in one or more species of animals but the utility of these naturally occurring models as research subjects is not well established. Many of the congenital diseases are associated with noncardiovascular defects and some of these may result in infertility, impotence, and other reproductive problems that preclude the breeding of these animals to obtain adequate numbers for research purposes. The advent of sophisticated genetic testing has made the identification of specific genes responsible for specific defects more practical, and this has led to the creation of specific transgenic animal models, knock-ins and knock-outs, that have advanced our understanding of both congenital defects and genetic predisposition for a variety of cardiovascular diseases.

The order of incidence of congenital cardiac defects diagnosed in all breeds of dogs is patent ductus arteriosus (PDA) > pulmonic stenosis (PS) > ventricular septal defect (VSD) > atrial septal defect (ASD) ≥ Tetralogy of Fallot > persistent right aortic arch > combined PS and PDA and a rare but nearly equal incidence of pericardial, arterial, and venous anomalies, mitral insufficiency, Ebstein's anomaly of the tricuspid valves, origin of both great vessels from the right ventricle, and partial anomalous pulmonary venous drainage into the right atrium.[1] Twenty-two of 52 dogs treated surgically for left-to-right shunting PDA were also found to have mitral valve regurgitation. Twenty-four of the 52 dogs (46.2%) had clinical signs of cardiac insufficiency and 56.3% had left atrial dilatation.[2] Boxer dogs exhibiting either a single congenital heart defect (53/105) or multiple defects (52/105) were included in a recent study. In these animals, ASD was most commonly diagnosed (56.2%), followed by mitral valve abnormalities (55.2%), and subaortic stenosis (SAS) (46.7%). Most of the dogs with ASD had a low intensity systolic murmur heard best at he left heart base, i.e., relative PS, while most of the SAS lesions were characterized by a high intensity murmur at the left base.[3]

Congenital cardiovascular disease has been reported in other species. Persistent left fourth aortic arch and VSD have been reported in chickens. A variety of intra cardiac anomalies have been reported in mice. VSDs have been found in rats, cattle,

D.R. Gross, *Animal Models in Cardiovascular Research*,
DOI: 10.1007/978-0-387-95962-7_8, © Springer Science + Business Media, LLC 2009

and horses; vestigial pulmonary artery and retro esophageal right subclavian artery in rabbits; endocardial fibroelastosis in cats; and a strain of miniature pigs has been diagnosed with hypoplastic left heart. Tricuspid atresia, congenital aortic valvular insufficiency, and supravalvular aortic stenosis have all been reported in foals.[1,4] Cor triatriatum sinister (CTS) characterized by partition of the left atrium and turbulent blood flow within the left atrium was diagnosed in a 5-month-old cat.[5] A similar lesion was found in a 3-year-old cat with a perforate membrane immediately above the mitral valve dividing the left atrium into proximal and distal chambers resulting in a functional supravalvular mitral stenosis. This lesion was not classified as CTS because the dividing membrane did not connect to the distal left atrial chamber.[6] Color Doppler echocardiography was used in 51 cats to characterize a localized, turbulent systolic jet located in the right ventricular outflow tract and originating just cranial to the tricuspid valve. There was systolic apposition of the RV free wall with the interventricular septum at the origin of the turbulent jets. The authors named this condition as "dynamic right ventricular obstruction".[7] Pulmonic stenosis (PS) and a more rare combination of PS and tricuspid valve dysplasia have been reported in cats.[8]

Genetically Engineered Models, General Information

Although the differences between mouse and human hearts are significant, the relative ease with which specifically engineered models can be created has resulted in an explosion of their use in cardiovascular research. Standard transgenic mice are created by random insertion of wild-type or mutated-type DNA from the transgene of interest into the mouse chromosomes, along with a promoter that determines the age and organ in which the inserted protein is overexpressed. The technique has limitations. The original gene remains in the system. The expression pattern of the transgene is different than the expression pattern of the native gene so when the transgene is overexpressed the animal must adjust by up- or downregulating other systems to maintain homeostasis. These adjustments can lead to spurious phenotypes. Finally, the overexpression of wild-type or mutated-type proteins can significantly mask other proteins or be directly toxic. An example of this toxicity is the dilated cardiomyopathy associated with the over expression of green fluorescent protein (GFP).[9]

Knock-out models are used to study cardiovascular diseases that have been associated with a partial or total loss of function of specific proteins. Knock-in models are used when the gene of interest can be identified and its expression pattern learned, then replaced with a related gene. This enables the study of subtle gene variations. It is also used to mimic human mutations leading to functional differences. The knock-out and knock-in techniques eliminate many of the problems associated with standard transgenic technology. The latter techniques use embryonic stem cells (ESC) produced from the inner cell mass of male blastocysts harvested after in vitro fertilization and culture. Most commonly these ESC are taken from SV129 mice and are homozygous for a dominant gene coding the agouti coat color.

Specific mutations are made in these ESC and the resultant cells are used to generate the transgenic mice.[9]

Knock-in mice can be generated using either single or double replacement strategies. The single technique introduces the DNA target construct into the ESC using an electric shock that makes the cell membranes leaky. Less than one per million of the cells thus exposed undergo homologous recombination that includes the desired gene or exon and an antibiotic resistant gene. The antibiotic resistant gene allows only those cells to grow in the presence of that antibiotic. PCR is used to confirm that the desired mutation is present. The antibiotic resistance is then removed by encoding cre recombinase into the ESC or by mating the mice with a transgenic mouse that expresses cre recombinase. The double replacement strategy involves removing the wild-type gene with a targeting vector and introducing the mutant gene with a second targeting vector. Another method uses recombinase-mediated cassette exchange to replace the second homologous recombination step. This is a very efficient way to replace the antibiotic resistance cassette with the mutant-type gene. ESC heterozygotes are expanded and usually injected into blastocysts from C57BL/6 mice with black hair coats. The injected blastocysts are implanted into pseudopregnant females. The chimeric offspring derived from a combination of the dominant agouti and black hair coat color are identified by their patchy hair coat coloring. The male chimeras are mated with female C57BL/6 mice and the germ-line of the ESC-derived sperm is identified by offspring with the agouti coat color. Heterozygous male and female mice are mated to yield homozygous mutant mice.[9]

Naturally Occurring Models of Valvular Disease

Angiectasis in the subendothelium of heart valves has been reported in many species including cattle, dogs, pigs, and mice. An incidence of 29.8% has been reported on the AV valves, predominately on the septal cusp of the tricuspid valve, in apparently normal 10–40-week-old Sprague–Dawley rats. These angiectases were single or multiple blood-filled dilatations, lined by endothelial cells, and ranging from 40 to 300 μm in diameter.[10]

Myxomatous degeneration of the mitral valve is the most common cardiac disease in dogs and rupture of the chordae tendinea is a potential complication. A 2007 study reported a 16.1% incidence of ruptured chordae tendinea (114/706), and/or mitral valve prolapse. A majority of the ruptured chordae cases are associated with severe mitral regurgitation (MR).[11,12] Structural change in the valves of dogs is characterized by interstitial cells becoming a mixture of myofibroblast and smooth muscle cells with a closer association between interstitial and endothelial cells. Cavalier King Charles Spaniels (Cavaliers) are predisposed to this disease and most of the affected individuals develop mitral valve disease prior to 10 years of age. This indicates a genetic predisposition. However, all breeds of dogs, including mixed breeds, can develop this disease and it is more prevalent in aged animals.[13–18]

Chronic MR leading to systolic dysfunction has been documented in experimental animal models and is frequently diagnosed clinically in pet dogs. Naturally occurring systolic dysfunction seems to be significantly less common in the smaller breeds of dogs even though mitral valve disease is more common in the smaller breeds. Mitral regurgitation accompanied by systolic dysfunction is more commonly diagnosed in the larger breeds. The smaller breeds seem to be able to compensate with left ventricular hypertrophy sufficient to avoid systolic dysfunction.[19,20] There is a classification scheme for heart failure in small animals (dogs and cats) devised by the International Small Animal Cardiac Health Council (ISACHC). The severity and prevalence of pulmonary hypertension associated with mitral valve disease increases in animals at higher ISACHC classifications. Pulmonary hypertension was diagnosed, from echocardiography-derived data, in 13.9% of dogs with mitral valve disease (86/617).[21] Dogs with naturally occurring tricuspid regurgitation (TR) have decreased right ventricular function correlated with the severity of the TR.[22]

Unlike humans Cavaliers with varying degrees of MR did not have increased plasma concentrations of asymmetric dimethylarginine (ADMA).[23] Plasma circulating levels of insulin-like growth factor-1 (IGF-1) are not altered before development of congestive heart failure (CHF) in dogs with naturally occurring MR.[24] Cavaliers with moderate to severe MR and dogs with SAS had longer closure times and a lower percentage of the largest von Willebrand factor multimers than control dogs indicating possible platelet dysfunction associated with the high shear rates of significant turbulent flow.[25] Dogs with myxomatous mitral valve disease demonstrate significant narrowing and atherosclerotic-like lesions of myocardial, pulmonary, and renal arterial vessels.[26] Dogs with mitral endocardiosis have an increase in antioxidant reactivity as determined by the ferric reducing ability of the plasma although measuring total antioxidant activity does not reflect this.[27] Forty-seven dogs with both physical and echocardiographic evidence of chronic valve disease had significantly increased concentrations of C-reactive protein when compared to 20 normal control dogs.[28]

In a recent study, heart murmurs were detected in 22 of 103 overtly healthy cats. Echocardiography was performed in 7 of the 22 but only one of the seven examined was diagnosed with valvular disease.[29]

Congenital cardiovascular abnormalities can be induced by homocysteine. Some of these homocysteine-induced abnormalities are also associated with the overexpression of human receptor-interacting serine-threonine kinase-3 (hRIP3).[30] Angiogenesis is a common finding in several types of cardiac valve disease. Chondromodulin-I apparently plays an important role in maintaining normal valvular form and function by preventing angiogenesis.[31] Anterior leaflets of mitral valves were compared from four dogs with myxomatous degeneration and four normal control dogs. The dogs with chronic mitral valve disease demonstrated, by a ≥2-fold difference, the upregulation of 159 transcripts and the downregulation of 70 transcripts when compared to the controls. A total of 152 different genes were specifically identified. The upregulated genes represented pathways involving cell signaling, inflammation, extracellular matrix, immune function, cell defense, and metabolism. Inflammatory cytokine pathways and the serotonin-transforming growth factor-β pathway seemed to be contributing to the pathology of the tissues.[32]

There are many naturally occurring infectious agents and other noxious substances that can result in valvular endocardiosis and myocarditis. Valvular lesions can also result from neoplasia or migrating larval forms of parasites. An example of this is found in aged horses where migrating *Strongyle* sp. larvae can cause aortic insufficiency. Heartworm disease, caused by the presence of adult *Dirofilaria immitis* in the right heart and pulmonary circulation, is characterized by pulmonary hypertension, right ventricular hypertrophy, and eventual right heart failure and is often accompanied by a functional mitral stenosis and/or regurgitation.[1]

Iatrogenic Models of Valvular Disease

A number of surgical techniques, both open and closed, have been used to create valvular pathology. Usually dogs or sheep are used as models for size considerations. Mitral insufficiency was created by cutting one or more chordae tendinea, usually of the free wall cusp, either by direct visualization during cardiopulmonary bypass or by using a special instrument inserted through the left ventricular apex and guiding the instrument by a finger inserted through the left atrium.[1,33–35] Tricuspid regurgitation was created percutaneously using a guide-wire loop to create papillary muscle avulsion in sheep.[36]

Ligation of coronary vessels supplying a large portion of the posterior left ventricular free wall of sheep cause asymmetric annular dilation of the mitral valve, a lack of coordination of papillary muscle relationships to the valve and almost immediate MR. When small posterior infarctions are created that include the posterior papillary muscle, MR develops more slowly as a result of annular and ventricular dilatation as the ventricle remodels.[37,38] When sheep were treated with the topical application of phenol to obliterate the anterior annular and leaflet muscles, there was dilatation of the mitral annulus in the intercommissural dimension with displacement of the anterior papillary muscle tip toward the annulus. However, these changes did not result in MR. MR, apparently, requires dilatation of the mitral annulus in the septolateral axis.[39]

Several techniques have been used to create aortic and/or pulmonary valve pathologies. Regurgitation has been created in rabbits by perforating the valve leaflets.[1] Similar surgical techniques were used in rats to create aortic valve regurgitation (AR). A somewhat surprising result of these studies was that female rats develop more left ventricular remodeling in response to the chronic AR than males.[40] Aortic stenosis has been accomplished by direct suturing or clipping of the aortic leaflets, plication of the noncoronary cusp, suturing small rolls of Teflon felt, covered with autologous pericardium into the sinuses of Valsalva below the coronary orifices. Aortic and pulmonary valve cusps can also be cauterized with silver nitrate sticks.[1] Supracoronary banding of the aorta has been used to simulate aortic stenosis in sheep and many other species.[1,4,41]

Rapid atrial or ventricular pacing can be used in many different species to create a model of cardiomyopathy. A significant number of these animals will also develop mitral annular dilatation and regurgitation.[42,43]

A number of transgenic mouse models have been shown to develop cardiac valve disease. Serotonin (5-hydroxytryptamine; 5-HT) overproduction is known to be responsible for cardiac valvular disease in patients with carcinoid neoplasias. The 5-HT transporter (5-HTT) is responsible for 5-HT uptake. 5-HTT-deficient mice (5-HTT$^{-/-}$) develop valvular pathologies along with other structural and/or functional cardiac abnormalities.[44] Twenty-four low-density lipoprotein receptor-deficient apolipoprotein B-100-only (LDLr$^{-/-}$ ApoB$^{100/100}$) mice were fed a standard mouse chow. At age 20.8 ± 0.9 months, these older animals were hypercholesterolemic with calcification and oxidative stress evident in the aortic valves accompanied by functional valvular disease.[45] Aortic valves of younger Apolipoprotein E-deficient mice, 30 weeks old, were compared to wild-type controls. The valves were thickened, contained macrophages and showed early dysfunction, the latter detected by MRI.[46] Fibulin-4 knockdown mice with a hypomorphic expression allele from a targeted disruption of the adjacent Mus81 endonuclease gene resulted in demonstrated dilation of the ascending aorta, a tortuous and stiffened aorta, and thickened aortic valvular leaflets associated with aortic valve stenosis and regurgitation. Some of these had aortic aneurysms.[47] Both wild-type and low-density lipoprotein receptor-deficient (LDLr$^{-/-}$) mice fed a high-fat/high carbohydrate diet demonstrate smaller aortic valve areas, high transvalvular velocities, and thicker valve leaflets infiltrated with lipids and macrophages. The lesions were more serious in the LDLr$^{-/-}$ mice.[48]

Spontaneously hypertensive rats eventually develop left ventricular hypertrophy, subendocardial fibrosis, and low ejection fractions. Aortic valve regurgitation is often associated with these lesions.[49]

Infectious Cardiovascular Disease

Bartonella sp

Infectious valvulitis, most commonly of the aortic valve, was diagnosed in human patients, 66% of whom had a history of contact with cats. *Bartonella henselae* was implicated.[50]

Borrelia sp

Intraperitoneal inoculation of 3-day-old Lewis rats, DC-1 mice, Syrian hamsters and 3-week-old American Dutch rabbits with *Borrelia burgdorferi* results in multisystemic infection characterized by arthritis and myocarditis. Pathogenicity is modulated by species and by the in vitro passage history of this spirochete that is responsible for Lyme disease.[51] *Borrelia burgdorferi sensu stricto* (B31, JD-1, 910255, and N40) were incorporated into *Ixodes scapularis* ticks. The ticks were then used to transmit the infection to mice. The mice developed subacute, multifocal, necrotizing myocarditis 6–18 weeks after tick infestation with the highest incidence

of lesions occurring 12 weeks after tick bite. The animals also developed concurrent urinary cystitis and arthritis.[52] *Borrelia burgdorferi sensu stricto* was recovered from 71.5% and 26.6% of specimens from mice infected with RST1 and RST3 isolates, respectively. Histological scores for both myocarditis and arthritis were significantly higher after 2 weeks of infection in mice infected with RST1 isolates than in mice infected with the RST3 isolates. The RST1 genotype is genetically homogeneous and could represent an evolved clonal lineage that is highly pathogenic in both humans and animals.[53] Nineteen grivet monkeys (*Cercopithecus aethiops*) were injected with the spirochete of louse-borne relapsing fever, *Borrelia recurrentis*. All developed histiocytic myocarditis. The monkeys also had multiple microabscesses replacing the nodular white pulp of the spleen and hepatitis with foci of midzonal necrosis.[54]

Coxsackievirus sp

Coxsackievirus B-3 (CVB-3) infections in BALB/c mice result in myocardial damage characterized by cardiomyocyte apoptosis. Viral replication in the cardiomyocytes seems to be responsible for some of the pathology in the early stages of disease.[55–58] The murine models of CVB-3-induced myocarditis seem to indicate that this infection initiates autoimmunity reactions and the substances released into the blood stream from these responses are the primary agents of myocardial and other tissue injury.[59,60] Inoculation of 25-day old male C3H/HeJ mice with either infectious or inactivated coxsackievirus B-2, followed 3 days later by inoculation with a myocarditic variant of CVB-3, resulted in a more intense myocardial inflammatory reaction and resultant tissue damage than was seen in age-matched mice inoculated with CVB-3 alone.[61] Following infection of BALB/c mice with either a mild strain of CVB3 (the Nancy strain) or a severe strain (the Woodruff strain) coronary flow reserve was reduced in proportion to the severity of the resulting myocarditis. Low coronary flow reserve was associated with progressive heart failure, an indication that coronary flow deficit may be a determinant of adverse outcomes in this disease.[56] CVB-3 injected into *Papio papio* (baboons) caused delayed hypersensitivity and myocarditis.[62]

Keshan disease is an endemic CVB-induced cardiomyopathy not infrequently seen in China. Selenium-deficient mice were more susceptible to the cardiopathologic effects of CVB3 and a normally benign strain of CVB3 becomes virulent in selenium-deficient mice. CVB4, isolated from a Keshan disease patient, resulted in greater damage to the myocardium when injected into selenium-deficient mice compared to mice with normal levels of selenium.[63,64]

Diphtheritic Myocarditis

Diphtheritic toxin was injected into the connective tissue of the anterior mediastinum of mice. The animals developed myocarditis along with significant lesions in the associated regional lymph nodes.[65]

Encephalomyocarditis Virus

Cyclosporine treatment did not have any effect on the development or progression of myocardial histopathology in 8-week-old DBA-2 mice inoculated with the encephalomyocarditis virus. All inoculated mice developed congestive cardiomyopathy pathologically similar to that seen in man.[66]

Autoimmune Myocarditis

The human HLA-DQ8 molecule was transfected into healthy HLA-DQ8 (+) RAG-$1^{-/-}$ $mII^{-/-}$ nonobese diabetic mice using lymphocytes. The result was the development of autoimmune myocarditis characterized by lymphocytic infiltration into the myocardium, cardiac myocyte destruction, circulating IgG autoantibodies against cardiac myosin heavy chain, and death from heart failure. These experiments provide evidence that spontaneous autoimmune myocarditis can occur in the absence of an infection and that expression of HLA-DQ8 confers susceptibility.[67]

TNF-α is necessary for adhesion molecule expression and to recruit leukocytes to the sites of inflammation. Following infection with the encephalomyocarditis virus, the survival of TNF-$\alpha^{-/-}$ mice was significantly lower than that of TNF-$\alpha^{+/+}$ and the injection of recombinant TNF-α into TNF-$\alpha^{-/-}$ mice resulted in a dose-dependent improvement.[68] Similar results were obtained with angiotensin converting enzyme inhibitors and angiotensin Pi receptor antagonists using the same animal model.[69]

The intravenous injection of some liposomal drugs, diagnostic agents, micelles, and other lipid-based nanoparticles can result in acute hypersensitivity reactions. These reactions have been reproduced and studied in pigs, dogs, and rats. The pig seems to be the most sensitive model. Small doses of phospholipid can result in anaphylactic shock characterized by pulmonary hypertension, systemic hypotension, decreased cardiac output, and major cardiac arrhythmias. Pigs also display flushing and a rash. Dogs are almost as sensitive as pigs to the hemodynamic changes from phospholipid injections but dogs also react to micellar lipids. Their response includes leukopenia followed by leukocytosis, thrombocytopenia, and fluid excretions. Rats are relatively insensitive demonstrating only hypotensive responses to significantly higher doses of phospholipid.[70]

Infectious Complications Following Burn Injury

Adult C57 BL6 mice were burned over 40% of their total body surface area, treated with fluid therapy and then given intratracheal inoculations of either *Streptococcus pneumoniae* or *Klebsiella pneumoniae*. Hearts from these animals were examined for contractile function in the Langendorff preparation 24 h after the bacterial challenge. There were significant reductions in contractility and evidence of significant inflammatory cytokine responses.[71]

Arrhythmic Cardiovascular Disease

Naturally Occurring Cardiac Arrhythmias

Various conduction disturbances without gross malformations can be found in specific breeds of dogs. Sinoatrial syncope is most commonly seen in Miniature Schnauzers. Jervelle and Lange-Nielsen syndrome characterized by prolonged Q-T intervals has been reported in Dalmatian dogs also afflicted with congenital deafness and in Harlequin Great Danes.[1] The Jervelle and Lange-Nielsen syndrome is a genetically heterogeneous inherited arrhythmia characterized by Q-T prolongation, abnormal T waves, syncope, seizures, and sudden death from ventricular arrhythmias including polymorphic ventricular tachycardias (VTs), torsades de pointes, and ventricular fibrillation. Malignant arrhythmias can be provoked in these animals by exercise, stress, or sleep.[9]

Twenty-four boxer dogs with right ventricular cardiomyopathy were included in a study to evaluate the effectiveness of fish oil, flax oil, or sunflower oil in reducing ventricular arrhythmias. Dogs with more than 95 ventricular premature contractions per 24 h were included in the study.[72] Four cases of endocardiosis of the mitral valve and complete AV block in dogs were examined for histological changes in the cardiac conduction system. Moderate to severe reduction of the conduction fibers due to fibrous or fibro-fatty replacement was found in the penetrating and branching portions of the AV bundle. There were also degenerative and fibrotic lesions in the upper portions of the left and right bundle branches.[12] Dogs with chronic MR and with CHF demonstrate structural remodeling of the atria accompanied by altered conduction leading to atrial fibrillation characterized by a stable high-frequency area from which the arrhythmia is initiated. Dogs with predominantly shortened refractoriness, without significant conduction abnormalities, demonstrate atrial fibrillation characterized by multiple high-frequency areas and multiple wavelets.[73] Marked degeneration and fibrous replacement of the AV conduction system were found in 13 cats with hypertrophic cardiomyopathy and complete AV block.[74]

Iatrogenic Cardiac Arrhythmias

Pigs are increasingly used as models of ventricular fibrillation for a variety of studies usually related to defibrillator development, design, and use. Two fibrillation induction techniques are most common, electrical induction and ischemic induction. The latter is usually accomplished in the closed-chest pig with balloon occlusion of the mid-left anterior descending coronary artery. Resuscitation from ischemic ventricular fibrillation is more difficult than from electrically induced fibrillation, and usually requires frequent refibrillation, the need to use a greater number of counter shocks, the need for higher doses of epinephrine during resuscitation, profound cardiac dysfunction, and a short-time survival rate that approaches that found in clinical

experience with human patients.[75] Rabbits are also used as models of electrical induction of ventricular fibrillation.[76] Electrolyte disturbances produced by intravenous infusions of strophanthin-K, $CaCl_2$, and aconitine produce arrhythmias in guinea pigs and rats.[77] Ligation of the coronary vasculature in rats is commonly used for ventricular fibrillation studies.[78–80] Cardiac sympathetic nerve activity burst size increased before the onset of VT and/or ventricular fibrillation in a sheep coronary ligation model.[81] Spontaneously hypertensive rats are more susceptible to atrial tachyarrhythmias induced by burst pacing.[82]

Continuous rapid atrial pacing is used to induce sustained atrial fibrillation in pigs. It usually results in atrial interstitial fibrosis. Myocytes harvested from pigs following rapid atrial pacing demonstrate significantly larger Na^+/Ca^{2+} exchanger currents probably as a result of autonomic nervous system modulation.[83]

Structural remodeling of the atrial myocardium and atrial fibrillation in dogs is induced by rapid atrial pacing (400 bpm for 3–6 weeks) or rapid ventricular pacing (240 bpm for 2 weeks).[73,84] There are time-dependent, qualitatively different, and temporally evolving patterns of mRNA expression-changes associated with the duration of rapid atrial and ventricular pacing in dogs.[85] Intermittent rapid atrial pacing results in paroxysmal atrial tachycardia and fibrillation. Simultaneous activation of the autonomic nervous system apparently triggers this response.[86] Autonomic tone also plays a critical role in the initiation of paroxysmal atrial fibrillation since stimulation of the right ganglionated plexus, subthreshold for atrial excitation, will convert isolated premature depolarizations into depolarizations capable of inducing atrial fibrillation.[87]

Atrial fibrillation is a common finding with CHF and CHF is associated with atrial structural remodeling and fibrosis. In canine models of pacing-induced CHF, angiotensin converting enzyme receptor blockade reduces the amount of atrial fibrosis and decreases the incidence of atrial fibrillation. The atrial fibrosis seen with atrial fibrillation may be induced by an antagonistic regulation between angiotensin converting enzymes I and II.[88]

Transforming growth factor-β (TGF-β) also seems to play an important role since dogs with CHF have increased TGF-β expression and transgenic mouse models that overexpress TGF-β develop significant atrial fibrosis and atrial fibrillation but have normal appearing ventricular architecture and function.[43] TGF-β stimulates α-smooth muscle actin expression and this reaction can apparently, be attenuated by antioxidant/anti-inflammatory agents such as simvastatin.[89]

Sodium channel blocking agents, including many tricyclic antidepressants, decrease inotropy and prolong conduction times. When sodium channel blockers are administered to animals with myocardial ischemia, conduction times are more prolonged resulting in nonuniform conduction and re-entry arrhythmias such as VT.[90,91]

The α-subunit of $KvLGT_1$ and the β-subunit of minK coassemble to form the channels responsible for the slow component of the repolarizing delayed rectifier K^+ current in the human heart. The $KCNE_1$ gene codes for minK and the loss of function of this gene can cause both the autosomal dominant long Q-T syndrome and the more severe autosomal recessive form associated with Jervelle and Lange-Nielsen syndrome. Mice lacking minK were deaf but did not have Q-T prolongation or arrhythmias at baseline.

It was found that minK expression was restricted to cells of the cardiac conduction system thus explaining the absence of the long Q-T phenotype in the $minK^{-/-}$.[9] Transgenic mice overexpressing Kv1.1N206Tag in the heart have prolonged Q-T intervals and VT.[92] Repression of ether-a-go-go gene (ERG) by miR-133 in hearts of a diabetes model in rabbits appears to be responsible for the slowing of repolarization and Q-T prolongation via depression of the I_{Kr} channel.[93]

Gap junctions couple cardiac cells allowing electrical, ion, and chemical communication. Six connexin subunits form a hemi channel and two hemi channels span the intercellular space to form functional gap junctions. Over 20 connexin genes have been identified but only four are expressed in the mammalian heart, Cx30.2, Cx40, Cx43, and Cx45. Homozygous knock-in mice in which Cx45 was replaced by lacZ did not survive embryogenesis but heterozygous $Cx45^{lacZ/WT}$ had lacZ expressed in the AV node, His bundle, and bundle branches. Knock-in mice in which one Cx40 allele was replaced by GFP demonstrated expression in the atrium, AV node, and his-Purkinje system. Mice lacking Cx40 have conduction disease and atrial fibrillation. $Cx43^{-/-}$ mice die as neonates from right ventricular outflow obstruction while conditional cardiac-restricted Cx43 knock-outs have structurally normal hearts but develop ventricular arrhythmias and sudden death prior to 2 months of age. $Cx^{31/31}$ mice did not survive to adults because of right ventricular outflow tract stenosis. Forty percent of $Cx43^{32/32}$ mice survived to adulthood with a lesser degree of outflow obstruction than $Cx43^{-/-}$ mice. The hearts of $Cx43^{40/40}$ homozygotes were structurally normal but there was significant occurrence of premature ventricular contractions and atrioventricular dissociation.[9]

Kv1.5 encodes the rapidly activating, slowly inactivating 4-aminopyridine-sensitive (4-AP) inward K^+ ion current (I_{Kslow1}) in the mouse ventricle. When the Kv1.5 channel was replaced with Kv1.1 from rats, the mice lacked the I_{Kslow1} and had no Q-T prolongation following exposure to 4-AP. The long Q-T3 form of Q-T prolongation is caused by mutations in the cardiac Na^+ channel (SCN5A). These mutations disrupt inactivation and lead to prolongation of the inward current, action potential, and QTc. Knock-in mice with a mutation of SCN5A demonstrate increased peak and late Na^+ current. $SCN5A^{KPQ/WT}$ mice demonstrate polymorphic VT especially after sinus pauses or AV block. Stimulation of protein kinase C with phenylephrine reduces the late Na^+ current in cells isolated from the $SCN5A^{KPQ/WT}$ mice indicating that α-adrenergic activity may be antiarrhythmic in the long QT-3 syndrome. Some cases of Brugada syndrome, characterized by ST elevation, arrhythmias, and increased risk of sudden death are caused by mutations in the SCN5A gene that decrease the inward Na^+ current. Mutations in SCN5A also cause some inherited forms of conduction disease. $SCN5A^{-/WT}$ mice have decreased Na^+ current in cardiac myocytes, delayed intramyocardial and AV conduction, increased ventricular effective refractory period, and inducible re-entrant ventricular tachy-arrhythmias. Progressive conduction defects and fibrosis accompany aging in these animals. Cardiac myocytes from $SCN5A^{1798insD/WT}$ mice demonstrate decreased total inward Na^+ current, persistent late inward Na^+ current, prolonged action potentials, decreased action potential upstroke velocities, and early afterdepolarizations. Isolated hearts from these same animals had longer effective refractory periods and decreased transverse conduction velocities.[9]

The cardiac ryanodine receptor (RyR2) regulates calcium release from the sarcoplasmic reticulum (SR). Mutations in this receptor result in catecholamine-induced polymorphic ventricular tachy-arrhythmias exacerbated by exercise. $RyR2^{R4496C/WT}$ mice have bidirectional VT, polymorphic VT, and ventricular fibrillation (VF) in response to epinephrine and caffeine or exercise stress followed by epinephrine. These responses were not prevented by propranolol. Cardiac myocytes from these animals display delayed after-depolarizations and triggered activity following pacing or exposure to isoproterenol. Calstabin-2 stabilizes RyR2. Calstabin-2-deficient mice develop exercise-induced ventricular arrhythmias. Mice with the $RyR2^{R176Q/WT}$ mutation respond to epinephrine and caffeine stimulation by developing VT. Isoproterenol administered during programmed stimulation resulted in more frequent and longer VT episodes. Cardiomyocytes from these animals had increased spontaneous oscillations of cytoplasmic Ca^{2+}. The RyR2 R176Q mutation appears sufficient to cause catecholamine-induced polymorphic VT.[9]

Overexpression of the hyperpolarization-activation cyclic nucleotide-gated channel gene in cardiac myocytes can be used to induce automaticity.[94] Mouse lines carrying a targeted mutation of the homeodomain transcription factor Shox2 were used to demonstrate that this factor plays a critical role in the recruitment of the sinus venosus myocardium comprising the SA nodal region. Heterozygous animals did not exhibit obvious defects but homozygotes led to severe hypoplasia of the sinus venosus myocardium and embryonic death.[95]

References

1. Gross DR. Animal Models in Cardiovascular Research, 2nd Revised Edition. Boston, MA: Kluwer Academic; 1994.
2. Bureau S, Monnet E, Orton EC. Evaluation of survival rate and prognostic indicators for surgical treatment of left-to-right patent ductus arteriosus in dogs: 52 cases (1995–2003). *J Am Vet Med Assoc*. 2005;227:1794–1799.
3. Chetboul V, Trolle JM, Nicolle A, et al. Congenital heart diseases in the boxer dog: A retrospective study of 105 cases (1998–2005). *J Vet Med A Physiol Pathol Clin Med*. 2006;53:346–351.
4 Gross DR. Unpublished data.
5. Koie H, Sato T, Nakagawa H, Sakai T. Cor triatriatum sinister in a cat. *J Small Anim Pract*. 2000;41:128–131.
6. Fine DM, Tobias AH, Jacob KA. Supravalvular mitral stenosis in a cat. *J Am Anim Hosp Assoc*. 2002;38:403–406.
7. Rishniw M, Thomas WP. Dynamic right ventricular outflow obstruction: A new cause of systolic murmurs in cats. *J Vet Intern Med*. 2002;16:547–552.
8. Hopper BJ, Richardson JL, Irwin PJ. Pulmonic stenosis in two cats. *Aust Vet J*. 2004;82:143–148.
9. Nilles KM, London B. Knockin animal models of inherited arrhythmogenic diseases: What have we learned from them? *J Cardiovasc Electrophysiol*. 2007;18:1117–1125.
10. Fang H, Howroyd PC, Fletcher AM, et al. Atrioventricular valvular angiectasis in Sprague-Dawley rats. *Vet Pathol*. 2007;44:407–410.
11. Serres F, Chetboul V, Tissier R, et al. Chordae tendineae rupture in dogs with degenerative mitral valve disease: Prevalence, survival, and prognostic factors (114 cases, 2001–2006). *J Vet Intern Med*. 2007;21:258–264.

12. Kaneshige T, Machida N, Yamamoto S, Nakao S, Yamane Y. A histological study of the cardiac conduction system in canine cases of mitral valve endocardiosis with complete atrioventricular block. *J Comp Pathol*. 2007;136:120–126.
13. Black A, French AT, Dukes-McEwan J, Corcoran BM. Ultrastructural morphologic evaluation of the phenotype of valvular interstitial cells in dogs with myxomatous degeneration of the mitral valve. *Am J Vet Res*. 2005;66:1408–1414.
14. Tarnow I, Kristensen AT, Olsen LH, Pedersen HD. Assessment of changes in hemostatic markers in cavalier King Charles spaniels with myxomatous mitral valve disease. *Am J Vet Res*. 2004;65:1644–1652.
15. Tarnow I, Olsen LH, Jensen MB, Pedersen KM, Pedersen HD. Determinants of weak femoral artery pulse in dogs with mitral valve prolapse. *Res Vet Sci*. 2004;76:113–120.
16. Freeman LM, Rush JE, Markwell PJ. Effects of dietary modification in dogs with early chronic valvular disease. *J Vet Intern Med*. 2006;20:1116–1126.
17. Tou SP, Adin DB, Estrada AH. Echocardiographic estimation of systemic systolic blood pressure in dogs with mild mitral regurgitation. *J Vet Intern Med*. 2006;20:1127–1131.
18. Kanno N, Kuse H, Kawasaki M, Hara A, Kano R, Sasaki Y. Effects of pimobendan for mitral valve regurgitation in dogs. *J Vet Med Sci*. 2007;69:373–377.
19. Borgarelli M, Tarducci A, Zanatta R, Haggstrom J. Decreased systolic function and inadequate hypertrophy in large and small breed dogs with chronic mitral valve insufficiency. *J Vet Intern Med*. 2007;21:61–67.
20. Teshima K, Asano K, Iwanaga K, et al. Evaluation of left ventricular tei index (index of myocardial performance) in healthy dogs and dogs with mitral regurgitation. *J Vet Med Sci*. 2007;69:117–123.
21. Serres FJ, Chetboul V, Tissier R, et al. Doppler echocardiography-derived evidence of pulmonary arterial hypertension in dogs with degenerative mitral valve disease: 86 cases (2001–2005). *J Am Vet Med Assoc*. 2006;229:1772–1778.
22. Teshima K, Asano K, Iwanaga K, et al. Evaluation of right ventricular Tei index (index of myocardial performance) in healthy dogs and dogs with tricuspid regurgitation. *J Vet Med Sci*. 2006;68:1307–1313.
23. Pedersen LG, Tarnow I, Olsen LH, Teerlink T, Pedersen HD. Body size, but neither age nor asymptomatic mitral regurgitation, influences plasma concentrations of dimethylarginines in dogs. *Res Vet Sci*. 2006;80:336–342.
24. Pedersen HD, Falk T, Haggstrom J, et al. Circulating concentrations of insulin-like growth factor-1 in dogs with naturally occurring mitral regurgitation. *J Vet Intern Med*. 2005;19:528–532.
25. Tarnow I, Kristensen AT, Olsen LH, et al. Dogs with heart diseases causing turbulent high-velocity blood flow have changes in platelet function and von Willebrand factor multimer distribution. *J Vet Intern Med*. 2005;19:515–522.
26. Falk T, Jonsson L, Olsen LH, Pedersen HD. Arteriosclerotic changes in the myocardium, lung, and kidney in dogs with chronic congestive heart failure and myxomatous mitral valve disease. *Cardiovasc Pathol*. 2006;15:185–193.
27. Hetyey CS, Manczur F, Dudas-Gyorki Z, et al. Plasma antioxidant capacity in dogs with naturally occurring heart diseases. *J Vet Med A Physiol Pathol Clin Med*. 2007;54:36–39.
28. Rush JE, Lee ND, Freeman LM, Brewer B. C-reactive protein concentration in dogs with chronic valvular disease. *J Vet Intern Med*. 2006;20:635–639.
29. Cote E, Manning AM, Emerson D, Laste NJ, Malakoff RL, Harpster NK. Assessment of the prevalence of heart murmurs in overtly healthy cats. *J Am Vet Med Assoc*. 2004;225:384–388.
30. Zhao L, Wang G, Lu D, et al. Homocysteine, hRIP3 and congenital cardiovascular malformations. *Anat Embryol (Berl)*. 2006;211:203–212.
31. Yoshioka M, Yuasa S, Matsumura K, et al. Chondromodulin-I maintains cardiac valvular function by preventing angiogenesis. *Nat Med*. 2006;12:1151–1159.
32. Oyama MA, Chittur SV. Genomic expression patterns of mitral valve tissues from dogs with degenerative mitral valve disease. *Am J Vet Res*. 2006;67:1307–1318.

33. Hankes GH, Ardell JL, Tallaj J, et al. Beta1-adrenoceptor blockade mitigates excessive norepinephrine release into cardiac interstitium in mitral regurgitation in dog. *Am J Physiol Heart Circ Physiol*. 2006;291:H147–H151.
34. Nakayama T, Nishijima Y, Miyamoto M, Hamlin RL. Effects of 4 classes of cardiovascular drugs on ventricular function in dogs with mitral regurgitation. *J Vet Intern Med*. 2007;21:445–450.
35. Bernal JM, Garcia I, Morales D, et al. The 'valve racket': A new and different concept of atrioventricular valve repair. *Eur J Cardiothorac Surg*. 2006;29:1026–1029.
36. Hoppe H, Pavcnik D, Chuter TA, et al. Percutaneous technique for creation of tricuspid regurgitation in an ovine model. *J Vasc Interv Radiol*. 2007;18:133–136.
37. Gorman JH, III, Gorman RC, Plappert T, et al. Infarct size and location determine development of mitral regurgitation in the sheep model. *J Thorac Cardiovasc Surg*. 1998;115:615–622.
38. Messas E, Bel A, Morichetti MC, et al. Autologous myoblast transplantation for chronic ischemic mitral regurgitation. *J Am Coll Cardiol*. 2006;47:2086–2093.
39. Green GR, Dagum P, Glasson JR, et al. Mitral annular dilatation and papillary muscle dislocation without mitral regurgitation in sheep. *Circulation.* 1999;100:II95–II102.
40. Drolet MC, Lachance D, Plante E, Roussel E, Couet J, Arsenault M. Gender-related differences in left ventricular remodeling in chronic severe aortic valve regurgitation in rats. *J Heart Valve Dis*. 2006;15:345–351.
41. Walther T, Schubert A, Wustmann T, et al. Reverse remodeling of cardiac collagen protein expression after surgical therapy for experimental aortic stenosis. *J Heart Valve Dis*. 2006;15:651–656.
42. Popovic ZB, Martin M, Fukamachi K, et al. Mitral annulus size links ventricular dilatation to functional mitral regurgitation. *J Am Soc Echocardiogr*. 2005;18:959–963.
43. Everett TH, IV, Olgin JE. Atrial fibrosis and the mechanisms of atrial fibrillation. *Heart Rhythm*. 2007;4:S24–S27.
44. Mekontso-Dessap A, Brouri F, Pascal O, et al. Deficiency of the 5-hydroxytryptamine transporter gene leads to cardiac fibrosis and valvulopathy in mice. *Circulation*. 2006;113:81–89.
45. Weiss RM, Ohashi M, Miller JD, Young SG, Heistad DD. Calcific aortic valve stenosis in old hypercholesterolemic mice. *Circulation*. 2006;114:2065–2069.
46. Aikawa E, Nahrendorf M, Sosnovik D, et al. Multimodality molecular imaging identifies proteolytic and osteogenic activities in early aortic valve disease. *Circulation*. 2007;115:377–386.
47. Hanada K, Vermeij M, Garinis GA, et al. Perturbations of vascular homeostasis and aortic valve abnormalities in fibulin-4 deficient mice. *Circ Res*. 2007;100:738–746.
48. Drolet MC, Roussel E, Deshaies Y, Couet J, Arsenault M. A high fat/high carbohydrate diet induces aortic valve disease in C57BL/6J mice. *J Am Coll Cardiol*. 2006;47:850–855.
49. Couet J, Gaudreau M, Lachance D, et al. Treatment of combined aortic regurgitation and systemic hypertension: Insights from an animal model study. *Am J Hypertens*. 2006;19:843–850.
50. Oteo JA, Castilla A, Arosey A, Blanco JR, Ibarra V, Morano LE. Endocarditis due to Bartonella spp. three new clinical cases and Spanish literature review. *Enferm Infecc Microbiol Clin.* 2006;24:297–301.
51. Moody KD, Barthold SW, Terwilliger GA. Lyme borreliosis in laboratory animals: Effect of host species and in vitro passage of borrelia burgdorferi. *Am J Trop Med Hyg*. 1990;43:87–92.
52. Zeidner NS, Schneider BS, Dolan MC, Piesman J. An analysis of spirochete load, strain, and pathology in a model of tick-transmitted Lyme borreliosis. *Vector Borne Zoonotic Dis*. 2001;1:35–44.
53. Wang G, Ojaimi C, Wu H, et al. Disease severity in a murine model of Lyme borreliosis is associated with the genotype of the infecting borrelia burgdorferi sensu stricto strain. *J Infect Dis*. 2002;186:782–791.
54. Judge DM, La Croix JT, Perine PL. Experimental louse-borne relapsing fever in the grivet monkey, cercopithecus aethiops. II. pathology. *Am J Trop Med Hyg.* 1974;23:962–968.
55. Saraste A, Arola A, Vuorinen T, et al. Cardiomyocyte apoptosis in experimental coxsackievirus B3 myocarditis. *Cardiovasc Pathol*. 2003;12:255–262.
56. Saraste A, Kyto V, Saraste M, Vuorinen T, Hartiala J, Saukko P. Coronary flow reserve and heart failure in experimental coxsackievirus myocarditis. A transthoracic Doppler echocardiography study. *Am J Physiol Heart Circ Physiol.* 2006;291:H871–H875.

57. Li J, Leschka S, Rutschow S, et al. Immunomodulation by interleukin-4 suppresses matrix metalloproteinases and improves cardiac function in murine myocarditis. *Eur J Pharmacol*. 2007;554:60–68.
58. Lee CK, Kono K, Haas E, et al. Characterization of an infectious cDNA copy of the genome of a naturally occurring, avirulent coxsackievirus B3 clinical isolate. *J Gen Virol*. 2005;86:197–210.
59. Leslie K, Blay R, Haisch C, Lodge A, Weller A, Huber S. Clinical and experimental aspects of viral myocarditis. *Clin Microbiol Rev*. 1989;2:191–203.
60. Anderson DR, Wilson JE, Carthy CM, Yang D, Kandolf R, McManus BM. Direct interactions of coxsackievirus B3 with immune cells in the splenic compartment of mice susceptible or resistant to myocarditis. *J Virol*. 1996;70:4632–4645.
61. Beck MA, Chapman NM, McManus BM, Mullican JC, Tracy S. Secondary enterovirus infection in the murine model of myocarditis. pathologic and immunologic aspects. *Am J Pathol.* 1990;136:669–681.
62. Paque RE, Gauntt CJ, Nealon TJ. Assessment of cell-mediated immunity against coxsackievirus B3-induced myocarditis in a primate model (Papio papio). *Infect Immun*. 1981;31:470–479.
63. Beck MA. Rapid genomic evolution of a non-virulent coxsackievirus B3 in selenium-deficient mice. *Biomed Environ Sci*. 1997;10:307–315.
64. Levander OA, Beck MA. Interacting nutritional and infectious etiologies of Keshan disease. Insights from Coxsackie virus B-induced myocarditis in mice deficient in selenium or vitamin E. *Biol Trace Elem Res.* 1997;56:5–21.
65. Zabejinski MM, Ivanova VV, Zaborov AM, Nasirov RA. New animal model of diphtheritic myocarditis. *Exp Toxicol Pathol*. 2000;52:67–70.
66. Monrad ES, Matsumori A, Murphy JC, Fox JG, Crumpacker CS, Abelmann WH. Therapy with cyclosporine in experimental murine myocarditis with encephalomyocarditis virus. *Circulation*. 1986;73:1058–1064.
67. Taylor JA, Havari E, McInerney MF, Bronson R, Wucherpfennig KW, Lipes MA. A spontaneous model for autoimmune myocarditis using the human MHC molecule HLA-DQ8. *J Immunol*. 2004;172:2651–2658.
68. Wada H, Saito K, Kanda T, et al. Tumor necrosis factor-alpha (TNF-alpha) plays a protective role in acute viralmyocarditis in mice: A study using mice lacking TNF-alpha. *Circulation*. 2001;103:743–749.
69. Godsel LM, Leon JS, Engman DM. Angiotensin converting enzyme inhibitors and angiotensin II receptor antagonists in experimental myocarditis. *Curr Pharm Des*. 2003;9:723–735.
70. Szebeni J, Alving CR, Rosivall L, et al. Animal models of complement-mediated hypersensitivity reactions to liposomes and other lipid-based nanoparticles. *J Liposome Res*. 2007;17:107–117.
71. Horton J, Maass D, White J, Sanders B. Effect of aspiration pneumonia-induced sepsis on postburn cardiac inflammation and function in mice. *Surg Infect (Larchmt)*. 2006;7:123–135.
72. Smith CE, Freeman LM, Rush JE, Cunningham SM, Biourge V. Omega-3 fatty acids in boxer dogs with arrhythmogenic right ventricular cardiomyopathy. *J Vet Intern Med*. 2007;21:265–273.
73. Everett TH, 4th, Wilson EE, Verheule S, Guerra JM, Foreman S, Olgin JE. Structural atrial remodeling alters the substrate and spatiotemporal organization of atrial fibrillation: A comparison in canine models of structural and electrical atrial remodeling. *Am J Physiol Heart Circ Physiol.* 2006;291:H2911–H2923.
74. Kaneshige T, Machida N, Itoh H, Yamane Y. The anatomical basis of complete atrioventricular block in cats with hypertrophic cardiomyopathy. *J Comp Pathol*. 2006;135:25–31.
75. Niemann JT, Rosborough JP, Youngquist S, Thomas J, Lewis RJ. Is all ventricular fibrillation the same? A comparison of ischemically induced with electrically induced ventricular fibrillation in a porcine cardiac arrest and resuscitation model. *Crit Care Med*. 2007;35:1356–1361.
76. Zhong JQ, Laurent G, So PP, Hu X, Hennan JK, Dorian P. Effects of rotigaptide, a gap junction modifier, on defibrillation energy and resuscitation from cardiac arrest in rabbits. *J Cardiovasc Pharmacol Ther*. 2007;12:69–77.
77. Spasov AA, Iezhitsa IN, Zhuravleva NV, Gurova NA, Sinolitskii MK, Voronin SP. Comparative study of the antiarrhythmic activity of l-, d- and dl-stereoisomers of potassium magnesium aspartate. *Eksp Klin Farmakol*. 2007;70:17–21.

78. Clements-Jewery H, Hearse DJ, Curtis MJ. Neutrophil ablation with anti-serum does not protect against phase 2 ventricular arrhythmias in anaesthetised rats with myocardial infarction. *Cardiovasc Res*. 2007;73:761–769.
79. Lorentzon M, Ramunddal T, Bollano E, Soussi B, Waagstein F, Omerovic E. In vivo effects of myocardial creatine depletion on left ventricular function, morphology, and energy metabolism - consequences in acute myocardial infarction. *J Card Fail*. 2007;13:230–237.
80. Fukushima S, Varela-Carver A, Coppen SR, et al. Direct intramyocardial but not intracoronary injection of bone marrow cells induces ventricular arrhythmias in a rat chronic ischemic heart failure model. *Circulation*. 2007;115:2254–2261.
81. Jardine DL, Charles CJ, Frampton CM, Richards AM. Cardiac sympathetic nerve activity and ventricular fibrillation during acute myocardial infarction in a conscious sheep model. *Am J Physiol Heart Circ Physiol*. 2007;293:H433–H439.
82. Choisy SC, Arberry LA, Hancox JC, James AF. Increased susceptibility to atrial tachyarrhythmia in spontaneously hypertensive rat hearts. *Hypertension*. 2007;49:498–505.
83. Wei SK, Ruknudin AM, Shou M, et al. Muscarinic modulation of the sodium-calcium exchanger in heart failure. *Circulation*. 2007;115:1225–1233.
84. Shiroshita-Takeshita A, Sakabe M, Haugan K, Hennan JK, Nattel S. Model-dependent effects of the gap junction conduction-enhancing antiarrhythmic peptide rotigaptide (ZP123) on experimental atrial fibrillation in dogs. *Circulation*. 2007;115:310–318.
85. Cardin S, Libby E, Pelletier P, et al. Contrasting gene expression profiles in two canine models of atrial fibrillation. *Circ Res*. 2007;100:425–433.
86. Chen PS, Tan AY. Autonomic nerve activity and atrial fibrillation. *Heart Rhythm*. 2007;4:S61–S64.
87. Zhou J, Scherlag BJ, Edwards J, Jackman WM, Lazzara R, Po SS. Gradients of atrial refractoriness and inducibility of atrial fibrillation due to stimulation of ganglionated plexi. *J Cardiovasc Electrophysiol*. 2007;18:83–90.
88. Pan CH, Lin JL, Lai LP, Chen CL, Stephen Huang SK, Lin CS. Downregulation of angiotensin converting enzyme II is associated with pacing-induced sustained atrial fibrillation. *FEBS Lett*. 2007;581:526–534.
89. Shiroshita-Takeshita A, Brundel BJ, Burstein B, et al. Effects of simvastatin on the development of the atrial fibrillation substrate in dogs with congestive heart failure. *Cardiovasc Res*. 2007;74:75–84.
90. Seger DL. A critical reconsideration of the clinical effects and treatment recommendations for sodium channel blocking drug cardiotoxicity. *Toxicol Rev*. 2006;25:283–296.
91. Tabo M, Kimura K, Ito S. Monophasic action potential in anaesthetized guinea pigs as a biomarker for prediction of liability for drug-induced delayed ventricular repolarization. *J Pharmacol Toxicol Methods*. 2007;55:254–261.
92. London B, Jeron A, Zhou J, et al. Long QT and ventricular arrhythmias in transgenic mice expressing the N terminus and first transmembrane segment of a voltage-gated potassium channel. *Proc Natl Acad Sci USA*. 1998;95:2926–2931.
93. Xiao J, Luo X, Lin H, et al. MicroRNA miR-133 represses HERG K + channel expression contributing to QT prolongation in diabetic hearts. *J Biol Chem*. 2007;282:12363–12367.
94. Zhou YF, Yang XJ, Li HX. Hyperpolarization-activated cyclic nucleotide-gated channel gene: The most possible therapeutic applications in the field of cardiac biological pacemakers. *Med Hypotheses*. 2007;69:541–544.
95. Blaschke RJ, Hahurij ND, Kuijper S, et al. Targeted mutation reveals essential functions of the homeodomain transcription factor Shox2 in sinoatrial and pacemaking development. *Circulation*. 2007;115:1830–1838.

Chapter 9
Iatrogenic Models of Ischemic Heart Disease

Ischemic heart disease is the most common cause of heart failure in humans. Ventricular dilation, hypertrophy, biochemical alterations, and edema formation are all consequences of the poor pumping capacity of the damaged myocardium. Two very different types of ischemia are studied. Global ischemia is associated with cardiac arrest usually iatrogenic during cardiopulmonary bypass surgery or from ventricular fibrillation although during the initial period of fibrillation coronary flow increases. Regional ischemia is associated with a localized myocardial infarction. The two types of ischemia differ significantly in their biochemical and electrophysiological characteristics.[1]

Global Ischemia

Surgically induced global ischemia in humans is usually accompanied by the use of cardioplegia formulations designed to minimize myocardial damage and much research has been directed at perfecting this protection. The insult is characterized by a relatively short duration of ischemia and is readily reversible when the aortic cross-clamp is removed and the myocardium is reperfused. Protective agents can be administered prior to, at the time of the induction of ischemia and/or during the ischemic insult. When global ischemia is the result of ventricular fibrillation or cardiac arrest, it is rarely possible to administer any kind of protective agent prior to the onset of injury. There is a considerable lack of experimental uniformity for the time of ischemia or for reperfusion prior to the various parameters of interest being monitored.[1]

Mice are used with increasing frequency to study global ischemia phenomena because of the ability to use specific knockout or knockin transgenic models. Isolated hearts from mice overexpressing catalase were perfused at constant flow (2.2 ml/min) for 30 min for equilibration. Flow was stopped for 20 min of ischemia and then the hearts were reperfused for 30 min at the same flow rate. The authors concluded that overexpressing catalase in endothelial cells only weakly protects the myocardium and vasculature from ischemia/reperfusion (I/R) injury but preserves

D.R. Gross, *Animal Models in Cardiovascular Research*,
DOI: 10.1007/978-0-387-95962-7_9, © Springer Science + Business Media, LLC 2009

the ability of the heart to respond to adrenergic stimulation.[2] Buffer-perfused hearts from apolipoprotein E/LDL receptor double knockout mice were equilibrated for 35 min, subjected to global ischemia for 35 min, and then reperfused for 30 min to study the effects of an endothelin antagonist.[3] A comparison of global I/R in young (2-4-month-old mice) and aged (16-18-month-old mice) was made. The isolated mouse hearts were subjected to 20 min of ischemia and 60 min of reperfusion. The insult resulted in more severe contractile impairment and cellular damage in the hearts from older animals.[4]

Isolated rat hearts have been used extensively to study the effects of global I/R. Isolated working hearts were subjected to 20 min of global ischemia prior to reperfusion.[5] In other studies isolated perfused rat hearts, not working, were made ischemic for 25 min, followed by 30 min of reperfusion.[6,7] Ikizler et al.[8] subjected Langendorff perfused isolated rat hearts to 120 min of arrest using crystalloid cardioplegia and then reperfused the hearts for 30 min to study the protective effects of trimetazidine an agent reported to protect against ischemia at the cellular level. Wischmeyer et al.[9] administered glutamine (alanine-glutamine dipeptide) to Sprague-Dawley rats 18 h before excising the hearts, perfusing them and then inducing global ischemia for 15 min and reperfusing for 60 min. Hearts from streptozotocin-induced diabetic rats were equilibrated and then subjected to 5 min of low-flow ischemia, 25 min of no-flow ischemia, and 30 min of reperfusion to study the effects of long-term treatment with glibenclamide on I/R injury in diabetes.[10] A similar diabetic rat model was used in an isolated heart preparation exposed to 30 min ischemia and 30 min reperfusion to study the role of translocation of protein kinase C during I/R injury.[11] The effects of dietary Magnesium restriction was studied on hearts isolated from Sprague-Dawley rats. These hearts were exposed to 40 min global ischemia and 30 min of reperfusion.[12]

The effects of resveratrol, a natural antioxidant found in grapes and red wine, were evaluated in Langendorff-perfused isolated rat hearts subjected to 60 min global ischemia and 60 min of reperfusion.[13] Dyck et al.[14] used an isolated working rat heart model in three different protocols, 60 min of aerobic perfusion, 30 min aerobic perfusion followed by 30 min of flow reduction to 35% of baseline, and 30 min aerobic perfusion, followed by 30 min of no-flow global ischemia, followed by 60 min of reperfusion to study the effects of malonyl coenzyme A decarboxylase inhibition. The effects of activating both neuronal ATP-sensitive K^+ channels and the extra neuronal monoamine transporter system were evaluated in isolated rat hearts subjected to 0.4 ml/min flow (low flow).[15]

Improving myocardial energy metabolism during 45 min of continuous normothermic global ischemia in isolated hearts from Japanese white rabbits appears to be cardioprotective.[16] Isolated isovolumic rabbit hearts were subjected to 15 min of global ischemia and 30 min of reperfusion to study “hyper contraction” a pheno menon that occurs at the beginning of reperfusion in stunned myocardium.[17]

Pigs are frequently used for myocardial I/R studies that more closely approximate the global ischemia experienced during cardiopulmonary bypass. Again the protocols for ischemia and reperfusion vary with the study. Castella et al.[18] subjected pigs to 30 min of normothermic global ischemia, followed by 30 min of aortic clamping

during either buffered or nonbuffered glutamate-aspartate-enriched blood cardioplegic solution infusion. Ischemic times ranging from 40 to 90 min to mimic the surgical experience have been used in our laboratory.[19-21] Newborn piglets were exposed to hypoxia by ventilation with 8% O_2 in nitrogen resulting in a hypoxic myocardial model. Myocardial damage was evaluated by measuring concentrations of cardiac troponin I in the blood of these animals.[22]

Regional Ischemia

It is essential that pump function be maintained during infarction or regional ischemia. A major effort in cardiovascular research has been, and still is, directed at the development of physical and/or pharmacological interventions to reduce infarct size, to assist the viable tissue in maintaining a normal level of contractile ability, to speed recovery of the damaged tissue, and to stimulate growth and/or regeneration of viable tissue. To accomplish these aims, it is essential that the model should mimic, as closely as possible, the clinical situation. Most experiments that have been conducted to evaluate tissue salvage and/or reduction of infarct size has assumed that, within the area of regional ischemia, tissue injury is heterogeneous with the most severely ischemic tissue in the core of the area affected. A "border zone" of intermediately injured tissue is presumed to exist around the severely injured core. This border zone is the target of most interventions. It appears that in many experimental models, particularly the acute infarction models, no such border zone exists. There is a sharp, but irregular transition, from normal to ischemic myocardium.[23] This absence of an area of intermediate injury is different from that seen in coronary artery disease in man and may pose a problem of applicability of acute infarction models in healthy animals.

Until recently the dog was the most commonly used animal model for coronary infarction and myocardial I/R injury studies but there seems to be little doubt that the pig coronary vascular system is more similar to that of man.[24] In the dog, the left circumflex coronary artery and left anterior descending (LAD) coronary artery each supply about 40% of the myocardium and the right coronary about 15%. In pigs, the right coronary and LAD are about equal and the left circumflex plays a relatively minor role, more similar to the situation in man.[1] There are also more similarities between man and the pig in intramural coronary artery branching patterns, coronary supply to the papillary muscles and to the nodal conduction tissues.[25,26] The dog has an extensive and recruitable coronary collateral system with 3-4 relatively large subepicardial collateral vessel anastomoses. Pigs have some small endocardial anastomoses between the right and left coronaries. Humans seem to fall somewhere between these two extremes, perhaps tending more toward the situation in pigs.[1] There is considerable evidence that a gradual narrowing of the coronary arteries is the greatest stimulus for formation of collaterals.[27] When the blood supply to one of the major coronary arteries is interrupted acutely in pigs, sheep, and rabbits, the anastomoses are generally not adequate to prevent necrosis and/or fatal ventricular arrhythmias.

In dogs, mice, and rats, a higher survivor rate is common following acute ligations.[1,28] The location of the coronary vasculature in rats and mice can be more subepicardial than epicardial making the exact identification of a specific coronary artery difficult. From a practical standpoint, acute ligation of the coronary vasculature is accomplished in these species by passing a suture through the myocardium in the general location of a coronary vessel and tightly ligating the entire area with the vessel included.[28]

Baboons have a coronary circulation very similar to humans, although the diagonal branches are grouped into a single "third primary" coronary. Acute coronary ligation in baboons results in a very well circumscribed lesion with a clearly defined edge and marked tissue changes. There is no apparent "border zone."[27] Diffuse myocardial necrosis and, on occasion, infarct-like lesions have been recorded in captured baboons without the presence of atherosclerotic coronary disease. These lesions are presumed to be endocrine/neurogenic from the stress and the massive catecholamine discharge, which the animals experienced during capture.[1]

Some very elaborate devices have been developed for creating coronary stenoses. These include a device with a hook-shaped stainless steel pressure plate and a silicone rubber-covered chromyl plunger bent to fit the pressure plate. To provide the flexibility needed for coronary arteries on a beating heart, the hook-shaped plate was silver soldered to a piece of 17 gauge thin-walled stainless steel tubing approximately 12 in. long. The upper end of the tubing was silver soldered into a collar rigidly fixed into a lucite mounting block with a setscrew. The chromyl plunger is freely movable within the thin wall tubing and is silver soldered to a second, spring-loaded metal collar that maintains a constant pressure against the spindle of the micrometer. The device is designed to create a linear compression of the cross-sectional area. There is also a direct drive lever included in this device that fully occludes the vessel when manually depressed. The device is reported to be precise, easily applied, and manipulated and reproduces a specific stenosis each time it is used.[1]

Another technique uses 00 nylon suture looped through a very small ring and held at each end by two blocks of plastic. The two plastic blocks are mounted on a pair of metal rods, one of which is moveable and alters the loop diameter. The distance between the blocks can be accurately measured with a Vernier caliper and the relationship between that distance and the radius of the loop is linear.[1] A 2-3-mm-wide band of umbilical tape can be passed around the artery, then through a stiff tube, and attached to a machinist's micrometer. This technique is reported to produce a reproducible stenosis.[1]

Coronary embolization has been accomplished in closed chest dogs by the injection of glass beads 50-100 μm in diameter. The technique seems to be most effective when multiple catheterizations are done, at least seven to ten, at 2-week intervals.[1]

A variety of intravascular polycarbonate plugs have been used, with or without flow channels. The outside diameter of the plug is matched to within 0.25 mm of the inside diameter of the vessel. These plugs can be made with complicated or streamlined channel geometries. If the exact geometry is well described and the flow through the device measured, it is possible to calculate the various fluid dynamic parameters and shear forces associated with the "lesion." Lexan plastic external cylinders have also been used to create stenoses.[1]

Helically shaped copper wires have been delivered into the coronary vasculature resulting in a vascular reaction, stenosis, and thrombus formation.[1] Electrical injury to the coronary endothelium will also produce a lesion and thrombus formation. This can be accomplished using anodal currents of 50-200 μA from a DC source. The current can be delivered rapidly at higher doses or more slowly at lower doses with the latter resulting in more slowly developing obstructive lesions. The injury induces platelet adhesion and aggregation a the lesion and with time there is further platelet aggregation and consolidation with the growing thrombus entrapping RBCs.[1]

It is also possible to induce a clot by removing the endothelium using external trauma with a forceps or internal trauma with an intravascular balloon. Following the endothelial injury, snare occluders are placed proximal and distal to the injury site and 10 units of thrombin are injected into the isolated segment of vessel, usually via a side branch into the isolated segment. Autologous blood (0.3-0.4 ml), mixed with $CaCl_2$ (0.05 M) is also injected into the isolated segment. This produces a stasis-type red clot superimposed on an injured blood vessel. After 2-5 min, the snares are released and a total occlusion usually occurs.[1]

Ameroid constrictors have been used in many different animal models to provide a gradual stenosis with time. The Ameroid casein material is hydrophilic resulting in expansion of the material. It is usually used inside a rigid encasement so as the material expands it encroaches inward on the vessel it surrounds. Some skill is necessary to fit the devices properly and 30% or more of the total constriction takes place within the first 48 h after application making it difficult to have a postoperative period for baseline control measurements. The degree of stenosis produced cannot be adjusted nor predicted.[1] Almost any material: hard plastic, Tygon® tubing, Saran Wrap® applied to the external surface of a vessel will stiffen the vessel and result in some degree of reaction, medial hypertrophy, and stenosis over time. The problem with these techniques is similar to that of the Ameroid constrictors in that the degree of stenosis cannot be regulated or predicted.[28]

Perhaps the most useful device for creating an acute vascular occlusion has been some version of the inflatable cuff described by Khouri and Gregg in 1967.[29] The basic design has been marketed as a hydraulic occluder sold by In Vivo Metric Systems, Healdsburg, CA. It is most useful when used in conjunction with a flowmeter transducer located downstream so the amount of occlusion can be quantified and reproduced.

Many different coronary ligation models have been described in dogs. A two-stage ligation of the LAD coronary, approximately 2 cm distal to its origin, allowed for a modicum of preconditioning.[1] Elzinga and Skinner[30] described a stepwise occlusion of coronary arteries using a U-shaped base that fits around the vessel, a plate and a screw inside a threaded portion. The screw is turned down pushing the plate and giving more control over the amount of stenosis created. There is no control over the geometry of the constriction and this is still an acute ligation model. A similar result can be obtained by the stepwise twisting of a copper wire placed around the vessel.[1] Lekx et al.[31] reduced LAD flow in dogs 72.4 ± 1.6% by applying a Doppler-flowmeter transducer and tightening a ligature until the desired level of reduced flow was achieved. The stenosis was maintained for 3 or 10 weeks. The perfusion reserve in this model, measured by adenosine infusion, was significantly reduced.

As previously mentioned, the protocols for the duration of ischemia and for reperfusion vary significantly and it is rare that any rationale is provided for either time. Dogs, for example, were subjected to 15 min of LAD occlusion followed by 60 min of reperfusion.[32] In another study, dogs were subjected to 60 min of LAD occlusion and 3 h of reperfusion[33] and in a study reported in 2005 the left circumflex coronary artery of dogs was occluded for 10 min and the hearts reperfused for 24 h.[34]

Snares were used to occlude the LAD in pigs for 45 min followed by 6 h of reperfusion.[35] Following an acute ligation of the proximal LAD, a left ventricle to coronary shunt using a stent provided sufficient blood flow to the epicardium but not to the mid- or endocardium.[36]

In another pig study, snares were placed around the left circumflex coronary artery and epicardial radio-opaque markers were applied. After the animals recovered from the surgical procedures, they were sedated and placed in a sling; baseline measurements were made; and the snares were tightened to cause a coronary occlusion. Six pigs developed refractory ventricular fibrillation within 45 min of the coronary occlusion and these were excluded from the study. Surviving animals were studied for 10 days postmyocardial infarction.[37] Another group studied pigs with permanent occlusion of the left circumflex for 2-3 weeks.[38] Ninety-four pigs had an Ameroid constrictor applied to the left circumflex.[39] A closed-chest model of nonocclusive coronary stenosis was created in pigs by inflating an angioplasty balloon in the proximal LAD.[40] More clinically relevant models were created in pigs by repeated (four times) balloon endothelial denudation of the epicardial LAD,[41] by coil embolization of the LAD,[42] and by a very unique technique that used a snare embedded with a 50% $FeCl_3$ solution. The $FeCl_3$ solution diffuses through the vascular wall damaging the endothelium and initiating a thrombus.[43]

A 2.8 F infusion catheter was placed in the LAD between the second and third diagonal branches in mini-pigs. Initially 1.5×10^5 polystyrene microspheres of 45 μm diameter were infused followed by incremental doses of microspheres until there was S-T segment deviation on the ECG indicating ischemia.[44] In acute experiments, the isolated LAD was perfused from the femoral artery of pigs using a roller pump. The controlled LAD flow was reduced by 20% and demand-induced ischemia produced by infusing dobutamine to increase the heart rate and contractility.[14]

Sheep have been used for experiments involving ligation of the left circumflex coronary artery[45] and the LAD.[46,47] Regional infarcts were created in rabbits subjected to 30 min of ischemia and 170 min of reperfusion[48] and 30 min ischemia and 120 min of reperfusion, the later following ischemic preconditioning of 5 min occlusions and 10 min reperfusions.[49] Rabbits were anesthetized and a thoracotomy performed. A cryoprobe with a 1.2 cm diameter was cooled to −70°C using circulating nitric oxide. After reaching temperature, the probe was applied to the epicardial surface of the anterolateral left ventricular free wall for 3 min. A transmural cryoinjury lesion ~1.5 cm in diameter resulted. The thorax was closed and the animals were allowed to recover for 2 weeks before being used in experiments to evaluate the intracardiac transplantation of a mixed population of bone marrow cells.[50]

The LAD was ligated in rats via a thoracotomy. The rats were allowed to recover and then used in an experimental protocol 3 weeks later[51] and 6 weeks later.[52]

Ligation of the left main coronary artery for 25 min was followed by reperfusion for 3 h and then the infarct size was assessed.[33] Isolated, perfused, and working or nonworking rat hearts were subjected to either global ischemia or regional ischemia. The latter for 35 min prior to reperfusion.[5,6] The protective effects of a synthetic xanthone derivative on myocardial injury was studied in rats subjected to 30 min coronary ligations and 120 min of reperfusion.[53] The effects of bone marrow derived mesenchymal stem cells were evaluated after they were injected directly into the center and border zones of infarcts created by 5 h of coronary ligation then reperfusion and recovery for 10 days prior to the transplantation of cells.[54]

An attempt has been made to model the clinical situation of a regional ischemia followed by ventricular fibrillation (global ischemia) in rats. The left coronary artery was constricted and 4 weeks later ventricular fibrillation was induced and then converted and the animals' myocardial function evaluated.[55] In a different study 4 weeks after coronary ligation hearts were harvested from the rats and used in Langendorff preparations with 25 min of global ischemia followed by 2 h of reperfusion.[56] Isolated perfused rat hearts were used to study the effect of I/R injury on apoptosis and infarct size. Ischemic preconditioning was accomplished in these hearts by 5 min of global ischemia repeated three times prior to occlusion of a coronary artery for 35 min followed by 120 min of reperfusion.[57]

Mouse models of myocardial infarction, as previously described, usually involve placing a suture through the myocardium in the general location of the LAD at a prescribed distance distal to the atrial-ventricular junction. The technique has been used to evaluate treatment with pioglitazone to block proinflammatory cytokines,[58] angiotensin II type 1 receptor blockade in streptozotocin-treated (diabetic) mice,[59] the effects of targeted deletion of p53 to prevent cardiac rupture using $p53^{+/-}$ compared to $p53^{+/+}$ mice,[60] and the role of inducible NO synthase using $iNOS^{-/-}$.[61]

Thakker et al.[62] used a mouse model of diet-induced obesity to study the effects of obesity on the inflammatory and healing responses following myocardial I/R. They occluded the LAD for 1 h then re-established blood flow and examined animals after 1, 3, and 7 days of reperfusion. Male CD1 mice were subjected to 30 min of coronary occlusion and 24 h of reperfusion to investigate the role of Rho A and Rho-kinase in I/R injury.[63] Isoflurane-induced myocardial protection was studied in mice following 30 min of coronary occlusion and either 2 h or 2 weeks of reperfusion.[64] TNF-$\alpha^{-/-}$ mice were used to investigate the role of TNF-α following LAD ligation followed by reperfusion for 3, 7, 14, or 28 days.[65]

Since coronary ligation frequently results in apical aneurisms of variable sizes van den Bos et al.[66] used a 2- or 3-mm cryoprobe to produce a highly reproducible, transmural, cone-shaped infarctions. Four weeks postinjury a 3 mm diameter cryoinfarction resulted in decreased LV fractional shortening, decreased global contractility, and progressive LV remodeling.

A mouse model of β-thalassemia has been developed that demonstrates the absence, or only very low levels of beta globin, and the clinical signs of both arterial and venous thrombosis, transient ischemic attacks, and microcirculatory obstructions. The investigators were able to make quantitative measurements of microcirculatory flow using high-frequency ultrasound imaging methods.[67]

References

1. Gross DR. *Animal Models in Cardiovascular Research, 2nd Revised Edition*. Boston: Kluwer Academic; 1994.
2. Wolkart G, Kaber G, Kojda G, Brunner F. Role of endogenous hydrogen peroxide in cardiovascular ischaemia/reperfusion function: Studies in mouse hearts with catalase-overexpression in the vascular endothelium. *Pharmacol Res.* 2006;54:50–56.
3. Gonon AT, Bulhak A, Broijersen A, Pernow J. Cardioprotective effect of an endothelin receptor antagonist during ischaemia/reperfusion in the severely atherosclerotic mouse heart. *Br J Pharmacol.* 2005;144:860–866.
4. Ashton KJ, Willems L, Holmgren K, Ferreira L, Headrick JP. Age-associated shifts in cardiac gene transcription and transcriptional responses to ischemic stress. *Exp Gerontol.* 2006;41:189–204.
5. du Toit EF, Rossouw E, Salie R, Opie LH, Lochner A. Effect of sildenafil on reperfusion function, infarct size, and cyclic nucleotide levels in the isolated rat heart model. *Cardiovasc Drugs Ther.* 2005;19:23–31.
6. Lochner A, Genade S, Hattingh S, Marais E, Huisamen B, Moolman JA. Comparison between ischaemic and anisomycin-induced preconditioning: Role of p38 MAPK. *Cardiovasc Drugs Ther.* 2003;17:217–230.
7. Khudairi T, Khaw BA. Preservation of ischemic myocardial function and integrity with targeted cytoskeleton-specific immunoliposomes. *J Am Coll Cardiol.* 2004;43:1683–1689.
8. Ikizler M, Dernek S, Sevin B, Kural T. Trimetazidine improves recovery during reperfusion in isolated rat hearts after prolonged ischemia. *Anadolu Kardiyol Derg.* 2003;3:303–308.
9. Wischmeyer PE, Jayakar D, Williams U, et al. Single dose of glutamine enhances myocardial tissue metabolism, glutathione content, and improves myocardial function after ischemia-reperfusion injury. *JPEN J Parenter Enteral Nutr.* 2003;27:396–403.
10. Takahashi N, Ooie T, Saikawa T, Iwao T, Yoshimatsu H, Sakata T. Long-term treatment with glibenclamide increases susceptibility of streptozotocin-induced diabetic rat heart to reperfusion-induced ventricular tachycardia. *Exp Biol Med (Maywood).* 2003;228:1234–1238.
11. Ooie T, Takahashi N, Nawata T, et al. Ischemia-induced translocation of protein kinase C-epsilon mediates cardioprotection in the streptozotocin-induced diabetic rat. *Circ J.* 2003;67:955–961.
12. Kramer JH, Mak IT, Phillips TM, Weglicki WB. Dietary magnesium intake influences circulating pro-inflammatory neuropeptide levels and loss of myocardial tolerance to postischemic stress. *Exp Biol Med (Maywood).* 2003;228:665–673.
13. Dernek S, Ikizler M, Erkasap N, et al. Cardioprotection with resveratrol pretreatment: Improved beneficial effects over standard treatment in rat hearts after global ischemia. *Scand Cardiovasc J.* 2004;38:245–254.
14. Dyck JR, Cheng JF, Stanley WC, et al. Malonyl coenzyme a decarboxylase inhibition protects the ischemic heart by inhibiting fatty acid oxidation and stimulating glucose oxidation. *Circ Res.* 2004;94:e78–e84.
15. Burgdorf C, Dendorfer A, Kurz T, et al. Role of neuronal KATP channels and extra neuronal monoamine transporter on norepinephrine overflow in a model of myocardial low flow ischemia. *J Pharmacol Exp Ther.* 2004;309:42–48.
16. Kawabata H, Ishikawa K. Cardioprotection with pioglitazone is abolished by nitric oxide synthase inhibitor in ischemic rabbit hearts - comparison of the effects of pioglitazone and metformin. *Diabetes Metab Res Rev.* 2003;19:299–305.
17. Gonzalez GE, Mangas F, Chauvin AD, et al. Diastolic behavior during postischemic hypercontraction phase in rabbit stunned myocardium. *Medicina (B Aires).* 2003;63:403–409.
18. Castella M, Buckberg GD, Saleh S, Tan Z, Ignarro LJ. A new role for cardioplegic buffering: Should acidosis or calcium accumulation be counteracted to salvage jeopardized hearts? *J Thorac Cardiovasc Surg.* 2003;126:1442–1448.

19. Gross DR, Dewanjee MK, Zhai P, Lanzo S, Wu SM. Successful prosthetic mitral valve implantation in pigs. *ASAIO J.* 1997;43:M382–M386.
20. Gross DR, Salley RK, Maley RH, Arden WA, Nammalwar P. Effects of internal mammary artery pedicle coronary artery bypass grafting on aortic valve leaflet positioning. *J Heart Valve Dis.* 1995;4:313–320.
21. Sparks DL, Gross DR, Hunsaker JC. Neuropathology of mitral valve prolapse in man and cardiopulmonary bypass (CPB) surgery in adolescent Yorkshire pigs. *Neurobiol Aging.* 2000;21:363–372.
22. Borke WB, Munkeby BH, Morkrid L, Thaulow E, Saugstad OD. Resuscitation with 100% O(2) does not protect the myocardium in hypoxic newborn piglets. *Arch Dis Child Fetal Neonatal Ed.* 2004;89:F156–F160.
23. Hearse DJ. Models and problems in the study of myocardial ischemia and tissue protection. *Eur Heart J.* 1983;4 Suppl C:43–48.
24. Verdouw PD, Wolffenbuttel BH, van der Giessen WJ. Domestic pigs in the study of myocardial ischemia. *Eur Heart J.* 1983;4 Suppl C:61–67.
25. Eckstein RW. Coronary interarterial anastomoses in young pigs and mongrel dogs. *Circ Res.* 1954;2:460–465.
26. Brooks H, Al-Sadir J, Schwartz J, Rich B, Harper P, Resnekov L. Biventricular dynamics during quantitated anteroseptal infarction in the porcine heart. *Am J Cardiol.* 1975;36:765–775.
27. Opie LH, Bruyneel KJ, Lubbe WF. What has the baboon to offer as a model of experimental ischemia? *Eur Heart J.* 1983;4 Suppl C:55–60.
28. Gross DR. Unpublished data.
29. Khouri EM, Gregg DE. An inflatable cuff for zero determination in blood flow studies. *J Appl Physiol.* 1967;23:395–397.
30. Elzinga WE, Skinner DB. Hemodynamic characteristics of critical stenosis in canine coronary arteries. *J Thorac Cardiovasc Surg.* 1975;69:217–222.
31. Lekx KS, Prato FS, Sykes J, Wisenberg G. The partition coefficient of Gd-DTPA reflects maintained tissue viability in a canine model of chronic significant coronary stenosis. *J Cardiovasc Magn Reson.* 2004;6:33–42.
32. Morillas P, Hernandez A, Pallares V, et al. Usefulness of trimetazidine in ischemia-reperfusion lesion. experimental study in myocardial stunning model. *Arch Cardiol Mex.* 2004;74:262–270.
33. Lubbers NL, Campbell TJ, Polakowski JS, et al. Postischemic administration of CGX-1051, a peptide from cone snail venom, reduces infarct size in both rat and dog models of myocardial ischemia and reperfusion. *J Cardiovasc Pharmacol.* 2005;46:141–146.
34. Nikolaidis LA, Doverspike A, Hentosz T, et al. Glucagon-like peptide-1 limits myocardial stunning following brief coronary occlusion and reperfusion in conscious canines. *J Pharmacol Exp Ther.* 2005;312:303–308.
35. Khalil PN, Neuhof C, Huss R, et al. Calpain inhibition reduces infarct size and improves global hemodynamics and left ventricular contractility in a porcine myocardial ischemia/reperfusion model. *Eur J Pharmacol.* 2005;528:124–131.
36. Engbers HM, de Zeeuw S, Visser T, Cramer MJ, Grundeman PF. Myocardial blood supply by left ventricle-to-coronary artery channel: An old idea revisited. *Int J Cardiol.* 2006;106:145–151.
37. Apple KA, Yarbrough WM, Mukherjee R, et al. Selective targeting of matrix metalloproteinase inhibition in post-infarction myocardial remodeling. *J Cardiovasc Pharmacol.* 2006;47:228–235.
38. Duncker DJ, Haitsma DB, Liem DA, Verdouw PD, Merkus D. Exercise unmasks autonomic dysfunction in swine with a recent myocardial infarction. *Cardiovasc Res.* 2005;65:889–896.
39. Radke PW, Heinl-Green A, Frass OM, et al. Evaluation of the porcine Ameroid constrictor model of myocardial ischemia for therapeutic angiogenesis studies. *Endothelium.* 2006;13:25–33.
40. Yip G, Khandheria B, Belohlavek M, et al. Strain echocardiography tracks dobutamine-induced decrease in regional myocardial perfusion in nonocclusive coronary stenosis. *J Am Coll Cardiol.* 2004;44:1664–1671.
41. Saitoh S, Muto M, Osugi T, et al. Repeated epicardial coronary artery endothelial injuries lead to a global spontaneous coronary artery spasm. *Coron Artery Dis.* 2004;15:137–145.

42. Thompson CA, Reddy VK, Srinivasan A, et al. Left ventricular functional recovery with percutaneous, transvascular direct myocardial delivery of bone marrow-derived cells. *J Heart Lung Transplant.* 2005;24:1385–1392.
43. Segers P, Tchana-Sato V, Leather HA, et al. Determinants of left ventricular preload-adjusted maximal power. *Am J Physiol Heart Circ Physiol.* 2003;284:H2295–H2301.
44. Zhang QY, Ge JB, Chen JZ, et al. Mast cell contributes to cardiomyocyte apoptosis after coronary microembolization. *J Histochem Cytochem.* 2006;54:515–523.
45. Ryan LP, Jackson BM, Parish LM, et al. Regional and global patterns of annular remodeling in ischemic mitral regurgitation. *Ann Thorac Surg.* 2007;84:553–559.
46. Pilla JJ, Blom AS, Brockman DJ, Ferrari VA, Yuan Q, Acker MA. Passive ventricular constraint to improve left ventricular function and mechanics in an ovine model of heart failure secondary to acute myocardial infarction. *J Thorac Cardiovasc Surg.* 2003;126:1467–1476.
47. Blom AS, Pilla JJ, Gorman RC, III, et al. Infarct size reduction and attenuation of global left ventricular remodeling with the CorCap cardiac support device following acute myocardial infarction in sheep. *Heart Fail Rev.* 2005;10:125–139.
48. Tracey WR, Magee WP, Oleynek JJ, et al. Novel N6-substituted adenosine 5′-N-methyluronamides with high selectivity for human adenosine A3 receptors reduce ischemic myocardial injury. *Am J Physiol Heart Circ Physiol.* 2003;285:H2780–H2787.
49. Flynn DM, Smith AH, Treadway JL, et al. The sulfonylurea glipizide does not inhibit ischemic preconditioning in anesthetized rabbits. *Cardiovasc Drugs Ther.* 2005;19:337–346.
50. Thompson RB, van den Bos EJ, Davis BH, et al. Intracardiac transplantation of a mixed population of bone marrow cells improves both regional systolic contractility and diastolic relaxation. *J Heart Lung Transplant.* 2005;24:205–214.
51. Woo YJ, Grand TJ, Berry MF, et al. Stromal cell-derived factor and granulocyte-monocyte colony-stimulating factor form a combined neovasculogenic therapy for ischemic cardiomyopathy. *J Thorac Cardiovasc Surg.* 2005;130:321–329.
52. Schwarz ER, Meven DA, Sulemanjee NZ, et al. Monocyte chemoattractant protein 1-induced monocyte infiltration produces angiogenesis but not arteriogenesis in chronically infarcted myocardium. *J Cardiovasc Pharmacol Ther.* 2004;9:279–289.
53. Dai Z, Jiang DJ, Hu GY, et al. 3,4,5,6-tetrahydroxyxanthone protects against myocardial ischemia-reperfusion injury in rats. *Cardiovasc Drugs Ther.* 2004;18:279–288.
54. Piao H, Youn TJ, Kwon JS, et al. Effects of bone marrow derived mesenchymal stem cells transplantation in acutely infarcting myocardium. *Eur J Heart Fail.* 2005;7:730–738.
55. Fang X, Tang W, Sun S, et al. Cardiopulmonary resuscitation in a rat model of chronic myocardial ischemia. *J Appl Physiol.* 2006;101:1091–1096.
56. Miki T, Miura T, Yano T, et al. Alteration in erythropoietin-induced cardioprotective signaling by post infarct ventricular remodeling. *J Pharmacol Exp Ther.* 2006;317:68–75.
57. Moolman JA, Hartley S, Van Wyk J, Marais E, Lochner A. Inhibition of myocardial apoptosis by ischaemic and beta-adrenergic preconditioning is dependent on p38 MAPK. *Cardiovasc Drugs Ther.* 2006;20:13–25.
58. Shiomi T, Tsutsui H, Hayashidani S, et al. Pioglitazone, a peroxisome proliferator-activated receptor-gamma agonist, attenuates left ventricular remodeling and failure after experimental myocardial infarction. *Circulation.* 2002;106:3126–3132.
59. Matsusaka H, Kinugawa S, Ide T, et al. Angiotensin II type 1 receptor blocker attenuates exacerbated left ventricular remodeling and failure in diabetes-associated myocardial infarction. *J Cardiovasc Pharmacol.* 2006;48:95–102.
60. Matsusaka H, Ide T, Matsushima S, et al. Targeted deletion of p53 prevents cardiac rupture after myocardial infarction in mice. *Cardiovasc Res.* 2006;70:457–465.
61. Liu YH, Carretero OA, Cingolani OH, et al. Role of inducible nitric oxide synthase in cardiac function and remodeling in mice with heart failure due to myocardial infarction. *Am J Physiol Heart Circ Physiol.* 2005;289:H2616–H2623.
62. Thakker GD, Frangogiannis NG, Bujak M, et al. Effects of diet-induced obesity on inflammation and remodeling after myocardial infarction. *Am J Physiol Heart Circ Physiol.* 2006;291: H2504–H2514.

63. Bao W, Hu E, Tao L, et al. Inhibition of Rho-kinase protects the heart against ischemia/reperfusion injury. *Cardiovasc Res.* 2004;61:548–558.
64. Tsutsumi YM, Patel HH, Lai NC, Takahashi T, Head BP, Roth DM. Isoflurane produces sustained cardiac protection after ischemia-reperfusion injury in mice. *Anesthesiology.* 2006;104:495–502.
65. Sun M, Dawood F, Wen WH, et al. Excessive tumor necrosis factor activation after infarction contributes to susceptibility of myocardial rupture and left ventricular dysfunction. *Circulation.* 2004;110:3221–3228.
66. van den Bos EJ, Mees BM, de Waard MC, de Crom R, Duncker DJ. A novel model of cryoinjury-induced myocardial infarction in the mouse: A comparison with coronary artery ligation. *Am J Physiol Heart Circ Physiol.* 2005;289:H1291–H1300.
67. Stoyanova E, Trudel M, Felfly H, Garcia D, Cloutier G. Characterization of circulatory disorders in {beta}-thalassemic mice by non-invasive ultrasound biomicroscopy. *Physiol Genomics.* 2007; 29:84–90.

Chapter 10
Iatrogenic, Transgenic, and Naturally Occurring Models of Cardiomyopathy and Heart Failure

Cardiomyopathy is a general term applied to a wide variety of conditions that result in myocardial lesions not related to specific disease states. The term encompasses a wide variety of conditions initiated by numerous etiologies. The disease usually presents as either hypertrophic or dilated cardiomyopathy (HCM or DCM). Naturally occurring cardiomyopathy seems to be caused by mutations in one or more sarcomeric proteins. Inherited DCM can result from mutations in the genes encoding cardiac troponin T, troponin C, and alpha-tropomyosin, while different mutations in the same genes cause HCM. DCM mutations depress myofibrillar function as a result of thin filament mutations while HCM has the opposite effect.[1]

Familial HCM is described as an autosomal dominant disorder that manifests as cardiac hypertrophy with myocyte disarray. Mutations in five different loci result in the disease. Beta cardiac myosin heavy-chain, alpha tropomyosin, and cardiac troponin T have been identified as distinct disease genes.[2-6] Liu et al.[7] compared the morphological features of spontaneously occurring HCM in 38 humans, 51 cats, and 10 dogs. They found that asymmetric hypertrophy of the ventricular septum, marked disorganization of myocardial cells, abnormal intramural coronary arteries, and myocardial fibrosis were common to all three species. Transgenic mice expressing cardiac troponin T (cTnT)-Q92 develop HCM characterized by enhanced systolic function and have higher levels of cardiac troponin I, cardiac alpha-actin, cardiac alpha-tropomyosin, and cardiac troponin than wild type.[8]

DCM, a putative autoimmune disease, kills males two to three times more commonly than females. Male mice immunized to the p406-425 peptide derived from mouse cardiac alpha-myosin heavy chain preferentially developed a predominant Th17 lineage response resulting in a high incidence of DCM accompanied by sustained T cell memory. Female mice treated identically developed a Th1 lineage response and were protected against DCM.[9] Transgenic mice expressing cTnT-W141 develop dilated hearts and decreased systolic function.[8]

Heart failure is, by definition, the inability of the heart to supply adequate tissue blood flow (left heart failure) or pulmonary alveolar blood flow (right heart failure) to meet the metabolic demands of the body. In man and other animals, chronic heart failure involves complex adaptive changes in the autonomic nervous system, the renin-angiotensin system, the adrenal steroids, and other physiological accommodations in

D.R. Gross, *Animal Models in Cardiovascular Research*,
DOI: 10.1007/978-0-387-95962-7_10, © Springer Science+Business Media, LLC 2009

an effort to reduce metabolic demand and/or increase cardiac output sufficient to maintain homeostasis. It is associated with subcellular abnormalities in myocardial cells directly affected by the underlying disease process. Other myocardial cells may be less affected or unaffected.[10]

Naturally Occurring Models of Cardiomyopathy

Heritable HCM in Cats

HCM is the most common heart disease of cats. It is particularly prevalent in Maine Coon and Maine Coon crossbred cats.[11-24] The cardiac myosin binding protein C (*MYBPC3*) gene has been reported as a mutation in both the Main Coon breed and in Ragdoll cats with HCM.[25] Cats with HCM have significantly higher serum concentrations of cTnI than control cats.[26,27] Cats with HCM typically demonstrate subendocardial and myocardial fibrosis. Theories of pathogenesis implicate coronary vascular occlusion resulting from a thickening of vessel walls, thromboembolism and/or vascular spasm. Also implicated are apoptosis of myocytes and hypertrophy beyond the ability of the coronary vasculature to provide adequate blood flow.[28] Increases in kidney renin values have been documented in cats with HCM, probably in response to impaired cardiac output and reduced blood pressures.[29]

Functionally, cats with HCM present with decreased late-systolic velocities along the longitudinal axis as measured with pulsed tissue Doppler imaging. There is also a decrease in early systolic acceleration of the mitral annulus. Six of 23 cats with HCM demonstrated postsystolic thickening of the left ventricular free wall.[16] Using cardiac magnetic resonance imaging, MacDonald et al.[30] documented significantly lower peak early diastolic velocities in HCM cats when compared with normal controls. When HCM cats were compared with cats with chronic systemic hypertension (SHT) and normal controls, using tissue Doppler imaging, systolic velocities and both radial and longitudinal diastolic velocities were similarly decreased in both HCM and SHT animals compared with controls.[15]

Cats with HCM can also present with conduction abnormalities. Thirteen feline cases of HCM with complete atrioventricular (AV) block were examined histologically. There was marked degeneration and fibrous replacement of the AV conduction system in the branching portion of the AV bundle and the upper portion of the left bundle branch. The pathological process and type of lesions observed with similar to those reported in aged human patients with complete AV block.[31] Arrhythmogenic right ventricular cardiomyopathy is an important cause of sudden death in humans. It is characterized by infiltration of the myocardium by adipose and fibrous tissue. Two cats with right ventricular failure presented with complete AV block and bilateral multiform ventricular ectopic beats. One of the cats also demonstrated ventricular tachycardia, ventricular bigeminy, and R-on-T phenomenon. Echocardiographically there was massive dilation and hypokinesis of both the right atria and right ventricles in both cats.[32]

Atrial natriuretic peptide (ANP) and brain natriuretic peptide (BNP) are endogenous peptides produced by myocardial cells and are part of the homeostatic mechanisms involved in fluid and electrolyte regulation. Plasma N-terminal immunoreactivity (ANP-IR) was not statistically different in HCM cats when compared with normal controls. There was a significant, but modest, correlation between plasma ANP-IR concentrations and thickness of the left ventricular posterior wall and a weak correlation with left atrial size. There was no appreciable correlation between plasma ANP-IR and any of the other echocardiographic variables measured.[33] The cardiac distribution of ANP and BNP is more diffuse in the atria of cats with HCM, and there is a novel expression of BNP in ventricular myocytes.[34]

Cats with HCM frequently suffer from arterial thromboembolism, especially with left atrial enlargement. Hyper-coagulability is diagnosed by two or more laboratory abnormalities reflecting coagulation factor excess (high fibrinogen concentrations or Factor VIII coagulant activity), inhibitor deficiency (low antithrombin activity) or thrombin generation (high thrombin-antithrombin complex (TAT) and d-dimer concentrations. Laboratory evidence of systemic hyper-coagulability was found in 45% of cats with asymptomatic HCM,[35] and over 50% of 43 cats in another study.[36] Chromogenic antithrombin activity was measured in 30 healthy controls cats, 30 ill cats (7 of the 30 were diagnosed with disseminated intravascular coagulation), and 13 cats with HCM. The HCM cats did not have significantly increased AT activities.[37] Three related cats were followed with serial echocardiograms until they developed end-stage HCM, died, and were then necropsied. Two of the three cats had large left atrial thrombi. All three animals died following thromboembolization of the aortic bifurcation and had subendocardial and myocardial fibrosis. One animal had acute, multifocal, myocardial infarcts with mononuclear inflammatory cell infiltrates.[28]

DCM in Dogs

Dogs with DCM demonstrate impaired contractility along both the long and short axis of the LV as well as impaired left ventricular freewall diastolic function and systolic RV function.[38,39] Large breed dogs, particularly Irish wolfhounds, are most commonly affected with a higher prevalence in males compared with females. A set of X chromosomal microsatellites was genotyped in Irish wolfhound families diagnosed with DCM. Statistical analysis of the microsatellite markers did not reveal any linkages to DCM and all the animals in the study were monomorphic for intron sequences of the *tafazzin* gene indicating that gene is unlikely to be responsible for DCM in this breed.[40] A mixed monogenic-polygenic model including a sex-dependent allele effect is a most likely explanation as a cause of DCM in Irish wolfhounds.[41]

Because there are more Doberman Pinschers than Irish wolfhounds, this breed accounts for most of the animals diagnosed with DCM. In this breed, the disease is typically adult onset with a familial etiology suggested. An autosomal dominant mode of inheritance has been defined by the appearance of the disease in multiple generations. There is equal gender representation in this breed and male-to-male transmission.

The causative gene or genes in Dobermans is not resolved.[42] Doberman Pinschers showed echocardiographic evidence of moderate diastolic dysfunction in animals with occult DCM and severe diastolic dysfunction with overt DCM. Shorter early transmitral flow deceleration times may be a useful predictor of the onset of congestive heart failure or sudden death.[43] Plasma big endothelin-1 (ET-1), norepinephrine (NE), aldosterone, and ANP were compared with 10 normal Dobermans, 10 with occult DCM, and 10 with overt DCM. Dogs with occult DCM had significantly higher ANP concentrations than normal dogs. Dogs with overt DCM had significantly higher plasma concentrations of all the neurohormones measured compared with the normal dogs. The authors concluded that high ANP concentrations could be useful in identifying dogs with advanced occult DCM while increased levels of big ET-1 or NE could be predictors of a poor prognosis.[44]

Spontaneous ventricular arrhythmias have been reported in German shepherds, Boxers, and Doberman Pinchers with DCM and could be a useful model for the study of arrhythmias. Arrhythmias have also been reported in large dogs with gastric dilatation or splenic torsion.[45]

Ten English Cocker Spaniels with DCM and pulsus alternans were studied. The pulsus alternans was an intermittent finding in all 10 dogs. This combination may be more prevalent in this breed and because of the intermittent nature might be more common than previously reported. The presence of pulsus alternans is usually associated with severe myocardial depression.[46] Dogs with Golden Retriever Muscular Dystrophy, a model of Duchenne muscular dystrophy, also present with Duchenne's DCM.[47]

Boxer dogs suffer from arrhythmogenic right ventricular dysplasia/cardiomyopathy (ARVD/C).[48] Genetic mutations responsible for ARVD/C lead to severe changes in mechanical and electrical cell/cell interactions. Significant reductions in gap junction formation may promote a substrate for malignant ventricular arrhythmias.[49] Boxers with ARVD/C have a significant increase in serum cTnI concentrations.[50]

The ferric reducing ability of the plasma (FRAP) is a measure of antioxidant reactivity. Dogs with DCM and with mitral endocardiosis demonstrated increased antioxidant reactivity as measured by FRAP, but not by total antioxidant activity. The magnitude of the increase seems to be related to the severity of the disease rather than the type of disease.[51]

Cattle with Cardiomyopathy and Woolly Hair Coat Syndrome

Naxos disease is characterized by arrhythmogenic right ventricular cardiomyopathy associated with wooly hair and palmoplantar keratoderma or similar skin problems in humans. There has also been reported a mutation of this condition in Ecuadorian families that truncates the intermediate filament-binding site of desmoplakin and results in a variant of Naxos disease with left ventricular cardiomyopathy (Caravajal syndrome). Polled Hereford calves have been diagnosed with a lethal autosomal recessive cardio-cutaneous syndrome demonstrating a similar

hair and cardiac phenotype. These animals present with arrhythmogenicity that increases with age and myocardial damage with lipid and/or fibrous tissue replacement of myocardial tissue in the subepicardial and medial layers of the left ventricle.[52] Morrow and McOrist[53] reported on calves that have a tight, curly hair coat at birth and usually die before reaching 6 months of age. Necropsy results documented focal, diffuse, and pale fibrous streaking of the entire myocardium and vascular congestion of the liver, spleen, and lungs. This cardiomyopathy of cattle is attributed to a lethal autosomal recessive gene present in both the Polled Hereford breed and in Japanese black cattle. The cardiac arrhythmias are attributed to the myocardial degeneration and fibrosis.[54,55]

Primates

Interstitial myocardial fibrosis was diagnosed in 66% of moustached tamarins (*Saguinus mystax*) that had been previously used in viral studies of hepatitis A and GB. These animals had a high incidence of spontaneous colitis cystica profunda, myocardial fibrosis, and membranoproliferative glomerulonephritis.[56] A wild-caught male *Aotus vociferans* (owl monkey) was diagnosed with spontaneous cardiomyopathy that resembled rheumatic heart disease. Several small myocardial arteries were replaced with fibrinoid necrosis and adjacent inflammation with infiltration of lymphocytes and large histiocytic cells.[57]

Whales

Necropsies were performed on adult pygmy sperm whales (*Kogia breviceps*) and dwarf sperm whales (*Kogia simus*) found stranded along the southeastern coast of the US. The whales had pale, flabby right ventricles characterized by moderate to extensive myocardial degeneration, atrophy, and fibrosis. Cardiomyopathic lesions were not present in sexually immature whales or whale calves.[58]

Iatrogenic Models of Cardiomyopathy and Heart Failure

Ventricular Arrhythmia

Ventricular arrhythmia models, with or without heart failure, can be induced in many species by intoxicating doses of digitalis glycoside and/or escalating doses of epinephrine. Programmed electrical stimulation has been used to detect an increased tendency for arrhythmia in conjunction with the testing of drugs for possible arrhythmogenic effects.[45]

Increasing the Ventricular Workload

This is the most common technique for inducing cardiomyopathies and heart failure. Four general methods are used: rapid cardiac pacing, pressure overload, volume overload, and creating a valvular insufficiency. The various techniques are most commonly used in dogs, cats, and rats but are also frequently reported in pigs, sheep, rabbits, primates, and other species. When the heart is exposed to an increase in ventricular workload it compensates by dilation and/or hypertrophy but this does not result in heart failure until the compensatory response is unable to meet the metabolic demands of the individual. All of the methods to be described produce some degree of dilatation and/or hypertrophy but the final level of failure and its rate of progression are beyond the control of the experiment.[10]

Rapid Cardiac Pacing

DCM is the third most common cause of heart failure in humans. It is characterized by progressive ventricular dilation and functional impairment without coronary artery disease or hypertension. The rapid pacing model has been most commonly reported in dogs,[59-64] sheep,[65-71] pigs,[72-75] and monkeys.[59] Either atrial or ventricular pacing at three to four times the normal heart rate for the particular individual, for a period of 3-4 weeks is usually sufficient to induce signs of DCM.

Pressure Overload

Pressure overload models are most commonly produced by banding, or partially ligating, the aorta or pulmonary artery. Hydraulic occluders are available for acute responses and a wide variety of materials have been used for both acute and chronic banding. It is also common to surgically band young animals loosely and allow them to grow into a more constricted state. The use of Saran$^{(R)}$ wrap or similar materials for a band results in a significant fibrotic response that stiffens the vessel and also results in a constriction. Banding the aorta results in a significant increase in LV afterload and work but because the coronary vasculature sees the increased pressure this does not mimic the most common forms of LV pressure overload seen clinically, i.e., aortic valvular stenoses or subvalvular stenoses wherein the coronary pressures are significantly lower than LV systolic pressures.[10]

Both chronic and intermittent pressure-overload, induced by aortic constriction, result in some degree of diastolic dysfunction, altered β-adrenergic receptor function, and vascular rarefaction prior to the development of ventricular hypertrophy in mice.[76-78] Dahl salt-sensitive rats fed a high salt diet started at 7 weeks of age develop diastolic heart failure with collagen accumulation but without LV dilatation. When the high salt diet is started at 8 weeks of age, the rats develop systolic heart failure. Both models demonstrate progressive LV fibrosis.[79] DCM has been induced using a 2-kidney, 1-clip hypertension model in rats with induced diabetes.[80] Aortic arch banding in cats can result in either a

compensated or uncompensated left ventricular hypertrophy.[81,82] Severe left ventricular outflow obstruction was surgically created in first-trimester sheep fetuses by banding the ascending aorta. About half of the surviving fetuses developed a compensatory left ventricular hypertrophy (7 of 13). The other six fetuses developed a noncompensatory left ventricular dilation with severe left ventricular dysfunction.[83] Hughes et al.[84] used aortic constriction to cause DCM in mice and demonstrated that copper supplementation improved cardiac function. Nitric oxide synthase-2 does not seem to play a critical role in prolonged pressure-overload heart failure in mice.[85] When subjected to aortic constriction the apoptosis-inducing factor-deficient harlequin, mouse mutant develops enhanced oxidative stress, cell death, accelerated progression to heart failure, and a reduced ability of sub-sarcolemmal mitochondria to scavenge free radicals.[86]

Volume Overload

Ventricular volume overload-induced failure can be accomplished acutely by volume overloading the subject with the rapid infusion of isotonic or hypertonic fluids. Chronic models include the creation of aortic-caval shunts (fistulas), femoral artery-vein shunts, left subclavian artery to pulmonary artery shunts, and shunts from the LV to the left atrium.[10]

Valvular Stenoses or Insufficiencies

Mitral insufficiency can be accomplished by transecting one or more chordae tendinea. Other surgical techniques that have been reported include perforation of the aortic valves, direct suturing, plication, or clipping of the aortic valves to cause aortic stenosis, cauterizing the pulmonic or aortic valves with silver nitrate. A simulated aortic valvular stenosis was created by rolling Teflon felt into a 4-5 mm diameter, 8-9 mm long, cylinder. The cylinder was then covered with autologous pericardium and sutured into the sinus of Valsalva proximal to the coronary orifices. Acute tricuspid regurgitation was produced by introducing a wire coiled into a spiral through the tricuspid valve, via a puncture incision in the right atrium. The wire was advanced until the valve became insufficient.[10]

Other Iatrogenic Models of Cardiomyopathy and Heart Failure

Anthracycline-Induced Cardiomyopathy

Doxorubicin-induced cardiomyopathy is partly mediated by stimulation of Toll-like receptors 2 and 4 that are expressed on cardiomyocytes.[87] Weanling rabbits were given weekly injections of doxorubicin for 4 months. They developed cardiomyopathy as did

rats and mice similarly treated.[88,89] Three-month old New Zealand rabbits developed cardiomyopathy after they were treated with doxorubicin (3 mg/kg).[90] Rats treated with adriamycin developed DCM[91] as did male Sprague-Dawley rats that received 6 weekly injections of doxorubicin, 2 mg/kg, subcutaneously,[92] or 2.5 mg/kg intravenously for 10 or 12 weeks.[93] Sheep developed cardiomyopathy following repeated intracoronary injections of doxorubicin (0.75 mg/kg) administered every 2 weeks until cardiac dysfunction was detected.[94] Doxorubicin-induced cardiomyopathy in mice is largely prevented by the prior administration of erythropoietin probably by the activation of phosphatidylinositol 3-kinase cell-survival pathways.[95]

Diabetic and Lipid-Toxic Models of Cardiomyopathy

Mice or rats treated with streptozotocin (50 mg/kg, i.p.) for 5 days develop diabetic cardiomyopathy.[96-98] Diabetic cardiomyopathy is exacerbated by surgically induced abdominal aortic coarctation.[99] Obese Zucker rats develop cardiac lipotoxicity and LV dysfunction as they age.[100] Streptozotocin-treated C57BL/6 mice develop type-1 diabetes that most commonly results in ischemic heart disease due to accelerated atherosclerosis. However, a percentage of mice thus treated will develop cardiomyopathy without clear evidence of ischemic disease.[101]

Chronic Myocardial Ischemia Models of Cardiomyopathy

Thakker et al.[102] combined a model of diet-induced obesity with myocardial ischemia-reperfusion to produce a DCM model. Chronic heart failure has been produced in sheep using multiple sequential bolus injections of (90 μm, $n = 25{,}000$) polysterol microspheres into the left main or the left circumflex coronary arteries. The injections were repeated up to three times with two- to three-week intervals until the animals demonstrate stable signs of heart failure.[103,104] A similar model has been created in sheep by ligation of the first two diagonal branches of the left anterior descending coronary artery resulting in a postinfarction DCM.[105] Porcine-derived gelfoam (Curaspon $^{(R)}$) has been found to be an efficient material for temporary occlusion of arteries in pigs.[106] Sequential ligation of the LAD and its first diagonal branch produces ischemic cardiomyopathy in goats.[107]

A wide variety of hydraulic occluders, microspheres, suture materials, and other materials have been used to constrict and/or occlude coronary vessels. These occlusions have been done singly or in stages, acutely or chronically, and using an array of external snares, internal plugs, and other innovative devices such as Ameroid constrictors. The myocardium has also been injured directly using electrical currents, thrombin-induced clots, thermal and ultrasonic injury.[10]

Toxicosis and Mineral-Deficient Models of Cardiomyopathy

Chronic iron-overload cardiomyopathy was created in mice.[108] Feeding a copper-deficient diet will result in HCM in mice.[109] Gousiekte is a plant-induced cardiac toxicosis that has been experimentally reproduced by dosing sheep with *Pachystigma pygmaeum, Fadogia homlei*, and *Pavetta harboril.* The cardiac lesions produced mimic those observed in humans with idiopathic DCM.[110] Calves given a single oral dose of monensin (20-40 mg/kg) develop a decrease in peak systolic blood pressure, an increase in central venous blood pressure, and mild LV dilation accompanied by swollen myocytes with loss of striation and sarcoplasmic vacuolization, necrotic fibers, infiltration with macrophages and neutrophils, and both local and generalized fibrosis.[111,112] Both spontaneous and experimental selenium-vitamin E (Se-E) deficiency results in necrosis and calcification in the left ventricular free wall and septum in calves. Other lesions include hyaline necrosis with or without calcification, macrophage infiltration, and fibrosis. Se-E deficiency in lambs, turkey poults, ducklings, and growing pigs, remarkably, results in different pathologies. In lambs, the lesions are more frequently found in the right ventricular subendocardium. In pigs, there are epicardial and myocardial hemorrhages, so-called "mulberry heart", characterized by fibrinoid necrosis of small arteries and arterioles and fibrin microthrombi in capillaries. Lesions in young pigs, turkeys, and ducks consist of cardiac myocyte multifocal hyaline necrosis with calcification, macrophage infiltration, and fibrosis. Ultrastructural lesions include mitochondrial swelling and mineralization, myofibrillar lysis, and contraction band necrosis.[113,114]

Autoimmune Models of Cardiomyopathy

Immunization of mice with the peptides derived from human adenine nucleotide translocator (ANT) result in DCM.[115] Anesthetized rats dosed with *Staphylococcus aureus* α-toxin demonstrated significant adverse changes in systemic hemodynamics, coronary perfusion pressures, ventricular function, and increased p53 expression with myocardial cell apoptosis.[116] Rabbits and mice immunized with a peptide corresponding to the sequence of the second extracellular loop of the β_1-adrenergic receptor [β_1-EC(II)] develop a progressive left ventricular dilation, systolic dysfunction, and apoptosis of the myocardial cells.[117,118] The autoimmune cardiomyopathy thus produced is enhanced by doses of NE.[118] Similar lesions, i.e. increased left ventricular systolic and diastolic pressures, increased inhibitory G protein levels, myocyte hypertrophy and interstitial fibrosis, were obtained following the immunization of Japanese white rabbits against sarcolemmal Na-K-ATPase.[119] Immunization of mice with cardiac myosin results in myocarditis characterized by DCM with mononuclear infiltration.[120]

Hyperthyroid and Hyper-Adrenergic Models of Cardiomyopathy

Senescent female B6D2F1 hybrid mice were injected with levothyroxine (10 μg/10 g body weight) daily for 8 days and developed diastolic dysfunction.[121] Rats treated with L-thyroxin (0.2 mg/kg/day, s.c.) for 10 days develop cardiomyopathy with a high incidence of ventricular arrhythmia.[122] Sympathetic hyperactivity will also induce heart failure in mice.[123]

Chronic Hypoxia Models of Cardiomyopathy

Chronic alveolar hypoxia in mice exposed to 10% oxygen for 4 weeks resulted in impaired ventricular relaxation and diastolic dysfunction in both the LV and RV.[124]

Liver Cirrhosis Models of Cardiomyopathy

When the bile duct is ligated rats develop liver cirrhosis and cirrhotic cardiomyopathy and myocardial dysfunction attributed, at least in part, to increased nuclear factor-kappaB (NF-kappaB) activity.[125]

Murine Cysticercosis Model of Cardiomyopathy

Wild-type mice infected with *Taenia crassiceps* developed bilateral DCM, decreased ventricular wall thickness, compensatory myocardial cell hypertrophy, and increased myocyte apoptosis. The pathology did not develop in Substance-P knockout mice similarly infected.[126]

Commercially Available Inbred-Rat Models of Cardiomyopathy and Heart Failure

The original NIH Veterinary Resources Branch breeding program developed a wide variety of rat strains but is now not functioning except for some preserved frozen embryos. Genetic Models, Inc. and Charles River Laboratories have rederived and established rat genetic models commercially. The SHROB strain is a cross between Sprague-Dawley and spontaneously hypertensive rats (SHR). They mature to be very obese, hyperlipidemic, and hyperinsulinemic. They develop atherosclerosis and dissecting aortic aneurysms. Rats that are homozygous for the autosomal recessive *cp*

gene (*cp/cp*) develop obesity, hyperlipidemia, and insulin resistance whereas heterozygous (*cp/+*) or homozygous normal (+/+) are normal. The SHHF/MccCrl-*Lepr*^{cp} strain of rats develop cardiomyopathy and heart failure as do the Crl:JCR(LA)-*Lepr*^{cp}, the Crl:ZUC-*Lepr*^{cp}, the ZDF/Crl-*Lepr*^{fa}, and the SHR/OBKOLCrl-*Lepr*^{cp} strains. More information about these and other strains of rats prone to cardiomyopathies is available at http://www.criver.com.[127] At least two mouse model strains of obesity, insulin resistance, and diabetes are available, ob/ob and db/db. Buchanan et al.[128] have shown that obesity alone does not cause contractile dysfunction in these models but loss of the hyper-contractile phenotype of obesity and up-regulation of peroxisomal proliferator-activated receptor (PPAR)-α-regulated genes occur with aging and are most pronounced in their adverse myocardial effects when hyperglycemia is chronic. Congenic SS-16/Mcwi rats develop severe cardiac HCM, even though they are normotensive and on a high-salt diet.[129]

Transgenic Models of Cardiomyopathy and Heart Failure

Mouse and Rat Models of Familial Hypertrophic Cardiomyopathy and HCM

Familial hypertrophic cardiomyopathy (FHC) is attributed to mutations in myosin heavy and light chains, actin, both T and I troponin, myosin-binding protein C, and α-tropomyosin.[130] Mutations in the β-myosin heavy chain gene are thought to result in HCM by acting as dominant negative alleles but truncated cardiac troponin T also causes HCM by altering the stoichiometry of contractile proteins.[5]

Using an amino acid substitution at codon 180 (Glu180Gly) that occurs in a troponin T binding region, Prabhakar et al.[130,131] and Jagatheesen et al.[132] created mice that demonstrate concentric ventricular hypertrophy, fibrosis, and atrial enlargement within the first month after birth. The disease progresses to heart failure and death in 4-6 months. A chimeric α^{-}/β^{-} TM (tropomyosin) protein mouse model was also developed. When the two models were mated the double-transgenic offspring exhibited normal cardiac morphology.[132] Transgenic rats with mutations Asp175Asn or Glu189Gly in α-tropomyosin develop FHC.[133]

Mice expressing three different truncated cardiac troponin T (TnT) mutations, Ile79Asn, Arg92Gln, and DeltaGlu160 all develop HCM. The studies suggest that TnT can change the rate of myosin cross-bridge detachment thereby playing a significant role in modulating muscle contractile performance. Cardiac pathology develops because of the increased energetic load on the myocardium.[134]

In humans, FHC is characterized by genetic and clinical heterogeneity and 5% of families have two FHC-causing mutations. When two mutations are involved there is an increased incidence of cardiac dysfunction and a higher incidence of sudden death. A double mutant mouse model of FHC, (TnI-203/MHC-403), was generated by crossbreeding Gly203Ser cTnI-203 mice with Arg403Gln α-myosin

heavy chain mice. The double-mutant mice suffered 100% mortality from heart failure before they were 21-days old.[135]

Muscle RING finger 1 (MuRF1) and MuRF3 are E3 ubiquitin ligases that cooperate with the E2 ubiquitin-conjugating enzymes UbcH5-a, UbcH5-b, and UbcH5-c to mediate the degradation of β-slow myosin heavy chain and MHCIIa via the ubiquitin proteasome system. Mice made deficient for MuRF1 and MuRF3 develop skeletal muscle dystrophy and HCM characterized by the sub-sarcolemmal accumulation of myosin heavy chain, myocardial fiber fragmentation, and myocardial dysfunction.[136] Another mouse model of FHC was generated by the introduction of an Arg403Gln mutation into the α-cardiac myosin heavy chain gene (MHC 403/+). In this model, ventricular dysfunction, myocyte disarray, hypertrophy, and fibrosis all increase as the mice age. Male MHC 403/+ mice are more susceptible to cardiac dysfunction than females.[137]

Fifty to 70% of transgenic mice carrying a p.Met532Arg mutant α-MHC gene, reported to be identical to the human β-MHC gene, develop LV hypertrophy by 2-3 months of age. Approximately, 25% of these transgenic mice develop LV dilatation by 18-months of age.[138]

Mice have two homologous genes for the intercalated disk protein Xin. These are identified as mXin-α and mXin-β. mXin-α-null mice [mXin-α (–/–)] develop HCM with intercalated disk disruption and myofilament disarray. These animals also have significantly prolonged QT intervals and altered localization and decreased expression of connexin 43.[139]

Caveolin-1 knockout mice develop increased vascular nitric oxide production, HCM, and pulmonary dysfunction. The pulmonary dysfunction is associated with alveolar cell hyper-proliferation. The myocyte hypertrophy, pulmonary hypertension, and alveolar cell changes seem to be a result of constitutive activation of p42/44 mitogen-activated protein kinase and Akt.[140]

Family 78 is a mutant mouse line from a C57BL6/J background intercrossed into the C3H/Hej strain background to map the mutation. A percentage of the progeny of this cross can develop severe fetal LV hypertrophy and neonatal lethality. Some of the adult mice die suddenly with HCM.[141]

Transgenic rats with a dominant-negative mutant of natriuretic peptide receptor-B (NPR-BDeltaKC) develop progressive ventricular hypertrophy without significantly increased aortic pressures. The rats also have increased resting heart rates. The hypertrophy is enhanced by chronic volume overloading resulting in HF.[142]

Mouse and Rat Models of DCM

Transgenic mice expressing an increase in mutant α-tropomyosin (TM) (Glu54Lys) demonstrated a decrease in endogenous α-TM levels but total myofilament TM levels remained the same. These animals developed DCM with progression to HF and usually died by 6 months of age.[143] E40K and E54K mutations in α-TM are reported to cause inherited DCM in humans.[1,144] Warren et al.[145] separated native,

mutant E54K and phosphorylated forms of TM from wild-type and transgenic mice and concluded that altered TM phosphorylation associated with the E54K mutation could be a significant cause of DCM in this model.

Diastolic dysfunction was documented in cardiac troponin-I [cTnI (193His)] mice.[146] Knock-in mice were created by deletion of three base pairs coding for K210 in cardiac troponin T (cTnT). The mutant mice showed significantly lower Ca^{2+}sensitivity probably contributing to the observed DCM.[147] Cardiac troponin Tnnt2 was ablated to produce heterozygous Tnnt2 (+/−) mice. These mice were crossbred to produce homozygous null Tnnt2 (−/−) embryos. Transgenic mice overexpressing wild-type or DCM mutant [TG (K210Delta)] Tnnt2 were also developed. Crossbreeding with the Tnnt2 (+/−) mice produced animals lacking one allele of Tnnt2, but carrying wild-type [Tnnt2 (+/−)] or mutant Tnn2 (+/−)/TG (K210Delta) transgenes. Tnnt2 (+/−) mice demonstrated normal hearts. Tnnt2 (+/−)/TG (K210Delta) developed severe DCM and TG (K210Delta) mice had moderate DCM.[148] The expression of mutant cTnT (R141W) in transgenic mice results in ventricular dilatation, systolic dysfunction, myocardial hypertrophy, and interstitial fibrosis characteristic of DCM.[149]

Mutations in myosin heavy chain (MHC) can result in HCM characterized by hypertrophy, contractile dysfunction, and sudden death.[150]β-myosin heavy chain (betaMHC) mutations have been identified in both hypertrophic and dilated cardiomyopathies in humans. Fifty to seventy percent of mice with a p.Met532Arg mutant α-MHC gene, identical to the p.Met531Arg mutation in the human beta-MHC, develop LV hypertrophy by 2-3 months of age and about 25% of these transgenic animals develop LV dilatation by 18 months of age.[138] Mice with a mutated, heart-specific, myosin light chain gene also develop DCM.[151]

Striated muscle activator of Rho signaling (STARS) is a muscle-specific actin-binding protein. It activates serum response factor (SRF)-dependent transcription by inducing nuclear translocation of myocardin-related SRF coactivators. Transgenic mice that overexpress STARS in their cardiomyocytes have increased sensitivity to pressure overload and calcineurin signaling and demonstrate an exaggerated hypertrophic response to these stimuli.[152]

Transgenic mice with ventricular myocyte-specific expression of angiotensin type II receptors (AT2) develop DCM and HF.[153,154] Mice with the muscle-specific deletion of Ptpn11, the gene that encodes the SH2 domain containing the specific protein tyrosine phosphatase (PTP) Shp2, develop a compensated DCM without the usual hypertrophic phase. Signs of myocardial dysfunction usually are manifest within the first two postnatal months.[155]

The *lamin A/C* gene encodes nuclear membrane proteins. Mutations in this gene can result in DCM. Transgenic mice with one normal allele of the A type lamin [Lmna (+/−)] had only half the normal levels of cardiac lamin A/C, early onset apoptosis of AV nodal myocytes and progressive adverse changes in electrical excitation processes along with the usual myocardial abnormalities associated with DCM.[156] Mouse lines that carry some of the same mutations of Lmna found in a variety of human diseases, including those associated with DCM, have been created by Stewart et al.[157]

Mdm2, a p53-negative regulator, has been shown to protect cardiomyocytes from ischemia-reperfusion injury. Mdm4 is a homologue of Mdm2 and inhibits p53 activity in many different cell types. Transgenic mice with a cardiomyocyte conditional knockout of Mdm4, via a specific Cre allele, were apparently normal at birth but developed DCM as adults with a median survival of 234 days. The onset of DCM occurs significantly earlier in male compared with female mice.[158]

Transgenic mice expressing the transcriptional repressor "Snail" in the heart display severe DCM, cardiac arrhythmias, and significantly reduced voltage-gated Na^+ currents. There is an associated decrease in expression of Scn5a, the major cardiomyocyte sodium channel gene that is a direct target of Snail.[159]

Transgenic mice with a deficiency in PDE4, a cAMP-specific phosphodiesterase with specific functions that regulates cardiovascular system performance, develop a progressive and age-related, cardiomyopathy. Following experimental coronary ligation and/or exercise-induced arrhythmias, these animals demonstrate accelerated heart failure.[160]

Female transgenic mice with a cardiomyocyte-specific deletion of stat3 develop postpartum cardiomyopathy (PPCM). Cardiac cathepsin D expression and activity is enhanced in these animals and is associated with the generation of a cleaved anti-angiogenic and proapoptotic 16 kDa form of prolactin.[161]

DCM has also been documented in transgenic mice deficient in dystrophin,[162-164] delta-sarcoglycan (Sgcd −/−),[165] dysferlin,[166] *Dicer*, a gene encoding a RNase III endonuclease essential for microRNA processing,[167] the lysosomal cysteine protease cathepsin L,[168] muscle LIM protein,[169] vinculin, a ubiquitously expressed multiliganded protein that links the actin cytoskeleton to the cell membrane,[170] apelin,[171] relaxin,[172] and delta-sarcoglycan (delta-sgc). The delta-sgc (−/−) is a mouse model of human limb girdle muscular dystrophy type 2F that also develops DCM.[173]

Cre-loxP-mediated deletion of peroxisome proliferator-activated receptor (PPAR)-gamma was created in transgenic mice. These PPAR gamma (−/−) animals developed progressive cardiac hypertrophy with mitochondrial oxidative damage and died from DCM at about 3 months of age.[174]

The mouse T-box family transcription factor gene, *TBX20*, guides cardiac development and is expressed in cardiac progenitor cells, differentiating cardiomyocytes and developing valvular tissues. TBX20 mutant mice develop DCM.[175]

Blocking the ErbB-2 or ErbB-4 tyrosine kinase receptors in transgenic mice results in DCM. When an ecdysone-inducible gene expression system was used to express a cardiomyocyte-specific, dominant-negative ErbB-1 mutant receptor in mice ErbB-2 signaling was blocked and the animals developed ventricular hypertrophy, dilatation, dysfunction, fibrosis, and other signs of DCM.[176]

ANP-null mice [Nppa (−/−)] develop ventricular hypertrophy. When these animals were challenged with pressure overload stress via surgically induced aortic constriction they rapidly progressed to heart failure.[177]

Mice with mutations in the voltage-regulated potassium channel KCNQ1 demonstrate K^+-channel dysfunction leading to long QT syndrome. This can lead to significant ventricular arrhythmias including ventricular fibrillation and cardiac arrest. Interestingly, these animals show similar concurrent problems to those

associated with humans with long QT syndrome including deafness, balance problems, and morphological abnormalities of the inner ear and GI tract.[178]

Overexpression Models

The TG9 mouse is generated by cardiac-specific overexpression of Cre-recombinase and displays typical signs of DCM. The DCM in this model is characterized by ventricular dilatation, systolic dysfunction, congestive heart failure, and premature death with a maximum lifespan of 13 weeks for males and 11 weeks for females. The animals develop signs of heart failure a few days before death but treatment with captopril or metoprolal will delay the progression of disease.[179]

G-alpha proteins are the α-subunits of heterotrimeric G proteins and play a major role in the determination of signaling selectivity. Adult transgenic mice with cardiac-directed overexpression of G-alpha(g) develop LV dysfunction, cardiomyopathy, and congestive heart failure.[180,181] However, transgenic rabbits with the same over expression of G-alpha exhibited increased heart rates and contractility but did not develop cardiomyopathy.[181] Transgenic mice that overexpress G (i)-coupled receptor (Ro1) also develop DCM.[182]

Transgenic mice that overexpress a number of different endogenous proteins and that develop cardiomyopathies have been reported. These include mice that overexpress tumor necrosis factor-alpha (TNF-α),[183,184] protein kinase C (PKC)-epsilon,[185,186] the cardiac-specific hR120GCryAB, analogous to the alphaB-crystallin gene in humans,[187] cardiac-specific calsequestrin,[188-190] erythropoietin, following high doses of NE,[191]β-tropomyosin,[192] myocardial creatine transporter,[193] the *cTnI* gene mutation Gly203Ser,[194] and the TRP cation channel, TRPC6.[195] Overexpression of β2-adrenergic receptor (AR) leads to fibrotic cardiomyopathy,[196] as does overexpression of α-1A AR.[197]

Mice with cardiac specific overexpression of glycosylphosphatidylinositol (GPI)-anchored human lipoprotein lipase (LpLGPI) develop dilated, lipotoxic cardiomyopathy associated with diabetes and severe obesity.[198] A similar lipotoxic cardiomyopathy can be generated in mice with cardiomyocyte-specific overexpression of the acyl CoA synthase gene.[199]

As noted previously mice with Cre-lox P-mediated deletion of peroxisome proliferator-activated receptor-gamma (PPAR-gamma) develop DCM. However, mice with cardiac-specific overexpression of the peroxisome proliferator-activated receptor-α (PPAR-α), a key driver of diabetes-related lipid metabolic dysregulation, also develop diastolic dysfunction, heart failure, prolonged QT intervals, and other arrhythmias.[200] PPAR-gamma1 transgenic mice develop DCM with increased lipid and glycogen stores, cardiomyocyte mitochondrial and cristae disruption.[201]

Mice that overexpress cardiac-specific serine-threonine kinase Akt develop ventricular hypertrophy at both the molecular and histological levels. The hypertrophy is associated with a significant increase in cardiomyocyte size.[202] Mice that overexpress the R120G mutation in the small heat shock-like protein αB-crystallin (CryAB

(R120G) develop cardiomyopathy at about 3 months of age and die from heart failure at 6-7 months of age.[203] Overexpression of matrix metalloproteinase-1, in the hearts of transgenic mice, causes cardiac hypertrophy, dilation, and systolic dysfunction.[204] Transgenic mice that overexpress sarcolemmal L-type Ca^{2+} channel proteins develop progressive cardiomyocyte necrosis, LV dysfunction, and premature death. The progression of disease can be enhanced by stimulation of β-adrenergic receptors.[205]

Glutathione peroxidase overexpression protects the hearts of animals made diabetic by the injection of streptozotocin (160 mg/kg, i.p.),[206] and overexpression of a mutant serum response factor preserved intracellular Ca^{2+} handling and the functional response to isoproterenol challenge.[207]

Human ET-1 cDNA was placed downstream of a promoter responsive to a doxycycline (DOX)-regulated transcriptional activator (tTA) in binary transgenic mice (BT, ET+/tTA+). Following DOX withdrawal, these animals start dying between 5 and 11 weeks of age from LV dilatation and contractile dysfunction. Histological examination of the mice revealed cardiac interstitial inflammatory infiltration with macrophages and T lymphocytes. The changes were associated with sequential increases in nuclear factor-kappaB translocation and expression of TNF-α, interferon-gamma, interleukin-1 (IL-1), and IL-6.[208]

Transgenic rats with mutations Asp175Asn and Glu180Gly in α-tropomyosin develop cardiomyopathy and sudden death with age. Prior to signs of cardiomyopathy animals with both mutations demonstrate an increase in the number of bradycardic and tachycardic fluctuations and decreased baroreflex sensitivity with exercise.[133]

References

1. Mirza M, Marston S, Willott R, Ashley C, Mogensen J, McKenna W, Robinson P, Redwood C, Watkins H. Dilated cardiomyopathy mutations in three thin filament regulatory proteins result in a common functional phenotype. *J Biol Chem.* 2005;280:28498–28506.
2. Thierfelder L, Watkins H, MacRae C, Lamas R, McKenna W, Vosberg HP, Seidman JG, Seidman CE. Alpha-tropomyosin and cardiac troponin T mutations cause familial hypertrophic cardiomyopathy: A disease of the sarcomere. *Cell.* 1994;77:701–712.
3. Watkins H, Seidman JG, Seidman CE. Familial hypertrophic cardiomyopathy: A genetic model of cardiac hypertrophy. *Hum Mol Genet.* 1995;4 Spec No:1721–1727.
4. Watkins H, Conner D, Thierfelder L, Jarcho JA, MacRae C, McKenna WJ, Maron BJ, Seidman JG, Seidman CE. Mutations in the cardiac myosin binding protein-C gene on chromosome 11 cause familial hypertrophic cardiomyopathy. *Nat Genet.* 1995;11:434–437.
5. Watkins H, Seidman CE, Seidman JG, Feng HS, Sweeney HL. Expression and functional assessment of a truncated cardiac troponin T that causes hypertrophic cardiomyopathy. Evidence for a dominant negative action. *J Clin Invest.* 1996;98:2456–2461.
6. Anan R, Greve G, Thierfelder L, Watkins H, McKenna WJ, Solomon S, Vecchio C, Shono H, Nakao S, Tanaka H. Prognostic implications of novel beta cardiac myosin heavy chain gene mutations that cause familial hypertrophic cardiomyopathy. *J Clin Invest.* 1994;93:280–285.
7. Liu SK, Roberts WC, Maron BJ. Comparison of morphologic findings in spontaneously occurring hypertrophic cardiomyopathy in humans, cats and dogs. *Am J Cardiol.* 1993;72:944–951.
8. Lombardi R, Bell A, Senthil V, Sidhu J, Noseda M, Roberts R, Marian AJ. Differential interactions of thin filament proteins in two cardiac troponin T mouse models of hypertrophic and dilated cardiomyopathies. *Cardiovasc Res.* 2008;79:109–117.

9. Jane-wit D, Altuntas CZ, Monti J, Johnson JM, Forsthuber TG, Tuohy VK. Sex-defined T-cell responses to cardiac self determine differential outcomes of murine dilated cardiomyopathy. *Am J Pathol.* 2008;172:11–21.
10. Gross DR. Animal Models in Cardiovascular Research, 2nd Revised Edition. Boston: Kluwer Academic Publishers; 1994.
11. MacDonald KA, Kittleson MD, Larson RF, Kass P, Klose T, Wisner ER. The effect of ramipril on left ventricular mass, myocardial fibrosis, diastolic function, and plasma neurohormones in Maine coon cats with familial hypertrophic cardiomyopathy without heart failure. *J Vet Intern Med.* 2006;20:1093–1105.
12. MacDonald KA, Wisner ER, Larson RF, Klose T, Kass PH, Kittleson MD. Comparison of myocardial contrast enhancement via cardiac magnetic resonance imaging in healthy cats and cats with hypertrophic cardiomyopathy. *Am J Vet Res.* 2005;66:1891–1894.
13. Gundler S, Tidholm A, Haggstrom J. Prevalence of myocardial hypertrophy in a population of asymptomatic Swedish Maine coon cats. *Acta Vet Scand.* 2008;50:22.
14. Fries R, Heaney AM, Meurs KM. Prevalence of the myosin-binding protein C mutation in Maine coon cats. *J Vet Intern Med.* 2008;22:893–896.
15. Carlos Sampedrano C, Chetboul V, Gouni V, Nicolle AP, Pouchelon JL, Tissier R. Systolic and diastolic myocardial dysfunction in cats with hypertrophic cardiomyopathy or systemic hypertension. *J Vet Intern Med.* 2006;20:1106–1115.
16. Koffas H, Dukes-McEwan J, Corcoran BM, Moran CM, French A, Sboros V, Simpson K, McDicken WN. Pulsed tissue Doppler imaging in normal cats and cats with hypertrophic cardiomyopathy. *J Vet Intern Med.* 2006;20:65–77.
17. Wall M, Calvert CA, Sanderson SL, Leonhardt A, Barker C, Fallaw TK. Evaluation of extended-release diltiazem once daily for cats with hypertrophic cardiomyopathy. *J Am Anim Hosp Assoc.* 2005;41:98–103.
18. Yang VK, Freeman LM, Rush JE. Comparisons of morphometric measurements and serum insulin-like growth factor concentration in healthy cats and cats with hypertrophic cardiomyopathy. *Am J Vet Res.* 2008;69:1061–1066.
19. Prosek R, Sisson DD, Oyama MA, Biondo AW, Solter PE. Measurements of plasma endothelin immunoreactivity in healthy cats and cats with cardiomyopathy. *J Vet Intern Med.* 2004;18:826–830.
20. Baty CJ. Feline hypertrophic cardiomyopathy: An update. *Vet Clin North Am Small Anim Pract.* 2004;34:1227–1234.
21. Nakagawa K, Takemura N, Machida N, Kawamura M, Amasaki H, Hirose H. Hypertrophic cardiomyopathy in a mixed breed cat family. *J Vet Med Sci.* 2002;64:619–621.
22. Bright JM, Herrtage ME, Schneider JF. Pulsed Doppler assessment of left ventricular diastolic function in normal and cardiomyopathic cats. *J Am Anim Hosp Assoc.* 1999;35:285–291.
23. Riesen SC, Kovacevic A, Lombard CW, Amberger C. Echocardiographic screening of purebred cats: An overview from 2002 to 2005. *Schweiz Arch Tierheilkd.* 2007;149:73–76.
24. Rush JE, Freeman LM, Fenollosa NK, Brown DJ. Population and survival characteristics of cats with hypertrophic cardiomyopathy: 260 cases (1990-1999). *J Am Vet Med Assoc.* 2002;220:202–207.
25. Meurs KM, Norgard MM, Ederer MM, Hendrix KP, Kittleson MD. A substitution mutation in the myosin binding protein C gene in ragdoll hypertrophic cardiomyopathy. *Genomics.* 2007;90:261–264.
26. Connolly DJ, Cannata J, Boswood A, Archer J, Groves EA, Neiger R. Cardiac troponin I in cats with hypertrophic cardiomyopathy. *J Feline Med Surg.* 2003;5:209–216.
27. Herndon WE, Kittleson MD, Sanderson K, Drobatz KJ, Clifford CA, Gelzer A, Summerfield NJ, Linde A, Sleeper MM. Cardiac troponin I in feline hypertrophic cardiomyopathy. *J Vet Intern Med.* 2002;16:558–564.
28. Cesta MF, Baty CJ, Keene BW, Smoak IW, Malarkey DE. Pathology of end-stage remodeling in a family of cats with hypertrophic cardiomyopathy. *Vet Pathol.* 2005;42:458–467.
29. Taugner FM. Stimulation of the renin-angiotensin system in cats with hypertrophic cardiomyopathy. *J Comp Pathol.* 2001;125:122–129.
30. MacDonald KA, Kittleson MD, Garcia-Nolen T, Larson RF, Wisner ER. Tissue Doppler imaging and gradient echo cardiac magnetic resonance imaging in normal cats and cats with hypertrophic cardiomyopathy. *J Vet Intern Med.* 2006;20:627–634.

31. Kaneshige T, Machida N, Itoh H, Yamane Y. The anatomical basis of complete atrioventricular block in cats with hypertrophic cardiomyopathy. *J Comp Pathol.* 2006;135:25–31.
32. Harvey AM, Battersby IA, Faena M, Fews D, Darke PG, Ferasin L. Arrhythmogenic right ventricular cardiomyopathy in two cats. *J Small Anim Pract.* 2005;46:151–156.
33. MacLean HN, Abbott JA, Ward DL, Huckle WR, Sisson DD, Pyle RL. N-terminal atrial natriuretic peptide immunoreactivity in plasma of cats with hypertrophic cardiomyopathy. *J Vet Intern Med.* 2006;20:284–289.
34. Biondo AW, Ehrhart EJ, Sisson DD, Bulmer BJ, De Morais HS, Solter PF. Immunohistochemistry of atrial and brain natriuretic peptides in control cats and cats with hypertrophic cardiomyopathy. *Vet Pathol.* 2003;40:501–506.
35. Bedard C, Lanevschi-Pietersma A, Dunn M. Evaluation of coagulation markers in the plasma of healthy cats and cats with asymptomatic hypertrophic cardiomyopathy. *Vet Clin Pathol.* 2007;36:167–172.
36. Stokol T, Brooks M, Rush JE, Rishniw M, Erb H, Rozanski E, Kraus MS, Gelzer AL. Hypercoagulability in cats with cardiomyopathy. *J Vet Intern Med.* 2008;22:546–552.
37. Brazzell JL, Borjesson DL. Evaluation of plasma antithrombin activity and D-dimer concentration in populations of healthy cats, clinically ill cats, and cats with cardiomyopathy. *Vet Clin Pathol.* 2007;36:79–84.
38. Chetboul V, Gouni V, Sampedrano CC, Tissier R, Serres F, Pouchelon JL. Assessment of regional systolic and diastolic myocardial function using tissue Doppler and strain imaging in dogs with dilated cardiomyopathy. *J Vet Intern Med.* 2007;21:719–730.
39. Freeman LM, Rush JE. Nutrition and cardiomyopathy: Lessons from spontaneous animal models. *Curr Heart Fail Rep.* 2007;4:84–90.
40. Philipp U, Broschk C, Vollmar A, Distl O. Evaluation of tafazzin as candidate for dilated cardiomyopathy in Irish wolfhounds. *J Hered.* 2007;98:506–509.
41. Distl O, Vollmar AC, Broschk C, Hamann H, Fox PR. Complex segregation analysis of dilated cardiomyopathy (DCM) in Irish wolfhounds. *Heredity.* 2007;99:460–465.
42. Meurs KM, Fox PR, Norgard M, Spier AW, Lamb A, Koplitz SL, Baumwart RD. A prospective genetic evaluation of familial dilated cardiomyopathy in the Doberman pinscher. *J Vet Intern Med.* 2007;21:1016–1020.
43. O'Sullivan ML, O'Grady MR, Minors SL. Assessment of diastolic function by Doppler echocardiography in normal Doberman pinschers and Doberman pinschers with dilated cardiomyopathy. *J Vet Intern Med.* 2007;21:81–91.
44. O'Sullivan ML, O'Grady MR, Minors SL. Plasma big endothelin-1, atrial natriuretic peptide, aldosterone, and norepinephrine concentrations in normal Doberman pinschers and Doberman pinschers with dilated cardiomyopathy. *J Vet Intern Med.* 2007;21:92–99.
45. Hamlin RL. Animal models of ventricular arrhythmias. *Pharmacol Ther.* 2007;113:276–295.
46. Moneva-Jordan A, Luis Fuentes V, Corcoran BM, French A, Dukes-McEwan J. Pulsus alternans in English cocker spaniels with dilated cardiomyopathy. *J Small Anim Pract.* 2007;48:258–263.
47. Chetboul V, Escriou C, Tessier D, Richard V, Pouchelon JL, Thibault H, Lallemand F, Thuillez C, Blot S, Derumeaux G. Tissue Doppler imaging detects early asymptomatic myocardial abnormalities in a dog model of Duchenne's cardiomyopathy. *Eur Heart J.* 2004;25:1934–1939.
48. Smith CE, Freeman LM, Rush JE, Cunningham SM, Biourge V. Omega-3 fatty acids in boxer dogs with arrhythmogenic right ventricular cardiomyopathy. *J Vet Intern Med.* 2007;21:265–273.
49. Oxford EM, Everitt M, Coombs W, Fox PR, Kraus M, Gelzer AR, Saffitz J, Taffet SM, Moise NS, Delmar M. Molecular composition of the intercalated disc in a spontaneous canine animal model of arrhythmogenic right ventricular dysplasia/cardiomyopathy. *Heart Rhythm.* 2007;4:1196–1205.
50. Baumwart RD, Orvalho J, Meurs KM. Evaluation of serum cardiac troponin I concentration in boxers with arrhythmogenic right ventricular cardiomyopathy. *Am J Vet Res.* 2007;68:524–528.
51. Hetyey CS, Manczur F, Dudas-Gyorki Z, Reiczigel J, Ribiczey P, Vajdovich P, Voros K. Plasma antioxidant capacity in dogs with naturally occurring heart diseases. *J Vet Med A Physiol Pathol Clin Med.* 2007;54:36–39.
52. Protonotarios N, Tsatsopoulou A. Naxos disease and Caravajal syndrome: Cardiocutaneous disorders that highlight the pathogenesis and broaden the spectrum of arrhythmogenic right ventricular cardiomyopathy. *Cardiovasc Pathol.* 2004;13:185–194.

53. Morrow CJ, McOrist S. Cardiomyopathy associated with a curly hair coat in poll Hereford calves in Australia. *Vet Rec.* 1985;117:312–313.
54. Watanabe S, Akita T, Itakura C, Goto M. Evidence for a new lethal gene causing cardiomyopathy in Japanese black calves. *J Hered.* 1979;70:255–258.
55. Whittington RJ, Cook RW. Cardiomyopathy and woolly haircoat syndrome of poll Hereford cattle: Electrocardiographic findings in affected and unaffected calves. *Aust Vet J.* 1988;65:341–344.
56. Gozalo AS, Cheng LI, St Claire ME, Ward JM, Elkins WR. Pathology of captive moustached tamarins (Saguinus mystax). *Comp Med.* 2008;58:188–195.
57. Gozalo A, Dagle GE, Montoya E, Weller RE. Spontaneous cardiomyopathy resembling acute rheumatic heart disease in an owl monkey. *J Med Primatol.* 1992;21:381–383.
58. Bossart GD, Odell DK, Altman NH. Cardiomyopathy in stranded pygmy and dwarf sperm whales. *J Am Vet Med Assoc.* 1985;187:1137–1140.
59. Recchia FA, Lionetti V. Animal models of dilated cardiomyopathy for translational research. *Vet Res Commun.* 2007;31 Suppl 1:35–41.
60. Bounhoure JP, Boveda S, Albenque JP. Arrhythmia-induced dilated cardiomyopathies. *Bull Acad Natl Med.* 2006;190:1225–35; discussion 1235-6.
61. Potter DD, Araoz PA, Ng LL, Kruger DG, Thompson JL, III, Hamner CE, Rysavy JA, Mandrekar JN, Sundt TM, III. Cardiotropin-1 and myocardial strain change heterogeneously in cardiomyopathy. *J Surg Res.* 2007;141:277–283.
62. Nishijima Y, Sridhar A, Viatchenko-Karpinski S, Shaw C, Bonagura JD, Abraham WT, Joshi MS, Bauer JA, Hamlin RL, Gyorke S, Feldman DS, Carnes CA. Chronic cardiac resynchronization therapy and reverse ventricular remodeling in a model of nonischemic cardiomyopathy. *Life Sci.* 2007;81:1152–1159.
63. Fuller GA, Bicer S, Hamlin RL, Yamaguchi M, Reiser PJ. Increased myosin heavy chain-beta with atrial expression of ventricular light chain-2 in canine cardiomyopathy. *J Card Fail.* 2007;13:680–686.
64. Liu X, Gu X, Li Z, Li X, Li H, Chang J, Chen P, Jin J, Xi B, Chen D, Lai D, Graham RM, Zhou M. Neuregulin-1/erbB-activation improves cardiac function and survival in models of ischemic, dilated, and viral cardiomyopathy. *J Am Coll Cardiol.* 2006;48:1438–1447.
65. Power JM, Raman J, Dornom A, Farish SJ, Burrell LM, Tonkin AM, Buxton B, Alferness CA. Passive ventricular constraint amends the course of heart failure: A study in an ovine model of dilated cardiomyopathy. *Cardiovasc Res.* 1999;44:549–555.
66. Raman JS, Byrne MJ, Power JM, Alferness CA. Ventricular constraint in severe heart failure halts decline in cardiovascular function associated with experimental dilated cardiomyopathy. *Ann Thorac Surg.* 2003;76:141–147.
67. Tibayan FA, Lai DT, Timek TA, Dagum P, Liang D, Zasio MK, Daughters GT, Miller DC, Ingels NB, Jr. Alterations in left ventricular curvature and principal strains in dilated cardiomyopathy with functional mitral regurgitation. *J Heart Valve Dis.* 2003;12:292–299.
68. Tibayan FA, Lai DT, Timek TA, Dagum P, Liang D, Daughters GT, Ingels NB, Miller DC. Alterations in left ventricular torsion in tachycardia-induced dilated cardiomyopathy. *J Thorac Cardiovasc Surg.* 2002;124:43–49.
69. Timek TA, Dagum P, Lai DT, Liang D, Daughters GT, Tibayan F, Ingels NB, Jr, Miller DC. Tachycardia-induced cardiomyopathy in the ovine heart: Mitral annular dynamic three-dimensional geometry. *J Thorac Cardiovasc Surg.* 2003;125:315–324.
70. Timek TA, Lai DT, Dagum P, Liang D, Daughters GT, Ingels NB, Jr, Miller DC. Mitral leaflet remodeling in dilated cardiomyopathy. *Circulation.* 2006;114:I518–I523.
71. Byrne MJ, Kaye DM, Mathis M, Reuter DG, Alferness CA, Power JM. Percutaneous mitral annular reduction provides continued benefit in an ovine model of dilated cardiomyopathy. *Circulation.* 2004;110:3088–3092.
72. Balaji S, Hewett KW, Krombach RS, Clair MJ, Ye X, Spinale FG. Inducible lethal ventricular arrhythmias in swine with pacing-induced heart failure. *Basic Res Cardiol.* 1999;94:496–503.
73. Spinale FG, Coker ML, Krombach SR, Mukherjee R, Hallak H, Houck WV, Clair MJ, Kribbs SB, Johnson LL, Peterson JT, Zile MR. Matrix metalloproteinase inhibition during the development of congestive heart failure: Effects on left ventricular dimensions and function. *Circ Res.* 1999;85:364–376.

74. Kostelec M, Covell J, Buckberg GD, Sadeghi A, Hoffman JI, Kassab GS. Myocardial protection in the failing heart: I. Effect of cardioplegia and the beating state under simulated left ventricular restoration. *J Thorac Cardiovasc Surg.* 2006;132:875–883.
75. Wei SK, Ruknudin AM, Shou M, McCurley JM, Hanlon SU, Elgin E, Schulze DH, Haigney MC. Muscarinic modulation of the sodium-calcium exchanger in heart failure. *Circulation.* 2007;115:1225–1233.
76. Perrino C, Naga Prasad SV, Mao L, Noma T, Yan Z, Kim HS, Smithies O, Rockman HA. Intermittent pressure overload triggers hypertrophy-independent cardiac dysfunction and vascular rarefaction. *J Clin Invest.* 2006;116:1547–1560.
77. Takahashi R, Asai T, Murakami H, Murakami R, Tsuzuki M, Numaguchi Y, Matsui H, Murohara T, Okumura K. Pressure overload-induced cardiomyopathy in heterozygous carrier mice of carnitine transporter gene mutation. *Hypertension.* 2007;50:497–502.
78. Zhang C, Yasuno S, Kuwahara K, Zankov DP, Kobori A, Makiyama T, Horie M. Blockade of angiotensin II type 1 receptor improves the arrhythmia morbidity in mice with left ventricular hypertrophy. *Circ J.* 2006;70:335–341.
79. Nishikawa N, Yamamoto K, Sakata Y, Mano T, Yoshida J, Miwa T, Takeda H, Hori M, Masuyama T. Differential activation of matrix metalloproteinases in heart failure with and without ventricular dilatation. *Cardiovasc Res.* 2003;57:766–774.
80. Zhang JN, Geng Q, Chen XJ, Fang WW, Wu XH, Yang D. Alteration of endothelin system and calcium handling protein in left ventricles following drug treatment in dilated cardiomyopathy rats. *Acta Pharmacol Sin.* 2003;24:1099–1102.
81. Jung AS, Kubo H, Wilson R, Houser SR, Margulies KB. Modulation of contractility by myocyte-derived arginase in normal and hypertrophied feline myocardium. *Am J Physiol Heart Circ Physiol.* 2006;290:H1756–H1762.
82. Ishikawa Y, Uechi M, Hori Y, Takashi E, Yamano S, Enomoto Y, Jun U. Effects of enalapril in cats with pressure overload-induced left ventricular hypertrophy. *J Feline Med Surg.* 2007;9:29–35.
83. Eghtesady P, Michelfelder E, Altaye M, Ballard E, Hirsh R, Beekman RH, III. Revisiting animal models of aortic stenosis in the early gestation fetus. *Ann Thorac Surg.* 2007;83:631–639.
84. Hughes WM, Jr, Rodriguez WE, Rosenberger D, Chen J, Sen U, Tyagi N, Moshal KS, Vacek T, Kang YJ, Tyagi SC. Role of copper and homocysteine in pressure overload heart failure. *Cardiovasc Toxicol.* 2008;8:137–144.
85. Hataishi R, Rodrigues AC, Morgan JG, Ichinose F, Derumeaux G, Bloch KD, Picard MH, Scherrer-Crosbie M. Nitric oxide synthase 2 and pressure-overload-induced left ventricular remodeling in mice. *Exp Physiol.* 2006;91:633–639.
86. van Empel VP, Bertrand AT, van Oort RJ, van der Nagel R, Engelen M, van Rijen HV, Doevendans PA, Crijns HJ, Ackerman SL, Sluiter W, De Windt LJ. EUK-8, a superoxide dismutase and catalase mimetic, reduces cardiac oxidative stress and ameliorates pressure overload-induced heart failure in the harlequin mouse mutant. *J Am Coll Cardiol.* 2006;48:824–832.
87. Kast RE, Foley KF, Focosi D. Doxorubicin cardiomyopathy via TLR-2 stimulation: Potential for prevention using current anti-retroviral inhibitors such as ritonavir and nelfinavir. *Hematol Oncol.* 2007;25:96–97.
88. Robert J. Long-term and short-term models for studying anthracycline cardiotoxicity and protectors. *Cardiovasc Toxicol.* 2007;7:135–139.
89. Robert J. Preclinical assessment of anthracycline cardiotoxicity in laboratory animals: Predictiveness and pitfalls. *Cell Biol Toxicol.* 2007;23:27–37.
90. Aupperle H, Garbade J, Schubert A, Barten M, Dhein S, Schoon HA, Mohr FW. Effects of autologous stem cells on immunohistochemical patterns and gene expression of metalloproteinases and their tissue inhibitors in doxorubicin cardiomyopathy in a rabbit model. *Vet Pathol.* 2007;44:494–503.
91. Ma GT, Xie XM, Wu XH, Chen XB, Fang YQ, He J. Short- and long-term therapeutic effects of combination therapy with perindopril and irbesartan in a rat model of dilated cardiomyopathy. *Zhong Nan Da Xue Xue Bao Yi Xue Ban.* 2007;32:594–598.
92. Berthiaume JM, Wallace KB. Persistent alterations to the gene expression profile of the heart subsequent to chronic doxorubicin treatment. *Cardiovasc Toxicol.* 2007;7:178–191.

93. Migrino RQ, Aggarwal D, Konorev E, Brahmbhatt T, Bright M, Kalyanaraman B. Early detection of doxorubicin cardiomyopathy using two-dimensional strain echocardiography. *Ultrasound Med Biol.* 2008;34:208–214.
94. Borenstein N, Chetboul V, Bruneval P, Hekmati M, Tissier R, Behr L, Derumeaux G, Montarras D. Non-cultured cell transplantation in an ovine model of non-ischemic heart failure. *Eur J Cardiothorac Surg.* 2007;31:444–451.
95. Kim KH, Oudit GY, Backx PH. Erythropoietin protects against doxorubicin-induced cardiomyopathy via a phosphatidylinositol 3-kinase-dependent pathway. *J Pharmacol Exp Ther.* 2008;324:160–169.
96. Westermann D, Rutschow S, Van Linthout S, Linderer A, Bucker-Gartner C, Sobirey M, Riad A, Pauschinger M, Schultheiss HP, Tschope C. Inhibition of p38 mitogen-activated protein kinase attenuates left ventricular dysfunction by mediating pro-inflammatory cardiac cytokine levels in a mouse model of diabetes mellitus. *Diabetologia.* 2006;49:2507–2513.
97. Westermann D, Van Linthout S, Dhayat S, Dhayat N, Schmidt A, Noutsias M, Song XY, Spillmann F, Riad A, Schultheiss HP, Tschope C. Tumor necrosis factor-alpha antagonism protects from myocardial inflammation and fibrosis in experimental diabetic cardiomyopathy. *Basic Res Cardiol.* 2007;102:500–507.
98. Van den Bergh A, Flameng W, Herijgers P. Type II diabetic mice exhibit contractile dysfunction but maintain cardiac output by favourable loading conditions. *Eur J Heart Fail.* 2006;8:777–783.
99. Belmadani S, Bernal J, Wei CC, Pallero MA, Dell'italia L, Murphy-Ullrich JE, Berecek KH. A thrombospondin-1 antagonist of transforming growth factor-beta activation blocks cardiomyopathy in rats with diabetes and elevated angiotensin II. *Am J Pathol.* 2007;171:777–789.
100. Toblli JE, Cao G, Rivas C, DeRosa G, Domecq P. Angiotensin-converting enzyme inhibition reduces lipid deposits in myocardium and improves left ventricular function of obese Zucker rats. *Obesity (Silver Spring).* 2006;14:1586–1595.
101. Shen X, Bornfeldt KE. Mouse models for studies of cardiovascular complications of type 1 diabetes. *Ann N Y Acad Sci.* 2007;1103:202–217.
102. Thakker GD, Frangogiannis NG, Bujak M, Zymek P, Gaubatz JW, Reddy AK, Taffet G, Michael LH, Entman ML, Ballantyne CM. Effects of diet-induced obesity on inflammation and remodeling after myocardial infarction. *Am J Physiol Heart Circ Physiol.* 2006;291:H2504–H2514.
103. Schmitto JD, Ortomann P, Vorkamp T, Heidrich F, Kolat P, Popov AF, Doerge H, Grossmann M, Seipelt R, Ramadori G, Schondube A. Histological changes in a model of chronic heart failure induced by multiple sequential coronary microembolization in sheep. *J Cardiovasc Surg (Torino).* 2008;49:533–537.
104. Monreal G, Gerhardt MA, Kambara A, Abrishamchian AR, Bauer JA, Goldstein AH. Selective microembolization of the circumflex coronary artery in an ovine model: Dilated, ischemic cardiomyopathy and left ventricular dysfunction. *J Card Fail.* 2004;10:174–183.
105. Moainie SL, Gorman JH, 3rd, Guy TS, Bowen FW, III, Jackson BM, Plappert T, Narula N, St John-Sutton MG, Narula J, Edmunds LH, Jr, Gorman RC. An ovine model of postinfarction dilated cardiomyopathy. *Ann Thorac Surg.* 2002;74:753–760.
106. Louail B, Sapoval M, Bonneau M, Wasseff M, Senechal Q, Gaux JC. A new porcine sponge material for temporary embolization: An experimental short-term pilot study in swine. *Cardiovasc Intervent Radiol.* 2006;29:826–831.
107. Kim WG, Cho SR, Sung SH, Park HJ. A chronic heart failure model by coronary artery ligation in the goat. *Int J Artif Organs.* 2003;26:929–934.
108. Bartfay WJ, Davis MT, Medves JM, Lugowski S. Milk whey protein decreases oxygen free radical production in a murine model of chronic iron-overload cardiomyopathy. *Can J Cardiol.* 2003;19:1163–1168.
109. Elsherif L, Ortines RV, Saari JT, Kang YJ. Congestive heart failure in copper-deficient mice. *Exp Biol Med (Maywood).* 2003;228:811–817.
110. Prozesky L, Bastianello SS, Fourie N, Schultz RA. A study of the pathology and pathogenesis of the myocardial lesions in gousiekte, a plant-induced cardiotoxicosis of ruminants. *Onderstepoort J Vet Res.* 2005;72:219–230.

111. Litwak KN, McMahan A, Lott KA, Lott LE, Koenig SC. Monensin toxicosis in the domestic bovine calf: A large animal model of cardiac dysfunction. *Contemp Top Lab Anim Sci.* 2005;44:45–49.
112. Shlosberg A, Perl S, Yakobson B, Klopfer U, Egyed MN, Nobel TA, Efron Y. The chronic course of a probable monensin toxicosis in cattle. *Vet Hum Toxicol.* 1986;28:230–233.
113. Cawley GD, Bradley R. Sudden death in calves associated with acute myocardial degeneration and selenium deficiency. *Vet Rec.* 1978;103:239–240.
114. Ferrans VJ, Van Vleet JF. Cardiac lesions of selenium-vitamin E deficiency in animals. *Heart Vessels Suppl.* 1985;1:294–297.
115. Wang ZH, Liao YH, Yuan J, Zhang L, Wang M, Zhang JH, Liu ZP, Dong JH. A therapeutic anti-CD4 monoclonal antibody inhibits T cell receptor signal transduction in mouse autoimmune cardiomyopathy. *Chin Med J (Engl).* 2007;120:1319–1325.
116. Buerke U, Carter JM, Schlitt A, Russ M, Schmidt H, Sibelius U, Grandel U, Grimminger F, Seeger1 W, Mueller-Werdan U, Werdan K, Buerke M. Apoptosis contributes to septic cardiomyopathy and is improved by simvastatin therapy. *Shock.* 2008;29:497–503.
117. Buvall L, Tang MS, Isic A, Andersson B, Fu M. Antibodies against the beta1-adrenergic receptor induce progressive development of cardiomyopathy. *J Mol Cell Cardiol.* 2007;42:1001–1007.
118. Mao W, Fukuoka S, Iwai C, Liu J, Sharma VK, Sheu SS, Fu M, Liang CS. Cardiomyocyte apoptosis in autoimmune cardiomyopathy: Mediated via endoplasmic reticulum stress and exaggerated by norepinephrine. *Am J Physiol Heart Circ Physiol.* 2007;293:H1636–H1645.
119. Baba A, Yoshikawa T, Iwata M, Anzai T, Nakamura I, Wainai Y, Ogawa S, Fu M. Antigen-specific effects of autoantibodies against sarcolemmal na-K-ATPase pump in immunized cardiomyopathic rabbits. *Int J Cardiol.* 2006;112:15–20.
120. Taneja V, Behrens M, Cooper LT, Yamada S, Kita H, Redfield MM, Terzic A, David C. Spontaneous myocarditis mimicking human disease occurs in the presence of an appropriate MHC and non-MHC background in transgenic mice. *J Mol Cell Cardiol.* 2007;42:1054–1064.
121. Taffet GE, Hartley CJ, Wen X, Pham T, Michael LH, Entman ML. Noninvasive indexes of cardiac systolic and diastolic function in hyperthyroid and senescent mouse. *Am J Physiol.* 1996;270:H2204–H2209.
122. Feng Y, Dai DZ, Na T, Cui B, Wang T, Zhang Y, Dai Y. Endothelin receptor antagonist CPU0213 suppresses ventricular fibrillation in L-thyroxin induced cardiomyopathy. *Pharmacol Rep.* 2007;59:306–314.
123. Medeiros A, Rolim NP, Oliveira RS, Rosa KT, Mattos KC, Casarini DE, Irigoyen MC, Krieger EM, Krieger JE, Negrao CE, Brum PC. Exercise training delays cardiac dysfunction and prevents calcium handling abnormalities in sympathetic hyperactivity-induced heart failure mice. *J Appl Physiol.* 2008;104:103–109.
124. Larsen KO, Sjaastad I, Svindland A, Krobert KA, Skjonsberg OH, Christensen G. Alveolar hypoxia induces left ventricular diastolic dysfunction and reduces phosphorylation of phospholamban in mice. *Am J Physiol Heart Circ Physiol.* 2006;291:H507–H516.
125. Liu H, Lee SS. Nuclear factor-kappaB inhibition improves myocardial contractility in rats with cirrhotic cardiomyopathy. *Liver Int.* 2008;28:640–648.
126. D'Souza M, Garza MA, Xie M, Weinstock J, Xiang Q, Robinson P. Substance P is associated with heart enlargement and apoptosis in murine dilated cardiomyopathy induced by Taenia crassiceps infection. *J Parasitol.* 2007;93:1121–1127.
127. Russell JC, Proctor SD. Small animal models of cardiovascular disease: Tools for the study of the roles of metabolic syndrome, dyslipidemia, and atherosclerosis. *Cardiovasc Pathol.* 2006;15:318–330.
128. Buchanan J, Mazumder PK, Hu P, Chakrabarti G, Roberts MW, Yun UJ, Cooksey RC, Litwin SE, Abel ED. Reduced cardiac efficiency and altered substrate metabolism precedes the onset of hyperglycemia and contractile dysfunction in two mouse models of insulin resistance and obesity. *Endocrinology.* 2005;146:5341–5349.
129. de Resende MM, Kriegel AJ, Greene AS. Combined effects of low-dose spironolactone and captopril therapy in a rat model of genetic hypertrophic cardiomyopathy. *J Cardiovasc Pharmacol.* 2006;48:265–273.

130. Prabhakar R, Boivin GP, Grupp IL, Hoit B, Arteaga G, Solaro JR, Wieczorek DF. A familial hypertrophic cardiomyopathy alpha-tropomyosin mutation causes severe cardiac hypertrophy and death in mice. *J Mol Cell Cardiol.* 2001;33:1815–1828.
131. Prabhakar R, Petrashevskaya N, Schwartz A, Aronow B, Boivin GP, Molkentin JD, Wieczorek DF. A mouse model of familial hypertrophic cardiomyopathy caused by a alpha-tropomyosin mutation. *Mol Cell Biochem.* 2003;251:33–42.
132. Jagatheesan G, Rajan S, Petrashevskaya N, Schwartz A, Boivin G, Arteaga GM, Solaro RJ, Liggett SB, Wieczorek DF. Rescue of tropomyosin-induced familial hypertrophic cardiomyopathy mice by transgenesis. *Am J Physiol Heart Circ Physiol.* 2007;293:H949–H958.
133. Wernicke D, Wessel N, Malberg H, Plehm R, Bauernschmitt R, Thierfelder L. Autonomic cardiac control in animal models of cardiovascular diseases II. Variability analysis in transgenic rats with alpha-tropomyosin mutations Asp175Asn and Glu180Gly. *Biomed Tech (Berl).* 2007;52:50–55.
134. Sweeney HL, Feng HS, Yang Z, Watkins H. Functional analyses of troponin T mutations that cause hypertrophic cardiomyopathy: Insights into disease pathogenesis and troponin function. *Proc Natl Acad Sci U S A.* 1998;95:14406–14410.
135. Tsoutsman T, Kelly M, Ng DC, Tan JE, Tu E, Lam L, Bogoyevitch MA, Seidman CE, Seidman JG, Semsarian C. Severe heart failure and early mortality in a double-mutation mouse model of familial hypertrophic cardiomyopathy. *Circulation.* 2008;117:1820–1831.
136. Fielitz J, Kim MS, Shelton JM, Latif S, Spencer JA, Glass DJ, Richardson JA, Bassel-Duby R, Olson EN. Myosin accumulation and striated muscle myopathy result from the loss of muscle RING finger 1 and 3. *J Clin Invest.* 2007;117:2486–2495.
137. Geisterfer-Lowrance AA, Christe M, Conner DA, Ingwall JS, Schoen FJ, Seidman CE, Seidman JG. A mouse model of familial hypertrophic cardiomyopathy. *Science.* 1996;272:731–734.
138. Kaneda T, Naruse C, Kawashima A, Fujino N, Oshima T, Namura M, Nunoda S, Mori S, Konno T, Ino H, Yamagishi M, Asano M. A novel beta-myosin heavy chain gene mutation, p.Met531Arg, identified in isolated left ventricular non-compaction in humans, results in left ventricular hypertrophy that progresses to dilation in a mouse model. *Clin Sci (Lond).* 2008;114:431–440.
139. Gustafson-Wagner EA, Sinn HW, Chen YL, Wang DZ, Reiter RS, Lin JL, Yang B, Williamson RA, Chen J, Lin CI, Lin JJ. Loss of mXinalpha, an intercalated disc protein, results in cardiac hypertrophy and cardiomyopathy with conduction defects. *Am J Physiol Heart Circ Physiol.* 2007;293:H2680–H2692.
140. Murata T, Lin MI, Huang Y, Yu J, Bauer PM, Giordano FJ, Sessa WC. Reexpression of caveolin-1 in endothelium rescues the vascular, cardiac, and pulmonary defects in global caveolin-1 knockout mice. *J Exp Med.* 2007;204:2373–2382.
141. Leatherbury L, Yu Q, Chatterjee B, Walker DL, Yu Z, Tian X, Lo CW. A novel mouse model of X-linked cardiac hypertrophy. *Am J Physiol Heart Circ Physiol.* 2008;294:H2701–H2711.
142. Langenickel TH, Buttgereit J, Pagel-Langenickel I, Lindner M, Monti J, Beuerlein K, Al-Saadi N, Plehm R, Popova E, Tank J, Dietz R, Willenbrock R, Bader M. Cardiac hypertrophy in transgenic rats expressing a dominant-negative mutant of the natriuretic peptide receptor B. *Proc Natl Acad Sci U S A.* 2006;103:4735–4740.
143. Rajan S, Ahmed RP, Jagatheesan G, Petrashevskaya N, Boivin GP, Urboniene D, Arteaga GM, Wolska BM, Solaro RJ, Liggett SB, Wieczorek DF. Dilated cardiomyopathy mutant tropomyosin mice develop cardiac dysfunction with significantly decreased fractional shortening and myofilament calcium sensitivity. *Circ Res.* 2007;101:205–214.
144. Mirza M, Robinson P, Kremneva E, Copeland O, Nikolaeva O, Watkins H, Levitsky D, Redwood C, El-Mezgueldi M, Marston S. The effect of mutations in alpha-tropomyosin (E40K and E54K) that cause familial dilated cardiomyopathy on the regulatory mechanism of cardiac muscle thin filaments. *J Biol Chem.* 2007;282:13487–13497.
145. Warren CM, Arteaga GM, Rajan S, Ahmed RP, Wieczorek DF, Solaro RJ. Use of 2-D DIGE analysis reveals altered phosphorylation in a tropomyosin mutant (Glu54Lys) linked to dilated cardiomyopathy. *Proteomics.* 2008;8:100–105.

146. Du J, Zhang C, Liu J, Sidky C, Huang XP. A point mutation (R192H) in the C-terminus of human cardiac troponin I causes diastolic dysfunction in transgenic mice. *Arch Biochem Biophys.* 2006;456:143–150.
147. Du CK, Morimoto S, Nishii K, Minakami R, Ohta M, Tadano N, Lu QW, Wang YY, Zhan DY, Mochizuki M, Kita S, Miwa Y, Takahashi-Yanaga F, Iwamoto T, Ohtsuki I, Sasaguri T. Knock-in mouse model of dilated cardiomyopathy caused by troponin mutation. *Circ Res.* 2007;101:185–194.
148. Ahmad F, Banerjee SK, Lage ML, Huang XN, Smith SH, Saba S, Rager J, Conner DA, Janczewski AM, Tobita K, Tinney JP, Moskowitz IP, Perez-Atayde AR, Keller BB, Mathier MA, Shroff SG, Seidman CE, Seidman JG. The role of cardiac troponin T quantity and function in cardiac development and dilated cardiomyopathy. *PLoS ONE.* 2008;3:e2642.
149. Juan F, Wei D, Xiongzhi Q, Ran D, Chunmei M, Lan H, Chuan Q, Lianfeng Z. The changes of the cardiac structure and function in cTnTR141W transgenic mice. *Int J Cardiol.* 2008;128:83–90.
150. Luckey SW, Mansoori J, Fair K, Antos CL, Olson EN, Leinwand LA. Blocking cardiac growth in hypertrophic cardiomyopathy induces cardiac dysfunction and decreased survival only in males. *Am J Physiol Heart Circ Physiol.* 2007;292:H838–H845.
151. Sze RW, Chan CB, Dardzinski BJ, Dunn S, Sanbe A, Schmithorst V, Robbins J, Holland SK, Strife JL. Three-dimensional MR microscopy of a transgenic mouse model of dilated cardiomyopathy. *Pediatr Radiol.* 2001;31:55–61.
152. Kuwahara K, Teg Pipes GC, McAnally J, Richardson JA, Hill JA, Bassel-Duby R, Olson EN. Modulation of adverse cardiac remodeling by STARS, a mediator of MEF2 signaling and SRF activity. *J Clin Invest.* 2007;117:1324–1334.
153. Yan X, Price RL, Nakayama M, Ito K, Schuldt AJ, Manning WJ, Sanbe A, Borg TK, Robbins J, Lorell BH. Ventricular-specific expression of angiotensin II type 2 receptors causes dilated cardiomyopathy and heart failure in transgenic mice. *Am J Physiol Heart Circ Physiol.* 2003;285:H2179–H2187.
154. Oudit GY, Kassiri Z, Patel MP, Chappell M, Butany J, Backx PH, Tsushima RG, Scholey JW, Khokha R, Penninger JM. Angiotensin II-mediated oxidative stress and inflammation mediate the age-dependent cardiomyopathy in ACE2 null mice. *Cardiovasc Res.* 2007;75:29–39.
155. Kontaridis MI, Yang W, Bence KK, Cullen D, Wang B, Bodyak N, Ke Q, Hinek A, Kang PM, Liao R, Neel BG. Deletion of Ptpn11 (Shp2) in cardiomyocytes causes dilated cardiomyopathy via effects on the extracellular signal-regulated kinase/mitogen-activated protein kinase and RhoA signaling pathways. *Circulation.* 2008;117:1423–1435.
156. Wolf CM, Wang L, Alcalai R, Pizard A, Burgon PG, Ahmad F, Sherwood M, Branco DM, Wakimoto H, Fishman GI, See V, Stewart CL, Conner DA, Berul CI, Seidman CE, Seidman JG. Lamin A/C haploinsufficiency causes dilated cardiomyopathy and apoptosis-triggered cardiac conduction system disease. *J Mol Cell Cardiol.* 2008;44:293–303.
157. Stewart CL, Kozlov S, Fong LG, Young SG. Mouse models of the laminopathies. *Exp Cell Res.* 2007;313:2144–2156.
158. Xiong S, Van Pelt CS, Elizondo-Fraire AC, Fernandez-Garcia B, Lozano G. Loss of Mdm4 results in p53-dependent dilated cardiomyopathy. *Circulation.* 2007;115:2925–2930.
159. Hesse M, Kondo CS, Clark RB, Su L, Allen FL, Geary-Joo CT, Kunnathu S, Severson DL, Nygren A, Giles WR, Cross JC. Dilated cardiomyopathy is associated with reduced expression of the cardiac sodium channel Scn5a. *Cardiovasc Res.* 2007;75:498–509.
160. Yan J, Zhu HB. Cyclic nucleotide phosphodiesterase IV expression, activity and targeting in cells of cardiovascular system. *Yao Xue Xue Bao.* 2007;42:571–575.
161. Hilfiker-Kleiner D, Kaminski K, Podewski E, Bonda T, Schaefer A, Sliwa K, Forster O, Quint A, Landmesser U, Doerries C, Luchtefeld M, Poli V, Schneider MD, Balligand JL, Desjardins F, Ansari A, Struman I, Nguyen NQ, Zschemisch NH, Klein G, Heusch G, Schulz R, Hilfiker A, Drexler H. A cathepsin D-cleaved 16 kDa form of prolactin mediates postpartum cardiomyopathy. *Cell.* 2007;128:589–600.
162. Spurney CF, Knoblach S, Pistilli EE, Nagaraju K, Martin GR, Hoffman EP. Dystrophin-deficient cardiomyopathy in mouse: Expression of Nox4 and lox are associated with fibrosis and altered functional parameters in the heart. *Neuromuscul Disord.* 2008;18:371–381.

163. Bostick B, Yue Y, Long C, Duan D. Prevention of dystrophin-deficient cardiomyopathy in twenty-one-month-old carrier mice by mosaic dystrophin expression or complementary Dystrophin/Utrophin expression. *Circ Res.* 2008;102:121–130.
164. Branco DM, Wolf CM, Sherwood M, Hammer PE, Kang PB, Berul CI. Cardiac electrophysiological characteristics of the mdx (5cv) mouse model of duchenne muscular dystrophy. *J Interv Card Electrophysiol.* 2007;20(1-2):1–7.
165. Bauer R, Macgowan GA, Blain A, Bushby K, Straub V. Steroid treatment causes deterioration of myocardial function in the {delta}-sarcoglycan-deficient mouse model for dilated cardiomyopathy. *Cardiovasc Res.* 2008;79:652–661.
166. Wenzel K, Geier C, Qadri F, Hubner N, Schulz H, Erdmann B, Gross V, Bauer D, Dechend R, Dietz R, Osterziel KJ, Spuler S, Ozcelik C. Dysfunction of dysferlin-deficient hearts. *J Mol Med.* 2007;85:1203–1214.
167. Chen JF, Murchison EP, Tang R, Callis TE, Tatsuguchi M, Deng Z, Rojas M, Hammond SM, Schneider MD, Selzman CH, Meissner G, Patterson C, Hannon GJ, Wang DZ. Targeted deletion of dicer in the heart leads to dilated cardiomyopathy and heart failure. *Proc Natl Acad Sci U S A.* 2008;105:2111–2116.
168. Spira D, Stypmann J, Tobin DJ, Petermann I, Mayer C, Hagemann S, Vasiljeva O, Gunther T, Schule R, Peters C, Reinheckel T. Cell type-specific functions of the lysosomal protease cathepsin L in the heart. *J Biol Chem.* 2007;282:37045–37052.
169. Gardiwal A, Klein G, Kraemer K, Durgac T, Koenig T, Niehaus M, Heineke J, Mohammadi B, Krampfl K, Schaefer A, Wollert KC, Korte T. Reduced delayed rectifier K+ current, altered electrophysiology, and increased ventricular vulnerability in MLP-deficient mice. *J Card Fail.* 2007;13:687–693.
170. Zemljic-Harpf AE, Miller JC, Henderson SA, Wright AT, Manso AM, Elsherif L, Dalton ND, Thor AK, Perkins GA, McCulloch AD, Ross RS. Cardiac-myocyte-specific excision of the vinculin gene disrupts cellular junctions, causing sudden death or dilated cardiomyopathy. *Mol Cell Biol.* 2007;27:7522–7537.
171. Kuba K, Zhang L, Imai Y, Arab S, Chen M, Maekawa Y, Leschnik M, Leibbrandt A, Markovic M, Schwaighofer J, Beetz N, Musialek R, Neely GG, Komnenovic V, Kolm U, Metzler B, Ricci R, Hara H, Meixner A, Nghiem M, Chen X, Dawood F, Wong KM, Sarao R, Cukerman E, Kimura A, Hein L, Thalhammer J, Liu PP, Penninger JM. Impaired heart contractility in apelin gene-deficient mice associated with aging and pressure overload. *Circ Res.* 2007;101:e32–e42.
172. Du XJ, Samuel CS, Gao XM, Zhao L, Parry LJ, Tregear GW. Increased myocardial collagen and ventricular diastolic dysfunction in relaxin deficient mice: A gender-specific phenotype. *Cardiovasc Res.* 2003;57:395–404.
173. Milner DJ, Kaufman SJ. Alpha7beta1 integrin does not alleviate disease in a mouse model of limb girdle muscular dystrophy type 2F. *Am J Pathol.* 2007;170:609–619.
174. Ding G, Fu M, Qin Q, Lewis W, Kim HW, Fukai T, Bacanamwo M, Chen YE, Schneider MD, Mangelsdorf DJ, Evans RM, Yang Q. Cardiac peroxisome proliferator-activated receptor gamma is essential in protecting cardiomyocytes from oxidative damage. *Cardiovasc Res.* 2007;76:269–279.
175. Kirk EP, Sunde M, Costa MW, Rankin SA, Wolstein O, Castro ML, Butler TL, Hyun C, Guo G, Otway R, Mackay JP, Waddell LB, Cole AD, Hayward C, Keogh A, Macdonald P, Griffiths L, Fatkin D, Sholler GF, Zorn AM, Feneley MP, Winlaw DS, Harvey RP. Mutations in cardiac T-box factor gene TBX20 are associated with diverse cardiac pathologies, including defects of septation and valvulogenesis and cardiomyopathy. *Am J Hum Genet.* 2007;81:280–291.
176. Rajagopalan V, Zucker IH, Jones JA, Carlson M, Ma YJ. Cardiac ErbB-1/ErbB-2 mutant expression in young adult mice leads to cardiac dysfunction. Am J Physiol Heart Circ Physiol. 2008.
177. Franco V, Chen YF, Feng JA, Li P, Wang D, Hasan E, Oparil S, Perry GJ. Eplerenone prevents adverse cardiac remodeling induced by pressure overload in atrial natriuretic peptide-null mice. *Clin Exp Pharmacol Physiol.* 2006;33:773–779.
178. Jespersen T, Grunnet M, Olesen SP. The KCNQ1 potassium channel: From gene to physiological function. *Physiology (Bethesda).* 2005;20:408–416.

179. McMullen JR, Amirahmadi F, Woodcock EA, Schinke-Braun M, Bouwman RD, Hewitt KA, Mollica JP, Zhang L, Zhang Y, Shioi T, Buerger A, Izumo S, Jay PY, Jennings GL. Protective effects of exercise and phosphoinositide 3-kinase(p110alpha) signaling in dilated and hypertrophic cardiomyopathy. *Proc Natl Acad Sci U S A.* 2007;104:612–617.
180. Rebolledo B, Lai NC, Gao MH, Takahashi T, Roth DM, Baird SM, Hammond HK. Adenylylcyclase gene transfer increases function of the failing heart. *Hum Gene Ther.* 2006;17:1043–1048.
181. Nishizawa T, Vatner SF, Hong C, Shen YT, Hardt SE, Robbins J, Ishikawa Y, Sadoshima J, Vatner DE. Overexpressed cardiac gsalpha in rabbits. *J Mol Cell Cardiol.* 2006;41:44–50.
182. McCloskey DT, Turcato S, Wang GY, Turnbull L, Zhu BQ, Bambino T, Nguyen AP, Lovett DH, Nissenson RA, Karliner JS, Baker AJ. Expression of a gi-coupled receptor in the heart causes impaired Ca2+ handling, myofilament injury, and dilated cardiomyopathy. *Am J Physiol Heart Circ Physiol.* 2008;294:H205–H212.
183. Matsusaka H, Ikeuchi M, Matsushima S, Ide T, Kubota T, Feldman AM, Takeshita A, Sunagawa K, Tsutsui H. Selective disruption of MMP-2 gene exacerbates myocardial inflammation and dysfunction in mice with cytokine-induced cardiomyopathy. *Am J Physiol Heart Circ Physiol.* 2005;289:H1858–H1864.
184. Kurrelmeyer KM, Michael LH, Baumgarten G, Taffet GE, Peschon JJ, Sivasubramanian N, Entman ML, Mann DL. Endogenous tumor necrosis factor protects the adult cardiac myocyte against ischemic-induced apoptosis in a murine model of acute myocardial infarction. *Proc Natl Acad Sci U S A.* 2000;97:5456–5461.
185. Xiao L, Zhao Q, Du Y, Yuan C, Solaro RJ, Buttrick PM. PKCepsilon increases phosphorylation of the cardiac myosin binding protein C at serine 302 both in vitro and in vivo. *Biochemistry.* 2007;46:7054–7061.
186. Hankiewicz JH, Goldspink PH, Buttrick PM, Lewandowski ED. Principal strain changes precede ventricular wall thinning during transition to heart failure in a mouse model of dilated cardiomyopathy. *Am J Physiol Heart Circ Physiol.* 2008;294:H330–H336.
187. Rajasekaran NS, Connell P, Christians ES, Yan LJ, Taylor RP, Orosz A, Zhang XQ, Stevenson TJ, Peshock RM, Leopold JA, Barry WH, Loscalzo J, Odelberg SJ, Benjamin IJ. Human alpha B-crystallin mutation causes oxido-reductive stress and protein aggregation cardiomyopathy in mice. *Cell.* 2007;130:427–439.
188. Le Corvoisier P, Park HY, Carlson KM, Marchuk DA, Rockman HA. Multiple quantitative trait loci modify the heart failure phenotype in murine cardiomyopathy. *Hum Mol Genet.* 2003;12:3097–3107.
189. Yang A, Sonin D, Jones L, Barry WH, Liang BT. A beneficial role of cardiac P2X4 receptors in heart failure: Rescue of the calsequestrin overexpression model of cardiomyopathy. *Am J Physiol Heart Circ Physiol.* 2004;287:H1096–H1103.
190. Shen JB, Cronin C, Sonin D, Joshi BV, Gongora Nieto M, Harrison D, Jacobson KA, Liang BT. P2X purinergic receptor-mediated ionic current in cardiac myocytes of calsequestrin model of cardiomyopathy: Implications for the treatment of heart failure. *Am J Physiol Heart Circ Physiol.* 2007;292:H1077–H1084.
191. Deten A, Shibata J, Scholz D, Briest W, Wagner KF, Wenger RH, Zimmer HG. Norepinephrine-induced acute heart failure in transgenic mice overexpressing erythropoietin. *Cardiovasc Res.* 2004;61:105–114.
192. Gaffin RD, Gokulan K, Sacchettini JC, Hewett T, Klevitsky R, Robbins J, Muthuchamy M. Charged residue changes in the carboxy-terminus of alpha-tropomyosin alter mouse cardiac muscle contractility. *J Physiol.* 2004;556:531–543.
193. Wallis J, Lygate CA, Fischer A, ten Hove M, Schneider JE, Sebag-Montefiore L, Dawson D, Hulbert K, Zhang W, Zhang MH, Watkins H, Clarke K, Neubauer S. Supranormal myocardial creatine and phosphocreatine concentrations lead to cardiac hypertrophy and heart failure: Insights from creatine transporter-overexpressing transgenic mice. *Circulation.* 2005;112:3131–3139.
194. Nguyen L, Chung J, Lam L, Tsoutsman T, Semsarian C. Abnormal cardiac response to exercise in a murine model of familial hypertrophic cardiomyopathy. *Int J Cardiol.* 2007;119:245–248.

195. Kuwahara K, Wang Y, McAnally J, Richardson JA, Bassel-Duby R, Hill JA, Olson EN. TRPC6 fulfills a calcineurin signaling circuit during pathologic cardiac remodeling. *J Clin Invest.* 2006;116:3114–3126.
196. Bathgate RA, Lekgabe ED, McGuane JT, Su Y, Pham T, Ferraro T, Layfield S, Hannan RD, Thomas WG, Samuel CS, Du XJ. Adenovirus-mediated delivery of relaxin reverses cardiac fibrosis. *Mol Cell Endocrinol.* 2008;280(1-2):30–38.
197. Chaulet H, Lin F, Guo J, Owens WA, Michalicek J, Kesteven SH, Guan Z, Prall OW, Mearns BM, Feneley MP, Steinberg SF, Graham RM. Sustained augmentation of cardiac alpha1A-adrenergic drive results in pathological remodeling with contractile dysfunction, progressive fibrosis and reactivation of matricellular protein genes. *J Mol Cell Cardiol.* 2006;40:540–552.
198. Park TS, Hu Y, Noh HL, Drosatos K, Okajima K, Buchanan J, Tuinei J, Homma S, Jiang XC, Abel ED, Goldberg IJ. Ceramide is a cardiotoxin in lipotoxic cardiomyopathy. *J Lipid Res.* 2008;49:2101–2112.
199. Lee Y, Naseem RH, Duplomb L, Park BH, Garry DJ, Richardson JA, Schaffer JE, Unger RH. Hyperleptinemia prevents lipotoxic cardiomyopathy in acyl CoA synthase transgenic mice. *Proc Natl Acad Sci U S A.* 2004;101:13624–13629.
200. Marionneau C, Aimond F, Brunet S, Niwa N, Finck B, Kelly DP, Nerbonne JM. PPARalpha-mediated remodeling of repolarizing voltage-gated K+ (kv) channels in a mouse model of metabolic cardiomyopathy. *J Mol Cell Cardiol.* 2008;44:1002–1015.
201. Son NH, Park TS, Yamashita H, Yokoyama M, Huggins LA, Okajima K, Homma S, Szabolcs MJ, Huang LS, Goldberg IJ. Cardiomyocyte expression of PPARgamma leads to cardiac dysfunction in mice. *J Clin Invest.* 2007;117:2791–2801.
202. Condorelli G, Drusco A, Stassi G, Bellacosa A, Roncarati R, Iaccarino G, Russo MA, Gu Y, Dalton N, Chung C, Latronico MV, Napoli C, Sadoshima J, Croce CM, Ross J, Jr. Akt induces enhanced myocardial contractility and cell size in vivo in transgenic mice. *Proc Natl Acad Sci U S A.* 2002;99:12333–12338.
203. Maloyan A, Gulick J, Glabe CG, Kayed R, Robbins J. Exercise reverses preamyloid oligomer and prolongs survival in alphaB-crystallin-based desmin-related cardiomyopathy. *Proc Natl Acad Sci U S A.* 2007;104:5995–6000.
204. Lee RT. Matrix metalloproteinase inhibition and the prevention of heart failure. *Trends Cardiovasc Med.* 2001;11:202–205.
205. Nakayama H, Chen X, Baines CP, Klevitsky R, Zhang X, Zhang H, Jaleel N, Chua BH, Hewett TE, Robbins J, Houser SR, Molkentin JD. Ca2+- and mitochondrial-dependent cardiomyocyte necrosis as a primary mediator of heart failure. *J Clin Invest.* 2007;117:2431–2444.
206. Matsushima S, Kinugawa S, Ide T, Matsusaka H, Inoue N, Ohta Y, Yokota T, Sunagawa K, Tsutsui H. Overexpression of glutathione peroxidase attenuates myocardial remodeling and preserves diastolic function in diabetic heart. *Am J Physiol Heart Circ Physiol.* 2006;291:H2237–H2245.
207. Azhar G, Zhang X, Wang S, Zhong Y, Quick CM, Wei JY. Maintaining serum response factor activity in the older heart equal to that of the young adult is associated with better cardiac response to isoproterenol stress. *Basic Res Cardiol.* 2007;102:233–244.
208. Yang LL, Gros R, Kabir MG, Sadi A, Gotlieb AI, Husain M, Stewart DJ. Conditional cardiac overexpression of endothelin-1 induces inflammation and dilated cardiomyopathy in mice. *Circulation.* 2004;109:255–261.

Chapter 11
Iatrogenic, Congenic, and Transgenic Models of Hypertension

Human essential hypertension is a multifactorial and complex disease involving several genes that have, thus far, defied complete characterization. Congenic models such as the spontaneously hypertensive stroke-prone rats are genetically homo geneous and thus aid the search for causative genes. The identification of quantitative trait loci (QTL) responsible for blood pressure regulation by genome-wide scanning is most commonly employed;[1] however, the identification of a QTL is just the first step to identify the gene(s) of interest. Congenic strains must be produced to verify the QTL and identify the chromosomal region that must then be reduced to an appropriate size for positional cloning of the gene(s). So-called "speed congenic strategies" have been used to confirm blood pressure QTLs on rat chromosome 2.[2]

The number of articles published each year suggests that the various animal models of hypertension are probably the most used in cardiovascular research. The volume of significant, i.e., leading to effective treatment of the human condition, research conducted using these models verifies their importance.

As early as 1889 Tigerstedt and Bergman demonstrated that extracts from the kidney could produce a pressor effect. They named the active substance "renin."[3] Goldblatt, Lynch, Hanzal, and Summerville published "The Production of Persistent Elevation of Systolic Blood Pressure by Means of Renal Ischemia" in the *Journal of Experimental Medicine* in 1934. Goldblatt and his colleagues produced persistent hypertension in dogs following a two-stage renal arterial constriction. A year earlier John Loesch had published a three-part article in a German journal entitled *A Contribution to Experimental Nephritis and to Arterial Hypertension*. The animal model Loesch used was intermittent cross-clamping of the canine renal pedicle.[4] Within a few years of the work of Goldblatt, Page and Helmer working in the USA and Braun-Menendez et al., working independently in Argentina, described the renin-angiotensin system much as we recognize it today. Various forms of the Goldblatt preparation, all involving surgically reducing blood flow to the kidney(s), are still widely used, with over 500 recent references identified. These models are usually identified as renovascular hypertension models and purport to mimic essential hypertension in humans.

D.R. Gross, *Animal Models in Cardiovascular Research*,
DOI: 10.1007/978-0-387-95962-7_11, © Springer Science + Business Media, LLC 2009

The spontaneously hypertensive rat (SHR) is the most widely used animal model of hypertension with over 17,000 articles cited in PubMed. However, this model reflects a rare subtype of human hypertension, primary hypertension inherited in a Mendelian fashion. When the natural history and response to antihypertensive drugs in different rat models of hypertension [SHR, Dahl, DOCA-salt, two-kidney one-clip, and the transgenic TGR(mRen2)27] were compared it was found that all of the models exhibited cardiac hypertrophy and impaired endothelium-dependent relaxation but the more severe forms of end-organ damage such as heart failure, stroke, and kidney failure occur only in some of the models and even then in a subset of the hypertensive rats. The effects of antihypertensive drugs varied even more in the different models. For example, endothelin-receptor antagonists are not effective in SHR but are effective in the deoxycorticosterone acetate (DOCA)-salt model. It was found that some antihypertensives only attenuate end-organ damage if they effectively reduce blood pressure while others do so in nonhypotensive doses. Other agents such as hydralazine in the SHR decrease blood pressure but do not prevent organ damage.[5]

Mice models of hypertension present some technical difficulties. The C57BL/6 strain of mice is almost ubiquitous as the genetic background for transgenic and gene knockout models, but it is somewhat resistant to renovascular hypertension. Successful models have been created using a combination of DOCA-salt and Angiotensin-II (Angio-II) infusion[6] and the renovascular two-kidney, one-clip (2K1C) and DOCA-salt combination.[7] However, Wiesel et al.[8] produced two different models of renovascular hypertension in male C57BL/6 mice with a single renin gene, a 2K1C and a one-kidney, one-clip (1K1C). Both models required the clip lumen diameter to be exactly 0.12 mm. Clips with a 0.11-mm lumen resulted in a high percentage of renal infarction and clips with a 0.13-mm lumen failed to produce hypertension. The 2K1C model is considered to be renin-dependent, that is, renin levels are consistently elevated during hypertension. The 1K1C model is characterized by increased plasma renin activity initially but within a few days plasma renin activity returns to normal while sodium retention and plasma volume increase and hypertension persists.[3]

Renovascular Hypertension

Several different variations of the original Goldblatt renovascular hypertensive model have been developed. As previously described the original model in dogs was a 2-kidney, 1-clip (2K1C) model. Both kidneys were left intact but the renal arterial flow to one kidney was significantly reduced by partial ligation. In dogs the 2K1C model has been well characterized. Following unilateral renal arterial constriction there is a decrease in extensibility of both arteries and veins during the first 24 h. The early stages of the dog model are characterized by an increase in arterial pressure, an increase in aortic flow, a decrease in total peripheral resistance, and enhanced responses to Angio-II and serotonin. As aortic flow continues to increase

the response to norepinephrine increases and the dilator responses to acetylcholine and nitroglycerine decrease. Aortic flow then decreases to baseline levels and the increase in aortic pressure is maintained by an increase in total peripheral resistance. Within 32 days vascular stiffness is further increased and there is a decrease in vascular smooth muscle (VSM) contractility.[3]

Greenberg et al. modified the classical 2K1C preparation by using a hydraulic occluder on a renal artery. They also instrumented the same renal artery with a flowmeter transducer. Initially it was necessary to reduce preconstriction flow by 5-15% to produce hypertension but it was necessary to adjust the hydraulic occluder several times over the first 4 h of occlusion to maintain that level of flow reduction since the kidney was able to autoregulate, with blood flow increasing again to normal levels despite the constriction.[3]

Renovascular hypertension has been demonstrated in 1K1C and 2K1C models, with and without wrapping, in most other animal species used for hypertension research. Surgical constriction (banding) of the mid-thoracic aorta, the thoracic aorta just proximal to the diaphragm, the abdominal aorta just proximal to the renal arteries, or between them have all been used to create hypertensive models. When 1-kidney or kidney wrapping models are created it can be accomplished as either a one-stage or two-stage procedure. The two-stage models usually involve unilateral nephrectomy first and when the animal recovers a second operation to create renal artery constriction or wrapping.[3,9]

2K1C and 1K1C Renovascular Hypertension in Rats

In the rat model of 2K1C hypertension one report claims that plasma Angio-II levels do not correlate directly with blood pressure changes although tissue Angio-II production is upregulated in the kidneys and adrenal glands and Angiotensin-II-type 1 (AT-1) receptor density is maintained in these tissues.[10] This point may be controversial since Gauer et al.[11] report that osteopontin is highly upregulated in many models of renal disease including 2K1C hypertension in rats and Angio-II seems to induce elevated osteopontin production in the nonclipped kidney. Osteopontin is involved in the induction of the nephrosclerosis associated with the 2K1C model. The nephrosclerosis is probably associated with augmented monocyte infiltration.

Plasma renin activity and aldosterone are more increased in 2K1C rats than in sham controls but blockade of the prorenin receptor does not improve target organ damage.[12] 2K1C rats demonstrate a decrease in isoprenaline-induced vasodilation most likely related to impaired modulation of sarcolemmal Ca^{2+} ATPase activity. K^+ ATP channels may play a compensatory role during isoprenaline-induced vascular relaxation in this model.[13] Treatment of 2K1C rats with the modified fatty acid tetradecylthioacetic acid (TTA) attenuated the development of hypertension, reduced the mRNA levels of renin in the clipped kidney, reduced plasma renin activity, and prevented organ damage. These effects were attributed to reducing circulating levels of Angio-II and 8-iso-prostaglandin F2α as well as inducing an increase in serum oleic acid levels.[14]

Immunoprotease subunit-7 (LMP-7) was upregulated in the clipped, atrophic kidneys of 2K1C rats but the unclipped kidney was hypertrophied and LMP-7 was not increased. These results suggest a direct link between LMP-7 and renal atrophy.[15] When rats were treated with L-arginine (10 mg/ml with an average intake of 300 mg/day) from the 7th to the 14th day following the 2K1C surgery systemic blood pressure was reduced compared with that in untreated rats. The antihypertensive effects of the L-arginine were attributed to increased nitric oxide (NO) formation and reduced Angio-II formation.[16]

When the subfornical organ (SFO), a forebrain circumventricular structure, was electrolytically lesioned the mean arterial pressure and the range of the baroreflex response of heart rate were significantly decreased in 2K1C rats. Circulating levels of Angio-II were unchanged.[17]

Tachycardia is a common occurrence in the 1K1C rat model of renovascular hypertension. This tachycardia has been attributed to intrinsic cardiac mechanisms and a shift in the sympatho vagal balance toward cardiac sympathetic stimulation and vagal suppression. These changes are associated with a decrease in baroreflex sensitivity.[18] When both renal arteries were constricted with ring-shaped silver clips a stroke-prone renovascular hypertension developed. Lesions were observed in the cerebral arteries and arterioles in these rats along with damage to cerebral capillaries - all associated with the hypertension. The incidence of spontaneous stroke was 56.4% within 40 weeks after bilateral renal artery constriction.[19]

In rats the clip-ablation model is produced by placement of a silver clip with a 0.13-mm lumen on a branch of the left renal artery that supplies one-third of that kidney. The right kidney is removed. This allows the effects of renin-dependent hypertension to be studied in glomeruli undergoing compensatory changes in response to renal mass. When these animals were compared with rats with one kidney removed and a one-third reduction of the remaining kidney mass at various intervals up to 28 days after surgery it was found that plasma renin activity was increased slightly at 3 days postoperation in the ablation model but returned to normal within 28 days whereas plasma renin activity continuously rose in the clip-ablation model. Systolic blood pressure increased with time in both models but the increase in clip-ablation model was greater. There was also more glomerular damage in the clip-ablation rats.[20]

Rats with renovascular (2K1C) hypertension were compared with those with hypertension produced by DOCA (15 mg/kg, s.c., two times/week) and *N*-nitro L-arginine methyl ester (L-NAME) (50 mg/kg/day, i.p., 10 weeks). There were increases in blood pressure and decreases in baroreflex sensitivity in all the three groups. Blood pressure variability was highest in the DOCA rats. The L-NAME rats had the lowest baroreflex sensitivity. Morphological changes were similar in the DOCA and L-NAME rats with relatively slight cardiac changes in the 2K1C rats. Endothelin-1 levels were highest in the DOCA group while Angio-II was increased in the 2K1C rats and decreased in DOCA rats.[21] When red blood cell (RBC) deformability and aggregation were compared in 1K1C, 2K1C, DOCA, and L-NAME rats it was found that RBC rheological properties were altered in all the four models of hypertension, which might play a role in its development. However,

the phenotypic alterations were not the same in the various models even though the length and magnitude of the hypertension were similar.[22]

It is also possible to produce significant hypertension in rats by partially occluding the aorta between the origins of the renal arteries. Approximately 8 days later the rats develop hypertension. The hypertension is not due to a mechanical increase in resistance from the coarctation but to increased renin release. This model can be reversed by the administration of angiotensin-converting enzyme inhibitors.[3] Another rat model was created in Sprague-Dawley rats by banding the abdominal aorta proximal to the renal arteries. This results in severe hypertension proximal but not distal to the coarctation and renal hypoperfusion. This activates the renin-angiotensin system and may promote the local induction of chemoattractant and inflammatory cytokines resulting in tubulointerstitial inflammation associated with leukocyte activation.[23]

2K1C and 1K1C Renovascular Hypertension Models in Mice

As previously discussed mice models of hypertension are most commonly used to identify mechanisms of hypertension development using transgenic knockouts or knock-ins. One of the technical problems associated with renal arterial constriction is the amount of constriction created. Kharin and Krandycheva[24] suggest a method involving pulling a loop of isolated renal artery into a thin plastic tube with a calibrated inner diameter. When bradykinin (BK) B2 receptor ($B2^{-/-}$, $B2^{+/+}$, and $B2^{+/-}$) mice were subjected to the 2K1C procedure it was found that kinins acting on the BK B2 receptor exerted a protective action against excessive hypertension during the early phases.[25]

When mice bearing 1, 2, 3, or 4 copies of the angiotensin (Angio) gene were made hypertensive by 2K1C there was no demonstrable effect of the Angio genotype on baseline or hypertensive blood pressures. However, there was a marked gene-dose effect on DOCA hypertensive mice. Treatment of 2K1C mice with an Angio-II type 1 receptor antagonist abolished the genotype effects on blood pressure and left ventricular hypertrophy.[26] The relative contributions of Angio-II subtype 1A and 1B receptors (ATR-1A & ATR-1B) to the development of 2K1C hypertension were evaluated in ATR-$1A^{-/-}$ and ATR-$1A^{+/+}$ mice. A significant and sustained hypertension was recorded in the ATR-$1A^{+/+}$ mice following 2K1C. Systolic blood pressure was significantly lower in the ATR-$1A^{-/-}$ mice and was not affected by the 2K1C procedure. Acute ATR-2 blockade with PD 123319 resulted in significant increases in mean arterial pressures in 2K1C/ATR-$1A^{-/-}$ mice. The results signify a critical role for ATR-1A in 2K1C hypertension in mice.[27] The same model was used to indicate that ATR-1B plays a minor role in Angiotensin-II-dependent hypertension and enhanced NO synthase activity plays a protective role by counteracting the vasoconstrictor effects of Angio-II.[28]

1K1C produced significantly higher degrees of hypertension and cardiac hypertrophy in mice deficient in the inducible isoform of heme oxygenase (HO-$1^{-/-}$). These animals also had higher mortality rates within 72 h of the 1K1C surgery.[29]

Transgenic eNOS$^{-/-}$ mice are hypertensive with fasting hyperinsulinemia, hyperlipidemia, and a 40% lower insulin-stimulated glucose uptake than control mice.[30] C57BL/6 mice overexpressing eNOS were created by the intravenous injection of recombinant adenovirus expressing the functional gene eNOS at the time of 2K1C or sham surgery. Overexpression of eNOS prevented the development of hypertension in the 2K1C animals.[31]

The apolipoprotein E-deficient mouse (ApoE$^{-/-}$) develops hypercholesterolemia and atherosclerosis. When 2K1C hypertension was induced in 8- to 9-week-old C57BL/6 and Apo E$^{-/-}$ mice they developed hypertension, tachycardia, and cardiac hypertrophy of similar magnitude.[32] When 2K1C Apo E$^{-/-}$ mice were compared with 1K1C Apo E$^{-/-}$ mice there was a marked increase in atherosclerotic plaque accumulation in the aortic sinus of the 2K1C animals accompanied by an enhanced accumulation of macrophages and a parallel increase in scavenger receptor-A expression on the macrophages. These results suggest that increased generation of Angio-II in the 2K1C model may initiate and promote atherosclerotic activity in the VSM cells (VSMCs).[33] High fat diet-fed ApoE$^{-/-}$ mice subjected to 2K1C surgery were unable to increase renin secretion or blood pressure compared with regular chow-fed ApoE$^{-/-}$ mice.[34]

G-protein-coupled receptor (GPCR) kinase 2 (GRK2) is a serine/theorine kinase that phosphorylates and desensitizes agonist-bound GPCRs. GRK2 is increased in both expression and activity in human hypertension and animal models of hypertension. When the GRK2ct (peptide inhibition) or VSM-selective GRK2 genes were ablated in mice with 2K1C hypertension there was a 30% increase in conscious blood pressure, a threefold increase in plasma norepinephrine levels, and a 50% increase in VSM GRK2 mRNA levels. GRK2 inhibition of expression or activity enhanced both α-adrenergic receptor-mediated vasoconstriction and β-adrenergic receptor-mediated vasodilation.[35]

When 5-week-old male CD-1 mice were subjected to interrenal aortic banding the resulting proximal hypertension resulted in LV hypertrophy and histopathological lesions in the coronary arteries and arterioles.[36] Suprarenal aortic banded and unbanded matrix metalloproteinase-1 (MMP-1) transgenic mice (overexpression of MMP-1) were compared with appropriately matched wild-type mice. MMP-1 attenuated the development of cardiac fibrosis in this model. It also prevented LV dilation and preserved cardiac function.[37]

Renovascular Hypertension Models in Rabbits

A common model in rabbits has been dubbed the 1-kidney, 1-wrap model. The surgical procedure involves removal of one kidney, usually the right kidney because the left is more accessible for wrapping, and then wrapping the remaining kidney with sterile cellophane or plastic wrap. This results in enormous increases in total peripheral resistance, a decrease in heart rate and stroke volume, and usually a greater than 35% decrease in cardiac output. This is a very different phenotype than the 2K1C model. It is possible to reverse the hypertension in this model by removing

the wrap and stripping the extensive fibrous thickening of the true renal capsule. This allows the compressed kidney to regain its normal compliance.[3,9]

Wrapping both kidneys with cellophane or plastic wrap can also produce hypertension. The hypertension produced is more moderate than in the 1-kidney, 1-wrap model and is maintained by an increase in total peripheral resistance.[3]

Central inhibition of the sympathetic nervous system of 1K1C rabbits using rilmenidine (5 mg/kg/day) for 6 weeks rapidly reverses cardiac hypertrophy and increases ventricular compliance while reducing blood pressure and heart rate.[38] 1K1C male rabbits demonstrated action potentials with longer durations both in the endocardial and epicardial surface of the LV and an increase in dispersion of repolarization than 1K1C females. The electrical remodeling was associated with an increased vulnerability to the induction of ventricular arrhythmias.[39]

Subcutaneous injection of renopressin into normal rabbits has been shown to produce a delayed, slow increase in blood pressure and then moderate but persistent hypertension after a few days. Renopressin has been detected in the kidney cortex of the 1K1C rabbit model.[3]

1K1C Renovascular Hypertension in Dogs

Both resting and open loop hemodynamic measurements were made in 1K1C untreated and enalapril-treated dogs at 1-3 weeks and at 4-6 weeks following surgery, as hypertension developed. The dose-response effects of acute intravenous infusions of vasopressin and phenylephrine were evaluated. It was concluded that hypertension in this model was not due to autonomic nervous system or Angio-II mechanisms, and there was no evidence of vascular amplification of the effects of the vasoconstrictors used.[40]

Renovascular Hypertension in Pigs

The 2K1C surgical model in pigs results in significant increases in mean blood pressure and renin activity. Following portalization of the clipped kidney both renin activity and blood pressure were reduced.[41]

A reinforced silicone vascular occluder was placed around the suprarenal aorta proximal to the diaphragm in pigs. When the occluder was sequentially inflated the pigs became hypertensive. The advantages of this model are that the occlusions are performed in awake animals; therefore, excessive occlusion of the aorta that could result in neurologic dysfunction or distress can be immediately corrected by reducing the amount of fluid in the occluder. The removal of the constriction and reversal of the hypertension can be accomplished without a second surgical procedure unlike other models.[42]

Porcine atherosclerotic renovascular disease was created by diet-induced hypercholesterolemia and 2K1C surgery. The pigs developed hypertension accompanied

by significant upregulation of renal transforming growth factor-β signaling and elicited epithelial-to-mesenchymal transition accompanied by glomerulosclerosis and renal fibrosis.[43]

Genetic Models of Hypertension

Spontaneously Hypertensive Rat

The SHR is the most commonly used model to study hypertension. This model is genetically related to the Wistar-Kyoto (WKY) rat, and it is widely accepted that the WKY is the most appropriate control for studies using the SHR. However, there is some concern about genetic differences between colonies of WKY and SHR rats. In the USA breeding stocks of WKY may have been distributed to major commercial suppliers as early as the F10 generation, and molecular evidence of genetic variability has been identified among WKY rats within and between breeding facilities.[44] The only way to establish that a genetic trait is an etiological factor in the development of hypertension is by studying F2 backcrosses between SHR and controls. A central reference strain was proposed using SHRs inbred at Kyoto University, where brother/sister inbreeding has been practiced for over 80 generations of rats.[45] It is not clear from the literature that this strategy has been carried out.

An autosomal and a Y chromosome component are the two major genetic components of SHR hypertension. Two substrains, SHR/a and SHR/y, were developed using a series of backcrosses to isolate each of these components. The SHR/a has the autosomal loci and X chromosome from the SHR strain and the Y chromosome from the WKY rat. The SHR/y substrain has only the Y chromosome from the SHR and autosomal loci and X chromosome from the WKY. The autosomal component in the SHR/a is sex-influenced with males having a significantly greater degree of hypertension than females.[46]

Expression of the SA gene in the kidney of the SHR occurs prior to hypertension. This gene was initially identified by differential hybridization in the SHR because it is expressed significantly higher in SHR than in WKY rats. The allele of the SA gene from SHR and other genetically hypertensive strains cosegregates with hypertension in F2 progeny derived from crosses with normotensive rats.[47] Four congenic substrains were derived from WKY/SHR-SA and SHR-WKY-SA backcrosses to WKY and SHR. All the substrains demonstrated higher blood pressures than their respective parental strains and the hypertension was similar in magnitude to the original congenic strains. These findings were interpreted as evidence that there are at least two QTLs affecting blood pressure in the region of rat chromosome-1. That chromosome houses the SA gene but it is likely that some portion of the blood pressure effects of this region of rat chromosome-1 is independent of the SA gene.[48] Somewhat later the same laboratory constructed and analyzed a SA-null mouse model in which exons 2 and 3 of the SA gene were deleted by homologous recombination.

Basal blood pressures were similar in $SA^{-/-}$ and $SA^{+/+}$ littermates. The $SA^{-/-}$ mice grew normally, were fertile, and had no overt negative phenotype. Feeding a high-salt diet for 4 weeks resulted in significant increases in blood pressure in both $SA^{-/-}$ and $SA^{+/+}$ animals. Treatment with an Angio-II blocker lowered blood pressure in both strains but the response was similar in both. The investigators concluded that the SA gene was not involved in the regulation of either basal or salt-stimulated blood pressure and that this lack of differential effect between the two strains was not related to compensatory activation of the renin-angiotensin system in this mouse model.[49] More recently, two distinct blood pressure QTLs, BP1 and BP2, have been demonstrated on rat chromosome-1. When two new mutually exclusive congenic substrains of BP1 were created and interrogated only one of them continued to demonstrate a blood pressure difference. A single gene (*Spon-1*) was identified that exhibited significant differential expression between the WKY and SHR genotypes. The *Spon-1* gene belongs to a family of genes with antiangiogenic properties and it should be investigated further.[50]

Loci within five or six genomic regions were found to explain about 43% of the total response to salt-loaded increases in systolic blood pressure in 188 F2 progeny from a cross between the Brown-Norway and SHR strains. This study provides further evidence of the multiplicity of genes involved in blood pressure control.[51]

The Okamoto-Aoki strain of SHR was used in crossbreeding studies that indicated that the reduction in renal blood flow and GFR in young SHR is genetically linked to the development of hypertension. It was concluded that endogenous Angio-II probably contributes to the renal vasoconstriction in young SHR, at least during the developmental stage of hypertension. This might involve an exaggerated reactivity to Angio-II in this model.[52] Inhibition of renin, angiotensinogen, angiotensin-converting enzyme, and angiotensin receptors using oligonucleotides or cDNA-encoding strategies results in prolonged blood pressure reductions in SHR. This work indicates a significant role for the renin-angiotensin system in hypertension in this model.[53] An F2 population of rats demonstrating the angiotensin-I-converting enzyme (ACE) genotype was derived from a cross between SHR and WKY rats. In males from this cross the ACE genotype accounted for about 20% of the difference in mean blood pressures between SHR and WKY. Females from this cross showed no blood pressure differences.[54]

When male WKY and SHR rats were subjected to sinoaortic denervation it was found that blood pressure variability is a more critical factor in determining myocardial injury, renal injury, and hypertrophy of the aorta than blood pressure levels.[55] Norepinephrine-induced cardiac oxidative stress has been identified as a mitigating factor in the development of myocardial hypertrophy in the SHR. Exercise training seems to reduce oxidative stress and increase nitric oxide (NO) bioavailability. This attenuates the response to norepi.[56] The gain of the volume-sensitive cardiopulmonary reflex has also been shown to be impaired in SHR but this seems to correlate better with the magnitude of cardiac hypertrophy than with the degree of hypertension.[57]

SHR demonstrates an exaggerated cardiovascular responsiveness to environmental stressors such as noise, vibration, overcrowding, and light. If the external stimuli are decreased the development of hypertension is delayed. This seems to

suggest an important role for the autonomic and/or central nervous system in the pathogenesis of hypertension in this model. When borderline hypertensive rats were exposed to air-jet stress for 10 days they developed sustained hypertension.[58] Borderline hypertensive rats resulting from the cross of normotensive WKY dams and SHR sires were exposed to 6 weeks of crowding stress (200 cm^2/rat) compared with controls maintained in cages with 480 cm^2/rat. Hypertension developed associated with reduced vascular NO synthesis and altered vascular function.[59]

Early increases in cardiac output in the SHR seem to be related to increases in central intravascular volume. Later increases in blood pressure and total peripheral resistance appear to be caused by an independent and secondary increase in vascular resistance. Renal denervation will delay the onset and attenuate the severity of hypertension in both the Okamoto-Aoki and New Zealand strains of SHR. Renal changes, characterized by a reduction in the glomerular filtration rate (GFR), may provide a mechanism for the permanent establishment of hypertension in the Milan SHR model. During the early phases of development, from weaning to 4 weeks postweaning, sodium is retained to a greater extent in the Milan SHR. Sodium retention appears to be the result of a significant decrease in urinary Na^+ excretion.[3]

Studies in the SHR show that the percentage of energy derived from protein in the diet may have marked effects on the development of hypertension and survival. When fed a low-protein, excess-salt diet the stroke-prone SHR (SHRSP) strains of this model show a marked decrease in the incidence of stroke. Methionine seems to be the most influential amino acid in this response and when supplied in high levels blood pressures are reduced. Lysine and proline have this effect as well but are less potent than methionine. The ACE inhibitor captopril effectively reduces blood pressure in the SHR but bilateral nephrectomy abolishes the antihypertensive effect of captopril.[3]

Hippocampal and hypothalamic abnormalities can be observed in SHR. When SHR were treated with a single estradiol benzoate pellet (14 mg), implanted subcutaneously, there was enhanced proliferation in the dentate gyrus, a decrease in the number of glial fibrillary acidic immunopositive actrocytes, increased density of neurons in the hilus of the dentate gyrus, and decreased hypothalamic arginine vasopressin mRNA expression. These results suggest that the neuronal and glial alterations in SHR may be reversible by estrogen treatment.[60] Numerous studies have demonstrated that endogenous Na^+ pump inhibitors in the brain mediate hypertension in SHR and other models of hypertension. Studies in gene-targeted mice suggest that the α-2 isoform of the catalytic-α subunit of Na^+/K^+ ATPase plays a critical role in mediating the hypertensive effects of ouabain-like substance circulating in the CNS.[61]

When SHRs were treated with the heme oxygenase inducer (hemin) blood pressure was decreased. The hemin treatment enhanced heme oxygenase activity, upregulated cyclic guanosine monophosphate-protein kinase G signaling, increased superoxide dismutase (SOD) activity, and potentiated total antioxidant capacity. Aldosterone activating protein-1 and nuclear factor-kappaB were reduced. Hemin also suppressed phospholipase C activity, attenuated inositol 1,4,5-triphosphate, and reduced resting intracellular Ca^{2+} in the aorta.[62]

Ashton and Balment[63] were able to introduce hypothalamic diabetes insipidus into the New Zealand genetically hypertensive rat (NZGH) and its normotensive

substrain (NZN) by crossbreeding males with female Brattleboro diabetes insipidus rats. Selective breeding of the resultant diabetic/hypertensive rats, based upon their maximum systolic blood pressures and degree of vasopressin deficiency, produced F6 rats with higher blood pressures at 10 weeks of age than in diabetic/normotensive controls but significantly lower pressures than in age-matched NZGH rats. Another genetic type II diabetic/hypertensive model was produced by crossbreeding the Cohen diabetic rat and the SHR. Sibling pairs with the highest spontaneous blood glucose and blood pressures were selectively mated. F6 animals resulting from this breeding demonstrated noninsulin-dependent overt diabetes and hypertension.[64]

SHRs have also been used as models for attention-deficit hyperactivity disorder. They are hyperactive in open field behavioral testing and show high terminal rates of responding to certain fixed-interval schedules. When SHR, NZGH, and WKY controls were tested the hypertensive strains showed increased terminal lever-pressing rates on a multiple fixed-interval schedule compared with the WKY. Further testing of the unrelated hypertensive rat strains suggested that the genetic loci for hypertension and responding to these particular behavior tests are close but distinct.[65] Two novel strains of rats were generated from hybrid crosses of SHR and WKY rats. Selection of the initial breeding pairs was based on two mutually exclusive phenotypic traits: hypertension but not hyperactive (WKHT) and hyperactive but not hypertensive (WKHA). Inbreeding of brother and sister littermates for more than 25 generations refined the strains. Immunogenetic analyses demonstrated that the WKY and WKHT rats were of the RT-1 haplotype and the SHR WKHA were of the k haplotype.[66]

Stroke-Prone SHR

A marker-assisted breeding strategy, using SHRSP as the recipient and WHY as the donor strains generated three congenic strains: SP.WKYGla2a, SP.WKYGla2c, and SP.WKYGla2k. The SP.WKYGla2k strain contains a 10-cM congenic interval encompassed within the larger (64-cM) SP.WKYGla2a congenic region. When expression data within the minimal congenic interval was examined the positional candidates EDG-1 and VCAM-1 demonstrated significantly elevated renal RNA expression levels in the SHRSP compared to the WKY and SP.WKYGla2a. This work identifies a suggestive minimal interval encompassing a 6-Mbp region on rat chromosome 2 that contains several physiological candidate genes for salt-sensitive hypertension in the SHRSP model.[67] Lindpaintner et al.[68] suggested a structural difference in the gene coding for renin between SHRSP and WKY. They found a deletion, approximately 700 bp in size, within the first intron in SHRSP compared with WKY. The restriction fragment length polymorphism affects a portion of the gene characterized by the presence of a multimeric tandem repeat element where the occurrence of insertional/deletional events could be expected. Using blood pressure measurements in conscious rats they ruled out a cosegregation of blood pressures with renin genotype.

SHRSP fatty rats, congenic rats resulting from the SHRSP.Z-Lepr (fa)/IzmDmcr) cross, were used to demonstrate that the combination of hypertension and obesity accelerates vascular remodeling, dyslipidemia, and insulin resistance in this model of the metabolic syndrome. The phenotype of the SHRSP fatty rat is similar to the human metabolic syndrome.[69] Ras-GTPase is at least partially responsible for hypertension, vascular reactivity, renal dysfunction, and cardiac dysfunction in SHR with streptozotocin-induced diabetes.[70]

There also exist stroke-resistant substrains of SHR as well as the arteriolipoidosis SHR and the obese SHR. The Smirk's genetic hypotensive strain originated from the New Zealand breeding efforts.[3]

Dahl Salt-Sensitive and Insensitive Rats

The Dahl genetic salt-sensitive rat was developed and characterized by selective inbreeding. Dahl and his associates produced two strains of rats, the salt-sensitive (Dahl SS) and the salt-resistant (Dahl SR), with opposite genetic propensities for developing hypertension following exposure to high levels of salt in food or, more commonly, drinking water. The two strains also showed opposite innate predispositions for developing experimental hypertension from DOCA and salt treatment, 2K1C without salt, cortisone treatment, or cortisone treatment of adrenalectomized rats.[3] The Dahl SS is also an animal model of insulin resistance as well as salt sensitivity. The Dahl SR is a model of insulin sensitivity and salt resistance.[71]

The Dahl strain of salt-sensitive rats only develops hypertension when provided with high levels of salt but the hypertension is then maintained if the salt is withdrawn. By comparison in most strains of SHR increased salt intake will exacerbate hypertension but salt restriction does not alter the normal course of high blood pressure development. In some models of hypertension salt loading can actually reverse experimentally induced malignant hypertension. When two Dahl rats, one from a salt-sensitive and the other from a salt-resistant strain, both exposed to high salt, are used in a parabiosis experiment involving an exchange of extracellular fluids, the salt-resistant rat rapidly develops chronic hypertension. The Dahl salt-sensitive rat is more sensitive than the salt-resistant strain to induction of hypertension by DOCA plus 7.3% NaCl, adrenal regeneration plus 1% NaCl, or cortisone treatment of adrenalectomized animals drinking 0.85% saline. The salt-sensitive rat is also more prone to hypertension in experiments without excess salt but with renal artery constriction, the injection of cadmium, or psychological stress. Dahl salt-sensitive rats maintained on a high-salt diet show a selective enhancement of vasoconstrictor responsiveness to sympathetic nerve stimulation. The fall in vascular resistance resulting from sympathetic denervation is also enhanced in Dahl salt-sensitive rats. The indications are that the Dahl salt-sensitive model might depend upon genetic transmission of hypersensitivity to both salt and stress.[3]

Multiple blood pressure QTLs have been reported on rat chromosome-10 by comparing the genomes of the Dahl salt-sensitive rats with that of the relatively

normotensive Lewis and Milan strains. The Dahl/Milan QTL-1 has been mapped to less than 2.6-cM as a differential segment between two congenic strains. When multiple congenic strains spanning the projected interval were studied the Milan alleles within the previously proposed differential segment did not lower the blood pressure of the Dahl rats. However, another congenic strain, Dahl/Milan (10) × 9, containing introgressed Milan alleles that are outside the previously proposed differential segment was found to be of interest. The introgressed alleles that seem to be responsible for lowered blood pressure are contained within a single congenic strain and overlap with the previously identified Dahl/Lewis BP QTL region.[72]

Hypertensive Dahl salt-sensitive rats develop ventricular hypertrophy within 11 weeks, myocardial dysfunction within 17 weeks, and die from cardiac failure at about 21 weeks. During the early hypertension phase messenger RNA levels of 93 genes previously identified as being associated with cardiac dysfunction were measured. The expression of three genes, atrial natriuretic peptide, brain natriuretic peptide, and endothelin-1 precursor, was significantly increased. Twenty-four other genes including SOD-2, sarco (endo) plasmic reticulum Ca^{2+} ATPase 2a, and ryanodine receptor-2 were downregulated. As the model progressed to the cardiac dysfunction phase the expression of an additional 20 genes including inducible NO synthase (iNOS), ACE, and IL-1β was increased and the expression of seven other genes was decreased. When the hypertensive phase was compared with the cardiac dysfunction phase 22 genes including prepro-endothelin-1, *ANP*, *ACE*, β1-adrenergic receptor, *SOD-2*, and endothelial NOS (*eNOS*) changed.[73]

Significant differences in kidney regional proteomic profiles were found between the Dahl salt-sensitive and the consomic SS-13 (BN) rats. The latter is genetically similar to the Dahl SS but exhibits a significant amelioration of salt-induced hypertension. The study demonstrated a potential role of heterogeneous nuclear ribonucleoprotein K in the regulation of angiotensinogen expression in the renal medulla.[74]

Renal phosphodiesterase 4B4 metabolizes cAMP and reduces β-adrenergic signaling in the kidney. The phosphorylated, active, form of this protein was found to be two times greater in Dahl SS rats than in SHR and Dahl SR (salt-resistant) strains.[75]

When Dahl SS and Dahl SR (control) rats were fed a high-salt diet the Dahl SS animals demonstrated significantly higher blood pressures, cardiac hypertrophy, and collagen-III mRNA levels. Plasma renin activity and plasma aldosterone concentrations were decreased concomitant with increased expression of cardiac angiotensinogen mRNA and decreased mRNA levels of ACE-2. In the Dahl SS rats blockade of aldosterone or Angio-II protects against cardiac hypertrophy and fibrosis by inactivation of the local renin-angiotensin-aldosterone system (RAAS).[76] Somatic gene transfer of human kallikrein or atrial natriuretic peptide attenuated hypertension and exerted a protective effect against renal damage and ventricular hypertrophy in Dahl SS rats after high salt loading.[53]

Renalase is a secreted amine oxidase found in the kidneys. It metabolizes catecholamines. Dahl SS rats are deficient in renalase.[77] Telmisartan is an Angio-II-receptor antagonist and a partial agonist of peroxisome-proliferator-activated receptor-gamma (PPAR-γ). Dahl SS hypertensive rats treated with telmisartan were partially protected against cardiac dysfunction possibly due to improvement of endothelial

function associated with PPAR-gamma-eNOS, reduced oxidative stress, and Rho-kinase pathway-related effects.[78]

Female Dahl SS rats fed a low-salt diet gradually develop hypertension at 6 months of age. Ovariectomy at 2 months of age accelerates the rate of hypertension development while estrogen replacement slows it. In this model the gradual development of hypertension stimulated extracellular matrix protein turnover by increasing the production of both metalloproteinases and tissue inhibitors of metalloproteinases while also stimulating extracellular matrix protein degradation. Estrogen loss or gain resulted in a shift in metalloproteinase profiles.[79]

Dahl SS hypertensive rats fed high-fructose or sucrose diets demonstrate accelerated cardiac systolic dysfunction and mortality compared with rats fed either a low-carbohydrate/high-fat or high-starch diet.[80] Endogenous Na^+ pump inhibitors and other endogenous ouabain-like substances in the brain also appear to mediate salt-dependent hypertension in the Dahl SS model.[61]

Other Salt-Sensitive (Salt-Induced) Models of Hypertension

Salt-sensitive hypertension has been described as a vascular diathesis characterized by reduced cardiovascular and renal NO bioavailability and local upregulation of Angio-II. It has also been demonstrated that local activation of the RAAS, by increasing the generation of reactive oxygen species (ROS), mediates cyclooxygenase-2 (COX-2) upregulation in salt-sensitive hypertensive rats.[81] WKY rats fed 8% NaCl in their diet demonstrated increases in blood pressure, tissue aldehyde conjugates, and cytosolic free Ca^{2+}. There are also pathological changes in the renal vasculature. WKY rats fed 4% NaCl in their diet for 10 weeks (moderately high sodium intake) did not demonstrate the same changes and may not have any adverse effects in this model.[82] Hooded (Aguti) rats given 8% salt for 6 weeks developed hypertension attributed to NO deficiency.[83]

C57BL/6J mice fed a high-salt diet demonstrated increased renal medullary COX-2 and microsomal prostaglandin E synthase-1 (mPGES-1) expression. This increases renal medullary PGE-2 synthesis that, in turn, promotes renal sodium excretion via the EP-2 receptor.[84]

The development of salt-sensitive hypertension has also been attributed to blunted activity of the endothelin (ET) and the RAA systems. Endothelin receptor subtype B null ($ETBR^{-/-}$) rats develop severe salt-sensitive hypertension when fed a high-salt diet.[85] When rats were fed a high-salt diet for 5 weeks, following a short-term infusion of Angio-II, they developed hypertension. The renal Angio-II concentrations and the number of tubulointerstitial Angio-II positive cells correlated well with blood pressure increases but plasma Angio-II levels correlated negatively with increases in blood pressure.[86]

The actions of ET-1 are mediated via activation of G-protein-coupled ET (A) and ET (B) receptors found in various cells of the cardiovascular and renal systems. Overexpression of ET-1 is a common finding in salt-sensitive models of hypertension. Males seem to have higher ET-1 levels, greater ET-1-mediated vasoconstriction,

and enhanced pressor responses compared with littermate females. These sex-associated differences may be related to differences in the number and functionality of ET (B) receptors.[87]

An imbalance between the production of NO and ROS in the kidney probably determines levels of oxidative stress. This influences renal hemodynamics and excretory function leading to sodium retention that could contribute to the development of salt-sensitive hypertension.[88]

There are documented differential effects of Na^+ and Cl^- loading on the long-term maintenance of hypertension in different experimental models. The kidneys and CNS are two major sites for salt sensing and do so utilizing at least four different mechanisms: (1) Chloride ion concentrations [Cl^-] are sensed in renal tubular fluids by Na^+-K^+-Cl^- cotransporter isoforms NKCC2B and NKCC2A. The expression of these proteins is mainly limited to macula densa cells. (2) [Na^+] sensing in the cerebrospinal fluid (CSF) by a novel isoform of Na^+ channels, Na (x) that are expressed in SFOs. (3) There is also sensing of the CSF osmolality by mechanosensitive, nonselective cation channels expressed in neuronal cells of the supraoptic and paraventricular nuclei. (4) Volume-regulated anion channels in glial cells of the supraoptic and paraventricular nuclei detect changes in osmolarity.[89]

High-salt intake did not result in hypertension in subtotally nephrectomized pregnant ewes, intact pregnant ewes in late gestation, or intact nonpregnant ewes. The subtotally nephrectomized pregnant ewes had higher arterial pressures and plasma creatinine levels than the intact pregnant ewes. Following high-salt concentrations (0.17 M NaCl) in their drinking water for 5 days the blood pressure did not change in the subtotally nephrectomized pregnant or intact pregnant groups of animals. The subtotal nephrectomized nonpregnant ewes showed increased blood pressures with the higher salt intake and there was a positive correlation between diastolic pressure and sodium balance. It was concluded that pregnancy offers protection against further rises in blood pressure induced by high-salt intake.[90]

Obese Zucker rats are more inclined than lean Zucker rats to develop a diet-induced hypertension when fed a moderately high-fat diet with 1% NaCl in the drinking water. The moderately high fat diet seems to induce defects in NO production that could promote the salt-sensitive increases in blood pressure in the obese Zucker rat model.[91]

Salt-induced hypertension promotes increased cerebral arterial phosphorylation of extracellular signal-regulated kinase 1-2 (ERK1/2) and expression of the proliferative marker Ki-67. These changes seem to be stimulated by Angio-II, regulated by ERK, and selectively regulated by JunB and CREB.[92]

Angiotensin-II-Induced Hypertension

Experimental models based on Angio-II infusion are reported to replicate human pathologies such as postmenopausal hypertension, preeclampsia, vascular remodeling, vascular aging, and neovascularization.[93] Many different dosing protocols have been published for Angio-II infusions that result in hypertension. Mice models usually

involve continuous infusions, via osmotic minipumps. These protocols include 2-4 weeks of infusion at 5.2 ng/10-g body weight per minute,[94] 490 ng/kg body weight per minute,[95] 14 days of infusion at 1,000 ng/kg body weight per minute,[96] 1 μg/kg body weight per minute,[97] and 400 ng/kg body weight per minute.[98]

Protocols used to create hypertension with Angio-II in rats also varied. Bruner and Fink[99] infused Angio-II directly into the intracerebroventricula for 5-7 days at 2 μg/h. Vasopressin release does not appear to contribute to the hypertension produced by chronic infusion of Angio-II into the intracerebral ventricles of rats. This model of hypertension is predominantly characterized by an increase in sympathetic vasoconstrictor tone and, perhaps, a small increase in circulating levels of Angio-II.[99] Neurons in the median preoptic nucleus seem to be involved in the central neural pathway that mediates the chronic hypertensive effects of Angio-II.[100] An intact area postrema appears to be necessary for the development of chronic, but not acute, hypertension during the intravenous infusion of Angio-II in rats.[101]

Osmotic minipumps were used to infuse 200 ng/kg/min of Angio-II subcutaneously in Sprague-Dawley rats for 6 days[102,103] or 120 ng/kg/min for 14 days.[104] Three different doses of Angio-II, 100, 200, and 300 ng/kg/min for 14 days, were used to better understand mechanisms of Angio-II-induced vascular hypertrophy.[105] Minipumps were used to subcutaneously infuse 76 ng/min for 10-14 days,[106] and were used 13 days at 40 ng/min,[107] and 14 days at 50 ng/min or 400 ng/min.[108] Male Sprague-Dawley rats were treated intravenously with 10 ng/kg body weight per minute for 10 days.[100] Another protocol was 5 μg/ml infused intravenously at 0.5-2.0 ml/h.[109]

Dogs were made hypertensive acutely by the intravenous infusion of 50 ng/kg/min of Angiotensin-I for 6 h[110] or a bolus IV injection of Angio-II of 1.25 mg.[111] Cats respond to intravenous infusions of 25 μg at 0.1 ml/min Angio-II with significant hypertension.[112]

Angio-II-induced hypertension is associated with an inflammatory response that contributes to the development of target organ damage. CC chemokine receptor-2 activation plays an important role in the development of hypertensive nephropathy by increasing oxidative stress and inflammation.[94] Homozygous osteopetrotic mice (Op/Op), deficient in macrophage colony-stimulating factor (m-CSF), developed less endothelial dysfunction, vascular remodeling, and oxidative stress induced by Angio-II than wild-type littermates.[96] Vascular reactive oxygen species (ROS) are increased in DOCA-salt-hypertensive rats. The generation of ROS is induced by endothelin-1 in the aorta and resistance arteries and, at least partly, originates from xanthine oxidase and mitochondria in the endothelial cells.[113]

Mice lacking T and B cells have a blunted hypertensive response to Angio-II and do not develop abnormalities of vascular function. Adoptive transfer of T, but not B, cells restored the Angio-II responses.[95] Kidney-specific induction of heme oxygenase-1 prevents the development of Angio-II-dependent hypertension.[97] Aged female follitropin receptor knockout mice (FORKO), a model of menopause, demonstrated enhanced responses to Angio-II infusion when compared with wild-type mice. The enhanced cardiac hypertrophy was associated with increased collagen content and

augmented ERK 1/2 phosphorylation. Cardiac thioredoxin expression and activity were decreased by Angio-II in FORKO but not in wild-type mice.[98]

The copper transporter Menkes ATPase (MNK) has an important role in modulating Angio-II-induced hypertension and endothelial function. It regulates SOD-3 activity and vascular superoxide anion production.[114] Angio-II-induced hypertension was attenuated in lectin-like oxidized low-density lipoprotein receptor-1 (LOX-$1^{-/-}$) knockout mice, as was cardiac remodeling.[115] Estrogen attenuates Angio-II-induced hypertension via action on the sympathetic nervous system and may involve interactions with the production of ROS.[116] Calponin gene expression in the aortic smooth muscle of rats is increased by both exogenous and endogenous Angio-II.[102]

Prolonged Angio-II infusion in rats results in hypertension, renal vasoconstriction, renal cortical hypoxia, reduced efficiency of O_2 usage for Na^+ transport, activation of renal cortical NADPH oxidase, increased expression of p22 (phox), and reduced expression of EC-SOD. The nitroxide SOD mimetic 4-hydroxy-2,2,6,6-tetramethylpiperidine 1-oxyl (Tempol) prevented these ROS effects.[103] Angio-II infusion in rats is accompanied by increased production of aldosterone and increased sympathetic tone.[106] The aldosterone release stimulated by Angio-II infusion may also mediate some of the adverse effects by increasing the amount of oxidative stress.[104] The treatment of rats with heparin directly interfered with the hypertrophy mechanism in mesenteric arteries.[105]

The endogenous tetrapeptide *N*-acetyl-seryl-aspartyl-lysyl-proline (Ac-SDKP) has an antifibrotic effect in the aorta of Angio-II infused rats. This effect may be due to inhibition of PKC activation. Reduced PKC can reduce oxidative stress, ICAM-1 expression, and macrophage infiltration. A portion of the Ac-SDKP effect could also be due to reduced expression of the profibrotic cytokine TGF-β and inhibition of Smad2 phosphorylation.[117]

Renal denervation of rats decreases the level of hypertension and afferent arteriolar responsiveness to chronic Angio-II infusion.[107] Female rats treated with Angio-II demonstrate enhancement of the vasodilatory arm of the RAAS, particularly stimulation of angiotensin-II-type-2 (ACE-2) receptors and angiotensin-converting enzyme-2 mRNA expression. These changes may help explain the sex-specific differences in response.[108]

Newborn rats treated with an Angio-II receptor antagonist during the nephrogenic period (first 2 weeks of age) have modified renal function and develop Angio-II-dependent hypertension. The hypertension becomes Na^+-sensitive as the animals age.[118]

Work done using male beagle dogs indicates that a significant increase in blood pressure following the use of ACE-2 inhibitors is only manifest after about 80% of the ACE activity is inhibited.[110] An intravenous bolus injection of 1.25-mg Angio-II in dogs results in hypertension-associated increases in cortical, brainstem, and cerebellum blood flows.[111] Hypothalamic blood flow remains unchanged following Angio-II intravenous infusion in cats but pretreatment with Naloxone induces a significant downward shift of the upper limits of autoregulation. Hypothalamic blood flow increases when the mean arterial pressure reaches 125-145 mmHg.

This suggests a role for endogenous opioid peptides in hypothalamic blood flow autoregulatory mechanisms in both hypotensive and hypertensive states in anesthetized cats.[112]

DOCA-Induced Hypertension

Two different animal models of DOCA-induced hypertension are most commonly used: DOCA plus added salt (DOCA-salt) and unilateral nephrectomy plus DOCA-salt. The unilateral nephrectomy-DOCA-salt model results in a faster onset, higher degree of hypertension, and more rapid end-organ damage. The DOCA-salt model results in hypertension via salt retention and resulting increases in circulating blood volumes.

DOCA-salt hypertension in mice has been created by implantation of a 50-mg DOCA tablet subcutaneously and 1% saline given as drinking water,[119] and by daily subcutaneous injections of 1-mg DOCA dissolved in 0.5-ml vehicle and 0.9% saline drinking water.[120] Following unilateral nephrectomy mice were injected subcutaneously three times per week with 75 mg/kg DOCA in corn oil and 1% NaCl was provided for drinking water,[121] or were implanted with a 50 mg/kg pellet and provided with 1% NaCl + 0.2% KCl drinking water.

DOCA-induced hypertension in rats has been reported following unilateral nephrectomy and the subcutaneous implantation of 60 day time-release 200-mg DOCA pellets.[122] Male Sprague-Dawley rats were uninephrectomized, and 200 mg/kg DOCA in a sealed silicone pellet was implanted subcutaneously. Postoperatively the rats were provided with 1% NaCl and 0.2% KCl drinking water.[123,124] A similar protocol was followed by O'Donaughy et al.[125] except that the subcutaneously implanted silicone pellet contained 65 mg of DOCA. DOCA implants delivering a dose of 250 mg/kg plus 1% saline drinking water were used by Viel et al.[113] Seven days after unilateral nephrectomy Swoap et al.[126] injected rats with 25 mg/kg DOCA dissolved in corn oil three times a week plus 1% saline drinking water.

Hypertension without unilateral nephrectomy was induced in male rats following the subcutaneous injection of DOCA, 20 mg/kg, twice weekly for 5 weeks, and concurrent with 1% saline drinking water.[127] A similar protocol used a DOCA dose of 15 mg/kg.[128]

When four strains of mice, 129/Sv, C57BL/6, and F1 and F2 intercrosses of the two were compared following DOCA-salt induction of hypertension it was found that 129/Sv mice were more susceptible to the development of hypertension and interstitial fibrosis than the C57BL/6 mice and that the intercrosses demonstrated a complex and nonuniform segregation of susceptibility.[129] Medullary blood flow autoregulation is significantly affected in DOCA-salt mice. The normal blood flow response to increased perfusion pressures is abolished and flow increases associated with increases in extracellular fluid volumes are diminished. These changes are associated with diminished pressure-natriuresis in this model.[119] Work done in heme oxygenase-1 knockout ($HO^{-/-}$) mice and hyperbilirubinemic mutant Gunn

rats suggests that HO^{-1} and bilirubin could exert countervailing effects in DOCA-salt-induced hypertension.[130]

In rats DOCA-salt-induced hypertension does not modify atrial natriuretic peptide receptor (NPR) types A or C. NPR-C-mediated inhibition of cAMP generation is not changed.[120] Vascular overproduction of ROS, via an NADPH oxidase subunit protein (gp91phox), is one of the crucial factors in the development of DOCA-salt-induced hypertension,[121] and TNF-α contributes to the increase in renal inflammation observed in this model in rats.[122]

The expression of tissue inhibitor of metalloproteinase-2 (TIMP-2) was significantly increased in the aorta of DOCA-salt-induced hypertensive rats but was barely detectable in vena caval samples from these animals.[123] DOCA-salt-induced hypertension in rats results in hypertonicity in the brain that supports the increase in blood pressure, partially by stimulating vasopressin secretion and partly by stimulating the sympathetic nervous system.[125] Protein kinase C has been shown to play a crucial role in the endothelial dysfunction associated with DOCA-salt-induced hypertension in Sprague-Dawley rats,[127] and magnesium supplementation prevents blood pressure elevation in this model.[128]

Both rat and mice knockout models of serotonin transporter protein (SERT) responded the same as wild-type controls to DOCA-salt protocols indicating no role for SERT in this model.[124] Caloric restriction appears to significantly reduce hypertension in the rodent unilateral nephrectomy-DOCA-salt-hypertensive model. The regulation of β-myosin heavy chain expression appears to be regulated by the development of hypertension and an independent pathway linked to caloric restriction in this model.[126]

When peroxisome proliferator-activated receptor-α (PPAR-α) is knocked out (PPAR-$\alpha^{-/-}$) in mice exposed to DOCA-salt-induced hypertension, renal tubular cytochrome P450-4a expression is decreased, 20-hydroxy-eicosatetranaeoic acid (20-HETE) production is decreased, sodium retention is decreased, and hypertension is decreased. Expression of the PPAR-α protein was greater in proximal tubules than in renal microvessels.[131]

Ablation of the transient receptor potential vanilloid type-1 (*TRPV1*) gene exacerbates the renal damage caused by DOCA-salt hypertension in the TRPV1$^{-/-}$ mouse. This seems to indicate that TRPV1 may be involved in protecting against end-organ damage resulting from hypertension.[132]

Normal 129/SvEvTac mice (controls) and mice lacking the bradykinin B2 receptor gene (B2$^{-/-}$) were made hypertensive with either DOCA-salt or aortic coarctation. DOCA-salt (volume expansion) and aortic constriction (renin-dependent) produced similar levels of hypertension in both control and B2$^{-/-}$ mice. Chronic ACE inhibition (Ramipil, 4 mg/kg/day) prevented the development of both hypertension and left ventricular hypertrophy in both models suggesting that kinins do not participate in the chronic antihypertensive and antihypertrophic effects of ACE-inhibition in these models.[133]

Sesamin, a lignan from sesame oil, was found to reduce blood pressures and inhibit the enhancement of aortic ROS production in DOCA-salt hypertensive rats.[134] Endothelin-1 (ET-1) stimulates inflammatory processes and contributes to

cardiovascular damage in DOCA-salt hypertension. DOCA-salt treated and control unilaterally nephrectomized rats were treated with the ET antagonist BMS182874. It was determined that ET-1 participates, via activation of ET antagonist receptors, in altered leukocyte-endothelial cell interactions, probably by modulating the expression of cell adhesion molecules.[135]

Axl$^{-/-}$, receptor tyrosine kinase knockout mice, and wild-type controls were made hypertensive with DOCA-salt. There was increased vascular apoptosis in the Axl$^{-/-}$ mice suggesting that this receptor could play a role in the development of hypertension in this mode.[136] RAG-1$^{-/-}$ mice lack both T and B cells. These animals demonstrate blunted hypertension and do not develop the vascular functional abnormalities identified in control animals.[95]

Abnormalities of the hippocampus and the hypothalamus are commonly observed in rats with DOCA-salt-induced hypertension, as in SHR. In the hippocampus changes include decreased cell proliferation in the dentate gyrus, astrogliosis, and decreased neuronal density in the hilus. In the hypothalamus expression of arginine vasopressin is markedly increased. Treatment with estradiol modifies these adverse effects.[60]

Endogenous ouabain-like substances in the brain mediate DOCA-salt hypertension in rats. Even if ouabain is administered parenterally it results in hypertension since it accumulates in the brain. Ouabain-initiated hypertension can be abolished in DOCA-salt rats by the intracerebroventricular administration of an anti-ouabain antibody but the antibody has no effect if administered intravenously. The hypertension can also be abolished by discrete excitotoxic lesions in the brain or by ganglionic blockade indicating that the response is neurally mediated.[61] In pigs the same, or a similar, endogenous digitalis-like factor (EDLF) was found to be involved in DOCA-salt hypertension but did not directly mediate mineralocorticoid escape.[137]

In an early study it was found that DOCA-salt hypertension does not aggravate the severity of ventricular dysfunction in streptozotocin (STZ)-induced diabetic rats.[138] The same lab found that DOCA-salt-hypertensive STZ-diabetic rats had similar hyperglycemia, milder hypoinsulinemia, and significantly lower rates of left ventricular relaxation and systolic blood pressure compared with nondiabetic DOCA-hypertensive rats.[139]

NO-Synthesis Blockade Hypertension

N-nitro-L-arginine methyl ester (L-NAME) can be supplied in the drinking water over time. Effective doses reported are 1 mg/ml of water for 6 days,[140] 1 g/l in tap water for 8 weeks,[141] 100 mg/kg/day for 40 days,[142] 100 mg/kg/day for 21 days,[143] 60 mg/kg/day for 6 weeks,[144] 60 mg/kg/day for 21 days,[145] and 60 mg/kg/day for 7 days[146]; L-NAME can also be injected (30 mg/kg, intravenously) to evaluate acute effects.[109,147]

L-NAME-induced hypertension is associated with increased activity in both the adrenal-medullary and renin-angiotensin systems. Resulting increases in Gs-adenylyl cyclase activity suggest that nitric oxide plays a modulatory role in the formation

of cyclic AMP. Angio-II seems to contribute to this mechanism via an Angio-II type-1 receptor-mediated mechanism.[142]

Significant hypertension develops following L-NAME treatment in male Munich-Wistar rats. There is also marked renal vasoconstriction and a decline in renal plasma flow but no change in GFR. There is no significant reduction of Na^+ excretion and both L-NAME-treated and control rats show similar increases in urinary Na^+ excretion after salt loading, with a similar ratio of Na^+ excreted/infused.[143] The level of resting sympathetic drive to the heart is increased in L-NAME-treated rats while the level of vagal tone is significantly decreased.[140] Albino rats treated with L-NAME show no differences between treated and control groups in tissue or blood levels of zinc or copper but magnesium concentrations are significantly lower in the hypertensive rats. This suggests that Mg^{+2} depletion might play a role in the development of hypertension in this model.[145]

Simultaneous treatment of rats with L-NAME-induced hypertension with L-carnitine (β-hydroxy-γ-*N*-trimethylammonium-butyrate), an antioxidant/anti-inflammatory agent, produces a decrease in IL-β, IL-6, and TNF-α in the treated animals. Plasma ACE activity is not different between treated and control groups and L-carnitine reversed the increased expression of ACE and angiotensin receptor-1 (ATR-1) enhancement by L-NAME.[148]

When thromboxane-receptor-deficient mice ($TP^{-/-}$) and wild-type ($TP^{+/+}$) mice were treated with L-NAME the severity of hypertension was less in the $TP^{-/-}$ mice but renal hypertrophy, the severity of glomerulosclerosis, tubule vacuolization, and interstitial chronic inflammation were all enhanced in the $TP^{-/-}$ animals. TP receptors apparently contribute to hypertension and cardiac hypertrophy but provide unexpected protection against renal damage in this model.[149]

Local neocortical blood flow and glucose utilization were compared in conscious rats made hypertensive with either L-NAME or Angio-II. When hypertension from Angio-II did not exceed 150 mmHg there were no significant effects on cortical blood flow, compared to controls. When blood pressures > 157±1 mmHg were achieved the blood flow was significantly increased especially in the parietal and occipital cortex while blood flow in the temporal and frontal areas of the renal cortex were unchanged. When L-NAME-produced hypertension reached levels > 164 mmHg, blood flow was significantly decreased in every cortical region except the parietal area where no change was measured. No significant differences in glucose utilization were noted between groups.[109]

Pregnant rats treated with L-NAME were compared with age-matched pregnant and nonpregnant rats that received only the vehicle. The study suggests that a significant decrease in plasma [Ca^{2+}] coupled with a concomitant increase in VSM $[Ca^{2+}]_i$ (intracellular free calcium) and altered blood pH are associated with preeclampsia in the pregnant rat.[147]

Chronic L-NAME treatment of $eNOS^{-/-}$ mice caused decreases in blood pressure while the same treatment in $eNOS^{+/+}$ and $eNOS^{+/-}$ mice resulted in hypertension. When L-NAME was discontinued pressures returned to normal levels. These results suggest that in $eNOS^{-/-}$ mice NO derived from nNOS increases blood pressure both acutely and chronically.[150]

The L-NAME-induced-hypertension model develops nephroangiosclerosis. When transgenic mice harboring the luciferase reporter gene under the control of the collagen I-α-2 chain promoter were treated with L-NAME the activation of collagen I gene within the renal vasculature preceded blood pressure increase and was accompanied by the appearance of sclerotic glomeruli and tubulointerstitial infiltration. The removal of L-NAME coupled with endothelin antagonism normalized collagen-I gene expression and improved renal morphology.[151] Dietary doses of nitrite may also offer some protection against renal damage induced by L-NAME in rats.[141]

Long-term treatment with amlodipine, a Ca^{2+} antagonist in L-NAME-hypertensive rats increases NOS activity and eNOS mRNA in the left ventricle. These changes are thought to play a role in the amelioration of coronary reserve and microvascular remodeling.[144] Exercise is associated with a significant increase in A/V oxygen content difference in L-NAME-hypertensive rats. This suggests that impaired NO release induces different cardiovascular adjustments to exercise.[146]

Glucocorticoid-Induced Hypertension

ACTH-induced-hypertension can be created in Sprague-Dawley rats - 0.2 mg/kg/day, administered subcutaneously (s.c.) for 11 days. Neither vitamin C nor E modified the resulting hypertension.[152] ACTH (0.2 mg/kg) or dexamethasone (20 μg/kg) injected s.c. for 12 days results in hypertension in male rats.[153] Both male Swiss Outbred and Quackenbush Swiss mice, as well as male Sprague-Dawley rats, develop hypertension following the injection of ACTH (500 μg/kg/day, s.c.) for 10 days.[154,155]

Products of the metabolism of arachidonic acid, including 20-hydroxy-eicosatetraneoic acid (20-HETE), regulate vascular tone. 20-HETE is a potent constrictor in small arteries and also has natriuretic properties. ACTH-induced, but not dexamethasone-induced, hypertension increases urinary excretion of 20-HETE in male Sprague-Dawley rats. This indicates that 20-HETE could play a role in ACTH-induced hypertension.[153]

Rats treated with endothelin-1 exhibit dose-dependent increases in blood pressure. These effects are blocked by the endothelin-1 antagonist bosentan. Bosentan treatment of ACTH-induced hypertension in rats has no effect on blood pressure or a variety of metabolic parameters including water intake, urine volume, food intake, and bodyweight. Endothelin probably does not play a major role in ACTH-induced hypertension in rats.[155]

When SHR and ACTH-induced hypertensive rats were compared by gene expression profiling of the saphenous artery it was determined that the majority of differences in gene expression reflect distinctive morphological and physiological alterations. Changes in caveolin-1 expression and G-protein signaling, through attenuation of Rgs2 and Rgs5, were common to both models. Augmentation of vasoconstrictor pathways could contribute to hypertension.[156]

Mutant mice expressing ouabain-resistant α(2)-Na^+-K^+-ATPase subunits do not develop hypertension when treated with ACTH. This suggests that there is a differential

sensitivity of renal, mesenteric, and cerebral circulations to ACTH and the response of each depends on the ouabain sensitivity of α(2)-Na^+-K^+-ATPase.[157]

Guinea pigs were unilaterally nephrectomized and then treated with aldosterone and a high-salt diet for 90 days. The treatment group developed hypertension, LV hypertrophy, increased plasma levels of norepinephrine, and decreased renin activity. Analysis of mRNA encoding the three α-isoforms and the β-1 subunit of Na^+, K^+-ATPase revealed that the aldosterone-salt treatment had no effect on levels of α-1 or β-1 mRNA, but α-2 mRNA was increased in both ventricles and α-3 was only increased in the hypertrophied left ventricle. Reciprocal expression of the Na^+/Ca^{2+} exchanger and Na^+, K^+- ATPase suggests a mechanism for adaptation that maintains an appropriate Na^+ gradient and [Ca^{2+}] in the hypertensive myocardium.[158]

ACTH-induced hypertension in sheep occurs within 4-6 h of treatment and is associated with changes in cardiac output and total peripheral resistance. In this model the autonomic nervous system and vasoactive prostanoids seem to buffer, rather than cause, the hypertension. It also appears that the renin-angiotensin system and serotonin are not involved and the effects of ACTH on blood pressure are not directly related to Na^+ balance or changes in fluid volumes. A possible explanation could be a direct effect on the CNS.[159,160]

Intrauterine Growth-Restricted Induced Hypertension

Epidemiological studies report an inverse relationship between birth weight and hypertension in humans. Experimental studies support this observation indicating that both cardiovascular and renal disease can originate in response to fetal adaptations to adverse in-utero conditions.[161] The mechanisms involved in fetal programming of disease are multifactorial and include alterations in the regulatory systems affecting long-term control of systemic blood pressure. Sex hormones may modulate the activity of these regulatory systems leading to a lower incidence of intrauterine growth-restricted (IUGR)-induced hypertension in females than in males.[162] Reduction in uterine perfusion pressure, induced by the placement of silver clips on the abdominal aorta and the ovarian arteries on the 14th day of pregnancy in rats, decreased innate antioxidant activity resulting in elevated oxidative stress, at least one of the mediating factors in this hypertension model.[163]

IUGR-induced hypertension seems to be related to developmental changes in the cardiac sympathetic activity in a maternal protein-restriction protocol in rats. Myocardial mRNA expression of β-2-adrenergic receptors was reported to be increased but only in female offspring.[164] In the rat variations in dietary nutrients, especially protein, during pregnancy seem to be the most important perturbation resulting in blood pressure changes in the offspring.

In the sheep model of nutrient restriction, birth weight rather than maternal diet seems to play the most critical role. Animal models of reduced uteroplacental perfusion during late gestation can also result in IUGR offspring. A reduction in nephron numbers in response to placental insufficiency, irrespective of cause, has

been noted in all species exposed to these protocols. However, a reduction in nephron numbers may not always be critical to the development of hypertension. Many studies indicate that the RAAS is significantly involved in the hypertension resulting from IUGR. This includes marked increases in ATR-1 expression in areas of the brain critical to regulation of the cardiovascular system. In the rat there is a reduction of intrarenal renin and Angio-II at birth followed by a postnatal upregulation of renal ATR-1.

After puberty the male offspring of rats exposed to IUGR remain hypertensive but female offspring stabilize their blood pressure within normal limits. The explanation for this seems to be increased estrogen levels after puberty.[165] Estradiol has been shown to downregulate tissue ACE and ATR-1 mRNA expression. A decrease in the bioavailability of antioxidants also seems to play an important role in IUGR. Hypertension is associated with an increase in urinary albuminuria, glomerulosclerosis, and histological evidence of renal tissue damage in the IUGR offspring.[166]

A modest level of protein restriction in the pregnant female rat produces male offspring that develop hypertension and a reduced number of glomeruli but female offspring do not show these changes. Severe maternal dietary protein restriction in pregnant rats (5% protein compared with a normal diet containing 19% protein) made both male and female adult offspring more susceptible to salt-induced hypertension.[167] Pregnant female rats were maintained on a low-protein diet throughout gestation. At delivery they were fed normal laboratory chow. At 10 weeks of age the F1 generation, those showing signs of hypertension and renal damage, was mated. This produced a second generation (F2) all maintained throughout on normal laboratory chow. The F2 generation also demonstrated the hypertensive effects of IUGR, passed down through both the maternal and paternal lines, but no effect was observed in the F3 generation.[168]

Prenatal exposure to dexamethasone during the last week of pregnancy in rats results in offspring with lower than normal birth weights and slightly lower than normal blood pressure as adults. The expected hypertensive phenotype is only observed when these offspring are subjected to stress, but even mild stress will invoke the response. With more severe stress the hypertension is magnified and maintained for a longer period of time. When endogenous catecholamine release is stimulated in these animals the hypertensive response was 77% higher than that observed in controls. Altered sympathetic responses obviously mediate the stress-induced hypertension in adult offspring resulting from dexamethasone exposure of dams during late pregnancy.[169]

IUGR following uteroplacental insufficiency reduces nephron numbers, predisposes toward renal insufficiency early in life, and increases the risk of hypertension in adult offspring. It significantly decreases renal COX-2, glucocorticoid receptor (GR) protein and mRNA, and 11β-HSD2 (11β-hydroxysteroid dehydrogenase type-2) in offspring at birth. The latter protects both the glucocorticoid receptor and the mineralocorticoid receptor from the actions of corticosterone. The expression of mineralocorticoid receptor (MR) protein and mRNA is upregulated at birth. Hypertension developed in both male and female offspring between 21 and 140 days of age. In this model, fetal COX-2 expression during the period of active nephrogenesis results in decreased nephron numbers and adult-onset hypertension.[170]

Serum- and glucocorticoid-inducible kinase (SGK-1) wild-type (SGK-$1^{+/+}$) male mice were mated with SGK-$1^{-/-}$ females and SGK-$1^{-/-}$ males with SGK-$1^{+/+}$ females, producing heterozygous offspring. When pregnant SGK-$1^{+/+}$ females were fed a protein-restricted diet the offspring gained weight slower and demonstrated hypertension following birth. A sexual dimorphism was found with higher fasting blood glucose and plasma corticosterone concentrations in female offspring. Prenatal protein restriction in SGK-$1^{-/-}$ females had no significant effect on postnatal weight gain, blood pressure, plasma glucose concentrations, or corticosterone levels, irrespective of sex. This work seems to offer evidence that maternal signals mediated by SGK-1 may play an important role in fetal programming IURG.[171]

Other Transgenic and Congenic Models of Hypertension

The mRen-2 Model

The most common transgenic models of hypertension involve manipulation of the renin-angiotensin-aldosterone system (RAAS). The most commonly used of these is the mREN-2 transgene rat model of tissue Angio-II. These animals overexpress mouse renin in extrarenal tissues and this leads to increased local synthesis of Angio-II. Estrogen depletion enhances the progression of hypertension and cardiac dysfunction in this model.[172-174] The mREN-2 transgenic rat has higher renal tissue omega-hydroxylase activity and urinary excretion of 20-HETE but has significantly lower renal epoxygenase activity and urinary excretion of epoxyeicosatrienoic acids (EETs) than controls.[175] When isolated aortic rings from mREN-2 and control rats were used to compare the vasoconstrictor effects of serotonin (5HT), Angio-II, and phenylephrine, with and without the addition of estrogen, only the response to 5HT was augmented. Phenylephrine effects were not affected by estrogen. The response to NO was dependent upon the nature of the vasoconstrictor and/or the presence of estrogen.[176] The aortas from mREN-2 rats exhibit greater NADPH oxidase activity, ROS levels, C-reactive protein, TNF-α expression, apoptosis, and wall thickness. These alterations are significantly attenuated by treatment with ATR-1 blockade (valsartan) or the SOD/catalase mimetic (tempol).[177] A single intra-arterial bolus injection of ATR-1 antisense into 30-day-old mREN-2 rats resulted in lowered blood pressures for 18 days but no differences were found in treated versus control animals at 100 days of age.[178]

ATR-1 Models

Transgenic mice expressing a constitutively activated ATR-1A receptor instead of the wild-type receptor were obtained by homologous recombination. The animals have a moderate hypertension and hypertrophy of the small renal arteries but no

ventricular hypertrophy. The major phenotypic trait of this model is the early and progressive development of cardiovascular fibrosis.[179]

Angio-II Overexpression Models

TG1306/1R mice exhibit cardiac-specific Angio-II overexpression and cardiac hypertrophy but are not hypertensive. There is a marked elevation of myocardial encephalin levels in these mice once cardiac hypertrophy is established but it is not elevated in the early phases of disease progression.[180]

G-Protein Models

Regulation of the cardiovascular system is accomplished by signaling through GPCRs. Normal physiological control involves hormones and neurotransmitters that activate GPCRs and are able to maintain blood pressure within normal limits despite rapid and large changes in cardiac output.[181] β-adrenergic receptors (β-ARs) are GPCRs that regulate inotropy and chronotropy in the heart. They also mediate vasodilation. GPCR kinases (GRKs), including GRK-2, phosphorylated and desensitized agonist-activated β-ARs. Transgenic mice that overexpress GRK-2 in VSM develop hypertension suggesting that GRK-2 plays an important role in vascular control.[182] Both heterozygous and knockout mice deficient in RGS-2, a GTPase-activating protein that accelerates the deactivation rate of heterotrimeric G-proteins, demonstrate hypertension, renovascular abnormalities, and persistent constriction of the resistance vasculature and prolonged responses of the vasculature to vasoconstrictors.[181] RGS-$2^{-/-}$ and RGS-$2^{+/+}$ mice demonstrate equal ATR (1A), ATR (1B), and ATR (2) gene expression. RGS-2 deletion appears to promote Angio-II-dependent hypertension via an increase in myogenic tone and vasoreactivity, possibly by sensitization of ATR (1).[183]

Transgenic mice overexpressing GRK5 in VSM are hypertensive with no gender difference in the degree of hypertension. However, in males overexpressing GRK-5 the elevation of blood pressure is mediated by Gi and, at least in part, by β-1 AR. In females the hypertension seems to be mediated by Angio-II receptors.[184]

The GTP binding protein Rac regulates a wide variety of cellular functions including the activation of NADPH oxidase. Transgenic mice overexpressing the human cDNA of the constitutively active mutant of Rac1 in smooth muscle cells develop moderate hypertension and ventricular hypertrophy.[185]

The G-proteins G (q)-G11 and G12-G13 stimulate phosphorylation of myosin light chain (MLC) via the Ca^{2+}/MLC kinase- and the Rho/Rho kinase-mediated signaling pathways, respectively. Genetically altered mice were developed that allow for the acute abrogation of both signaling pathways using inducible Cre/loxP-mediated mutagenesis in smooth muscle cells. G (q)-G11-mediated signaling in

VSM is necessary for the maintenance of basal blood pressures and for the development of salt-induced hypertension. Lack of G12-G13 and lack of their major effector, the leukemia-associated Rho guanine nucleotide exchange factor (LARG), did not have an effect on the regulation of blood pressure but did block the development of salt-induced hypertension.[186]

Spinophilin controls the intensity and duration of GPCR signaling influencing synaptic activity. Spinophilin-deficient mice ($SPL^{-/-}$) have increased central sympathetic outflow and hypertension. The hypertension was also associated with attenuated baroreflex sensitivity and parasympathetic withdrawal.[187]

Lysophosphatidic acid (LPA) receptors couple to multiple G-proteins to convey their intracellular signaling cascades. The LPA receptors are important mediators for cell migration, proliferation, and survival, among others. VSMCs from transgenic mice that express a peptide inhibitor of G (q), G (q1) express both LPA-1 and LPA-2 receptors. Rat VSMCs express LPA-1 and LPA-3. SM22-G (q1) did not alter LPA-induced migration but was sufficient to attenuate LPA-induced proliferation. G (q1) expression also attenuated LPA-induced ERK1/2 and Akt activation. Transient expression of G (q1) using adenovirus encoding demonstrated that G (q1) was capable of inhibiting both LPA-induced migration and proliferation in VSMCs isolated from both rats and mice.[188]

eNOS Models

Transgenic $eNOS^{-/-}$ mice are hypertensive, demonstrate fasting hyperinsulinemia, hyperlipidemia, and 40% lower insulin-stimulated glucose uptake than $eNOS^{+/+}$ (wild type) mice from the C57BL/6J strain.[30] Cardiovascular changes during pregnancy appear to be similar in C57BL/6J mice and humans. Using $eNOS^{-/-}$ and $eNOS^{+/+}$ mice it was determined that eNOS plays a critical role in increasing stroke volume in late gestation by promoting cardiac remodeling.[189]

Endothelin Models

The collecting duct endothelin system regulates blood pressure and Na^+ excretion. Collecting duct (CD)-specific $ET\text{-}1^{-/-}$ (CD $ET\text{-}1^{-/-}$) mice are hypertensive. CD $ETAR^{-/-}$ (collecting duct-specific endothelin A receptor knockout) mice have normal blood pressures but CD $ETBR^{-/-}$ (CD endothelin B receptor knockout) mice are hypertensive but do not have blood pressures as high as CD $ET\text{-}1^{-/-}$ animals. CD $ETBR^{-/-}$ hypertension is salt-sensitive and the associated Na^+ retention is related to the animals' inability to suppress the RAAS. When CD $ETAR^{-/-}$/CD $ETBR^{-/-}$ double transgenics were produced it was apparent that CD ETAR and CD ETBR exert a combined hypotensive effect that exceeds that of either alone.[190] Amiri et al.[191] specifically targeted overexpression of the human *preproET-1* gene to the endothelium

using the Tie-2 promoter in C57BL/6 mice. The resulting transgenic mice had threefold increases in vascular tissue ET-1 mRNA and sevenfold increases in ET-1 plasma levels compared with wild-type controls but did not demonstrate hypertension. Despite normal blood pressures these animals exhibited marked hypertrophic remodeling and oxidant excess-dependent endothelial dysfunction of resistance vessels, changes from normal ET-1 and ET-3 vascular responses, and significant increases in ETBR expression compared with wild-type littermates. The transgenic mice also generated significantly higher oxidative stress. This suggests that these changes might not be inextricably tied to hypertension - a novel idea.

Chronic activation of endothelin type-B receptors (ETBR) in rats using the selective agonist sarafotoxin 6c results in sustained hypertension. The hypertension is partially mediated by excitation of sympathetic drive to the splanchnic vasculature driven by increased oxidative stress in the prevertebral sympathetic ganglia.[192]

Chromogranin-A Models

Genetic ablation of the chromogranin-A gene in mice ($Chga^{-/-}$) results in hypertension. Chromogranin-A is the endogenous precursor to catestatin, a 21-amino acid residue, cationic, and hydrophobic peptide costored and coreleased with catecholamines from the storage vesicles in adrenal chromaffin cells and adrenergic neurons. This is yet another example of simultaneous physiological stimulation/inhibition with resulting "fine-tune" control. Pretreatment of $Chga^{-/-}$ with human chromogranin-A 352-372 prevented hypertension. $Chga^{-/-}$ mice demonstrate myocardial depression and depressed responses to β-adrenergic and ET-1 stimulation. This model might be an excellent candidate for the study of hypertensive cardiomyopathy.[193,194]

PPAR-α Models

Peroxisome proliferator-activated receptor-α knockout (PPAR-$\alpha^{-/-}$) mice demonstrate defective fatty acid oxidation but are not hypertensive unless placed on a high-salt diet. Studies using this model have shown that PPAR-α participates in pressure natriuresis and regulates Na^+ transport via amiloride- and thiazide-sensitive mechanisms.[195]

Bradykinin-2 Models

Bradykinin-2 receptor knockout ($B2R^{-/-}$) mice develop hypertension and maladaptive cardiac hypertrophy characterized by eNOS downregulation in the myocardium and mitogen-activated protein kinase (MAPK) upregulation. Simvastatin, a NO-synthase

activator, reverses the hypertension and cardiac hypertrophy. This is another example of multiple and redundant systems that accomplish the same or similar end result.[196]

Estrogen Models

ER-$\beta^{-/-}$ mice have vascular dysfunction and hypertension. Tsutsumi et al.[197] examined the differential regulation of iNOS using ER-α and ER-β knockouts. They found that iNOS transcription is positively regulated by ER-β and negatively regulated by ER-α in VSMCs. Female follitropin-receptor knockout (FOR$^{-/-}$) mice demonstrate obesity and age-related hypertension. They have an impaired natriuretic peptide system that probably contributes to the age-related hypertension that develops. Hypertension can be reversed in this model by the injection of estradiol.[198]

Corin Models

Corin is a transmembrane serine protease that converts proatrial natriuretic peptide (pro-ANP) to active ANP in a sequence-specific manner. Corin$^{-/-}$ mice are not able to effectively produce ANP and develop salt-sensitive hypertension.[199]

Vitamin D Receptor Models

Vitamin D receptor knockout (VDR$^{-/-}$) mice, or absence of the key activating enzyme, 25-OHD-1-α-hydroxylase, demonstrate a bone and growth plate phenotype that mimics humans with the same congenital disease or those with severe vitamin D deficiency. Among all the other abnormalities in this model the mice develop high renin hypertension, cardiac hypertrophy, and increased thrombogenicity.[200]

Glucocorticoid Receptor Models

The glucocorticoid receptor gene plays a role in the activity of the hypothalamic-pituitary-adrenal (HPA) axis and can be associated with hypertension and susceptibility to metabolic disease. Heterozygous glucocorticoid receptor (GR β-geo/+) mice were generated from embryonic stem cells with a gene trap integration of a β-galactosidase-neomycin phosphortransferase (β-geo) cassette into the GR gene. This created a transcriptionally inactive GR fusion protein. Although the GR β-geo/+ mice have half of the functional GR of control animals they have normal lipid and glucose homeostasis because of a compensatory HPA axis activation but

they are hypertensive due to activation of the RAAS. A high-fat diet in control and GR β-geo/+ mice resulted in HPA activation and increased blood pressure in controls but these responses were attenuated or abolished in the GR β-geo/+ mice. The conclusion is that reduced GR density balanced by HPA activation leaves glucocorticoid functions unchanged, but mineralocorticoid functions are increased, resulting in the hypertension. Reduced GR limits HPA and blood pressure adaptations to an obesity-generating diet.[201]

Smoothelin Models

Smoothelin-A is an actin-binding protein abundantly expressed in healthy visceral smooth muscle. Smoothelin-B is expressed in healthy VSM. Smoothelin-B knockout (Smtn-$B^{-/-}$) mice demonstrated decreased arterial contractility, moderate hypertension, cardiac hypertrophy, and normal autonomic tone. Surprisingly, isobaric pulse wave velocity and pulse pressure measurements indicated normal aortic distensibility in these animals leaving a valid explanation for the hypertension open.[202]

Adiponectin Models

Adiponectin exhibits defensive properties against type-2 diabetes and hypertension. Plasma adiponectin levels are decreased in obesity. Subtotal nephrectomy was performed in adiponectin knockout ($APN^{-/-}$) and wild-type ($APN^{+/+}$) mice. Two-thirds of the left kidney (upper and lower poles) were resected, taking care to leave the adrenal gland undisturbed. The mice were allowed to recover for 1 week and then the right kidney was totally removed. This procedure resulted in significant accumulation of adiponectin in the glomeruli and interstitium in the remnant kidney. Urinary albumin excretion, glomerular hypertrophy, and tubulointerstitial fibrosis were significantly worse in the $APN^{-/-}$ mice. Intraglomerular macrophage infiltration and mRNA levels of vascular cell adhesion molecule (VCAM)-1, MCP-1, TNF-α, TGF-β-1, collagen type I/III, and NADPH oxidase components were all significantly increased in the knockout versus wild-type animals. The authors concluded that adiponectin accumulates in the injured kidneys and prevents glomerular and tubulointerstitial injury by modulating inflammation and oxidative stress.[203]

Aryl Hydrocarbon Models

Aryl hydrocarbon receptor (AHR) is a basic helix-loop-helix Per-Arnt-Sim transcription factor that mediates the induction of metabolic enzymes, the toxicity of some environmental pollutants, and mild degrees of hypoxia. The $AHR^{-/-}$ mouse responds

to modest decreases in the partial pressure of inspired oxygen, and resultant mild hypoxia, by increasing plasma ET-1. Systemic hypertension develops but pulmonary prepro-ET-1 expression is unchanged.[204]

Parathyroid Hormone Type 1 Receptor Models

Transgenic mice overexpressing parathyroid hormone type-1 receptor (PTH1R) in smooth muscle demonstrate hypotension and decreased renal tone along with unexpected decreases in heart rate. PTH1R mediates the vasodilatory, cardiac stimulatory, and renin-activating effects of exogenous PTH/PTH-related protein (PTHrP). However, PTHrP/PTH1R$^{-/-}$ mice do not survive, so they are not available for study. The intravenous administration of PTH/PTHrP type-1 receptor cDNA to adult rats decreased heart rate, blood pressure, and renal tone, as well as RAAS and stress-induced cardiovascular responses. Endogenous PTHrP also inhibits renin release. Human PTH1R injected intravenously to rats resulted in a generalized expression of hPTH1R, both mRNA and protein, in blood vessels, liver, heart, kidney, and CNS. PTH1R overexpression markedly reduces the liver production and circulatory levels of angiotensinogen, and because of this plasma renin activity is significantly reduced.[205]

Profilin Models

Transgenic FVB/N mice were created to selectively overexpress profilin-1 or the mutant form, 88R/L, in VSMCs. The aortas of profilin-1 overexpressed mice demonstrated activation of the hypertrophic signaling cascades. Phospho-ERK1/2 was significantly higher in profilin-1 overexpressed mice than in 88R/L and control mice as were increases in phospho-JNK. Levels of the two kinases in 88R/L mice were not different than in controls. This study suggests that increased actin polymerization in blood vessels triggers activation of the hypertrophic signaling cascades, and this results in the development of hypertension as the mice age.[206]

Oligodeoxynucleotide Models

The transcription factor hypoxia inducible factor (HIF)-1α is abundantly expressed in the renal medulla and regulates many oxygen-sensitive genes such as NO synthase, *COX-2*, and heme oxygenase-1. All of these genes play important roles in the control of arterial pressure. HIF-1α decoy oligodeoxynucleotides (ODNs) or scrambled ODNs were transfected into the renal medulla in uninephrectomized rats. Two weeks later the HIF-1α binding activities were significantly inhibited and when exposed to a high-salt intake the rats developed significant hypertension. The results suggest

that when the HIF-1α-mediated gene is activated it plays an important role in the regulation of renal medullary function and long-term arterial blood pressure.[207]

Multiple Transgenic Models

Double transgenic mice expressing the human renin and Angio-II genes were fed with a polyunsaturated fatty acid ethyl-ester diet (Omacor; 25 gm/kg) or treated with a direct renin inhibitor (aliskiren, 3 mg/kg/day). There was no effect of either agent on the degree of hypertension or the development of cardiac hypertrophy but both improved electrical remodeling, arrhythmia induction, and connexin 43 expression.[208]

The cyp-1 a-1 ren-2 transgenic rat model allows for chronic dose-dependent upward titration of arterial blood pressures by the oral administration of indole-3-carbinol.[209] In double transgenic mice that express the human renin and angiotensin genes (h-Ang 204/1 h REN 9) there are significant microanatomic variations in the pulmonary, renal, and cardiac distribution and the cellular localization of COX-1, COX-2, mPGES-1, and mPGES-2. However, there are no differences in expression of these endogenous substances between genders.[210] The Tsukuba hypertensive mouse expresses the entire human RAAS. It is a model of hypertension and atherosclerosis with high circulating Angio-II and aldosterone levels.[211]

The A-ZIP/F1 transgenic mouse is a model of lipoatrophic diabetes that exhibits hypertension despite the lack of white adipose tissue and its hormones. These animals also demonstrate a significant reduction of adrenal zona glomerulosa but plasma aldosterone levels and aldosterone synthase mRNA expression are unchanged. Lipoatrophic mice present with elevated corticosterone levels but no adrenocortical hyperplasia.[212]

Apoe triple-knockout (Apoe 3KO) mice are deficient in apolipoprotein E, express exclusively apolipoprotein B-100 [Apob (100/100)], and express no leptin [Lep(ob/ob)]. These animals are designated ($Apoe^{-/-}$) Apob (100/100) Lep (ob/ob). Ldlr triple-knockout (Ldlr 3KO) mice are deficient in low-density lipoprotein receptor, exclusively express Apob (100/100), and do not express leptin. These animals are designated ($Ldlr^{-/-}$) Apob (100/100) Lep (ob/ob). Both transgenic lines become obese and develop hyperinsulinemia, hyperlipidemia, hypertension, and atherosclerosis. The Apoe 3KO mice are hyperglycemic and glucose intolerant and are more obese than the Ldlr 3KO mice.[213]

Congenic Models

Db/db mice have been extensively used as a model of type-2 diabetes. It was recently reported that arterial blood pressures were significantly increased in db/db mice. An analysis of continuous 72-h blood pressure data revealed that both the power and the amplitude of the 24-h period length rhythm were significantly

decreased in db/db mice when compared with controls. The circadian rhythms of heart rate and locomotor activity were also disrupted in this model. Analysis of the clock genes *DBP* and *Bmall* indicated that their oscillations were significantly suppressed in the db/db mouse aorta but the clock gene *Perl* was not. Db/db mice are hypertensive and develop disruptions in blood pressure, heart rate, and locomotor circadian rhythms.[214]

Substitution of Brown Norway (BN) chromosome 13 or 18, but not 20 into the Dahl salt-sensitive rat genome significantly attenuates salt-induced hypertension and albuminuria.[215] A complete chromosome substitution panel of consomic rats in which each of the 20 autosomes and the X and Y chromosomes were individually transferred from the Brown Norway rat onto the Dahl SS/Mcwi genetic background was used to examine the genetic basis of hypertension and renal disease in Dahl SS/Mcwi rats. Substitution of chromosomes 1, 5, 7, 8, 13, or 18 from the BN onto the Dahl SS/Mcwi background attenuated the development of hypertension, proteinuria, and albuminuria in male rats. In female rats substitution of chromosomes 1 and 5 also decreased blood pressure, protein excretion, and albumin excretion. Several chromosomes in males and others in females reduced albuminuria without changing blood pressure.[216]

The mREN.Lewis rat is a congenic in which males exhibit higher systolic pressures than females along with higher Angio-I and Angio-II levels but plasma Angio (1-7) was higher in female congenics. The male mREN.Lewis also exhibited higher circulating levels of renin, ACE activity, and angiotensinogen than female littermates.[217]

The VSM-derived hypertensive mouse developed by Harris et al.[218] has been used to demonstrate that inhibition of G-protein (q) attenuates the hypertension, attenuates VSM reactivity to Angio-II, and reverses VSM hypertrophy. The male F1 hybrids of the NZW X BXSB cross of systemic lupus erythematosus (SLE) mice have an early onset of glomerulonephritis, progressive hypertension, and a higher incidence of degenerative cardiovascular disease with myocardial infarcts than their female counterparts or other strains of SLE mice. The hypertension and coronary artery disease in the F1 hybrid males seem to originate from immunological abnormalities.[219]

Other Models of Systemic Hypertension

Rats fed 10% w/v fructose in their drinking water have increased systolic blood pressures and triglyceride levels and decreased mesenteric vasodilatory prostanoids release response. Dehydroepiandrosterone (DHEA) treatment (30 mg/kg/48 h) prevented the hypertension and increased triglyceride levels and decreased vasoconstrictor prostanoids levels in fructose-overloaded rats. DHEA also normalized the diminished PGI_2/thromboxane (TX) ratio in this model.[220]

Male Sprague-Dawley rats were treated with glycyrrhizic acid for 3 weeks. These rats developed hypertension characterized by increases in both mRNA and protein expression of mineralocorticoid receptor (MR) in the kidney along with the

protein expression of eNOS and iNOS. The expression of atrial natriuretic peptide (ANP) mRNA was increased but natriuretic peptide receptor (NPR)-A and NPR-C mRNA were unchanged. The cGMP production provoked by treatment with ANP or sodium nitroprusside was not different between treated and control groups. The increased expression of kidney MR could contribute to the glycyrrhizic acid-induced hypertension but the enhanced expression of NOS and ANP are probably compensatory responses.[221]

Leptin treatment of rats (0.5 mg/kg/day) resulted in hypertension, increased renal Na^+, K^+-ATPase activity, and reduced fractional Na^+ excretion. These effects were prevented by treatment with the NADPH oxidase inhibitor apocynin. Initial changes in glutathione redox status induced a decrease in the SOD/glutathione peroxidase (GPx) ratio. The decrease in SOD/GPx results in a greater amount of superoxide species versus H_2O_2 in the later phases of leptin treatment. This seems to shift the mechanisms of hypertension development from H_2O_2 extracellular signal-regulated kinases (ERK) to superoxide NO-dependent mechanisms.[222]

The intravenous injection of acetaldehyde produces hypotension in pentobarbital-anesthetized rats but equal doses in pithed rats produce hypertension. These hypertensive effects of acetaldehyde in pithed rats were significantly attenuated by pretreatment with reserpine or treatment with prazosin or phentolamine. The results suggest that the hypertensive response to acetaldehyde in pithed rats is due to the release of catecholamines.[223]

GTP cyclohydrolase-1 (GTPCH-1) is the rate-limiting enzyme in de novo synthesis of tetrahydrobiopterin (BH4). BH4 is an essential cofactor for eNOS and plays a role in dictating the balance of NO and superoxide produced by this enzyme. BH4 reduction induced by the injection of GTPCH-1 siRNA in C57BL6 mice increased their aortic levels of superoxide, 3-nitrotyrosine, ICAM-1, and VCAM-1, as well as causing significant hypertension.[224]

Pulmonary Hypertension

Hypoxia-Induced Pulmonary Hypertension

Chronic hypoxia (10% O_2 for 5 weeks) results in pulmonary hypertension in Balb/c mice. The animals also have increased plasma levels of stromal cell-derived factor-1 (SDF-1) and mobilization of its ligand, CXC chemokine receptor-4 (CXCR-4). Vascular endothelial growth factor receptor (VEGFR)-2 (+)/c-kit (+) cells migrate from bone marrow to the pulmonary arterial adventitia. These results can be significantly reduced by simultaneous oral treatment with pravastatin (2 mg/kg/day). The results suggest that pravastatin ameliorates hypoxia-induced pulmonary hypertension by suppression of SDF-1/CXCR-4 and ICAM-1/CD18 pathways. There is a resultant reduction in the mobilization and homing of bone marrow-derived progenitor cells.[225]

Thirty-six proteins that exhibited significantly altered expression were identified following exposure of mice to hypoxia. The protein identified as Fh1-1, known to be involved in muscle development, was one of the most prominently upregulated of this group. Regulation of Fh1-1 was hypoxia-inducible transcription factor dependent. Abrogation of Fh1-1 expression in primary human pulmonary artery smooth muscle cells by small-interfering RNA suppressed, while Fh1-1 overexpression increased, migration and proliferation. Coimmunoprecipitation experiments identified Talin-1 as a new interacting partner of Fh1-1.[226] Na^+/H^+ exchanger activity plays an essential role in pulmonary arterial smooth muscle cell proliferation and the development of hypoxia-induced pulmonary hypertension and vascular remodeling.[227]

When wild-type and transgenic sickle cell disease (SCD) mice were exposed to 8% O_2 for 7 days there was an increased inflammatory response and activation of the endothelin-1 system in the SCD mice. In this model hypoxia significantly increased phosphodiesterase (PDE)-4 and -1 gene expression. The PDE-4 inhibitor rolipram prevented the hypoxia-induced PDE-4 and -1 upregulation and interfered with the development of pulmonary hypertension.[228]

The classic naturally occurring animal model of hypoxia-induced hypertension is high-altitude (brisket) disease in cattle. There is an inheritable predilection to develop this sensitivity to hypoxia in cattle. The disease is characterized by significantly increased pulmonary arterial pressures leading to congestive right heart failure and the marked subcutaneous edema characteristic of the condition in cattle. The term brisket disease derives from the subcutaneous edema that tends to accumulate along the ventral thorax and abdomen.[3]

Monocrotaline-Induced Pulmonary Hypertension

Pulmonary hypertension can be induced in adult Wistar rats injected with monocrotaline (MCT), 60 mg/kg, subcutaneously. Chronic administration of etanercept, an anti-TNF-α monoclonal antibody, resulted in only a slight increase in right ventricular relaxation velocity with no effect on pulmonary hypertension or right ventricular hypertrophy in this model.[229] Male Sprague-Dawley rats were given the same dose of monocrotaline (60 mg/kg/day) to examine the effects of total ginsenoside (TG)compounds reported to release NO and decrease intracellular Ca^{2+} in the cardiovascular system. TG proved to be effective in protecting against MCT-induced right ventricular hypertrophy and reduced the level of pulmonary hypertension. Multiple molecular mechanisms seem to be involved in this response including the suppression of MCT-activated calcineurin and ERK signaling pathways.[230]

The COX-2 inhibitor celecoxib (25 mg/kg/day) reduced MCT-induced pulmonary hypertension and right ventricular hypertrophy in rats. The beneficial effects might be because of its effects on pulmonary artery thickening and hypertrophy but there were no measured effects on pulmonary arterial vasorelaxation, whole lung eNOS expression, or apoptosis.[231] Thymulin, a zinc-dependent thymic hormone, prevented morphological, hemodynamic, and inflammatory changes associated with MCT-induced pulmonary

hypertension; however, some degree of these same effects was seen with MCT-treated animals injected with the same zinc containing vehicle.[232]

Dual endothelin (ET) receptor inhibition did not have more of an effect on pulmonary vasoconstriction than selective ET(A) inhibition following MCT-induced pulmonary hypertension. ET-3 significantly contributes to pulmonary vascular constriction by activating the ET(B) receptors at low concentrations and the ET(A) receptors at high concentrations.[233]

Transgenic Models of Pulmonary Hypertension

Heterozygous bone morphogenetic protein receptor-II-knockout (BMPR-$2^{+/-}$) mice have a similar genetic trait as seen in some idiopathic pulmonary hypertensive human patients. The BMPR-2 gene was deleted in pulmonary endothelial cells using BMPR-2 conditional knockout mice and a novel endothelial Cre transgenic mouse line. Conditional or homozygous BMPR-2 deletion in pulmonary endothelial cells predisposes mice to pulmonary hypertension.[234] BMPR-$2^{+/-}$ and wild-type (BMPR-$2^{+/+}$) mice were subjected to two injections of MCT combined with intratracheal instillation of replication-deficient adenovirus expressing 5-lipoxygenase. One week after the challenge the BMPR-$2^{+/-}$ mice demonstrated twice as high right ventricular systolic pressures as BMPR-$2^{+/+}$ controls. The pulmonary hypertension continues for 3 weeks before the animals developed right ventricular failure. The BMPR-$2^{+/-}$ animals also exhibited greater endothelial injury and enhanced inflammatory response.[235]

Transgenic and knockout mice with graded vascular elastin compositions ranging from 45 to 120% of that seen in wild-type mice were evaluated for pulmonary circulatory changes. Pulmonary arterial and right ventricular peak systolic pressures were significantly elevated in mice with elastin levels below those seen in control mice.[236]

References

1. Graham D, McBride MW, Brain NJ, Dominiczak AF. Congenic/consomic models of hypertension. *Methods Mol Med.* 2005;108:3–15.
2. Jeffs B, Negrin CD, Graham D, et al. Applicability of a "speed" congenic strategy to dissect blood pressure quantitative trait loci on rat chromosome 2. *Hypertension.* 2000;35:179–187.
3. Gross DR. Animal Models in Cardiovascular Research, Second Revised Edition. Boston: Kluwer Academic; 1994.
4. Glodny B, Glodny DE. John Loesch, discoverer of renovascular hypertension, and Harry Goldblatt: Two great pioneers in circulation research. *Ann Intern Med.* 2006;144:286–295.
5. Pinto YM, Paul M, Ganten D. Lessons from rat models of hypertension: From goldblatt to genetic engineering. *Cardiovasc Res.* 1998;39:77–88.
6. Kirchhoff F, Krebs C, Abdulhag UN, et al. Rapid development of severe end-organ damage in C57BL/6 mice by combining DOCA salt and angiotensin II. *Kidney Int.* 2008;73:643–650.
7. Johns C, Gavras I, Handy DE, Salomao A, Gavras H. Models of experimental hypertension in mice. Hypertension. 1996;28:1064–1069.

8. Wiesel P, Mazzolai L, Nussberger J, Pedrazzini T. Two-kidney, one clip and one-kidney, one clip hypertension in mice. Hypertension. 1997;29:1025–1030.
9. Gross DR. Unpublished data.
10. Sadjadi J, Puttaparthi K, Welborn MB III, et al. Upregulation of autocrine–paracrine renin–angiotensin systems in chronic renovascular hypertension. J Vasc Surg. 2002;36:386–392.
11. Gauer S, Hartner A, Hauser IA, Fierlbeck W, Eberhardt W, Geiger H. Differential regulation of osteopontin expression in the clipped and nonclipped kidney of two-kidney, one-clip hypertensive rats. Am J Hypertens. 2003;16:214–222.
12. Muller DN, Klanke B, Feldt S, et al. (Pro)renin receptor peptide inhibitor "handle-region" peptide does not affect hypertensive nephrosclerosis in Goldblatt rats. Hypertension. 2008;51:676–681.
13. Callera GE, Yeh E, Tostes RC, Caperuto LC, Carvalho CR, Bendhack LM. Changes in the vascular beta-adrenoceptor-activated signaling pathway in 2 kidney-1 clip hypertensive rats. Br J Pharmacol. 2004;141:1151–1158.
14. Gudbrandsen OA, Hultstrom M, Leh S, et al. Prevention of hypertension and organ damage in 2-kidney, 1-clip rats by tetradecylthioacetic acid. Hypertension. 2006;48:460–466.
15. Ostrowska H, Kruszewski K, Kasacka I. Immuno-proteasome subunit LMP7 is up-regulated in the ischemic kidney in an experimental model of renovascular hypertension. *Int J Biochem Cell Biol.* 2006;38:1778–1785.
16. Gouvea SA, Bissoli NS, Moyses MR, Cicilini MA, Pires JG, Abreu GR. Activity of angiotensin-converting enzyme after treatment with l-arginine in renovascular hypertension. *Clin Exp Hypertens.* 2004;26:569–579.
17. Maliszewska-Scislo M, Chen H, Augustyniak RA, Seth D, Rossi NF. Subfornical organ differentially modulates baroreflex function in normotensive and two-kidney, one-clip hypertensive rats. *Am J Physiol Regul Integr Comp Physiol.* 2008;295:R741–R750.
18. Souza HC, Martins-Pinge MC, da Silva VJD, et al. Heart rate and arterial pressure variability in the experimental renovascular hypertension model in rats. *Auton Neurosci.* 2008;139:38–45.
19. Zeng J, Huang R, Su Z. Stroke-prone renovascular hypertensive rats. *Chin Med J (Engl).* 1998;111:741–744.
20. Olson JL, Boitnott JK, Heptinstall RH. Clip-ablation. A model of experimental hypertension in the rat. *Lab Invest.* 1987;57:291–296.
21. Wang DS, Xie HH, Shen FM, Cai GJ, Su DF. Blood pressure variability, cardiac baroreflex sensitivity and organ damage in experimentally hypertensive rats. *Clin Exp Pharmacol Physiol.* 2005;32:545–552.
22. Hacioglu G, Yalcin O, Bor-Kucukatay M, Ozkaya G, Baskurt OK. Red blood cell rheological properties in various rat hypertension models. *Clin Hemorheol Microcirc.* 2002;26:27–32.
23. Rodriguez-Iturbe B, Quiroz Y, Kim CH, Vaziri ND. Hypertension induced by aortic coarctation above the renal arteries is associated with immune cell infiltration of the kidneys. *Am J Hypertens.* 2005;18:1449–1456.
24. Kharin SN, Krandycheva VV. Method of experimental constriction of renal artery for modeling of renovascular hypertension in rats. *Bull Exp Biol Med.* 2004;138:103–105.
25. Madeddu P, Milia AF, Salis MB, et al. Renovascular hypertension in bradykinin B2-receptor knockout mice. *Hypertension.* 1998;32:503–509.
26. Handtrack C, Cordasic N, Klanke B, Veelken R, Hilgers KF. Effect of the angiotensinogen genotype on experimental hypertension in mice. *J Mol Med.* 2007;85:343–350.
27. Cervenka L, Horacek V, Vaneckova I, et al. Essential role of AT1A receptor in the development of 2K1C hypertension. *Hypertension.* 2002;40:735–741.
28. Cervenka L, Vaneckova I, Huskova Z, et al. Pivotal role of angiotensin II receptor subtype 1A in the development of two-kidney, one-clip hypertension: Study in angiotensin II receptor subtype 1A knockout mice. *J Hypertens.* 2008;26:1379–1389.
29. Wiesel P, Patel AP, Carvajal IM, et al. Exacerbation of chronic renovascular hypertension and acute renal failure in heme oxygenase-1-deficient mice. *Circ Res.* 2001;88:1088–1094.
30. Duplain H, Burcelin R, Sartori C, et al. Insulin resistance, hyperlipidemia, and hypertension in mice lacking endothelial nitric oxide synthase. *Circulation.* 2001;104:342–345.
31. Gava AL, Peotta VA, Cabral AM, Vasquez EC, Meyrelles SS. Overexpression of eNOS prevents the development of renovascular hypertension in mice. *Can J Physiol Pharmacol.* 2008;86:458–464.

32. Nogueira BV, Peotta VA, Meyrelles SS, Vasquez EC. Evaluation of aortic remodeling in apolipoprotein E-deficient mice and renovascular hypertensive mice. *Arch Med Res.* 2007;38:816–821.
33. Heo HJ, Yun MR, Jung KH, et al. Endogenous angiotensin II enhances atherogenesis in apoprotein E-deficient mice with renovascular hypertension through activation of vascular smooth muscle cells. *Life Sci.* 2007;80:1057–1063.
34. Mazzolai L, Korber M, Bouzourene K, et al. Severe hyperlipidemia causes impaired renin-angiotensin system function in apolipoprotein E deficient mice. *Atherosclerosis.* 2006;186:86–91.
35. Cohn HI, Harris DM, Pesant S, et al. Inhibition of vascular smooth muscle G protein-coupled receptor kinase 2 enhances {alpha}1DAR constriction. Am J Physiol Heart Circ Physiol. 2008.
36. Higashiyama H, Sugai M, Inoue H, et al. Histopathological study of time course changes in inter-renal aortic banding-induced left ventricular hypertrophy of mice. *Int J Exp Pathol.* 2007;88:31–38.
37. Foronjy RF, Sun J, Lemaitre V, D'Armiento JM. Transgenic expression of matrix metalloproteinase-1 inhibits myocardial fibrosis and prevents the transition to heart failure in a pressure overload mouse model. *Hypertens Res.* 2008;31:725–735.
38. Signolet IL, Bousquet PP, Monassier LJ. Improvement of cardiac diastolic function by long-term centrally mediated sympathetic inhibition in one-kidney, one-clip hypertensive rabbits. *Am J Hypertens.* 2008;21:54–60.
39. Biagetti MO, Quinteiro RA. Gender differences in electrical remodeling and susceptibility to ventricular arrhythmias in rabbits with left ventricular hypertrophy. *Heart Rhythm.* 2006;3:832–839.
40. Anderson WP, Shweta A, Evans RG, Edgley AJ, Gao Y. Total peripheral resistance responsiveness during the development of secondary renal hypertension in dogs. *J Hypertens.* 2007;25:649–662.
41. Katsenis K, Vlahakos DV, Antoniadis P, et al. Renal-portal shunt ameliorates renovascular hypertension in pigs. *Artif Organs.* 2005;29:333–337.
42. Fossum TW, Baltzer WI, Miller MW, et al. A novel aortic coarctation model for studying hypertension in the pig. *J Invest Surg.* 2003;16:35–44.
43. Chade AR, Zhu XY, Grande JP, Krier JD, Lerman A, Lerman LO. Simvastatin abates development of renal fibrosis in experimental renovascular disease. *J Hypertens.* 2008;26:1651–1660.
44. Kurtz TW, Montano M, Chan L, Kabra P. Molecular evidence of genetic heterogeneity in Wistar-Kyoto rats: Implications for research with the spontaneously hypertensive rat. *Hypertension.* 1989;13:188–192.
45. Louis WJ, Howes LG. Genealogy of the spontaneously hypertensive rat and Wistar-Kyoto rat strains: Implications for studies of inherited hypertension. *J Cardiovasc Pharmacol.* 1990;16 Suppl 7:S1–S5.
46. Turner ME, Johnson ML, Ely DL. Separate sex-influenced and genetic components in spontaneously hypertensive rat hypertension. *Hypertension.* 1991;17:1097–1103.
47. Samani NJ, Lodwick D. SA gene and hypertension. *J Hum Hypertens.* 1995;9:501–503.
48. Frantz S, Clemitson JR, Bihoreau MT, Gauguier D, Samani NJ. Genetic dissection of region around the sa gene on rat chromosome 1: Evidence for multiple loci affecting blood pressure. *Hypertension.* 2001;38:216–221.
49. Walsh V, Somody L, Farrell A, et al. Analysis of the role of the SA gene in blood pressure regulation by gene targeting. *Hypertension.* 2003;41:1212–1218.
50. Clemitson JR, Dixon RJ, Haines S, et al. Genetic dissection of a blood pressure quantitative trait locus on rat chromosome 1 and gene expression analysis identifies SPON1 as a novel candidate hypertension gene. *Circ Res.* 2007;100:992–999.
51. Schork NJ, Krieger JE, Trolliet MR, et al. A biometrical genome search in rats reveals the multigenic basis of blood pressure variation. *Genome Res.* 1995;5:164–172.
52. Arendshorst WJ, Chatziantoniou C, Daniels FH. Role of angiotensin in the renal vasoconstriction observed during the development of genetic hypertension. *Kidney Int Suppl.* 1990;30:S92–S96.
53. Chao J, Wang C, Chao L. Gene therapy for hypertension: A review of potential targets. *BioDrugs.* 1999;11:43–53.
54. Zhang L, Summers KM, West MJ. Angiotensin I converting enzyme gene cosegregates with blood pressure and heart weight in F2 progeny derived from spontaneously hypertensive and normotensive Wistar-Kyoto rats. *Clin Exp Hypertens.* 1996;18:753–771.

55. Miao CY, Xie HH, Zhan LS, Su DF. Blood pressure variability is more important than blood pressure level in determination of end-organ damage in rats. *J Hypertens.* 2006;24:1125–1135.
56. Bertagnolli M, Schenkel PC, Campos C, et al. Exercise training reduces sympathetic modulation on cardiovascular system and cardiac oxidative stress in spontaneously hypertensive rats. *Am J Hypertens.* 2008;21:1188–1193.
57. de Andrade TU, Abreu GR, Moyses MR, de Melo Cabral A, Bissoli NS. Role of cardiac hypertrophy in reducing the sensitivity of cardiopulmonary reflex control of renal sympathetic nerve activity in spontaneously hypertensive rats. *Clin Exp Pharmacol Physiol.* 2008;35: 1104–1108.
58. Coste SC, Qi Y, Brooks VL, McCarron DA, Hatton DC. Captopril and stress-induced hypertension in the borderline hypertensive rat. *J Hypertens.* 1995;13:1391–1398.
59. Bernatova I, Csizmadiova Z. Effect of chronic social stress on nitric oxide synthesis and vascular function in rats with family history of hypertension. *Life Sci.* 2006;78:1726–1732.
60. Pietranera L, Saravia FE, Roig P, Lima A, De Nicola AF. Protective effects of estradiol in the brain of rats with genetic or mineralocorticoid-induced hypertension. *Psychoneuroendocrinology.* 2008;33:270–281.
61. Van Huysse JW. Endogenous brain na pumps, brain ouabain-like substance and the alpha2 isoform in salt-dependent hypertension. *Pathophysiology.* 2007;14:213–220.
62. Ndisang JF, Lane N, Jadhav A. Crosstalk between the heme oxygenase system, aldosterone, and phospholipase C in hypertension. *J Hypertens.* 2008;26:1188–1199.
63. Ashton N, Balment RJ. Blood pressure and renal function in a novel vasopressin-deficient, genetically hypertensive rat strain. *J Physiol.* 1989;410:21–34.
64. Cohen AM, Rosenmann E, Rosenthal T. The cohen diabetic (non-insulin-dependent) hypertensive rat model. Description of the model and pathologic findings. *Am J Hypertens.* 1993;6:989–995.
65. Wickens JR, Macfarlane J, Booker C, McNaughton N. Dissociation of hypertension and fixed interval responding in two separate strains of genetically hypertensive rat. *Behav Brain Res.* 2004;152:393–401.
66. Deschepper CF, Prescott G, Hendley ED, Reudelhuber TL. Genetic characterization of novel strains of rats derived from crosses between Wistar-Kyoto and spontaneously hypertensive rats, and comparisons with their parental strains. *Lab Anim Sci.* 1997;47:638–646.
67. Graham D, McBride MW, Gaasenbeek M, et al. Candidate genes that determine response to salt in the stroke-prone spontaneously hypertensive rat: Congenic analysis. *Hypertension.* 2007;50:1134–1141.
68. Lindpaintner K, Takahashi S, Ganten D. Structural alterations of the renin gene in stroke-prone spontaneously hypertensive rats: Examination of genotype-phenotype correlations. *J Hypertens.* 1990;8:763–773.
69. Ueno T, Takagi H, Fukuda N, et al. Cardiovascular remodeling and metabolic abnormalities in SHRSP.Z-lepr(fa)/IzmDmcr rats as a new model of metabolic syndrome. *Hypertens Res.* 2008;31:1021–1031.
70. Yousif MH, Benter IF, Abul AH, Abraham S, Walther T, Akhtar S. Inhibition of ras-GTPase signaling by FPTIII ameliorates development of cardiovascular dysfunction in diabetic-hypertensive rats. *Vascul Pharmacol.* 2008;49:151–157.
71. Shehata MF. Important genetic checkpoints for insulin resistance in salt-sensitive (S) Dahl rats. *Cardiovasc Diabetol.* 2008;7:19.
72. Saad Y, Toland EJ, Yerga-Woolwine S, Farms P, Joe B. Congenic mapping of a blood pressure QTL region on rat chromosome 10 using the Dahl salt-sensitive rat with introgressed alleles from the milan normotensive strain. *Mamm Genome.* 2008;19:85–91.
73. Koyanagi T, Wong LY, Inagaki K, Petrauskene OV, Mochly-Rosen D. Alteration of gene expression during progression of hypertension-induced cardiac dysfunction in rats. *Am J Physiol Heart Circ Physiol.* 2008;295:H220–H226.
74. Tian Z, Greene AS, Usa K, et al. Renal regional proteomes in young Dahl salt-sensitive rats. *Hypertension.* 2008;51:899–904.
75. Tawar U, Kotlo K, Jain S, Shukla S, Setty S, Danziger RS. Renal phosphodiesterase 4B is activated in the Dahl salt-sensitive rat. *Hypertension.* 2008;51:762–766.

76. Takeda Y, Zhu A, Yoneda T, Usukura M, Takata H, Yamagishi M. Effects of aldosterone and angiotensin II receptor blockade on cardiac angiotensinogen and angiotensin-converting enzyme 2 expression in Dahl salt-sensitive hypertensive rats. *Am J Hypertens.* 2007;20:1119–1124.
77. Xu J, Desir GV. Renalase, a new renal hormone: Its role in health and disease. *Curr Opin Nephrol Hypertens.* 2007;16:373–378.
78. Kobayashi N, Ohno T, Yoshida K, et al. Cardioprotective mechanism of telmisartan via PPAR-gamma-eNOS pathway in Dahl salt-sensitive hypertensive rats. *Am J Hypertens.* 2008;21:576–581.
79. Dai Q, Lin J, Craig T, Chou YM, Hinojosa-Laborde C, Lindsey ML. Estrogen effects on MMP-13 and MMP-14 regulation of left ventricular mass in Dahl salt-induced hypertension. *Gen Med.* 2008;5:74–85.
80. Sharma N, Okere IC, Barrows BR, et al. High-sugar diets increase cardiac dysfunction and mortality in hypertension compared to low-carbohydrate or high-starch diets. *J Hypertens.* 2008;26:1402–1410.
81. Jaimes EA, Zhou MS, Pearse DD, Puzis L, Raij L. Upregulation of cortical COX-2 in salt-sensitive hypertension: Role of angiotensin II and reactive oxygen species. *Am J Physiol Renal Physiol.* 2008;294:F385–F392.
82. Vasdev S, Gill VD, Parai S, Gadag V. Effect of moderately high dietary salt and lipoic acid on blood pressure in Wistar-Kyoto rats. *Exp Clin Cardiol.* 2007;12:77–81.
83. Mojiminiyi FB, Anigbogu CN, Sofola OA, Adigun SA. Role of nitric oxide in salt and water excretion in experimental hypertension in hooded (aguti) rats. *Niger Postgrad Med J.* 2007;14:99–104.
84. Chen J, Zhao M, He W, et al. Increased dietary NaCl induces renal medullary PGE2 production and natriuresis via the EP2 receptor. *Am J Physiol Renal Physiol.* 2008;295:F818–F825.
85. Caprioli J, Mele C, Mossali C, et al. Polymorphisms of EDNRB, ATG, and ACE genes in salt-sensitive hypertension. *Can J Physiol Pharmacol.* 2008;86:505–510.
86. Franco M, Martinez F, Quiroz Y, et al. Renal angiotensin II concentration and interstitial infiltration of immune cells are correlated with blood pressure levels in salt-sensitive hypertension. *Am J Physiol Regul Integr Comp Physiol.* 2007;293:R251–R256.
87. Tostes RC, Fortes ZB, Callera GE, et al. Endothelin, sex and hypertension. *Clin Sci (Lond).* 2008;114:85–97.
88. Majid DS, Kopkan L. Nitric oxide and superoxide interactions in the kidney and their implication in the development of salt-sensitive hypertension. *Clin Exp Pharmacol Physiol.* 2007;34:946–952.
89. Orlov SN, Mongin AA. Salt-sensing mechanisms in blood pressure regulation and hypertension. *Am J Physiol Heart Circ Physiol.* 2007;293:H2039–H2053.
90. Gibson KJ, Boyce AC, Thomson CL, Chinchen S, Lumbers ER. Interactions between subtotal nephrectomy and salt: Effects on blood pressure and renal function in pregnant and nonpregnant ewes. *Am J Physiol Regul Integr Comp Physiol.* 2008;294:R1227–R1233.
91. Morrison RG, Mills C, Moran AL, et al. A moderately high fat diet promotes salt-sensitive hypertension in obese zucker rats by impairing nitric oxide production. *Clin Exp Hypertens.* 2007;29:369–381.
92. Rose P, Bond J, Tighe S, et al. Genes overexpressed in cerebral arteries following salt-induced hypertensive disease are regulated by angiotensin II, JunB, and CREB. *Am J Physiol Heart Circ Physiol.* 2008;294:H1075–H1085.
93. Qin Z. Newly developed angiotensin II-infused experimental models in vascular biology. *Regul Pept.* 2008;150:1–6.
94. Liao TD, Yang XP, Liu YH, et al. Role of inflammation in the development of renal damage and dysfunction in angiotensin II-induced hypertension. *Hypertension.* 2008;52:256–263.
95. Guzik TJ, Hoch NE, Brown KA, et al. Role of the T cell in the genesis of angiotensin II induced hypertension and vascular dysfunction. *J Exp Med.* 2007;204:2449–2460.
96. De Ciuceis C, Amiri F, Brassard P, Endemann DH, Touyz RM, Schiffrin EL. Reduced vascular remodeling, endothelial dysfunction, and oxidative stress in resistance arteries of angiotensin II-infused macrophage colony-stimulating factor-deficient mice: Evidence for a role in inflammation in angiotensin-induced vascular injury. *Arterioscler Thromb Vasc Biol.* 2005;25:2106–2113.

97. Vera T, Kelsen S, Stec DE. Kidney-specific induction of heme oxygenase-1 prevents angiotensin II hypertension. *Hypertension.* 2008;52:660–665.
98. Ebrahimian T, Sairam MR, Schiffrin EL, Touyz RM. Cardiac hypertrophy is associated with altered thioredoxin and ASK1 signaling in a mouse model of menopause. *Am J Physiol Heart Circ Physiol.* 2008;295:H1481–H1488.
99. Bruner CA, Fink GD. Neurohumoral contributions to chronic angiotensin-induced hypertension. *Am J Physiol.* 1986;250:H52–H61.
100. Ployngam T, Collister JP. Role of the median preoptic nucleus in chronic angiotensin II-induced hypertension. *Brain Res.* 2008;1238:75–84.
101. Fink GD, Bruner CA, Mangiapane ML. Area postrema is critical for angiotensin-induced hypertension in rats. *Hypertension.* 1987;9:355–361.
102. Castoldi G, di Gioia CR, Pieruzzi F, et al. Angiotensin II modulates calponin gene expression in rat vascular smooth muscle cells in vivo. *J Hypertens.* 2001;19:2011–2018.
103. Welch WJ, Blau J, Xie H, Chabrashvili T, Wilcox CS. Angiotensin-induced defects in renal oxygenation: Role of oxidative stress. *Am J Physiol Heart Circ Physiol.* 2005;288:H22–H28.
104. Virdis A, Neves MF, Amiri F, Viel E, Touyz RM, Schiffrin EL. Spironolactone improves angiotensin-induced vascular changes and oxidative stress. *Hypertension.* 2002;40:504–510.
105. Dilley RJ, Nataatmadja MI. Heparin inhibits mesenteric vascular hypertrophy in angiotensin II-infusion hypertension in rats. *Cardiovasc Res.* 1998;38:247–255.
106. Luft FC, Wilcox CS, Unger T, et al. Angiotensin-induced hypertension in the rat: Sympathetic nerve activity and prostaglandins. *Hypertension.* 1989;14:396–403.
107. Ichihara A, Inscho EW, Imig JD, Michel RE, Navar LG. Role of renal nerves in afferent arteriolar reactivity in angiotensin-induced hypertension. *Hypertension.* 1997;29:442–449.
108. Sampson AK, Moritz KM, Jones ES, Flower RL, Widdop RE, Denton KM. Enhanced angiotensin II type 2 receptor mechanisms mediate decreases in arterial pressure attributable to chronic low-dose angiotensin II in female rats. *Hypertension.* 2008;52:666–671.
109. Kelly PA, Thomas CL, Ritchie IM, Arbuthnott GW. Cerebrovascular autoregulation in response to hypertension induced by NG-nitro-L-arginine methyl ester. *Neuroscience.* 1994;59:13–20.
110. Hutter JF, Dehn A, Schmidt W. Hemodynamic effects of new angiotensin converting enzyme inhibitors during continuous angiotensin I infusion on conscious dogs. *Arzneimittelforschung.* 1988;38:896–901.
111. Werner C, Kochs E, Hoffman WE, Blanc IF, Schulte AM, Esch J. Cerebral blood flow and cerebral blood flow velocity during angiotensin-induced arterial hypertension in dogs. *Can J Anaesth.* 1993;40:755–760.
112. Komjati K, Velkei-Harvich M, Toth J, Dallos G, Nyary I, Sandor P. Endogenous opioid mechanisms in hypothalamic blood flow autoregulation during haemorrhagic hypotension and angiotensin-induced acute hypertension in cats. *Acta Physiol Scand.* 1996;157:53–61.
113. Viel EC, Benkirane K, Javeshghani D, Touyz RM, Schiffrin EL. Xanthine oxidase and mitochondria contribute to vascular superoxide anion generation in DOCA-salt hypertensive rats. *Am J Physiol Heart Circ Physiol.* 2008;295:H281–H288.
114. Qin Z, Gongora MC, Ozumi K, et al. Role of Menkes ATPase in angiotensin II-induced hypertension. A key modulator for extracellular superoxide dismutase function. *Hypertension.* 2008;52:945–951.
115. Hu C, Dandapat A, Sun L, et al. Modulation of angiotensin II-mediated hypertension and cardiac remodeling by lectin-like oxidized low-density lipoprotein receptor-1 deletion. *Hypertension.* 2008;52:556–562.
116. Xue B, Zhao Y, Johnson AK, Hay M. Central estrogen inhibition of angiotensin II-induced hypertension in male mice and the role of reactive oxygen species. *Am J Physiol Heart Circ Physiol.* 2008;295:H1025–H1032.
117. Lin CX, Rhaleb NE, Yang XP, Liao TD, D'Ambrosio MA, Carretero OA. Prevention of aortic fibrosis by N-acetyl-seryl-aspartyl-lysyl-proline in angiotensin II-induced hypertension. *Am J Physiol Heart Circ Physiol.* 2008;295:H1253–H1261.

118. Salazar F, Reverte V, Saez F, Loria A, Llinas MT, Salazar FJ. Age- and sodium-sensitive hypertension and sex-dependent renal changes in rats with a reduced nephron number. *Hypertension.* 2008;51:1184–1189.
119. Gross V, Lippoldt A, Bohlender J, Bader M, Hansson A, Luft FC. Cortical and medullary hemodynamics in deoxycorticosterone acetate-salt hypertensive mice. *J Am Soc Nephrol.* 1998;9:346–354.
120. Li X, Woodard GE, Brown J, Rosado JA. Renal atrial natriuretic peptide receptors binding properties and function are resistant to DOCA-salt-induced hypertension in rats. *Regul Pept.* 2006;137:114–120.
121. Fujii A, Nakano D, Katsuragi M, et al. Role of gp91phox-containing NADPH oxidase in the deoxycorticosterone acetate-salt-induced hypertension. *Eur J Pharmacol.* 2006;552:131–134.
122. Elmarakby AA, Quigley JE, Imig JD, Pollock JS, Pollock DM. TNF-alpha inhibition reduces renal injury in DOCA-salt hypertensive rats. *Am J Physiol Regul Integr Comp Physiol.* 2008;294:R76–R83.
123. Watts SW, Rondelli C, Thakali K, et al. Morphological and biochemical characterization of remodeling in aorta and vena cava of DOCA-salt hypertensive rats. *Am J Physiol Heart Circ Physiol.* 2007;292:H2438–H2448.
124. Ni W, Zhou H, Diaz J, Murphy DL, Haywood JR, Watts SW. Lack of the serotonin transporter does not prevent mineralocorticoid hypertension in rat and mouse. *Eur J Pharmacol.* 2008;589:225–227.
125. O'Donaughy TL, Qi Y, Brooks VL. Central action of increased osmolality to support blood pressure in deoxycorticosterone acetate-salt rats. *Hypertension.* 2006;48:658–663.
126. Swoap SJ, Boddell P, Baldwin KM. Interaction of hypertension and caloric restriction on cardiac mass and isomyosin expression. *Am J Physiol.* 1995;268:R33–R39.
127. Fatehi-Hassanabad Z, Fatehi M, Shahidi MI. Endothelial dysfunction in aortic rings and mesenteric beds isolated from deoxycorticosterone acetate hypertensive rats: Possible involvement of protein kinase C. *Eur J Pharmacol.* 2004;494:199–204.
128. Kh R, Khullar M, Kashyap M, Pandhi P, Uppal R. Effect of oral magnesium supplementation on blood pressure, platelet aggregation and calcium handling in deoxycorticosterone acetate induced hypertension in rats. *J Hypertens.* 2000;18:919–926.
129. Hartner A, Cordasic N, Klanke B, Veelken R, Hilgers KF. Strain differences in the development of hypertension and glomerular lesions induced by deoxycorticosterone acetate salt in mice. *Nephrol Dial Transplant.* 2003;18:1999–2004.
130. Nath KA, d'Uscio LV, Juncos JP, et al. An analysis of the DOCA-salt model of hypertension in HO-1$^{-/-}$ mice and the gunn rat. *Am J Physiol Heart Circ Physiol.* 2007;293:H333–H342.
131. Zhou Y, Luo P, Chang HH, et al. Colfibrate attenuates blood pressure and sodium retention in DOCA-salt hypertension. *Kidney Int.* 2008;74:1040–1048.
132. Wang Y, Babankova D, Huang J, Swain GM, Wang DH. Deletion of transient receptor potential vanilloid type 1 receptors exaggerates renal damage in deoxycorticosterone acetate-salt hypertension. *Hypertension.* 2008;52:264–270.
133. Rhaleb NE, Peng H, Alfie ME, Shesely EG, Carretero OA. Effect of ACE inhibitor on DOCA-salt- and aortic coarctation-induced hypertension in mice: Do kinin B2 receptors play a role? *Hypertension.* 1999;33:329–334.
134. Nakano D, Itoh C, Ishii F, et al. Effects of sesamin on aortic oxidative stress and endothelial dysfunction in deoxycorticosterone acetate-salt hypertensive rats. *Biol Pharm Bull.* 2003;26:1701–1705.
135. Callera GE, Montezano AC, Touyz RM, et al. ETA receptor mediates altered leukocyte-endothelial cell interaction and adhesion molecules expression in DOCA-salt rats. *Hypertension.* 2004;43:872–879.
136. Korshunov VA, Daul M, Massett MP, Berk BC. Axl mediates vascular remodeling induced by deoxycorticosterone acetate-salt hypertension. *Hypertension.* 2007;50:1057–1062.
137. Hamlyn JM. Increased levels of a humoral digitalis-like factor in deoxycorticosterone acetate-induced hypertension in the pig. *J Endocrinol.* 1989;122:409–420.
138. Dai S, McNeill JH. Myocardial performance of STZ-diabetic DOCA-hypertensive rats. *Am J Physiol.* 1992;263:H1798–H1805.

139. Schenk J, Hebden RA, Dai S, McNeill JH. Integrated cardiovascular function in the conscious streptozotocin-diabetic deoxycorticosterone-acetate-hypertensive rats. *Pharmacology.* 1994;48:211–215.
140. Cunha RS, Cabral AM, Vasquez EC. Evidence that the autonomic nervous system plays a major role in the L-NAME-induced hypertension in conscious rats. *Am J Hypertens.* 1993;6: 806–809.
141. Kanematsu Y, Yamaguchi K, Ohnishi H, et al. Dietary doses of nitrite restore the circulating nitric oxide level and improve renal injury in L-NAME-induced hypertensive rats. *Am J Physiol Renal Physiol.* 2008;295:F1457–F1462.
142. K-Laflamme A, Foucart S, Moreau P, Lambert C, Cardinal R, de Champlain J. Sympathetic functions in NG-nitro-L-arginine-methyl-ester-induced hypertension: Modulation by the renin-angiotensin system. *J Hypertens.* 1998;16:63–76.
143. Rodriguez-Perez JC, Brenner BM. Renal effects of an acute NaCl load in chronic nitric oxide blockade-induced hypertensive rats. *J Physiol Biochem.* 1998;54:127–133.
144. Kobayashi N, Yanaka H, Tojo A, Kobayashi K, Matsuoka H. Effects of amlodipine on nitric oxide synthase mRNA expression and coronary microcirculation in prolonged nitric oxide blockade-induced hypertensive rats. *J Cardiovasc Pharmacol.* 1999;34:173–181.
145. Senturk UK, Kaputlu I, Gunduz F, Kuru O, Gokalp O. Tissue and blood levels of zinc, copper, and magnesium in nitric oxide synthase blockade-induced hypertension. *Biol Trace Elem Res.* 2000;77:97–106.
146. De Angelis K, Ogawa T, Sanches IC, Rigatto KV, Krieger EM, Irigoyen MC. Impairment on cardiac output and blood flow adjustments to exercise in L-NAME-induced hypertensive rats. *J Cardiovasc Pharmacol.* 2006;47:371–376.
147. Ebose EJ, Campbell PI, Okorodudu AO. Electrolytes and pH changes in pre-eclamptic rats. *Clin Chim Acta.* 2007;384:135–140.
148. Miguel-Carrasco JL, Mate A, Monserrat MT, Arias JL, Aramburu O, Vazquez CM. The role of inflammatory markers in the cardioprotective effect of L-carnitine in L-NAME-induced hypertension. *Am J Hypertens.* 2008;21:1231–1237.
149. Francois H, Makhanova N, Ruiz P, et al. A role for the thromboxane (tp) receptor in L-NAME hypertension. *Am J Physiol Renal Physiol.* 2008;295:F1096–F1102.
150. Kurihara N, Alfie ME, Sigmon DH, Rhaleb NE, Shesely EG, Carretero OA. Role of nNOS in blood pressure regulation in eNOS null mutant mice. *Hypertension.* 1998;32:856–861.
151. Placier S, Boffa JJ, Dussaule JC, Chatziantoniou C. Reversal of renal lesions following interruption of nitric oxide synthesis inhibition in transgenic mice. *Nephrol Dial Transplant.* 2006;21:881–888.
152. Schyvens CG, Andrews MC, Tam R, et al. Antioxidant vitamins and adrenocorticotrophic hormone-induced hypertension in rats. *Clin Exp Hypertens.* 2007;29:465–478.
153. Zhang Y, Hu L, Mori TA, Barden A, Croft KD, Whitworth JA. Arachidonic acid metabolism in glucocorticoid-induced hypertension. *Clin Exp Pharmacol Physiol.* 2008;35:557–562.
154. Schyvens CG, Mangos GJ, Zhang Y, McKenzie KU, Whitworth JA. Telemetric monitoring of adrenocorticotrophin-induced hypertension in mice. *Clin Exp Pharmacol Physiol.* 2001;28:758–760.
155. Fraser TB, Mangos GJ, Turner SW, Whitworth JA. Adrenocorticotrophic hormone-induced hypertension in the rat: Effects of the endothelin antagonist bosentan. *Clin Exp Pharmacol Physiol.* 1999;26:628–633.
156. Grayson TH, Ohms SJ, Brackenbury TD, et al. Vascular microarray profiling in two models of hypertension identifies caveolin-1, Rgs2 and Rgs5 as antihypertensive targets. *BMC Genomics.* 2007;8:404.
157. Lorenz JN, Loreaux EL, Dostanic-Larson I, et al. ACTH-induced hypertension is dependent on the ouabain-binding site of the alpha2-Na^+-K^+-ATPase subunit. *Am J Physiol Heart Circ Physiol.* 2008;295:H273–H280.
158. Ramirez-Gil JF, Trouve P, Mougenot N, Carayon A, Lechat P, Charlemagne D. Modifications of myocardial Na^+,$K(^+)$-ATPase isoforms and Na^+/Ca^{2+} exchanger in aldosterone/salt-induced hypertension in guinea pigs. *Cardiovasc Res.* 1998;38:451–462.

159. Scoggins BA, Allen KJ, Coghlan JP, et al. Haemodynamics of ACTH-induced hypertension in sheep. *Clin Sci (Lond).* 1979;57 Suppl 5:333s–336s.
160. Scoggins BA, Coghlan JP, Congiu M, et al. Alterations in osmotic but not pressor responses to ACTH by optic recess lesions in sheep. *Hypertension.* 1982;4:154–158.
161. Ojeda NB, Grigore D, Alexander BT. Intrauterine growth restriction: Fetal programming of hypertension and kidney disease. *Adv Chronic Kidney Dis.* 2008;15:101–106.
162. Grigore D, Ojeda NB, Alexander BT. Sex differences in the fetal programming of hypertension. *Gend Med.* 2008;5 Suppl A:S121–S132.
163. Sedeek M, Gilbert JS, Lamarca BB, et al. Role of reactive oxygen species in hypertension produced by reduced uterine perfusion in pregnant rats. *Am J Hypertens.* 2008;21:1152–1156.
164. Elmes MJ, Haase A, Gardner DS, Langley-Evans SC. Sex differences in sensitivity to beta-adrenergic agonist isoproterenol in the isolated adult rat heart following prenatal protein restriction. Br J Nutr. 2008:1-10.
165. Ojeda NB, Grigore D, Robertson EB, Alexander BT. Estrogen protects against increased blood pressure in postpubertal female growth restricted offspring. *Hypertension.* 2007;50:679–685.
166. Ojeda NB, Grigore D, Alexander BT. Developmental programming of hypertension: Insight from animal models of nutritional manipulation. *Hypertension.* 2008;52:44–50.
167. Woods LL, Weeks DA, Rasch R. Programming of adult blood pressure by maternal protein restriction: Role of nephrogenesis. *Kidney Int.* 2004;65:1339–1348.
168. Harrison M, Langley-Evans SC. Intergenerational programming of impaired nephrogenesis and hypertension in rats following maternal protein restriction during pregnancy. Br J Nutr. 2008:1-11.
169. O'Regan D, Kenyon CJ, Seckl JR, Holmes MC. Prenatal dexamethasone 'programmes' hypotension, but stress-induced hypertension in adult offspring. *J Endocrinol.* 2008;196:343–352.
170. Baserga M, Hale MA, Wang ZM, et al. Uteroplacental insufficiency alters nephrogenesis and downregulates cyclooxygenase-2 expression in a model of IUGR with adult-onset hypertension. *Am J Physiol Regul Integr Comp Physiol.* 2007;292:R1943–R1955.
171. Rexhepaj R, Boini KM, Huang DY, et al. Role of maternal glucocorticoid inducible kinase SGK1 in fetal programming of blood pressure in response to prenatal diet. *Am J Physiol Regul Integr Comp Physiol.* 2008;294:R2008–R2013.
172. Hayden MR, Chowdhury N, Govindarajan G, Karuparthi PR, Habibi J, Sowers JR. Myocardial myocyte remodeling and fibrosis in the cardiometabolic syndrome. *J Cardiometab Syndr.* 2006;1:326–333.
173. DeMarco VG, Habibi J, Whaley-Connell AT, et al. Oxidative stress contributes to pulmonary hypertension in the transgenic (mRen2)27 rat. *Am J Physiol Heart Circ Physiol.* 2008;294: H2659–H2668.
174. Chappell MC, Westwood BM, Yamaleyeva LM. Differential effects of sex steroids in young and aged female mRen2.lewis rats: A model of estrogen and salt-sensitive hypertension. *Gen Med.* 2008;5 Suppl A:S65–S75.
175. Chabova VC, Kramer HJ, Vaneckova I, et al. Effects of chronic cytochrome P-450 inhibition on the course of hypertension and end-organ damage in ren-2 transgenic rats. *Vascul Pharmacol.* 2007;47:145–159.
176. Brosnihan KB, Li P, Figueroa JP, Ganten D, Ferrario CM. Estrogen, nitric oxide, and hypertension differentially modulate agonist-induced contractile responses in female transgenic (mRen2)27 hypertensive rats. *Am J Physiol Heart Circ Physiol.* 2008;294:H1995–H2001.
177. Wei Y, Whaley-Connell AT, Chen K, et al. NADPH oxidase contributes to vascular inflammation, insulin resistance, and remodeling in the transgenic (mRen2) rat. *Hypertension.* 2007;50:384–391.
178. Vaneckova I, Kopkan L, Huskova Z, et al. AT1 receptor antisense therapy transiently lowers blood pressure in ren-2 transgenic rats. *Vascul Pharmacol.* 2007;47:63–67.
179. Billet S, Aguilar F, Baudry C, Clauser E. Role of angiotensin II AT(1) receptor activation in cardiovascular diseases. *Kidney Int.* 2008;74:1379–1384.
180. van den Brink OW, Delbridge LM, Pedrazzini T, Rosenfeldt FL, Pepe S. Augmented myocardial methionine-enkephalin in a murine model of cardiac angiotensin II-overexpression. *J Renin Angiotensin Aldosterone Syst.* 2007;8:153–159.

181. Heximer SP, Knutsen RH, Sun X, et al. Hypertension and prolonged vasoconstrictor signaling in RGS2-deficient mice. *J Clin Invest.* 2003;111:445–452.
182. Eckhart AD, Ozaki T, Tevaearai H, Rockman HA, Koch WJ. Vascular-targeted overexpression of G protein-coupled receptor kinase-2 in transgenic mice attenuates beta-adrenergic receptor signaling and increases resting blood pressure. *Mol Pharmacol.* 2002;61:749–758.
183. Hercule HC, Tank J, Plehm R, et al. Regulator of G protein signaling 2 ameliorates angiotensin II-induced hypertension in mice. *Exp Physiol.* 2007;92:1014–1022.
184. Keys JR, Zhou RH, Harris DM, Druckman CA, Eckhart AD. Vascular smooth muscle overexpression of G protein-coupled receptor kinase 5 elevates blood pressure, which segregates with sex and is dependent on gi-mediated signaling. *Circulation.* 2005;112:1145–1153.
185. Hassanain HH, Gregg D, Marcelo ML, et al. Hypertension caused by transgenic overexpression of Rac1. *Antioxid Redox Signal.* 2007;9:91–100.
186. Wirth A, Benyo Z, Lukasova M, et al. G12-G13-LARG-mediated signaling in vascular smooth muscle is required for salt-induced hypertension. *Nat Med.* 2008;14:64–68.
187. da Costa-Goncalves AC, Tank J, Plehm R, et al. Role of the multidomain protein spinophilin in blood pressure and cardiac function regulation. *Hypertension.* 2008;52:702–707.
188. Kim J, Keys JR, Eckhart AD. Vascular smooth muscle migration and proliferation in response to lysophosphatidic acid (LPA) is mediated by LPA receptors coupling to gq. *Cell Signal.* 2006;18:1695–1701.
189. Kulandavelu S, Qu D, Adamson SL. Cardiovascular function in mice during normal pregnancy and in the absence of endothelial NO synthase. *Hypertension.* 2006;47:1175–1182.
190. Ge Y, Bagnall AJ, Stricklett PK, Webb DJ, Kotelevtsev YV, Kohan DE. Combined knockout of collecting duct endothelin A and B receptors causes hypertension and sodium retention. *Am J Physiol Renal Physiol.* 2008;295:F1635–F1640.
191. Amiri F, Virdis A, Neves MF, et al. Endothelium-restricted overexpression of human endothelin-1 causes vascular remodeling and endothelial dysfunction. *Circulation.* 2004;110:2233–2240.
192. Li MW, Dai X, Watts SW, Kreulen DL, Fink GD. Increased superoxide levels in ganglia and sympathoexcitation are involved in sarafotoxin 6c-induced hypertension. *Am J Physiol Regul Integr Comp Physiol.* 2008;295:R1546–R1554.
193. Angelone T, Quintieri AM, Brar BK, et al. The antihypertensive chromogranin A-derived peptide catestatin as a novel endocrine/paracrine modulator of cardiac function: Inotropic and lusitropic actions on the rat heart. *Endocrinology.* 2008;149:4780–4793.
194. Mahapatra NR. Catestatin is a novel endogenous peptide that regulates cardiac function and blood pressure. *Cardiovasc Res.* 2008;80:330–338.
195. Obih P, Oyekan AO. Regulation of blood pressure, natriuresis and renal thiazide/amiloride sensitivity in PPARalpha null mice. *Blood Press.* 2008;17:55–63.
196. Osorio JC, Cheema FH, Martens TP, et al. Simvastatin reverses cardiac hypertrophy caused by disruption of the bradykinin 2 receptor. *Can J Physiol Pharmacol.* 2008;86:633–642.
197. Tsutsumi S, Zhang X, Takata K, et al. Differential regulation of the inducible nitric oxide synthase gene by estrogen receptors {alpha}and {beta}. *J Endocrinol.* 2008;199:267.
198. Belo NO, Sairam MR, Dos Reis AM. Impairment of the natriuretic peptide system in follitropin receptor knockout mice and reversal by estradiol: Implications for obesity-associated hypertension in menopause. *Endocrinology.* 2008;149:1399–1406.
199. Wu Q, Xu-Cai YO, Chen S, Wang W. Corin: New insights into the natriuretic peptide system. *Kidney Int.* 2009;75:142–146.
200. Bouillon R, Carmeliet G, Verlinden L, et al. Vitamin D and human health: Lessons from vitamin D receptor null mice. *Endocr Rev.* 2008;29:726–776.
201. Michailidou Z, Carter RN, Marshall E, et al. Glucocorticoid receptor haploinsufficiency causes hypertension and attenuates hypothalamic-pituitary-adrenal axis and blood pressure adaptions to high-fat diet. *FASEB J.* 2008;22:3896–3907.
202. Rensen SS, Niessen PM, van Deursen JM, et al. Smoothelin-B deficiency results in reduced arterial contractility, hypertension, and cardiac hypertrophy in mice. *Circulation.* 2008;118:828–836.

203. Ohashi K, Iwatani H, Kihara S, et al. Exacerbation of albuminuria and renal fibrosis in subtotal renal ablation model of adiponectin-knockout mice. *Arterioscler Thromb Vasc Biol.* 2007;27:1910–1917.
204. Lund AK, Agbor LN, Zhang N, et al. Loss of the aryl hydrocarbon receptor induces hypoxemia, endothelin-1, and systemic hypertension at modest altitude. *Hypertension.* 2008;51:803–809.
205. Fritsch S, Lindner V, Welsch S, et al. Intravenous delivery of PTH/PTHrP type 1 receptor cDNA to rats decreases heart rate, blood pressure, renal tone, renin angiotensin system, and stress-induced cardiovascular responses. *J Am Soc Nephrol.* 2004;15:2588–2600.
206. Moustafa-Bayoumi M, Alhaj MA, El-Sayed O, et al. Vascular hypertrophy and hypertension caused by transgenic overexpression of profilin 1. *J Biol Chem.* 2007;282:37632–37639.
207. Li N, Chen L, Yi F, Xia M, Li PL. Salt-sensitive hypertension induced by decoy of transcription factor hypoxia-inducible factor-1alpha in the renal medulla. *Circ Res.* 2008;102:1101–1108.
208. Fischer R, Dechend R, Qadri F, et al. Dietary n-3 polyunsaturated fatty acids and direct renin inhibition improve electrical remodeling in a model of high human renin hypertension. *Hypertension.* 2008;51:540–546.
209. Peters B, Grisk O, Becher B, et al. Dose-dependent titration of prorenin and blood pressure in Cyp1a1ren-2 transgenic rats: Absence of prorenin-induced glomerulosclerosis. *J Hypertens.* 2008;26:102–109.
210. Radi ZA, Ostroski R. Pulmonary and cardiorenal cyclooxygenase-1 (COX-1), -2 (COX-2), and microsomal prostaglandin E synthase-1 (mPGES-1) and -2 (mPGES-2) expression in a hypertension model. *Mediators Inflamm.* 2007;2007:85091.
211. Tordjman KM, Semenkovich CF, Coleman T, et al. Absence of peroxisome proliferator-activated receptor-alpha abolishes hypertension and attenuates atherosclerosis in the Tsukuba hypertensive mouse. *Hypertension.* 2007;50:945–951.
212. Lamounier-Zepter V, Bornstein SR, Kunes J, et al. Adrenocortical changes and arterial hypertension in lipoatrophic A-ZIP/F-1 mice. *Mol Cell Endocrinol.* 2008;280:39–46.
213. Lloyd DJ, McCormick J, Helmering J, et al. Generation and characterization of two novel mouse models exhibiting the phenotypes of the metabolic syndrome: Apob48−/−Lepob/ob mice devoid of ApoE or ldlr. *Am J Physiol Endocrinol Metab.* 2008;294:E496–E505.
214. Su W, Guo Z, Randall DC, Cassis LA, Brown DR, Gong MC. Hypertension and disrupted blood pressure circadian rhythm in type 2 diabetic db/db mice. *Am J Physiol Heart Circ Physiol.* 2008;295:H1634–1641.
215. Liang M, Lee NH, Wang H, et al. Molecular networks in Dahl salt-sensitive hypertension based on transcriptome analysis of a panel of consomic rats. *Physiol Genomics.* 2008;34:54–64.
216. Mattson DL, Dwinell MR, Greene AS, et al. Chromosome substitution reveals the genetic basis of Dahl salt-sensitive hypertension and renal disease. *Am J Physiol Renal Physiol.* 2008;295:F837–F842.
217. Pendergrass KD, Pirro NT, Westwood BM, Ferrario CM, Brosnihan KB, Chappell MC. Sex differences in circulating and renal angiotensins of hypertensive mRen(2).lewis but not normotensive lewis rats. *Am J Physiol Heart Circ Physiol.* 2008;295:H10–H20.
218. Harris DM, Cohn HI, Pesant S, Zhou RH, Eckhart AD. Vascular smooth muscle G(q) signaling is involved in high blood pressure in both induced renal and genetic vascular smooth muscle-derived models of hypertension. *Am J Physiol Heart Circ Physiol.* 2007;293:H3072–H3079.
219. Hang L, Stephen-Larson PM, Henry JP, Dixon FJ. Transfer of renovascular hypertension and coronary heart disease by lymphoid cells from SLE-prone mice. *Am J Pathol.* 1984;115:42–46.
220. Peredo HA, Mayer M, Faya IR, Puyo AM, Carranza A. Dehydroepiandrosterone (DHEA) prevents the prostanoid imbalance in mesenteric bed of fructose-induced hypertensive rats. *Eur J Nutr.* 2008;47:349–356.
221. Ma SK, Bae EH, Kim IJ, et al. Increased renal expression of nitric oxide synthase and atrial natriuretic peptide in rats with glycyrrhizic-acid-induced hypertension. *Phytother Res.* 2009;23:206–211.
222. Beltowski J, Jamroz-Wisniewska A, Wojcicka G, Lowicka E, Wojtak A. Renal antioxidant enzymes and glutathione redox status in leptin-induced hypertension. *Mol Cell Biochem.* 2008;319:163–174.

223. Satoh Y, Ide Y, Sugano T, Koda K, Momose Y, Tagami M. Hypotensive and hypertensive effects of acetaldehyde on blood pressure in rats. *Nihon Arukoru Yakubutsu Igakkai Zasshi.* 2008;43:188–193.
224. Wang S, Xu J, Song P, et al. Acute inhibition of guanosine triphosphate cyclohydrolase 1 uncouples endothelial nitric oxide synthase and elevates blood pressure. *Hypertension.* 2008;52:484–490.
225. Satoh K, Fukumoto Y, Nakano M, et al. Statin ameliorates hypoxia-induced pulmonary hypertension associated with down-regulated stromal cell-derived factor-1. *Cardiovasc Res.* 2009;81:226–234.
226. Kwapiszewska G, Wygrecka M, Marsh LM, et al. Fhl-1, a new key protein in pulmonary hypertension. *Circulation.* 2008;118:1183–1194.
227. Yu L, Quinn DA, Garg HG, Hales CA. Deficiency of the NHE1 gene prevents hypoxia-induced pulmonary hypertension and vascular remodeling. *Am J Respir Crit Care Med.* 2008;177:1276–1284.
228. De Franceschi L, Platt OS, Malpeli G, et al. Protective effects of phosphodiesterase-4 (PDE-4) inhibition in the early phase of pulmonary arterial hypertension in transgenic sickle cell mice. *FASEB J.* 2008;22:1849–1860.
229. Henriques-Coelho T, Brandao-Nogueira A, Moreira-Goncalves D, Correia-Pinto J, Leite-Moreira AF. Effects of TNF-alpha blockade in monocrotaline-induced pulmonary hypertension. *Rev Port Cardiol.* 2008;27:341–348.
230. Qin N, Gong QH, Wei LW, Wu Q, Huang XN. Total ginsenosides inhibit the right ventricular hypertrophy induced by monocrotaline in rats. *Biol Pharm Bull.* 2008;31:1530–1535.
231. Rakotoniaina Z, Guerard P, Lirussi F, et al. Celecoxib but not the combination of celecoxib + atorvastatin prevents the development of monocrotaline-induced pulmonary hypertension in the rat. *Naunyn Schmiedebergs Arch Pharmacol.* 2008;378:241–251.
232. Henriques-Coelho T, Oliveira SM, Moura RS, et al. Thymulin inhibits monocrotaline-induced pulmonary hypertension modulating interleukin-6 expression and suppressing p38 pathway. *Endocrinology.* 2008;149:4367–4373.
233. Sauvageau S, Thorin E, Villeneuve L, Dupuis J. Endothelin-3-dependent pulmonary vasoconstriction in monocrotaline-induced pulmonary arterial hypertension. *Peptides.* 2008;29:2039–2045.
234. Hong KH, Lee YJ, Lee E, et al. Genetic ablation of the BMPR2 gene in pulmonary endothelium is sufficient to predispose to pulmonary arterial hypertension. *Circulation.* 2008;118:722–730.
235. Song Y, Coleman L, Shi J, et al. Inflammation, endothelial injury, and persistent pulmonary hypertension in heterozygous BMPR2-mutant mice. *Am J Physiol Heart Circ Physiol.* 2008;295:H677–H690.
236. Shifren A, Durmowicz AG, Knutsen RH, Faury G, Mecham RP. Elastin insufficiency predisposes to elevated pulmonary circulatory pressures through changes in elastic artery structure. *J Appl Physiol.* 2008;105:1610–1619.

Chapter 12
Naturally Occurring, Iatrogenic and Transgenic Models of Atherosclerotic Disease

Atherosclerosis in humans is a complex, multifactorial process usually occurring in large conduit arteries over prolonged periods of time. It is a chronic inflammatory disease, the result of interaction between atherogenic stimuli and the response of the arterial wall. Immune responses play a major role. There are predisposing genetic factors and a number of risk factors involved including hyperlipidemia, hypertension, obesity, smoking, and type-1 (insulin-dependent) and type-2 (noninsulin-dependent) diabetes.

Mouse models of atherosclerotic disease usually fail to mimic the cardiovascular complications of diabetes seen in humans. The Animal Models of Diabetic Complications Consortium, working under the auspices of the NIH, has been working to develop suitable mouse models and to standardize the methods used to assess metabolic and cardiovascular end points with the purpose of quantifying diabetes and its macrovascular complications. The consortium shares the animal models developed and the accumulation of phenotype information with scientists working in this area.[1]

The correlation between diabetes and atherosclerosis is a serious public health issue. Eighty percent of type-2 diabetes patients, who usually have concurrent obesity and metabolic syndrome, die from complications of atherosclerotic disease. Human diabetes is characterized by a reduced ability to use glucose in peripheral tissues. This inability to use glucose effectively is linked to insulin resistance and/or the loss of insulin production by pancreatic islet cells. Type-1 diabetes is a chronic disease triggered by the autoimmune destruction of pancreatic insulin-producing β-cells. It is associated with polymorphisms in HLA class II, but environmental factors including pathogens, toxins, drugs, and viruses can also play a role. Type-2 diabetes is associated with an inability of the pancreas to produce sufficient insulin to cope with increasing metabolic demand. In adult humans β-cell mass is plastic, and a balance of insulin supply and metabolic demand is dependent upon the ability of the β-cells to grow and survive. This ability eventually fails in type-2 patients and β-cell mass declines. Type-2 diabetes usually coexists with the metabolic syndrome and is characterized by abdominal obesity, hyperglycemia, hyperinsulinemia, insulin resistance, hypertension, dyslipidemia, and microalbuminuria.

D.R. Gross, *Animal Models in Cardiovascular Research*,
DOI: 10.1007/978-0-387-95962-7_12, © Springer Science + Business Media, LLC 2009

Increased triglyceride and free fatty acid levels, decreased HDL-cholesterol, and an increase in small dense low-density lipoproteins (LDLs) characterize changes in the plasma of diabetes patients and presage atherosclerosis.[2]

Animal models of type-1 diabetes can be created by treatment with streptozotocin (STZ), a monofunctional nitrosourea derivative isolated from *Streptomyces achromogenes*, that is toxic to pancreatic β-cells. However, the action of STZ is not restricted to β-cells. Rats and dogs treated with STZ do develop diabetes but also display higher than normal levels of protein kinase C (PKC) and diacilglycerol (DAG) in the heart and aorta. When these animals are treated with insulin to attain normal glucose levels the plasma, PKC, and DAG levels return to normal.[2]

The etiology of atherosclerosis probably involves endothelial insult(s) resulting in endothelial dysfunction characterized by changes in endothelial homeostatic mechanisms and increased permeability. LDL cholesterol, very low-density lipoprotein (VLDL) cholesterol, and other lipoproteins accumulate in the wall of the artery initiating and/or associated with smooth muscle cell proliferation. The accumulation of lipoprotein is continuous and dynamic, with influx and deposition exceeding elimination by a variety of mechanisms.[3,4]

Cholesterol acyltransferase 1 (ACAT1) and ACAT2 are membrane-spanning proteins found in the endoplasmic reticulum of cells. ACAT2 is closely associated with plasma cholesterol levels while ACAT1 is more or less ubiquitous serving a more general role in cholesterol homeostasis at the cellular level. ACAT2 also contributes cholesteryl esters to newly secreted VLDL.[5-7] LDL-cholesterol concentrations and composition of the LDL, including size and fatty acid composition, are important determinants of the degree of atherogenicity. Small dense LDL has been correlated with increased risk of coronary arterial disease.[8]

When LDL cholesterol oxidizes the process seems to activate endothelial cells to express vascular cell adhesion molecule-1 (VCAM-1). VCAM-1 binds lymphocytes and monocytes that invade by transendothelial movement into the developing lesion. Other adhesion molecules are released from the endothelial and subendothelial cells including intercellular adhesion molecule (ICAM)-1 (E-selectin) and monocyte chemotactic protein (MCP)-1. Once these molecules migrate into the vessel wall leucocytes become lipid-laden macrophages (foam cells); the transformation is thought to involve macrophage scavenger receptors (MSRs). The foam cells and endothelial cells present in the lesion express a variety of inflammatory cytokines and growth factors including interleukin (IL)-1, angiotensin (Ang)-II, tumor necrosis factor (TNF)-α, vascular endothelial growth factor (VEGF), and endothelin (ET0-1). These cause smooth muscle cells (SMC) to migrate from the media to the intima where they proliferate and help form a neointima and fibroproliferative plaques with large amounts of extracellular matrix.[4] The foam cells also release enzymes including matrix metaloproteinases (MMPs). MMPs begin degradation of the connective tissue matrix of the vessel. A fibrous cap-covered plaque develops and over time it becomes an even more complex lesion. As the disease progresses necrosis may occur, especially at the base of the lesion, along with damage to the media of the vessel. An inflammatory response occurs and the fibrous plaque thins, making the plaque unstable and susceptible to rupture.[3,9]

Characteristics of Plaque Rupture and Resulting Thrombosis

Atherosclerosis was traditionally viewed as a disease of uncontrolled plaque growth with growth-related end points such as atherosclerotic burden, lesion size, cell number, smooth muscle cell proliferation, lipid accumulation, extracellular matrix accumulation, growth factor gene expression, etc. More recently it has been observed that occlusion of the arterial lumen is more commonly an acute event caused by plaque rupture and thrombosis rather than by uncontrolled plaque growth. It is not essential that the plaque is large but that it is prone to rupture and thrombosis, that it is "vulnerable." Rupture of the plaque is a result of physical factors such as fluid shear rates, strains, or pressure forces exceeding the tensile strength of the plague in a mechanically weak region.[10]

The extracellular matrix particularly the fibrillar collagen and extracellular lipids contained within the plaque determine its mechanical properties. Plaques with a thin fibrous cap and a large lipid/necrotic core ratio are most vulnerable to rupture. The consistency of the lipid core depends upon lipid composition and temperature with a soft core considered more vulnerable. The collagen content, distribution, and cross-linkage determine mechanical properties of the cap. Collagen content is also the end result of a dynamic balance between synthesis and degradation with degradation driven by proteinases, mostly MMPs and cathepsins, synthesized by macrophages and SMC and stimulated by macrophage-derived cytokines. SMC are also the main source of collagen synthesis, so SMC accumulation is associated with plaque stability. In this context SMC number and apoptosis-driven death rates can serve as end points to characterize plaque vulnerability. T cells may exacerbate plaque vulnerability via inhibition of collagen production.[10]

The plethora of experimental approaches used to provide appropriate animal models of this disease while creating a vulnerable plaque as a complication of an existing atherosclerotic process and duplicating the precise mechanisms of plaque rupture is problematic. An ideal animal model of the disease would provide lesions that would allow experiments devised to study plaque stability and either spontaneous or induced plaque rupture with resulting thrombosis. Some features of plaque vulnerability have been reported but there does not seem to be a single, gold standard available.[10,11]

Implication of New "Players" in the Pathogenesis of Atherosclerotic Disease

Insulin-like growth factor-1 (IGF-1) plays a role in the progression of atherosclerosis in animal models. IGF binding protein-4 (IGFBP-4) binds to IGF-I and prevents receptor binding. Protease-resistant forms of IGFBP-4 inhibit atherosclerotic lesion development in mouse and pig models.[12]

Fractalkine (CX3CL1) and CXCL16 (SR-PSOX) are small chemotaxtic polypeptides synthesized as transmembrane molecules that can be cleaved from

endothelial cell surfaces by disintegrin and metalloproteinase-10 (ADAM-10). These molecules are enhanced by activation of the enzyme ADAM17 to produce soluble chemoattractants. Leukocyte subtypes have receptors, CX3CR1 and CXCR6, that interact with these chemoattractants. The result is cell-to-cell adhesion. There is increasing evidence that CX3CL1, CXCL16, and other members of the CXC family of chemokines including IL-8/CCL8, IP-10/CXCL10, and SDF-1/CXCL12, as well as members of the CC chemokine family such as MCP-1/CCL2, contribute to the pathogenesis of atherosclerosis.[13,14] Cathepsin-S (CTSS) is an elastolytic cysteine protease that has also been implicated in the development of atherosclerotic lesions in animal models.[15]

There is recent evidence that vasa vasorum (VV) may contribute to early atherosclerotic lesions by providing nutrient and oxygen supply to the plaque and by their role as conduits of inflammatory cells. Blocking plaque neovascularization using angiostatin reduced the progression of atherosclerosis in apoE$^{-/-}$ knockout mice. The density of VV is highly correlated with the extent of inflammatory cells but not the size of atheromatous lesions. The VV also seem to play a role in plaque stability. Plaque neovascularization is an important aspect of plaque development and could be a source of intraplaque hemorrhage.[16]

Local treatment with adiponectin, an adipocytokine, suppressed the development of atherosclerosis in the abdominal aortas in a rabbit hypercholesterolemia model. The result was due, in part, to the treatment attenuating the expression of VCAM-1 and ICAM-1 in the vessel walls.[17]

Animal Models

General

A.C. Ignatowski fed rabbits a special diet rich in meat, milk, and eggs to produce the first animal model used in atherosclerosis research in 1908.[3] Vesselinovitch listed the requirements for an ideal animal model for atherosclerosis research. The ideal model must be easily available and inexpensive, easy to maintain and manipulate, of a proper size, available as genetically pure-bred lines, reproduce easily in captivity, develop typical lesions with relative ease in a practical length of time, have a low incidence of other spontaneous diseases, have some similarity to human anatomy, physiology, and biochemistry including serum lipoprotein and lipid metabolism similar to humans, similar pathogenesis of lesions to humans, similar topography of lesions to humans, lesion components similar to those found in humans, and demonstrating clinical complications of lesion rupture similar to those seen in humans.[3]

The search for appropriate animal models has led to high-fat diet feeding, alone and in combination with physical, chemical, and/or immunologic injury to the endothelium. More recently the generation of models has exploded using selective breeding or transgenic technology. There always seem to be some features of the iatrogenic

disease in these animal models that differ from the naturally occurring disease in humans. It is therefore necessary to make some sort of compromise when selecting an animal model. The goal is to seek the model that provides the closest fit for the specific hypothesis being tested. Because there is a strong link between glucose metabolism, diabetes, and atherosclerosis new animal models are being used to help define the details of these interrelationships.

Placing a silicone, Tygon®, acrylic, or any other plastic collar around an artery in most species will induce intimal hyperplasia. If the animal is fed an atherogenic diet an atherosclerotic lesion will develop at the site along with characteristic changes in vascular reactivity, such as increased sensitivity to serotonin.[18,19]

Naturally Occurring Animal Models of Atherosclerosis

Nonhuman primates are phylogenetically close to humans, eat a similar omnivorous diet, have similar metabolism, and can develop atherosclerotic lesions as they age. Primates are expensive to maintain and can carry viral zoonoses dangerous to humans, and their use stimulates animal rights activism relating to ethical issues concerning their use in experimental paradigms.[3,20] Naturally occurring atherosclerotic lesions have been reported during routine necropsies of swine, ducks, domestic chickens, pigeons, parrots, some marsupials including kangaroos, and occasionally in seals, sea lions, and other pinnipeds and in bears.[3]

Primate Models of Atherosclerosis

Male rhesus monkeys were made diabetic with intravenous alloxan. They developed marked hyperglycemia and increased serum triglycerides and free fatty acids. When vasectomy was combined with diabetes there was a significant increase in the atherosclerotic plaque score in the coronary and renal arteries.[21]

When primates are fed high-fat high-cholesterol diets for prolonged periods they develop atherosclerotic lesions associated with hypercholesterolemia. Thomas et al.[22] fed primates high-cholesterol diets plus saturated, monounsaturated, or polyunsaturated fatty acids for 5 years. Lipid extracts from atherosclerotic plaque in the iliac arteries were analyzed for cholesterol, cholesteryl esters, fatty acid composition, and F-2-isoprostane, a marker of lipid oxidation. They found that F-2-isoprostane accumulation did not depend on the concentration of oxidizable lipids accumulated in the lesions. N-3 polyunsaturated fat added to the diet of African green monkeys reduced HDL-cholesterol concentration by increasing the fractional catabolic rate of medium-sized HDL particles.[23] Male African green monkeys were fed diets with either cis monounsaturated fatty acids or a diet with trans isomers (trans fatty acids) for 6 years. The monkeys fed with the trans fat gained more weight and had increased intra-abdominal fat, postprandial hyperinsulinemia, and elevated fructosamine blood levels.

A significant reduction in muscle insulin-stimulated/threonine protein kinase suggested that a change in carbohydrate metabolism might be responsible.[24]

Peroxisome proliferator-activated receptor (PPAR) agonists increased plasma HDL-C, apoA-I, and apoA-II concentrations and increased the size of HDL particles in St. Kitts vervet monkeys.[25] Cholesterol ester transfer protein (CETP) activity did not differ in St. Kitts vervets fed diets enriched in saturated, monounsaturated, or *n*-6 polyunsaturated fatty acids but was significantly higher when cholesterol was added to the diets. Significant negative associations were observed between CETP activity and HDL cholesterol and significant positive correlations of CETP activity with LDL particle diameter.[26]

When rhesus monkeys were fed 30% less calories for more than 2 years plasma lipoprotein A (LpA) levels were reduced significantly in males but not in females. Males were fed the control diet that had close to twice as high LpA levels as females on the same diet. LpA levels were closely correlated with total cholesterol and LDL cholesterol measurements.[27] Dietary cholesterol sufficient to cause hypercholesterolemia resulted in a threefold increase of acyl-CoA:cholesterol acyltransferase-2 (ACAT-2) protein mass while ACAT-2 mRNA was not as responsive in cynomolgus monkeys. Neither marker was increased significantly by feeding twice the concentration of cholesterol to African green monkeys.[28]

Swine Models of Atherosclerosis

Domestic swine are also susceptible to atherosclerosis. They are omnivorous and their cardiovascular system and metabolism are similar to that of humans. Unfortunately, mature pigs can be as large as 300 kg and thus pose significant management problems. Miniature pigs have been developed and used but these pigs are still not very small since adults of some strains easily reach 100+ kg. Sinclair Research has recently acquired breeding colonies of Hanford and Yucatan miniature pigs as well as the Sinclair strain they are known for.[20] When these miniature breeds are used in atherosclerosis experiments lesions distribute in patterns very similar to those seen in humans and can be developed in as little as 16-18 weeks by feeding high-cholesterol and/or high-sugar diets.[29,30] Pigs treated with alloxan or STZ develop a quasi type I diabetes and develop atheroma as part of the metabolic syndrome, especially if fed a cholesterol-containing diet.[20]

A strain of pigs with inherited LDL cholesterolemia has been identified. At 39-54 months of age these animals demonstrated spontaneous hemorrhage and rupture of coronary artery lesions.[10]

Dog and Cat Models

Dogs and cats are carnivores so they have a natural resistance to high-lipid diets and atherosclerosis. These species also have an extensive coronary collateral circulation system, significantly more extensive than seen in most other animal species, and are

thus further protected against myocardial infarctions. Dogs and cats have been useful models for the study of mechanisms of response to ischemia and reperfusion injury but the results need to be extrapolated to humans with care. Because of their status as beloved pets and increasingly restrictive anthropomorphic attitudes about their use in research their use has declined significantly in recent years. The justification for their use in very specific experimental paradigms needs to be extensive and well argued to be acceptable.

Rabbit Models

The high-cholesterol diet fed rabbit model will have been used for over 100 years by the time this text is available. Because they are herbivores rabbits seldom, if ever, develop spontaneous true atherosclerotic lesions. They do develop some unusual types of degenerative medial lesions in the aortic arch and thoracic aorta characterized by mineralization of the tunica media. The lesions resemble those associated with Monckeberg's medial sclerosis in humans and animals selectively bred for these lesions.

When rabbits are fed regular rabbit chow with the addition of as little as 2% animal origin cholesterol they will go from normal total plasma cholesterol levels of 50-70 mg/dl to >1,500 mg/dl in 6-8 weeks. The cells of the reticuloendothelial system, particularly in the liver, become massively engorged with cholesterol. The kidneys and other organs are also severely affected. These lesions are reminiscent of a lipid storage disorder and the rabbits are obviously ill. If allowed to progress a percentage of the animals will die of liver and/or renal failure. The rabbits also accumulate cholesterol within the intima of the large-conduit arteries but the content of the lesions and the sites of distribution are not the same as in atherosclerosis in humans. The amount of cholesterol and the amount and type of fat in the diet play a direct role in the severity and composition of the lesions in rabbits. Simple substitution of casein for soy protein in the diet can result in arterial lesions in rabbits. Microscopically rabbit lesions resemble thick fatty streaks with most of the lipid localized in foam cells. When the duration of hypercholesterolemia is extended the lipid eventually will accumulate extracellularly. It is rare for rabbits to develop fibrosis, hemorrhage, ulceration, and/or thrombosis. Depending on the diet used some lesions may become significantly fibrocellular in composition. Because rabbits are easy to feed, care for and handle, and are both relatively inexpensive and available they are still frequently used in atherosclerosis research.[3,20,31]

Kondo and Watanabe isolated a mutation in the LDL receptor in rabbits that corresponds to the defect found in familial hypercholesterolemia in humans. These rabbits have a defective LDL receptor (LDLR) due to a spontaneous four-amino-acid deletion in the cysteine-rich ligand-binding domain of the receptor (7) in exon-4 of the *LDLR* gene. The Watanabe heritable hyperlipidemic rabbits develop massive hypercholesterolemia, hyperinsulinemia, and fulminating atherosclerosis even when fed a cholesterol-free diet.[3,20,32] When Watanabe heritable hyperlipidemic

rabbits were challenged with Russel's viper venom, combined with serotonin or angiotensin II by intraperitoneal injection, they developed acute myocardial infarctions in some animals, but there was no correlation between coronary atherosclerosis and myocardial infarction in this model.[10]

A hybrid hare, heterozygous for glucose-6-phosphate dehydrogenase has been described and used to study clonal characteristics of arterial lesions in cholesterol-induced atherosclerosis.[33-35] Shimoda et al.[36] recently described a new line of rabbit designated TGH. These animals have significantly higher concentrations of plasma triglyceride and cholesterol than control Japanese white rabbits. The TGH rabbits demonstrate severe atherosclerotic lesions throughout the aorta and especially in the aortic arch. The TGH rabbits also have significantly higher arterial pulse pressures, as measured in the femoral artery, suggesting a less compliant arterial vasculature compared with the control animals.

Since it is commonly accepted that the initiation of atherosclerosis is inflammatory in nature it is attractive to hypothesize that causative agent(s) may be involved, viral and/or bacterial. One candidate is *Chlamydia pneumonieae* in humans. Rabbits with *C. pneumoniae* infection have demonstrated exacerbated development of arterial lesions. A common respiratory disease of caged rabbits (snuffles), caused by *Pasteurella multocida*, has atherogenic consequences. Specific pathogen-free rabbits fed with a high-cholesterol diet failed to develop significant aortic lesions.[20]

Accelerated atherosclerotic-like lesions can be developed in rabbits by a combination of balloon injury and hypercholesterolemia.[10] When alloxan-induced diabetic rabbits are subjected to balloon injury they demonstrate increased neointimal thickening.[2] A rupture vulnerable model can be created in rabbits by allowing an inflatable balloon to become embedded in a plaque and then inflating the balloon when convenient to study plaque rupture. The pressure required to inflate the balloon and cause the rupture can be used as a measure of the mechanical strength of the plaque.

Transgenic Rabbit Models

New Zealand white rabbits were fed 0.1% cholesterol included in their isocaloric diets. The latter included saturated fats, monounsaturated fats, or *n*-6 polyunsaturated fats. Half of the rabbits in each group were supplemented with 2,500 IU α-tocopherol/kg of the diet. The other half of the animals received 25 IU α-tocopherol. The high supplement groups had total plasma cholesterol levels 31% lower than those animals that received the low dose. Differences in mean esterified cholesterol concentrations from samples of the arteries of these animals paralleled differences in total plasma cholesterol levels and indicate that atherosclerosis can be diminished in this model.[37] Conjugated linoleic acid has also been shown to inhibit cholesterol-induced atherosclerosis in rabbits.[38]

Human transgenes for apoA I, apoB100, apoE2, apoE3, apo(a), cluster AI/CIII/AIV, HL, LCAT, LPL, and SRB1 have been transvected into New Zealand White rabbits. ApoA I, LCAT, apo(a), and LPL have been transvected into Watanabe rabbits.[4]

Rat Models

The first well-characterized strain of rats was developed at the Wistar Institute in the 1920s. Rats are social, highly adaptive, and omnivorous. They resemble humans in their metabolism and many aspects of their physiology but the normal rat is resistant to the development of atherosclerosis. With the recent sequencing of the rat genome there is renewed interest in developing transgenic rat models for many kinds of biomedical research.

Hypercholesterolemia is difficult to produce in the rat since lipid metabolism is focused on HDL, rather than on LDL as it is in humans. Feeding cholesterol, as high as 10% on a weight/weight basis, is not usually enough to produce hypercholesterolemia without the use of thiopropyluracil to cause concurrent hypothyroidism.

As in other species there is a link between diabetes and atherosclerosis in rats. Male Wistar rats were given an i.p. injection of 45 mg/kg STZ. They demonstrated elevated plasma levels of glucose, thiobarbituric acid reactive substances, hydroperoxides, serum triglycerides, phospholipids, free fatty acids, total cholesterol, VLDL, high-density lipoprotein-cholesterol (HDL-C), and LDL-cholesterol. The percentage of HDL-C to total cholesterol was decreased.[39]

The fatty Zucker rat incorporates a spontaneous mutant *fa* gene that affects the action of leptin. When homozygous for the *fa* gene the Zucker rat develops a variant of metabolic syndrome and becomes obese, moderately insulin-resistant, and hypertriglyceridemic, but does not progress to diabetes or atherosclerosis.[20] The Zucker diabetic fatty rat (ZDF) does develop diabetes. The onset seems to be related to the loss of GLUT-2 from the β cells in the pancreas and GLUT-4 transporters in muscle indicating that the diabetes develops from both impaired insulin secretion and impaired peripheral glucose transporter function. These rats develop microvascular damage leading to glomerular sclerosis and retinopathy but do not develop atherosclerosis. There are reports of vascular dysfunction in the aorta, coronary and mesenteric arteries in middle-aged, obese ZDF rats and they mimic the transition to type-2 diabetes with the development of microvascular lesions.[20]

Koletsky[40] reported the isolation of a mutation from a rat line produced by crossing Sprague-Dawley rats with spontaneously hypertensive rats (SHR). These animals become obese, hypertensive, and hyperinsulinemic and developed atherosclerosis and dissecting aortic aneurysms. Charles River Laboratories breeds these animals commercially. A number of congenic strains have been developed that incorporate genetic mutations on various inbred backgrounds from these animals. Rats of strains that are homozygous for the autosomal recessive *cp* gene become obese, hyperlipidemic, and insulin resistant. When a normotensive strain, designated LA/N-*cp*, was outbred the animals developed atherosclerosis and ischemic myocardial lesions spontaneously. This outbred strain also develops the metabolic abnormalities found in other *cp* strains. The strain was redesignated as JCR:LA-*cp*. Many of these strains have now been rederived and new genetic animal models have been established by Charles River Laboratories (www.criver.com). Some are available commercially. Because many of these strains are fully congenic they are highly inbred. Some of the highly inbred strains have maintained the *cp* gene and obese phenotype but have lost

the atherosclerosis and cardiovascular disease-prone characteristics. However, the JCR:LA-*cp* strain has been maintained as a closed outbred colony and has kept the high insulin resistance and atherosclerosis-prone traits. It mimics the clinical sequence seen in human patients with metabolic syndrome developing vascular damage and dysfunction early during asymptomatic stages.[20,41,42] JCR:LA-*cp* rats have an elevated level of cAMP phosphodiesterase (PDE) activity but only PDE3B activity is elevated.[43] The lesions found in these animals include dead endothelial cells, polygonal cells, varying areas of desquamation with attached blood elements, frank ulcerated lesions, and old, rechannelized, thromboses. The lesions are present in both homozygous cp and heterozygous animals, but are more frequent and severe in the homozygous animals.[44]

The *cp/cp* male rat phenotype develops spontaneous coronary artery atherosclerosis, thrombosis, and stress-induced myocardial infarcts that can be fatal. Extensive atherosclerotic lesions can be found in the major arteries of the middle-aged *cp/cp* male. Female *cp/cp* rats have lower blood levels of plasminogen activator inhibitor-1 (PAI-1) and less severe arterial lesions. Hyperinsulinemia is a significant factor in the development of vasculopathy in this model and the vasculopathy can be modulated by the reduction of circulating levels of insulin suggesting a significant role for insulin in endothelial damage and atherosclerosis development in this model. The spontaneous ischemic lesions found in the hearts of *cp/cp* rats are probably due to a sequence of vasospasm and associated thrombosis that accompany occlusive coronary lesions. The coronary flow response to bradykinin is reduced.[20,45] Both male and female *cp/cp* rats have elevated triglyceride levels (282-512 mg/100 ml) and moderate increases in total cholesterol (74-84 mg/100 ml). There are large triacylglycerol-rich and apoprotein-poor VLDL fragments that contain both apolipoproteins Bh and B1 and increased phospholipid-rich HDL. There are elevations in serum apolipoproteins B and E and apolipoproteins A-I are 2.7-3.0-fold higher. The levels of VLDL are significantly higher in females but the levels of intermediate-density lipoproteins (IDL) and HDL are significantly lower than in the more atherosclerosis-prone males. LDL, similar to that seen in normal rats, is heterogeneous and contains apolipoproteins Bh, E, A-I, and C and is significantly higher in males than in females. However, LDL represents less than 13% of the total serum cholesterol and less than 6% of the total serum lipids in 3-month-old animals.[46]

Hyperlipidemia in the *cp/cp* rat is primarily due to hepatic hypersecretion of VLDL and its effects on the LDL and HDL fractions. The result is high triglyceride levels and moderate effects on cholesterol. The hypersecretion of VLDL in this model seems to be a compensatory response by the liver to large amounts of glucose absorbed by these hyperphagic animals from a high carbohydrate diet. The insulin-resistant/hyperinsulinemic state in this model is associated with enhanced circulating levels of two different classes of atherogenic lipid particles and has a hyperlipidemic profile similar to that found in prediabetic humans.[20]

An atherosclerosis calcification model was created in rats with the combination of excessive vitamin D and a high cholesterol diet.[47] BB Wistar diabetic rats have increased neointimal hyperplasia following balloon injury of the carotid artery or aorta.[2]

Transgenic Rat Models

Cholesterol ester transfer protein (CETP) transgenic rats have been developed by the transfer of simian and human CETP into the normally CETP-deficient Fisher rat. In this transgenic animal, a high-sucrose diet induces large increases in non-HDL lipids with implications for reverse cholesterol transport and the development of atherosclerosis. The CETP transgenic Dahl-salt-sensitive (Tg25) male rats have marked dyslipidemia and advanced coronary artery disease compared to females. [20]

Mouse Models

Normally mice are short-lived and resistant to the development of atherosclerotic disease. However, a number of genetic mouse models based on either a spontaneous mutation or genetic manipulation have been developed. Deletion mouse models for Apolipoproteins AI, AII, AIV, AV, B100, B48, CI, CII, CIII, E and Cluster AI/CIII/AIV as well as overexpression models for AII, AIV, and AV have been described. Mice have been used with deletion of lipoprotein lipase, hepatic lipase, hormone-sensitive lipase, lecithin-cholesterol acyltransferase, phospholipid transfer protein, cholesterol 7-alpha-OH, acyl CoA:cholesterol acyltransferase-1 and -2, and sterol 27-OH. An overexpression model of hepatic lipase has been used as well as mice with receptor deletions for LDL, LDL receptor-related protein, VLDL, MSR A, and combined LDL/LRP/VLDLR and CD 36 receptor. Overexpression mice models of VLDLR and CD 36 have been used. Transport protein deletions for ATP-binding cassette transporter A1 (ABCA1), scavenger receptor class B type1 (SRB1), and microsomal transfer protein were developed in mice as well as overexpression models of ABCA1 and SRB1.[4]

Transgenic mouse "knock-in" models for lipoprotein metabolism and atherosclerosis research have included human apolipoproteins AI, AII, AIV, AV, B, CI, CII, CIII, E and clusters of AI/CIII/AIV and AI/CIII/AIV/AV. Human enzyme genes for LPL, HL, HSL, LCAT, PLTP, Sterol 27-OH, and cholesterol 7-alpha-OH have also been knocked-in to mice along with receptors for LDL and VLDL and CETP (cholesteryl ester transfer protein) and ABCA1 transport proteins.[4]

Mice Models of Glucose Intolerance

The *db/db* mouse contains a spontaneous mutation of the leptin obR system analogous to the *cp* gene. Homozygous *db* mice (*db/db*) have a defective leptin binding receptor and develop obesity, insulin resistance, hyperinsulinemia, hypertriglyceridemia, and a severe hyperglycemia that differs from the stable hyperinsulinemia and normoglycemia seen in *cp/cp* rats. The *db/db* mice have impaired endothelial and vascular function, abnormal cardiac metabolism and function, retinal damage,

and glomerular sclerosis. They do not seem to develop atherosclerosis or ischemic cardiovascular disease.[20]

The *ob/ob* mouse has a mutation that results in the production of a structurally defective leptin unable to bind to the ob receptor. These animals are obese, insulin-resistant, hypertriglyceridemic but normoglycemic. They demonstrate vascular dysfunction and some cardiac functional defects but atherosclerosis or related myocardial infarction has not been reported. The model is most useful for studying the role of leptin in metabolism of glucose and lipids.[20] Adipose tissue of obese mice is hypoxic and local adipose tissue hypoxia deregulates the production of adipocytokines.[48]

Mice homozygous for the spontaneous autosomal recessive diabetes mutation *db* (Lepr*db/db*) and animals of the same C57BL/KsJ strain designated (Lep*ob/ob*) display early-onset obesity, extreme insulin resistance, a more efficient conversion of food to lipid, and a slower rate of catabolism when fasted. Double mutants (Lep*ob/ob*:LDLR$^{-/-}$) demonstrate increased atherosclerosis compared with wild-type, LDLR$^{-/-}$, Lep*ob/ob*, or Lep*ob/ob*:LDLR$^{+/-}$ controls when all were fed a normal diet. The Lep*ob/ob*:LDLR$^{-/-}$ mice have severe hypercholesterolemia and hypertriglyceridemia. Lep*ob/ob*:ApoE$^{-/-}$ and Lep*ob/ob*:LDLR$^{-/-}$ fed standard rations demonstrate similar levels of obesity, but the ApoE$^{-/-}$ double mutants have lower triglyceride levels, higher nonesterified fatty acid levels, and higher insulin levels. The Lep*ob/ob*:ApoE$^{-/-}$ mice transport cholesterol primarily on VLDL while the Lep*ob/ob*:LDLR$^{-/-}$ transport on LDL. Atherosclerosis was greater in both than in single mutant ApoE$^{-/-}$ and LDLR$^{-/-}$ controls. Both atheroma size and collagen content were significantly greater in the Lep*ob/ob*:ApoE$^{-/-}$ mice.[2]

Insulin receptor substrate -2 (IRS)$^{-/-}$ female mice are infertile and demonstrate signs of type 2 diabetes and metabolic syndrome with severe obesity. Male IRS-2$^{-/-}$ mice are extremely diabetic by 6-8 weeks of age. When IRS-2$^{-/-}$:ApoE$^{-/-}$ animals are fed a fatty diet they develop hypercholesterolemia and accelerated atherosclerosis.[2]

The apoE Lipoprotein Knockout

The most widely used mouse model is the apoE$^{-/-}$ "knockout" strain. These mice have total plasma cholesterol concentrations of 11 mM, compared with 2 mM for the parent C57BL/6 mouse. They develop advanced intimal lesions largely confined to the aortic root. When fed a high-cholesterol diet the apoE$^{-/-}$ mice develop a more widely distributed pattern of atherosclerosis, similar to that found in humans, and have plasma cholesterol concentrations that can approach 30 mM. The C57BL/6 strain of mice will also develop some atherosclerosis, mostly confined to the aortic root, when fed a high-fat or high-cholesterol diet. The apoE$^{-/-}$ mouse is generally considered to be a model for untreated, severely dyslipidemic, humans.[20,49-59]

ApoE$^{-/-}$ mice 42-54-weeks old have both a high frequency of intraplaque hemorrhage and a fibrotic conversion of necrotic zones with loss of the fibrous cap in the innominate artery. When animals 37-59-weeks old were fed a diet supplemented with 21% lard and 0.15% cholesterol they died spontaneously with luminal thrombi and ruptured plaques. Platelet- and fibrin-rich thrombi can be induced by direct mechanical injury of the aorta in apoE$^{-/-}$ mice.[10,59,60]

ApoE$^{-/-}$ mice fed a normal diet also exhibit accelerated atherosclerosis when treated with STZ. The enhanced atherosclerotic response is associated with increased macrophage-foam cell formation with an increased capacity of these cells to take up oxidized LDL. When STZ treatment is superimposed on LDLR$^{-/-}$ mice fed a high-fat diet for 6 months the mice exhibit enhanced arterial production of advanced glycation end products and higher levels of blood glucose and VLDL cholesterol compared with nondiabetic controls. Some workers have reported the same degree of atherosclerosis in both groups of mice while others doing similar experiments found larger atherosclerotic lesions in the aortic root in the STZ-treated animals.[2]

Hypercholesterolemic apoE$^{-/-}$:LDR$^{-/-}$ double knockout mice are frequently used in atherosclerosis research.[61-63] Animals with coronary atherosclerotic lesions were subjected to mental stress or hypoxia and developed acute myocardial infarction with ischemia followed by inflammation and fibrosis in the myocardium. The pathological changes were prevented when an endothelin type-A receptor blocker was used. No signs of plaque rupture or plaque-associated thrombosis were described in this study.[10] When apoE$^{-/-}$:LDLR$^{-/-}$ mice are treated with STZ the resulting diabetic animals can be used to study accelerated atherosclerosis and cardiomyopathy.[64]

Double knockout apoE$^{-/-}$ and acyl CoA:cholesterol acyltransferase 2 (ACAT2)$^{-/-}$ mice were used to demonstrate that ACAT2 deficiency leads to a compensatory increase in the activity of lecithin cholesterol acyltransferase, the major plasma cholesterol esterification enzyme that increases HDL cholesterol esters.[65] However, cholesterol absorption is not completely inhibited in ACAT2$^{-/-}$ mice.[6,7,66,67]

ApoE$^{-/-}$:P-selectin$^{-/-}$ double knockouts show significantly reduced atherosclerosis and leukocyte recruitment in the plaque that forms.[68] Without apoA-I and HDL, apoE$^{-/-}$:apoA-I$^{-/-}$ double knockouts demonstrate the same amount of aortic cholesteryl ester as apoE$^{-/-}$ mice.[69] Double knockout apoE$^{-/-}$:pregnancy-associated plasma protein-A (PAPP-A)$^{-/-}$ mice were used to demonstrate that PAPP-A plays a critical role in lesion development in the apoE$^{-/-}$ mouse model. This is due, in part, to amplification of local IGF-I bioavailability.[70]

ApoE$^{-/-}$:glutathione peroxidase-1 (GPx1)$^{-/-}$ mice were treated with STZ. GPx1 is an antioxidant and the double knockouts demonstrated significantly increased atherosclerotic lesion formation in the aortic sinus, aortic arch, and thoracic and abdominal aorta compared with apoE$^{-/-}$ treated with STZ controls.[71]

Mouse strains deficient in the HDL scavenger receptor Class B Type 1 (SR-B1), with and without apoE deficiency and fed a normal laboratory mouse diet do not demonstrate atherogenesis. When fed a high fat/high cholesterol diet these animals will develop coronary lesions with total plasma cholesterol concentrations in the 40 mM range. The combination of abnormal metabolism due to the genetic defects and the abnormal diet results in advanced vasculopathy similar to those seen in rare human genetic disorders but does not mimic the disease progression seen in humans with common metabolic syndrome or type-2 diabetes.[20]

Glucose-6-phosphate dehydrogenase (G6PD) mutant mice with G6PD activity 20% of normal were crossed with apoE$^{-/-}$ mice and were fed a high-fat diet for 11 weeks. They were compared with G6PD wild-type (E-WT) and G6PD hemizygous (E-Hemi) animals.

The blood pressure was significantly higher in the E-Hemi mice but superoxide anion release, nitro tyrosine, VCAM-1, and iNOS immunohistochemical staining were less in the E-Hemi than in E-WT animals. Serum cholesterol level was lower in E-Hemi animals but lesion area was decreased.[72]

A bile-acid-activated member of the nuclear receptor superfamily designated farnesoid X receptor (FXR) is essential for the regulation of bile acid, cholesterol, and triglycerides. ApoE$^{-/-}$:FXR$^{-/-}$ female mice were found to have less atherosclerotic lesion area than apoE$^{-/-}$ controls even though serum cholesterols and triglycerides were higher. There seems to be a disconnection between serum lipid levels and the degree of atherosclerotic deposition in this model.[73]

Tumor necrosis factor-alpha (TNF-α) also seems to contribute to the atherosclerotic process. When interposition carotid artery grafting was performed using TNF-α-1R$^{-/-}$ and congenic (C57B1/6) wild-type (WT) mice as graft donors and congenic normal diet-fed apoE$^{-/-}$ mice as recipients advanced atherosclerotic lesions developed in the grafts within 8 weeks. The WT grafts demonstrated twice as much atherosclerosis as the TNF-α-1$^{-/-}$ grafts. Fourteen-month-old apoE$^{-/-}$:TNF-α-1$^{-/-}$ double knockout mice had less atherosclerosis than apoE$^{-/-}$ controls.[74]

Grb2 is a ubiquitous linker protein that couples growth factor receptor activation to downstream mitogen-activated protein kinase (MAPK) cascades. Deletion of Grb2 is lethal but Grb2 heterozygous mice appear normal. ApoE$^{-/-}$:Grb2$^{+/-}$ mice fed a high-fat diet had less atherosclerotic plaque formation than apoE$^{-/-}$ mice suggesting that Grb2 is needed for plaque formation.[75]

ApoE$^{-/-}$ mice were crossed with mice overexpressing eNOS (eNOS-Tg) and with mice overexpressing GTP-cyclohydrolase I (GCH-Tg). GTP-cyclohydrolase is the rate-limiting enzyme in BH4 synthesis. The ApoE$^{-/-}$:eNOS-Tg:GCH-Tg mice had significantly more atherosclerosis than apoE$^{-/-}$ controls.[76]

The LDL Receptor Knockout

The LDLR$^{-/-}$ mouse is a model for human familial hyperlipidemia (FH). These mice have only mildly elevated plasma cholesterol levels when fed a normal chow diet but when fed a 1.25% cholesterol diet homozygotes develop plasma cholesterol levels in the +40 mM range similar to FH humans and have xanthomas and extensive atherosclerosis in the large conduit arteries.[20,77-81]

Insulin resistance and hyperinsulinemia do not appear to enhance atherosclerosis in severely hypercholesterolemic male LDLR$^{-/-}$ mice but feeding a fat- and sucrose-enriched diet to these animals for 16 weeks produced significant obesity, hyperglycemia, hypertriglyceridemia, hypercholesterolemia, and hyperleptinemia. C57BL/6ApoE$^{-/-}$ mice fed a similar diet became obese but did not demonstrate these changes in blood profiles or atherosclerotic deposition.

Joven et al.[82] studied 128 male Apo E$^{-/-}$ and 128 LDLR$^{-/-}$ mice. Equal numbers of each were assigned to a control diet group or five other groups that were fed different levels of fat and cholesterol. Animals from each group were euthanized after 10, 16, 24, and 32 weeks on their respective diets. There were significant

differences between strains, particularly in the constitutive expression of liver genes, glucose tolerance, and body weight. Both strains had signs of steatohepatitis but the signs were more severe in the LDLR$^{-/-}$ mice. The authors concluded that there were enough differences found so that investigators need to carefully consider not only the animal model but also the choice of diet and how long it is fed.

When the LDLR$^{-/-}$ mouse is crossed with the *ob/ob* mouse the strain has very high plasma concentrations of both triglycerides and cholesterol and when fed a low-cholesterol diet still the strain develops advanced atherosclerotic disease by 6 months of age.[20]

LDLR$^{-/-}$:RAG1$^{-/-}$ mice are immunodeficient and atherosclerosis-susceptible. When natural killer T (NKT) cells from Valpha14Jalphal8 T-cell receptor transgenic mice were transferred into LDLR$^{-/-}$:RAG1$^{-/-}$ mice fed a high-fat diet for 12 weeks there was a significant increase in aortic root atherosclerotic plaque compared with the same double knockouts receiving NKT cell-deficient splenocytes from CD1d$^{-/-}$ controls.[83]

Acyl-coenzymeA:cholesterol O-acyltransferase-2 (ACAT2) synthesizes cholesteryl esters from cholesterol and fatty acyl-CoA. These are incorporated into apoB-containing lipoproteins secreted into the blood stream. LDLR$^{-/-}$:ACAT2$^{-/-}$ double knockout mice fed an atherosclerotic diet for 20 weeks had less atherosclerosis than LDLR$^{-/-}$ controls.[81]

LDLR$^{-/-}$:ApoB Cl$^{-/-}$ mice were used to investigate gene-gene interactions and the effects of a high-fat diet. Five-month-old male and female double knockouts were fed either the high-fat diet or normal mouse chow for 3 months. Male mice had 54 different genes and female mice 77 genes perturbed by the high-fat diet. Glycolysis, fat transport, and steroid hormone biosynthesis pathways were upregulated as were a number of stress-response genes. Several genes involved in calcium signaling and bone formation were also upregulated.[84]

LOX-1 is an endothelial receptor for oxidized LDL. LOX-1$^{-/-}$ were compared with LDLR$^{-/-}$:LOX-1$^{-/-}$ double knockouts after feeding a 4% cholesterol/10% cocoa butter diet for 18 weeks. Atherosclerotic lesions covered 61 ± 2% of the aorta in the LDLR$^{-/-}$ but only 36 ± 3% of the aorta in the double knockouts.[85]

Other Knockout Models

The murine plasma fibrinolytic system is more resistant to activation than the human system probably due to a relative resistance of murine plasminogen to tissue-type plasminogen activator (t-PA) and a shorter plasma half-life of mouse t-PA. Mice lacking t-PA (t-PA$^{-/-}$) have delayed clearance of intravascular fibrin after vascular injury and develop severe generalized thrombosis. ApoE$^{-/-}$:t-PA$^{-/-}$ mice have enhanced atherosclerosis compared with apoE$^{-/-}$ controls.[86]

VCAM-1$^{-/-}$ fetus die in utero since $\alpha_4\beta_1$ interaction with VCAM-1 is essential for fetal development. Mice with a D4D mutation lack one of the two VCAM-1 ligand-binding sites but still have enough VCAM-1 expression to survive. When mice with this genotype were crossed with LDLR$^{-/-}$ mice and the animals were fed a high-fat diet atherosclerotic lesion size was significantly greater in the crosses.[9]

LR11 (also designated sorLA) is a member of the LDL receptor family and is highly expressed in intimal SMC. When arteries were balloon-denuded in vivo macrophage filtration into the injury site was markedly reduced in LR11$^{-/-}$ mice.[87]

SM Cx43$^{-/-}$ mice lack smooth muscle cell connexin 43. This model was used in studies in which the animals were fed a high-fat diet and the carotid endothelium was injured using an occlusion or a wire. In the SM Cx43$^{-/-}$ mice there was accelerated growth of the neointima and of the adventitia indicating that smooth muscle Cx43 gap junctions play a multifaceted role in modulating the in vivo response to injury.[88] Aquaporin 7 (AQP7)$^{-/-}$ knockout mice have been used to demonstrate a linkage between adventitial inflammation and atherosclerotic lesions.[89]

Lipoclin-type prostaglandin D(2) synthase (L-PGDS)$^{-/-}$ mice are glucose intolerant and develop insulin resistance. They have larger adipocytes than C57BL/6 controls. When fed a diabetogenic high-fat diet for 20 weeks the L-PGDS$^{-/-}$ mice demonstrate renal pathology and thickening of the aorta similar to that seen in early atherosclerosis.[2]

Other Transgenic Mouse Models

When bone marrow cells from a lupus-prone strain of mice were transplanted into LDLR$^{-/-}$ mice the result was accelerated atherosclerotic plaque formation compared with LDLR$^{-/-}$ mice transplanted with bone marrow cells from WT mice.[90] Bone marrow cells from C57BL/6 mice overexpressing human ORP1L were transplanted into LDLR$^{-/-}$ mice and the animals were fed a high-fat diet. There was a more than twofold increase in atherosclerosis lesion size in these mice than in LDLR$^{-/-}$ animals that received bone marrow cells from WT littermates.[91]

Thiol oxidative stress has been implicated in the development of atherosclerosis. LDLR$^{-/-}$ mice received transplants of bone marrow cells infected with retroviral vectors expressing green fluorescent protein (GFP), GFP-fusion protein of cytosolic glutathione reductase (cyto-GR-GFP), or mitochondrial GR (mito-GR-GFP). Five weeks after bone marrow transplant the animals were fed a high-fat diet for 10 weeks. There were no differences in plasma cholesterol or triglyceride levels between the three groups but both cyto-GR and mito-GR mice had significantly less atherosclerotic lesion areas.[92]

Human paraoxonase 3 (PON3) is an HDL-associated protein that can prevent oxidation of LDL in vitro. ApoE$^{-/-}$ mice were injected with adenovirus expressing human PON3. Three weeks following the injections atherosclerotic lesion areas were significantly lower in transgenic PON3 mice than in apoE$^{-/-}$ controls.[93]

Transgenic mice expressing human apolipoprotein B (ApoB) were crossed with mice heterozygous for lipoprotein lipase (LPL1) and/or with transgenic mice expressing human cholesteryl ester transfer protein (CETP). The purpose was to generate a more human-like lipoprotein profile since wild-type mice have low ApoB levels and no CETP. These mice, designated HuB/LPL1/CETP, had decreased HDL and increased VLDL and IDL/LDL. When HuB/LPL1 mice were treated with STZ they became more diabetic, severely hyperlipidemic with higher triglyceride

levels as well as higher total cholesterol, VLDL, and IDL/LDL levels and had increased atherosclerotic deposition.[2]

Transgenic mice that express the lymphocytic choriomeningitis virus (LCMV) suffer an immune reaction that specifically destroys the glycoprotein (GP) expressing β-cells and results in rapid onset type 1 diabetes. When these animals are bred with $LDLR^{-/-}$ the offspring are atherosclerosis-prone with type 1 diabetes ($LDLR^{-/-}$:GP). They are hyperlipidemic; the atherosclerotic lesions have increased macrophage proliferation and the lesions have extensive hemorrhages.[2]

The nonobese diabetic mouse (NOD) demonstrates type 1 diabetes resulting from an autoimmune process culminating in spontaneous hyperglycemia results from the destruction of pancreatic β-cells. When fed a high-fat diet these animals did not develop aortic atherosclerotic lesions despite hyperlipidemia.[2]

Diabetogenic diets can induce type 2 diabetes in some strains of mice, but not all. C57BL/6 mice fed such a diet become obese, hyperglycemic, hyperinsulinemic, and insulin resistant, but A/J mice are resistant. A high-fat diet fed to C57BL/6, C3H/He, BALB/c, and seven recombinant inbred strains did not induce the same response in all strains but a diabetogenic diet enriched in fat and sucrose but lacking cholesterol and bile acids caused obesity, diabetes, and increased plasma lipoprotein concentrations in the C57BL/6 mice. Forty percent of these animals had small aortic fatty streaks not observed in control animals fed a standard diet.

Other Induced Models

A single peripheral injection of gold thioglycose (GTG) rapidly destroys leptin receptor-positive hypothalamic neurons including those that regulate energy expenditure and food intake. A certain percentage of $ApoE^{-/-}$ mice, but not all, respond to GTG injection by developing type 2 diabetes but these animals develop less atherosclerosis than $ApoE^{-/-}$ nonresponders who remain lean or saline-injected ad libitum fed $ApoE^{-/-}$ mice.

Mice fed a high-methionine diet develop high homocysteine (Hcy) plasma levels. Methionyl-tRNA synthetase preferentially selects Hcy rather than methionine during protein biosynthesis in the mouse, and this results in the formation of Hcy-thiolactone resulting in extremely high levels of plasma and urinary Hcy-thiolactone. High plasma Hcy-thiolactone levels initiate a pathological pathway that has been implicated in human vascular disease.[94]

Graft Vasculopathy

Graft vasculopathy is a robust form of atherosclerosis that develops rapidly in transplanted organs. Transgenic mice ubiquitously expressing LacZ (LacZ-mice) were transplanted with heterotopic hearts from wild-type mice. Four weeks after transplantation the allografts were stained with 5-bromo-4-chloro-3-indolyl-beta-D-galactopyranoside

(X-gal) to identify LacZ-expressing cells. Large epicardial arteries as well as their smaller branches and arterioles demonstrated hyperplastic growth of neointimal cells, most of which expressed LacZ. Transplanted hearts also had some medial SMC and endothelial cells replaced by LacZ-expressing recipient cells. The model seems to have great potential for studying graft vasculopathy.[95]

Hamsters

The Golden Syrian hamster is sensitive to high-fat/high-cholesterol diets. A significant portion of the plasma cholesterol is present in the LDL lipoprotein fraction in these animals, resembling humans rather than other rodents. When on an atherosclerotic diet the hamsters develop mild atherosclerosis made more severe when NO synthesis is inhibited. However, the aortic lesions are most commonly fatty streaks and they do not usually develop advanced intimal lesions, thrombosis, or myocardial infarcts. When pancreatic β cells are ablated using STZ the result is quasi type-1 diabetes with significant atherosclerosis and glomerular sclerosis in hamsters fed the high-fat/high-cholesterol diet. With time these animals will develop advanced aortic lesions.[20] Male Golden Syrian hamsters fed a diet containing 0.2% cholesterol and 20% butter developed high ratios of VLDL + IDL + LDL/HDL ratios and a plasma lipoprotein cholesterol profile associated with a high risk for atherosclerosis.[96]

Sand Rats

These animals, native to the deserts of the Middle East and North Africa, normally live off of a local plant, the salt bush. When fed an energy-rich diet such as laboratory chow it becomes obese, insulin-resistant, develops high VLDL levels and, eventually, type-2 diabetes. However, even when fed a high cholesterol diet they do not develop advanced atherosclerotic lesions, just fatty streaks. Females of the species develop vascular hyper-contractility and impaired endothelium-dependent relaxation during the insulin-resistant phase when fed high-energy diets and the effect is exacerbated when the animals become diabetic.[20]

References

1. Hsueh W, Abel ED, Breslow JL, et al. Recipes for creating animal models of diabetic cardiovascular disease. *Circ Res.* 2007;100:1415–1427.
2. Gonzalez-Navarro H, Burks DJ, Andres V. Murine models to investigate the influence of diabetic metabolism on the development of atherosclerosis and restenosis. *Front Biosci.* 2007;12:4439–4455.
3. Gross DR. Animal Models in Cardiovascular Research, 2nd Revised Edition. Boston: Kluwer Academic; 1994.

4. Fievet C, Fruchart JC, Staels B. Genetically-engineered animals as research models for atherosclerosis: Their use for the characterization of PPAR agonists in the treatment of cardio metabolic disorders. *Front Biosci.* 2007;12:4132–4156.
5. Lee RG, Willingham MC, Davis MA, Skinner KA, Rudel LL. Differential expression of ACAT1 and ACAT2 among cells within liver, intestine, kidney, and adrenal of nonhuman primates. *J Lipid Res.* 2000;41:1991–2001.
6. Lee RG, Shah R, Sawyer JK, Hamilton RL, Parks JS, Rudel LL. ACAT2 contributes cholesteryl esters to newly secreted VLDL, whereas LCAT adds cholesteryl ester to LDL in mice. *J Lipid Res.* 2005;46:1205–1212.
7. Temel RE, Hou L, Rudel LL, Shelness GS. ACAT2 stimulates cholesteryl ester secretion in apoB-containing lipoproteins. *J Lipid Res.* 2007;48:1618–1627.
8. Lada AT, Rudel LL. Associations of low density lipoprotein particle composition with atherogenicity. *Curr Opin Lipidol.* 2004;15:19–24.
9. Preiss DJ, Sattar N. Vascular cell adhesion molecule-1: A viable therapeutic target for atherosclerosis? *Int J Clin Pract.* 2007;61:697–701.
10. Rekhter MD. How to evaluate plaque vulnerability in animal models of atherosclerosis? *Cardiovasc Res.* 2002;54:36–41.
11. Schapira K, Heeneman S, Daemen MJ. Animal models to study plaque vulnerability. *Curr Pharm Des.* 2007;13:1013–1020.
12. Nichols TC, Busby WH, Jr, Merricks E, et al. Protease resistant IGFBP-4 inhibits IGF-I actions and neointimal expansion in a porcine model of neointimal hyperplasia. *Endocrinology.* 2007;148:5002–5010.
13. Ludwig A, Weber C. Transmembrane chemokines: Versatile 'special agents' in vascular inflammation. *Thromb Haemost.* 2007;97:694–703.
14. Braunersreuther V, Mach F, Steffens S. The specific role of chemokines in atherosclerosis. *Thromb Haemost.* 2007;97:714–721.
15. Taleb S, Clement K. Emerging role of cathepsin S in obesity and its associated diseases. *Clin Chem Lab Med.* 2007;45:328–332.
16. Langheinrich AC, Kampschulte M, Buch T, Bohle RM. Vasa vasorum and atherosclerosis - Quid novi? *Thromb Haemost.* 2007;97:873–879.
17. Li CJ, Sun HW, Zhu FL, et al. Local adiponectin treatment reduces atherosclerotic plaque size in rabbits. *J Endocrinol.* 2007;193:137–145.
18. Yasa M, Kerry Z, Reel B, Anacak GY, Ertuna E, Ozer A. The effects of calcium channel blockers are not related to their chemical structure in the collar model of the rabbit. *J Int Med Res.* 2007;35:59–71.
19. Gross DR. Unpublished data.
20. Russell JC, Proctor SD. Small animal models of cardiovascular disease: Tools for the study of the roles of metabolic syndrome, dyslipidemia, and atherosclerosis. *Cardiovasc Pathol.* 2006;15:318–330.
21. Bansal N, Majumdar S, Chakravarti RN. Frequency and size of atherosclerotic plaques in vasectomized diabetic monkeys. *Int J Fertil.* 1986;31:298–304.
22. Thomas MJ, Chen Q, Sorci-Thomas MG, Rudel LL. Isoprostane levels in lipids extracted from atherosclerotic arteries of nonhuman primates. *Free Radic Biol Med.* 2001;30:1337–1346.
23. Huggins KW, Colvin PL, Burleson ER, et al. Dietary n-3 polyunsaturated fat increases the fractional catabolic rate of medium-sized HDL particles in African green monkeys. *J Lipid Res.* 2001;42:1457–1466.
24. Kavanagh K, Jones KL, Sawyer J, et al. Trans fat diet induces abdominal obesity and changes in insulin sensitivity in monkeys. *Obesity (Silver Spring).* 2007;15:1675–1684.
25. Wallace JM, Schwarz M, Coward P, et al. Effects of peroxisome proliferator-activated receptor alpha/delta agonists on HDL-cholesterol in vervet monkeys. *J Lipid Res.* 2005;46:1009–1016.
26. Fusegawa Y, Kelley KL, Sawyer JK, Shah RN, Rudel LL. Influence of dietary fatty acid composition on the relationship between CETP activity and plasma lipoproteins in monkeys. *J Lipid Res.* 2001;42:1849–1857.
27. Edwards IJ, Rudel LL, Terry JG, et al. Caloric restriction lowers plasma lipoprotein (a) in male but not female rhesus monkeys. *Exp Gerontol.* 2001;36:1413–1418.

28. Rudel LL, Davis M, Sawyer J, Shah R, Wallace J. Primates highly responsive to dietary cholesterol up-regulate hepatic ACAT2, and less responsive primates do not. *J Biol Chem.* 2002;277:31401–31406.
29. van Oort G, Gross DR, Spiekerman AM. Effects of eight weeks of physical conditioning on atherosclerotic plaque in swine. *Am J Vet Res.* 1987;48:51–55.
30. Burattini R, Montanari L, Mulligan LJ, Cannon MS, Gross DR. Evaluation of hypercholesterol diet-induced changes in viscoelastic properties of carotid circulation in pigs. *Am J Physiol.* 1992;263:H1919–H1926.
31. Ribichini F, Joner M, Ferrero V, et al. Effects of oral prednisone after stenting in a rabbit model of established atherosclerosis. *J Am Coll Cardiol.* 2007;50:176–185.
32. Roy H, Bhardwaj S, Babu M, et al. VEGF-A, VEGF-D, VEGF receptor-1, VEGF receptor-2, NF-kappaB, and RAGE in atherosclerotic lesions of diabetic watanabe heritable hyperlipidemic rabbits. *FASEB J.* 2006;20:2159–2161.
33. Lee KT, Janakidevi K, Thomas WA. Study of monotypism in atherosclerotic lesions from glucose-6-phosphate dehydrogenase (G-6-PD) heterozygotes. *Artery.* 1980;8:581–586.
34. Lee KT, Thomas WA, Janakidevi K, Kroms M, Reiner JM, Borg KY. Mosaicism in female hybrid hares heterozygous for glucose-6-phosphate dehydrogenase (G-6-PD). I. General properties of a hybrid hare model with special reference to atherogenesis. *Exp Mol Pathol.* 1981;34:191–201.
35. Pearson TA, Dillman J, Malmros H, Sternby N, Heptinstall RH. Cholesterol-induced atherosclerosis. Clonal characteristics of arterial lesions in the hybrid hare. *Arteriosclerosis.* 1983;3:574–580.
36. Shimoda T, Ishihata A, Aita T, et al. Progression of severe atherosclerosis and increased arterial pulse pressure in the newly developed heritable mixed hyperlipidaemic rabbits. *Clin Exp Pharmacol Physiol.* 2006;33:221–226.
37. Schwenke DC, Rudel LL, Sorci-Thomas MG, Thomas MJ. Alpha-tocopherol protects against diet induced atherosclerosis in New Zealand white rabbits. *J Lipid Res.* 2002;43:1927–1938.
38. Kritchevsky D. Antimutagenic and some other effects of conjugated linoleic acid. *Br J Nutr.* 2000;83:459–465.
39. Saravanan R, Pari L. Effect of a novel insulinotropic agent, succinic acid monoethyl ester, on lipids and lipoproteins levels in rats with streptozotocin-nicotinamide-induced type 2 diabetes. *J Biosci.* 2006;31:581–587.
40. Koletsky S. Obese spontaneously hypertensive rats - A model for study of atherosclerosis. *Exp Mol Pathol.* 1973;19:53–60.
41. Pederson RA, Campos RV, Buchan AM, Chisholm CB, Russell JC, Brown JC. Comparison of the enteroinsular axis in two strains of obese rat, the fatty zucker and the JCR:LA-corpulent. *Int J Obes.* 1991;15:461–470.
42. Russell JC, Amy RM, Dolphin PJ. Effect of dietary n-3 fatty acids on atherosclerosis prone JCR:LA-corpulent rats. *Exp Mol Pathol.* 1991;55:285–293.
43. Netherton SJ, Jimmo SL, Palmer D, et al. Altered phosphodiesterase 3-mediated cAMP hydrolysis contributes to a hypermotile phenotype in obese JCR:LA-cp rat aortic vascular smooth muscle cells: Implications for diabetes-associated cardiovascular disease. *Diabetes.* 2002;51:1194–1200.
44. Russell JC, Amy RM. Early atherosclerotic lesions in a susceptible rat model: The LA/N-corpulent rat. *Atherosclerosis.* 1986;60:119–129.
45. Russell JC, Kelly SE, Schafer S. Vasopeptidase inhibition improves insulin sensitivity and endothelial function in the JCR:LA-cp rat. *J Cardiovasc Pharmacol.* 2004;44:258–265.
46. Dolphin PJ, Stewart B, Amy RM, Russell JC. Serum lipids and lipoproteins in the atherosclerosis prone LA/N corpulent rat. *Biochim Biophys Acta.* 1987;919:140–148.
47. Tang F, Wu X, Wang T, et al. Tanshinone II A attenuates atherosclerotic calcification in rat model by inhibition of oxidative stress. *Vascul Pharmacol.* 2007;46:427–438.
48. Hosogai N, Fukuhara A, Oshima K, et al. Adipose tissue hypoxia in obesity and its impact on adipocytokine dysregulation. *Diabetes.* 2007;56:901–911.
49. Arbones-Mainar JM, Navarro MA, Guzman MA, et al. Selective effect of conjugated linoleic acid isomers on atherosclerotic lesion development in apolipoprotein E knockout mice. *Atherosclerosis.* 2006;189:318–327.

50. Johnson J, Carson K, Williams H, et al. Plaque rupture after short periods of fat feeding in the apolipoprotein E-knockout mouse: Model characterization and effects of pravastatin treatment. *Circulation.* 2005;111:1422–1430.
51. Bro S, Binder CJ, Witztum JL, Olgaard K, Nielsen LB. Inhibition of the renin-angiotensin system abolishes the proatherogenic effect of uremia in apolipoprotein E-deficient mice. *Arterioscler Thromb Vasc Biol.* 2007;27:1080–1086.
52. Haghighat A, Weiss D, Whalin MK, Cowan DP, Taylor WR. Granulocyte colony-stimulating factor and granulocyte macrophage colony-stimulating factor exacerbate atherosclerosis in apolipoprotein E-deficient mice. *Circulation.* 2007;115:2049–2054.
53. Thorngate FE, Rudel LL, Walzem RL, Williams DL. Low levels of extrahepatic nonmacrophage ApoE inhibit atherosclerosis without correcting hypercholesterolemia in ApoE-deficient mice. *Arterioscler Thromb Vasc Biol.* 2000;20:1939–1945.
54. Sugita M, Sugita H, Kaneki M. Farnesyltransferase inhibitor, manumycin A, prevents atherosclerosis development and reduces oxidative stress in apolipoprotein E-deficient mice. *Arterioscler Thromb Vasc Biol.* 2007;27:1390–1395.
55. Monetti M, Canavesi M, Camera M, et al. Rosuvastatin displays anti-atherothrombotic and anti-inflammatory properties in apoE-deficient mice. *Pharmacol Res.* 2007;55:441–449.
56. George J, Afek A, Keren P, et al. Functional inhibition of ras by S-trans,trans-farnesyl thiosalicylic acid attenuates atherosclerosis in apolipoprotein E knockout mice. *Circulation.* 2002;105:2416–2422.
57. Johnson JL, Baker AH, Oka K, et al. Suppression of atherosclerotic plaque progression and instability by tissue inhibitor of metalloproteinase-2: Involvement of macrophage migration and apoptosis. *Circulation.* 2006;113:2435–2444.
58. Johnson JL, Fritsche-Danielson R, Behrendt M, et al. Effect of broad-spectrum matrix metalloproteinase inhibition on atherosclerotic plaque stability. *Cardiovasc Res.* 2006;71:586–595.
59. Johnson JL, Jackson CL. Atherosclerotic plaque rupture in the apolipoprotein E knockout mouse. *Atherosclerosis.* 2001;154:399–406.
60. Williams H, Johnson JL, Carson KG, Jackson CL. Characteristics of intact and ruptured atherosclerotic plaques in brachiocephalic arteries of apolipoprotein E knockout mice. *Arterioscler Thromb Vasc Biol.* 2002;22:788–792.
61. Langheinrich AC, Michniewicz A, Sedding DG, et al. Quantitative X-ray imaging of intraplaque hemorrhage in aortas of apoE(-/-)/LDL(-/-) double knockout mice. *Invest Radiol.* 2007;42:263–273.
62. Fukao H, Ijiri Y, Miura M, et al. Effect of trans-resveratrol on the thrombogenicity and atherogenicity in apolipoprotein E-deficient and low-density lipoprotein receptor-deficient mice. *Blood Coagul Fibrinolysis.* 2004;15:441–446.
63. Zadelaar S, Kleemann R, Verschuren L, et al. Mouse models for atherosclerosis and pharmaceutical modifiers. *Arterioscler Thromb Vasc Biol.* 2007;27:1706–1721.
64. Shen X, Bornfeldt KE. Mouse models for studies of cardiovascular complications of type 1 diabetes. *Ann N Y Acad Sci.* 2007;1103:202–217.
65. Willner EL, Tow B, Buhman KK, et al. Deficiency of acyl CoA:Cholesterol acyltransferase 2 prevents atherosclerosis in apolipoprotein E-deficient mice. *Proc Natl Acad Sci USA.* 2003;100:1262–1267.
66. Temel RE, Lee RG, Kelley KL, et al. Intestinal cholesterol absorption is substantially reduced in mice deficient in both ABCA1 and ACAT2. *J Lipid Res.* 2005;46:2423–2431.
67. Rudel LL, Lee RG, Parini P. ACAT2 is a target for treatment of coronary heart disease associated with hypercholesterolemia. *Arterioscler Thromb Vasc Biol.* 2005;25:1112–1118.
68. Woollard KJ, Chin-Dusting J. Therapeutic targeting of P-selectin in atherosclerosis. *Inflamm Allergy Drug Targets.* 2007;6:69–74.
69. Thorngate FE, Yancey PG, Kellner-Weibel G, Rudel LL, Rothblat GH, Williams DL. Testing the role of apoA-I, HDL, and cholesterol efflux in the atheroprotective action of low-level apoE expression. *J Lipid Res.* 2003;44:2331–2338.
70. Harrington SC, Simari RD, Conover CA. Genetic deletion of pregnancy-associated plasma protein-A is associated with resistance to atherosclerotic lesion development in apolipoprotein E-deficient mice challenged with a high-fat diet. *Circ Res.* 2007;100:1696–1702.

71. Lewis P, Stefanovic N, Pete J, et al. Lack of the antioxidant enzyme glutathione peroxidase-1 accelerates atherosclerosis in diabetic apolipoprotein E-deficient mice. *Circulation.* 2007;115:2178–2187.
72. Matsui R, Xu S, Maitland KA, et al. Glucose-6-phosphate dehydrogenase deficiency decreases vascular superoxide and atherosclerotic lesions in apolipoprotein E(–/–) mice. *Arterioscler Thromb Vasc Biol.* 2006;26:910–916.
73. Guo GL, Santamarina-Fojo S, Akiyama TE, et al. Effects of FXR in foam-cell formation and atherosclerosis development. *Biochim Biophys Acta.* 2006;1761:1401–1409.
74. Zhang L, Peppel K, Sivashanmugam P, et al. Expression of tumor necrosis factor receptor-1 in arterial wall cells promotes atherosclerosis. *Arterioscler Thromb Vasc Biol.* 2007;27:1087–1094.
75. Proctor BM, Ren J, Chen Z, et al. Grb2 is required for atherosclerotic lesion formation. *Arterioscler Thromb Vasc Biol.* 2007;27:1361–1367.
76. Takaya T, Hirata K, Yamashita T, et al. A specific role for eNOS-derived reactive oxygen species in atherosclerosis progression. *Arterioscler Thromb Vasc Biol.* 2007;27:1632–1637.
77. Petrovan RJ, Kaplan CD, Reisfeld RA, Curtiss LK. DNA vaccination against VEGF receptor 2 reduces atherosclerosis in LDL receptor-deficient mice. *Arterioscler Thromb Vasc Biol.* 2007;27:1095–1100.
78. Powell-Braxton L, Veniant M, Latvala RD, et al. A mouse model of human familial hypercholesterolemia: Markedly elevated low density lipoprotein cholesterol levels and severe atherosclerosis on a low-fat chow diet. *Nat Med.* 1998;4:934–938.
79. Cyrus T, Yao Y, Ding T, Dogne JM, Pratico D. A novel thromboxane receptor antagonist and synthase inhibitor, BM-573, reduces development and progression of atherosclerosis in LDL receptor deficient mice. *Eur J Pharmacol.* 2007;561:105–111.
80. Kanter JE, Johansson F, LeBoeuf RC, Bornfeldt KE. Do glucose and lipids exert independent effects on atherosclerotic lesion initiation or progression to advanced plaques? *Circ Res.* 2007;100:769–781.
81. Bell TA, III, Brown JM, Graham MJ, Lemonidis KM, Crooke RM, Rudel LL. Liver-specific inhibition of acyl-coenzyme A: Cholesterol acyltransferase 2 with antisense oligonucleotides limits atherosclerosis development in apolipoprotein B100-only low-density lipoprotein receptor–/– mice. *Arterioscler Thromb Vasc Biol.* 2006;26:1814–1820.
82. Joven J, Rull A, Ferre N, et al. The results in rodent models of atherosclerosis are not interchangeable: The influence of diet and strain. *Atherosclerosis.* 2007;195:e85–e92.
83. VanderLaan PA, Reardon CA, Sagiv Y, et al. Characterization of the natural killer T-cell response in an adoptive transfer model of atherosclerosis. *Am J Pathol.* 2007;170:1100–1107.
84. Dutta R, Singh U, Li TB, Fornage M, Teng BB. Hepatic gene expression profiling reveals perturbed calcium signaling in a mouse model lacking both LDL receptor and Apobec1 genes. *Atherosclerosis.* 2003;169:51–62.
85. Mehta JL, Sanada N, Hu CP, et al. Deletion of LOX-1 reduces atherogenesis in LDLR knockout mice fed high cholesterol diet. *Circ Res.* 2007;100:1634–1642.
86. Fay WP, Garg N, Sunkar M. Vascular functions of the plasminogen activation system. *Arterioscler Thromb Vasc Biol.* 2007;27:1231–1237.
87. Ohwaki K, Bujo H, Jiang M, Yamazaki H, Schneider WJ, Saito Y. A secreted soluble form of LR11, specifically expressed in intimal smooth muscle cells, accelerates formation of lipid-laden macrophages. *Arterioscler Thromb Vasc Biol.* 2007;27:1050–1056.
88. Liao Y, Regan CP, Manabe I, et al. Smooth muscle-targeted knockout of connexin43 enhances neointimal formation in response to vascular injury. *Arterioscler Thromb Vasc Biol.* 2007;27:1037–1042.
89. He ZQ, Liang C, Wang H, Wu ZG. Dysfunction of AQP7 in the periadventitial fat: A novel trigger of atherosclerosis. *Med Hypotheses.* 2008;70:92–95.
90. Gautier EL, Huby T, Ouzilleau B, et al. Enhanced immune system activation and arterial inflammation accelerates atherosclerosis in lupus-prone mice. *Arterioscler Thromb Vasc Biol.* 2007;27:1625–1631.
91. Yan D, Jauhiainen M, Hildebrand RB, et al. Expression of human OSBP-related protein 1L in macrophages enhances atherosclerotic lesion development in LDL receptor-deficient mice. *Arterioscler Thromb Vasc Biol.* 2007;27:1618–1624.

92. Qiao M, Kisgati M, Cholewa JM, et al. Increased expression of glutathione reductase in macrophages decreases atherosclerotic lesion formation in low-density lipoprotein receptor-deficient mice. *Arterioscler Thromb Vasc Biol.* 2007;27:1375–1382.
93. Ng CJ, Bourquard N, Hama SY, et al. Adenovirus-mediated expression of human paraoxonase 3 protects against the progression of atherosclerosis in apolipoprotein E-deficient mice. *Arterioscler Thromb Vasc Biol.* 2007;27:1368–1374.
94. Chwatko G, Boers GH, Strauss KA, Shih DM, Jakubowski H. Mutations in methylenetetrahydrofolate reductase or cystathionine beta-synthase gene, or a high-methionine diet, increase homocysteine thiolactone levels in humans and mice. *FASEB J.* 2007;21:1707–1713.
95. Iwata H, Sata M. Potential contribution of bone marrow-derived precursors to vascular repair and lesion formation: Lessons from animal models of vascular diseases. *Front Biosci.* 2007;12:4157–4167.
96. Lock AL, Horne CA, Bauman DE, Salter AM. Butter naturally enriched in conjugated linoleic acid and vaccenic acid alters tissue fatty acids and improves the plasma lipoprotein profile in cholesterol-fed hamsters. *J Nutr.* 2005;135:1934–1939.

Chapter 13
Animal Models for the Study of Neurohumeral and Central Neural Control of the Cardiovascular System

Studies investigating the integrative central control of the locomotor and cardiovascular system have mostly been conducted in rats. These studies have shown that control of cardiovascular responses is located in neurons in close proximity, if not overlapping or possibly identical to, neurons responsible for respiratory and locomotor control. In rats cardiorespiratory and locomotor centers have been identified in the periaqueductal gray (PAG), posterior hypothalamic area (PHA), nucleus tractus solitarius (NTS), rostral ventrolateral medulla (rVLM), and the cuneiform nucleus (CnF). Of these, the PH has been clearly identified as both a locomotor and cardiovascular center.[1]

The CnF, with the pedunculopontine nucleus, has been identified as the mesencephalic locomotor center.[2,3] The spinal cord and the lateral tegmental field (LTF) have been identified as integration sites for cardiorespiratory and locomotor responses.[4] Interestingly, exercise training induced attenuation of dendritic fields of neurons in the exercising rat model.[1]

Rats that spontaneously trained on running wheels for 80–100 days were compared to sedentary rats. A single test bout of exercise resulted in significantly less activation in the exercised trained group, as indicated by Fos labeling, in both colliculi of the midbrain, the PH, PAG, NTS, rVLM, the parabrachial nucleus (PBN), and the CnF.[5, 6] Seventy days of exercise training in rats resulted in dendritic attenuation in the PH, PAG, CnF, and NTS. These changes were completely reversed after 50 days of rest.[7]

Other cardiorespiratory centers identified in male Sprague-Dawley rats include the caudal ventrolateral medulla (cVLM) and the hypothalamic paraventricular nucleus (HVN). These areas, along with the NTS, comprise noradrenergic neurons that initiate and modulate hypothalamic-pituitary-adrenal axis responses to a wide variety of stressors via noradrenergic projections from the hindbrain to the hypothalamus.[8] The medial paralemniscal nucleus (MPL) in rats receives afferent neuronal connections from a large number of CNS locations including the RVLM, CVLM, PAG, and CnF. This suggests a possible role in cardiovascular control for the MPL.[9] Stimulation of the insular cortex (IC) in primates and rats elicits cardiovascular responses. In the rat the cardiovascular region is located caudally in the IC while in primates it is located in the anterior region. The IC projects to the lateral hypothalamus (LH), caudal nucleus of the NTS, the PBN, and the medullary reticular formation

D.R. Gross, *Animal Models in Cardiovascular Research*,
DOI: 10.1007/978-0-387-95962-7_13, © Springer Science+Business Media, LLC 2009

region (MRFR) through the amygdala. Cardiovascular responses of this system, via the autonomic nervous system, are clearly modulated by muscular contraction.[10]

The cat has proven to be a valuable experimental model for the study of reflex responses to exercise. Because the ventral roots in cats are easily dissected and stimulated the preparation provides a controlled stimulus of muscular contraction. This contraction simulates the reflex effects of exercise as evoked from Group III (small myelinated) and Group IV (unmyelinated) muscle afferents. The relatively large size also facilitates close arterial injections of substances that can influence the function of these afferent fibers, and this ability has resulted in the elucidation of the chemical nature of the metabolites. The basic findings are that, generally, Group III afferents respond to mechanical events while Group IV afferents respond to a host of chemical stimuli. Using tracer studies these signals have been shown to affect many of the central nuclei previously identified.[4]

Electrical stimulation of the posterior hypothalamic locomotor region (PHLR) in decorticated cats elicited increases in glucose production, plasma glucose levels, plasma epinephrine and norepinephrine levels, heart rate, and blood pressure. In intact anesthetized cats stimulation of the PHLR caused increases in glucose production, plasma glucose, blood pressure, and heart rate but catecholamine and insulin plasma concentrations were not changed.[11]

Activation of caudal vestibular nucleus (CVN) neurons can induce a pressor response. Projections from the CVN to the RVLM, via the NTS, comprise an indirect vestibulo-cardiovascular pathway in the brain stem.[12] Activation of the CnF, located in the midbrain, produces hypertension.[13] The stria terminalis is a band of fibers running along the lateral margin of the ventricular surface of the thalamus. It is a major output pathway of the amygdala. The bed nucleus of the stria terminalis (BST) plays a prominent role in the integration of acute and chronic stress responses, including those affecting the cardiovascular system in male Sprague-Dawley rats.[14] Selective activation of the ponto-medullary nucleus reticularis gigantocellularis (PMNGC) in anesthetized cats can depress both respiratory and cardiovascular activity.[15] Electrical stimulation of the inferior olivary nucleus (ION) or unilateral microinjections of kainic acid, D-L-homocysteic acid, or glutamate into this structure increases arterial pressure but does not modulate the baroreceptor reflex in anesthetized cats.[16]

In male Sprague-Dawley rats a decrease in melatonin and an increase in melatonin type-2 (MT-2) receptors in the anterior hypothalamic area (AHA) are involved in stress-induced hypertension.[17] The locus coeruleus (LC), a nucleus in the brain stem, is also involved with physiological responses, such as hypertension, to stress and panic.[18] The dorsomedial hypothalamus (DMH) integrates physiological responses to psychological stressors. The cardiovascular components of these responses include hypertension, tachycardia, and increased sympathetic nerve stimulation to the kidneys, skin, and brown adipose tissue.[19]

So far we have listed at least 20 different areas of the brain that are purported to exert some sort of control over cardiovascular function. There is also recent evidence that at least 29 genes, including transcription factor, growth factors, and membrane receptors, are upregulated in the suprachiasmatic nucleus (SCN), and peripheral tissues by clock genes and thus demonstrate circadian oscillation.[20]

We also know that the brain plays a significant role in regulating the osmolality of body fluids. Recently the transient receptor potential vanilloid (TRPV) family of cation channels has been identified as osmo-mechanoreceptors that mediate the neuronal responses to changes in tonicity.[21]

The Autonomic Nervous System in Blood Pressure Homeostasis and Cardiorespiratory Reflex Responses

The rat rVLM was first shown to be the principal direct sympatho-excitatory pathway from the brainstem to the intermediolateral cell column (IML). It has been shown to be responsible for a loss of sympatho-excitatory function including the maintenance of resting blood pressure and the sympathetic portion of the baroreflex.[4]

The parapyramidal region (PPR) is also an important medullary control region for sympathetic excitation in chloralose-anesthetized cats. This area also has direct projections to the IML and is thought to be important for the maintenance of blood pressure.[22]

Afferent fibers from the canine carotid sinus, and their presumptive terminals, were found bilaterally in the caudal NTS, the PH, and the LTF, reaching the area of the nucleus ambiguus. There was also sparse labeling in the ipsilateral spinal trigeminal nucleus (SPV) and lateral Cu. These results suggest that there are multiple pathways by which peripheral baroreceptor inputs can influence central neurons influencing cardiovascular responses. Although the relays in the NTS are classically described carotid sinus afferents may also directly affect neurons in other brain stem areas.[23] The LTF, in addition to its function as a pressor response region, has a major role in sympathetic nerve discharge rhythmicity in chloralose-urethane-anesthetized cats. This area of the brain may help synchronize sympathetic nerve discharge during muscular contractions but its contribution to basal rhythms may not be required for the pressor responses observed during hindlimb muscular contractions or hypothalamic stimulation. It is also identifiable with the ponto medullary locomotor "strip" and may thus be an integrative cardiorespiratory and locomotor site.[24]

In anesthetized rats brain pathways involved in the baroreceptor reflex were identified in the NTS, the primary termination of baroreceptor afferents. The RVLM, the lateral PBN, the PVN, the supraoptic nucleus (SON), and the central amygdaloid nucleus (CEA) all receive either direct or indirect inputs from the NTS.[25]

Cardiopulmonary chemoreceptor-activated vagal reflexes (the von Bezold-Jarisch reflex) and predominantly cardiac high-pressure mechanoreceptor-activated vagal reflexes (ramp baroreflex) were impaired in conscious, previously instrumented, 24-month-old rats when compared with 6-month-old rats. The deficit was ameliorated by atrial natriuretic peptide infusion or chronic neutral endopeptidase inhibition.[26] Rho-kinase is activated in the brainstem 10 days following coronary artery occlusion in mice. The increase in brainstem Rho-kinase enhances sympathetic drive contributing to hypertension.[27]

In 1K,1C rabbits with renovascular hypertension central inhibition of the sympathetic nervous system (rilmenidine) reverses left ventricular hypertrophy and problems

associated with the loss of left ventricular compliance without affecting inotropy.[28] Feeding a high-salt diet to SHR and WKY rats enhances sympathetic nervous activity significantly. Reflex inhibition of renal sympathetic nerve activity by stimulation of the aortic depressor nerve was augmented in WKY and attenuated in SHR suggesting that differential modulation of the CNS involved in the baroreflex control of sympathetic activity may account for the differences in baroreflex response between SHR and their normal controls.[29]

Reflex cardio-inhibitory responses were evaluated in chloralose-urethane-anesthetized cats following stimulation of the carotid body chemoreceptors by intracarotid injections of cyanide. The arterial baroreflex was perturbed by controlled elevations of blood pressure. Cardiac receptors were stimulated by left atrial injections of veratridine. Pulmonary C fibers and J receptors were stimulated by injections of phenylbiguanide into the right atrium. The effects of central inspiratory neuronal activity on pulse interval were assessed by comparing the values observed during the inspiratory and expiratory phases of the respiratory cycle in the control state and during stimulation of four cardiovascular receptor groups. Carotid chemoreceptor-induced bradycardia during expiration was reduced during inspiration. Central inspiratory drive was less effective in altering the reflex responses from the arterial baroreceptors and cardiac receptors. Bradycardia evoked by pulmonary C fiber stimulation was not affected by the central inspiratory drive. This differential modulation by central inspiratory drive was independent of the integrity of the sympathetic nerve supply to the heart indicating parasympathetic involvement in these reflexes.[30]

Aged (22-month old) rats with stress-hypertension demonstrate sustained increases in central sympathetic outflow to ganglia. This provides the repeated high-frequency presynaptic activity required for induction of long-term potentiation of sympathetic ganglia.[31] The carotid body chemoreflex is enhanced in animal models of congestive heart failure. This contributes to the observed tonic elevation in sympathetic nerve activity. Adaptive changes occur in both the afferent and central nervous system pathways of the reflex arc. Multiple adaptive mechanisms involving Angio-II and NO, in both the carotid body and the central nervous system, are probably redundant but enhance carotid body chemoreflexes during congestive heart failure.[32]

Dissecting and transecting the aortic depressor nerve and cervical sympathetic nerves and then stripping the carotid arteries of all connective tissue result in a "neurogenic" model of hypertension. This selective aortic baroreceptor deafferentation produces a persistent hypertension with increased neurogenic renal vasoconstrictor activity. No pressure diuresis or natriuresis is observed during the first week after these procedures are completed.[33]

Rostal and Caudal Ventrolateral Medulla

As previously described the rVLM is the primary excitatory brainstem pathway of the sympathetic nervous system. It sends excitatory fibers to the sympathetic, preganglionic neurons in the spinal cord. Neurons in the RVLM receive afferent

information from baroreceptors and other sources.[34] The rVLM receives GABAergic receptors from the cVLM. Thus, the rVLM and cVLM neurons demonstrate both excitatory and inhibitory responses to stimulation by sympathetic afferents. They mediate multiphase reflex responses of the sympathetic nerve by regulating the activity of sympathetic preganglionic neurons.[35]

Early work indicated that chemical stimulation of the dorsal VLM evoked both pressor and depressor responses. The pressor sites are located caudal to the depressor sites in cats.[36] More recently it has been shown that direct stimulation of the rVLM increases arterial blood pressure and sympathetic nerve activity while the same perturbation of the cVLM has the opposite effect. A significant proportion of sympathetic tonic activity arising from the rVLM is actually driven by neurons in another portion of the VLM, the caudal pressor area, located at the extreme caudal part of the VLM.[37] Local injection of L-glutamate into the caudal pressor area of chloralose-anesthetized male SHR resulted in a greater pressor response than in control WKY.[38] Neurons in the VLM also respond to muscular contractions and most likely have a role in the pressor reflex associated with exercise.[39]

The rVLM premotor neurons release several neurotransmitters including glutamate, various amines, and neuropeptides. The latter two classes act on metabotropic receptors with long-term effects on cell function. γ-Aminobutyric acid (GABA) provides the inhibitory effects counteracting glutamate-induced stimulatory effects.[40, 41] There are also indirect excitatory pathways from two areas of the vestibular nucleus, the medial vestibular nucleus (MVe), and the spinal vestibular nucleus (SpVe). These connect via the NTS and PBN to the RVLM. In the NTS and PBN pathways *N*-methyl-D-aspartate (NMDA) receptors are implicated in the responses of the MVe. Glutamate-stimulated responses seem to be responsible elsewhere in the system.[12] Cold pressor test-induced increases in sympathetic outflow in rats are mediated by activation of ionotropic glutamate receptors in the RVLM and spinal cord. Activation of GABA receptors, i.e., inhibitory withdrawal, in the nucleus ambiguus also contributes to the sympathetic outflow increase observed as a result of the cold pressure test.[42] The injection of Neuropeptide Y (NPY) into the RVLM exerts excitatory effects on sympathetic tone but inhibits responses to muscular stimulation. This result is probably due to differential expression of NPY receptor subtypes in the RVLM.[43]

Angiotensin-II (Angio-II), acting on angiotensin type-1 receptors (ATR-1), in the RVLM of rats plays a role in the development of hypertension. This occurs as a result of Angio-II activating NADPH oxidase-producing reactive oxygen species (ROS).[44] In rabbits the intracerebroventricular (i.v.c.) infusion of Angio-II induces ATR-1 upregulation by the induction of oxidant stress and activation of activator protein-1.[45] Microinjection of ANG-1-7 and Angio-II into the CVLM produces a differential modulation of the baroreflex control of heart rate. Injections into the RVLM produce increases in pressor effects but no change in heart rate.[46] Feeding high-salt diets to male Sprague-Dawley rats enhances the sympathoexcitatory actions of Angio-II in the RVLM by changing the intrinsic properties of the RVLM neurons.[47] ATR-1 in the RVLM play an important role in modulating cardiovascular function during static exercise in anesthetized rats.[48] Rats with chronic heart failure

demonstrate upregulation of ATR-1 in the RVLM and a downregulation of ATR-2. These changes combine to increase sympathetic outflow in this model.[49] Overexpression of ATR-2 in the RVLM of conscious rats decreases nocturnal arterial blood pressures, increases 24-h urine excretion, and decreases 24-h urine excretion and concentration of norepinephrine.[50]

Tyrosine hydroxylase (TH) is a key enzyme for catecholamine and angiotensinogen synthesis in the VLM.[18] Pituitary adenylate cyclase-activating polypeptide (PACAP) was found in 84% of TH-immunoreactive (TH-ir) neurons in the RVLM. Intrathecal infusion of PACAP in rats results in a prolonged excitation of the sympathetic nervous system.[51]

The DMH is an essential location for the integration of physiological responses to a wide variety of psychological stressors, including panic. The cardiovascular components of these responses include hypertension, tachycardia, and increased sympathetic outflow to the kidneys, skin, and brown adipose tissue. Neurons in the RVLM, and in the region of the medullary raphe, are important components of the descending pathways that control cardiovascular responses following activation of the DMH. Activation of 5-hydroxytryptamine-1A [5-HT(1A)] receptors in the brain suppresses the cardiac and sympathetic vasomotor components of the DMH-evoked response from the lower brainstem but not from the rVLM.[19] However, serotonergic inputs into the VLM play an important role in the expression of the 10-Hz rhythmic component of basal inferior cardiac sympathetic nerve discharge in urethane-anesthetized, baroreceptor-denervated cats.[52]

Both nitric oxide synthase (NOS) and nitric oxide (NO) are widely distributed in the RVLM and contribute to regulation of the cardiovascular system. nNOS and iNOS apparently have opposite effects on rVLM modulation of sympathetic outflow in rats.[53]NO signaling in the rVLM is cGMP-dependent and this pathway is impaired with hypertension in rats.[54] Overproduction of NO by gene transduction of eNOS in the rVLM of SHR results in a temporary reduction of arterial pressure followed by a rebound hypertension. The mechanism for this is an interactive action between NO and ROS on mitochondrial respiratory enzyme complex-1 in the rVLM.[55] Attenuation of cardiovascular responses during muscle contraction in rats subjected to transitory occlusion of the middle cerebral artery (stroke model) may be partly due to a reduction in eNOS expression in the ipsilateral rVLM and an overexpression of eNOS in the ipsilateral cVLM.[56]

Nicotinic acetylcholine (ACh) receptors (nAChRs) mediate numerous visceral functions via medullary catecholamines (CA) found in the VLM, NTS, and dorsal motor nucleus of the vagus (DMV). All CA neurons expressed β-2 mRNA but α-2 mRNA was absent. α-6 and β-3 mRNA expression was more or less restricted to the VLM, and α-4, α-5, and α-7 mRNA expression was greater in the rVLM than in the cVLM. These variations in nAChR subunit mRNA expression in rats suggest that different receptor subtypes may produce function-specific regulation of medullary catecholamine systems.[57]

The brain contains high concentrations of polyunsaturated fatty acids, targets for ROS. Thiobarbituric acid-reactive substances (TBARS) are an indirect marker of oxidative stress. They are increased in the rVLM in stroke-prone spontaneously

hypertensive rats (SHRSP). The intensity of electron spin resonance signals from the rVLM decreases more rapidly in the rVLM of SHRSP, another indicator of increased oxidative stress in this region. This could be another mechanism for hypertension in this model.[58]

Resveratrol is a phytoalexin produced by a wide variety of plants. It is commonly found in the skin of red grapes, red wine, and Japanese knotweed. Microinjection of resveratrol into the RVLM of anesthetized male rats inhibited sympathetic discharge. It was thought that these effects might be mediated by NO synthesis and a decrease in Ca^{2+} influx involving protein tyrosine kinase.[59]

Nucleus Tractus Solitarius

The NTS, located in the caudal medulla, is a gateway for a variety of cardiopulmonary related afferents. This would include well-known afferents from baroreceptors as well as a population that apparently receives stimuli from somatic structures such as muscle and skin.[60, 61]

The NTS also receives cardiopulmonary A- and C-fiber afferents with differing capsaicin sensitivities. Distinct intrinsic and synaptic long-term depression mechanisms in the NTS, specific for the relay of A- or C-fiber afferents, are responsible for the changes seen in response to persistent afferent fiber hyperactivity. Afferent fiber hyperactivity is associated with various noxious signals, disease states, or pathological perturbations.[62] Afferent transmission within the medial NTS differs according to the capsaicin sensitivity of the axons but there are no differences based on the source of the axon, i.e., baroreceptor vs. nonbaroreceptor.[63] Baroreceptor inputs provide a major stimulus for NTS-mediated excitation of the cVLM. Glutamate activates the cVLM to reduce sympathetic nerve activity independent of the NTS.[41] Lipopolysaccharide-induced hypotension is mediated by vagal nerve conduction to the NST that stimulates catecholamine release within the AHA.[64]

In awake rats atrial mechanoreceptors, sensitive to stretch, contribute to the regulation of heart rate and intravascular volume sending signals to the NTS and from there to the PVN. The PVN neurons synthesize corticotropin-releasing factor (CRF), vasopressin (AVP), and oxytocin (OT). The CRF-releasing neurons show an increase in Fos expression induced by stimulation of right atrial mechanoreceptors indicating a role for CRF in the cardiovascular reflex adjustments to volume loading. Osmotic stimulation modulates activation of CRF neurons in the NTS.[65]

Cholecystokinin (CCK) is a peptide released as a hormone by the proximal gut in response to the presence of peptones and fatty acids in the lumen. CCK is also widely distributed throughout the mammalian brain where it functions as a neurotransmitter and neuromodulator. It may act directly to activate central vagal afferent terminal inputs to the NTS. It does this by provoking increases in intracellular Ca^{2+} in vagal afferent terminals via a complex interaction between protein kinase A and phospholipase C transduction mechanisms. This opens L-type Ca^{2+} channels and stimulates Ca^{2+} release from the endoplasmic reticulum.[66]

In the rat nerve growth factor (NGF) and brain-derived neurotrophic factor (BDNF) attenuate Angio-II-induced facilitation of voltage-dependent Ca^{2+} channels (VDCCs) but do not attenuate glutamate-induced facilitation of the L-type VDCC current in the NTS. NGF attenuates Angio-II-induced facilitation of L-type VDCCs mediated by tyrosine kinase A receptors in NTS neurons.[67]

In adult rats the transcription factor Phox2b is expressed exclusively within a subpopulation of glutamatergic neurons in the NTS and is necessary for the development of this structure. NTS neurons express the enzyme 11-β-hydroxysteroid dehydrogenase type-2, and nuclear Phox2b is found in virtually all of these neurons suggesting that the Phox2b neurons are responsible for the release of the excitatory neurotransmitter glutamate.[68] The release of glutamate from the NTS is directly correlated with extracellular glucose concentrations. 5-HT3 receptors on synaptic connections between vagal afferent nerve terminals and NTS neurons may be a strong candidate as a site for glucose to act.[69] Hexokinase-I is the first enzyme required for the metabolism of glucose in the CNS and strong hexokinase-I mRNA labeling is found in the NTS, along with the Purkinje and granular cells of the cerebellar cortex, neurons of the medulla oblongata area postrema, reticular nucleus, nucleus cuneatus, and several motor nuclei in rats.[70]

The injection of ACh into the NTS of conscious rats induces hypotension and bradycardia. These effects seem to be partly mediated by NO produced in the NTS neurons.[57, 71]

μ-, δ-, and κ-opioid receptors are the main opioid receptors found in the CNS and periphery. In the rat brain mu receptor mRNA has been identified in the NTS and other nuclei associated with cardiovascular control including the medial preoptic area, dorsal raphe, nucleus cuneatus, and the dorsal motor neurons of the vagus, along with many other specific locations not directly related to cardiovascular control. Cellular localization of delta receptor mRNA was in the VLM and different loci than mu and kappa receptor mRNA. Kappa mRNA was found in different loci than mu and delta but in most hypothalamic nuclei and again in the NTS.[72, 73]

Japanese monkeys (*Macaca fuscata*) have three opioid peptide neuronal systems: propiomelanocortin (POMC), proenkephalin A, and proenkephalin B. POMC-related immunoreactive material was found in only one area related to cardiovascular control, the NTS, but was well distributed otherwise. Proenkephalin A-related immunoreactive neuronal perikarya were detected in the NTS, and densely packed immunoreactive fibers were found in the periaqueductal central gray, nucleus cuneatus, and were widely distributed in noncardiovascular areas. Cardiovascular areas containing neuronal perikarya stained for proenkephalin B were the PCG and NTS, but there was wide distribution elsewhere in the CNS.[74]

The phosphatidylinositol 3-kinase (PI3K)-Akt-nitric oxide synthate (NOS) signaling pathway has important functions in the central control of cardiovascular effects in the NTS of normotensive WKY rats. Both Akt-dependent and Akt-independent signaling pathways are defective in 16-week-old SHR.[75]

In Sprague-Dawley rats two component proteins of the adrenomedullin-1 (ADM-1) receptor complex, calcitonin receptor-like receptor and receptor activity-modifying protein, are uniformly distributed and highly colocalized in the NTS. Microinjection of ADM into the NTS significantly increased baroreceptor response

and sensitivity in a time- and dose-responsive manner but without effect on arterial blood pressure or heart rate. It was determined that ADM enhances baroreceptor response via activation of a cAMP/PKA-dependent mechanism acting on site-specific ADM-1 receptors in the NTS in this model.[76] Adrenomedullin-2 (ADM-2) is a novel member of the calcitonin gene-related peptide family. When it is injected into the NTS of rats there is an increase in arterial pressure and heart rate, and this effect is significantly attenuated by an antagonist of receptor components for ADM-2 that were found to be abundant in the rat NTS.[77]

Hypoxia activates neuronal ATP-sensitive K^+ channels (KATP) in the NTS. Chronic exposure to either sustained or intermittent hypoxia reduces KATP channel function in NTS neurons of rats. It is suggested that this is a neuronal adaptation preserving neuronal excitability in crucial relay neurons in peripheral chemoreflex pathways.[78] Chemosensory glomus cells of the carotid body detect changes in O_2. Carotid sinus nerve fibers, originating from peripheral sensory neurons located within the petrosal ganglion, innervate the carotid body. Transmitter released from glomus cells activates sensory afferent fibers transmitting information to the NTS. At least four different voltage-gated K^+ channels [Kv1.4, Kv1.5, Kv4.3, and K (Ca)-BK] shape the action potential and the frequency of discharge in the sensory afferent fibers in rats.[79] Enhanced cardiac sympathetic afferent input contributes to the excitatory effects seen in chemoreflex function in rats with congestive heart failure. These changes are mediated by an ATR-1-dependent mechanism in the NTS.[80]

In rats with streptozotocin-induced diabetes for 8 or 16 weeks there is reduced activity in the afferent baroreceptor input to the NTS. This is consistent with diabetes-induced damage to baroreceptor afferent nerves and may be at least partly responsible for the increased cardiovascular morbidity and mortality seen in diabetic patients.[81]

The NTS was microdissected from 15-week-old male SHR and WKY control rats. Gene expression of gp39 precursor and monocyte chemoattractant protein-1 were higher in the NTS of SHR but interleukin-6 was lower in the NTS of SHR than in the NTS of controls. There were no significant differences in the expression of IL-1-β, TNF-α, or TGF-β1.[82] Another study from the same lab reported overexpression of junctional adhesion molecule-1, a leukocyte adhesion molecule, in the NTS of SHR.[83]These studies suggest that the NTS of the SHR demonstrates a rather specific inflammatory state.

Following 7 days of experimental hypertension resulting from aortic coarctation TH and angiotensinogen mRNA expression in the NTS increases. Similar increases were seen in other areas involved in the central control of cardiovascular reflexes including the VLM, locus coeruleus (LC), and the PVN. The results suggest that norepi and Angio-II might participate in the modulation and maintenance of coarctation hypertension.[18]

Hypothalamic Paraventricular Nucleus

The PVN regulates several homeostatic variables. In tetrapods it is composed of magnocellular neurons that project to the posterior pituitary and parvicellular neurons that project to numerous sites in the CNS. The homeodomain transcription

factor Orthopedia (Otp) is expressed in several different hypothalamic sites including the PVN. Otp expression was compared in mice, chicks, frogs, and axolotol (*Ambystoma mexicanum*). Otp-positive cells were found in the PVN and were continuous with cells found in the medial amygdala. Otp-positive cells were also observed in the arcuate nucleus and oblique perimammillary band. The PVN is relatively unevaginated in the amphibian brain, barely evaginated in the chick, and fully evaginated in the mouse.[84]

The PVN contains aggregations of glucagon-like peptide-1 (GLP-1) in neurons in its hypophysiotrophic zones. GLP-1 modulates neuroendocrine and autonomic function and exerts excitatory action on adrenocorticotropin release. GLP-1 also influences oxytocin secretion and controls outflow to brainstem cardiovascular relays.[85] The PVN contains a highly heterogeneous distribution of distinct neurons that are able to access cGMP to produce constitutive NO. NO effects in the PVN involve intricate cell-to-cell interactions and heterogeneous signaling modalities.[86] Also in rats the central administration of urotensin-II (UII) causes tachycardia, increases ventricular contractility, and increases plasma levels of epinephrine and glucose. The administration of U-II centrally increased Fos immunoreactivity in the PVN, the NTS, and the CEA, but the PVN increase was over a longer time course. It was concluded that U-II acts on specific nuclei in the brain to stimulate the hypothalamic-pituitary-adrenal axis and to stimulate adrenal sympathetic nerve activity.[87]

The PVN contributes to both sympatho-excitation and hypertension in renovascular hypertension. The transient outward K^+ current in patch-clamped RVLM-projecting PVN neurons exhibited diminished transient outward K^+ currents in hypertensive rats and this contributes to the aberrant neuronal function.[88]

Animal models of salt-sensitive hypertension demonstrate differential effects of Na^+ and Cl^- loading on the long-term maintenance of hypertension. Salt sensing occurs in renal tubular fluids in the macula densa cells. Sodium ion concentration is sensed in the cerebrospinal fluid (CSF) by a novel isoform of Na^+ channels that are expressed in subfornical organs. There is also sensing of CSF osmolality by mechanosensitive, nonselective cation channels expressed in neuronal cells of the PVN and supraoptic nuclei. Volume-regulated anion channels located in glial cells of the PVN and supraoptic nuclei also respond to changes in osmolality.[89] When rats were exposed to 7 days of i.c.v. insulin treatment, the PVN was still able to amplify neuronal hypotensive and natriuretic pathways and counteracted the known peripheral antinatriuretic effects of insulin.[90]

Periaqueductal Gray

As has been previously described the PAG contains well-characterized pressor and depressor sites[7] that are structurally distinct longitudinal columns of cells.[91, 92]The PAG, along with the amygdala and the medial hypothalamus, are thought to be responsible for the generation and elaboration of unconditional fear in rats. The neuronal structures in these areas are under tonic inhibitory control exerted by GABA

mechanisms.[93] In mice glutamate-NMDA receptor activation in the PAG results in antinociceptive, autonomic, and behavioral responses that characterize the reaction to fear. Recent work indicates that PAG synthesis of NO does not play a role in these responses.[94] Other neurotransmitters play a role in PAG anxiety responses including glutamate and 5-HT (1A) (serotonin) as well as NMDA receptors in rats.[95] Hypothalamic processing of predatory threats in rats takes place in the dorsal premammillary nucleus where input signals are amplified and transmitted to the PAG where antipredatory unconditioned and conditioned behavioral responses, including cardiovascular adaptations, are initiated.[96] Oxytocin receptor activation in the ventrocaudal PAG is an important consequence of contact with infants in mother rats. It seems to reduce some anxiety-related behaviors.[97]

Anesthetized rats were used to study the effects of mechanical, heat, and cold nociception on cardiovascular responses. It was found that eNOS within the dorsolateral (dl)-PAG plays a differential role on the cardiovascular system during heat- and cold-mediated nociception via modulating glutamatergic/GABAergic neurotransmission. Mechanical stimulation had no effect on cardiovascular responses when an eNOS antagonist was infused into the PAG.[98] Air jet stress in rats provokes the DMH to initiate responses that result in tachycardia, hypertension, and increased levels of circulating ACTH. There is evidence that the dl-PAG acts as a descending relay for this response and neurons within this structure are activated and contribute to the cardiovascular responses.[99]

The PAG is also involved in many gonadal steroid-sensitive behaviors in rats, including the response to pain. The PAG projects to the RVLM and comprises the primary circuit driving pain inhibition. There is direct evidence for the expression of steroid receptors in the PAG and the descending pathway driving pain inhibition in both male and female rats.[100] Significant decreases in regional cerebral blood flow (rCBF) were seen in the PAG, as well as in the thalamus, PBN, hypothalamus, and pons following colorectal distension (visceral pain stimulus) in conscious, unrestrained, male rats. As expected, rCBF was increased in response to this stimulus in sensory, limbic, and paralimbic regions of the brain.[101]

A transgenic mouse, in which a 12.2-kb fragment of the human renin promoter was used to drive expression of Cre-recombinase, was crossed with the ROSA26-lac Z reporter mouse strain. Cre-recombinase-mediated excision of the floxed stop cassette resulted in expression of the reporter protein, β-galactosidase. The reporter protein was found to be colocalized with the neuronal marker NeuN. The PAG was among those areas of the brain that were labeled with this marker, indicating that renin could have broader actions in the brain. There is the potential for interaction with the (pro)-renin receptor or production of a ligand for non-ATR-1 or ATR-2 receptors to play a role in PAG function.[102]

Natriuretic peptide receptor type C (NPR-C) binds all natriuretic peptides and is considered to be involved in the clearance of these substances as well as being essential for their neuromodulatory effects. NPR-C immunoreactivity was found in the PAG and in many other regions of the rat brainstem indicating an important role for natriuretic peptides in neuroendocrine regulation and central cardiovascular integration.[103]

Alpha-2-delta is a membrane-spanning auxiliary protein subunit of voltage-gated Ca^{2+} channels. Rat brains stained with a monoclonal antibody to α-2-delta demonstrated a number of areas of dense staining and few with moderate staining. The PAG was moderately stained but the significance of these findings is not yet clear.[104]

Anterior and Posterior Hypothalamic Areas

Both a decrease of melatonin (MT) and an increase in the melatonin-2 (MTR-2) receptor in the AHA are involved in stress-induced hypertension in rats. Both MTR-1 and MTR-2 receptors participate in the antihypertensive effects of MT in the AHA. The antihypertensive effect of MT is also related to decreased excitatory amino acid glutamate and increased inhibitory amino acids taurine and BABA in the RVLM via communication from the AHA.[17]

An intact PHA is necessary for the development of chronic, but not acute, hypertension following intravenous infusion of Angio-II in rats.[105] Significant differences were found in *per2* and *bmall* (clock genes) expression in the PHA between control rats and mREN-2 (hypertensive) rats. Clock gene expression was also affected in mREN-2 rats in the nucleus ambiguus. This area receives direct innervation from the PHA.[106]

Median Preoptic Nucleus

Subpopulations of neurons in the median preoptic nucleus (MnPo), located within the lamina terminalis, contribute to thermoregulation, cardiovascular and hydro mineral homeostasis, and sleep promotion. The MnPo is innervated by lateral hypothalamic neurons that synthesize and secrete arousal-promoting and excitatory orexin neuropeptides. Rat brain slices were used to demonstrate that in addition to a direct postsynaptic receptor-mediated excitation, orexins are able to increase the excitability of MnPo neurons by increasing their excitatory inputs via an orexin receptor-mediated excitation of local glutamatergic neurons whose axons project to the MnPo neurons.[107] The MnPo appears to be a downstream site of activation following binding of Angio-II at the subfornical organ and organum vasculosum of the lamina terminalis. Neurons of the MnPo are thus involved in the central neural pathway mediating the chronic hypertensive effects of increased Angio-II.[108]

Nucleus Cuneatus

The ability of thalamic neurons in the ventrobasal complex to show adaptive changes in receptive field properties following the loss of projections from the Cu was examined in rats exposed to air jet stimulation stress. The receptive field structure

of individual neurons showed adaptive properties immediately after loss of predominant ascending inputs. This is yet another example of plasticity.[109]

Lateral Parabrachial Nucleus and the Dorsal Raphe Nucleus

Serotonergic mechanisms in a key pathway that links the lateral parabrachial nucleus (LPBN) and dorsal raphe nucleus (DRN) are involved in the regulation of renal and hormonal responses to the control of blood volume within physiological set points in rats.[110]

Caudal Vestibular Nucleus

Activation of CVN neurons can induce a pressor response. In anesthetized rats injection of 1-glutamate (5 nmol) into the MVe and SpVe resulted in a slight increase in arterial blood pressure. Local pretreatment with a NMDA-receptor antagonist attenuated this pressor response indicating a role for NMDA receptors. Glutamatergic CVN pathways to the NTS and PBN and projections from the CVN to the RVLM via the NTS comprise an indirect vestibulo-cardiovascular pathway in the rat brainstem.[12]

Gender Effects on Central Control of Cardiovascular Responses

In the VLM of both male and female rats with a nonfunctional mutation of the androgen receptor (testicular feminization mutation, Tfm) there is a significant sexual dimorphism in control animals and a decrease of nNOS-positive elements in Tfm males. This suggests that androgens, via the action of androgen receptors, may play an important role in the organization and modulation of nNOS activity in the hypothalamus.[111]

Bulbospinal neurons in the RVLM are involved in the tonic regulation of arterial pressure. Angio-II acting on ATR-1 in RVLM neurons has been implicated in the development of hypertension. Female rats with TH-positive RVLM neurons display more ATR-1 immunoreactivity and less p47 immunoreactivity than males. This counterbalance of ATR-1 and p47 results in similar levels of Angio-II-induced ROS production in males and females. However, Angio-II-induced L-type Ca^{2+} currents are increased in females, possibly as a result of gender differences in Ca^{2+} channel densities or dynamics.[44] In mice the central actions of estrogen are involved in the protection of Angio-II-induced hypertension perhaps involving interactions with ROS production.[112]

Extranuclear estrogen receptors (ER) have been identified in the rVLM,[113] and ER-α-immunoreactive cells, now called nucleus para-retroambiguus (NPRA), are

found in the cVLM of rats.[114] The ratio of axon terminal surface/dendrite surface was significantly increased in the NPRA during the estrous phase of normal female Golden hamsters compared with ovarioectomized females and the diestrous periods of intact females. Remodeling of axon terminals due to axonal sprouting into large terminal fields filled with pleomorphic vesicles was the cause of this structural plasticity.[114] Progestins apparently modulate neurons in the rVLM and NTS by presynaptic mechanisms involving GABAergic transmission, and progestin receptor activation could contribute to gender differences in cardiovascular regulation and progestin effects on blood pressure during pregnancy in Sprague-Dawley rats.[115]

Following estrogen treatment of 7-week-old ovarioectomized rats there was differential regulation of neuronal nAChR, $GABA_A$-receptor delta, serotonin receptor-6, and GABA transporter-2 in the preoptic area and the ventromedial nucleus of the hypothalamus. There was differential regulation of these genes by estrogen between the anterior and posterior parts of the hypothalamus.[116]

Single unit activity was recorded from cells located in the arcuate nucleus and medial preoptic area of anesthetized, intact, male rats treated with testosterone or 17-β-estradiol. It was concluded that both physiological and supraphysiological concentrations of testosterone can rapidly affect single unit activity in the arcuate nucleus and the medial preoptic area - the latter to a lesser degree.[117]

Neurohumeral Control

The brain controls circulating hormones. Some of these can influence the brain by binding to brain neurons that lie outside the blood-brain barrier. So-called cardiovascular hormones are synthesized and released in the brain as neurotransmitters or neuromodulators. Some of these can pass the blood-brain barrier and circulate.[118]

Renin-Angiotensin System

The intrinsic renin-angiotensin system in the brain plays a critical role in the control of blood pressure. Brain Angio-II affects other neurons both through activation of angiotensin receptors and the generation of NO and ROS. Circulating Angio-II activates endothelial-derived NO that crosses the blood-brain barrier and modulates neuronal activity in various cardiovascular control nuclei.[118]

Serotonin

Serotonin (5-HT) receptors have been identified in every important nucleus of cardiovascular control, and 5-HT-induced changes in cardiovascular system function have been linked to activation of these receptors. A variety of studies have linked

5-HT to the maintenance of hypertension but there are other studies that demonstrate the ability of 5-HT to reduce elevated blood pressures.[119, 120] Central 5-HT(1A), 5-HT(3), and 5-HT(7) receptors play an important role in the regulation of cardiovascular reflexes by controlling parasympathetic stimulatory activity to the heart. Activity in the sympathetic system can be inhibited by central 5-HT(1A) receptors resulting in a decrease in blood pressure. 5-HT(2) can excite receptors to increase blood pressure and may be involved in the development of DOCA-salt hypertension via their ability to control AVP release.[121]

Vasopressin

Hypertonicity in the brain stimulates AVP secretion in rats.[122] In SHR or rats with mineralocorticoid/salt-induced hypertension the hypothalamic expression of AVP is significantly elevated.[123]

Endogenous Ouabain-Like Substance

This substance is produced endogenously in the brain and acts as a Na^+, K^+-ATPase pump inhibitor. When exogenous ouabain is administered to rats hypertension develops and is of CNS origin. It can be blocked by the i.c.v. administration of an anti-ouabain antibody, but this is not effective if the antibody is given intravenously. Ouabain-induced hypertension can also be blocked by discrete excitotoxic lesions in CNS cardiovascular control centers or by ganglionic blockade. The brain ouabain-like substance (OLS) system has also been shown to activate the brain renin-angiotensin system. There are three isoforms of the catalytic α subunit of the Na^+, K^+-ATPase in the brain and cardiovascular system but it is not known which brain isoform(s) mediate the hypertensive effects of OLS. Preliminary studies in gene-targeted mice suggest that the α-2 isoform may play a critical role.[124] In Wistar rats chronic increases in CSF [Na^+] may increase hypothalamic aldosterone and activate CNS pathways involving both mineralocorticoid and OLC. This leads to increases in ATR-1 and angiotensin-converting-enzyme (ACE) densities in CNS cardiovascular control centers.[125]

Opioids

Hypothalamic blood flow autoregulation was studied in anesthetized, artificially ventilated, temperature-controlled cats made hypotensive or hypertensive. The autoregulatory range was significantly narrowed following the administration of a general opiate receptor antagonist suggesting an important role for endogenous

opioid peptides in hypothalamic blood flow autoregulation both in hypotensive and hypertensive cats.[126] High fat diet-induced obesity and hypertension is associated with increased hypothalamic mu-opioid receptors in response to s-endorphins in conscious rats.[127]

Tyrosine Hydroxylase and Phenylethanolamine N-Methyltransderase

The TH- and PNMT-immunoreactive cells of the medulla are closely associated with cardiovascular control in cats, rats, and dogs although some species variations in location do exist.[128]

Neuropeptide Y

The same neural circuits that regulate energy balance appear to regulate the secretion of triglycerides (TG) into the plasma of fasting rats. NPY signaling in the CNS was modulated by the i.c.v. injection of NPY, a NPY receptor antagonist, and a NPY receptor agonist. A single i.c.v. injection of NPY increased plasma TG by 2.5-fold. Activating NPY signaling in downstream neurons with a NPY-Y5 receptor agonist saw the same effect. A NPY-Y1 receptor antagonist decreased NPY-induced elevations in TG.[129]

Leptin

Leptin has powerful antidiabetic actions in insulin-deficient rats. It acts directly on the CNS independent of increased peripheral α-1-, β-1-, β-2-, and β-3-adrenergic activity. It also exerts long-term cardiovascular effects that are partially mediated by activation of α-1- and β-1/β-2-adrenergic receptors.[130]

Dopamine-β-Hydroxylase

Mice with a homozygous deletion of dopamine-β-hydroxylase (DBH) ($Dbh^{-/-}$) have a selective and complete lack of norepinephrine. The density of α-1-AR in $Dbh^{-/-}$ mice is similar to that in $Dbh^{+/-}$ mice in most brain regions but there is upregulation of these receptors in the hippocampus. There are modest decreases in α-2-AR in the septum, hippocampus, and amygdala, but no change in α-2-AR function. The density of β-AR is upregulated, to varying degrees, in most brain

regions in $Dbh^{-/-}$ mice than in $Dbh^{+/-}$. The conclusion is that in the brain the regulation of noradrenergic receptors by endogenous epinephrine is dependent upon receptor type and their neuroanatomical location.[131]

11-β-Hydroxylase and Aldosterone Synthase

There is transcription of 11-β-hydroxylase (CYP11B1) and aldosterone synthase (CYP11B2) throughout the CNS in rats. Gene transcription of these enzymes is regulated by ACTH and by circulating corticosteroid levels.[132]

Orexin

Orexins (hypothalamic neuropeptides) act as neurotransmitters or neuromediators in the brain. They regulate autonomic and neuroendocrine function. In the pig orexin B immunoreactive neurons are localized in the perifornical area, dorsomedial hypothalamic nucleus, zona incerta, and the PHA. About 30% of gonadotropin-releasing hormone neurons were in close contact with orexin B immunoreactive fibers.[133] Orexin A is a member of a wider family of orexigenic neuropeptides produced by a small group of neurons located in the posterior hypothalamus, the ventromedial hypothalamus, the lateral hypothalamic region, the HVN, and the dorsomedial nucleus, all cardiovascular control centers. Orexin A injected i.c.v. in rats resulted in significant increases in food consumption but subcutaneous or intravenous injections produced changes in insulin plasma concentrations and cardiovascular changes. The same results were produced in pigs.[134] Norepinephrine, dopamine, and epinephrine all directly hyperpolarize orexin neurons but in a very complex manner.[135]

Urotensin-II

UII is a vasoactive peptide primarily expressed in motor neurons of the brainstem and spinal cord. In rats UII receptor mRNA and UII binding sites have been identified in the hypothalamus, locus coeruleus, NTS, DMV, inferior olive, SON, paraventricular nucleus, ventromedial nucleus, and the arcuate nucleus.[136] UII and UII-related peptide (URP) are paralog neuropeptides. In the mouse brain the UII-immunoreactive molecule corresponds to the UII (17) isoform. Calcium mobilization assays indicate that UII (17) and URP are equally potent in stimulating UII receptors. UII and URP appear to have redundant biological effects but URP may be more specific in participating in autonomic, cardiovascular, and reproductive functions.[137]

Cholecystokinin

CCK was first identified as a gastrointestinal hormone released from enteroendocrine cells lining the intestinal mucosa. It was recently demonstrated that CCK differentially influences the discharge rate of presympathetic vasomotor neurons in the RVLM.[138] CCK peptides induce neurogenic vasodilation both in cerebral and mesenteric vessels. These effects are mediated by NO and seem to be presynaptic.[139]

References

1. Nelson AJ, Juraska JM, Musch TI, Iwamoto GA. Neuroplastic adaptations to exercise: Neuronal remodeling in cardiorespiratory and locomotor areas. J Appl Physiol. 2005;99:2312–2322.
2. Plowey ED, Kramer JM, Beatty JA, Waldrop TG. In vivo electrophysiological responses of pedunculopontine neurons to static muscle contraction. Am J Physiol Regul Integr Comp Physiol. 2002;283:R1008–R1019.
3. Bedford TG, Loi PK, Crandall CC. A model of dynamic exercise: The decerebrate rat locomotor preparation. J Appl Physiol. 1992;72:121–127.
4. Kaufman MP, Forster HV. Reflexes controlling circulatory, ventilatory, and airway responses to exercise. In: Roweland LB, Shepherd JT, eds. Handbook of Physiology, Section 12: Exercise, Regulation and Integration of Multiple Systems. New York: Oxford University Press; 1996:381–446.
5. Iwamoto GA, Wappel SM, Fox GM, Buetow KA, Waldrop TG. Identification of diencephalic and brainstem cardiorespiratory areas activated during exercise. Brain Res. 1996;726:109–122.
6. Ichiyama RM, Gilbert AB, Waldrop TG, Iwamoto GA. Changes in the exercise activation of diencephalic and brainstem cardiorespiratory areas after training. Brain Res. 2002;947:225–233.
7. Nelson AJ, Iwamoto GA. Reversibility of exercise-induced dendritic attenuation in brain cardiorespiratory and locomotor areas following exercise detraining. J Appl Physiol. 2006;101:1243–1251.
8. Bienkowski MS, Rinaman L. Noradrenergic inputs to the paraventricular hypothalamus contribute to hypothalamic-pituitary-adrenal axis and central fos activation in rats after acute systemic endotoxin exposure. Neuroscience. 2008;156:1093–1102.
9. Varga T, Palkovits M, Usdin TB, Dobolyi A. The medial paralemniscal nucleus and its afferent neuronal connections in rat. J Comp Neurol. 2008;511:221–237.
10. Ichiyama RM, Waldrop TG, Iwamoto GA. Neurons in and near insular cortex are responsive to muscular contraction and have sympathetic and/or cardiac-related discharge. Brain Res. 2004;1008:273–277.
11. Vissing J, Iwamoto GA, Rybicki KJ, Galbo H, Mitchell JH. Mobilization of glucoregulatory hormones and glucose by hypothalamic locomotor centers. Am J Physiol. 1989;257:E722–E728.
12. Cai YL, Ma WL, Wang JQ, Li YQ, Li M. Excitatory pathways from the vestibular nuclei to the NTS and the PBN and indirect vestibulo-cardiovascular pathway from the vestibular nuclei to the RVLM relayed by the NTS. Brain Res. 2008;1240:96–104.
13. Verberne AJ. Cuneiform nucleus stimulation produces activation of medullary sympathoexcitatory neurons in rats. Am J Physiol. 1995;268:R752–R758.
14. Choi DC, Furay AR, Evanson NK, et al. The role of the posterior medial bed nucleus of the stria terminalis in modulating hypothalamic-pituitary-adrenocortical axis responsiveness to acute and chronic stress. Psychoneuroendocrinology. 2008;33:659–669.
15. Stremel RW, Waldrop TG, Richard CA, Iwamoto GA. Cardiorespiratory responses to stimulation of the nucleus reticularis gigantocellularis. Brain Res Bull. 1990;24:1–6.
16. Waldrop TG, Iwamoto GA. Point: Supraspinal locomotor centers do contribute significantly to the hyperpnea of dynamic exercise. J Appl Physiol. 2006;100:1077–1079.
17. Xia CM, Shao CH, Xin L, et al. Effects of melatonin on blood pressure in stress-induced hypertension in rats. Clin Exp Pharmacol Physiol. 2008;35:1258–1264.

18. Maximino JR, Ferrari MF, Coelho EF, Fior-Chadi DR. Time course analysis of tyrosine hydroxylase and angiotensinogen mRNA expression in central nervous system of rats submitted to experimental hypertension. Neurosci Res. 2006;55:292–299.
19. Horiuchi J, McDowall LM, Dampney RA. Role of 5-HT(1A) receptors in the lower brainstem on the cardiovascular response to dorsomedial hypothalamus activation. Auton Neurosci. 2008;142:71–76.
20. Maemura K, Takeda N, Nagai R. Circadian rhythms in the CNS and peripheral clock disorders: Role of the biological clock in cardiovascular diseases. J Pharmacol Sci. 2007;103:134–138.
21. Verbalis JG. How does the brain sense osmolality? J Am Soc Nephrol. 2007;18:3056–3059.
22. Swiatkowski K, Dellamano LM, Vissing J, Rybicki KJ, Kozlowski GP, Iwamoto GA. Differential effects from parapyramidal region and rostral ventrolateral medulla mediated by substance P. Am J Physiol. 1999;277:R1120–R1129.
23. Ruiz-Pesini P, Tome E, Balaguer L, Romano J, Yllera M. The projections to the medulla of neurons innervating the carotid sinus in the dog. Brain Res Bull. 1995;37:41–46.
24. Iwamoto GA, Waldrop TG. Lateral tegmental field neurons sensitive to muscular contraction: A role in pressor reflexes? Brain Res Bull. 1996;41:111–120.
25. Wei S, Lei M, Tong M, Ding J, Han Q, Xiao M. Acute baroreceptor unloading evokes fos expression in anesthetized rat brain. Brain Res Bull. 2008;76:63–69.
26. Thomas CJ, McAllen RM, Salo LM, Woods RL. Restorative effect of atrial natriuretic peptide or chronic neutral endopeptidase inhibition on blunted cardiopulmonary vagal reflexes in aged rats. Hypertension. 2008;52:696–701.
27. Ito K, Kimura Y, Hirooka Y, Sagara Y, Sunagawa K. Activation of rho-kinase in the brainstem enhances sympathetic drive in mice with heart failure. Auton Neurosci. 2008;142:77–81.
28. Signolet IL, Bousquet PP, Monassier LJ. Improvement of cardiac diastolic function by long-term centrally mediated sympathetic inhibition in one-kidney, one-clip hypertensive rabbits. Am J Hypertens. 2008;21:54–60.
29. Ono A, Kuwaki T, Kumada M, Fujita T. Differential central modulation of the baroreflex by salt loading in normotensive and spontaneously hypertensive rats. Hypertension. 1997;29:808–814.
30. Daly MD. Some reflex cardioinhibitory responses in the cat and their modulation by central inspiratory neuronal activity. J Physiol. 1991;439:559–577.
31 Alzoubi KH, Aleisa AM, Alkadhi KA. In vivo expression of ganglionic long-term potentiation in superior cervical ganglia from hypertensive aged rats. Neurobiol Aging. 2008 July 21 [Epub ahead of print].
32. Schultz HD, Li YL. Carotid body function in heart failure. Respir Physiol Neurobiol. 2007;157:171–185.
33. Gross DR. Animal Models in Cardiovascular Research, 2nd Revised Edition. Boston, MA: Kluwer Academic; 1994.
34. Ma Y, Yang ZM, Kang YM. Brain renin-angiotensin-aldosterone system contributes to sympatho-excitation in heart failure. Sheng Li Ke Xue Jin Zhan. 2008;39:105–108.
35. Koganezawa T, Shimomura Y, Terui N. The role of the RVLM neurons in the viscero-sympathetic reflex: A mini review. Auton Neurosci. 2008;142:17–19.
36. Iwamoto GA, Brtva RD, Waldrop TG. Cardiorespiratory responses to chemical stimulation of the caudal most ventrolateral medulla in the cat. Neurosci Lett. 1991;129:86–90.
37. Campos RR, Carillo BA, Oliveira-Sales EB, et al. Role of the caudal pressor area in the regulation of sympathetic vasomotor tone. Braz J Med Biol Res. 2008;41:557–562.
38. Yajima Y, Ito S, Komatsu K, Tsukamoto K, Matsumoto K, Hirayama A. Enhanced response from the caudal pressor area in spontaneously hypertensive rats. Brain Res. 2008;1227:89–95.
39. Bauer RM, Iwamoto GA, Waldrop TG. Discharge patterns of ventrolateral medullary neurons during muscular contraction. Am J Physiol. 1990;259:R606–R611.
40. Pilowsky PM, Abbott SB, Burke PG, et al. Metabotropic neurotransmission and integration of sympathetic nerve activity by the rostral ventrolateral medulla in the rat. Clin Exp Pharmacol Physiol. 2008;35:508–511.
41. Mandel DA, Schreihofer AM. Glutamatergic inputs to the CVLM independent of the NTS promote tonic inhibition of sympathetic vasomotor tone in rats. Am J Physiol Heart Circ Physiol. 2008;295:H1772–H1779.

42. Nakamura T, Kawabe K, Sapru HN. Cold pressor test in the rat: Medullary and spinal pathways and neurotransmitters. Am J Physiol Heart Circ Physiol. 2008;295:H1780–H1787.
43. Kashihara K, McMullan S, Lonergan T, Goodchild AK, Pilowsky PM. Neuropeptide Y in the rostral ventrolateral medulla blocks somatosympathetic reflexes in anesthetized rats. Auton Neurosci. 2008;142:64–70.
44. Wang G, Milner TA, Speth RC, et al. Sex differences in angiotensin signaling in bulbospinal neurons in the rat rostral ventrolateral medulla. Am J Physiol Regul Integr Comp Physiol. 2008;295:R1149–R1157.
45. Liu D, Gao L, Roy SK, Cornish KG, Zucker IH. Role of oxidant stress on AT1 receptor expression in neurons of rabbits with heart failure and in cultured neurons. Circ Res. 2008;103:186–193.
46. Alzamora AC, Santos RA, Campagnole-Santos MJ. Baroreflex modulation by angiotensins at the rat rostral and caudal ventrolateral medulla. Am J Physiol Regul Integr Comp Physiol. 2006;290:R1027–R1034.
47. Adams JM, McCarthy JJ, Stocker SD. Excess dietary salt alters angiotensinergic regulation of neurons in the rostral ventrolateral medulla. Hypertension. 2008;52:932–937.
48. Patel D, Bohlke M, Phattanarudee S, Kabadi S, Maher TJ, Ally A. Cardiovascular responses and neurotransmitter changes during blockade of angiotensin II receptors within the ventrolateral medulla. Neurosci Res. 2008;60:340–348.
49. Gao L, Wang WZ, Wang W, Zucker IH. Imbalance of angiotensin type 1 receptor and angiotensin II type 2 receptor in the rostral ventrolateral medulla: Potential mechanism for sympathetic overactivity in heart failure. Hypertension. 2008;52:708–714.
50. Gao L, Wang W, Wang W, Li H, Sumners C, Zucker IH. Effects of angiotensin type 2 receptor overexpression in the rostral ventrolateral medulla on blood pressure and urine excretion in normal rats. Hypertension. 2008;51:521–527.
51. Farnham MM, Li Q, Goodchild AK, Pilowsky PM. PACAP is expressed in sympathoexcitatory bulbospinal C1 neurons of the brain stem and increases sympathetic nerve activity in vivo. Am J Physiol Regul Integr Comp Physiol. 2008;294:R1304–R1311.
52. Orer HS, Gebber GL, Barman SM. Role of serotonergic input to the ventrolateral medulla in expression of the 10-Hz sympathetic nerve rhythm. Am J Physiol Regul Integr Comp Physiol. 2008;294:R1435–R1444.
53. Xia CM, Chen J, Wang J, et al. Differential expressions of nNOS and iNOS in the rostral ventrolateral medulla induced by electroacupuncture in acute myocardial ischemia rats. Sheng Li Xue Bao. 2008;60:453–461.
54. Powers-Martin K, Barron AM, Auckland CH, et al. Immunohistochemical assessment of cyclic guanosine monophosphate (cGMP) and soluble guanylate cyclase (sGC) within the rostral ventrolateral medulla. J Biomed Sci. 2008;15:801–812.
55. Kung LC, Chan SH, Wu KL, Ou CC, Tai MH, Chan JY. Mitochondrial respiratory enzyme complexes in rostral ventrolateral medulla as cellular targets of nitric oxide and superoxide interaction in the antagonism of antihypertensive action of eNOS transgene. Mol Pharmacol. 2008;74:1319–1332.
56. Ally A, Maher TJ. Endothelial NOS expression within the ventrolateral medulla can affect cardiovascular function during static exercise in stroked rats. Brain Res. 2008;1196:33–40.
57. O'Leary KT, Loughlin SE, Chen Y, Leslie FM. Nicotinic acetylcholine receptor subunit mRNA expression in adult and developing rat medullary catecholamine neurons. J Comp Neurol. 2008;510:655–672.
58. Hirooka Y. Role of reactive oxygen species in brainstem in neural mechanisms of hypertension. Auton Neurosci. 2008;142:20–24.
59. Ma HJ, Cao YK, Liu YX, Wang R, Wu YM. Microinjection of resveratrol into rostral ventrolateral medulla decreases sympathetic vasomotor tone through nitric oxide and intracellular Ca^{2+} in anesthetized male rats. Acta Pharmacol Sin. 2008;29:906–912.
60. Potts JT, Waldrop TG. Discharge patterns of somatosensitive neurons in the nucleus tractus solitarius of the cat. Neuroscience. 2005;132:1123–1134.
61. Toney GM, Mifflin SW. Sensory modalities conveyed in the hindlimb somatic afferent input to nucleus tractus solitarius. J Appl Physiol. 2000;88:2062–2073.

62. Bantikyan A, Song G, Feinberg-Zadek P, Poon CS. Intrinsic and synaptic long-term depression of NTS relay of nociceptin- and capsaicin-sensitive cardiopulmonary afferents hyperactivity. Pflugers Arch. 2009;457:1147–1159.
63. Andresen MC, Peters JH. Comparison of baroreceptive to other afferent synaptic transmission to the solitary tract nucleus. Am J Physiol Heart Circ Physiol. 2008;295:H2032–H2042.
64. Yilmaz MS, Goktalay G, Millington WR, Myer BS, Cutrera RA, Feleder C. Lipopolysaccharide-induced hypotension is mediated by a neural pathway involving the vagus nerve, the nucleus tractus solitarius and alpha-adrenergic receptors in the preoptic anterior hypothalamic area. J Neuroimmunol. 2008;203:39–49.
65. Benedetti M, Rorato R, Castro M, Machado BH, Antunes-Rodrigues J, Elias LL. Water deprivation increases fos expression in hypothalamic corticotropin-releasing factor neurons induced by right atrial distension in awake rats. Am J Physiol Regul Integr Comp Physiol. 2008;295:R1706–R1712.
66. Rogers RC, Hermann GE. Mechanisms of action of CCK to activate central vagal afferent terminals. Peptides. 2008;29:1716–1725.
67. Endoh T, Sato D, Wada Y, et al. Nerve growth factor and brain-derived neurotrophic factor attenuate angiotensin-II-induced facilitation of calcium channels in acutely dissociated nucleus tractus solitarii neurons of the rat. Arch Oral Biol. 2008;53:1192–1201.
68. Geerling JC, Chimenti PC, Loewy AD. Phox2b expression in the aldosterone-sensitive HSD2 neurons of the NTS. Brain Res. 2008;1226:82–88.
69. Wan S, Browning KN. Glucose increases synaptic transmission from vagal afferent central nerve terminals via modulation of 5-Ht3 receptors. Am J Physiol Gastrointest Liver Physiol. 2008;295:G1050–G1057.
70. Jacobsson G, Meister B. Hexokinase I messenger RNA in the rat central nervous system. Mol Cell Neurosci. 1994;5:658–677.
71. da Silva LG, Dias AC, Furlan E, Colombari E. Nitric oxide modulates the cardiovascular effects elicited by acetylcholine in the nts of awake rats. Am J Physiol Regul Integr Comp Physiol. 2008;295:R1774–1781.
72. Mansour A, Fox CA, Burke S, et al. Mu, delta, and kappa opioid receptor mRNA expression in the rat CNS: An in situ hybridization study. J Comp Neurol. 1994;350:412–438.
73. Mansour A, Fox CA, Thompson RC, Akil H, Watson SJ. Mu-opioid receptor mRNA expression in the rat CNS: Comparison to mu-receptor binding. Brain Res. 1994;643:245–265.
74. Ibuki T, Okamura H, Miyazaki M, Yanaihara N, Zimmerman EA, Ibata Y. Comparative distribution of three opioid systems in the lower brainstem of the monkey (macaca fuscata). J Comp Neurol. 1989;279:445–456.
75. Hsiao M, Lu PJ, Huang HN, et al. Defective phosphatidylinositol 3-kinase signaling in central control of cardiovascular effects in the nucleus tractus solitarii of spontaneously hypertensive rats. Hypertens Res. 2008;31:1209–1218.
76. Ho LK, Chen K, Ho IC, et al. Adrenomedullin enhances baroreceptor reflex response via cAMP/PKA signaling in nucleus tractus solitarii of rats. Neuropharmacology. 2008;55:729–736.
77. Cui H, Kohsaka A, Waki H, et al. Adrenomedullin 2 microinjection into the nucleus tractus solitarius elevates arterial pressure and heart rate in rats. Auton Neurosci. 2008;142:45–50.
78. Zhang W, Carreno FR, Cunningham JT, Mifflin SW. Chronic sustained and intermittent hypoxia reduce the function of ATP-sensitive potassium channels in the nucleus of the solitary tract. Am J Physiol Regul Integr Comp Physiol. 2008;295:R1555–R1562.
79. Buniel M, Glazebrook PA, Ramirez-Navarro A, Kunze DL. Distribution of voltage-gated potassium and hyperpolarization-activated channels in sensory afferent fibers in the rat carotid body. J Comp Neurol. 2008;510:367–377.
80. Wang WZ, Gao L, Wang HJ, Zucker IH, Wang W. Interaction between cardiac sympathetic afferent reflex and chemoreflex is mediated by the NTS AT1 receptors in heart failure. Am J Physiol Heart Circ Physiol. 2008;295:H1216–H1226.
81. Gouty S, Regalia J, Helke CJ. Attenuation of the afferent limb of the baroreceptor reflex in streptozotocin-induced diabetic rats. Auton Neurosci. 2001;89:86–95.
82. Waki H, Gouraud SS, Maeda M, Paton JF. Gene expression profiles of major cytokines in the nucleus tractus solitarii of the spontaneously hypertensive rat. Auton Neurosci. 2008;142:40–44.

83. Waki H, Gouraud SS, Maeda M, Paton JF. Specific inflammatory condition in nucleus tractus solitarii of the SHR: Novel insight for neurogenic hypertension? Auton Neurosci. 2008;142:25–31.
84. Bardet SM, Martinez-de-la-Torre M, Northcutt RG, Rubenstein JL, Puelles L. Conserved pattern of OTP-positive cells in the paraventricular nucleus and other hypothalamic sites of tetrapods. Brain Res Bull. 2008;75:231–235.
85. Tauchi M, Zhang R, D'Alessio DA, Stern JE, Herman JP. Distribution of glucagon-like peptide-1 immunoreactivity in the hypothalamic paraventricular and supraoptic nuclei. J Chem Neuroanat. 2008;36:144–149.
86. Powers-Martin K, Phillip JK, Biancardi VC, Stern JE. Heterogeneous distribution of basal cyclic guanosine monophosphate within distinct neuronal populations in the hypothalamic paraventricular nucleus. Am J Physiol Regul Integr Comp Physiol. 2008;295:R1341–R1350.
87. Watson AM, McKinley MJ, May CN. Effect of central urotensin II on heart rate, blood pressure and brain fos immunoreactivity in conscious rats. Neuroscience. 2008;155:241–249.
88. Sonner PM, Filosa JA, Stern JE. Diminished A-type potassium current and altered firing properties in presympathetic PVN neurones in renovascular hypertensive rats. J Physiol. 2008;586:1605–1622.
89. Orlov SN, Mongin AA. Salt-sensing mechanisms in blood pressure regulation and hypertension. Am J Physiol Heart Circ Physiol. 2007;293:H2039–H2053.
90. Menegon LF, Zaparolli A, Boer PA, de Almeida AR, Gontijo JA. Long-term effects of intracerebroventricular insulin microinjection on renal sodium handling and arterial blood pressure in rats. Brain Res Bull. 2008;76:344–348.
91. Behbehani MM. Functional characteristics of the midbrain periaqueductal gray. Prog Neurobiol. 1995;46:575–605.
92. Keay KA, Bandler R. Anatomical evidence for segregated input from the upper cervical spinal cord to functionally distinct regions of the periaqueductal gray region of the cat. Neurosci Lett. 1992;139:143–148.
93. Santos JM, Macedo CE, Brandao ML. Gabaergic mechanisms of hypothalamic nuclei in the expression of conditioned fear. Neurobiol Learn Mem. 2008;90:560–568.
94. Miguel TT, Nunes-de-Souza RL. Anxiogenic-like effects induced by NMDA receptor activation are prevented by inhibition of neuronal nitric oxide synthase in the periaqueductal gray in mice. Brain Res. 2008;1240:39–46.
95. Moraes CL, Bertoglio LJ, Carobrez AP. Interplay between glutamate and serotonin within the dorsal periaqueductal gray modulates anxiety-related behavior of rats exposed to the elevated plus-maze. Behav Brain Res. 2008;194:181–186.
96. Cezario AF, Ribeiro-Barbosa ER, Baldo MV, Canteras NS. Hypothalamic sites responding to predator threats - The role of the dorsal premammillary nucleus in unconditioned and conditioned antipredatory defensive behavior. Eur J Neurosci. 2008;28:1003–1015.
97. Figueira RJ, Peabody MF, Lonstein JS. Oxytocin receptor activity in the ventrocaudal periaqueductal gray modulates anxiety-related behavior in postpartum rats. Behav Neurosci. 2008;122:618–628.
98. Chaitoff KA, Patel D, Ally A. Effects of endothelial NOS antagonism within the periaqueductal gray on cardiovascular responses and neurotransmission during mechanical, heat, and cold nociception. Brain Res. 2008;1236:93–104.
99. de Menezes RC, Zaretsky DV, Sarkar S, Fontes MA, Dimicco JA. Microinjection of muscimol into the periaqueductal gray suppresses cardiovascular and neuroendocrine response to air jet stress in conscious rats. Am J Physiol Regul Integr Comp Physiol. 2008;295:R881–R890.
100. Loyd DR, Murphy AZ. Androgen and estrogen (alpha) receptor localization on periaqueductal gray neurons projecting to the rostral ventromedial medulla in the male and female rat. J Chem Neuroanat. 2008;36:216–226.
101. Wang Z, Bradesi S, Maarek JM, et al. Regional brain activation in conscious, nonrestrained rats in response to noxious visceral stimulation. Pain. 2008;138:233–243.
102. Allen AM, O'Callaghan EL, Hazelwood L, et al. Distribution of cells expressing human renin-promoter activity in the brain of a transgenic mouse. Brain Res. 2008;1243:78–85.
103. Abdelalim EM, Masuda C, Bellier JP, et al. Distribution of natriuretic peptide receptor-C immunoreactivity in the rat brainstem and its relationship to cholinergic and catecholaminergic neurons. Neuroscience. 2008;155:192–202.

104. Taylor CP, Garrido R. Immunostaining of rat brain, spinal cord, sensory neurons and skeletal muscle for calcium channel alpha2-delta (alpha2-delta) type 1 protein. Neuroscience. 2008;155:510–521.
105. Fink GD, Bruner CA, Mangiapane ML. Area postrema is critical for angiotensin-induced hypertension in rats. Hypertension. 1987;9:355–361.
106. Monosikova J, Herichova I, Mravec B, Kiss A, Zeman M. Effect of upregulated renin-angiotensin system on per2 and bmal1 gene expression in brain structures involved in blood pressure control in TGR(mREN-2)27 rats. Brain Res. 2007;1180:29–38.
107. Kolaj M, Coderre E, Renaud LP. Orexin peptides enhance median preoptic nucleus neuronal excitability via postsynaptic membrane depolarization and enhancement of glutamatergic afferents. Neuroscience. 2008;155:1212–1220.
108. Ployngam T, Collister JP. Role of the median preoptic nucleus in chronic angiotensin II-induced hypertension. Brain Res. 2008;1238:75–84.
109. Alloway KD, Aaron GB. Adaptive changes in the somatotopic properties of individual thalamic neurons immediately following microlesions in connected regions of the nucleus cuneatus. Synapse. 1996;22:1–14.
110. Margatho LO, Godino A, Oliveira FR, Vivas L, Antunes-Rodrigues J. Lateral parabrachial afferent areas and serotonin mechanisms activated by volume expansion. J Neurosci Res. 2008;86:3613–3621.
111. Martini M, Di Sante G, Collado P, Pinos H, Guillamon A, Panzica GC. Androgen receptors are required for full masculinization of nitric oxide synthase system in rat limbic-hypothalamic region. Horm Behav. 2008;54:557–564.
112. Xue B, Zhao Y, Johnson AK, Hay M. Central estrogen inhibition of angiotensin II-induced hypertension in male mice and the role of reactive oxygen species. Am J Physiol Heart Circ Physiol. 2008;295:H1025–H1032.
113. Milner TA, Lubbers LS, Alves SE, McEwen BS. Nuclear and extranuclear estrogen binding sites in the rat forebrain and autonomic medullary areas. Endocrinology. 2008;149:3306–3312.
114. Gerrits PO, Kortekaas R, Veening JG, et al. Estrous cycle-dependent neural plasticity in the caudal brainstem in the female golden hamster: Ultrastructural and immunocytochemical studies of axo-dendritic relationships and dynamic remodeling. Horm Behav. 2008;54:627–639.
115. Milner TA, Mitterling KL, Iadecola C, Waters EM. Ultrastructural localization of extranuclear progestin receptors relative to C1 neurons in the rostral ventrolateral medulla. Neurosci Lett. 2008;431:167–172.
116. Xu Q, Hamada T, Kiyama R, Sakuma Y, Wada-Kiyama Y. Site-specific regulation of gene expression by estrogen in the hypothalamus of adult female rats. Neurosci Lett. 2008;436:35–39.
117. Jansen HT, Popiela CL, Jackson GL, Iwamoto GA. A re-evaluation of the effects of gonadal steroids on neuronal activity in the male rat. Brain Res Bull. 1993;31:217–223.
118. Carlson SH, Wyss JM. Neurohormonal regulation of the sympathetic nervous system: New insights into central mechanisms of action. Curr Hypertens Rep. 2008;10:233–240.
119. Watts SW. Henry pickering bowditch award the love of a lifetime: 5-HT in the cardiovascular system. Am J Physiol Regul Integr Comp Physiol. 2009; 296(2):R252–R256.
120. Watts SW, Rondelli C, Thakali K, et al. Morphological and biochemical characterization of remodeling in aorta and vena cava of DOCA-salt hypertensive rats. Am J Physiol Heart Circ Physiol. 2007;292:H2438–H2448.
121. Ramage AG, Villalon CM. 5-hydroxytryptamine and cardiovascular regulation. Trends Pharmacol Sci. 2008;29:472–481.
122. O'Donaughy TL, Qi Y, Brooks VL. Central action of increased osmolality to support blood pressure in deoxycorticosterone acetate-salt rats. Hypertension. 2006;48:658–663.
123. Pietranera L, Saravia FE, Roig P, Lima A, De Nicola AF. Protective effects of estradiol in the brain of rats with genetic or mineralocorticoid-induced hypertension. Psychoneuroendocrinology. 2008;33:270–281.
124. Van Huysse JW. Endogenous brain na pumps, brain ouabain-like substance and the alpha2 isoform in salt-dependent hypertension. Pathophysiology. 2007;14:213–220.
125. Huang BS, Cheung WJ, Wang H, Tan J, White RA, Leenen FH. Activation of brain renin-angiotensin-aldosterone system by central sodium in wistar rats. Am J Physiol Heart Circ Physiol. 2006;291:H1109–H1117.

126. Komjati K, Velkei-Harvich M, Toth J, Dallos G, Nyary I, Sandor P. Endogenous opioid mechanisms in hypothalamic blood flow autoregulation during haemorrhagic hypotension and angiotensin-induced acute hypertension in cats. Acta Physiol Scand. 1996;157:53–61.
127. Hill-Pryor C, Dunbar JC. The effect of high fat-induced obesity on cardiovascular and physical activity and opioid responsiveness in conscious rats. Clin Exp Hypertens. 2006;28:133–145.
128. Iwamoto GA, Mitchell JH, Sadeq M, Kozlowski GP. Localization of tyrosine hydroxylase and phenylethanolamine N-methyltransferase immunoreactive cells in the medulla of the dog. Neurosci Lett. 1989;107:12–18.
129. Stafford JM, Yu F, Printz R, Hasty AH, Swift LL, Niswender KD. Central nervous system neuropeptide Y signaling modulates VLDL triglyceride secretion. Diabetes. 2008;57:1482–1490.
130. da Silva AA, Tallam LS, Liu J, Hall JE. Chronic antidiabetic and cardiovascular actions of leptin: Role of CNS and increased adrenergic activity. Am J Physiol Regul Integr Comp Physiol. 2006;291:R1275–R1282.
131. Sanders JD, Szot P, Weinshenker D, Happe HK, Bylund DB, Murrin LC. Analysis of brain adrenergic receptors in dopamine-β-hydroxylase knockout mice. Brain Res. 2006;1109:45–53.
132. Ye P, Kenyon CJ, Mackenzie SM, et al. Effects of ACTH, dexamethasone, and adrenalectomy on 11β-hydroxylase (CYP11B1) and aldosterone synthase (CYP11B2) gene expression in the rat central nervous system. J Endocrinol. 2008;196:305–311.
133. Su J, Lei Z, Zhang W, Ning H, Ping J. Distribution of orexin B and its relationship with GnRH in the pig hypothalamus. Res Vet Sci. 2008;85:315–323.
134. Papakonstantinou P, Tziris N, Kesisoglou I, et al. The effect of porcine orexin A on insulin plasma concentrations in pigs. J Biol Regul Homeost Agents. 2007;21:115–124.
135. Yamanaka A, Muraki Y, Ichiki K, et al. Orexin neurons are directly and indirectly regulated by catecholamines in a complex manner. J Neurophysiol. 2006;96:284–298.
136. Jegou S, Cartier D, Dubessy C, et al. Localization of the urotensin II receptor in the rat central nervous system. J Comp Neurol. 2006;495:21–36.
137. Dubessy C, Cartier D, Lectez B, et al. Characterization of urotensin II, distribution of urotensin II, urotensin II-related peptide and UT receptor mRNAs in mouse: Evidence of urotensin II at the neuromuscular junction. J Neurochem. 2008;107:361–374.
138. Sartor DM, Verberne AJ. Abdominal vagal signalling: A novel role for cholecystokinin in circulatory control? Brain Res Rev. 2008;59:140–154.
139. Ruiz-Gayo M, Gonzalez MC, Fernandez-Alfonso S. Vasodilatory effects of cholecystokinin: New role for an old peptide? Regul Pept. 2006;137:179–184.

Chapter 14
Other Transgenic Animal Models Used in Cardiovascular Studies

Previous chapters have described a large number of transgenic animal models used to study specific cardiovascular syndromes. This chapter will fill in some gaps. Many of these transgenic animals were developed to study normal and/or abnormal physiological responses in other organ systems, or to study basic biochemical and molecular reactions or pathways. These models were then discovered to also have effects on the cardiovascular system, some of them unanticipated.

A word of caution, particularly when highly inbred mouse strains are used to develop transgenic models - not all strains of a particular species are created equal. When cardiovascular parameters of age- and sex-matched A/J and C57BL/6J inbred mice were compared the C57BL/6J mice demonstrated eccentric physiologic ventricular hypertrophy, increased ventricular function, lower heart rates, and increased exercise endurance.[1]

It is also important to note that different species will react differently to the introduction of promoter genes. Human ICAM-2 promoter produces strong and uniform endothelial expression in all organs examined in mice. When the identical promoter was used to generate transgenic pigs only two of the pigs showed expression and that was significantly weaker than in the mice and restricted to vascular endothelium in the heart and kidney.[2]

Transgenic animals that harbor luciferase or other marker/reporter proteins have proven to be very useful when used to define in vivo responses to specific perturbations. The reporter protein in these transgenics is under the control of a specific promoter. A few examples of these transgenic animals include the development of CD2-enhanced green fluorescence protein transgenic mice used to characterize lymphocyte trafficking during inflammation.[3] Placier et al.[4] used transgenic mice harboring the luciferase reporter gene under the control of the collagen I-α-2 chain promoter to show that the combination of removing L-NAME and blocking endothelin in the L-NAME model of hypertension normalized collagen-I gene expression and reversed nephroangiosclerosis without marked changes in blood pressure. Pichler et al.[5] describe a universal transgenic reporter mouse strain that expresses firefly luciferase under the regulatory control of a concatenated Gal-4 promoter. They use an adenovirus to deliver a fused binding-domain-activator chimera to induce bioluminescence in tissues that take up the Ga1-4 promoter. Beta-gal expression of the

D.R. Gross, *Animal Models in Cardiovascular Research*,
DOI: 10.1007/978-0-387-95962-7_14, © Springer Science+Business Media, LLC 2009

lacZ gene was used in two transgenic models (cGATA6/lacZ and cardiac conduction system/lacZ) and two targeted gene knock-in models (minK/lacZ and Hop/lacZ) in an attempt to mark portions of the proximal and distal atrioventricular conduction system (AVCS) in mice. Beta-gal expression was consistently observed in the proximal and distal AVCS but it was also observed in the working myocardium outside the AVCS. The reporter system was not expressed in the SA node, and thus it limits the technique.[6]

Sex-Related Responses

Studies using estrogen deletion,[7] phytoestrogen feeding,[8] genetic models, and estrogen receptor antagonists and agonists have demonstrated that both estrogen receptor subtypes (α and β) protect against various forms of cardiovascular disease including ischemia-reperfusion injury, hypertension, ventricular hypertrophy, and chronic heart failure.[9] When low-density lipoprotein LDL$^{-/-}$ female mice were treated with estrogen (E2) there was a delay in atherosclerotic plaque formation. This delay was associated with an increase in DNA strand breaks in the arterial wall. When the same mouse model was fed a high-cholesterol diet and ovarioectomized there was an increase in atherogenesis.[10]

Aromatase knockout mice, both males and females, suffer from a variety of abnormalities including loss of fertility and libido, bone loss, cardiovascular and cerebrovascular problems, and development of metabolic syndrome.[11] Treating arteries from male estrogen receptor-α knockout (ERKO) mice with specific aromatase short-interfering RNA for 72 h knocked down the aromatase mRNA and protein associated with elimination of epoxyeicosatrienoic acid (EET) mediation of flow-induced dilation. This indicates that flow-induced dilation in male ERKO mice arteries is maintained by an EDHF/EET-mediated mechanism compensating for reduced NO because of reduced estrogen aromatized from testosterone.[12]

We were able to demonstrate the important role of estrogen receptor-α in cardiac ischemia-reperfusion injury.[13] Nuclear ER-α$^{-/-}$ (ERKO) mice were used to show that ER-α target genes involved in energy substrate oxidation, ATP synthesis, and phosphate transfer are downregulated at baseline and following pressure overload. The results indicate that ER-α is required for the adaptive bioenergetic response to pressure overload heart failure.[14] During acute lipopolysaccharide (LPS)-induced inflammatory responses ER-α mediates NO synthesis and the vascular responses to NO involving soluble guanylate cyclase.[15]

ER-β$^{-/-}$ (BERKO) mice were used to show that ER-β-mediated mechanisms protect against left ventricular hypertrophy.[16] E2 (estrogen) mitigates Angio-II signaling that produces hypertrophy and fibrosis in female BERKO mice.[17] BERKO mice are protected against high-fat diet-induced insulin resistance and glucose intolerance. The protection involves augmented PPAR-γ signaling in adipose tissue and overexpression of nuclear coactivators such as SRC1 and TIF2.[18] ER-β also plays a role in the cardioprotective effects of estrogen following global, warm ischemia-reperfusion injury.[19] Myocardial infarction-induced heart failure in female

BERKO mice resulted in increased mortality, increased levels of clinical and biochemical markers of heart failure, and impaired expression of Ca^{2+}-handling proteins.[20] Estrogenic effects on Ca^{2+} currents in isolated ventricular cardiomyocytes from WT, ERKO, and BERKO mice show that the inhibition of Ca^{2+} currents and decreased contractility are not dependent upon ER-α or β.[21]

ERKO and BERKO mice were used to reveal that ER-α- and ER-β-dependent pathways regulate distinct, and mostly nonoverlapping, sets of genes that function as an estrogen-regulatory transcriptional network in the vasculature.[22] ER-β seems to modify adrenergic control of small artery tone in males but not in females. This is demonstrated by a gender-specific (male) enhanced response to phenylephrine[23] and reduced endothelium-derived hyperpolarizing factor (EDHF)-mediated relaxation via gap junction communication.[24] NO appears to contribute to the vasodilation response to E2 in femoral arteries from BERKO but not WT mice.[25] ERs play a sex-specific role in small mesenteric arterial estrogen-mediated flow responses and distensibility. Deletion of ER-β affects arterial structure only in male BERKO.[26]

In vascular smooth muscle cells (VSMC) human-inducible nitric oxide synthase (iNOS) transcription is positively regulated by ER-β and negatively regulated by ER-α.[27] Knocking out the gene encoding the catabolic enzyme CYP7B1 decreased estrogen-dependent expression of NOS and repressed carotid artery reendothelialization following endothelial injury.[28]

Female follitropin-receptor knockout (FORKO) mice have an impaired natriuretic peptide system. This could contribute to the susceptibility to develop age-related hypertension in female FORKO mice. This model shows a relationship between estrogen, adipose tissue, and ANP, and it is used as a model for menopause.[29] Aged FORKO mice developed higher levels of Angio-II-induced hypertension, ventricular hypertrophy, and myocardial fibrosis than age-matched WT controls. The Angio-II-induced ventricular hypertrophy and myocardial fibrosis are associated with down-regulation of the endogenous antioxidant thioredoxin (Trx) and upregulation of apoptosis-signal-regulated kinase-1 (ASK-1)/caspase signaling in the FORKO mice.[30]

Kinases

Transgenic mice overexpressing cardiac-specific Lats2, a serine/threonine kinase, have significantly reduced left and right ventricular mass whereas transgenic mice overexpressing dominant-negative Lats2 demonstrate biventricular hypertrophy.[31] G-protein-coupled receptor (GPCR) kinase 2 (GRK-2) is also a serine/threonine kinase. It phosphorylates and desensitizes agonist-bound GPCRs. GRK-2 levels in VSMC are increased in animal models of hypertension. In GRK-2 knockout mice β-adrenergic receptor-mediated dilation was increased while α-adrenergic-mediated vasoconstriction was also increased.[32] Confocal studies of cardiac tissue from transgenic mice overexpressing GRK-2 show a clear increase in relative fluorescence intensity of GRK-2 in the arrhythmia-prone subepicardial border zone following coronary artery ligation.[33] Myocardial thrombin signaling, as assessed by p42/p44 mitogen-activated protein kinase activation, was significantly attenuated in transgenic

mice with cardiac specific overexpression of GRK-3.[34] Transgenic mice overexpressing cardiac-specific dominant-negative glycogen synthase kinase-β (GSK-3-β DN) were produced. Persistent inhibition of GSK-3-β induced compensatory hypertrophy, inhibited apoptosis and fibrosis, and increased cardiac contractility. The antiapoptosis effects of GSK-3-β inhibition are mediated by myeloid cell leukemia-1.[35] When GSK-3-β was used to create a double-transgenic mouse by breeding with a mouse model of hypertrophic cardiomyopathy (HCM) the male animals had reduced contractility, reduced sarcoplasmic (endo) reticulum Ca^{2+}-ATPase expression, elevated ANF expression, and premature death. Female HCM/GSK-3-β double-transgenic mice demonstrated cardiac histology, function, and survival the same as their female HCM littermates.[36]

Hypertension was induced using uninephrectomy and DOCA-salt in Axl (a receptor tyrosine kinase) knockout ($Axl^{-/-}$) mice. The results indicate a likely mechanism for Axl-dependent effects on hypertension.[37] Studies conducted in serum- and glucocorticoid-inducible kinase-1 knockout mice ($SGK\text{-}1^{-/-}$) indicate that this kinase may play a decisive role in fetal programming of hypertension induced by prenatal protein restriction.[38]

Reactive oxygen species (ROS) generated during ischemic preconditioning could be responsible for altering mitochondrial metabolism by oxidizing key mitochondrial enzymes in the hearts of protein kinase C-delta knockout ($PKC\text{-}delta^{-/-}$) mice. Metabolic adaptation to preconditioning is also impaired in this animal model.[39] In transgenic mice that overexpress specific cardiomyocyte Ca^{2+}/calmodulin-dependent myosin light chain kinase-increased regulatory light chain phosphorylation was not responsible for cardiac hypertrophy. It apparently inhibits hypertrophy by contributing to enhanced contractility and myocardial efficiency.[40]

The hearts of transgenic mice overexpressing the regulatory γ-subunit of AMP-activated protein kinase (PPKAG2) resist low-flow ischemic injury better than controls. This resistance was associated with increased consumption of glycogen but this was unrelated to AMP-activated protein kinase activation.[41] The intimal thickness-related receptor (ITR) is expressed in rabbit aortic smooth muscle cells following injury. The sequence contains a motif common to the Rhodopsin-like GPCR superfamily. ITR seems to be a novel receptor that could play a role in vascular remodeling.[42]

Cardiac-specific transgenic mice with increased or decreased phosphoinositide 3-kinase (PI3K) activity were crossed with a transgenic mouse model of dilated cardiomyopathy (DCM). Exercise training and increased PI3K activity prolonged survival in the DCM model by 15-20%. Reduced PI3K activity shortened survival by about 50%.[43]

Oxidases and Oxygenases

Transgenic mice deficient in gp91phox, an NADPH oxidase subunit protein, designated $gp91^{-/-}$ mice were used to define mechanisms involved in DOCA-salt-induced hypertension. The findings indicated that vascular superoxide ion overproduction

via gp91phox-containing NADPH oxidase is involved in the development of hypertension in this model.[44] Using mice lacking the p47phox subunit of the NADPH oxidase (p47phox$^{-/-}$) Salguero et al.[45] show that in WT mice 2K1C hypertension was associated with a fourfold increase in endothelial progenitor cells (EPCs). In p47phox$^{-/-}$ mice there was a significantly less increase in arterial pressures and no change in EPCs.

Coronary ligation was performed in gp91phox$^{-/-}$ and WT mice. Mortality was significantly higher in the gp91phox$^{-/-}$ mice but the progression of left ventricular remodeling was not affected by phenotype. Systemic oxidative stress was not reduced in gp91phox$^{-/-}$ mice since there was a significant increase in lipid peroxides probably mediated by the observed increase of the NADPH subunit nox-1 in gp91phox$^{-/-}$ mice.[46]

Heme oxygenase is a cytoprotective enzyme that degrades heme to generate carbon monoxide, bilirubin, and iron. Two rodent models, Gunn rats (hyperbilirubinemic) and heme oxygenase-1 knock out (HO-1$^{-/-}$) mice, were used to evaluate DOCA-salt hypertension. Uninephrectomized WT rats treated with DOCA-salt had significantly increased arterial pressures but the response was attenuated in Gunn rats. The response in the Gunn rats was not due to a greater induction of HO-1 in the vasculature or due to an increase in renal Na^+ excretion. Using HO-1$^{-/-}$ mice Wiesel et al.[47] reported that chronic deficiency of HO-1 does not alter basal blood pressure, but when the HO-1$^{-/-}$ mice were exposed to 1K1C there was more severe renovascular hypertension and cardiac hypertrophy, an increase in ischemic damage, and higher mortality rates. DOCA-salt induced HO-1 protein in HO-1$^{+/+}$ mice but there was no increase in arterial pressures. The same DOCA-salt regimen in HO-1$^{-/-}$ mice produced significant increases in arterial pressures.[48]

Adenosine and Adrenergic Receptors

Adenosine receptors belong to a large family of GPCRs containing four receptor subtypes. In keeping with the physiological model of yin and yang (accelerator and brake), receptor subtypes designated A1R and A3R mediate *inhibition* of adenylyl cyclase and subtypes A2aR and A2bR mediate *stimulation* of adenylyl cyclase. All of the identified receptor subtypes have now been used to create knockout mouse models and some have been used in overexpression models. Various activities related to normal cardiovascular function and to CNS regulation of CV function have been identified using these transgenic models. Some responses are reduced and others enhanced depending upon the specific receptor that has been deleted or overexpressed.[49] Some examples are as follows: in the mouse heart, A1R inhibits β-adrenergic-induced myocardial contractility whereas A2aR opposes the action of A1R and enhances myocardial contractility. During low-flow myocardial ischemia A2aR supports myocardial contractility.[50] Mice with deletion of adenylyl cyclase type V (AC-V$^{-/-}$) demonstrate enhanced basal left ventricular function than WT controls, but there is a reduced response to β-adrenergic stimulation.[51]

In the subcommissural bed nucleus of the stria terminalis norepinephrine (NE)-induced decreases in synaptic transmission are markedly reduced in α2-adrenergic receptor knockout (α2-AR$^{-/-}$) mice.[52] α2-ARs directly regulate the release of NE, but not dopamine, at the terminal level in the nucleus accumbens in mice. α2-AR$^{-/-}$ mice have been used to show that these receptors regulate dopamine indirectly via their effects on dopamine neurons in the ventral tegmental area. The mechanism(s) for this indirect regulation were yet to be described in 2004.[53] In WT mice rilmenidine, moxonidine, and clonidine all produce dose-dependent decreases in blood pressure and heart rate. In D79N α2-AR$^{-/-}$ mice there were no responses to these agents indicating that α2-ARs are responsible for the cardiovascular effects of these drugs.[54] α2c-AR overexpression increased the development of behavioral despair and associated cardiovascular responses associated with increased corticosterone levels following stress. α-2c$^{-/-}$ mice demonstrated attenuated corticosterone levels and cardiovascular responses when exposed to equal levels of stress.[55]

The effects of alterations in the level of myocardial β-adrenergic receptor kinase (β-ARK-1) were studied in β-ARK-1$^{+/-}$ (heterozygous) mice and a mouse model heterozygous for β-ARK-1 and transgenic for cardiac-specific overexpression of β-ARK-1 COOH-terminal inhibitor peptide (β-ARK-1$^{+/-}$/β-ARK-1ct). These studies suggest that the level of β-ARK-1 activity can modulate contractile function. Even partial inhibition of β-ARK-1 activity enhances β-adrenergic receptor signaling and results in improved catecholamine responsiveness.[56]

Dopamine (D2)-receptor knockout (D2R$^{-/-}$) mice were used to demonstrate that pituitary vascular endothelial growth factor (VEGF) expression is under dopaminergic control and may be critical for pituitary angiogenesis via paracrine actions in female D2R$^{-/-}$ mice.[57] "Beta-less" mice are triple adrenoreceptor knockouts (β-1/β-2/β-3 AR$^{-/-}$). In these animals the lipolytic response to NE and β-AR agonists is blunted, but a residual low-affinity lipolytic effect is observed in the presence of catecholamines and β-3-AR agonists but not β-1- or β-2-AR agonists. The residual lipolytic effect is attributed to an unknown GPCR with low affinity for catecholamines.[58]

Nitric Oxide Synthase

In eNOS$^{-/-}$ mice, chronically treated with L-NAME, blood pressure decreased while eNOS$^{+/-}$ and eNOS$^{+/+}$ mice both developed hypertension.[59] eNOS$^{-/-}$ mice also develop fasting hyperinsulinemia, hyperlipidemia, and decreased insulin-stimulated glucose uptake.[60] Pulmonary endothelial cells were isolated from eNOS$^{-/-}$ mice and grown without E2. In control WT cells E2 significantly increased telomerase activity but in the eNOS$^{-/-}$ cells exogenous eNOS or an NO donor were needed to normalize the level of telomerase activity.[61] Billon et al.[62] used eNOS$^{-/-}$ mice to document that the presence, but not the enzymatic activity, of eNOS is necessary for estrogen signaling in the endothelium.

Transgenic mice that overexpress eNOS were used to discover that ventilator-induced lung injury could be reduced significantly by excess eNOS. The mechanism

for this protection seems to be inhibition of the production of inflammatory chemokines and cytokines associated with neutrophilic infiltration.[63] eNOS overexpression is also able to prevent the development of 2K1C renovascular hypertension in mice.[64] At the University of Missouri-Columbia transgenic pigs carrying an endogenous eNOS gene driven by a Tie-2 promoter and tagged with a V5 His tag have been developed.[65]

Metabolic Syndrome

Obesity and obesity-linked insulin resistance are significant causes of the metabolic syndrome characterized by adipocyte hypertrophy. Adipose tissue is an important regulator of energy homeostasis. It functions as an endocrine organ secreting adipokines including adiponectin (APN). Studies using adiponectin transgenic (overexpression) and knockout mice demonstrate that adiponectin is an insulin-sensitizing adipokine and that obesity can result in insulin resistance and diabetes. At least two different adiponectin receptors have been cloned (AdipoR1 and ApipoR2) comprising a novel cell-surface receptor family acting as receptors for globular and full-length adiponectin. These receptors mediate increased activity of AMP-activated protein kinase, and PPAR-α, as well as glucose uptake and fatty-acid oxidation by adiponectin.[66,67] Intraglomerular macrophage infiltration and mRNA levels of VCAM-1, MCP-1, TNF-α, TGF-β, collagen type I/III, and NADPH oxidase are all increased in adiponectin knockout ($APN^{-/-}$) mice than in WT, when subjected to subtotal nephrectomy and the resulting hypertension. Changes in the $APN^{-/-}$ mice resulted in glomerular and tubulointerstitial injury from increased inflammation and oxidative stress.[68] Studies conducted on transgenic mice overexpressing native full-length APN, targeted to white adipose tissue, revealed that adipose mass and adipocyte size were reduced while caloric intake was maintained constant. $APN^{-/-}$ mice also show decreases in preadipocyte factor-1 mRNA and increased CCAAT/enhancer binding protein-α in white adipose tissue.[69] Shinmura et al.[70] compared adiponectin antisense transgenic mice with WT to demonstrate that the cardioprotective effects of short-term caloric restriction are mediated by increased production of adiponectin and the resulting activation of AMP-activated protein kinase.

The insulin receptor knockout ($IR^{-/-}$) mouse is a genetic model of resistance to insulin's indirect effects on hepatic glucose production. This model demonstrates high levels of adiponectin in the blood with normal adiponectin receptor levels and was used to provide evidence that adiponectin potentiates hepatic insulin sensitivity.[71]

Carvalho et al.[72] crossed glucose transporter-4 knockout ($GLUT\text{-}4^{-/-}$) mice with mice overexpressing GLUT-4 only in adipose tissue (AG-4-TG). Overexpression of GLUT-4 reduces fasting hyperglycemia and glucose intolerance in $GLUT\text{-}4^{-/-}$ mice to subnormal levels and reduces whole body insulin resistance without restoring glucose transport in muscle.

Adipose fatty acid binding protein knockout (A-FABP$^{-/-}$) mice have increased fat mass, decreased lipolysis, increased muscle glucose oxidation, and attenuated insulin resistance. Mice overexpressing epithelial FABP in adipose tissue have the exact opposite phenotype. These observations suggest that the balance between adipocyte lipolysis and lipogenesis is remodeled in animal models that reprogram adipokine expression in fat cells and plasma adipokine homeostasis.[73]

Transgenic mice that overexpress protein phosphatase-1 (PP-1) glycogen-targeting subunit (PTG), driven by the adipocyte fatty acid binding protein promoter (PTG-TG), were found to have exogenous PTG in gonadal, perirenal, and brown fat depots, but not in any of the other tissues studied. PTG overexpression was associated with a modest redistribution of PP-1 to glycogen particles. The results of these experiments suggest that in vivo mechanisms may exist to maintain adipocyte glycogen storage at physiological set points.[74]

Regucalcin is a multifunctional regulatory protein in intracellular signaling pathways. Female regucalcin transgenic (RC-TG) rats were compared at 7 and 50 weeks of age. As these animals age disorders of lipid metabolism in adipose tissue and liver are observed and levels of gene expression of leptin and adiponectin are reduced.[75]

Hemochromatosis gene knockout (Hfe$^{-/-}$) mice have increased plasma adiponectin levels and increased activation of AMP-dependent kinase. Following glucose challenge these animals have decreased glucose excursions compared with WT controls. The decreased glucose excursions are mediated by insulin-independent increased glucose disposal.[76]

Feeding a high-fat diet to low-density lipoprotein receptor knockout (LDL-R$^{-/-}$) mice results in obesity, hyperglycemia, hyperlipidemia, and upregulation of serum TNF-α. Mice with augmented vascular TNF-α, produced by a transgene (SM22-TNF-α-TG) driven by the SM22 promoter, had upregulated aortic Msx2, Wnt3a, and Wnt7a transcription proteins that contribute to the aortic calcification seen in type-II diabetic mouse models.[77]

Infusion of a large number of CD4+ helper T (Th) cells overcomes ovalbumin (OVA)-specific immune tolerance in transgenic rat insulin promoter (RIP)-mOVA mice. This results in CD+ cytotoxic T lymphocyte-mediated destruction of pancreatic islet cells and diabetes. Major histocompatibility complex (MHC) gene knockout (MHC-II$^{-/-}$) mice lack CD4+ T cells. When CD4+ Th cells are injected into MHC-II$^{-/-}$ mice the OVA-specific CD8+ T-cell response is stimulated. These findings could have significant implications in autoimmunity, antitumor immunity, and regulatory T-cell-dependent immune suppression, important in xenotransplantation studies.[78]

Xenotransplantation

Research in xenotransplantation is directed at solving the ever-increasing shortage of organs for human transplantation. It also offers new information related to the development of cell- and tissue-based therapies. Real progress in xenotransplantation has been delayed by the presence of xenoreactive natural antibodies that bind to the

foreign cell surface and activate complement resulting in graft rejection. Genetic engineering of donor cells and animals to express human complement inhibitors such as hCD59 has significantly prolonged graft survival. Expression of human α, 2-fucosyltransferase (HT) in pigs modifies the cell-surface carbohydrate phenotype and results in reduced G-α-1, 3-Gal expression and decreased antibody binding. Hearts from transgenic pigs that coexpress hCD59 and HT were perfused with human blood. These hearts demonstrated increased resistance to human serum-mediated lysis.[79]

Targeting xenograft rejection using single genetic modifications has proven to be ineffective. This led to development of pigs that express human decay accelerating factor (hDAF). Hearts from hDAF transgenic pigs seem to be protected during perfusion with human blood or blood components. They are metabolically stable and maintain acceptable hemodynamic function longer than previous models.[80-83] Expression of human complement regulating factor (hCRF) in pig organs seems to prevent hyperacute rejection of these organs after xenotransplantation to nonhuman primates. Arteries from pigs transgenic for human CD46 expression demonstrate augmented endothelium-dependent relaxation responses to bradykinin mediated by the release of endothelium-derived relaxing factors other than NO.[84]

Pigs transgenic for human membrane cofactor protein (hMCP) were crossed with pigs heterozygous for hDAF. Endothelial cells from this cross were exposed to complement-mediated damage. Cells expressing both hMCP and hDAF were not better protected than cells expressing only hDAF.[85]

Transgenic CMy-mOVA mice were subjected to adoptive transfer of OVA-specific CD8+ effector T cells expressing OVA in cardiac myocytes. The studies conducted on these animals indicate that granulocytic inflammation sustains CD8+ T-cell-mediated myocarditis. This is important knowledge related to allograft rejection.[86]

Hearts from transgenic mice expressing viral interleukin (vIL-10), encoded in the Epstein-Barr virus genome, were transplanted as vascularized allografts into unmodified MHC full-mismatched or MHC class II-disparate mice. Results from these studies indicate that a high level of expression of vIL-10 in grafts can exacerbate immunological rejection.[87]

Liver sinusoidal endothelial cells are capable of selectively suppressing the expansion of IFN-γ-producing cells but are also capable of promoting the outgrowth of IL-4-expression in T helper (Th) cells thus creating an immune suppressive milieu in the liver.[88] Donor hearts from B6.C-H2 mice were transplanted into WT and IL-10 transgenic recipients. In IL-10 TG recipients murine IL-10 is produced under control of the human IL-2 promoter. IL-10 expression inhibited the development of allograft vasculopathy.[89] Hearts from IL-4 transgenic mice, under the control of a cardiac α-myosin heavy chain promoter, were transferred into unmodified recipients. Although the investigators were able to establish that Th-2 bias may contribute to allograft acceptance in this model, probably by inducing the down-regulation of Th-1-cytokine mRNAs, they were not able to conclude that those reactions were able to confer long-term graft survival.[90]

Two lines of transgenic mice express β-galactosidase (β-gal) exclusively in endothelial cells (EC). TIE2-lacZ mice express β-gal in all EC and VWF-lacZ mice

express β-gal only in the microvascular EC of the heart and brain. Using these animal models Rothermel et al.[91] found that EC express intracellular "self" proteins to the immune system but this antigen expression does not delete or stimulate a large population of specific lymphocytes that respond to the same protein following conventional immunization with protein or expression vector DNA. The results of these experiments indicate that context sensitivity in the immune recognition of EC exists and that this phenomena needs to be considered in the context of xenotransplantation.

Na^+/Ca^{2+} and Na^+/H^+ Exchangers

Studies on transgenic mice overexpressing canine cardiac Na^+/Ca^{2+} exchanger (cNCX) indicate that this exchanger could be an important Ca^{2+} transport mechanism in myocardial dysfunction. During ischemia-reperfusion injury increased $[Ca^{2+}]$ in the sarcoplasmic reticulum, the result of increased Na^+/Ca^{2+} exchange activity, can compromise contractile performance and result in cardiac hypertrophy and heart failure.[92] The *NCX* gene contains at least three promoters, H1, K1, and Br1, resulting in multiple tissue-specific variants of the NCX. The H1 promoter directs cardiac-specific expression of NCX in both the embryo and adult and is probably responsible for upregulation of cNCX in response to pressure overload.[93]

Postrest potentiation was compared in transgenic mice overexpressing cNCX and mice with a deletion mutant of cNCX (Delta680-685). The Delta680-685 mice are devoid of intracellular Na^+- and Ca^{2+}-dependent regulatory properties. Postrest potentiation was greater in Delta680-685 mice than in the cNCX animals indicating that ionic regulation of sodium/calcium exchange plays a significant functional role in myocardial contractility.[94] Other studies using isolated myocytes from the same models suggest that beat-to-beat changes in cNCX function can occur in vivo.[95]

Overexpression of cNCX in isolated myocytes from transgenic mice appears to accelerate the decline of $[Ca^{2+}]i$ during relaxation. Increased Ca^{2+} influx also appears to occur.[96] Null mutation of the *cNCX* gene is lethal resulting in embryonic death (9.0-9.5 days). When transgenic mice expressing canine cNCX were bred to $cNCX^{+/-}$ mice this did not prevent the lethal results.[97] Isolated thoracic aortic rings from transgenic mice that specifically overexpress NCX in smooth muscle were used to show that NCX was involved in the forskolin-induced reduction of tension resulting from decreased $[Ca^{2+}]i$.[98] The reverse NCX current was measured in isolated ventricular myocytes from WT and transgenic mice overexpressing NCX. Currents were significantly higher (>twofold) in the transgenic myocytes.[99]

Transgenic mice that overexpress the human sarcolemmal Na^+/H^+ exchanger (hNHX), with high cardiac activity, develop hypertrophy, contractile dysfunction, and heart failure. These changes are mainly the result of activation of calmodulin-dependent protein kinase-II (CaMK-II)-dependent phorphorylation of phospholamban (PLB).[100]

Inflammatory Cytokines

Several laboratories have reported the results of experiments using transgenic mice overexpressing cardiac-specific TNF-α or β using a variety of different strategies and/or promoters.[101-107] These animals develop concentric ventricular hypertrophy,[101,102] modify desmin so that it loses its intercalated disk localization and forms aggregates that colocalize with heat shock protein 25 and ubiquitin,[106] and demonstrate atrial structural remodeling, downregulation of connexin-40, and an increased incidence of atrial arrhythmias.[104]

Sekiguchi et al.[105] were able to demonstrate that overexpression of TNF-β signaling pathways suppresses PPAR-α activity and reduces cardiac fatty acid β-oxidation in cardiac myocytes. Increased matrix metalloproteinase (MMP)-3 in male TNF-α transgenic mice might regulate activation of MMP-9/gelatinase initiating the progression of cardiac remodeling and the development of heart failure.[103] Sustained proinflammatory signaling in the hearts of adult transgenic mice overexpressing TNF-β is associated with a profibrotic phenotype that activates Smad 2/3 leading to increased myocardial fibrosis and loss of compliance in the left ventricle.[107]

Transgenic mice with murine IL-10 under the control of the human IL-2 promoter fed a high-fat diet demonstrate decreased atherosclerotic lesions compared with WT controls.[108] Overexpression of IL-10 by T cells inhibits atherogenesis in $LDLR^{-/-}$ mice fed a high-fat diet.[109]

Willuweit et al.[110] generated transgenic mice expressing a noncleavable transmembrane form of TNF under control of the endothelial-specific tie2 promoter. These mice develop chronic inflammatory disease in kidney and liver but were protected from immune-mediated liver injury following Con A-induced acute hepatitis. Interferon-γ transgenic mice constitutively express IFN-γ in their livers and therefore have high circulating serum levels and develop chronic active myocarditis.[111]

LPS-induced toxicosis is characterized by hypermetabolism and anorexia in mice. TNF-$\alpha^{-/-}$ mice show a reduction in the amount of LPS-induced hypermetabolism but no change in anorexia. Lymphotoxin-$\alpha^{-/-}$ mice show the same responses to LPS as the TNF-$\alpha^{-/-}$ mice. Results from experiments using soluble tumor necrosis factor receptor-1 fusion protein (TNFR1-$IgG^{-/-}$) transgenic mice indicate that the hypermetabolic and anorexic responses are independently regulated. Interferon-γ receptor knockout mice showed the strongest anorexic response following LPS exposure.[112] TNF-$\alpha^{-/-}$ mice show a reduction in reactive stenosis following endothelial injury.[113]

Intercellular adhesion molecule-1 knockout (ICAM-$1^{-/-}$) mice were subjected to myocardial ischemia and reperfusion at 2 h, 1 week, and 3 weeks. The absence of ICAM-1 expression was associated with less myocardial damage following early reperfusion but the size of the infarction or scar formation was not changed.[114] β-1-integrin knockout (β-$1^{-/-}$) mice subjected to myocardial ischemia-reperfusion injury demonstrated reduced neutrophil infiltration in the ischemic regions but there was no effect on the severity of myocardial damage.[115]

Peroxisome Proliferator-Activated Receptor

Peroxisome proliferator-activated receptor (PPAR) alpha (PPAR-α) is a key driver of diabetes-related lipid metabolic dysregulation. Transgenic mice overexpressing PPAR-α (PPAR-α-TG) have decreased GLUT-4 mRNA levels and decreased glucose uptake.[116] PPAR-α-TG mice also demonstrate reduced β-adrenergic responses in contractility and chronotropy compared with WT controls.[117] Electrophysiological experiments conducted on myocytes from both the left and right ventricles of PPAR-α-TG and WT control mice reveal marked K^+ current remodeling in the mice overexpressing PPAR-α.[118]

DOCA-salt hypertension was induced in WT controls and PPAR-$\alpha^{-/-}$ mice. These studies reveal that the PPAR-α pathway induces renal tubular 20-hydroxyeicosatetranenoic acid (20-HETE) production regulating Na^+ retention and blood pressure.[119] The Na^+ and blood pressure regulation in PPAR-$\alpha^{-/-}$ mice is also affected via amiloride- and thiazide-sensitive mechanisms, so this model is not hypertensive but develops salt-sensitive hypertension despite defective fatty acid oxidation.[120]

Transgenic mice expressing PPAR-γ1 in the heart, via the cardiac α-myosin heavy chain promoter, have increased cardiac expression of fatty acid oxidation genes and increased lipoprotein triglyceride uptake. Heart glucose gransporter-4 (GLUT-4) mRNA expression and glucose uptake are not decreased. These animals develop DCM associated with increased lipid and glycogen stores, and abnormal ultrastructural changes in the mitochondria and cristae. Loss of PPAR-γ in myeloid cells impairs alternative macrophage activation and predisposes PPAR-$\gamma^{-/-}$ mice to the development of diet-induced obesity, insulin resistance, and glucose intolerance.[121]

Renin-Angiotensin System

Transgenic mice overexpressing angiotensinogen have decreased caspase recruitment domain (ARC), catalase expression, and protein kinase-2 (CK-2) levels. Catalase, CK-2, and ARC are an antihypertrophic pathway in the heart.[122] Transgenic mice that overexpress rat angiotensinogen in their proximal tubule cells were used to demonstrate that the intrarenal renin-angiotensin system (RAS) stimulates proximal tubule cell apoptosis and tubulointerstitial fibrosis, at least in part, by enhanced NADPH oxidase activity and ROS generation independent of hypertension.[123]

Double-transgenic rats harboring both human renin and human angiotensinogen genes were compared with Sprague-Dawley normal controls in experiments with and without a p38 inhibitor. The p38 mitogen-activated protein kinase inhibitor improved survival, target organ damage, and arrhythmogenic potential in these double-transgenic rats.[124]

Angio-II subtype 1A receptor (ATR-1A)$^{-/-}$ and WT mice were subjected to 2K1C renovascular hypertension and were compared. Arterial blood pressures were significantly lower in the ATR-1A$^{-/-}$ mice. Clip placement, ATR-2 blockade, and NOS activity did not alter the hypertension in this knockout model.[125,126]

Bradykinin-2 Receptor

Myocardial eNOS and mitogen-activated protein kinases (MAPK), including ERK, p38, and JNK, protein expression were measured in bradykinin-2 receptor (BR-2) knockout (BR-2$^{-/-}$) mice. Disruption of BR-2 resulted in maladaptive cardiac hypertrophy with downregulation of eNOS and upregulation of MAPK. These results were reversed by treatment with a NOS inhibitor.[127] BR-2$^{-/-}$ and their normal 129/SvEvTac WT controls were compared to evaluate the hypertensive effects of DOCA-salt and aortic coarctation. In this model kinins, acting via B-2 receptors, do not participate in the maintenance of normal arterial pressures or the establishment and maintenance of hypertension resulting from either treatment. Both BR-2$^{-/-}$ and WT mice reacted similarly to DOCA-salt and aortic coarctation when treated with angiotensin-converting enzyme inhibition, i.e., hypertension and ventricular hypertrophy were prevented.[128] However, Madeddu et al.[129] used BR-2$^{-/-}$ and WT to conclude that kinins, acting on the BR-2, exert protection against excessive hypertension in the early phases of 2K1C.

Apolipoprotein-E and Low-Density Lipoprotein Knockout Models

Apolipoprotein-E (ApoE$^{-/-}$), C57BL/6 WT, and sham-operated mice were compared following 2K1C renovascular hypertension. ApoE$^{-/-}$ mice developed less of an increase in aortic wall area than that seen early in the WT controls but the aortic lumen area was increased to a similar magnitude in both 2K1C models.[130] The effects of 1K1C and 2K1C renovascular hypertension were compared in ApoE$^{-/-}$ mice. 2K1C animals developed significantly more atherosclerotic lesion area and enhanced accumulation of macrophages, accompanied by a parallel increase in scavenger receptor-A expression in the macrophages, in the aortic sinus than did the 1K1C mice. This suggests that increased generation of Angio-II in the 2K1C model may initiate and promote atherosclerosis via activation of VSMC.[131] When ApoE$^{-/-}$ mice were fed a high-fat diet and subjected to 2K1C renovascular hypertension they were unable to increase renin secretion and blood pressure in response to diminished renal perfusion compared with ApoE$^{-/-}$ mice fed a regular diet.[132]

ABCG1 is a member of the G subfamily of ATP-binding cassette (ABC) transporters. Overexpression of ABCG1 alone can induce cholesterol efflux to HDL. When bone marrow from ABCG1$^{-/-}$ mice is transplanted into ApoE$^{-/-}$ or LDL$^{-/-}$ mice the amount of atherosclerotic lesion developed is reduced. ABCG1$^{-/-}$ mice were crossed with LDL$^{-/-}$ mice and the offspring (ABCG1/LDL$^{-/-}$) were compared with LDL$^{-/-}$ mice after both were placed on a high-fat diet. No major differences were observed in total plasma lipids but IDL-LDL cholesterol was significantly increased in the double-knockout mice as was the amount of atherosclerotic lesions. Plasma levels of MCP-1 and TNF-α were also increased in the double-knockout mice.[133]

BACH-1 is a nuclear protein that directly interacts with the highly conserved C-terminal BRCT repeats of the tumor suppressor BRCA-1. BACH-1/ApoE$^{-/-}$ (double knockout) mice were generated by crossing BACH-1$^{-/-}$ and ApoE$^{-/-}$ mice. These mice were fed a high-fat diet for 8 weeks. The double-knockout mice had significantly less atherosclerotic lesion formation, a result of upregulation of heme oxygenase-1 in the endothelium and, to a lesser extent, in the vascular smooth muscle.[134]

Mice transgenic for lysozyme (LZ-TG) are resistant to both acute and chronic oxidative stress. They display decreased circulating levels of pro-oxidant advanced glycation end products (AGEs). The degree of atherosclerosis was evaluated in LZ-TG mice crossed with ApoE$^{-/-}$ mice (LZ/ApoE$^{-/-}$). Serum levels of LZ were increased, levels of AGE and 8-isoprostanes were decreased, but hyperlipidemia was similar to ApoE$^{-/-}$ controls. The LZ/ApoE$^{-/-}$ transgenic mice had significantly less atherosclerotic plaque, neointimal lesions, and inflammatory infiltrates than the controls, and femoral arterial lesions following injury were also reduced.[135]

Toll-Like Receptors

Two strains of toll-like receptor TLR-4$^{-/-}$ mice (C57/BL10 ScCr and C3H/HeJ) were compared with control strains (C57/BL10 ScSn and C3H/OuJ). All four groups were subjected to 1 h of coronary ligation followed by 24 h of reperfusion. The TLR-4$^{-/-}$ animals had less infarcted area, less neutrophilic infiltration, less myeloperoxidase activity, and fewer lipid peroxides and complement deposition than controls.[136] TLR-4$^{-/-}$ mice demonstrate improved left ventricular function and reduced LV remodeling following coronary ischemia-reperfusion injury than WT controls.[137] When TLR-2$^{-/-}$ mice were compared with WT controls, following coronary ischemia-reperfusion injury, survival rates were significantly higher in the TLR-2$^{-/-}$ mice but infarct size and degree of inflammatory cell infiltration were similar. There were significantly less myocardial fibrosis, TGF-β, and collagen type-I mRNA expressions in the noninfarct area of the knockout mice.[138] The same laboratory found that inflammatory responses and neointimal hyperplasia were reduced in TLR-2$^{-/-}$ mice following the placement of an external cuff around the femoral artery.[139]

Caveolin-1 (Cav-1)

Ectonucleoside triphosphate diphosphohydrolase-1 (CD39) is a plasma membrane ectoenzyme that regulates purinergic receptor signaling by controlling the levels of extracellular nucleotides. Using Cav-1$^{-/-}$ mice Papanikolaou et al.[140] demonstrated that caveolae are not essential for the enzymatic activity of CD39 or for its targeting to plasma membrane. Cav-1 TG mice that overexpress Cav-1 show that endothelial-specific expression of Cav-1 impairs endothelial NOS activation, endothelial

barrier function, and the angiogenic response to exogenous VEGF and ischemia. VEGF-mediated phosphorylation of Akt and eNOS were significantly reduced in Cav-1 TG mice compared WT littermates.[141]

Long QT Syndrome

Transgenic rabbits that lack slowly activating delayed rectifier K^+ currents (IKs), designated LQT-1 (long QT-1), and another rabbit model that generates repolarizing K^+ currents (IKr) (long QT-2)[142] have been generated. These TG rabbits were produced by expression of pore mutants of the human genes designated *KCNQ1* (KvLQT1-Y315S) and *KCNH2* (HERG-G628S) in the heart. Both TG rabbits demonstrate prolongation of the QT interval and prolonged action potentials associated with the elimination of IKs and IKr currents. In these animals the elimination of one repolarizing current was associated with downregulation of the reciprocal repolarizing current. This is different from the compensatory upregulation that has been observed in long QT syndrome (LQTS) mouse models.[143-145]

Nuclear Factor Kappa-B

Mice expressing a luciferase reporter, whose transcription is dependent upon nuclear factor kappa-B (NF-κB) activation, were studied after myocardial infarction. A significant increase in NF-κB activity was observed with the maximum response 3 days following infarction.[146] Mice with NF-κB subunit p50 knocked out (p50/NF-$\kappa B^{-/-}$) were compared with WT controls following coronary artery ligation and ischemia-reperfusion injury. Ventricular dilation, early mortality, and ischemia-reperfusion injury were significantly reduced in the p50/NF-$\kappa B^{-/-}$ animals compared WT controls.[46,147,148] Pharmacological inhibition of aldose reductase, or knockdown of the enzyme by small interfering RNA, prevents the activation of NF-κB and the release of TNF-α and increased survival in mice injected with lethal doses of LPS.[149]

Transgenic Cre/lox mice with endothelial cell-restricted NF-κB super-repressor IkappaBalphaDeltaN (Tie-1-DeltaN) overexpression were subjected to hypertension by feeding a high-salt diet and L-NAME plus infusion of Angio-II. Both Tie-1-DeltaN and control mice demonstrated equal levels of hypertension. Tie-1-DeltaN mice developed less renal injury, reduced inflammatory responses, and less albuminuria than controls. There was also a significantly reduced expression of ICAM-1 and VCAM-1, targets of NF-κB. The investigators concluded that in vivo NF-κB suppression in endothelial cells blocks a signaling cascade leading to reduced hypertension-induced renal damage in the face of hypertension.[150]

A20 was first described as a TNF-inducible gene in human umbilical vein endothelial cells that inhibits NF-κB signaling and protects against apoptosis, inflammation, and cardiac hypertrophy. Transgenic mice containing the human *A20*

gene, under the control of the α-myosin heavy chain promoter, exhibit cardiac-specific overexpression of A20. Following acute coronary artery ligation these mice have improved cardiac function and less cardiac remodeling, apoptosis, inflammation, and fibrosis than controls.[151]

Orphan Nuclear Receptors

Orphan nuclear receptors, ERR-α and ERR-γ, act as nonobligatory heterodimers and target a common set of promoters involved in energy substrate uptake, the production and transport of ATP across mitochondrial membranes, intracellular fuel sensing, Ca^{2+} handling, and myocardial contractility.[152] Disruption of the *ERR-γ* gene, highly expressed in fetal and postnatal hearts of mice, results in lactatemia, cardiac arrhythmias, and mortality during the first week of life.[153]

Steroid receptor coactivator-1 (SRC-1) is a transcriptional coactivator for nuclear receptors including estrogen receptors (ER). SRC-$1^{-/-}$ mice were used in studies to demonstrate that SRC-1 is expressed in endothelial cells, VSMC, and neointimal cells. Neointimal growth, induced by injury to the common carotid artery, was almost completely inhibited by estrogen in WT mice but only partially inhibited in the SRC-$1^{-/-}$ mice.

Troponin

Troponin T (TnT) is essential to the Ca^{2+} regulatory system of striated muscle. Three specific fiber-type TnT genetic isoforms encoding cardiac, slow- and fast-twitch skeletal muscle have been identified. Intact cardiac muscle strips from transgenic mice overexpressing fast-twitch skeletal muscle TnT show decreased contractility at acidic pH than the same preparations from WT control mice.[154]

Transgenic mice that overexpress cardiac troponin-I (TnI) have serine residues normally targeted by protein kinase A (PKA) that are mutated to aspartic acid and mimic constitutive phorphorylation. These animals have slightly enhanced basal systolic and diastolic left ventricular function but display a marked increase in frequency-dependent inotropy and relaxation compared with control mice.[155]

Hemodynamic studies were conducted in mice that express normal levels of PLB and express either cardiac troponin-I (PBL/cTnI) or the slow skeletal isoform of TnI (PBL/ssTnI). The latter cannot be phosphorylated by PKA. Another construct of mice that do not express PBL and express either cTnI ($PBL^{-/-}$/cTnI) or ssTnI ($PBL^{-/-}$/ssTnI) was also studied. PBL/ssTnI hearts demonstrated a significant reduction in -dP/dt compared with PLB/cTnI hearts. β-adrenergic stimulation increased HR similarly in both groups but at the highest levels of stimulation -dP/dt was significantly less in PLB/ssTnI than in PLB/cTnI hearts. The authors concluded that phosphorylation of cTnI significantly contributes to the enhanced rate of left ventricular relaxation during β-adrenergic stimulation.[156]

Chromogranin A

Genetic ablation of the chromogranin A (*Chga−/−*) gene in mice results in hypertension, reduced myocardial function, and reduced responses to β-adrenergic and ET-1 stimulation. Pretreatment of $Chga^{-/-}$ mice with catestatin (human chromogranin A352-372) prevents the adverse effects of removing this gene.[157,158]

Lectin-Like Oxidized Low-Density Lipoprotein Receptor

ATR-1 activation upregulates the expression of lectin-like oxidized low-density lipoprotein receptor LOX-1. LOX-1 activation upregulates ATR-1 expression. Angio-II-induced hypertension, but not NE-induced hypertension, was attenuated in $LOX\text{-}1^{-/-}$ mice. This indicates that LOX-1 is a key modulator of Angio-II-induced hypertension and cardiac remodeling.[159]

$LOX\text{-}5^{-/-}$ mice were used to demonstrate that the loss of this receptor has no effect on cardiac ischemia-reperfusion injury, but neutrophil infiltration and TNF-α expression were greater in the $LOX\text{-}5^{-/-}$ animals.[160]

Junctin

Junctin (JCN) is a transmembrane protein located in the cardiac junctional sarcoplasmic reticulum (SR). It binds to the ryanodine receptor [calsequestrin (CSQ)] and to triadin-1. Atria from 3-week-old transgenic mice that overexpress junctin (JCN-TG) demonstrate reduced expression of triadin-1. This results in a higher SR Ca^{2+} load but no changes in contractility or HR. Atria from 6-week-old JCN-TG show a compensatory downregulation of the ryanodine receptor that seems to offset the effects of junctin overexpression. In 18-week-old JCN-TG the progressive decrease in ryanodine receptor density seems to contribute to decreases in atrial contractility and HR during stress.[161] JCN-TG mice demonstrate impaired myocardial relaxation possibly as a result of reduced NCX expression and/or increased leak of SR Ca^{2+}. Altered shortening-frequency excitation-contraction coupling in these animals may be a consequence of impaired excitation-contraction coupling with depressed SR Ca^{2+} release at higher stimulation rates.[162] Transgenic mice overexpressing canine junctin also show changes in the packing of CSQ in the junctional SR and a facilitation of the association of SR and T tubules.[163]

Crossbreeding of mice with heart-specific overexpression of both triadin and junctin resulted in offspring (JxT-TG) with a stable threefold expression of total triadin but normal levels of junctin. These animals display cardiac hypertrophy, prolonged basal relaxation, depressed responses to β-adrenergic stimulation, and altered Ca^{2+} transients.[164]

Connexin

Connexins (Cx) are labeled with a number that represents the molecular mass of the amino acid sequences, in kDa. When identical connexin isotypes form both Connexins of a gap junction a homomeric gap junction channel is formed. When different connexin isotypes combine a heteromeric channel is produced. In the mammalian heart seven connexins have been identified: Cx37, Cx40, Cx43, Cx45, Cx46, Cx50, and Cx57. The $Cx40^{-/-}$ mouse has been used to study mechanisms of arrhythmogenesis.[165,166]

Aside from being components of gap junctions, connexins can also comprise large, nonselective pores known as hemi channels. The Cx30.3/lacZ transgenic approach was used to identify Cx30.3 in the renal medulla in mice, rats, and rabbits.[167] Cx45 expression has been found in the juxtaglomerular apparatus (JGA), as well as in the heart. Transgenic mice that express lacZ coding DNA under the control of the Cx45 promoter were used to discover that Cx45 is involved in the propagation of JGA vascular signals and thus in the regulation of renin release and the control of blood pressure.[168]

$Cx40^{-/-}$ mice have a misdirection of renin-expressing cells from the medial layer of afferent arterioles to the perivascular tissue, extraglomerular mesangium, and periglomerulular and peritubular interstitium. The aberrant renin-producing cells in these animals also express significant amounts of COX-2 mRNA and this, apparently, contributes to the renin secretion.[169] $Cx40^{-/-}$ mice were also used to show that renin-secreting cells are coupled to each other and to endothelial cells by Cx40-containing channels.[170] Transgenic mice were produced in which the coding region for Cx43 was replaced by Cx26. Both neonatal and adult Cx43 knock-in Cx26 mice demonstrated slowed ventricular conduction patterns, and both males and females were infertile from impaired gametogenesis.[171]

Calrectin is a Ca^{2+}-binding protein of the endoplasmic reticulum and plays an essential role in cardiac development. Cre-loxP transgenic mice with spatiotemporal overexpression of calrectin were created. Protein levels of Cx40, Cx43, and myocyte-enhancer factor-2C were lower than the level of these proteins in control hearts.[172] The overexpression of calrectin and decreased levels of Cx were associated with arrhythmias, ventricular dilatation, and sudden death in 6-10-week-old offspring, and marked edema at 7 weeks of age. The expression of hyperpolarization-activated cyclic nucleotide-gated channel-1, an essential component for cardiac pacemaker activity, was also decreased in the hearts of these mice.

Phospholamban

Mouse studies have shown that PLB is a key regulator of SR Ca^{2+} cycling and cardiac function but mice differ significantly from humans in how they regulate calcium. Rabbits have proven to be a better model for the study of calcium handling. Transgenic rabbits that overexpress PLB die early from severe skeletal muscle

wasting and myocardial dysfunction. A viable transgenic line exhibiting only a 30% increase in cardiac PLB shows isolated foci of cardiac pathology but cardiac function and response to β-adrenergic stimulation are normal.[173] PLB phosphorylation is a CaMKII-dependent process. Mice with transgenic overexpression of CaMKII-delta-C (chronic overexpression) develop heart failure with impaired SR Ca^{2+} loading during late acidosis compared with WT controls. This response may be associated with decreased SR Ca-ATPase and decreased PLB expression. However, adenovirus-mediated gene transfer of CaMKII-delta-C in isolated mouse and rabbit cardiomyocytes (acute overexpression) actually slightly improves recovery following increased SR Ca^{2+} loading during late acidosis.[174]

Fas Ligand

Fas ligand (FasL) is a potent proapoptotic type-II transmembrane protein. Its forced expression can induce a dramatic inflammatory response.[175] Transgenic mice with cardiac-specific expression of soluble Fas (sFas), a competitive inhibitor of FasL, were injected with either LPS or control vehicle. Neutralization of FasL by expression of sFas significantly preserved cardiac function and reduced inflammatory responses to LPS in the heart.[176]

Mice with cardiac-specific expression of sFas and double homozygous TG mice that express both monocyte chemoattractant protein-1 (MCP-1) and sFas were used to show that FasL released from infiltrating monocytes plays a critical role in the adverse effects of MCP-1 expression. The results suggest that Fas/FasL signaling could be a novel therapeutic target for certain types of heart failure.[177,178]

Proteases, Metalloproteinases, and ATPases

A novel class of protease-activated receptors (PARs) characterized by seven transmembrane G-protein-coupled domains are activated by serine proteases such as thrombin, trypsin, and tryptase. PAR-1, PAR-2, and PAR-4 have been implicated in vascular development via studies using transgenic mice and synthetically tethered ligand domains.[179] PAR-$4^{-/-}$ mice have prolonged bleeding times because of the lack of PAR-4 function in platelets and are thereby protected against thrombosis.[180] Male PAR-$2^{-/-}$ mice have a moderate elevation of systolic arterial and pulse pressures, but no change in diastolic pressures along with a lack of hypertensive response to high-salt diet. This model displays only a subtle difference in the time course of hypertension in response to Angio-II infusion.[181]

Extravascular inflammation was induced by injection of recombinant soluble murine tissue factor (TF) in the hind paw of PAR-$1^{-/-}$, PAR-$2^{-/-}$, PAR-$3^{-/-}$, and PAR-$4^{-/-}$ mice. There was no effect on the inflammatory response in PAR-$1^{-/-}$, PAR-$2^{-/-}$, or PAR-$3^{-/-}$ mice but the PAR-$4^{-/-}$ mice demonstrated significantly less

soluble TF (sTF)-induced swelling of the injected paw. These results indicate that sTF induces inflammation via a thrombin-dependent pathway, and both fibrin deposition and platelet activation are essential steps with the activation of PAR-4 essential to the process.[182]

Corin is a transmembrane serine protease that has been isolated from the heart. It is responsible for converting proatrial natriuretic peptide (pro-ANP) to active ANP. Corin$^{-/-}$ mice do not convert pro-ANP to ANP resulting in salt-sensitive hypertension. Interestingly the hypertension is exacerbated in pregnant corin$^{-/-}$ mice.[183]

Matrix metalloproteases (MMPs) are enzymes that regulate matrix remodeling in response to hypertension. Transgenic mice that overexpress cardiac MMP-1 and matched WT were subjected to hypertension induced by suprarenal banding of the aorta. Overexpression of MMP-1 attenuated the development of myocardial fibrosis, prevented left ventricular dilatation, and preserved myocardial function.[184] Transgenic rabbits that overexpress human matrix metalloproteinase-12 (hMMP-12-TG) were fed a 1% cholesterol diet for 6 weeks. They developed larger atherosclerotic plaques, more significant degradation of the aortic internal elastic layer, and increased numbers of infiltrating macrophages and smooth muscle cells into the atherosclerotic lesions than WT control rabbits.[185] Tissue inhibitor of metalloprotease-3 (TIMP-3) inhibits MMP and regulates angiogenesis. TIMP-3$^{-/-}$ mice demonstrate enhanced MMP activity in the retinal choroids and develop abnormal vessels with dilated capillaries.[186]

Strain differences are demonstrated between FVB and B6 mice where disintegrin and metalloproteinase-17 (ADAM-17) mRNA expression is higher in the liver, macrophages, and aorta in FVB.LDLR$^{-/-}$ mice than in B6.LDLR$^{-/-}$ mice. Macrophages from FVB.LDLR$^{-/-}$ mice demonstrate fivefold increases in PMA-induced shedding of TNF-α and 32% increases in release of TNF-receptor-I than B6.LDLR$^{-/-}$ animals.[187]

The copper transporter Menkes ATPase (MNK) is overexpressed in MNK-mutant mice. This model was used to demonstrate that MNK plays an important role in modulating Angio-II-induced hypertension and endothelial function by regulating extracellular superoxide dismutase (SOD-3) activity and vascular superoxide production.[188]

Binary Calsequestrin/P2Xr-Purinergic Receptor (CSQ/P2X4R) Transgenics

P2X4R is a ligand-gated ion channel. When activated by extracellular ATP it allows Ca^{2+} influx. Transgenic cardiac overexpression of human P2X4R results in increased ventricular contractility. Transgenic mice with cardiac overexpression of canine CSQ have ventricular hypertrophy, heart failure, and early mortality. Crossing P2X4R-TG with CSQ-TG produced CSQ/P2X4R-TG offspring with prolonged survival, less ventricular hypertrophy, and restored β-adrenergic responsiveness.[189]

pro-ANP Gene Disrupted Mouse

$ANP^{-/-}$ mice received either vehicle or an Angio-II type-2 receptor (ATR-2) antagonist. Both groups were placed on a high-salt diet. The studies indicate that ATR-2 blockade in salt-sensitive hypertensive/ventricular hypertrophic $ANP^{-/-}$ mice results in changes in myocardial extracellular matrix components that translate into decreased ventricular hypertrophy.[190]

Macrophage Colony-Stimulating Factor

Homozygous osteopetrotic mice (Op/Op) are deficient in macrophage colony-stimulating factor (M-CSF). Adult Op/Op, heterozygous ($Op/^{+}$), and WT mice were subjected to 14 days of Angio-II (1,000 ng/kg/min) or vehicle infusion. Op/Op mice demonstrated less endothelial dysfunction, less vascular remodeling, and less oxidative stress than WT.[191] M-CSF has also been shown to stimulate differentiation and proliferation of monocyte/macrophage lineage and is involved in neointimal formation following vascular injury. Recombinant human M-CSF (500 μg/kg/day) or vehicle was administered for 10 consecutive days, starting 4 days prior to mechanical injury to the femoral artery, in C57BL/6 mice. M-CSF accelerated early neointimal formation after vascular injury suggesting that inhibition of this system might have therapeutic potential in the treatment of a number of cardiovascular diseases.[192]

Endothelin-1

Endothelin-1 (ET-1) is a potent endogenous vasoconstrictor that contributes to vascular remodeling in hypertension and other cardiovascular diseases. Amiri et al.[193] targeted expression of the human *pre-pro-ET-1* gene to the endothelium using the Tie-2 promoter in C57BL/6 mice. Compared with WT littermates the TG mice exhibited threefold higher vascular tissue ET-1 mRNA and sevenfold higher ET-1 plasma levels, but there was no significant difference in blood pressures between the two groups. Higher ET-1 levels resulted in structural remodeling and endothelial dysfunction in resistance vessels. The experiments conducted suggest a direct, nonhemodynamic, effect of ET-1 on the vasculature involving activation of vascular NADPH-oxidase.

Aryl hydrocarbon receptor (AHR) knockout ($AHR^{-/-}$) mice develop cardiac hypertrophy of unknown origin. When $AHR^{-/-}$ mice were exposed to a modest decrease in inspired pO_2 they became hypoxic and hypertensive and plasma ET-1 levels were significantly increased. The hypertension was not associated with increased pulmonary pre-pro-ET-1 mRNA expression.[194]

Elastin

Mice harboring targeted deletion of the elastin (*ELN*) gene ($ELN^{+/-}$) show many of the same features of supravalvular aortic stenosis (SVAS) seen in humans, including changes in cardiovascular hemodynamics and arterial wall structure. $ELN^{+/-}$ mice are hypertensive at birth compared with WT counterparts. The inner diameters of arteries from $ELN^{+/-}$ mice are smaller at any given intravascular pressure than that of WT mice.[195,196]

Exact modeling of SVAS and other elastin gene abnormality diseases in mice is difficult because of structural differences between the human and mouse genes. A humanized elastin mouse with elastin production controlled by the human elastin gene has been developed. The human elastin protein appears to interact with the mouse elastin to form functional elastic fibers. When the h-ELN is expressed in the elastin haploinsufficient background ($ELN^{+/-}$) the hypertension and cardiovascular changes are reversed.[197]

α-2-Antiplasmin

α-2-Antiplasmin (α-2-AP) is the major circulating inhibitor of plasmin. Plasmin plays a significant role in the regulation of intravascular fibrinolysis. Angio-II-induced arterial wall thickening, vascular cell proliferation, apoptosis, c-Myc, and collagen-I expression are all significantly decreased, along with perivascular fibrosis, in α-2-$AP^{-/-}$ mice compared to WT mice.[198]

cAMP Response Element Binding Protein

cAMP response element binding protein (CREB), at serine-133, regulates gene expression in the heart. The functional significance of CREB-S133 phosphorylation was studied by comparing TG mice in which a phosphorylation-resistant (CREB-S133A) mutant, containing either an intact or a mutated leucine zipper domain (CREB-S133A-LZ), was expressed in the heart. The 1-year survival of mice from two CREB-S133A-LZ (TG) lines was equivalent to non-TG littermate controls. TG CREB-S133A mice died from heart failure at about 30 weeks of age. CREB-S133A mice demonstrate altered gene expression characteristic of heart failure whereas the CREB-S133A-LZ mice did not.[199]

Fatty Acid Transport Protein: CD36

Hearts from otherwise normal aged mice show intramyocardial lipid accumulation, reduced fatty acid and glucose oxidation, and deterioration in supplies of cardiac ATP. These changes accompany myocardial remodeling and impaired myocardial function.

Hearts from CD36$^{-/-}$ mice have lower levels of intramyocardial lipids, improved mitochondrial-derived ATP production, improved myocardial function, and a blunted hypertrophic response compared with age-matched WT. This indicates CD36 is a potential mediator of these aging-associated functional, structural, and metabolic changes.[200]

Clotting Factor XIII

Clotting factor XIII (FXIII) is a transglutaminase involved in wound healing. FXIII$^{-/-}$ and FXIII$^{+/-}$ mice suffer left ventricular rupture and die within 5 days following ligation of the left coronary artery. FXIII$^{-/-}$ mice receiving intravenous FXIII replacement therapy for 5 days have normal survival rates but still have adverse ventricular remodeling compared with WT controls.[201]

Apelin

Apelin describes a novel endogenous peptide system thought to be involved in a number of physiological processes, including cardiovascular development and function, control of fluid homeostasis, and obesity. It is also a catalytic substrate for ACE (angiotensin-converting enzyme)-2. Endogenous Apelin is essential for the maintenance of cardiac contractility during pressure overload and aging. Apelin$^{-/-}$ mice develop a progressive loss of cardiac contractility associated with systolic dysfunction, but without histological abnormalities, or heart failure. Pressure overload normally induces upregulation of Apelin expression in the heart, but when Apelin$^{-/-}$ mice were exposed to pressure-overload-induced heart failure there was no significant difference in the LV hypertrophy response compared with WT.[202]

T-Box Transcription Factor

Mutations in human TBX-5, a member of the T-box transcription factor gene family, are associated with congenital cardiac septal defects and isomerism in the autosomal dominant Holt-Oram syndrome. Overexpression of TBX-5 in embryonic chick hearts inhibits myocardial growth and trabeculation and suppresses embryonic cardiomyocyte proliferation.[203]

Thrombospondin-1 and Its Receptor CD47

Thrombospondin-1 is a key regulator of NO signaling. It limits the angiogenic activity of NO in EC, its vasodilator activity in VSMC, and its antithrombotic activity in platelets. Thrombospondin-1$^{-/-}$ or CD47$^{-/-}$ mice have hyperdynamic responses to NO and improved ability to respond to ischemic stress.[204]

Polyomavirus Middle T Antigen

The pronuclear microinjection method was used to introduce purified polyomavirus middle T antigen (PyMT) transgene into the chromosomes of fertilized mice ova. The transgenic positive animals were used to develop future generations by hybridization. PyMT expression in the F1 generation produced mice with venous malformations.[205]

Thrombopoietin Receptor

Mice that express a full-length thrombopoietin receptor (Mpl) transgene, in the absence of other Mpl isoforms, were generated under the control of a 2-kb Mpl promoter in $Mpl^{-/-}$ background animals. Transgene expression was decreased during late megakaryocyte maturation. This resulted in diminished Mpl expression in platelets. Platelets exert a negative feedback on thrombopoiesis by binding and consuming thrombopoietin in the circulation via the action of Mpl. The significant reduction of Mpl protein in platelets from Mpl-TG mice results in a marked elevation of the numbers of megakaryocytes and platelets during the steady state.[206]

Vascular Endothelial Growth Factor

A VEGF transgenic mouse, rhodopsin promoter, model (tro29VEGF) that mimics nonproliferative diabetic retinopathy and mild proliferative diabetic retinopathy was used to characterize early stages of concomitant vascular and neural retinal damage. Rhodopsin was detected at postnatal day (P)-5 and reached mature levels by P-15. VEGF protein expression was transient but peaked at P-10 to P-15. In tro29VEGF mice the formation of capillary beds was accelerated compared with that in WT controls. Vascular lesions were more numerous by P-28 in the TG mice. Retinal layer thinning tracked abnormal vessel growth.[207]

Osteopontin

Osteopontin (OPN) is a noncollagenous adhesion molecule protein identified in atherosclerotic lesions. OPN-TG and OPN-WT mice fed a 1.25% cholesterol diet for 16 weeks develop atherosclerotic lesion but the lesions in the OPN-TG mice were significantly larger. This study also showed that OPN induces fatty-streak lesion formation and inhibits IL-10 production by macrophages.[208]

ATP-Binding Membrane Cassette Transporter-A1

Atherosclerotic disease involves a host of processes including reverse cholesterol transport (RCT). RCT is a pathway for transport of cholesterol that has accumulated in the vessel wall to the liver where it can be excreted. Major constituents of RCT include HDL and apolipoprotein A-I (ApoA-I), considered acceptors, and enzymes including cholesterol acyltransferase (LCAT), phospholipid transfer protein (PLTP), hepatic lipase (HL), and cholesterol ester transfer protein (CETP). A critical portion of this process is cholesterol efflux. Accumulated cholesterol is removed from macrophages in the subintima of the vessel wall by ATP-binding membrane cassette transporter-A1 (ABC-A1), or by other mechanisms including passive diffusion, scavenger receptor-B1, caveolins, and sterol 27-hydroxylase. The cholesterol is then available to be collected by HDL and/or ApoA-I. Studies in ABC-A1$^{-/-}$ mice demonstrate that disruption of *ABC-A1* genes induces atherosclerosis and that proinflammatory cytokines exert atherosclerotic effects, at least partially, by impairing RCT and cholesterol efflux.[209]

The K^+/Cl^- Cotransporter KCC3

Mice with a targeted disruption of the *KCC3* gene (KCC3$^{-/-}$) develop neurodegeneration of the peripheral and CNS and develop hypertension similar to Andermann syndrome in humans. Data from these animals indicate that local control of vascular myogenic tone does not require KCC3. The hypertension that develops is, apparently, dependent upon increased sympathetic tone.[210]

Aldosterone Synthase Overexpression

TG mice overexpressing the terminal enzyme of aldosterone biosynthesis, aldosterone synthase (AS), in cardiac tissue were developed by gene targeting with the α-myosin heavy chain promoter. When compared with WT, TG AS mRNA was increased 100-fold and aldosterone concentrations were increased 1.7-fold. This increased cardiac production of aldosterone-induced major dysfunction in coronary arteries, independent of the endothelium but there were no changes in myocardial function or structure.[211]

Cysteine and Glycine-Rich Protein-2 (CSRP-2)

A gene disruption cassette was cloned into exon 4, and a mouse strain lacking functional cysteine and glycine-rich protein-2 (CSRP-2) (CSRP-2$^{-/-}$) was created. CSRP-2$^{-/-}$ mice have subtle alterations in cardiac ultrastructure including changes in myocardiocyte thickness and hypertrophy.[212]

Parathyroid Hormone Type-1 Receptor and PTH/PTH-Related Protein

Transgenic mice that overexpress parathyroid hormone type-1 receptor (PTH1R) in smooth muscle have been used to demonstrate that the PTH/PTH-related protein (PTHrP)/PTH1R system is an important regulator of cardiovascular function. Unfortunately, PTHrP/TTH1R$^{-/-}$ mice are not viable, so this model is unavailable for study. Three weeks after the intravenous administration of either human-PTH1R or hPTH1R tagged with green-fluorescence protein there was generalized expression of both hPTH1R mRNA and protein, particularly in blood vessels, liver, heart, kidney, and CNS. PTH1R overexpression decreased blood pressure and renal tone but also decreased HR. The TG mice demonstrated marked reductions in the production of angiotensinogen in the liver and in circulating levels of both renin activity and angiotensinogen.[213]

Vitamin D Receptor

Absence of a functional vitamin D receptor (VDR), or the key activating enzyme, 25-OHD-1-α-hydroxylase (CYP27B1), in mice results in a bone and growth plate phenotype that mimics humans with congenital CYP27B1 mutations or severe vitamin D deficiency. VDR$^{-/-}$ mice also develop increased renin activity resulting in hypertension, myocardial hypertrophy, and increased thrombogenicity.[214]

Thromboxane Receptor (Tp)

Tp$^{-/-}$ and WT control mice were exposed to 21 weeks of L-NAME and a 6% salt diet. Hypertension and myocardial hypertrophy were attenuated in the Tp$^{-/-}$ mice but renal hypertrophy and the severity of glomerulosclerosis, tubule vacuolization, and chronic inflammation of the interstitium were enhanced.[215]

T and B Cells

Mice lacking T and B cells (RAG-1$^{-/-}$) exposed to Angio-II infusion- or DOCA-salt-induced hypertension exhibit a blunted hypertensive response and do not develop functional abnormalities of the vascular system. This result is, apparently, due to the lack of T cells.[216]

Vanilloid Type-1 Receptors (TRPV-1)

Hypertension was produced by uninephrectomy and DOCA-salt in WT and TRPV-1$^{-/-}$ mice. There was no difference in the level of hypertension produced between the two groups but there were significant increases in the urinary excretion of albumin and 8-isoprostane, glomerulosclerosis, renal cortical tubulointerstitial injury, nuclear antigen-positive cells, and renal monocyte/macrophage infiltration in the TRPV-1$^{-/-}$ animals.[217]

Serotonin Transporter (SERT)

Negative results are also important. SERT$^{-/-}$ mice and rats have the same basal arterial pressures as WT controls and the same response to DOCA-salt hypertension. SERT does not seem to be involved in the regulation of arterial blood pressure.[218]

CC Chemokine Receptor-2 (CCR-2)

CCR-2$^{-/-}$ and age-matched WT control mice were infused continuously with either Angio-II (5.2 ng/10 g/min) or vehicle for 2 or 4 weeks. Angio-II infusion resulted in similar degrees of hypertension and LV hypertrophy in both strains. CCR-2$^{-/-}$ mice with Angio-II-induced hypertension had significant decreases in oxidative stress, macrophage infiltration, albuminuria, and renal damage. GFR was significantly greater in CCR-2$^{-/-}$ than in the WT controls.[219]

Thymosin β-4

Hinkel et al.[220] have shown that the retrograde infusion of embryonic eEPCs into zones of myocardial ischemia provides rapid paracrine protection against ischemia-reperfusion injury. Intact pigs were subjected to 60 min of ischemia via percutaneous occlusion of the LAD. After 55 min of ischemia control eEPCs or cells transfected with thymosin β-4 (T-β-4) shRNA or T-β-4 alone were infused retrograde into the anterior interventricular vein. These studies demonstrate that the short-term cardioprotection resulting from retrograde infusion of eEPCs is, at least partially, due to T-β-4.

References

1. Hoit BD, Kiatchoosakun S, Restivo J, et al. Naturally occurring variation in cardiovascular traits among inbred mouse strains. *Genomics.* 2002;79:679–685.
2. Cowan PJ, Shinkel TA, Fisicaro N, et al. Targeting gene expression to endothelium in transgenic animals: A comparison of the human ICAM-2, PECAM-1 and endoglin promoters. *Xenotransplantation.* 2003;10:223–231.
3. Singbartl K, Thatte J, Smith ML, Wethmar K, Day K, Ley K. A CD2-green fluorescence protein-transgenic mouse reveals very late antigen-4-dependent CD8+ lymphocyte rolling in inflamed venules. *J Immunol.* 2001;166:7520–7526.
4. Placier S, Boffa JJ, Dussaule JC, Chatziantoniou C. Reversal of renal lesions following interruption of nitric oxide synthesis inhibition in transgenic mice. *Nephrol Dial Transplant.* 2006;21:881–888.
5. Pichler A, Prior JL, Luker GD, Piwnica-Worms D. Generation of a highly inducible Gal4→Fluc universal reporter mouse for in vivo bioluminescence imaging. *Proc Natl Acad Sci USA.* 2008;105:15932–15937.
6. Viswanathan S, Burch JB, Fishman GI, Moskowitz IP, Benson DW. Characterization of sinoatrial node in four conduction system marker mice. *J Mol Cell Cardiol.* 2007;42:946–953.
7. Zhai P, Eurell TE, Cotthaus R, Jeffery EH, Bahr JM, Gross DR. Effect of estrogen on global myocardial ischemia-reperfusion injury in female rats. *Am J Physiol Heart Circ Physiol.* 2000;279:H2766–H2775.
8. Zhai P, Eurell TE, Cotthaus RP, Jeffery EH, Bahr JM, Gross DR. Effects of dietary phytoestrogen on global myocardial ischemia-reperfusion injury in isolated female rat hearts. *Am J Physiol Heart Circ Physiol.* 2001;281:H1223–H1232.
9. Arias-Loza PA, Jazbutyte V, Pelzer T. Genetic and pharmacologic strategies to determine the function of estrogen receptor alpha and estrogen receptor beta in cardiovascular system. *Gend Med.* 2008;5 Suppl A:S34–S45.
10. Seli E, Guzeloglu-Kayisli O, Kayisli UA, Kizilay G, Arici A. Estrogen increases apoptosis in the arterial wall in a murine atherosclerosis model. *Fertil Steril.* 2007;88:1190–1196.
11. Simpson ER, Jones ME. Of mice and men: The many guises of estrogens. *Ernst Schering Found Symp Proc.* 2006;1:45–67.
12. Sun D, Yan C, Jacobson A, Jiang H, Carroll MA, Huang A. Contribution of epoxyeicosatrienoic acids to flow-induced dilation in arteries of male ERalpha knockout mice: Role of aromatase. *Am J Physiol Regul Integr Comp Physiol.* 2007;293:R1239–R1246.
13. Zhai P, Eurell TE, Cooke PS, Lubahn DB, Gross DR. Myocardial ischemia-reperfusion injury in estrogen receptor-alpha knockout and wild-type mice. *Am J Physiol Heart Circ Physiol.* 2000;278:H1640–H1647.
14. Huss JM, Imahashi K, Dufour CR, et al. The nuclear receptor ERRα is required for the bioenergetic and functional adaptation to cardiac pressure overload. *Cell Metab.* 2007;6:25–37.
15. Corbacho AM, Eiserich JP, Zuniga LA, Valacchi G, Villablanca AC. Compromised aortic vasoreactivity in male estrogen receptor-alpha-deficient mice during acute lipopolysaccharide-induced inflammation. *Endocrinology.* 2007;148:1403–1411.
16. Babiker FA, Lips D, Meyer R, et al. Estrogen receptor beta protects the murine heart against left ventricular hypertrophy. *Arterioscler Thromb Vasc Biol.* 2006;26:1524–1530.
17. Pedram A, Razandi M, Lubahn D, Liu J, Vannan M, Levin ER. Estrogen inhibits cardiac hypertrophy: Role of estrogen receptor-beta to inhibit calcineurin. *Endocrinology.* 2008;149:3361–3369.
18. Foryst-Ludwig A, Clemenz M, Hohmann S, et al. Metabolic actions of estrogen receptor beta (ERbeta) are mediated by a negative cross-talk with PPARgamma. *PLoS Genet.* 2008;4:e1000108.
19. Wang M, Crisostomo PR, Markel T, Wang Y, Lillemoe KD, Meldrum DR. Estrogen receptor beta mediates acute myocardial protection following ischemia. *Surgery.* 2008;144:233–238.
20. Pelzer T, Loza PA, Hu K, et al. Increased mortality and aggravation of heart failure in estrogen receptor-beta knockout mice after myocardial infarction. *Circulation.* 2005;111:1492–1498.

21. Ullrich ND, Krust A, Collins P, MacLeod KT. Genomic deletion of estrogen receptors ERalpha and ERbeta does not alter estrogen-mediated inhibition of Ca^{2+} influx and contraction in murine cardiomyocytes. *Am J Physiol Heart Circ Physiol.* 2008;294 :H2421–H2427.
22. O'Lone R, Knorr K, Jaffe IZ, et al. Estrogen receptors alpha and beta mediate distinct pathways of vascular gene expression, including genes involved in mitochondrial electron transport and generation of reactive oxygen species. *Mol Endocrinol.* 2007;21:1281–1296.
23. Luksha L, Poston L, Gustafsson JA, Aghajanova L, Kublickiene K. Gender-specific alteration of adrenergic responses in small femoral arteries from estrogen receptor-beta knockout mice. *Hypertension.* 2005;46:1163–1168.
24. Luksha L, Poston L, Gustafsson JA, Hultenby K, Kublickiene K. The oestrogen receptor beta contributes to sex related differences in endothelial function of murine small arteries via EDHF. *J Physiol.* 2006;577:945–955.
25. Cruz MN, Douglas G, Gustafsson JA, Poston L, Kublickiene K. Dilatory responses to estrogenic compounds in small femoral arteries of male and female estrogen receptor-beta knockout mice. *Am J Physiol Heart Circ Physiol.* 2006;290:H823–H829.
26. Douglas G, Cruz MN, Poston L, Gustafsson JA, Kublickiene K. Functional characterization and sex differences in small mesenteric arteries of the estrogen receptor-beta knockout mouse. *Am J Physiol Regul Integr Comp Physiol.* 2008;294:R112–R120.
27. Tsutsumi S, Zhang X, Takata K, et al. Differential regulation of the inducible nitric oxide synthase geneby estrogen receptors {alpha}and {beta}. J Endocrinol. 2008; 199(2):267–273.
28. Umetani M, Domoto H, Gormley AK, et al. 27-Hydroxycholesterol is an endogenous SERM that inhibits the cardiovascular effects of estrogen. *Nat Med.* 2007;13:1185–1192.
29. Belo NO, Sairam MR, Dos Reis AM. Impairment of the natriuretic peptide system in follitropin receptor knockout mice and reversal by estradiol: Implications for obesity-associated hypertension in menopause. *Endocrinology.* 2008;149:1399–1406.
30. Ebrahimian T, Sairam MR, Schiffrin EL, Touyz RM. Cardiac hypertrophy is associated with altered thioredoxin and ASK1 signaling in a mouse model of menopause. Am J Physiol Heart Circ Physiol. 2008.
31. Matsui Y, Nakano N, Shao D, et al. Lats2 is a negative regulator of myocyte size in the heart. *Circ Res.* 2008;103:1309–1318.
32. Cohn HI, Harris DM, Pesant S, et al. Inhibition of vascular smooth muscle G protein-coupled receptor kinase 2 enhances {alpha}1DAR constriction. *Am J Physiol Heart Circ Physiol.* 2008;295:H1695–H1704.
33. Yu X, Huang S, Patterson E, et al. Proteasome degradation of GRK2 during ischemia and ventricular tachyarrhythmias in a canine model of myocardial infarction. *Am J Physiol Heart Circ Physiol.* 2005;289:H1960–H1967.
34. Iaccarino G, Rockman HA, Shotwell KF, Tomhave ED, Koch WJ. Myocardial overexpression of GRK3 in transgenic mice: Evidence for in vivo selectivity of GRKs. *Am J Physiol.* 1998;275:H1298–H1306.
35. Hirotani S, Zhai P, Tomita H, et al. Inhibition of glycogen synthase kinase 3β during heart failure is protective. *Circ Res.* 2007;101:1164–1174.
36. Luckey SW, Mansoori J, Fair K, Antos CL, Olson EN, Leinwand LA. Blocking cardiac growth in hypertrophic cardiomyopathy induces cardiac dysfunction and decreased survival only in males. *Am J Physiol Heart Circ Physiol.* 2007;292:H838–H845.
37. Korshunov VA, Daul M, Massett MP, Berk BC. Axl mediates vascular remodeling induced by deoxycorticosterone acetate-salt hypertension. *Hypertension.* 2007;50:1057–1062.
38. Rexhepaj R, Boini KM, Huang DY, et al. Role of maternal glucocorticoid inducible kinase SGK1 in fetal programming of blood pressure in response to prenatal diet. *Am J Physiol Regul Integr Comp Physiol.* 2008;294:R2008–R2013.
39. Mayr M, Metzler B, Chung YL, et al. Ischemic preconditioning exaggerates cardiac damage in PKC-delta null mice. *Am J Physiol Heart Circ Physiol.* 2004;287:H946–H956.
40. Huang J, Shelton JM, Richardson JA, Kamm KE, Stull JT. Myosin regulatory light chain phosphorylation attenuates cardiac hypertrophy. *J Biol Chem.* 2008;283:19748–19756.

41. Ofir M, Arad M, Porat E, et al. Increased glycogen stores due to gamma-AMPK overexpression protects against ischemia and reperfusion damage. *Biochem Pharmacol.* 2008;75:1482–1491.
42. Tsukada S, Iwai M, Nishiu J, et al. Inhibition of experimental intimal thickening in mice lacking a novel G-protein-coupled receptor. *Circulation.* 2003;107:313–319.
43. McMullen JR, Amirahmadi F, Woodcock EA, et al. Protective effects of exercise and phosphoinositide 3-kinase(p110alpha) signaling in dilated and hypertrophic cardiomyopathy. *Proc Natl Acad Sci USA.* 2007;104:612–617.
44. Fujii A, Nakano D, Katsuragi M, et al. Role of gp91phox-containing NADPH oxidase in the deoxycorticosterone acetate-salt-induced hypertension. *Eur J Pharmacol.* 2006;552:131–134.
45. Salguero G, Akin E, Templin C, et al. Renovascular hypertension by two-kidney one-clip enhances endothelial progenitor cell mobilization in a p47phox-dependent manner. *J Hypertens.* 2008;26:257–268.
46. Frantz S, Brandes RP, Hu K, et al. Left ventricular remodeling after myocardial infarction in mice with targeted deletion of the NADPH oxidase subunit gp91PHOX. *Basic Res Cardiol.* 2006;101:127–132.
47. Wiesel P, Patel AP, Carvajal IM, et al. Exacerbation of chronic renovascular hypertension and acute renal failure in heme oxygenase-1-deficient mice. *Circ Res.* 2001;88:1088–1094.
48. Nath KA, d'Uscio LV, Juncos JP, et al. An analysis of the DOCA-salt model of hypertension in HO-1−/− mice and the Gunn rat. *Am J Physiol Heart Circ Physiol.* 2007;293:H333–H342.
49. Yaar R, Jones MR, Chen JF, Ravid K. Animal models for the study of adenosine receptor function. *J Cell Physiol.* 2005;202:9–20.
50. Tikh EI, Fenton RA, Dobson JG, Jr. Contractile effects of adenosine A1 and A2A receptors in isolated murine hearts. *Am J Physiol Heart Circ Physiol.* 2006;290:H348–H356.
51. Tang T, Lai NC, Roth DM, et al. Adenylyl cyclase type V deletion increases basal left ventricular function and reduces left ventricular contractile responsiveness to beta-adrenergic stimulation. *Basic Res Cardiol.* 2006;101:117–126.
52. Egli RE, Kash TL, Choo K, et al. Norepinephrine modulates glutamatergic transmission in the bed nucleus of the stria terminalis. *Neuropsychopharmacology.* 2005;30:657–668.
53. Ihalainen JA, Tanila H. In vivo regulation of dopamine and noradrenaline release by alpha2A-adrenoceptors in the mouse nucleus accumbens. *J Neurochem.* 2004;91:49–56.
54. Zhu QM, Lesnick JD, Jasper JR, et al. Cardiovascular effects of rilmenidine, moxonidine and clonidine in conscious wild-type and D79N alpha2A-adrenoceptor transgenic mice. *Br J Pharmacol.* 1999;126:1522–1530.
55. Sallinen J, Haapalinna A, MacDonald E, et al. Genetic alteration of the alpha2-adrenoceptor subtype c in mice affects the development of behavioral despair and stress-induced increases in plasma corticosterone levels. *Mol Psychiatry.* 1999;4:443–452.
56. Rockman HA, Choi DJ, Akhter SA, et al. Control of myocardial contractile function by the level of beta-adrenergic receptor kinase 1 in gene-targeted mice. *J Biol Chem.* 1998;273:18180–18184.
57. Cristina C, Diaz-Torga G, Baldi A, et al. Increased pituitary vascular endothelial growth factor-a in dopaminergic D2 receptor knockout female mice. *Endocrinology.* 2005;146:2952–2962.
58. Tavernier G, Jimenez M, Giacobino JP, et al. Norepinephrine induces lipolysis in beta1/beta2/beta3-adrenoceptor knockout mice. *Mol Pharmacol.* 2005;68:793–799.
59. Kurihara N, Alfie ME, Sigmon DH, Rhaleb NE, Shesely EG, Carretero OA. Role of nNOS in blood pressure regulation in eNOS null mutant mice. *Hypertension.* 1998;32:856–861.
60. Duplain H, Burcelin R, Sartori C, et al. Insulin resistance, hyperlipidemia, and hypertension in mice lacking endothelial nitric oxide synthase. *Circulation.* 2001;104:342–345.
61. Grasselli A, Nanni S, Colussi C, et al. Estrogen receptor-alpha and endothelial nitric oxide synthase nuclear complex regulates transcription of human telomerase. *Circ Res.* 2008; 103:34–42.
62. Billon A, Lehoux S, Lam Shang Leen L, et al. The estrogen effects on endothelial repair and mitogen-activated protein kinase activation are abolished in endothelial nitric-oxide (NO) synthase knockout mice, but not by NO synthase inhibition by N-nitro-L-arginine methyl ester. *Am J Pathol.* 2008;172:830–838.

63. Takenaka K, Nishimura Y, Nishiuma T, et al. Ventilator-induced lung injury is reduced in transgenic mice that overexpress endothelial nitric oxide synthase. *Am J Physiol Lung Cell Mol Physiol.* 2006;290:L1078–L1086.
64. Gava AL, Peotta VA, Cabral AM, Vasquez EC, Meyrelles SS. Overexpression of eNOS prevents the development of renovascular hypertension in mice. *Can J Physiol Pharmacol.* 2008;86:458–464.
65. Hao YH, Yong HY, Murphy CN, et al. Production of endothelial nitric oxide synthase (eNOS) over-expressing piglets. *Transgenic Res.* 2006;15:739–750.
66. Kadowaki T, Yamauchi T. Adiponectin and adiponectin receptors. *Endocr Rev.* 2005;26:439–451.
67. Otabe S, Yuan X, Fukutani T, et al. Overexpression of human adiponectin in transgenic mice results in suppression of fat accumulation and prevention of premature death by high-calorie diet. *Am J Physiol Endocrinol Metab.* 2007;293:E210–E218.
68. Ohashi K, Iwatani H, Kihara S, et al. Exacerbation of albuminuria and renal fibrosis in subtotal renal ablation model of adiponectin-knockout mice. *Arterioscler Thromb Vasc Biol.* 2007;27:1910–1917.
69. Bauche IB, El Mkadem SA, Pottier AM, et al. Overexpression of adiponectin targeted to adipose tissue in transgenic mice: Impaired adipocyte differentiation. *Endocrinology.* 2007;148:1539–1549.
70. Shinmura K, Tamaki K, Saito K, Nakano Y, Tobe T, Bolli R. Cardioprotective effects of short-term caloric restriction are mediated by adiponectin via activation of AMP-activated protein kinase. *Circulation.* 2007;116:2809–2817.
71. Lin HV, Kim JY, Pocai A, et al. Adiponectin resistance exacerbates insulin resistance in insulin receptor transgenic/knockout mice. *Diabetes.* 2007;56:1969–1976.
72. Carvalho E, Kotani K, Peroni OD, Kahn BB. Adipose-specific overexpression of GLUT4 reverses insulin resistance and diabetes in mice lacking GLUT4 selectively in muscle. *Am J Physiol Endocrinol Metab.* 2005;289:E551–E561.
73. Hertzel AV, Smith LA, Berg AH, et al. Lipid metabolism and adipokine levels in fatty acid-binding protein null and transgenic mice. *Am J Physiol Endocrinol Metab.* 2006;290:E814–E823.
74. Jurczak MJ, Danos AM, Rehrmann VR, Allison MB, Greenberg CC, Brady MJ. Transgenic overexpression of protein targeting to glycogen markedly increases adipocytic glycogen storage in mice. *Am J Physiol Endocrinol Metab.* 2007;292:E952–E963.
75. Yamaguchi M, Nakagawa T. Change in lipid components in the adipose and liver tissues of regucalcin transgenic rats with increasing age: Suppression of leptin and adiponectin gene expression. *Int J Mol Med.* 2007;20:323–328.
76. Huang J, Gabrielsen JS, Cooksey RC, et al. Increased glucose disposal and AMP-dependent kinase signaling in a mouse model of hemochromatosis. *J Biol Chem.* 2007;282:37501–37507.
77. Al-Aly Z, Shao JS, Lai CF, et al. Aortic Msx2-wnt calcification cascade is regulated by TNF-alpha-dependent signals in diabetic ldlr–/– mice. *Arterioscler Thromb Vasc Biol.* 2007;27:2589–2596.
78. Ye Z, Ahmed KA, Hao S, et al. Active CD4+ helper T cells directly stimulate CD8+ cytotoxic T lymphocyte responses in wild-type and MHC II gene knockout C57BL/6 mice and transgenic RIP-mOVA mice expressing islet beta-cell ovalbumin antigen leading to diabetes. *Autoimmunity.* 2008;41:501–511.
79. Costa C, Zhao L, Burton WV, et al. Transgenic pigs designed to express human CD59 and H-transferase to avoid humoral xenograft rejection. *Xenotransplantation.* 2002;9:45–57.
80. Smolenski RT, Forni M, Maccherini M, et al. Reduction of hyperacute rejection and protection of metabolism and function in hearts of human decay accelerating factor (hDAF)-expressing pigs. *Cardiovasc Res.* 2007;73:143–152.
81. Lee JM, Tu CF, Tai HC, et al. The hDAF exogene protects swine endothelial and peripheral blood mononuclear cells from xenoreactive antibody mediated cytotoxicity in hDAF transgenic pigs. *Transplant Proc.* 2006;38:2270–2272.
82. Brandl U, Erhardt M, Michel S, et al. Soluble galalpha(1,3)gal conjugate combined with hDAF preserves morphology and improves function of cardiac xenografts. *Xenotransplantation.* 2007;14:323–332.
83. Brandl U, Jockle H, Erhardt M, et al. Reduced fibrin deposition and intravascular thrombosis in hDAF transgenic pig hearts perfused with tirofiban. *Transplantation.* 2007;84:1667–1676.

84. Warnecke G, Severson SR, Ugurlu MM, et al. Endothelial function in pigs transgenic for human complement regulating factor. *Transplantation.* 2002;73:1060–1067.
85. Zhou CY, McInnes E, Parsons N, et al. Production and characterization of a pig line transgenic for human membrane cofactor protein. *Xenotransplantation.* 2002;9:183–190.
86. Grabie N, Hsieh DT, Buono C, et al. Neutrophils sustain pathogenic CD8+ T cell responses in the heart. Am J Pathol. 2003;163:2413–2420.
87. Adachi O, Yamato E, Kawamoto S, et al. High-level expression of viral interleukin-10 in cardiac allografts fails to prolong graft survival. Transplantation. 2002;74:1603–1608.
88. Klugewitz K, Blumenthal-Barby F, Schrage A, Knolle PA, Hamann A, Crispe IN. Immunomodulatory effects of the liver: Deletion of activated CD4+ effector cells and suppression of IFN-gamma-producing cells after intravenous protein immunization. J Immunol. 2002; 169:2407–2413.
89. Fischbein MP, Yun J, Laks H, et al. Regulated interleukin-10 expression prevents chronic rejection of transplanted hearts. J Thorac Cardiovasc Surg. 2003;126:216–223.
90. Takeuchi T, Ueki T, Sunaga S, et al. Murine interleukin 4 transgenic heart allograft survival prolonged with down-regulation of the Th1 cytokine mRNA in grafts. Transplantation. 1997;64:152–157.
91. Rothermel AL, Wang Y, Schechner J, et al. Endothelial cells present antigens in vivo. BMC Immunol. 2004;5:5.
92. Reuter H, Philipson KD. Sodium-calcium exchanger overexpression in the heart - Insights from a transgenic mouse model. Basic Res Cardiol. 2002;97 Suppl 1:131–135.
93. Muller JG, Isomatsu Y, Koushik SV, et al. Cardiac-specific expression and hypertrophic upregulation of the feline Na(+)-Ca(2+) exchanger gene H1-promoter in a transgenic mouse model. Circ Res. 2002;90:158–164.
94. Maxwell K, Scott J, Omelchenko A, et al. Functional role of ionic regulation of Na+/Ca2+ exchange assessed in transgenic mouse hearts. Am J Physiol. 1999;277:H2212–H2221.
95. Weber CR, Ginsburg KS, Philipson KD, Shannon TR, Bers DM. Allosteric regulation of Na/Ca exchange current by cytosolic Ca in intact cardiac myocytes. J Gen Physiol. 2001;117:119–131.
96. Yao A, Su Z, Nonaka A, et al. Effects of overexpression of the Na+-Ca2+ exchanger on [Ca2+]i transients in murine ventricular myocytes. Circ Res. 1998;82:657–665.
97. Cho CH, Lee SY, Shin HS, Philipson KD, Lee CO. Partial rescue of the Na+-Ca2+ exchanger (NCX1) knock-out mouse by transgenic expression of NCX1. Exp Mol Med. 2003;35:125–135.
98. Karashima E, Nishimura J, Iwamoto T, et al. Involvement of Na+-Ca2+ exchanger in cAMP-mediated relaxation in mice aorta: Evaluation using transgenic mice. Br J Pharmacol. 2007;150: 434–444.
99. Su Z, Bridge JH, Philipson KD, Spitzer KW, Barry WH. Quantitation of Na/Ca exchanger function in single ventricular myocytes. *J Mol Cell Cardiol.* 1999;31:1125–1135.
100. Nakamura TY, Iwata Y, Arai Y, Komamura K, Wakabayashi S. Activation of Na^+/H^+ exchanger 1 is sufficient to generate Ca^{2+} signals that induce cardiac hypertrophy and heart failure. *Circ Res.* 2008;103:891–899.
101. Dibbs ZI, Diwan A, Nemoto S, et al. Targeted overexpression of transmembrane tumor necrosis factor provokes a concentric cardiac hypertrophic phenotype. *Circulation.* 2003;108: 1002–1008.
102. Huber SA, Feldman AM, Sartini D. Coxsackievirus B3 induces T regulatory cells, which inhibit cardiomyopathy in tumor necrosis factor-alpha transgenic mice. *Circ Res.* 2006;99:1109–1116.
103. Mori S, Gibson G, McTiernan CF. Differential expression of MMPs and TIMPs in moderate and severe heart failure in a transgenic model. *J Card Fail.* 2006;12:314–325.
104. Sawaya SE, Rajawat YS, Rami TG, et al. Downregulation of connexin40 and increased prevalence of atrial arrhythmias in transgenic mice with cardiac-restricted overexpression of tumor necrosis factor. *Am J Physiol Heart Circ Physiol.* 2007;292:H1561–H1567.
105. Sekiguchi K, Tian Q, Ishiyama M, et al. Inhibition of PPAR-alpha activity in mice with cardiac-restricted expression of tumor necrosis factor: Potential role of TGF-beta/Smad3. *Am J Physiol Heart Circ Physiol.* 2007;292:H1443–H1451.

106. Panagopoulou P, Davos CH, Milner DJ, et al. Desmin mediates TNF-alpha-induced aggregate formation and intercalated disk reorganization in heart failure. *J Cell Biol.* 2008;181:761–775.
107. Sakata Y, Chancey AL, Divakaran VG, Sekiguchi K, Sivasubramanian N, Mann DL. Transforming growth factor-beta receptor antagonism attenuates myocardial fibrosis in mice with cardiac-restricted overexpression of tumor necrosis factor. *Basic Res Cardiol.* 2008;103:60–68.
108. Pinderski Oslund LJ, Hedrick CC, Olvera T, et al. Interleukin-10 blocks atherosclerotic events in vitro and in vivo. *Arterioscler Thromb Vasc Biol.* 1999;19:2847–2853.
109. Pinderski LJ, Fischbein MP, Subbanagounder G, et al. Overexpression of interleukin-10 by activated T lymphocytes inhibits atherosclerosis in LDL receptor-deficient mice by altering lymphocyte and macrophage phenotypes. *Circ Res.* 2002;90:1064–1071.
110. Willuweit A, Sass G, Schoneberg A, Eisel U, Tiegs G, Clauss M. Chronic inflammation and protection from acute hepatitis in transgenic mice expressing TNF in endothelial cells. *J Immunol.* 2001;167:3944–3952.
111. Reifenberg K, Lehr HA, Torzewski M, et al. Interferon-gamma induces chronic active myocarditis and cardiomyopathy in transgenic mice. *Am J Pathol.* 2007;171:463–472.
112. Arsenijevic D, Garcia I, Vesin C, et al. Differential roles of tumor necrosis factor-alpha and interferon-gamma in mouse hypermetabolic and anorectic responses induced by LPS. *Eur Cytokine Netw.* 2000;11:662–668.
113. Monraats PS, Pires NM, Schepers A, et al. Tumor necrosis factor-alpha plays an important role in restenosis development. *FASEB J.* 2005;19:1998–2004.
114. Metzler B, Mair J, Lercher A, et al. Mouse model of myocardial remodelling after ischemia: Role of intercellular adhesion molecule-1. *Cardiovasc Res.* 2001;49:399–407.
115. Metzler B, Haubner B, Conci E, et al. Myocardial ischaemia-reperfusion injury in haematopoietic cell-restricted {beta}1 integrin knockout mice. *Exp Physiol.* 2008;93:825–833.
116. Son NH, Park TS, Yamashita H, et al. Cardiomyocyte expression of PPARgamma leads to cardiac dysfunction in mice. *J Clin Invest.* 2007;117:2791–2801.
117. Cresci S, Jones PG, Sucharov CC, et al. Interaction between PPARA genotype and beta-blocker treatment influences clinical outcomes following acute coronary syndromes. *Pharmacogenomics.* 2008;9:1403–1417.
118. Marionneau C, Aimond F, Brunet S, et al. PPARalpha-mediated remodeling of repolarizing voltage-gated K+ (kv) channels in a mouse model of metabolic cardiomyopathy. *J Mol Cell Cardiol.* 2008;44:1002–1015.
119. Zhou Y, Luo P, Chang HH, et al. Colfibrate attenuates blood pressure and sodium retention in DOCA-salt hypertension. *Kidney Int.* 2008;74:1040–1048.
120. Obih P, Oyekan AO. Regulation of blood pressure, natriuresis and renal thiazide/amiloride sensitivity in PPARalpha null mice. *Blood Press.* 2008;17:55–63.
121. Odegaard JI, Ricardo-Gonzalez RR, Goforth MH, et al. Macrophage-specific PPARgamma controls alternative activation and improves insulin resistance. *Nature.* 2007;447:1116–1120.
122. Murtaza I, Wang HX, Feng X, et al. Down-regulation of catalase and oxidative modification of protein kinase CK2 lead to the failure of apoptosis repressor with caspase recruitment domain to inhibit cardiomyocyte hypertrophy. *J Biol Chem.* 2008;283:5996–6004.
123. Liu F, Wei CC, Wu SJ, et al. Apocynin attenuates tubular apoptosis and tubulointerstitial fibrosis in transgenic mice independent of hypertension. *Kidney Int.* 2009;75:156–166.
124. Park JK, Fischer R, Dechend R, et al. p38 Mitogen-activated protein kinase inhibition ameliorates angiotensin II-induced target organ damage. *Hypertension.* 2007;49:481–489.
125. Cervenka L, Horacek V, Vaneckova I, et al. Essential role of AT1A receptor in the development of 2K1C hypertension. *Hypertension.* 2002;40:735–741.
126. Cervenka L, Vaneckova I, Huskova Z, et al. Pivotal role of angiotensin II receptor subtype 1A in the development of two-kidney, one-clip hypertension: Study in angiotensin II receptor subtype 1A knockout mice. *J Hypertens.* 2008;26:1379–1389.
127. Osorio JC, Cheema FH, Martens TP, et al. Simvastatin reverses cardiac hypertrophy caused by disruption of the bradykinin 2 receptor. *Can J Physiol Pharmacol.* 2008;86:633–642.
128. Rhaleb NE, Peng H, Alfie ME, Shesely EG, Carretero OA. Effect of ACE inhibitor on DOCA-salt- and aortic coarctation-induced hypertension in mice: Do kinin B2 receptors play a role? *Hypertension.* 1999;33:329–334.

129. Madeddu P, Milia AF, Salis MB, et al. Renovascular hypertension in bradykinin B2-receptor knockout mice. *Hypertension.* 1998;32:503–509.
130. Nogueira BV, Peotta VA, Meyrelles SS, Vasquez EC. Evaluation of aortic remodeling in apolipoprotein E-deficient mice and renovascular hypertensive mice. *Arch Med Res.* 2007;38:816–821.
131. Heo HJ, Yun MR, Jung KH, et al. Endogenous angiotensin II enhances atherogenesis in apoprotein E-deficient mice with renovascular hypertension through activation of vascular smooth muscle cells. *Life Sci.* 2007;80:1057–1063.
132. Mazzolai L, Korber M, Bouzourene K, et al. Severe hyperlipidemia causes impaired renin-angiotensin system function in apolipoprotein E deficient mice. *Atherosclerosis.* 2006; 186:86–91.
133. Basso F, Amar MJ, Wagner EM, et al. Enhanced ABCG1 expression increases atherosclerosis in LDLr-KO mice on a western diet. *Biochem Biophys Res Commun.* 2006;351:398–404.
134. Watari Y, Yamamoto Y, Brydun A, et al. Ablation of the bach1 gene leads to the suppression of atherosclerosis in bach1 and apolipoprotein E double knockout mice. *Hypertens Res.* 2008;31:783–792.
135. Liu H, Zheng F, Li Z, et al. Reduced acute vascular injury and atherosclerosis in hyperlipidemic mice transgenic for lysozyme. *Am J Pathol.* 2006;169:303–313.
136. Oyama J, Blais C, Jr, Liu X, et al. Reduced myocardial ischemia-reperfusion injury in toll-like receptor 4-deficient mice. *Circulation.* 2004;109:784–789.
137. Riad A, Jager S, Sobirey M, et al. Toll-like receptor-4 modulates survival by induction of left ventricular remodeling after myocardial infarction in mice. *J Immunol.* 2008;180:6954–6961.
138. Shishido T, Nozaki N, Yamaguchi S, et al. Toll-like receptor-2 modulates ventricular remodeling after myocardial infarction. *Circulation.* 2003;108:2905–2910.
139. Shishido T, Nozaki N, Takahashi H, et al. Central role of endogenous toll-like receptor-2 activation in regulating inflammation, reactive oxygen species production, and subsequent neointimal formation after vascular injury. *Biochem Biophys Res Commun.* 2006;345:1446–1453.
140. Papanikolaou A, Papafotika A, Murphy C, et al. Cholesterol-dependent lipid assemblies regulate the activity of the ecto-nucleotidase CD39. *J Biol Chem.* 2005;280:26406–26414.
141. Bauer PM, Yu J, Chen Y, et al. Endothelial-specific expression of caveolin-1 impairs microvascular permeability and angiogenesis. *Proc Natl Acad Sci USA.* 2005;102:204–209.
142. Odening KE, Hyder O, Chaves L, et al. Pharmacogenomics of anesthetic drugs in transgenic LQT1 and LQT2 rabbits reveal genotype-specific differential effects on cardiac repolarization. *Am J Physiol Heart Circ Physiol.* 2008;295:H2264–H2272.
143. Brunner M, Peng X, Liu GX, et al. Mechanisms of cardiac arrhythmias and sudden death in transgenic rabbits with long QT syndrome. *J Clin Invest.* 2008;118:2246–2259.
144. Koren G. Electrical remodeling and arrhythmias in long-QT syndrome: Lessons from genetic models in mice. *Ann Med.* 2004;36 Suppl 1:22–27.
145. Killeen MJ, Thomas G, Sabir IN, Grace AA, Huang CL. Mouse models of human arrhythmia syndromes. *Acta Physiol (Oxf).* 2008;192:455–469.
146. Tillmanns J, Carlsen H, Blomhoff R, et al. Caught in the act: In vivo molecular imaging of the transcription factor NF-kappaB after myocardial infarction. *Biochem Biophys Res Commun.* 2006;342:773–774.
147. Frantz S, Hu K, Bayer B, et al. Absence of NF-kappaB subunit p50 improves heart failure after myocardial infarction. *FASEB J.* 2006;20:1918–1920.
148. Frantz S, Tillmanns J, Kuhlencordt PJ, et al. Tissue-specific effects of the nuclear factor kappaB subunit p50 on myocardial ischemia-reperfusion injury. *Am J Pathol.* 2007;171:507–512.
149. Ramana KV, Willis MS, White MD, et al. Endotoxin-induced cardiomyopathy and systemic inflammation in mice is prevented by aldose reductase inhibition. *Circulation.* 2006;114:1838–1846.
150. Henke N, Schmidt-Ullrich R, Dechend R, et al. Vascular endothelial cell-specific NF-kappaB suppression attenuates hypertension-induced renal damage. *Circ Res.* 2007;101:268–276.
151. Li HL, Zhuo ML, Wang D, et al. Targeted cardiac overexpression of A20 improves left ventricular performance and reduces compensatory hypertrophy after myocardial infarction. *Circulation.* 2007;115:1885–1894.

152. Dufour CR, Wilson BJ, Huss JM, et al. Genome-wide orchestration of cardiac functions by the orphan nuclear receptors ERRalpha and gamma. *Cell Metab.* 2007;5:345–356.
153. Alaynick WA, Kondo RP, Xie W, et al. ERRgamma directs and maintains the transition to oxidative metabolism in the postnatal heart. *Cell Metab.* 2007;6:13–24.
154. Nosek TM, Brotto MA, Jin JP. Troponin T isoforms alter the tolerance of transgenic mouse cardiac muscle to acidosis. *Arch Biochem Biophys.* 2004;430:178–184.
155. Takimoto E, Soergel DG, Janssen PM, Stull LB, Kass DA, Murphy AM. Frequency- and afterload-dependent cardiac modulation in vivo by troponin I with constitutively active protein kinase A phosphorylation sites. *Circ Res.* 2004;94:496–504.
156. Pena JR, Wolska BM. Troponin I phosphorylation plays an important role in the relaxant effect of beta-adrenergic stimulation in mouse hearts. *Cardiovasc Res.* 2004;61:756–763.
157. Angelone T, Quintieri AM, Brar BK, et al. The antihypertensive chromogranin A-derived peptide catestatin as a novel endocrine/paracrine modulator of cardiac function: Inotropic and lusitropic actions on the rat heart. Endocrinology. 2008; 149(10):4780–4793.
158. Mahapatra NR. Catestatin is a novel endogenous peptide that regulates cardiac function and blood pressure. *Cardiovasc Res.* 2008;80:330–338.
159. Hu C, Dandapat A, Sun L, et al. Modulation of angiotensin II-mediated hypertension and cardiac remodeling by lectin-like oxidized low-density lipoprotein receptor-1 deletion. *Hypertension.* 2008;52:556–562.
160. Adamek A, Jung S, Dienesch C, et al. Role of 5-lipoxygenase in myocardial ischemia-reperfusion injury in mice. *Eur J Pharmacol.* 2007;571:51–54.
161. Kirchhefer U, Baba HA, Hanske G, et al. Age-dependent biochemical and contractile properties in atrium of transgenic mice overexpressing junctin. *Am J Physiol Heart Circ Physiol.* 2004;287:H2216–H2225.
162. Kirchhefer U, Hanske G, Jones LR, et al. Overexpression of junctin causes adaptive changes in cardiac myocyte Ca(2+) signaling. *Cell Calcium.* 2006;39:131–142.
163. Zhang L, Franzini-Armstrong C, Ramesh V, Jones LR. Structural alterations in cardiac calcium release units resulting from overexpression of junctin. *J Mol Cell Cardiol.* 2001;33:233–247.
164. Kirchhefer U, Klimas J, Baba HA, et al. Triadin is a critical determinant of cellular Ca cycling and contractility in the heart. *Am J Physiol Heart Circ Physiol.* 2007;293:H3165–H3174.
165. Hagendorff A, Schumacher B, Kirchhoff S, Luderitz B, Willecke K. Conduction disturbances and increased atrial vulnerability in Connexin40-deficient mice analyzed by transesophageal stimulation. *Circulation.* 1999;99:1508–1515.
166. Hagendorff A, Kirchhoff S, Kruger O, et al. Electrophysiological characterization of connexin 40 deficient hearts - In vivo studies in mice. *Z Kardiol.* 2001;90:898–905.
167. Hanner F, Schnichels M, Zheng-Fischhofer Q, et al. Connexin 30.3 is expressed in the kidney but not regulated by dietary salt or high blood pressure. *Cell Commun Adhes.* 2008;15:219–230.
168. Hanner F, von Maltzahn J, Maxeiner S, et al. Connexin45 is expressed in the juxtaglomerular apparatus and is involved in the regulation of renin secretion and blood pressure. *Am J Physiol Regul Integr Comp Physiol.* 2008;295:R371–R380.
169. Wagner C, de Wit C, Gerl M, Kurtz A, Hocherl K. Increased expression of cyclooxygenase 2 contributes to aberrant renin production in connexin 40-deficient kidneys. *Am J Physiol Regul Integr Comp Physiol.* 2007;293:R1781–R1786.
170. Krattinger N, Capponi A, Mazzolai L, et al. Connexin40 regulates renin production and blood pressure. *Kidney Int.* 2007;72:814–822.
171. Winterhager E, Pielensticker N, Freyer J, et al. Replacement of connexin43 by connexin26 in transgenic mice leads to dysfunctional reproductive organs and slowed ventricular conduction in the heart. *BMC Dev Biol.* 2007;7:26.
172. Hattori K, Nakamura K, Hisatomi Y, et al. Arrhythmia induced by spatiotemporal overexpression of calreticulin in the heart. *Mol Genet Metab.* 2007;91:285–293.
173. Pattison JS, Waggoner JR, James J, et al. Phospholamban overexpression in transgenic rabbits. *Transgenic Res.* 2008;17:157–170.

174. Sag CM, Dybkova N, Neef S, Maier LS. Effects on recovery during acidosis in cardiac myocytes overexpressing CaMKII. *J Mol Cell Cardiol.* 2007;43:696–709.
175. Purevjav E, Nelson DP, Varela JJ, et al. Myocardial fas ligand expression increases susceptibility to AZT-induced cardiomyopathy. *Cardiovasc Toxicol.* 2007;7:255–263.
176. Niu J, Azfer A, Kolattukudy PE. Protection against lipopolysaccharide-induced myocardial dysfunction in mice by cardiac-specific expression of soluble fas. *J Mol Cell Cardiol.* 2008;44:160–169.
177. Niu J, Azfer A, Kolattukudy PE. Monocyte-specific bcl-2 expression attenuates inflammation and heart failure in monocyte chemoattractant protein-1 (MCP-1)-induced cardiomyopathy. *Cardiovasc Res.* 2006;71:139–148.
178. Niu J, Azfer A, Deucher MF, Goldschmidt-Clermont PJ, Kolattukudy PE. Targeted cardiac expression of soluble fas prevents the development of heart failure in mice with cardiac-specific expression of MCP-1. *J Mol Cell Cardiol.* 2006;40:810–820.
179. Barnes JA, Singh S, Gomes AV. Protease activated receptors in cardiovascular function and disease. *Mol Cell Biochem.* 2004;263:227–239.
180. Hamilton JR, Cornelissen I, Coughlin SR. Impaired hemostasis and protection against thrombosis in protease-activated receptor 4-deficient mice is due to lack of thrombin signaling in platelets. *J Thromb Haemost.* 2004;2:1429–1435.
181. McGuire JJ, Van Vliet BN, Halfyard SJ. Blood pressures, heart rate and locomotor activity during salt loading and angiotensin II infusion in protease-activated receptor 2 (PAR2) knockout mice. *BMC Physiol.* 2008;8:20.
182. Busso N, Chobaz-Peclat V, Hamilton J, Spee P, Wagtmann N, So A. Essential role of platelet activation via protease activated receptor 4 in tissue factor-initiated inflammation. *Arthritis Res Ther.* 2008;10:R42.
183. Wu Q, Xu-Cai YO, Chen S, Wang W. Corin: New insights into the natriuretic peptide system. *Kidney Int.* 2009;75:142–146.
184. Foronjy RF, Sun J, Lemaitre V, D'Armiento JM. Transgenic expression of matrix metalloproteinase-1 inhibits myocardial fibrosis and prevents the transition to heart failure in a pressure overload mouse model. *Hypertens Res.* 2008;31:725–735.
185. Yamada S, Wang KY, Tanimoto A, et al. Matrix metalloproteinase 12 accelerates the initiation of atherosclerosis and stimulates the progression of fatty streaks to fibrous plaques in transgenic rabbits. *Am J Pathol.* 2008;172:1419–1429.
186. Janssen A, Hoellenriegel J, Fogarasi M, et al. Abnormal vessel formation in the choroid of mice lacking tissue inhibitor of metalloprotease-3. *Invest Ophthalmol Vis Sci.* 2008;49:2812–2822.
187. Holdt LM, Thiery J, Breslow JL, Teupser D. Increased ADAM17 mRNA expression and activity is associated with atherosclerosis resistance in LDL-receptor deficient mice. *Arterioscler Thromb Vasc Biol.* 2008;28:1097–1103.
188. Qin Z, Gongora MC, Ozumi K, et al. Role of menkes ATPase in angiotensin II-induced hypertension. A key modulator for extracellular superoxide dismutase function. *Hypertension.* 2008;52:945–951.
189. Yang A, Sonin D, Jones L, Barry WH, Liang BT. A beneficial role of cardiac P2X4 receptors in heart failure: Rescue of the calsequestrin overexpression model of cardiomyopathy. *Am J Physiol Heart Circ Physiol.* 2004;287:H1096–H1103.
190. Angelis E, Tse MY, Adams MA, Pang SC. Effect of AT2 blockade on cardiac hypertrophy as induced by high dietary salt in the proatrial natriuretic peptide (ANP) gene-disrupted mouse. *Can J Physiol Pharmacol.* 2006;84:625–634.
191. De Ciuceis C, Amiri F, Brassard P, Endemann DH, Touyz RM, Schiffrin EL. Reduced vascular remodeling, endothelial dysfunction, and oxidative stress in resistance arteries of angiotensin II-infused macrophage colony-stimulating factor-deficient mice: Evidence for a role in inflammation in angiotensin-induced vascular injury. *Arterioscler Thromb Vasc Biol.* 2005;25:2106–2113.
192. Shiba Y, Takahashi M, Yoshioka T, et al. M-CSF accelerates neointimal formation in the early phase after vascular injury in mice: The critical role of the SDF-1-CXCR4 system. *Arterioscler Thromb Vasc Biol.* 2007;27:283–289.

193. Amiri F, Virdis A, Neves MF, et al. Endothelium-restricted overexpression of human endothelin-1 causes vascular remodeling and endothelial dysfunction. *Circulation.* 2004;110:2233–2240.
194. Lund AK, Agbor LN, Zhang N, et al. Loss of the aryl hydrocarbon receptor induces hypoxemia, endothelin-1, and systemic hypertension at modest altitude. *Hypertension.* 2008;51:803–809.
195. Dietz HC, Mecham RP. Mouse models of genetic diseases resulting from mutations in elastic fiber proteins. *Matrix Biol.* 2000;19:481–488.
196. Faury G, Pezet M, Knutsen RH, et al. Developmental adaptation of the mouse cardiovascular system to elastin haploinsufficiency. *J Clin Invest.* 2003;112:1419–1428.
197. Hirano E, Knutsen RH, Sugitani H, Ciliberto CH, Mecham RP. Functional rescue of elastin insufficiency in mice by the human elastin gene: Implications for mouse models of human disease. *Circ Res.* 2007;101:523–531.
198. Hou Y, Okada K, Okamoto C, Ueshima S, Matsuo O. Alpha2-antiplasmin is a critical regulator of angiotensin II-mediated vascular remodeling. *Arterioscler Thromb Vasc Biol.* 2008;28:1257–1262.
199. Huggins GS, Lepore JJ, Greytak S, et al. The CREB leucine zipper regulates CREB phosphorylation, cardiomyopathy, and lethality in a transgenic model of heart failure. *Am J Physiol Heart Circ Physiol.* 2007;293:H1877–H1882.
200. Koonen DP, Febbraio M, Bonnet S, et al. CD36 expression contributes to age-induced cardiomyopathy in mice. *Circulation.* 2007;116:2139–2147.
201. Nahrendorf M, Hu K, Frantz S, et al. Factor XIII deficiency causes cardiac rupture, impairs wound healing, and aggravates cardiac remodeling in mice with myocardial infarction. *Circulation.* 2006;113:1196–1202.
202. Kuba K, Zhang L, Imai Y, et al. Impaired heart contractility in apelin gene-deficient mice associated with aging and pressure overload. *Circ Res.* 2007;101:e32–e42.
203. Hatcher CJ, Kim MS, Mah CS, et al. TBX5 transcription factor regulates cell proliferation during cardiogenesis. *Dev Biol.* 2001;230:177–188.
204. Isenberg JS, Frazier WA, Krishna MC, Wink DA, Roberts DD. Enhancing cardiovascular dynamics by inhibition of thrombospondin-1/CD47 signaling. *Curr Drug Targets.* 2008;9:833–841.
205. Wang YA, Zheng JW, Fei ZL, et al. A novel transgenic mice model for venous malformation. *Transgenic Res*. 2009; 18(2):193–201.
206. Tiedt R, Coers J, Ziegler S, et al. Pronounced thrombocytosis in transgenic mice expressing reduced levels of mpl in platelets and terminally differentiated megakaryocytes. *Blood.* 2009;113:1768–1777.
207. van Eeden PE, Tee LB, Lukehurst S, et al. Early vascular and neuronal changes in a VEGF transgenic mouse model of retinal neovascularization. *Invest Ophthalmol Vis Sci.* 2006;47:4638–4645.
208. Isoda K, Kamezawa Y, Ayaori M, Kusuhara M, Tada N, Ohsuzu F. Osteopontin transgenic mice fed a high-cholesterol diet develop early fatty-streak lesions. *Circulation.* 2003;107:679–681.
209. Ohashi R, Mu H, Wang X, Yao Q, Chen C. Reverse cholesterol transport and cholesterol efflux in atherosclerosis. *QJM.* 2005;98:845–856.
210. Rust MB, Faulhaber J, Budack MK, et al. Neurogenic mechanisms contribute to hypertension in mice with disruption of the K-cl cotransporter KCC3. *Circ Res.* 2006;98:549–556.
211. Garnier A, Bendall JK, Fuchs S, et al. Cardiac specific increase in aldosterone production induces coronary dysfunction in aldosterone synthase-transgenic mice. *Circulation.* 2004;110:1819–1825.
212. Sagave JF, Moser M, Ehler E, et al. Targeted disruption of the mouse Csrp2 gene encoding the cysteine- and glycine-rich LIM domain protein CRP2 result in subtle alteration of cardiac ultrastructure. *BMC Dev Biol.* 2008;8:80.
213. Fritsch S, Lindner V, Welsch S, et al. Intravenous delivery of PTH/PTHrP type 1 receptor cDNA to rats decreases heart rate, blood pressure, renal tone, renin angiotensin system, and stress-induced cardiovascular responses. *J Am Soc Nephrol.* 2004;15:2588–2600.
214. Bouillon R, Carmeliet G, Verlinden L, et al. Vitamin D and human health: Lessons from vitamin D receptor null mice. *Endocr Rev.* 2008;29:726–776.
215. Francois H, Makhanova N, Ruiz P, et al. A role for the thromboxane (tp) receptor in l-NAME hypertension. *Am J Physiol Renal Physiol.* 2008;295:F1096–F1102.

216. Guzik TJ, Hoch NE, Brown KA, et al. Role of the T cell in the genesis of angiotensin II induced hypertension and vascular dysfunction. *J Exp Med.* 2007;204:2449–2460.
217. Wang Y, Babankova D, Huang J, Swain GM, Wang DH. Deletion of transient receptor potential vanilloid type 1 receptors exaggerates renal damage in deoxycorticosterone acetate-salt hypertension. *Hypertension.* 2008;52:264–270.
218. Ni W, Zhou H, Diaz J, Murphy DL, Haywood JR, Watts SW. Lack of the serotonin transporter does not prevent mineralocorticoid hypertension in rat and mouse. *Eur J Pharmacol.* 2008;589:225–227.
219. Liao TD, Yang XP, Liu YH, et al. Role of inflammation in the development of renal damage and dysfunction in angiotensin II-induced hypertension. *Hypertension.* 2008;52:256–263.
220. Hinkel R, El-Aouni C, Olson T, et al. Thymosin beta4 is an essential paracrine factor of embryonic endothelial progenitor cell-mediated cardioprotection. *Circulation.* 2008;117:2232–2240.

Index

H

I

O

W